Multi-Players Bandit Algorithms for Internet of Things Networks

Lilian Besson

UNIVERSITE BRETAGNE LOIRE / MATHSTIC

CentraleSupélec

THESE DE DOCTORAT DE

CENTRALESUPELEC RENNES
COMUE UNIVERSITE BRETAGNE LOIRE

ECOLE DOCTORALE N° 601
Mathématiques et Sciences et Technologies de l'Information et de la Communication
Spécialité : *Télécommunications*

Par

Lilian Besson

Algorithmes de Bandits Multi-Joueurs pour les Réseaux de l'Internet des Objets

Multi-Players Bandit Algorithms for Internet of Things Networks

Thèse présentée et soutenue à *Rennes*, le mercredi *20 novembre 2019*
Unité de recherche : UMR 6164 – IETR (équipe SCEE)
Thèse N° : 2019CSUP0005

Rapporteurs avant soutenance :

Nathalie Mitton	Directrice de Recherche Inria, Inria Lille Nord-Europe (*Lille*) **Présidente du jury**
Vianney Perchet	Professeur / École Normale Supérieure de Paris-Saclay (*Cachan*)

Composition du Jury :

Richard Combes	Maître de Conférence CentraleSupélec (*Gif-sur-Yvette*)
Patrick Maillé	Professeur IMT Atlantique *(Rennes)*
Raphaël Féraud	Chercheur Orange Labs (*Lannion*)
Christophe Moy	Professeur Université Rennes 1 (*Rennes*) *Directeur de thèse*
Émilie Kaufmann	Chargée de Recherche CNRS Université de Lille (*Lille*) *Co-encadrante de thèse*

À mes très chers frères, mes deux plus grands modèles.

À mes très chers parents, mes deux plus grands soutiens.

Cette thèse est aussi dédiée à la mémoire du regretté T., qui nous a quitté bien trop jeune.

– Je ne vous ai pas demandé d'en faire des bandits *non plus…*
– Des bandits*? Nooon…Des gars futés !*
Le Roi Arthur et Venec, interprétés par Alexandre Astier et Loïc Varraut,
Kaamelott, Livre II, Épisode 16, "Les tuteurs".

– Y a pas trente-six solutions. Arturus ? Hein ? Fais semblant ! Fais semblant de mériter ton grade. Si tu fais bien semblant, un jour tu verras, t'auras plus besoin !
L'Empereur César, interprété par Pierre Mondy,
Kaamelott, Livre VI, Épisode 5, "Dux Bellorum".

Acknowledgements

I would like to acknowledge and thank the following people, and also the various fundings which supported our works during the last three years and made this thesis possible.

My PhD was founded by the French Ministry of Higher Education and Research (MENESR), thanks to a "contrat doctoral spécifique normalien" obtained while I was a "normalien" student at École Normale Supérieure de Cachan (now ENS de Paris-Saclay). This work has also been supported by the French National Research Agency (ANR), under the projects BADASS, SOGREEN and EPHYL (grants *N ANR-16-CE40-0002*, *N ANR-14-CE28-0025-02* and *N ANR-16-CE25-0002-03*), by CNRS under the PEPS project BIO, by European Union, through the European Regional Development Fund (ERDF), and by Région Bretagne and Rennes Métropole, through the CPER Project *SOPHIE / STIC & Ondes*.

My thoughts then go to my two PhD advisors:

First, thanks to Christophe Moy who welcomed me in the SCEE team, in the IETR lab and in CentraleSupélec campus of Rennes, a nice and warm environment for research and day-to-day life. Christophe was very supportive on every aspect of my work as a PhD student, and he was also helpful during difficult moments in the last three years. Many thanks for being so nice and dynamic, and always comprehensive, especially regarding my teaching activities. Christophe was helpful for his expertise on wireless communications and engineering, and especially on cognitive radio. Regardless of what we did together, whether it was debugging a GNU Radio block [BBM18, BBM19], writing a paper by night while Christophe was in a plane coming back from India [MB19], chatting at a barbecue or playing "palets bretons" together along the ocean in Vannes, I was lucky to collaborate with and be around Christophe.

Then, thanks to Émilie Kaufmann, who accepted to co-supervise my thesis, and who did an amazing job in the last four years. Émilie was highly motivated by our collaboration, and she always pushed me further, to explore the mathematical aspects of my PhD work, to keep faith in the research world, and to keep a strong rigour in every part of our exchanges and productions. Visiting the SequeL team at Inria Lille on regular occasions was a rich experience, and I enjoyed working in close collaboration with Émilie during these visits. Our intensive white board sessions proved to be fruitful, giving the research work that I am the most proud of [BK18a], and rich research papers that join her rigorous expertise in statistical learning and mathematical analysis of bandit algorithms with my passion for numerical experiments, simulations and algorithm designs [BK18a, BK18b, BK19b].

Then I would like to thank the dear members of my PhD committee. It was interesting to be able to discuss with them on regular occasions, and these discussions have been very useful for some of our works. Many thanks to Vianney Perchet and Nathalie Mitton for accepting to review my thesis during the summer 2019, and for their very valuable comments. Thanks to Patrick Maillé and Raphaël Féraud for following our work since Spring 2017, and to Richard Combes as well for being part of my jury. Some of their research works were strong inspirations for our own works, and I wish to also thank their co-authors, and in particular the Masters or PhD students, and useful discussions we had whenever we met: thanks to Claire Vernade, Réda Alami, Étienne Boursier, Frédéric Loge-Munerel and Pratik Gajane, and others I could not meet (*e.g.*, Viktor Toldov or Robin Allesiardo).

Of course on a more personal level, my thoughts are strongly dedicated to my family. I first want to thank my older brother Florian, who has always been my main model and who has been a constant support during all my life and in my studies. His rigour, dedication and seriousness kept pushing me further, and I am immensely proud of him. Some of our board game nights were brain teasers comparable with some maths problems solved for this thesis! I also thank my younger brother Fabian, for being an inspiration for other (highly important) directions of my life. *Tes voyages, ton courage et ta force m'inspirent quotidiennement, merci beaucoup !* I sincerely thank my parents C. & P., for being the best parents since the last 26 years, and for their (vital) moral support. *Merci infiniment de nous avoir offert cette curiosité, merci d'être si gentils, et merci de votre soutien constant et de votre amour !* Very warm thanks then go to M., to my cousin L. and my grand-parents, J. & J.-M. and J., to my uncle J. and aunt B.! *Merci enfin à M., N. & B. pour votre accueil à La Gouesnière !*

I would then like to thank my closest friends, sorted in chronological order of our first encounter in the tall grass[1]: Guillaume, Florian, Marian, Hélène, Lucie, Lætitia and Julia in Briançon, Mayotte and Pierre in Marseille, Laurent, Simon, Tristan, Ludovic, Jessica, Romain, Benjamin, Angèle, Clément in Cachan, Jill-Jênn, Alain, Claire, Édouard, Loïc and Damien also in Cachan, Kumudham and Priscilla in India, Thibault, Sébastien, Sélim, Valentin again in Cachan, and Audrey, Rémi, Marine, Adrien, Bastien, Claire and Lola in Rennes. *J'ai une pensée particulière pour Hélène, merci pour ta foi, ton énergie et ta détermination, notamment en 2018-19.*

Thanks to my wonderful colleagues during these three years: Rémi☕, Pascal☕, Yves, Amor, Carlos Faouzi, Jacques P., Jacques W., Ali C., Haïfa, Marwa, Navik, Quentin☕, Vincent☕, Rami☕, Pierre H., Muhammad, Cristo☕, Adrien☕, Esteban☕, Ali Z., Éloïse☕, Nabil☕, Bastien☕, Corentin☕, Julio, Georgios, Morgane☕ in Rennes ; and Alessandro, Ronan, Julien P., Odalric-Ambrym, Philippe, Olivier, Florian, Xuedong, Guillaume, Benjamin, Julien S., Mathieu, Matteo, Mahsa, Nicolas, Sadegh, Édouard, Yannis and Omar in Lille. I want to especially thank the "coffee friends☕" in Rennes, for our daily interesting discussions. Thanks to the *"futsal"* players on Wednesday lunch, I haven't been useful, but it's been a lot of fun to play with you guys!

[1] Sorry if I forgot you, it's harder to keep track of wild encounters in the tall grass without a Pokédex!

In the last few years, some friends thanked me in their own PhD thesis, and it is a pleasure to do the same, and cross-link to their own PhD thesis. In a chronological order, I thank Jill-Jênn Vie (thesis link ↗), Navikkumar Modi (↗), Quentin Bodinier (↗), Florian Besson[2], Jessica Guérand (↗), Romain Ducasse (↗), Simon Abelard (↗), Ludovic Sacchelli (↗), Claire Brécheteau (↗), Damien Allonsius (↗), Rémi Bonnefoi, and Rami Othman.

For their administrative support regarding research, travelling or teaching, thanks to Karine, Jeannine, Grégory, Anne, Cécile, Maud, Frédéric, Gabriel (and others) at CentraleSupélec campus of Rennes, Amélie at Inria Lille and Maryline (and others) at CRIStAL in Lille. Thanks to the nice people at Sodexo in our campus, especially to Martine and J.-B.!

During my PhD, I was lucky to teach regularly in Mathematics and Computer Science. I warmly thank David Pichardie for his trust and support, and also François Schwarzentruber, Nathalie Bertrand and David Cachera at ENS de Rennes, and Romaric Gaudel and his colleagues at ENSAI. Thanks to them, I loved to teach these 3×64 hours. Thanks to my amazing students, I am proud of you and of our interesting exchanges. I am thankful to Amélie Stainer and Gilbert Gabillard at Lycée Chateaubriand and Joliot-Curie for useful discussions.

I am grateful to amazing professors who passed on their passion for mathematics and computer science to me, including Hubert P. in Briançon (2006-09), Yassine D. (2009-10) and Agnès B. (2010-11) in Lycée Thiers in Marseille. Then at ENS de Cachan (2011-16), I especially think about Frédéric P., Alain T., Claudine P., Florian de V. and Nicolas V. in Maths, to Hubert C.-L., Jean G.-L., Sylvain S., Paul G., Serge H. in Computer Science, and to Carine S.-P., Delphine L. and Nicolas P.† for their support. Thanks to Didier C. and Vijaysekhar C. in Hyderabad (2014-15), Michael U. and Julien F. in Lausanne (2016) for our collaborations.

I would also like to thank some unusual things. I thank my bike which I enjoyed riding everyday, despite the too many accidents and frequent rain, my enthusiastic daily cooking that gave me smiles and energy, and my favorite open-soure technological tools: git, GitHub and Bitbucket, LaTeX, Bash, Julia and Python, GNU/Linux and (X)Ubuntu, Firefox, Konsole and Visual Studio Code, and many other great free and open-source tools. Some people thank (a/some) God in their thesis, I feel that I prefer to thank *the Earth*, and apologize for the too many times I took a plane for a conference abroad, and in general apologize for the environmental impact of this research work. I am trying hard to do better from now on!

Je suis désolé si je vous ai oublié, merci de corriger : Je remercie sincèrement ..... pour ..... *I am sorry I forgot you, please fix this mistake*: I warmly thank ..... for .....

Deseo terminar este agradecimiento con un pensamiento especial para mi gatita L., *quien me apoyó diariamente, me sorprendió con su entusiasmo y me consoló con sus risas y su amor, durante el año pasado. ¡Muchísimas gracias, gatita!*

[2] Que je remercie deux fois plus que ce qu'il me remerciait dans sa propre thèse ! Pour répondre à la question, deux ans plus tard, tu remerciais Tom et moi un nombre non nul $x \in \mathbb{N} \cup \{+\infty\}$ satisfaisant $x = 2x$, soit $x = +\infty$, et je t'en remercie $2x$ fois !

Résumé

Dans cette thèse de doctorat, nous étudions les réseaux sans fil et les appareils reconfigurables qui peuvent accéder à des réseaux de type radio intelligente, dans des bandes non licenciées et sans supervision centrale. Nous considérons notamment des réseaux actuels ou futurs de l'Internet des Objets (IoT), avec l'objectif d'augmenter la durée de vie de la batterie des appareils, en les équipant d'algorithmes d'apprentissage machine peu coûteux mais efficaces, qui leur permettent d'améliorer automatiquement l'efficacité de leurs communications sans fil. Nous proposons deux modèles de réseaux IoT, et nous montrons empiriquement, par des simulations numériques et une validation expérimentale réaliste, le gain que peuvent apporter nos méthodes, qui se reposent sur l'apprentissage par renforcement. Les différents problèmes d'accès au réseau sont modélisés avec des Bandits Multi-Bras (MAB), mais l'analyse de la convergence d'un grand nombre d'appareils jouant à un jeu collaboratif sans communication ni aucune coordination reste délicate, lorsque les appareils suivent tous un modèle d'activation aléatoire. Le reste de ce manuscrit étudie donc deux modèles restreints, d'abord des bandits multi-joueurs dans des problèmes stationnaires, puis des bandits mono-joueur non stationnaires. Nous détaillons également une autre contribution, la bibliothèque Python open-source SMPyBandits, qui permet des simulations numériques de problèmes MAB, qui couvre les modèles étudiés et d'autres.

Abstract

In this PhD thesis, we study wireless networks and reconfigurable end-devices that can access Cognitive Radio networks, in unlicensed bands and without central control. We focus on Internet of Things networks (IoT), with the objective of extending the devices' battery life, by equipping them with low-cost but efficient machine learning algorithms, in order to let them automatically improve the efficiency of their wireless communications. We propose different models of IoT networks, and we show empirically on both numerical simulations and real-world validation the possible gain of our methods, that use Reinforcement Learning. The different network access problems are modeled as Multi-Armed Bandits (MAB), but we found that analyzing the realistic models was intractable, because proving the convergence of many IoT devices playing a collaborative game, without communication nor coordination is hard, when they all follow random activation patterns. The rest of this manuscript thus studies two restricted models, first multi-players bandits in stationary problems, then non-stationary single-player bandits. We also detail another contribution, SMPyBandits, our open-source Python library for numerical MAB simulations, that covers all the studied models and more.

Resumé des Travaux de Thèse

Ce manuscrit conclut ma thèse de doctorat, qui a débuté en octobre 2016 et s'est terminée en novembre 2019. Mes recherches se sont déroulées au laboratoire IETR à Rennes en France, dans l'équipe SCEE hébergée sur le campus de Rennes de l'école d'ingénieurs CentraleSupélec. J'étais supervisé par le professeur Christophe Moy, à Rennes, et j'étais également co-encadré par la docteure Émilie Kaufmann, à qui j'ai souvent rendu visite à Inria Lille Nord Europe.

Contexte de cette thèse

Les problèmes sous-jacents qui motivent cette thèse sont les questions du réchauffement climatique et de l'augmentation de la population mondiale. Au cours des 150 dernières années, l'humanité a développé de nombreuses technologies de communication différentes, et depuis la fin des années 1890, les télécommunications sans fil entre des appareils fabriqués par l'homme ont été rendues possibles, et de plus en plus fréquentes dans nos vies. Avec l'avènement des réseaux de l'Internet des Objets (IdO), des milliards d'objets à basse consommation devraient être déployés dans le monde entier, permettant un large éventail de nouvelles applications. Il existe aujourd'hui un consensus mondial sur le fait qu'avec la tendance actuelle à l'accroissement démographique et la crise énergétique, toute nouvelle technologie déployée doit être à la fois bon marché et efficace sur le plan énergétique, ainsi qu'adaptée pour desservir un grand nombre de personnes et d'appareils. Ces technologies des nouveaux réseaux sans fil de l'IdO devraient pouvoir s'adapter automatiquement à différents environnements et différents contextes d'application, et être aussi efficaces que possible. C'est pourquoi, en plus de l'effort habituel de recherche et développement pour concevoir de nombreux systèmes d'accès radio efficaces, couvrant tous les cas possibles, le moment est venu de le combiner avec un apprentissage machine peu coûteux, dans le but d'atteindre le niveau de gain de performance nécessaire pour que les promesses de l'IdO deviennent réalité.

C'est ainsi que nous avons décidé de nous intéresser dans cette thèse à l'amélioration de la durée de vie des batteries des objets de l'IdO et la réduction du coût énergétique des réseaux de l'IdO. Nous proposons d'atteindre ces deux objectifs conjointement, en intégrant une prise de décision décentralisée à faible coût, directement dans les futurs objets de l'IdO.

Ma thèse de doctorat porte donc sur les applications possibles de l'intégration d'un certain type d'algorithmes d'apprentissage machine (des algorithmes de type bandits multi-bras), afin de permettre aux objets de l'IdO d'optimiser leurs communications sans fil et d'apprendre à s'organiser automatiquement et sans contrôle central ni coordination.

Des anciens téléviseurs aux standards de l'IdO. Historiquement, trois grandes familles de systèmes de communication sans fil ont été déployées dans les grands réseaux commerciaux : d'abord, la radiodiffusion centralisée (*e.g.*, radio ou télédiffusion), puis les systèmes bidirectionnels centralisés (*e.g.*, 4G ou Wi-Fi), et aujourd'hui la collecte décentralisée de données pour les réseaux de l'Internet des Objets (*e.g.*, réseaux capteurs). Ce troisième type de systèmes peut être désigné comme décentralisé : même si une station de base centrale est toujours en charge de nombreux objets (ou appareils), ce sont les objets qui déclenchent l'envoi de paquets radio, et les seules données descendantes qu'ils peuvent recevoir sont de courts accusés de réception (ou acquittements, en anglais *acknowledgements*, noté *Ack*), envoyés par la station de base pour indiquer le succès ou l'échec de chaque paquet envoyé. Cette famille de systèmes sans fil est appelée Internet des Objets (IdO, ou *Internet of Things*, IoT), et un exemple typique d'application de tels réseaux de l'IdO est celui des réseaux sans fil de capteurs.

Pour le développement futur des « réseaux intelligents » (*smart grid*), des « villes intelligentes » (*smart cities*), des « maisons intelligentes » (*smart homes*) ou de « l'agriculture intelligente » (*smart agriculture*), des réseaux de capteurs devraient être largement déployés. Deux exemples d'applications futures qui sont déjà en cours de déploiement, en France ou à l'étranger, sont les « bâtiments connectés » et « l'agriculture connectée ». Pour les bâtiments, l'objectif principal est de réduire le coût de chauffage des bâtiments vides en utilisant des réseaux de capteurs afin d'obtenir des données précises et régulières sur la température dans toutes les pièces et tous les étages, pour permettre au contrôle centralisé du chauffage de minimiser son coût et sa consommation énergétique. Pour l'agriculture, un exemple peut être d'équiper chaque tête de bétail (dans les grandes fermes) de capteurs qui émettent régulièrement des informations biologiques, telles que la température corporelle ou le niveau de stress, afin d'optimiser l'heure de traite des vaches, de surveiller la santé des animaux, etc.

Ce troisième type de systèmes sans fil est caractérisé par sa nature décentralisée, puisque les communications sont initialisées et régulées par les objets, et non par un système de contrôle centralisé. En effet, un contrôle central nécessite des paquets de signalisation très réguliers, qui ont été identifiés comme trop lourds pour ce type de systèmes. Dans les réseaux de l'IdO actuels et futurs, de nombreux objets hétérogènes utilisent la même station de base (aussi appelée point d'accès, ou *base station*, *access point* ou *gateway*) pour des applications différentes. Un problème commun est la forte contrainte en terme de consommation énergétique de ces objets, car la plupart d'entre eux seront déployés sans alimentation directe et fonctionneront sur une batterie minuscule, dont la durée de vie devrait être maximisée. Ainsi, la plupart des

entreprises promettant des solutions d'IdO vendent aujourd'hui des objets ayant une durée de vie supérieure à 10 ans, comme SIGFOX [CVZZ16]. Une autre contrainte commune aux objets de l'IdO est leur faible besoin en communication, car la plupart des applications n'auront besoin d'envoyer qu'un ou quelques messages chaque jour, en nette opposition avec le débit de données élevé recherché pour les systèmes centralisés (tels que 4G/5G et Wi-Fi). De nombreuses normes différentes pour les réseaux de l'IdO ont été proposées ces dernières années, et elles consistent en une spécification à la fois pour la couche *PHY*sique et la couche *M*edium *A*ccess *C*ontrol (*MAC*). Pour citer quelques exemples de normes pouvant être utilisées pour des réseaux de type IdO, ZigBee, Z-Wave ou Bluetooth visent des communications à courte portée (jusqu'à 2 m), tandis que LoRaWAN, SIGFOX, Ingenu ou Weightless sont destinés aux communications à plus longue portée (jusqu'à 50 km). Nous référons à l'article [CVZZ16] pour plus de détails, et les références dans [AC18] ou notre dernier travail [MBDT19].

Épuisement du spectre radio. Un problème majeur des technologies sans fil actuelles est la question de l'épuisement du spectre radio : dans la plupart des bandes de fréquences, la totalité du spectre de radio fréquences (RF) est désormais attribuée et les bandes libres n'existent plus, ce qui limite la possibilité d'ajouter de nouveaux usages. Comme le montre la Figure 1.1 ci-dessous, presque tout le spectre est affecté à divers usages, qui vont de la radio-navigation maritime (historiquement le premier usage des radio-communications, *e.g.*, dans le Titanic), à la recherche spatiale, les communications inter satellitaire, la téléphonie mobile et de nombreuses autres applications. Les organismes de réglementation dans le monde, comme l'Union Internationale des Télécommunications (*ITU*, voir `www.ITU.int`), la Commission Fédérale des Communications aux États-Unis d'Amérique du Nord (*FCC*, voir `FCC.gov`) ou la Conférence Européenne des Administrations des Postes et des Télécommunications en Europe (*CEPT*, voir `CEPT.org`), ainsi que différentes campagnes de mesure indépendantes, ont montré que la plupart des fréquences du spectre des fréquences radio-électriques sont utilisées de manière inefficace. Cela signifie qu'une bande peut être attribuée à un certain usage unique, mais qu'elle peut être libre de tout utilisateur à certains moments et/ou endroits. Nous nous référons à [PPS11] pour une étude sur l'utilisation mondiale du spectre, et à [VMB+10] pour la situation en Europe.

Les bandes des réseaux cellulaires (2G/3G/4G/5G) sont surchargées dans la plupart des régions du monde, mais d'autres bandes de fréquences (comme les fréquences militaires ou de radio amateures) sont moins utilisées. Des études indépendantes réalisées dans certains pays ont confirmé cette observation et conclu que l'utilisation du spectre peut fortement dépendre à la fois du moment et du lieu, comme le montre [LBCU+09] par exemple. En outre, l'attribution fixe du spectre empêche l'introduction de nouveaux services, en particulier pour les objets à bas prix ou pour les marchés de niche. C'est ainsi qu'au cours des quinze dernières années, grâce à un lobbying actif de la communauté de la radio intelligente, les organismes de réglementation dans le monde se sont demandé s'il fallait permettre un nouveau paradigme de

communication sans fil : permettre aux utilisateurs non titulaires d'une licence d'utiliser des bandes sous licence s'ils ne causent pas d'interférence aux utilisateurs payants, titulaires d'une licence. Ces initiatives sont examinées par la **Radio Intelligente** (RI, ou *Cognitive Radio*, CR), que nous détaillons ci-dessous, et en particulier pour l'**Accès Dynamique au Spectre** (ADS, ou *Dynamic Spectrum Access*, DSA), pour lesquelles nous renvoyons aux articles [ALVM06, GB12] pour plus de détails.

Radio Intelligente et Bandits Multi-Bras

Dans cette thèse, nous étudions les réseaux Internet des Objets à longue portée, caractérisés principalement par trois contraintes essentielles : faible consommation d'énergie (ou longue durée de vie des batteries), longue portée, et un faible cycle d'utilisation (*i.e.*, faible à très faible nombres de messages par jour). Plus précisément, nous étudions les interconnexions possibles entre **Radio Intelligente** et **l'apprentissage statistique** appliquées aux réseaux de l'IdO. Définissons et détaillons les deux concepts séparément.

Des TIC à la Radio Intelligente (RI). Nous pouvons affiner le premier champ d'étude de cette thèse, étape par étape : des technologies de l'information et communication (TIC), aux télécommunications, aux communications sans fil, puis à la Radio Intelligente, et enfin à la Radio Logicielle (RL, ou *Software Defined Radio*, SDR). La transition de l'approche historique de la radio matérielle aux architectures RL est un processus graduel, qui a commencé au début des années 1990 et s'est accéléré dans les années 2000. Une RL est un système de radiocommunication où les composants qui ont été traditionnellement implémentés par du matériel dédiés (*e.g.*, mélangeurs, filtres, modulateurs/démodulateurs, détecteurs, etc) sont de plus en plus implémentés au moyen de logiciels sur un processeur. Même si le paradigme de la RI a été initié par des recherches de l'armée des États-Unis d'Amérique du Nord dans les années 1980, l'industrie civile a commencé à s'intéresser à la RI au cours des vingt dernières années, et la RI a également suscité beaucoup d'intérêt de la part du milieu universitaire. Comme la RI n'est pas une technologie standard, elle n'a pas de définition unique, commençons donc par citer la définition de deux chercheurs dont les travaux ont été à l'origine du développement de la RI, dont le premier vient de paraître il y a vingt ans.

- J. Mittola, en 1999, a proposé que « *une radio vraiment intelligente qui serait autonome, sensible aux RF et à l'utilisateur, et qui inclurait la technologie logicielle et les capacités d'apprentissage machine ainsi qu'une grande connaissance de l'environnement radio haute-fidélité* » [MM99].
- Puis S. Haykin en 2005 a aussi dit que « *une radio intelligente (RI) est un système de communication sans fil intelligent qui est capable de connaître son environnement, d'apprendre et d'adapter ses paramètres de fonctionnement* (e.g., *puissance d'émission et fréquence porteuse*)

à la volée, dans le but de fournir une communication fiable à tout moment, en tout lieu et efficace sur le plan spectral » [Hay05].

- L'encyclopédie Wikipédia dit ceci « *une RI est une radio qui peut être programmée et configurée dynamiquement pour utiliser les meilleurs canaux sans fil à proximité afin d'éviter les interférences et la congestion des utilisateurs. Une telle radio détecte automatiquement les canaux disponibles dans le spectre radio, puis modifie en conséquence ses paramètres de transmission ou de réception pour permettre plus de communications sans fil simultanées dans une bande de spectre donnée à un endroit donné* ». (`en.Wikipedia.org/wiki/Cognitive_radio`)

L'une des façons possibles d'envisager la flexibilité du spectre est la suivante. Dans les bandes sous licences, il y a des utilisateurs primaires (UP) qui paient un abonnement pour accéder au réseau, par exemple n'importe qui doit payer pour avoir un numéro de téléphone mobile et utiliser le réseau. Comme nous l'avons vu dans les définitions ci-dessus de la philosophie de la CR, nous pouvons imaginer que si le réseau n'est utilisé par aucun UP à un certain endroit et à une certaine heure, les utilisateurs non licenciés, appelés utilisateurs secondaires (US), pourraient l'utiliser aussi, éventuellement en payant un abonnement auprès de l'opérateur du réseau. La réglementation stipule que les UP ont une priorité stricte, mais même si les bandes RF sont attribuées, les mesures dans le monde réel montrent souvent que certaines bandes ne sont pas utilisées de manière intensive, et donc si un US était équipé d'une capacité de détection spectrale efficace, il pourrait analyser son environnement, et utiliser une bande sous licence si et seulement si elle est exempte de tout UP. Ceci définit le concept d'**Accès Opportuniste au Spectre** (AOS, ou *Opportunistic Spectrum Access*, OSA), pour lequel nous nous référons à l'article [ZS07] pour plus de détails.

Des statistiques ou de l'apprentissage machine aux bandits multi-bras. Nous sommes intéressés par l'apprentissage séquentiel et en particulier par les Bandits Multi-Bras (BMB), qui sont apparus comme des problèmes intéressants au sein de la communauté des statistiques et de l'apprentissage séquentiel, comme le montrent les travaux pionniers de [Tho33, Rob52, LR85]. Les BMB sont également inclus dans le concept plus général d'apprentissage par renforcement (ApR, ou *Reinforcement Learning*, RL), lui-même un des domaines de l'apprentissage machine (AM, ou *Machine Learning*, ML). Le livre de référence sur l'ApR est [SB18], citons donc la définition qu'en donnent R. Sutton et A. Barto : « *l'apprentissage par renforcement, c'est apprendre quoi faire – comment faire le lien entre les situations et les actions – pour maximiser un signal de récompense numérique. L'apprenant n'est pas informé des mesures à prendre mais doit plutôt découvrir quelles actions sont les plus gratifiantes en les essayant* ».

Nous illustrons ci-dessous l'idée d'un cycle d'apprentissage, alternant entre action et réaction, en Figure 1. Un-e joueur-se (ou un-e apprenant-e) interagit avec son environnement en prenant une action $A(t)$ (*e.g.*, un choix dans un ensemble fini, $A(t) \in \{1, \dots, K\}$, ou un vecteur $A(t) \in \mathbb{R}^d$), et ensuite en observant une récompense $r(t)$, qui est une certaine mesure

du succès de cette action, fournie par l'environnement (*e.g.*, $r(t) \in \{0, 1\}$ pour échec/succès binaire, ou $r(t) \in \mathbb{R}$). Le but de la joueuse est de maximiser ses récompenses, par des essais et des erreurs (*i.e.*, actions et récompenses). De nombreux problèmes du monde réel peuvent être présentés comme des problèmes d'apprentissage par renforcement, comme l'illustrent l'article [BR19] et la Section 2.2, par exemple apprendre à marcher, à conduire, à jouer à un jeu vidéo, découvrir quel traitement est efficace pour guérir une certaine maladie, etc.

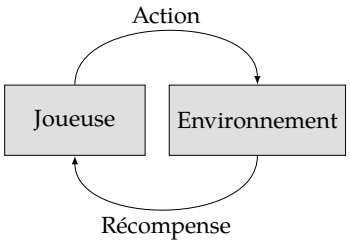

Figure 1 – Cycle de l'apprentissage par renforcement : un-e joueur-se interagit avec son environnement par des actions, et observe une récompense, de façon itérative.

Comme cette thèse se concentre sur les modèles d'apprentissage par renforcement, il est important de souligner que dans de tels modèles de prise de décision, l'apprenant n'a pas accès à l'ensemble des réactions possibles de l'environnement après avoir choisi son action. En d'autres termes, la joueuse ne voit que la récompense donnée par son action à chaque tour, et non la récompense qui aurait été donnée si elle avait choisi une des autres actions. Ce genre de rétroaction limitée s'appelle l'information de type bandit (*bandit feedback*), et nous discutons de l'histoire et du concept des *bandits* (BMB) en détails dans le prochain Chapitre 2. Les essais cliniques et l'identification du meilleur traitement ont été historiquement les premières applications des BMB depuis les années 1930, avec les premiers travaux de W. Thompson [Tho33], car les BMB sont un exemple simple mais puissant du dilemme bien connu entre *exploration et exploitation*. Lorsqu'il est confronté à un ensemble de K actions dont les effets sur l'environnement sont inconnus, l'apprenant doit trouver un équilibre entre explorer les actions inconnues, afin de recueillir plus d'informations à leur sujet, et en exploitant la meilleure action, selon ses connaissances actuelles. Les problèmes de bandits ont été étudiés à la fois dans la communauté de l'apprentissage machine et de la statistique, depuis les années 1950 avec des pionniers comme H. Robbins [Rob52], et c'est un domaine de recherche actif depuis les années 1990 [AVW87a, AVW87b, ACBFS95, Agr95]. La recherche sur les bandits a produit une vaste littérature durant les années 2000 [ACBF02, ACBFS02, AB09] et continue d'être un sujet actif, comme l'illustrent les livres [BCB12, LS19, Sli19] et les nombreuses applications des bandits les dernières années [BR19].

Accès Opportuniste au Spectre (AOS). Les deux communautés de l'AOS et des bandits ont commencé à interagir, et les travaux qui en ont résulté ont suscité un grand intérêt de la part des deux communautés, depuis la fin des années 2000 et le début des années 2010, avec des

travaux pionniers comme [LZ08, LZ10, JEMP09, JEMP10]. L'accent est mis sur un US accédant à un spectre sous licence, occupé par un UP, qui a une priorité stricte sur l'US, qui doit suivre un schéma d'accès de type « écoute avant de transmettre ». Les hypothèses sont les suivantes : l'US est équipé d'une capacité de détection, et considère un ensemble fixe et fini de K canaux orthogonaux, *i.e.*, différentes bandes de fréquences dans un spectre sous licence. Par exemple, il peut s'agir d'un ensemble de $K = 3$ canaux Wi-Fi à différentes fréquences, émis par la même station Wi-Fi. Une autre hypothèse est que UP et US sont synchronisés dans le temps, en subdivisant le temps en pas de temps discrets. Ainsi, si l'US passe un peu de temps au début de chaque plage horaire pour essayer de détecter un UP, il peut rechercher la présence ou l'absence d'un UP, avant de transmettre pendant le reste de la plage horaire, sans entrer en collision avec l'UP. Si l'US était capable d'analyser tous les K canaux, il pourrait simplement émettre dans l'un des canaux libres s'il y en avait, ou ne pas émettre si tous les canaux sont utilisés à un pas de temps donné. Cependant, on sait que la *détection spectrale* est coûteuse en énergie, en particulier pour la détection à large bande, comme le montrent les articles [YA09, SB11] (*spectrum sensing*). C'est pourquoi la plupart des travaux sur l'AOS limitent la capacité de détection de l'US à un seul canal à la fois. Cette hypothèse, ainsi que l'hypothèse selon laquelle les UP ne peuvent pas être perturbés (sans laquelle aucune réglementation ne sera jamais acceptée pour l'AOS), impose à l'US de transmettre dans le canal qu'il a analysé, si et seulement s'il a été détectée sans aucun UP, et ce à chaque pas de temps.

En se concentrant sur un US s'insérant dans un réseau permettant l'AOS, il doit décider séquentiellement d'un canal à analyser (dans l'ensemble des canaux, $[K] = \{1, \dots, K\}$), puis il écoute ce canal et effectue une détection de PU, et enfin il transmet dans ce canal s'il a été détecté libre. Le but de l'US est de minimiser sa consommation d'énergie (nous rappelons que nous nous concentrons sur la radio intelligente « écologique », *green radio*) et de maximiser son débit de données sur la liaison montante, ou de façon équivalente, de maximiser son nombre de transmissions réussies. Si les différents canaux ne sont pas uniformément occupés par les UP, et si l'on suppose une certaine stationnarité sur le trafic des UP, alors l'objectif de l'US se résume à explorer les différents canaux et à exploiter les meilleurs. Le problème de l'AOS est donc un problème d'exploration/exploitation, avec un ensemble fini d'actions (les canaux, également appelés *bras*), dans un cycle séquentiel d'action-réponse (les pas de temps sont $t \in \mathbb{N}^*$), sous l'information de rétroaction partielle (*i.e.*, l'US reçoit l'information concernant un seul canal parmi K). Ces trois hypothèses sont celles qui limitent le cadre général de l'apprentissage séquentiel au cas spécifique des bandit multi-bras (voir Figure 1).

BMB pour l'AOS, et un bref historique de ces recherches par l'équipe SCEE. Les travaux antérieurs de notre équipe SCEE ont montré que les BMB peuvent être utilisés pour modéliser le problème de prise de décision de l'AOS : les bandes de fréquences orthogonales (ou canaux) sont modélisées par des bras $k \in \{1, \dots, K\}$, et la récompense obtenue par l'objet après avoir analysé le canal k au temps t est modélisée par une récompense $r(t) \in \{0, 1\}$. En effet, $r(t) = 1$

indique qu'aucun utilisateur primaire n'a été détecté (et donc qu'un message d'US peut être envoyé), alors que $r(t) = 0$ indique que le canal k est occupé durant l'intervalle de temps t, et qu'aucun message d'US ne doit être envoyé, jusqu'à la fin de cet intervalle. Ce modèle a d'abord été étudié par W. Jouini lors de sa thèse de doctorat avec C. Moy [Jou17], il y a dix ans, d'abord dans l'article [JEMP09] puis avec [JEMP10, JMP12].

Leurs travaux ont été parmi les premiers à proposer l'utilisation de l'apprentissage par renforcement pour la radio intelligente et le problème AOS, notamment le modèle BMB et l'algorithme UCB_1, en parallèle des premiers travaux de Q. Zhao et de son équipe, par exemple [LZ08, LZ10]. Peu de temps après, en 2014, C. Moy et son étudiant C. Robert [RMZ14, Moy14, Moy14] ont développé des preuves de concept utilisant du matériel radio réaliste et la radio logicielle, avec des cartes USRP et le logiciel MATLAB/Simulink. Dans une seconde thèse, N. Modi a étudié de 2014 à 2017 l'impact sur la durée de vie des batteries d'un objet sans fil de l'utilisation des algorithmes BMB pour optimiser la sélection des canaux, [Mod17]. Le compromis entre des reconfigurations fréquentes, qui coûtent en énergie, mais qui permettent d'apprendre rapidement est étudié de façon empirique dans [DMNM16].

En 2017, C. Moy a continué à travailler dans cette direction, avec un étudiant post-doctoral, S. Darak, qui a mené à des publications telles que [DNMP16, DMP16]. Par exemple, des preuves de concepts comme [KDY+16] ont prouvé la capacité de telles approches sur des signaux radio réels pour l'AOS. Certaines analyses de réelles mesures radio effectuées pour les canaux ionosphériques HF ont également prouvé que les solutions basées sur l'apprentissage BMB sont appropriées et résolvent efficacement ce type de problèmes de prise de décision sur les signaux sans fil du monde réel [MGMM+15]. Depuis 2017, S. Darak et son équipe à l'IIIT Delhi en Inde, ont travaillé activement dans la recherche sur la radio intelligente à l'aide de bandits multi-bras. Par héritage de son travail au sein de l'équipe SCEE, certains de leurs travaux récents sont également illustrés par des démonstrations réalistes utilisant USRP et le système MATLAB/Simulink [KYDH18, SKHD18, JKYD18]. Pour plus de détails sur l'état de la recherche sur la radio intelligente, nous renvoyons aux enquêtes [GB12, MM12].

Limitations et spécificités des réseaux de l'IdO. La littérature susmentionnée a essentiellement montré que les algorithmes BMB peuvent être appliqués avec succès au problème de l'AOS. Toutefois, si l'on considère des objets de RI qui ne peuvent pas effectuer de détection spectrale active, tels que des objets à faible coût et à faible consommation d'énergie conçus pour les futurs réseaux de l'IdO, le modèle BMB qui utilise cette détection active pour vérifier l'absence d'UP dans le cadre de l'AOS ne peut plus être appliqué. En outre, dans la plupart des cas, les réseaux de l'IdO utilisent des bandes non licenciées et il n'y a donc plus de distinction entre UP et US. En d'autres termes, il n'y a plus de priorité entre les utilisateurs des réseaux de l'IdO. Les autres spécificités des réseaux de l'IdO peuvent être énumérées comme suit, et nous nous référons à l'article [CVZZ16] pour plus de détails.

- La plupart des objets sont à faible coût, fonctionnent sur du matériel de mauvaise qualité et ont des capacités logicielles et d'alimentation limitées (c'est-à-dire de minuscules batteries). Cela signifie que même s'ils ne sont pas équipés de capacités de détection particulières, ils sont équipés d'un émetteur ainsi que d'un récepteur (Tx et Rx, *i.e.*, un émetteur-récepteur), et ils ont des capacités de stockage et de calcul peu complexes (petits processeurs embarqués),
- une seule station de base IdO devra gérer un très grand nombre d'objets, et ne peut leur envoyer des ordres de coordination afin d'optimiser le réseau,
- les objets ont des cycles de fonctionnement faibles à très faibles (seulement quelques messages par minute ou par mois), et sont en charge d'initier leurs communications en voie montante (*up-link*).

Une coordination centrale des objets avec leur station de base est donc impossible car il faudrait qu'ils communiquent en permanence avec la station de base, ce qui viole les deux dernières contraintes. De plus, en raison de leur matériel limité (Rx/Tx), de leur puissance de calcul limitée et de la durée de vie limitée de leur batterie, bien que les objets soient capables d'utiliser leur antenne de réception pour écouter dans un canal occasionnellement (pendant quelques intervalles de temps après chaque message envoyé), ils ne peuvent pas effectuer de détection spectrale à chaque instant, comme cela est envisagé pour l'AOS (*i.e.*, au début de chaque intervalle, dans un schéma de type « écoute avant de transmettre »).

On pourrait penser qu'en l'absence de détection spectrale, l'apprentissage par renforcement n'est plus applicable, mais n'importe quel objet d'un vrai réseau de l'IdO reçoit encore des informations sur son environnement, après certaines ou toutes ses transmissions. Dans la plupart des normes IdO, un message (sur la voie montante) envoyé à une station de base doit être suivi d'un message (sur la voie descendante) renvoyé par la station de base pour indiquer si le message a été bien reçu, décodé et compris. En utilisant cette rétroaction, qui consiste en un *acquittement* (ou *acknowledgement*, *Ack*) reçu peu après chaque transmission réussie, ou en l'absence d'*Ack* après une transmission échouée, il est possible qu'un objet de l'IdO puisse également optimiser ses communications, grâce à un algorithme d'apprentissage par renforcement correctement conçu.

Nos contributions

Nous commençons par formuler le problème étudié dans cette thèse, puis nous développons notre approche. Si nous résumons les problèmes étudiés en une seule question, ce pourrait être la suivante : « *peut-on adapter les outils de prise de décision déjà appliqués avec succès à la Radio Intelligente* (*RI*) *pour l'Accès Opportuniste au Spectre* (*AOS*) *aux besoins spécifiques de la RI pour les* (*futurs*) *réseaux de l'Internet des Objets* (*IdO*) *?* ». Nous répondons partiellement à cette problématique par les étapes de recherche suivantes.

Explorer la jungle des algorithmes BMB

Nous avons commencé par explorer la riche littérature des bandits multi-bras, car il existe de nombreux algorithmes différents, avec de nombreuses variantes du problème présenté ci-dessus. Nous commençons donc la première partie de cette thèse par le Chapitre 2, qui présente le modèle BMB et passe en revue les algorithmes les plus importants conçus pour résoudre les problèmes stochastiques et stationnaires de bandits. Afin de bien comprendre quels algorithmes pourraient être adaptés aux contraintes susmentionnées de la RI pour les réseaux de l'IdO, nous ne nous sommes pas seulement intéressés par la mesure habituelle des performances d'un algorithme BMB (*i.e.*, son regret, voir ci-dessous en Section 2.3), mais aussi par leurs performances empiriques en termes de complexité de calcul et de stockage, tant du point de vue des analyses théoriques que des mesures réelles.

Notre exploration du grand nombre d'algorithmes et de modèles BMB développés dans la littérature récente nous a donné l'ambition d'écrire un seul logiciel permettant à n'importe quel-le chercheur-euse d'implanter facilement de nouveaux modèles et algorithmes, afin de comparer les modèles existants et d'explorer empiriquement les performances de nouveaux algorithmes. Pour atteindre cet objectif, nous avons développé une bibliothèque de simulation des problèmes BMB, dans le langage populaire Python. À notre connaissance, nous avons écrit la bibliothèque libre de simulation la plus exhaustive pour les problèmes BMB, appelée SMPyBandits [Bes18, Bes19], qui est publiée en ligne sous licence libre (open-source) et qui est hébergée sur `GitHub.com/SMPyBandits`. Nous présentons en détail son architecture et ses fonctionnalités dans le Chapitre 3. Une documentation complète est disponible en ligne, ainsi que des instructions pour reproduire les simulations présentées dans la suite de cette thèse.

Étant donné le grand nombre d'algorithmes BMB disponibles, nous nous intéressons aussi à la question de savoir comment un-e ingénieur-e peut choisir l'algorithme à mettre en œuvre, dans un objet de l'IdO donné, afin de doter cet objet de la capacité de s'adapter de manière robuste à son futur environnement. Pour répondre à cette question, nous présentons deux approches. La première est une comparaison empirique d'algorithmes existants, se focalisant sur les plus efficaces et les mieux connus, en Section 3.3 et 3.4. Nous confirmons que les algorithmes les plus utilisés, tels que UCB [ACBF02], l'échantillonage de Thompson (*Thompson sampling*) [Tho33] et kl-UCB [CGM+13], sont les plus efficaces en termes de regret, et offrent un bon équilibre entre regret et complexité (temps et mémoire). La seconde approche est la sélection d'algorithme en ligne, consistant à agréger un ensemble (fini) d'algorithmes et à découvrir automatiquement lequel est le plus efficace, contre un problème donné, avec notre contribution Aggregator que nous détaillons en Chapitre 4. Ce travail sur l'agrégation des algorithmes BMB était motivé par le cadre AOS, pour lequel les travaux antérieurs ne considéraient que l'algorithme UCB_1 sans vraiment justifier ce choix. Cette contribution a été présentée à la conférence IEEE WCNC à Barcelone, en Espagne, en avril 2018.

Nos modèles de réseaux de l'IdO et de BMB décentralisé

Dans la deuxième partie de cette thèse, nous commençons par proposer et étudier différents modèles de réseaux de l'IdO, avec des simulations et un prototype réel (*i.e.*, une preuve de concept), puis nous étudions des questions intéressantes sur deux modèles mathématiques de bandits, issues de la simplification de notre premier modèle.

Nous étudions deux modèles de réseaux de l'IdO dans le Chapitre 5. Le premier modèle considère que les objets ont simplement des données à envoyer régulièrement à une station de base, à des moments imprévisibles ou aléatoires. De tels objets utilisent les acquittements comme un retour d'information, afin d'optimiser leurs communications sur la liaison montante, en accédant aux meilleurs canaux, c'est-à-dire le canal le moins occupé par le trafic ambiant. L'objectif de ce premier modèle est d'améliorer la qualité de service (QdS, ou *Quality of Service*, QoS) de l'application de ce réseau de l'IdO, en appliquant un ApR décentralisé (côté objet), afin de réduire le taux d'échec de transmission. La station de base recevra donc plus de paquets de liaison montante des objets desservis, s'ils peuvent apprendre par eux-mêmes un accès efficace au spectre. Cela implique aussi que le réseau peut accepter plus d'objets tout en maintenant la même QdS. Notre deuxième modèle considère ensuite les retransmissions de paquets, et bien que les deux modèles soient similaires, l'application d'un algorithme d'apprentissage décentralisé efficace permet dans ce cas d'augmenter la durée de vie des batteries de chacun des objets, ainsi que la QdS de l'ensemble du réseau, puisque moins de retransmissions réduisent aussi la charge locale du spectre.

Le premier modèle sans retransmission est issu du premier article écrit au cours de cette thèse, qui a initié une collaboration avec R. Bonnefoi, un autre doctorant de notre équipe SCEE. Nous l'avons présenté à la conférence EAI CROWNCOM à Lisbonne, au Portugal, en septembre 2017, où il a obtenu le « prix du meilleur papier » [BBM+17]. La preuve de concept (PdC) a continué notre collaboration fructueuse, et a été montrée pendant trois jours à la conférence IEEE ICT à Saint-Malo, France, en juin 2018 [BBM18], et aussi à la conférence IEEE WCNC à Marrakech, Maroc, en avril 2019 [BBM19]. Notre deuxième modèle, avec retransmissions, correspond à la dernière collaboration avec R. Bonnefoi, qui a été présentée à l'atelier MoTION, également pendant la conférence IEEE WCNC 2019 [BBMVM19].

Dans les deux modèles de réseaux de l'IdO présentés ci-dessus, l'idée maîtresse est de laisser chaque objet dynamique d'un tel réseau exécuter un algorithme d'apprentissage de manière totalement décentralisée, afin d'optimiser le système complet. Il est important de noter que chaque objet ne communique, et donc n'apprend, qu'à quelques unes et non à toutes les étapes, en suivant son propre processus d'activation aléatoire (nous nous limitons à un processus d'activation purement aléatoire, Bernoulli de probabilité p). Cela signifie que chaque objet vise son propre objectif local, qui est de maximiser sa récompense cumulée, d'une manière égoïste et complètement agnostique des autres objets ayant le même objectif. Il est

bien connu en théorie des jeux que jouer égoïstement peut être désastreux pour la mesure de performance centralisée, on peut penser aux « dilemmes » populaires, tels que le dilemme du prisonnier. Il était donc assez surprenant que nos simulations numériques, ainsi que la preuve de concept réaliste, aient montré que l'apprentissage BMB décentralisé et égoïste conduisait à une coordination efficace entre les objets, dans tous les scénarios considérés, malgré le fait que ces objets ne peuvent communiquer directement entre eux, et reçoivent seulement un indicateur de collision depuis la station de base à laquelle ils sont associés.

Nous avons donc d'abord essayé d'analyser la performance de cet algorithme décentralisé, que nous appelons Selfish, dans le modèle de la Section 5.2, mais en raison du nombre aléatoire d'objets actifs à chaque pas de temps (*i.e.*, dès que la probabilité p d'activation est $p < 1$), nous n'avons pas pu développer une analyse propre. C'est la raison pour laquelle nous affaiblissons l'hypothèse d'avoir $M \gg K$ (ou même simplement $M > K$) dans un réseau avec un canal sans fil orthogonal K dans le Chapitre 6, qui est équivalent à avoir $p < 1$, et nous considérons le cas d'objets actifs à chaque étape de temps (*i.e.*, $p = 1$), et nous nous limitons donc à $M \leq K$ objets. Le modèle que nous avons étudié comporte différentes variantes, selon le niveau de rétroaction, et couvre à la fois le cas AOS (*i.e.*, avec détection des UP) ou le cas IdO (*i.e.*, sans détection). L'objectif était de comprendre l'heuristique du Chapitre 5, Selfish, dans le cadre plus simple des BMB multi-joueurs, qui a été étudié auparavant pour le cas de l'AOS, comme étudié par exemple par [LZ10, AMT10, AMTA11]. Le cas AOS couvert par notre modèle peut sembler légèrement différent de celui considéré par [JEMP10] et d'autres travaux antérieurs, car notre modèle exige qu'un *Ack* soit renvoyé par la station de base si la transmission a réussi, même dans le cas où l'information de détection est indisponible. Il est en fait équivalent aux modèles précédemment étudiés d'applications des BMB pour l'AOS, puisqu'ils ne prennent en compte que des objets synchronisés, un US et des UP, et donc si la détection indique qu'un canal est libre pour un intervalle de temps, le message envoyé par l'US sera certainement reçu avec succès par la station de base (dans le modèle idéal), donc il n'y aura aucun risque de collision, donc il n'a pas besoin d'*Ack*.

D'une part, dans le cadre de l'AOS, nous n'avons pas réussi à obtenir de résultat positif pour l'algorithme Selfish, car nous avons prouvé que dans certains petits problèmes (*e.g.*, $K = 3$ et $M = 2$), Selfish-UCB peut présenter un regret linéaire avec une faible probabilité, et donc souffre d'un regret moyen linéaire. Ce résultat a ensuite été confirmé et analysé par d'autres chercheurs dans [BP18] (Annexe F). D'autre part, nous avons été en mesure de proposer de nouveaux algorithmes pour ce problème de bandit multi-joueurs (avec informations de détection), et nous avons analysé notre proposition, appelée MCTopM, pour montrer qu'elle atteint une borne supérieure de regret logarithmique à temps fini, qui améliore considérablement les résultats précédents. Notre algorithme atteint également un nombre logarithmique de collisions et de changements de bras, et permet à un groupe fixe de M objets d'apprendre efficacement à utiliser les M meilleurs canaux orthogonalement pour presque toutes leurs communications montantes. Ce fort résultat théorique dépend fortement de la

présence d'une information de détection spectrale et, par conséquent, nos résultats ne sont pas (encore) applicables au modèle IdO sans détection.

Comme expliqué plus haut, le modèle de Chapitre 5 s'est révélé trop complexe à analyser, principalement parce que nous considérons un réseau d'IdO avec de nombreux objets, chacun suivant des profils d'activation aléatoires. La difficulté ne réside pas dans le fait que nous essayons d'analyser des algorithmes de bandits, conçus pour résoudre des problèmes stationnaires, appliqués à un problème non stationnaire, mais plutôt que nous considérons des algorithmes qui jouent tous à différents instants d'activations (aléatoires), ce qui donne des sous-ensembles différents et imprédictibles des pas de temps synchronisés globaux. Généraliser à différentes probabilités d'activation conduirait à un modèle encore plus difficile à analyser, et imposer un maximum de $M \leq K$ objets n'est en fait pas vraiment réaliste pour les réseaux de l'IdO, même si cela conduit au modèle du Chapitre 6.

D'une part, si le profil d'activation de tous les périphériques peut être corrigé, par exemple en se basant sur une affectation centralisée des périphériques à différents créneaux horaires, alors le modèle de bandit multi-joueurs du Chapitre 6 peut être utilisé pour permettre à chaque groupe de $M \leq K$ périphériques d'apprendre une affectation orthogonale optimale dans les K canaux (*e.g.*, les groupes peuvent être le jeu des périphériques que tous émettent au même instant). Cependant, même si nous continuons à supposer un temps synchronisé dans tout le reste de la thèse, il est difficile de soutenir que cette hypothèse d'un calendrier centralisé pour les objets peut être réaliste, car nous étudions le cas de l'apprentissage décentralisé pour l'AOS et l'IdO précisément afin d'éviter un surcoût dû à une signalisation régulière et un contrôle central des objets par la station de base, comme nous l'avons expliqué précédemment.

D'autre part, une autre façon d'affaiblir l'hypothèse de non stationnarité est de prendre le point de vue d'un seul objet, comme dans le cas de l'AOS mentionné ci-dessus, où l'accent est mis sur un US entouré de plusieurs UP ayant des comportements stochastiques et stationnaires. Si nous nous concentrons sur un objet de l'IdO, son environnement (*i.e.*, les autres objets) est non stationnaire, ce qui signifie que ses propriétés moyennes peuvent fluctuer dans le temps, mais les environnements réels présentent généralement des non-stationnarité avec une certaine structure. C'est pourquoi nous considérons l'hypothèse de stationnarité par intervalles de temps, dans la dernière contribution et le dernier chapitre de cette thèse.

Afin de bien comprendre également comment les algorithmes BMB se comportent dans un environnement non stationnaire, nous avons étudié la littérature sur les BMB adverses ou non stationnaires, principalement pour les deux cas d'environnements variant lentement ou changeant brusquement. Nous commençons notre dernier Chapitre 7 en passant en revue les travaux existants, et nous avons choisi de nous concentrer sur les problèmes de bandits stationnaires par morceaux, ce qui signifie que le problème de bandit sous-jacent est stationnaire sur certains intervalles, séparés par des points de changement situés à des moments inconnus. Supposer que l'environnement est stationnaire par morceaux est en effet cohérent pour les

applications aux réseaux sans fil, où un point de changement peut par exemple correspondre à l'arrivée d'un nouveau groupe d'objets dans le réseau. Des exemples d'une telle situation peuvent être une nouvelle entreprise arrivant sur le marché dans une ville (par exemple, les compteurs Linky qui sont installés aujourd'hui en France), ou l'agriculteur voisin installant des capteurs sur son propre troupeau de vaches, etc. Deux grandes familles d'algorithmes ont été proposées pour les problèmes stationnaires par morceaux, qui consistent généralement à combiner un algorithme efficace conçu pour le problème des bandits stationnaires (*e.g.*, Thompson Sampling ou kl-UCB), avec un moyen de s'adapter aux changements dans les distributions des bras. Les algorithmes passivement adaptatives utilisent une fenêtre de taille fixe ou évolutive [GM11], ou un facteur d'oubli, pour oublier les observations passées [KS06, GGCA11], tandis que les algorithmes activement adaptatifs utilisent un test statistique pour détecter les points de changement [MS13, AF15]. Comme la littérature récente a montré que cette dernière approche est généralement plus compétitive, en obtenant de meilleurs résultats tant sur le plan empirique que théorique, nous avons choisi de développer notre propre algorithme activement adaptatif.

Suite à deux travaux précédents récents [LLS18, CZKX19], nous combinons une stratégie d'indices efficace (kl-UCB) et un test efficace de détection des points de changement, dans l'hypothèse de récompenses bornées. Nous nous appuyons sur des résultats très récents à propos du Test du Rapport de Vraisemblance Généralisé (*Generalized Likelihood Ratio Test*, GLRT) pour les variables gaussiennes et sous-gaussiennes [Mai19], mais nous nous concentrons plutôt sur les récompenses bornées et les distributions de Bernoulli. Les récompenses bornées sont en effet généralement plus appropriées pour les applications de RI, comme nous l'avons discuté ci-dessus. En utilisant le fait que les variables bornées dans $[0, 1]$ ne sont pas seulement $1/4$ sous-Gaussiennes mais aussi sous-Bernoulli, nous prouvons les premières garanties à temps fini pour le GLRT pour des variables bornées. Nous montrons d'abord des bornes à temps finis à la fois sur la probabilité de fausse alarme de notre test, et sur son délai de détection, sous des hypothèses raisonnables sur la longueur des séquences stationnaires. Notre algorithme est alors présenté en deux variantes, selon que les points de changement soient locaux (*i.e.*, une seule moyenne de bras change à chaque point de changement) ou globaux (*i.e.*, peut-être que toutes les moyennes des bras changent à la fois). Nous prouvons qu'en combinant l'algorithme kl-UCB, asymptotiquement optimale pour les problèmes stationnaires, et notre nouvelle analyse du GLRT pour les récompenses bornées, nous obtenons des garanties de pointe sur le regret de notre algorithme proposé, noté GLR-klUCB. Nous considérons la même hypothèse que nos concurrents, en supposant que la longueur des intervalles stationnaires est « assez longue » pour que les points de changement soient détectables. La meilleure borne supérieure de regret est obtenue lorsque l'algorithme connaît à l'avance l'horizon et le nombre de points de changement, mais notre algorithme n'a pas besoin d'avoir d'autres connaissances sur la difficulté du problème pour être paramétré de manière optimale. La performance de GLR-klUCB est également illustrée par des expériences numériques sur

des données synthétiques, où il est démontré qu'il surpasse tous les algorithmes passivement adaptatifs ainsi que les précédents algorithmes activement adaptatifs. Ce dernier chapitre est basé sur un de nos derniers travaux, publié à la conférence GRETSI à Lille, en août 2019 [BK19a]. Notre travail a aussi mené à une version longue [BK19b], qui sera complétée avec des résultats plus récents, afin de le soumettre bientôt à une revue (probablement le Journal of Machine Learning Research) avant décembre 2019.

Ce manuscrit se termine par une liste d'abréviations et de notations, puis de figures, d'algorithmes, de morceaux de code et de tableaux, et enfin des références bibliographiques.

Contributions

Nous pouvons énumérer les points suivants pour résumer les principales contributions de cette thèse. Elles se situent à trois niveaux : des modèles BMB pour plusieurs contextes radio liés à la radio intelligente et l'IdO ; des preuves théoriques associées aux problèmes d'apprentissages correspondants ; et enfin des implantations d'algorithmes à but de simulations, de partage avec la communauté, et de validation par des démonstrations radio réalistes.

Nous signalons le chapitre, ainsi que les conférences nationales ou internationales dans lesquelles ont été publiés les résultats correspondants.

- Nous avons écrit la bibliothèque de simulation pour les problèmes BMB la plus complète, appelée SMPyBandits, qui est écrite en Python et publiée en ligne sous une licence open-source [Bes18, Bes19]. Nous présentons en détail son architecture et ses fonctionnalités dans le Chapitre 3, ainsi que différents exemples de son utilisation. Une documentation complète est disponible en ligne, ainsi que des instructions exhaustives pour reproduire les simulations numériques utilisées tout au long de ce manuscrit de thèse.

- Nous présentons le problème du choix de l'algorithme qu'un-e ingénieur-e devrait utiliser, ou de la sélection d'algorithme parmi la riche collection des différents algorithmes de bandits dans la littérature, dans le Chapitre 4. Nous présentons un algorithme d'agrégation d'algorithmes, appelé Aggregator, comme une solution en ligne au problème de sélection d'algorithmes, et nous montrons par des simulations numériques qu'il peut atteindre de bonnes performances empiriques ([BKM18], publié à WCNC 2018).

- Nous proposons différents modèles pour les réseaux de l'Internet des Objets (IdO), dans le Chapitre 5, où les objets dotés de capacités de radio intelligente peuvent mettre en œuvre de leur côté des algorithmes BMB, pour augmenter automatiquement la durée de vie de leur batterie. Cela permet également à davantage d'objets d'utiliser le même réseau tout en maintenant un taux élevé d'accès au spectre sans souffrir de collisions radio (publiés à CROWNCOM 2017 [BBM+17], démonstration ICT 2018 [BBM18], WCNC 2019 [BBM19] et MOTIoN 2019 [BBMVM19]).

- Nous avons réalisé une démonstration réaliste du modèle proposé ci-dessus [BBM18, BBM19], présentée à ICT 2018, et nous la détaillons en Section 5.3. Nous avons aussi réalisé une vidéo de présentation de six minutes, hébergée sur `youtu.be/HospLNQhcMk`.
- Nous formalisons le modèle du bandit multi-joueur, pour lequel nous avons introduit deux variantes, dans le Chapitre 6. Pour le cas avec information de détection spectrale (*spectral sensing*), nous proposons deux algorithmes, et nous analysons notre algorithme MCTopM, pour prouver qu'il est très efficace, à temps fini et asymptotiquement. Nous présentons aussi des expériences numériques approfondies pour montrer qu'il est bien plus efficace que les autres algorithmes de la littérature. Notre travail [BK18a], publié à ALT 2018, a également contribué à un nouvel élan à la recherche sur les bandits multi-joueurs, certains travaux de recherche récents s'étant construits sur nos résultats.
- Nous donnons une revue détaillée de la littérature sur les différentes extensions du modèle BMB multi-joueurs, particulièrement active ces deux dernières années.
- Nous présentons ensuite le modèle de bandits multi-bras stationnaire par morceaux, dans le Chapitre 7, et une vue détaillée de l'état de l'art de la recherche sur ce modèle ([BK19a] publié à GRETSI 2019, [BK19b]). Nous proposons un nouvel algorithme activement adaptatif, pour ces problèmes stationnaires par morceaux, GLR-klUCB, qui atteint des performances empiriques et des garanties théoriques comparables à l'état de l'art, tout en utilisant des hypothèses plus faibles car notre approche n'a pas besoin de connaître de borne sur la difficulté du problème à part le nombre de points de ruptures.

Organisation du manuscrit

L'ordre de lecture du manuscrit peut suivre n'importe quel chemin, entre l'introduction donnée dans le Chapitre 1, et la conclusion générale qui constitue le dernier Chapitre 8. Comme le montre le graphique de la Figure 2 ci-dessous, la thèse est organisée en deux parties, correspondant aux deux lignes intermédiaires de la figure suivante.

- Dans la Partie I, nous commençons par le Chapitre 2 qui présente les modèles de bandits multi-bras (BMB), les concepts et les notations utilisés dans tout ce document. Ce premier chapitre est nécessaire à la lecture du reste du manuscrit. Le Chapitre 3 présente notre bibliothèque de simulations SMPyBandits, qui est utilisée par les Chapitres 2, 4, 6 et 7 pour leurs simulations numériques. Nous terminons cette première partie par le Chapitre 4, qui détaille la première contribution : un nouvel algorithme pour la sélection séquentielle d'algorithmes BMB.
- La deuxième Partie II contient ensuite trois chapitres, qui sont inclus à la fois dans l'ordre logique et chronologique, mais peuvent être lus quasiment indépendamment.

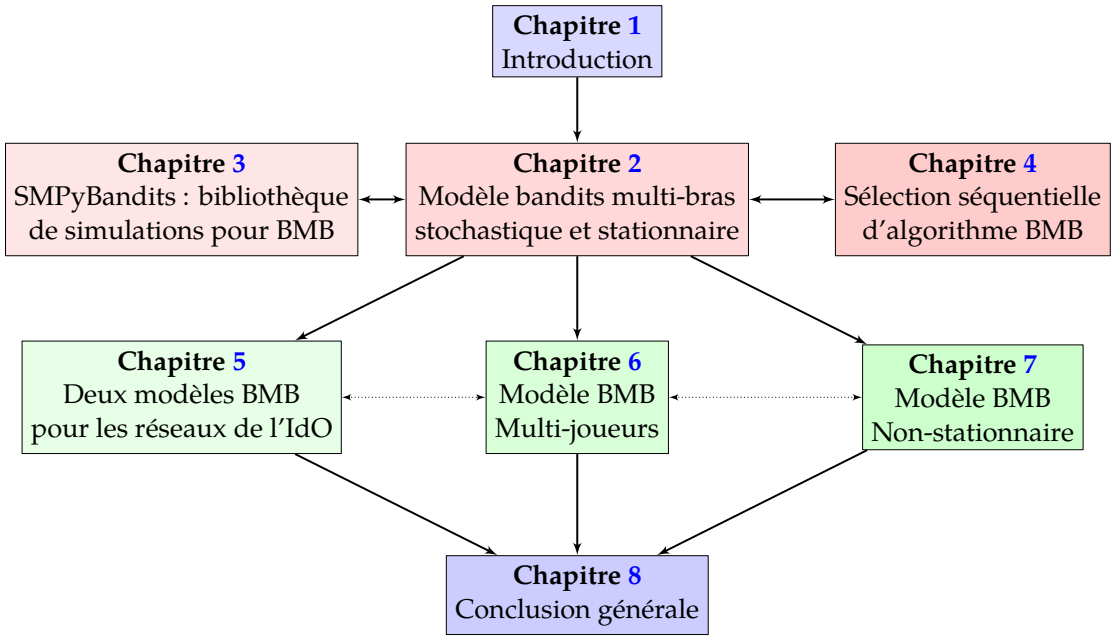

Figure 2 – Organisation de la thèse. Cette thèse peut se lire en suivant n'importe quel chemin contenant le Chapitre 1, le Chapitre 2, au moins un des trois Chapitres 5, 6 ou 7, et la Conclusion.

Le Chapitre 5 commence par proposer et étudier différents modèles de réseaux de l'IdO, pour lesquels nous montrons que les algorithmes BMB peuvent être utilisés avec succès. Nos deux modèles sont intéressants et proches de la réalité, mais ils se sont révélés trop complexes pour proposer une analyse mathématique de la bonne performance empirique des solutions envisagées. Pour cette raison, nous simplifions les modèles précédents dans la suite du document, afin d'établir des preuves mathématiques garantissant la convergence, ainsi que les gains en performance apportés par ces algorithmes de bandit. Les deux Chapitres 6 et 7 étudient chacun un modèle intermédiaire, situé entre le modèle BMB stationnaire à un joueur du Chapitre 2 et les modèles de réseaux de l'IdO du Chapitre 5. Ces deux études ont chacune donné des résultats théoriques à la pointe de la recherche, sur les deux modèles de bandits multi-joueurs et de bandits stationnaires par morceaux, que nous avons aussi validé par des expériences numériques.

Note sur le droit intellectuel. Ce document et les ressources additionnelles requises pour le générer (notamment les fichiers LaTeX, les morceaux de code Python, les figures etc) sont distribuées publiquement, selon les termes de la *licence MIT* open-source, en ligne sur `GitHub.com/Naereen/phd-thesis/`.

Table of Contents

Chapter 1

Introduction

This manuscript concludes my doctoral thesis, which started in October 2016 and finished in November 2019. My research took place at the IETR laboratory in Rennes (France), in the SCEE team, hosted on the Rennes campus of the engineering school CentraleSupélec. I was supervised by Professor Christophe Moy, in Rennes, and I was also co-supervised by Doctor Émilie Kaufmann, whom I visited many times at Inria Lille Nord Europe in Lille (France).

1.1 Context of this thesis

The root of the problems motivating this thesis are the questions of global warming and the increase of the world population. In the last 150 years, humankind has developed different communication technologies, and since the late 1890s, wireless communications between manufactured devices have been made possible, and more and more frequent in our lives. With the advent of Internet of Things networks (IoT), billions of autonomous low-power devices are expected to be deployed worldwide, allowing a wide range of different applications. It is now a world-wide consensus that with the current trend of population increase and with the ongoing energy crisis, any newly deployed technology should be both cheap and energy efficient, as well as adapted to serve a large number of people and devices. Such IoT technologies should be able to adapt automatically to different environments and application contexts, and be as efficient as possible. In addition to the usual Research and Development effort to design different efficient radio access schemes, covering all the possible cases, now the time has come to combine it with cheap and promising Machine Learning in order to (try to) attain the level of performance gain necessary for the IoT promises to become reality.

That is why we are interested in this thesis about improving the battery life of IoT end-devices and reducing the energy cost of IoT networks. We propose to attain these two goals jointly, by embedding low-cost decentralized decision making on directly into the future IoT

devices. Our focus in this PhD thesis is thus on the possible applications of embedding a certain kind of Machine Learning algorithms (Multi-Armed Bandit algorithms), in order to let the IoT devices optimize their wireless communications and learn to be self-organized automatically and without central control nor coordination.

From old TV to the IoT standards. Historically, three main families of wireless communication systems have been deployed in massive commercial networks: first, centralized broadcasting (*e.g.*, radio or TV broadcasting), then centralized bi-directional systems (*e.g.*, 4G or Wi-Fi), and nowadays decentralized data harvesting for the Internet of Things (IoT) networks (*e.g.*, sensor networks). This third kind of systems can be designed as decentralized: because even if a central base station is still in charge of many devices, the devices initiate the sending of up-link packets, and the only down-link data they can receive are short acknowledgements, sent from the base-station to indicate success or failure of every up-link packet. This family of wireless systems are referred to as Internet of Things (IoT), and a typical example of application of such IoT networks is for sensor wireless networks.

For the future development of "smart grids", "smart cities", "smart homes", or "smart agriculture", sensor networks are promised to be widely deployed. Two examples of future applications that are already in deployment, in France or other countries, are "connected buildings" and "connected agriculture". For buildings, the main goal is to reduce the cost of heating empty buildings and use sensor networks to get accurate and regular data about the temperature in all rooms and floors, and let the centralized heat control optimize its cost and energy consumption. For agriculture, one example can be to equip every cow (in large farms) with sensors that regularly emit biological information, such as body temperature or stress level etc, in order to optimize the time of milking, to monitor the health of the animals etc.

This third kind of wireless systems is characterized by its decentralized nature, where communications are initialized and regulated by the devices, not by a centralized control systems. Indeed, a central control requires signaling packets that have been identified as too heavy for these kinds of systems. In the present and future IoT networks, many devices of heterogeneous natures are using the same antenna for different applications. A common problem is the strong constraint that such IoT devices have on their power consumption, as most of them will be deployed without a direct power access and will run on a tiny battery, which lifespan should be maximized. Most commercial IoT companies nowadays indeed sell a lifespan larger than 10 years, like SIGFOX [CVZZ16]. Another common constraint for IoT devices is their low duty cycles, as most applications target a need for one or a few messages to send every day, in strike opposition to the high data-rate pursued for centralized systems (such as 4G/5G and Wi-Fi). Many different standards for IoT networks have been proposed in the recent years, and they consist in a specification for both the *PHY*sical and the *M*edium *A*ccess *C*ontrol (*MAC*) layers. To quote some examples of IoT standards, ZigBee, Z-Wave or

Bluetooth are targeting short-range communications (up-to 2 m), while LoRaWAN, SIGFOX, Ingenu or Weightless are designed for long-range communications (up-to 50 km). We refer to the survey [CVZZ16] and references in our recent articles [MB19, MBDT19] for more details.

Spectrum Scarcity. A major problem of current wireless technologies is the issue of spectrum scarcity: in most kinds of frequency bands, the entire RF spectrum is now allocated and free bands no longer exist, and this limits the possibility of adding any new usage. As illustrated in Figure 1.1 below, almost the entire spectrum is allocated to various usages, that goes from maritime radio-navigation (historically the first usage of radio telecommunication, *e.g.*, in the Titanic), to space research, inter-satellite, mobile telephony and many other applications. Regulatory bodies in the world, like the International Telecommunication Union (see `www.ITU.int`), the Federal Communications Commission in the United States of North America (see `FCC.gov`) or the European Conference of Postal and Telecommunications Administrations in Europe (see `CEPT.org`), as well as different independent measurement campaigns, found that most radio frequency spectrum are inefficiently utilized. This means that while a band can be allocated to a certain unique usage, it can be free from any user in certain times and/or places. We refer to [PPS11] for a survey on the worldwide spectrum utilization, and to [VMB+10] for the situation in Europe.

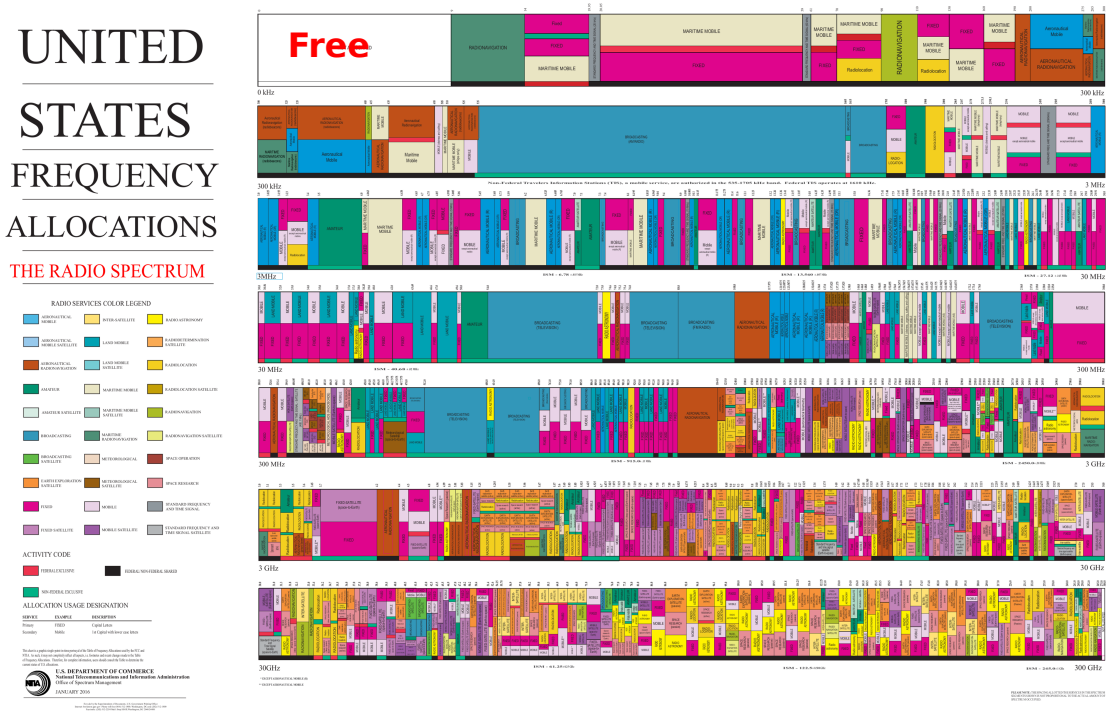

Figure 1.1 – A chart representing the allocation of radio spectrum in the United States of North America in 2016. © United States of North America, Department of Commerce, published online at `www.ntia.doc.gov/files/ntia/publications/january_2016_spectrum_wall_chart.pdf`.

Cellular network bands are overloaded in most parts of the world (2G/3G/4G/5G), but other frequency bands (such as military, amateur radio and paging frequencies) are less utilized. Independent studies performed in some countries confirmed that observation, and concluded that spectrum usage highly depends on both time and place, as shown by [LBCU+09] for instance. Moreover, the fixed spectrum allocation prevents the introduction of new services, especially for low-cost or small markets equipment. Therefore, in the last 15 years, thanks to an active lobbying by the cognitive radio community, regulatory bodies all over the world have been considering whether to allow a new wireless communication paradigm: enable unlicensed users in licensed bands, if they would not cause any interference to the (paying) licensed users. These initiatives are considered by the **Cognitive Radio** field that we detail below, and especially for **Dynamic Spectrum Access** (**DSA**), for which we refer to the surveys [ALVM06, GB12] for more details.

1.2 Cognitive Radio and Multi-Armed Bandits

In this thesis, we study Internet of Things networks characterized by mainly three essential constraints: low power consumption (or long battery life), long-range communications, and low duty cycle. More precisely, we study the possible interconnections between **Cognitive Radio** and **Machine Learning** applied for IoT networks. Let us define and detail both concepts.

From IT to Cognitive Radio. We can narrow down the first field of study of this thesis, steps by steps: from Information Technologies (IT), to Telecommunications, to Wireless Communications, then to Cognitive Radio (CR), and finally to Software Defined Radio (SDR). The transition from the historical approach of hardware-based radio to SDR architectures is a gradual process, that started in the early 1990s and has accelerated in the 2000s. A SDR is a radio communication system where components that have been traditionally implemented in hardware (*e.g.*, mixers, filters, modulators/demodulators, detectors, etc) are more and more implemented by means of software on a processor. Even though the SDR paradigm was initiated by the United States of North America defense research in the 1980s, over the past 20 years the civil industry has started to be interested by SDR, and CR has got significant attention from the academia as well. As CR is not a standard technology, it does not have a single definition, so let us start by quoting the definition of two researchers whose works constitutes the roots of the development of CR, the first one having appeared just 20 years ago.

- J. Mittola in 1999 proposed that *"a really smart radio that would be self-, RF- and user-aware, and that would include software technology and machine learning capabilities along with a lot of high-fidelity knowledge of the radio environment"* [MM99].
- Then S. Haykin in 2005 also said that *"a CR is an intelligent wireless communication system that is capable of being aware of its surroundings, learning, and adapting its operating parameters*

(e.g., *transmit power and carrier frequency*) *on the fly with an objective of providing reliable anytime, anywhere, and spectrally efficient communication"* [Hay05].

- The Wikipedia encyclopedia states *"a CR is a radio that can be programmed and configured dynamically to use the best wireless channels in its vicinity to avoid user interference and congestion. Such a radio automatically detects available channels in wireless spectrum, then accordingly changes its transmission or reception parameters to allow more concurrent wireless communications in a given spectrum band at one location"*. (`en.Wikipedia.org/wiki/Cognitive_radio`)

One possible way of considering spectrum flexibility is the following. In licensed bands, there are Primary Users (PU) paying to access the network, for instance anybody has to pay to have a mobile phone number and use cellular networks. As exposed in the definition above of the CR philosophy, we could imagine that if the network is unused by any PU in a certain location and time, then non licensed users, referred to as Secondary User (SU), could use it, possibly by also paying some rent to the network operator. Regulation states that PU have a strict priority, but even though the RF bands are allocated, real world measurements often show that some bands are not densely used, and thus if a SU was equipped with an efficient *spectrum sensing* capacity, it could analyze its environment, and use a licensed band if and only if it is free of any PU. This defines the concept of **Opportunistic Spectrum Access** (OSA), for which we refer to the survey [ZS07] for more details.

From Statistics or Machine Learning to Multi-Armed Bandits. We are interested by Multi-Armed Bandits (MAB) learning, which emerged as an interesting problem in the statistics community and among researchers interested by sequential learning, as shown by the pioneer works of [Tho33, Rob52, LR85]. It is also included in the more general concept of Reinforcement Learning (RL), itself one of the field of Machine Learning (ML). The reference book on RL is [SB18], so let us quote the definition of RL given by R. Sutton and A. Barto: *"Reinforcement learning is learning what to do - how to map situations to actions - so as to maximize a numerical reward signal. The learner is not told which actions to take, but instead must discover which actions yield the most reward by trying them"*.

We illustrate below the idea of a *learning cycle*, alternating between action and feedback, in Figure 1.2. A player (or learner) interacts with its environment by taking an action $A(t)$ (*e.g.*, a choice in a finite set, $A(t) \in \{1, \dots, K\}$, or a vector $A(t) \in \mathbb{R}^d$), and then by observing a reward $r(t)$, which is a certain measure of success of this action, produced by the environment (*e.g.*, $r(t) \in \{0, 1\}$ for binary failure/success, or $r(t) \in \mathbb{R}$). The goal of the player is to maximize its rewards, by trials and errors (*i.e.*, actions and rewards). Many real-world problems can be framed as Reinforcement Learning problems, as illustrated by the survey [BR19] and Section 2.2, for instance learning to walk, to drive, to play a board or computer game, discovering which treatment is efficient in healing a certain disease (clinical trial), etc.

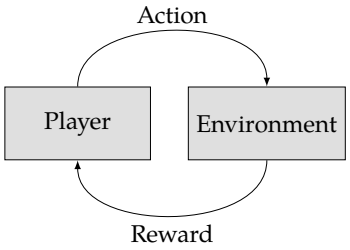

Figure 1.2 – Reinforcement learning cycle: a learner interacts with its environment through actions, and observes a reward, iteratively.

As this thesis focuses on Reinforcement Learning models, it is important to highlight that in such decision making models, the learner does not have access to the entire reaction of the environment after taking its action. In other words, the player only sees the reward generated by playing its action at every round, and not the reward that would have been given if she chose any other action. This kind of limited feedback is called *bandit information*, and we discuss the history and the concept of MAB in details in the next Chapter 2. Clinical trials and treatment discovery were historically the first application of MAB since the 1930s, with the early work of W. Thompson [Tho33], as MAB are indeed a simple yet powerful example of the well-known *exploration vs exploitation dilemma*. When facing a set of K actions whose effects on the environment are unknown, a learner must balance between exploring the unknown actions, in order to collect more information about them, and exploiting the best action, according to its current knowledge. The MAB problem has been studied in both the machine learning and the statistics communities, since the 1950s with pioneers like H. Robbins [Rob52], and more recently it is an active field of research, since the late 1990s [AVW87a, AVW87b, ACBFS95, Agr95]. The research on MAB has produced a vast literature in the 2000s [ACBF02, ACBFS02, AB09] and continues to be a topic of high interest, as illustrated by the surveys and books [BCB12, LS19, Sli19], and the wide range of applications of MAB in the recent years [BR19].

Opportunistic Spectrum Access. The two communities of OSA and MAB have started to interact, and the resulting works have received a great interest from both communities, since the late 2000s and early 2010s, with pioneers works like [LZ08, LZ10, JEMP09, JEMP10]. The focus is on one SU accessing a licensed spectrum, occupied by PU that have a strict priority over the SU, which has to follow a "listen-before-talk" access scheme. The following hypotheses are made: the SU is equipped with a spectrum sensing capability, and considers a fixed and finite set of K orthogonal channels, *i.e.*, different frequency bands in a licensed spectrum. For instance, it can be a set of $K = 3$ Wi-Fi channels at different frequencies, emitted by the same Wi-Fi station. Another hypothesis is that both PU and SU are synchronized in time, by sub-dividing the time in discrete time steps (or rounds). Thus if the SU spends a short time in the beginning of each time slot to perform sensing, it can scan for the presence or

absence of any PU before transmitting, without colliding with the PU during the rest of the time slot. If the SU was able to sense for all the K frequency bands, it could simply transmit in one of the free channels if any, or not transmit if all channels are used at a given time step. However, sensing is known to be costly, in terms of energy consumption, especially for wide-band sensing, as detailed in the surveys [YA09, SB11], thus most works on OSA limit the sensing capacity of SU to sensing only one channel at a time. This assumption, along with the hypothesis that PU cannot be disturbed (without which no regulation will ever be accepted for OSA), enforces the SU to transmit in the channel that it sensed, if and only if it was sensed free from any PU.

Focusing on one SU in an OSA network, it has to sequentially decide a channel to sense (in the set of channels, $[K] = \{1, \dots, K\}$), then it performs spectrum sensing, and finally it transmits in this channel if it was sensed free. The goal of the SU is to minimize its energy consumption (we remind that we focus on "green" cognitive radio) and to maximize its up-link data rate, or equivalently, to maximize its number of successful transmission. If the different channels are not uniformly used by the PU, and if we assume a stationary hypothesis on the PU traffic, then the goal of the SU boils down to exploring the different channels and exploiting the best ones. This frames the Opportunistic Spectrum Access problem as an exploration/exploitation problem, with a finite set of actions (the channels, also called *arms*), in a sequential action-then-feedback cycle (time steps are $t \in \mathbb{N}^*$), under partial information feedback (*i.e.*, the player receives sensing feedback about only one channel over K). These three hypotheses are the ones that restrict from the general sequential learning framework to the specific MAB case (see Figure 1.2).

MAB for OSA, and a short history of these researches at the SCEE team. Previous works of our SCEE team showed that MAB can be used to model the OSA problem: orthogonal frequency bands (or channels) are modeled by arms $k \in \{1, \dots, K\}$, and the feedback obtained by the CR-equipped device after sensing the channel k at time t is modeled by a reward of $r(t) \in \{0, 1\}$. Indeed, $r(t) = 1$ indicates that no Primary User was sensed (and thus the SU can send a message), while a reward of $r(t) = 0$ indicates that the channel k is busy during the time slot t, and no message should be sent, until the end of that slot. This model was first studied by W. Jouini during his PhD thesis with C. Moy [Jou17], about ten years ago, first in the article [JEMP09] and later in [JEMP10, JMP12].

Their works were among the first ones to propose to use Reinforcement Learning for Cognitive Radio and the OSA problem, especially the MAB model and the UCB_1 algorithm, along with the early works of Q. Zhao and her team, for instance with [LZ08, LZ10]. Shortly after in 2014, proof-of-concepts using real-world radio hardware and Software Defined Radio were developed by C. Moy and his student C. Robert, using USRP boards and the MATLAB/Simulink software [RMZ14, Moy14]. In a second PhD thesis, N. Modi studied from 2014 to 2017 the

impact on the battery life of a wireless device of using MAB algorithms to optimize channel selections [Mod17]. The trade-off between rapid software reconfigurations that cost energy but allow to learn quickly is studied empirically in [DMNM16].

In 2017, C. Moy continued to work on this direction, with a post-doctoral student, S. Darak, leading to publications such as [DNMP16, DMP16]. For example, proof-of-concepts like [KDY+16] have proven the capability of such approaches on real radio signals for OSA. Some analysis on real radio measurements made for HF ionospheric channels have also proven that solutions based on MAB learning are appropriate, and solve efficiently this kind of decision-making problems on real-world wireless signals [MGMM+15]. Since 2017, S. Darak, and his team at IIIT Delhi in India, have actively worked in the research on cognitive radio using multi-armed bandits. Inheriting from his work with the SCEE team, some of their recent works are also illustrated with realistic demos using USRP and the MATLAB/Simulink system [KYDH18, SKHD18, JKYD18]. For more details on the state of research on Cognitive Radio, we refer to the surveys [GB12, MM12].

Limitations and specifities of IoT networks. The aforementioned literature has essentially shown that MAB algorithms can be applied successfully on the SU side for the OSA problem. However, if we consider CR-ready devices that cannot perform spectrum sensing, such as low-cost and low energy-consumption end-devices designed for the future Internet of Things networks, the MAB model that uses sensing to detect PU in the OSA case can no longer be applied. Moreover, in most cases, the IoT networks use unlicensed bands, and as such there is no longer a distinction between PU and SU. In other words, there is no longer any priority between users in IoT networks. The other specificities of IoT networks can be listed as follows, and we refer to the survey [CVZZ16] for more details.

- most IoT devices are very low-cost devices, run on low-quality hardware, and have limited software and power capabilities (*i.e.*, tiny batteries). It means that even if they are not equipped with particular spectrum sensing capabilities, they are equipped with a transmitter as well as with a receiver (Tx and Rx, *i.e.*, a transceiver), and they have low-complexity storage and computation capabilities (*i.e.*, small embedded processors),
- a single IoT base station will have to handle a very large number of devices, and cannot send coordination orders to them in order to optimize the network,
- IoT devices have low to very low duty cycles (few messages every minute to only a few every month), and are in charge of initiating their up-link communications.

A central coordination of the devices with their base station is thus impossible as it would require them to communicate continuously with the base station, which violates the two last constraints. Moreover, due to both their limited hardware (Rx/Tx), limited computational power and limited battery life, the IoT devices are able to use their received antenna to sense one channel occasionally (typically, for a few time slots after every single up-link message),

but they cannot perform spectrum sensing like it is considered for OSA and CR (*i.e.*, at the beginning of a time slot, in a "listen-before-talk" scheme).

One could think that in the absence of sensing, Reinforcement Learning is no longer possible, but any real IoT device still receives some information about its environment after some or every of its transmissions. In most IoT standards an up-link message sent to a base station can be followed by a down-link message sent back by the base station, to indicate if the up-link message was successfully received and understood. By using this feedback, which consists in an *acknowledgement* (*Ack*) message received shortly after every successful transmission, or in an absence of *Ack* after a failed transmission, it is possible that an IoT end-device can also use a well-designed RL algorithm, in order to optimize its communications.

1.3 Our contributions

We start by formulating the problem studied in this thesis, and then we develop the organization of the contributions. If we sum-up the studied problems and summarize them in one question, it could be the following: *"Can we adapt the decision making tools, already successfully applied to Cognitive Radio for Opportunistic Spectrum Access, to the specific needs of CR for the (future) Internet of Things networks?"* We answer partially to this problematic by the following steps.

1.3.1 Exploring the Jungle of MAB algorithms

We started by exploring the rich literature of multi-armed bandits, as many different algorithms exist, with lots of variants on the simple problem presented above. We thus start the first part of this thesis with Chapter 2, which presents the MAB model and reviews the most important algorithms designed to solve stochastic and stationary MAB problems. In order to clearly understand which algorithms could be adapted to the aforementioned constraints of CR for IoT networks, we were not only interested by the usual measure of performance of any MAB algorithm (its regret, see below in Section 2.3), but also by their empirical performances in terms of computational complexity and storage requirements, from the points of view of both theoretical analyses and real-world measurements.

Our exploration of the large number of MAB algorithms and models developed in the recent literature has given us the ambition to write a single software allowing anyone to easily implement new models and algorithms, in order to compare the existing ones and empirically explore the performances of newly proposed algorithms. To tackle this goal, we developed a library of simulation of MAB problems, in the Python language. To the best of our knowledge, we wrote the most exhaustive open-source library for bandits. Our library SMPyBandits is published online, under an open-source licence [Bes18, Bes19], and hosted on

GitHub.com/SMPyBandits. We present in details its architecture and its features in Chapter 3, along with different examples of its usage. A full documentation is available online, as well as exhaustive instructions to reproduce the simulations presented in the rest of this thesis.

Because there are so many MAB algorithms available, we are also interested by the question of how an engineer can choose the algorithm to implement, in a given IoT object, in order to equip this object with the capacity to adapt robustly to any environment. To answer this question, we present two approaches. The first one is an empirical comparison of the most efficient and well known existing algorithms, in Sections 3.3 and 3.4. We confirm that widely used and not too sophisticated algorithms, such as UCB [ACBF02], Thompson sampling [Tho33] and $\mathrm{kl\text{-}UCB}$ [CGM+13], are the most efficient in terms of regret, and offer a good balance between regret and (time and memory) complexity. The second approach is online algorithm selection, consisting in aggregating a (finite) set of algorithms and automatically discovering which one performs the most efficiently, against a given problem, with our contribution $\mathrm{Aggregator}$ that we detail in Chapter 4. This work on aggregating MAB algorithms was motivated for the OSA case of CR, where many previous research works only considered the UCB_1 algorithm without really justifying their choice. This contribution was presented in the IEEE WCNC conference in Barcelona, Spain, in April 2018.

1.3.2 Two models of IoT networks and decentralized MAB

In the second part of this thesis, we start by proposing and studying different models of IoT networks, with simulations and a real-world proof-of-concept, and then we study interesting questions on two mathematical models of MAB, arising from simplification of our first model.

We study two models of IoT networks in Chapter 5. The first model considers IoT devices that simply have data to regularly send to a base station, at unpredictable or random times. Such devices use acknowledgements as feedback, in order to optimize their up-link communications, by accessing more the best channels, *i.e.*, the channel less occupied by the surrounding traffic. The goal of this first model is to increase the Quality of Service (QoS) of such IoT network, by applying decentralized RL on the device side in order to reduce the rate of failed transmissions. The base station will thus receive more up-link packets from the devices being served, if they can successfully learn by themselves an efficient spectrum access scheme. It implies that the network can serve more end-devices while maintaining the same QoS. Our second model then considers packet retransmissions, and while the two models are similar, the application of an efficient decentralized learning algorithm now results in both an increased battery life for each of the devices, and an increased QoS for the entire network, as less retransmissions reduce the local spectrum load.

The model without retransmission comes from the first article written during this thesis, which initiated a collaboration with R. Bonnefoi, another PhD student of our team SCEE. We

presented it at the EAI CROWNCOM conference in Lisboa, Portugal in September 2017, where it obtained the "best paper award" [BBM+17]. The proof-of-concept (PoC) continued the fruitful collaboration, and was demonstrated during three days at the IEEE ICT conference in Saint-Malo, France, in June 2018 [BBM18], and later at the IEEE WCNC conference in Marrakech, Morocco, in April 2019 [BBM19]. The second model with retransmissions concluded our collaboration with R. Bonnefoi, and resulted in a paper presented in the 1st MoTION workshop, also during the IEEE WCNC 2019 conference [BBMVM19].

In both models of IoT networks presented above, the core idea is to let every dynamic device run a learning algorithm in a fully decentralized way, in order to optimize the entire system. We highlight that each device communicates, and thus learns, only at some rounds and not at all the time steps, by following its own random activation process (we restrict to a purely random Bernoulli activation process of probability p). This means that each of them target its own local objective, which is to maximize its cumulated reward, in a selfish way and by being agnostic about the other devices following the same objective. It is well known in game theory that playing selfishly can be disastrous for the centralized performance measure, one can think of popular "dilemmas", such as the prisoner dilemma. So it was quite surprising that the numerical simulations, as well as the realistic PoC, showed that decentralized selfish MAB learning leads to efficient coordination between devices in all the considered scenarios, despite the fact that these IoT objects cannot communicate directly with each other, and receive only a collision feedback from the base station they are associated to.

That is why we first tried to analyze the performance of this decentralized algorithm, that we refer to as Selfish, in the model of Section 5.2, but due to the random number of active devices at each time step (*i.e.*, as soon as the probability p of activation is $p < 1$), we were unable to develop a clean analysis. That is the reason why we relax the hypothesis of having $M \gg K$ (or even simply $M > K$) devices in a network with K orthogonal wireless channel in Chapter 6, that is equivalent to having $p < 1$, and we consider the case of IoT devices communicating at every time step (*i.e.*, $p = 1$), and so we restrict to only up-to $M \leq K$ devices. The model we studied comes with different variants, depending on the feedback level, and covers both the OSA case (*i.e.*, with sensing of PU) or the IoT case (*i.e.*, without sensing). The goal was to understand the heuristic of Chapter 5, Selfish, in the simpler framework of multi-player MAB, which has been studied before for the case of OSA, for instance by [LZ10, AMT10, AMTA11]. The OSA case covered by the studied model can seem to slightly differ with the one exposed above, from [JEMP10] and other previous works, as our model requires that an *Ack* is sent back by the base station if the transmission was successful, even in the case where sensing information is available. It is actually equivalent to the previously studied models of applying MAB for OSA, as they only considered synchronized devices, only one SU and PU, and thus if the sensing indicates that one channel is free at one time slot, the up-link message sent by the SU device is sure to be successfully received by the base station (in the ideal model), so there is no risk of collision, and thus no need for an *Ack*.

On the one hand, in the OSA setting, we failed to obtain positive result for the Selfish policy, as we proved that in some limited settings (*e.g.*, $K = 3$ channels and $M = 2$ devices), Selfish-UCB can suffer from linear regret with a small probability, and thus suffers from linear mean regret. This result was later confirmed and analyzed by other researchers in [BP18] (Appendix F). On the other hand, we were able to propose new algorithms for this multi-player bandit problem with sensing information, and we analyzed our proposal MCTopM to show that it achieves a finite-time logarithmic regret upper bound, and improves significantly over previous state-of-the-art results. Our algorithm also achieves a logarithmic number of collisions and arm switches, and allows a fixed group of M devices to efficiently learn to use the M best channels orthogonally for almost all their up-link communications. This strong theoretical result heavily depends on the presence of sensing feedback, and as such our results are not (yet) applicable to the IoT model without sensing.

As explained above, the model of Chapter 5 was found intractable to analyze, mainly because we consider an IoT network with many end-devices, all following random activation patterns. The difficulty does not reside in the fact that we are trying to analyze MAB algorithms, designed to tackle stationary problems, applied on a non-stationary problem, but rather that we consider algorithms which are all playing in different (random) activation times, subsets of the global synchronized time steps. Generalizing to different activation probabilities would lead to a model even harder to analyze, and enforcing at most $M \leq K$ devices is in fact not really realistic for IoT networks, even though this leads to the interesting model of Chapter 6.

On the one hand, if the activation pattern of all devices could be fixed, for instance based on a centralized affectation of the devices to different time slots, then the model of multi-player bandit from Chapter 6 can be used to let every group of $M \leq K$ devices learn an optimal orthogonal affectation in the K channels (*e.g.*, groups can be the set of devices that all emit at the same time). However, even if we continue to assume a synchronized time in all the rest of the thesis, it is hard to argue that this hypothesis of a centralized time schedule for the end-devices can be realistic, because we study the case of decentralized learning for OSA and IoT precisely in order to avoid signaling and any central control of the devices by the base station, as we explained before.

On the other hand, another way to relax the non-stationary hypothesis is to take the point-of-view of a single device, like in the OSA case mentioned above, where the focus is on one SU surrounded by many PU having stationary behaviors. If we focus on one IoT device, its environment (*i.e.*, the surrounding devices) is non-stationary, meaning that its average properties can fluctuate with time, but real environments usually present non-stationarities with certain structures. It is thus interesting and realistic to enforce stationarity on some time intervals, and this leads to the last contribution and the last chapter of this thesis.

In order to also understand precisely how MAB algorithms behave under non-stationary environment, we studied the literature on adversarial and on non-stationary MAB, for the two

cases of slowly-varying and abruptly-changing environments. We begin the last Chapter 7 by reviewing the existing works, and we chose to focus on the piece-wise stationary problem (*i.e.*, abruptly-changing), meaning that the underlying bandit problem is stationary on consecutive intervals, separated by change-points located at unknown times. Assuming the environment to be piece-wise stationary indeed makes sense for applications to wireless networks, where a change-point can for instance corresponds to the arrival of a new group of end-devices in the network. Examples of such a situation can be a new company arriving on the market in one city (*e.g.*, the Linky counters being set-up nowadays in France), or the neighbor farmer installing sensors on his own herd of cows, etc. Two main families of algorithms have been proposed for the piece-wise stationary problem, that usually consists in combining an efficient policy designed for the stationary MAB problem (*e.g.*, Thompson Sampling or kl-UCB) and a way to adapt to changes in the arms distributions. Passively adaptive policies use a window of a fixed or evolving size [GM11], or a discount factor, in order to forget about the past observations [KS06, GGCA11], while actively adaptive policies use a statistical test to detect the change-points [MS13, AF15]. As the recent literature showed that the later approach is usually more competitive, by obtaining better results from both empirical and theoretical aspects, we chose to develop our own actively adaptive algorithm.

Following two recent previous works [LLS18, CZKX19], we combine an efficient index policy (kl-UCB) and an efficient change-point detection test, under the assumption of bounded rewards. We build on very recent results on the Generalized Likelihood Ratio test (GLRT) for Gaussian and sub-Gaussian variables [Mai19], but we instead focus on bounded rewards and Bernoulli distributions. Bounded rewards are indeed usually more appropriate for Cognitive Radio applications, as shown above. Using the fact that bounded variables in $[0, 1]$ are not only $1/4$ sub-Gaussian but also sub-Bernoulli, we prove the first finite-time guarantees for the GLRT for bounded variables. We first show finite-time bounds on both the false alarm probability of the test, and its detection delay, under mild assumptions on the lengths of the stationary sequences. Our algorithm is then presented in two variants, whether change-points are local (*i.e.*, only one arm mean changes at each change-point) or global (*i.e.*, possibly all the arm means change at a time). We prove that by combining the policy kl-UCB, efficient for stationary problems, and our new analysis of the GLRT for bounded rewards, we obtain state-of-the-art guarantees on the regret of the proposed algorithm, denoted GLR-klUCB. We consider the same hypothesis as our competitors, by assuming that the length of the stationary intervals to be "long enough" for the change-points to be detectable. The best regret upper-bound is obtained when the algorithm knows before-hand the horizon and the number of change-points, but our algorithm does not need to have any other knowledge of the problem difficulty to be tuned optimally. The performance of GLR-klUCB is also illustrated on numerical experiments on synthetic data, where it is shown to outperform all the passively adaptive policies as well as the previous actively adaptive policies. This last chapter is based on our last work, published at the GRETSI conference in Lille, France, in August 2019 [BK19a].

This work also leads to the long version article [BK19b], that will be partially rewritten and completed with more recent results, in order to submit it soon to a journal (probably the Journal of Machine Learning Research) in 2020.

This manuscript ends with a list of abbreviations and notations, then with lists of figures, algorithms, code samples and tables, and finally the list of the bibliographical references.

1.3.3 Summary of the contributions

We can list the following points to summarize the main contributions of this thesis.

- We developed SMPyBandits, an exhaustive open-source simulation library for MAB problems, that we published on-line under an open-source licence (MIT) [Bes18, Bes19]. We present it in details in Chapter 3.
- We present in Chapter 4 an algorithm called $\mathrm{Aggregator}$ for aggregation of algorithms as an online solution to the algorithm selection problem, and numerical simulations to illustrate that it achieves state-of-the-art empirical performances [BKM18].
- We propose different models for IoT networks, in Chapter 5, where end-devices with cognitive radio capabilities can implement MAB algorithms on their side, to automatically increase their battery life and allow more devices to use the same network while maintaining a high Quality of Service [BBM+17, BBM19, BBMVM19, MB19, MBDT19].
- We implemented a proof-of-concept of the aforementioned model [BBM18], and we present it in Section 5.3, and in a 6-minute video, hosted at `youtu.be/HospLNQhcMk`.
- We present three variants of the multi-players bandit model in Chapter 6. For the case with sensing information, we propose two new algorithms, and we give an analysis for our algorithm MCTopM to show it is order-optimal, as well as extensive numerical experiments to demonstrate its excellent performance in comparison with the rest of the literature. Some recent research works built up on our results, and the research on multi-players bandits has been quite active since its publication [BK18a].
- We also present the piece-wise stationary MAB model, in Chapter 7, and a detailed literature review of the research on non-stationary MAB [BK19b, BK19a]. We propose a new actively adaptive algorithm for the piece-wise stationary problem, $\mathrm{GLR\text{-}klUCB}$, that achieves state-of-the-art performance, while requiring no prior knowledge on the problem difficulty other than the number of break-points.

1.4 Organization of the thesis

The reading order of the manuscript can be any top-down path between the Introduction in the current Chapter 1, and the Conclusion in the last Chapter 8. The thesis is organized in two parts, corresponding to the two intermediate lines of the following Figure 1.3.

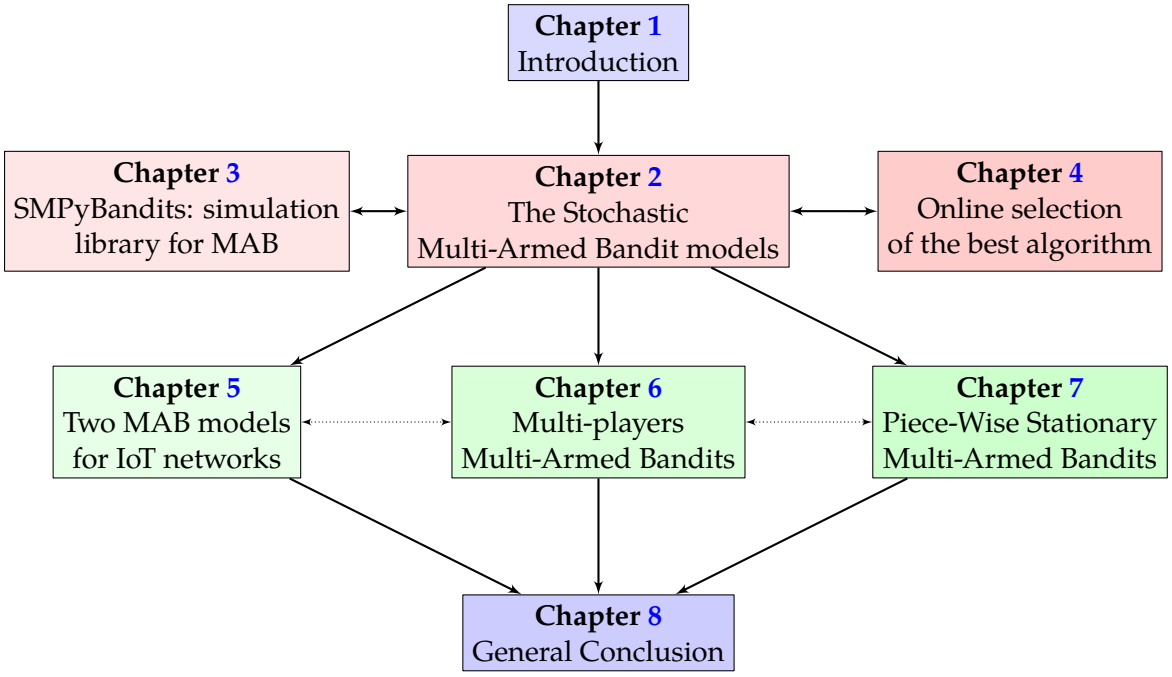

Figure 1.3 – A reading map of the thesis. Any top-down path containing Chapter 1, Chapter 2, at least one of the three Chapters 5, 6 and 7, and the Conclusion is a self contained way to read this thesis.

First, in Part I (second line), we start by the next Chapter 2, required for the rest of the document, as we introduce the MAB models and the notations used in this thesis. Conversely, even if Chapters 2, 6 and 7 use numerical simulations based on our simulation library SMPyBandits, the Chapter 3 where we present SMPyBandits is not required to understand them. We conclude this part with Chapter 4, where we detail one of the first contributions of this thesis, a new algorithm for online MAB algorithms selection.

Then, the second Part II contains three chapters (third line), that are included in both the logical and chronological orders, but can be read almost independently. Chapter 5 starts by presenting different models of IoT networks where we show that MAB algorithms can be used with success. Our two models are interesting and close to reality, but they appeared to be too general to propose a mathematical analysis of the good empirical performance of the considered solutions. For this reason, we weaken the models for the rest of the document, and both Chapters 6 and 7 study an intermediate model, lying between the stationary single-player MAB model from Chapter 2 and the intractable IoT networks models from Chapter 5.

1.5 List of publications

We conclude this chapter with a list of works published during my PhD. All the following works are published entirely and freely, on the HAL platform (on `HAL.Archives-Ouvertes.fr`). The complete list can be found on `CV.Archives-Ouvertes.fr/lilian-besson`. The following publications are ordered historically, from the most recent to the oldest.

Publications in international conferences with proceedings

- *Decentralized Spectrum Learning for IoT Wireless Networks Collision Mitigation*, by Christophe Moy & **Lilian Besson**. 1st International ISIoT workshop, at *Conference on Distributed Computing in Sensor Systems*, Santorini, Greece, May 2019. See Section 5.3. [MB19]
- *Upper-Confidence Bound for Channel Selection in LPWA Networks with Retransmissions*, by Rémi Bonnefoi, **Lilian Besson**, Julio Manco-Vasquez & Christophe Moy. 1st International MOTIoN workshop, at *IEEE WCNC*, Marrakech, Morocco, April 2019. See Section 5.4. [BBMVM19]
- *GNU Radio Implementation of MALIN: "Multi-Armed bandits Learning for Internet-of-things Networks"*, by **Lilian Besson**, Rémi Bonnefoi & Christophe Moy. *Wireless Communication and Networks Conference*, Marrakech, Morocco, April 2019, See Section 5.3. [BBM19]
- *Multi-Player Bandits Revisited*, by **Lilian Besson** & Émilie Kaufmann. *Algorithmic Learning Theory*, Lanzarote, Spain, April 2018, See Chapter 6. [BK18a]
- *Aggregation of Multi-Armed Bandits learning algorithms for Opportunistic Spectrum Access*, by **Lilian Besson**, Émilie Kaufmann & Christophe Moy. *Wireless Communication and Networks Conference*, Barcelona, Spain, April 2018, See Chapter 4. [BKM18]
- *Multi-Armed Bandit Learning in IoT Networks and non-stationary settings*, by Rémi Bonnefoi, **Lilian Besson**, Christophe Moy, Émilie Kaufmann & Jacques Palicot. *Conference on Cognitive Radio Oriented Wireless Networks*, Lisboa, Portugal, September 2017, **Best Paper Award**. See Section 5.2. [BBM+17]

Demonstrations in international conferences

- *MALIN: "Multi-Arm bandit Learning for Iot Networks" with GRC: A TestBed Implementation and Demonstration that Learning Helps*, by **Lilian Besson**, Rémi Bonnefoi, Christophe Moy. Demonstration presented in *International Conference on Telecommunications*, Saint-Malo, France in June 2018. See `YouTu.be/HospLNQhcMk` for a 6-minutes presentation video. See Section 5.3. [BBM18]

French language conferences with proceedings

- *Analyse non asymptotique d'un test séquentiel de détection de ruptures et application aux bandits non stationnaires* (in French), by **Lilian Besson** & Émilie Kaufmann, GRETSI 2019, August 2019, See Chapter 7. [BK19a]

Submitted works

- *Decentralized Spectrum Learning for Radio Collision Mitigation in Ultra-Dense IoT Networks: LoRaWAN Case Study and Measurements*, by Christophe Moy, **Lilian Besson**, Guillaume Delbarre & Laurent Toutain, July 2019. See Chapter 5. [MBDT19]
  Submitted for a special volume of the Annals of Telecommunications journal, on "Machine Learning for Intelligent Wireless Communications and Networking".

- *SMPyBandits: an Open-Source Research Framework for Single and Multi-Players Multi-Arms Bandits (MAB) Algorithms in Python*, by **Lilian Besson** and others, active development since October 2016, `HAL.Inria.fr/hal-01840022`. It currently consists in about 45000 lines of code, hosted on `GitHub.com/SMPyBandits`, and a complete documentation accessible on `SMPyBandits.rtfd.io` or `SMPyBandits.GitHub.io`.
  See Chapter 3. [Bes18, Bes19]
  Submitted for a special track of the Journal of Machine Learning Research, for Machine Learning Open-Source Software (MLOSS), in October 2019.

- *The Generalized Likelihood Ratio Test meets klUCB: an Improved Algorithm for Piece-Wise Non-Stationary Bandits*, by **Lilian Besson** & Émilie Kaufmann, February 2019.
  See Chapter 7. Preprint at `HAL.Inria.fr/hal-02006471`. [BK19b]
  An updated version is in writing, with Julien Seznec and Odalric-Ambrym Maillard.

In progress works waiting for a new submission

- *What Doubling-Trick Can and Can't Do for Multi-Armed Bandits*, by **Lilian Besson** & Émilie Kaufmann, September 2018. Preprint at `HAL.Inria.fr/hal-01736357`. [BK18b]

Part I

Exploring the Jungle of Multi-Armed Bandit algorithms

Chapter 2

Stochastic Multi-Armed Bandits

As explained in Chapter 1, we focus in this thesis on Reinforcement Learning (RL), and especially on decision-making models with a finite number of resources, called arms, and under a stochastic hypothesis: an arm being associated to a binary or real-valued distribution. In this chapter, we present the common base of the more sophisticated mathematical models studied in this thesis: the stochastic multi-armed bandit (MAB) model, by restricting to the single-player and stationary stochastic case. We motivate this model and discuss its application to and beyond Cognitive Radio (CR). We define the notion of regret of an algorithm, and present important results of regret lower-bound from the literature, which quantify what no algorithm can achieve. A short review of the most important families of MAB algorithms is then given, and we highlight some algorithms that are crucially used in the rest of this thesis, like UCB, kl-UCB and Thompson sampling, which all achieve logarithmic regret upper-bounds for our main target of interest, that are binary distributed problems.

– *C'est cool ça, des* bandits *haha !*
Le Barbare, John Lang, *Le Donjon de Naheulbeuk*,
Saison III, Épisode 37 : "La stratélique".

Contents

2.1 The stochastic Multi-Armed Bandit model

Multi-Armed Bandits (MAB) models were introduced by Thompson as early as in 1933 [Tho33], and later studied from the 1950s by Robbins [Rob52] and others. This family of models was first proposed for clinical trials, and later applied to a wide range of different problems. Their name refers to one-armed bandits found in casinos, as shown in Figure 2.2 below. We now formally introduce the model.

A MAB refers to a decision-making game, where a *player* has to sequentially select one action in a usually finite set of actions (or arms), and only receives a (random) feedback about the selected action, also called a *reward*. **We always consider $K \in \mathbb{N}, K \geq 2$ arms, and discrete times** $t \in \mathbb{N}^*$. We denote $[K]$ the set $\{1, \dots, K\}$. Each arm $k \in [K]$ is associated with a stream of rewards $(Y_{k,t})_{t \in \mathbb{N}^*}$, and when the player decides at time t to play (or pull) the arm $A(t) \in [K]$, she receives a reward $r(t) \doteq Y_{A(t),t}$ from this stream. She keeps playing an arm and observing a reward iteratively, and so on for a finite number of steps t (or rounds), from $t = 1$ until $t = T$ for an *horizon* T. A commonly studied goal for the player is to maximize its sum of received rewards, $\sum_{t=1}^{T} r(t)$ (or its *mean* in stochastic and stationary models).

The difficulty of this decision-making game comes from balancing the trade-off between *exploration*, because the player has to observe as much as possible all the arms to get more knowledge about the distributions of their rewards, and *exploitation*, because she also has to select as much as possible the best arm in insight. The MAB model is a famous example of a **reinforcement learning** model, where the decision-making process has to adapt to an unknown environment using noisy observations, alternating between decisions and observations. We illustrate this cycle in Figure 2.1 below. For more details on reinforcement learning, in particular about more generic models, we refer to the famous book [SB18].

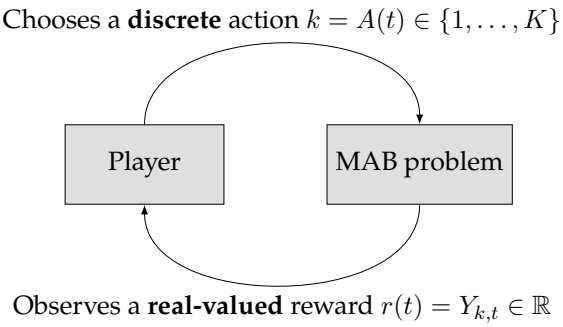

Figure 2.1 – Reinforcement learning cycle in a MAB model, for time steps $t = 1, \dots, T$.

This quantity $\sum_{t=1}^{T} r(t)$ can indeed be random, and it usually depends on two aspects. First, the rewards may depend on the randomness of the environment, *i.e.*, the unknown and unpredictable values $r(t) = Y_{A(t),t}$. Then this quantity also depends on the player's decision-making policy, *i.e.*, the choices $A(t)$, that are based on (all) the *past* observations,

i.e., $A(1), Y_{A(1),1}, \ldots, A(t-1), Y_{A(t-1),t-1}$, and possibly on an external source of randomness. Without loss of generality, it can be given by a sequence $U_0, U_1, \ldots$ of *i.i.d.* random values, uniformly distributed on $[0,1]$, and that has to be independent from the samples $Y_{k,t}$. External randomness is used in most MAB algorithms, *e.g.*, to uniformly break ties in an index policy.

About notations. We use in this thesis the usual notations from the MAB literature, and a summary is included in the Nomenclature, in the Appendix (Page 254).

Main references for the curious reader. For more details and a more formal introduction to multi-armed bandits, we suggest the interested reader to work on a very recent text-book by Slivkins [Sli19]. Another excellent but reasonably short survey is the book by Bubeck and Cesa-Bianchi [BCB12], while the more recent book by Lattimore and Szepesvári [LS19] is the most complete resource about bandit algorithms. Finally, we recommend [BR19] for a short but good survey on applications of MAB.

2.1.1 Finite arms and stochastic rewards

In all this thesis, we focus on the model with finite arms, that is $A(t) \in \{1, \ldots, K\}$ for a fixed and known number of arms $K \in \mathbb{N}, K \geq 2$. We focus on the **stochastic** MAB, in which the reward stream is drawn from some (unknown) distributions, before the beginning of the game. We associate a real-valued distribution to each arm, denoted ν_k for arm $k \in [K]$. We assume that rewards are stationary, meaning that $(Y_{k,t})_{t \in \mathbb{N}^*}$ is independent and identically distributed (*i.i.d.*), and $Y_{k,t} \sim \nu_k$ for any $t \geq 1$. We only consider binary rewards, *i.e.*, $Y_{k,t} \in \{0,1\}$, or real-valued rewards, *i.e.*, $Y_{k,t} \in \mathbb{R}$, and in all this thesis rewards are one-dimensional.

The most common objective for the player is to maximize its expected rewards $\mathbb{E}[\sum_{t=1}^{T} r(t)] = \sum_{t=1}^{T} \mathbb{E}[Y_{A(t),t}]$. The expectation $\mathbb{E}[\bullet]$ is taken on the rewards $(Y_{k,t})_{k,t}$, as well as on the external random variables $(U_s)_s$, *i.e.*, on the algorithm's decisions. Other commonly studied objectives include best-arm identification (BAI) [ABM10], risk- or cost-aware reward maximization etc.

An interactive demo to discover the MAB problem (for the novice). If you are discovering here the concept of bandits, we would like to recommend you to go online and play a few times with an interactive demonstration. On this demo, you will be facing a MAB problem with $K = 5$ arms, and you have $T = 100$ decisions to make. The demo is hosted on my website, at `perso.crans.org/besson/phd/MAB_interactive_demo/`, and it is illustrated below.

The web-page looks like Figure 2.2 below. The arms follow Bernoulli distributions, *i.e.*, $\nu_k = \mathcal{B}(\mu_k)$, of unknown means $\mu_k \in [0,1]$ (this means that $\forall k \in [K], \forall t \in [T], \mathbb{P}(Y_{k,t} = 1) = \mu_k$ and $\mathbb{P}(Y_{k,t} = 0) = 1 - \mu_k$). Your goal in this interactive demonstration is to obtain the highest possible cumulated reward in $T = 100$ steps, *i.e.*, to maximize $\sum_{t=1}^{100} r(t)$. Your decisions are

	Arm 1	Arm 2	Arm 3	Arm 4	Arm 5
Rewards:	6	2	2	2	2
Pulls:	8	4	4	4	4
Estimated Probs:	0.750	0.500	0.500	0.500	0.500
UCBs:	1.641	1.761	1.761	1.761	1.761

Figure 2.2 – Screenshot of the demonstration available on my website, for a current step of $t = 24$.

made sequentially: at time t, you pick one of the arms, $A(t) \in \{1, 2, 3, 4, 5\} = [5]$, then the demo shows the random reward obtained from this (virtual) casino machine (in yellow), *i.e.*, the binary value $r(t) \in \{0, 1\}$, that is sampled *i.i.d.* from ν_k. The UI of the demo also shows the current value of t ("total plays") and $\sum_{s=1}^{t} r(s)$ the "total reward". For each arm, we show the sum of rewards obtained from that arm, *i.e.*, $X_k(t) \doteq \sum_{s=1}^{t} r(s)\mathbb{1}(A(s) = k)$, in the "Rewards" line, and the number of pulls of that arm, *i.e.*, $N_k(t) \doteq \sum_{s=1}^{t} \mathbb{1}(A(s) = k)$ in the "Pulls" line. The demo also shows the estimated probability of each arm, that is $\widehat{\mu_k}(t) \doteq X_k(t)/N_k(t)$ (when $N_k(t) > 0$), in the "Estimated Probs" line.

In the first Figure 2.2, the current state of the game is shown at time $t = 24$. At this step, the player has collected a sum of rewards of 14, by observing $X(t) = [6, 2, 2, 2, 2]$ rewards of value 1 in the $K = 5$ different arms. Arms were sampled $N(t) = [8, 4, 4, 4, 4]$ times, meaning that the value 0 was seen respectively $[2, 2, 2, 2, 2]$ times, and currently arm 1 appears to be the best one. The true means of the arms are $\boldsymbol{\mu} = [0.6, 0.2, 0.55, 0.7, 0.5]$, and (much) more samples are needed before the player can accurately identify arm 4 as the best arm. In the second Figure 2.3 below, we display the result of an example of run, when the player was following the UCB_1 algorithm from [ACBF02] (we present it below in Section 2.4.2). After $T = 100$ steps, the player obtained a cumulated reward of 56, by playing mostly arms $4, 3, 5, 1, 0$ (in decreasing order of number of plays). The empirical means $\widehat{\mu_k}(T)$ correctly identify the best arm (arm 4), but do not correctly rank the arms as arms 1 and 3 obtained means of $\widehat{\mu_1}(T) = 0.5 < \widehat{\mu_3}(T) = 0.6$ but the true means are $\mu_3 = 0.55 < \mu_1 = 0.6$. Other examples of such results, for different algorithms, and $T = 100$ or $T = 10000$, are given in Section 2.4.5.

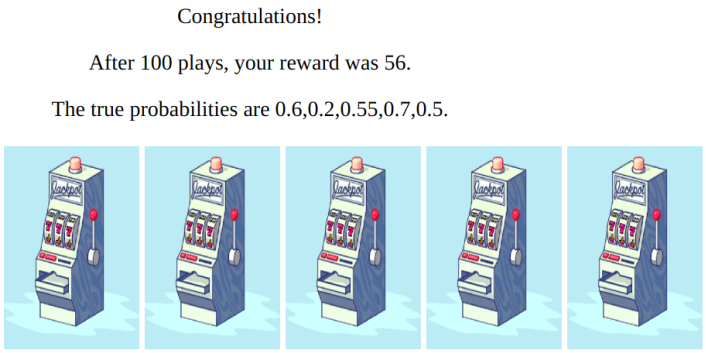

	Arm 1	Arm 2	Arm 3	Arm 4	Arm 5
Rewards:	9	0	15	21	11
Pulls:	18	6	25	31	20
Estimated Probs:	0.500	0.000	0.600	0.677	0.550
UCBs:	1.215	1.239	1.207	1.222	1.229

Figure 2.3 – Screenshot of the demonstration, at the end of the game after $T = 100$ steps, where the player suffers from an empirical regret of $R_T^{\mathrm{UCB}_1} = \mu^* T - 56 = 0.7T - 56 = 14$ after following the UCB_1 algorithm. You can try it online at `perso.crans.org/besson/phd/MAB_interactive_demo/`

Decisions can (and should) depend on the past observations. A *bandit algorithm* $\mathcal{A}$ is also referred to as a strategy or a policy. The algorithm $\mathcal{A}$ selects an arm $A(t)$ at time t, possibly by using the past observations and the past external randomness. As shown below, being oblivious to the past yields very poor performance (cf. the pure exploration policy in Section 2.4.1), so efficient policies indeed depend on the successive feedbacks. More formally, an algorithm can be defined as a sequence of *measurable* functions $(\mathcal{A}_t)_{t\geq 1}$, where $\mathcal{A}_t$ maps the past observations $O_t \doteq (U_0, Y_{A(1),1}, U_1, \dots, Y_{A(t-1),t-1}, U_{t-1})$ to an arm $\mathcal{A}_t(O_t) \doteq A(t) \in [K]$ (we remind that we denote $r(s) = Y_{A(s),s}$ the s-th reward). The initial information is reduced to $O_1 = (U_0)$, and the first decision is $A(1) = \mathcal{A}_1(O_1)$. Usually, most algorithms start by selecting $A(1) = 1, \dots, A(K) = K$ (or a permutation of the K arms) in the K first steps $t = 1, \dots, K$ (*e.g.*, Algorithm 2.3). An algorithm is said to be *deterministic* if it does not depend on the external randomness $U_0, U_1, \dots$, but in this thesis **we only use non-deterministic algorithms** (in particular, index policies need U_t to break ties in the $\arg\max$, see Algorithm 2.3 below).

2.1.2 Common assumptions on the reward distributions

In the example above, we consider Bernoulli distributions, but other real-valued distributions have been studied in the literature. From now on and until the last chapter of this thesis, **we only consider stochastic rewards**. The piece-wise stationary model is studied in Chapter 7. **We also focus only on real-valued rewards**, meaning that $Y_{k,t} \in \mathbb{R}$ for all arm k and time t.

An important hypothesis is whether rewards are bounded or not, and whether the player knows if they are bounded or not before starting the bandit game. Moreover, if rewards are known to be bounded, let say in an interval $[a, b]$, another important hypothesis is whether the player knows the values of a and b or not. Intuitively, the bandit game is easier if the player knows the support of the distributions, and we restrict to this case in all the thesis, *i.e.*, *a, b are always supposed to be known*. Most of the algorithms proposed in the literature follow this hypothesis as well. The mostly used infinitely supported distributions are Gaussian, exponential and Poisson, while in the literature, the Bernoulli distribution is the most common case of finitely supported distributions. Continuous-valued distributions with finite support also included truncated versions of infinitely supported distributions, in particular *truncated* Gaussian are used for numerical experiments in some research articles.

The normalization trick. If the player knows that rewards are bounded in an interval $[a, b]$, and if she knows a and b (for $a < b$), then with no loss of generality we can restrict to the interval $[0, 1]$, as if $r \in [a, b]$, the player can instead consider the normalized reward $r' = \frac{r-a}{b-a}$ that lies in $[0, 1]$. Note that this "normalization trick" is implemented for any policy in our library SMPyBandits, with the `lower` and `amplitude` optional arguments, respectively representing a the lower-bound on rewards and $b - a$ the length of the interval of possible values of rewards.

One-dimensional exponential family. In the literature, parametric assumptions on the rewards are sometimes considered, typically the assumption is that rewards belong to a real-valued distribution lying in an exponential family. One-dimensional exponential families include Bernoulli and Poisson distributions, as well as Gaussian distributions with a fixed variance. In most cases, our main interest is Bernoulli distributions, but we prefer to present the more general notations of exponential families in one dimension.

Given a measure λ, that is usually the natural Lebesgue measure on $\mathbb{R}$, an exponential family of probability distributions is defined as the distributions whose density (relative to λ) can be written as $\mathbb{P}_\eta(x|\lambda) = h(x) \exp(\eta x - A(\eta))$, for a parameter η (the canonical parameter), and a function h. The cumulant function $A(\eta)$ is entirely determined by η and h, as $A(\eta) = \ln(\int h(x) \exp(\eta x) \lambda(\mathrm{d}x))$. The natural parameter space is the set of values of η such that this integral $A(\eta)$ is finite, and usually the literature focuses on regular and minimal exponential families (*i.e.*, when the natural parameter space is a non-empty open set in $\mathbb{R}$).

We mention two important results on exponential families:

1. *A distribution in such a family is entirely characterized by its parameter η.* And the mapping $\eta \mapsto \mathbb{E}_\eta[X]$ is one-to-one, if $\mathbb{E}_\eta$ is the expectation under the probabilistic model $\mathbb{P}_\eta$. That is why one-dimensional distributions are entirely characterized by their mean, $\mu = \mathbb{E}_\eta[X]$.

2. A second important result is a simplified form for the *Kullback-Leibler divergence* [KL51], for two distributions lying in the same exponential family. The KL divergence is also called the *relative entropy*, and it is a measure of how one probability distribution is different from a second, reference probability distribution.

Definition 2.1. *The* Kullback-Leibler divergence *between distributions with densities d_1 and d_2, wrt to λ, is defined as*

$$\mathrm{KL}\left(d_1, d_2\right) \doteq \int d_1 \ln\left(\frac{d_2}{d_1}\right) \lambda(\mathrm{d}x) = \mathbb{E}_{d_1}\left[\ln\left(\frac{d_2}{d_1}\right)\right] \in \mathbb{R}_+ \cup \{+\infty\}. \tag{2.1}$$

Following this Definition 2.1 for two distributions $d_1 = \mathbb{P}(x|\eta_1)$ and $d_2 = \mathbb{P}(x|\eta_2)$ in the same exponential family $\mathcal{E}$, we can use a shorter notation and write $\mathrm{KL}(\eta_1, \eta_2) \doteq \mathrm{KL}(\mathbb{P}(x|\eta_1), \mathbb{P}(x|\eta_2))$, which can be simplified to use only the two parameters η_1 and η_2 of d_1 and d_2, and $\mu_1 = \mathbb{E}_{\eta_1}[X]$ the mean of distribution d_1, $\mathrm{KL}_{\mathcal{E}}\left(\eta_1, \eta_2\right) = \mathbb{E}_{d_1}[(\eta_1 - \eta_2)X] - A(\eta_1) + A(\eta_2) = (\eta_1 - \eta_2)\mu_1 - A(\eta_1) + A(\eta_2)$. Without diving more in the details of exponential families, it is interesting to illustrate this definition and the notations with two important examples:

- **Bernoulli distributions** can be seen as an exponential family with $h(x) = 1$, and for a Bernoulli distribution of mean $\mu \in [0, 1]$, denoted $B(\mu)$, the parameter is $\eta = \mu/(1-\mu)$, giving $A(\eta) = \ln(1 + \mathrm{e}^{\eta})$ (with the limit behavior $\eta = +\infty$ if $\mu = 1$).

  The KL divergence between $\mathcal{B}(x)$ and $\mathcal{B}(y)$, of parameters η, η' is given by $\mathrm{kl}(x, y) \doteq \mathrm{KL}_{\mathcal{B}}(\eta, \eta') = x\ln(x/y) + (1-x)\ln((1-x)/(1-y))$, and it is also called the *relative binary entropy*. It satisfies $\mathrm{kl}(x, y) \geq d_{1/4}(x, y)$ (Pinsker's inequality).

- **Gaussian distributions of a known variance** are a one-dimensional exponential family, and in this thesis we do not consider Gaussian with an unknown variance. For a variance of σ^2, the family uses $h(x) = 1/\sqrt{2\pi\sigma^2}\exp(-x^2/(2\sigma^2))$, and for a Gaussian distribution with mean $\mu \in \mathbb{R}$, denoted $\mathcal{N}(\mu, \sigma^2)$, the parameter is $\eta = \mu/\sigma^2$, giving $A(\eta) = \mu^2/(2\sigma^2)$.

  The KL divergence between $\mathcal{N}(x, \sigma^2)$ and $\mathcal{N}(y, \sigma^2)$, of parameters η, η' is given by $d_{\sigma^2}(x, y) \doteq \mathrm{KL}_{\mathcal{N},\sigma^2}(\eta, \eta') = (x-y)^2/(2\sigma^2)$ (see Chapter 8 of [Jor10]).

Hypotheses in this thesis. In the rest of this thesis, **we only consider bounded rewards in the mathematical developments**, and we mostly focus on Bernoulli distributions, because they are usually the most relevant choice for the considered applications. In Chapter 5, we only study models with binary rewards. Then, when we study multi-players bandits in Chapter 6, we explain that restricting to the Bernoulli case is interesting and not restrictive, as it is actually the hardest case (since continuous distributions has a null mass on $Y_{k,t} = 0$, they yield a much simpler problem as the sensing/no sensing distinction no longer makes sense), but this

work can be extended to any one-dimensional exponential families. Finally, in Chapter 7 we analyze our proposed algorithm for bounded distributions, without restricting to Bernoulli distributions, but we use the fact that bounded distributions on $[0, 1]$ are sub-Bernoulli, and our analysis use the Bernoulli Kullback-Leibler divergence kl.

Sub-Gaussian and sub-Bernoulli distributions. A lot of research works considers rewards distributions that are not Gaussian but sub-Gaussian, meaning distributions whose moment generating function is dominated by that of a Gaussian distribution with the same mean (and a known variance). For instance, bounded distributions on $[0, 1]$ are known to be $1/4$ sub-Gaussian, and this fact is used for instance in [Mai19]. In Chapter 7, we instead consider sub-Bernoulli distributions, formally introduced in Definition 7.1. Such hypothesis is also proposed for other families of distributions, for instance the recent article [KT19] analyses their Follow-the-Perturbed-Leader algorithm for perturbations following any sub-Weibull distribution, that generalize both sub-Gaussian and sub-Exponential distributions.

About Markov models. Finally, we note that Markov bandit models have also been considered for Cognitive Radio applications [LZ08]. They are not studied in this thesis, even though we did implement them in SMPyBandits. They were introduced in the 1980s, by Whittle in [Whi88] and Anantharam and others in [AVW87b]. A Markov MAB model maps an arm to a Markov chain [Nor98], instead of a distribution, and thus they are no longer stochastic. A Markov model exists in two flavors: rested or restless. For K arms, each Markov chain has a finite number of states s, each corresponding to a (constant) reward that the player obtains if she selects this arm while its Markov chain is in state s. Rested Markov models means that only the state of the selected arm's Markov chain can change, following its Markov transition matrix. Restless models remove this hypothesis, making them harder to track and solve. Such models were less studied than stationary or adversarial models, but some interesting works applied Markov models to Cognitive Radio in the last 10 years For instance, [MGMM+15] proposed a CR model mixing MAB and Hidden Markov Models (HMM), solved by a mixed policy called UCB-HMM. A reader curious about Markov chains could start to read Chapter 3 of [LS19] (Section 3.2) and then refer to [Nor98].

2.2 Applications of stochastic MAB

The blooming success of the research on multi-armed bandits is easily explained by the different possibilities of applying MAB models to real-world discrete-time decision making problems. This research field has been very active since the years 2010s, but it started as early as 1933 with [Tho33], and was active since the 1980s and the seminal works by Lai and Robbins

[LR85] and by Anantharam and others [AVW87a]. MAB have been applied successfully to various decision making problems, like the following:

Clinical trials have been the first historical application of MAB models, where an arm represents a treatment, and the distribution associated with such treatment can be a Bernoulli distribution: a reward of 0 means the treatment did not heal the disease, and a reward of 1 indicates a success. The mean of an arm, in this application, represents the mean success rate of a treatment. Following the "best arm identification" model, the goal of a doctor in a clinical trial is to identify the best treatment, *i.e.*, the arm with highest mean, in a number of trials as short as possible. And following our model of interest, maximizing the rewards corresponds to maximizing the number of patients being successfully treated.

MAB can also be applied to a broader setting of **online content recommendation**. The seminal work of [LCLS10] studies the application of contextual bandit to news articles recommendation, as it is used in practice on platforms such as Microsoft's Bing news website. Other famous examples include online advertisement or in other kinds of content recommendation, such as for video streaming platforms like YouTube or Netflix. In such models, the arms correspond to items to recommend (*e.g.*, ads, articles or movies), and the contexts contain features about each user of the system. An interesting work is [LRC+16], who studies slowly-varying non-stationary models applied to recommender systems.

Using bandit algorithms for **improved machine learning** models or algorithms has been an active research domain for the last ten years or so. As presented below in Chapter 4, a certain "leader" bandit algorithm can be used to select on the run the best bandit algorithm from a pool of "followers" algorithms. Other possible use cases include hyper-parameter optimization, or features selection. Hyper-parameters include real-valued parameters, for instance for supervised machine learning we can think of the step size multiplier γ in a gradient descent, the width ρ of a Radial Based Function (RBF) kernel, the margin C in a Support Vector Machines (SVM), etc. Discrete-valued parameters are also common, like a choice in a fixed set of kernel functions or the depth of neural networks, and higher dimensional or more complex hyper-parameters can for instance be the entire architecture of a neural network.

Applications for Cognitive Radio. As highlighted in Chapter 1, the focus of this work is on cognitive radio and IoT networks, where arms can represent wireless orthogonal channels, but more generally any resource characterizing the communication between a wireless device and a gateway (*e.g.*, the spreading factor for LoRa [KAF+18], the power allocation for NOMA [Z. 19], etc). In the model of Opportunistic Spectrum Access (OSA) with sensing [JEMP09, JEMP10], the samples $Y_{k,t}$ represent the feedback obtained by the CR-equipped device after sensing the channel k, at the beginning of its t-th transmission slot. A reward of $r(t) = 1$ indicates that no Primary User was sensed, while a reward of $r(t) = 0$ indicates that the channel k is busy at time t and no up-link message can be sent. We study a similar model of using MAB for

Cognitive Radio but without the OSA structure of Primary and Secondary users, *i.e.*, without sensing information but only a collision indicator, in Chapters 5 and 6.

The different applications discussed in this section are still active research directions, and a curious reader can find other interesting applications of MAB models and algorithms in [BR19], such as game tree search or network routing in Section 1.2 of [LS19].

2.3 Measuring the performance of a MAB algorithm

As explained above, the main objective of a player facing a bandit game is to maximize its (expected) cumulated reward. In particular, an efficient algorithm should see its mean reward converge to the maximum reward, if the horizon grows. In the bandit literature, the performance of an algorithm is often measured in terms of regret, a performance measure that we now introduce.

2.3.1 Introducing the (mean) regret

Let us first introduce some notations. We consider a stochastic and stationary MAB problem, with K arms of distributions $\nu_1, \dots, \nu_K = (\nu_k)_k$, that generate *i.i.d.* samples $Y_{k,t} \sim \nu_k$, for any time t. We focus on distributions fully characterized by their means, that can be Bernoulli or any one-dimensional exponential family. We denote $\mu_k \doteq \mathbb{E}[Y_{k,t}] \in \mathbb{R}$ the mean of the distribution of arm k (it will be referred to as the *mean of arm* k). To define the regret, we first need to distinguish between *optimal* and *sub-optimal* arms.

Definition 2.2. *Consider a bandit problem of K arms with distributions of means $\boldsymbol{\mu} = \mu_1, \dots, \mu_k$. Denote $\mu^* \doteq \max_k \mu_k$ the largest mean. The best arm can be non unique, and any arm k having $\mu_k = \mu^*$ is said to be* optimal*, while arms satisfying $\mu_k < \mu^*$ are called* sub-optimal*.*

If the goal of the player is to maximize $\mathbb{E}\left[\sum_{t=1}^{T} r(t)\right]$, the optimal strategy for this bandit problem is to always pull one of the optimal arms (it can be not unique), but it is unrealistic as the player does not know the true means, nor the optimal arms (as long as they are not all optimal, *i.e.*, in nontrivial problems). Comparing the difference between the performance of a fixed baseline and that of the player is a common approach in machine learning research, and here we can compare with the oracle strategy that always obtains an (expected) reward of μ^*. For a fixed horizon T, if k^* denotes the index of any optimal arm, let us introduce the (mean) regret $R_T^{\mathcal{A}}$ of an algorithm $\mathcal{A}$ as $R_T^{\mathcal{A}} \doteq \mathbb{E}\left[\sum_{t=1}^{T}(Y_{k^*,t} - r(t))\right]$. As the rewards from arm k^* are *i.i.d.* (as for all arms), and by linearity of the expectation, we can rewrite this expression to obtain the following definition of the regret.

Definition 2.3 (Regret). *For an algorithm $\mathcal{A}$, a bandit problem of K arms characterized by their means $\mu_1, \dots, \mu_K$, with $\mu^* \doteq \max_k \mu_k$, then its* (mean) regret *at horizon T is $R_T^{\mathcal{A}}$ defined as*

$$R_T^{\mathcal{A}} = \mathbb{E}\left[\sum_{t=1}^{T}(Y_{k^*,t} - r(t))\right] = \mathbb{E}\left[\sum_{t=1}^{T} \underbrace{Y_{k^*,t}}_{\text{i.i.d. } \textit{from } \nu_{k^*}}\right] - \mathbb{E}\left[\sum_{t=1}^{T} r(t)\right] \tag{2.2}$$

$$= T \times \mathbb{E}\left[Y_{k^*,1}\right] - \sum_{t=1}^{T}\mathbb{E}\left[r(t)\right] = T\mu^* - \sum_{t=1}^{T}\mathbb{E}\left[r(t)\right]. \tag{2.3}$$

One first need to observe that $R_T^{\mathcal{A}} \geq 0$ for any T and $\mathcal{A}$, and that $R_T^{\mathcal{A}} \leq \mu^* T$, in particular $R_T^{\mathcal{A}} \leq T$ if the rewards lie in $[0, 1]$. Thus any algorithm has $R_T^{\mathcal{A}} = \mathcal{O}(T)$, which justifies why we are interested in efficient algorithms that achieve at least a sub-linear regret, *i.e.*, $R_T^{\mathcal{A}} = o(T)$.

A useful decomposition of the regret. Recall that $N_k(t) \doteq \sum_{s=1}^{t} \mathbb{1}(A(s) = k)$ denotes the number of times arm k was selected between times 1 and t, and that the samples $Y_{k,t}$ are all *i.i.d.* of mean μ_k. The *gap* between any arm $k \in [K]$ and an optimal arm is defined as $\Delta_k \doteq \mu^* - \mu_k$ (an arm k is thus sub-optimal if and only if $\Delta_k > 0$), and thus we can write the following decomposition on the regret. *Its proof is simple and it is not a contribution, but we include it below for readers that are unfamiliar with conditioning arguments.*

Proposition 2.4 (Regret decomposition). *The (mean) regret $R_T^{\mathcal{A}}$ can be decomposed as a sum of the number of selections of sub-optimal arms k, weighted by their gaps:*

$$R_T^{\mathcal{A}} = \sum_{k=1}^{K} \Delta_k \, \mathbb{E}[N_k(T)] = \sum_{\substack{k=1,\dots,K \\ \Delta_k > 0}} \Delta_k \, \mathbb{E}[N_k(T)]. \tag{2.4}$$

Proof. We use the chain rule of expectation and a conditioning on O_t, because the expectation is taken on the randomness of the (*i.i.d.*) samples $(Y_{k,t})_t$ and on the decisions of the player $(A(t))_t$, which are measurable wrt to the past observations $O_t = (U_0, Y_{A(1),1}, U_1, \dots, Y_{A(t-1),t-1}, U_{t-1})$. Thus we can rewrite the expected cumulated reward as follows:

$$\mathbb{E}\left[\sum_{t=1}^{T} r(t)\right] = \mathbb{E}\left[\sum_{t=1}^{T}\sum_{k=1}^{K} Y_{k,t}\mathbb{1}(A(t) = k)\right] = \sum_{k=1}^{K}\sum_{t=1}^{T}\mathbb{E}\left[Y_{k,t}\mathbb{1}(A(t) = k)\right]$$

$$= \sum_{k=1}^{K} \sum_{t=1}^{T} \mathbb{E}\Big[\mathbb{E}\left[Y_{k,t}|O_t\right] \mathbb{1}(A(t) = k)\Big] = \sum_{k=1}^{K} \sum_{t=1}^{T} \mathbb{E}\Big[\mathbb{E}\left[Y_{k,1}\right] \mathbb{1}(A(t) = k)\Big]$$
$$= \sum_{k=1}^{K} \underbrace{\mathbb{E}\left[Y_{k,1}\right]}_{\mu_k} \underbrace{\sum_{t=1}^{T} \mathbb{E}\left[\mathbb{1}(A(t) = k)\right]}_{=N_k(T)} = \sum_{k=1}^{K} \mu_k \mathbb{E}\left[N_k(T)\right].$$

Thus $R_T^{\mathcal{A}} = T\mu^* - \sum_{t=1}^{T} \mathbb{E}\left[r(t)\right] = T\mu^* - \sum_{k=1}^{K} \mu_k \mathbb{E}[N_k(T)] = \sum_{k=1}^{K} (\mu^* - \mu_k)\mathbb{E}[N_k(T)]$, as $\sum_{k=1}^{K} \mathbb{E}[N_k(T)] = T$. The sum is then simplified to only count sub-optimal arms. □

Consequences. Such a decomposition of the regret can be useful for at least two reasons:

On the one hand, from a numerical simulation point-of-view, when we run a finite number of repetitions of the same stochastic experiment, if we want to compute and visualize the regret, we can either use the definition with the rewards, or the decomposition and simply sum the product of the gaps Δ_k with the number of sub-optimal draws. Both quantities are indeed equal *in expectation*, but with only a finite number of experiments and observations, the first estimate is more noisy than the second one, since the randomness on the rewards is (partially) removed in the decomposition (2.4) (thanks to the conditioning on O_t done in the proof). In our library SMPyBandits, we implement both estimators, and all values of regret used in this thesis are based on the one using the decomposition of Proposition 2.4, because it gives faster convergence, and also "smoother" plots.

On the other hand, this decomposition is necessary as theoretical analyses of the regret of (single-player) MAB algorithms are usually based on controlling the sub-optimal draws $N_k(T)$ and not directly the regret $R_T^{\mathcal{A}}$. Even if we prove that controlling $N_k(T)$ is no longer sufficient to obtain low regret for the multi-players case, we extend this decomposition in Chapter 3 (in Lemma 6.5), and it is the first quantity we prove to be bounded by $\mathcal{O}(\ln(T))$ when we prove the regret upper-bound of our proposal MCTopM-kl-UCB.

2.3.2 Regret lower-bounds

We include here two well-known results about what bandit algorithms *cannot* do. First, a *problem-dependent lower-bound* states that any algorithm suffers a regret at least $\Omega(\ln T)$ on any parametric problem [LR85]. Then, a *worst-case result* states that for any algorithm, there exists a certain problem instance such that the algorithm can perform as badly as $\Omega(\sqrt{KT})$ [ACBFS02]. In certain families of problems, *e.g.*, K Bernoulli distributed arms, the difficulty of a problem is characterized by a constant that depends only on the arms means. This measure of difficulty of a problem is hidden in the Ω notation in these lower-bounds.

In all this section, we restrict to stationary stochastic problems with $K \geq 2$ arms. We do not give proofs of the following theorems, as they can be found in the historical papers, and

simpler proofs are given in recent references, such as [BCB12], [LS19], or Chapter 2 in [Sli19] for instance. Let $\mathcal{I}$ denote the set of all problem instances, with $K \geq 2$ arms. We assume that rewards lie in $[0, 1]$, to present the lower-bounds, we prefer to focus on Bernoulli distributions, for simplicity. To specify the dependency on an instance $I \in \mathcal{I}$, we denote the regret of $\mathcal{A}$ on instance I and horizon T by $R_T^{\mathcal{A}}(I)$. We also index the Landau notations $o(\dots)$ and $\mathcal{O}(\dots)$ by I, for instance $R_T^{\mathcal{A}}(I) = o_I(\ln(T))$ means $R_T^{\mathcal{A}}(I) = o(c_I \ln(T))$ where the "constant" c_I can depend on the problem instance I (*e.g.*, on its means and on K) but *not* on the time horizon T.

Problem-dependent lower-bound in $\Omega(\ln T)$. The following two theorems were proven in [LR85]. These lower-bounds are of highest interest to design efficient algorithms, and a significant part of the research on MAB algorithms has focused on finding algorithms that match the Lai and Robbins' lower-bound asymptotically [LR85]. This means that a finite-time or an asymptotic upper-bound is proven on the regret of algorithm $\mathcal{A}$, that asymptotically matches the lower-bound. When the regret upper-bound matches the lower-bound with the same constant as in the big-$\mathcal{O}$ notation, we say that the algorithm is asymptotically *optimal*, otherwise the algorithm is said to be *order-optimal* if it matches the lower-bound with a larger constant.

Theorem 2.5. No algorithm $\mathcal{A}$ can achieve *a (mean) regret* $R_T^{\mathcal{A}}(I) = o_I(\ln(T))$ *for all Bernoulli problem instances* $I \in \mathcal{I}$. [*Sli19, Theorem 2.12*]

We consider uniformly efficient[1] algorithms, to rule out algorithms achieving low regret on some problem instances while achieving linear regret on other instances. In particular, it is necessary to rule out algorithms that always pick the same arm, as on some problem instances such fixed-arm algorithms can achieve zero regret.

Definition 2.6. *An algorithm $\mathcal{A}$ is* uniformly efficient *if its (mean) regret satisfies* $R_T^{\mathcal{A}}(I) = o_I(T^{\alpha})$, *for any value* $\alpha > 0$ *and any problem instance* $I \in \mathcal{I}$.

This family is non-empty, as it contains for instance the UCB_1 algorithm, since its regret is proven to be logarithmic on any Bernoulli problem instance (in Theorem 2.12 below). Now we can state the second logarithmic lower-bound, for algorithms in this family.

Theorem 2.7. *If $\mathcal{A}$ is uniformly efficient, then for any arbitrary Bernoulli problem instance I, its regret is asymptotically lower-bounded by $C_I \ln(T)$, or in other words,* $\liminf_{T\to\infty} \frac{R_T^{\mathcal{A}}(I)}{\ln(T)} \geq C_I$. [*Sli19, Theorem 2.13*],

[1] This notion is then extended to "*strongly uniformly efficient* algorithms", in the multi-players case with Definition 6.7, where we also include a notion of (expected) fairness.

Theorem 2.12 from [Sli19] specifies a possible value for the constant C_I. Note that the lower-bound of Lai and Robbins, proven in [LR85], is more general and applies to any one-dimensional exponential family $\mathcal{E}$, by replacing the Bernoulli Kullback-Leibler divergence kl with the KL divergence of this family, $\mathrm{kl}_{\mathcal{E}}$.

Theorem 2.8. *If $\mathcal{A}$ is uniformly efficient, and I an arbitrary Bernoulli problem instance.*

- *The bound from Theorem 2.7 holds with $C_I = \sum_{k:\Delta_k>0} \frac{\Delta_k}{\mathrm{kl}(\mu_k,\mu^*)}$.*
- *For any $\varepsilon > 0$, the bound also holds at finite time with $C'_I = C_I - \varepsilon$, meaning that there exists a constant C'_I depending only on I, and a time T_0 such that $\forall T \geq T_0, \quad R_T^{\mathcal{A}}(I) \geq C'_I \ln(T)$.*

It is interesting to note that the first lower-bound of Theorem 2.8 can be directly used to design efficient algorithms[2], as thanks to the regret decomposition given in Proposition 2.4 above, the expression of C_I essentially says that any efficient algorithm should sample each sub-optimal arm k about $\ln(T)/\mathrm{kl}(\mu_k, \mu^*)$ times in the total of T time steps. Many algorithms have been proven to achieve logarithmic regret in the stochastic case, and in particular it is the case of the algorithms used in the rest of thesis, UCB_1 from [ACBF02], Thompson sampling from [Tho33] and analyzed in [AG12, KKM12], and kl-UCB from [GC11, CGM+13]. Such bounds are valid in different settings: UCB_1 is order-optimal for bounded rewards or one-dimensional exponential families (*i.e.*, it matches the asymptotic lower-bound of [LR85]), while Thompson sampling is optimal for binary rewards, and kl-UCB and KL-UCB have been proven to be optimal respectively for both cases. Chapter 16 of [LS19] contains more details.

Worst-case lower-bound in $\Omega(\sqrt{T})$. For a fixed horizon T, it is interesting to note that one can find instances I that are so "hard" that a logarithmic regret (lower or upper) bound that uses a constant C_I no longer brings any information. Indeed, we can naively bound the regret by $R_T^{\mathcal{A}} \leq (\max_k \Delta_k)T$, and thus if $(\max_k \Delta_k)$ can be taken so small that $C_I \ln(T) \gg (\max_k \Delta_k)T$, a regret upper bound like $R_T^{\mathcal{A}} \leq C_I \ln(T)$ is useless.

For this reason, another family of regret bounds is relevant, that are not problem-dependent but worst-case, or also called minimax [AB09, AB10] or problem-independent. We give an example of such a result below. The following theorem is from [ACBFS02], and [Sli19, Theorem 2.1]. We also refer to Chapter 15 of [LS19].

[2] Tracking this quantity, by using empirical estimates of the means, is used for instance in the OSSB algorithm proposed in [CMP17], which is proven to attain the lower-bound for a wider range of problems (for problems called structured stochastic bandits).

Theorem 2.9. *Fix the number of arms K, and an algorithm $\mathcal{A}$. Then for any horizon T, there exists a Bernoulli problem instance I_T on which $\mathcal{A}$ suffers at least a regret $R_T^{\mathcal{A}}(I_T) \geq \Omega(\sqrt{KT})$.*

Similarly to what is considered for the first lower-bound, a natural question is to know if there is an algorithm achieving a regret upper-bound of the form $R_T^{\mathcal{A}}(I) \leq \mathcal{O}\left(\sqrt{KT}\right)$ for any instance, independently on the problem difficulty. The question has been answered since the early 2000s, as it is for instance the case for the Exp3 algorithm from [ACBF02]. In the last decade, some algorithms were shown to achieve both a problem-dependent logarithmic and a minimax upper-bounds, like MOSS from [AB09] or recently kl-UCB^{++} from [MG17], and such results are usually referred to as "best of both worlds".

2.3.3 Other measures of performances

In the rest of this thesis, the theoretical performance analysis of an algorithm that we obtained are all expressed in terms of the mean regret $R_T^{\mathcal{A}}$ (in Chapters 6 and 7), but we quickly mention other measures of performances that we consider in our works and in this manuscript.

First, when doing numerical experiments about bandits, if one studies the regret as an empirical mean based on a "large" number of random repetitions (*e.g.*, $N = 1000$ repetitions), it is important to not only show the mean value but also the variance of the values taken by the regret on each repetition, to verify that all algorithms perform consistently. Indeed, by only visualizing the mean of 1000 values, it is possible that we miss some "bad runs": if 1 run out of the 1000 gives linear regret (*i.e.*, $R_T^{\mathcal{A}} \propto T$) and the 999 other give logarithmic regret, then the mean will appear logarithmic. This is the case of the Selfish algorithm that is defined and explored in Chapter 6. On the contrary, for efficient algorithms, we can visualize the entire *distribution* as a histogram, or the variance of the values of $R_T^{\mathcal{A}}$, and if the number N is reasonably large, we can verify that the regret appears logarithmic for all runs.

The **switching cost** $\mathrm{SC}^{\mathcal{A}}(T)$ counts how many times the player's decision has changed from one round to the next one, *i.e.*, $\mathrm{SC}^{\mathcal{A}}(T) \doteq \sum_{t=1}^{T-1} \mathbb{1}(A(t) \neq A(t+1))$. It has recently gained interest in the literature, for instance the authors of [TRY17] proposed an algorithm that adaptively tries to balance the trade-off between minimizing the regret and minimizing the switching cost. Indeed, in single-player models it is easy to show that achieving logarithmic regret directly implies a logarithmic upper-bound on the switching cost, and conversely the lower-bound from [LR85] also gives an asymptotic logarithmic lower-bound. Even if $\mathrm{SC}^{\mathcal{A}}(T) = \Theta(\ln T)$ for an efficient algorithm, it can be interesting to numerically evaluate this quantity, as a large value might indicate an algorithm that is alternating too much between the optimal arm and other arms. It is relevant for cognitive radio applications, as a hardware reconfiguration costs energy, and so changing channel from two consecutive time steps has a nontrivial energy cost,

as highlighted in [DMNM16]. We also find interesting to study $\mathrm{SC}^{\mathcal{A}_1,\dots,\mathcal{A}_M}(T)$, the sum of the switching costs of the M players in a multi-players bandit game (if player j uses algorithm $\mathcal{A}_j$ for $j = 1, \dots, M$), as studied in Chapter 6. Our proposed algorithm, MCTopM, achieves order-optimal logarithmic regret as well as a logarithmic number of switches.

Finally, another interesting measure of performance is the **fairness**. It was not studied much for single-player problems, and usually it means that each arm must be explored at least a given fraction of the total horizon T (*i.e.*, "arm-wise fairness"). It was studied in a very recent article [PGNN19], where a different notion of regret is introduced to account for the fairness constraint. The authors show that different algorithms, based on UCB_1 or Thompson sampling, can achieve logarithmic regret while respecting the fairness constraints. In this thesis, we only consider fairness in the multi-players bandit models, in Chapter 6, where fairness refers to a different notion (*i.e.*, "cooperative fairness"), in Section 6.3.2.

2.4 Review of stochastic MAB algorithms

This Section reviews the most important families of stochastic MAB algorithms, from naive and simple strategies, to strategies based on the optimism or the Bayesian principles, to recent "best-of-both-worlds" strategies.

Implementation. We describe our library SMPyBandits in more details in Chapter 3. All the algorithms described in this chapter are implemented in SMPyBandits, in the `Policies` module, alongside with many more algorithms (there are about 65 for single-player stochastic problems). A complete list of the implemented policies can be found on the following web page on the documentation, `SMPyBandits.GitHub.io/docs/Policies.html`.

2.4.1 Naive or simple strategies

Pure exploitation or pure exploration. Let us first describe two naive strategies, that both fail dramatically. We recall the notations introduced above in Section 2.1.1, the sums of rewards are $X_k(t) \doteq \sum_{s=1}^{t} r(s)\mathbb{1}(A(s) = k)$, and the numbers of samples are $N_k(t) \doteq \sum_{s=1}^{t} \mathbb{1}(A(s) = k)$. The estimated means, or empirical averages, are $\widehat{\mu_k}(t) \doteq X_k(t)/N_k(t)$ (when $N_k(t) > 0$).

– The uniform strategy always plays the K arms uniformly at random, $\forall t \in [T], A(t) \sim \mathcal{U}([K])$, where $\mathcal{U}(S)$ denotes the uniform distribution on a set S, and $\mathcal{U}([K])$ the uniform distribution on $[K] = \{1, \dots, K\}$ (*i.e.*, $\forall t, \forall k \in [K], \mathbb{P}(A(t) = k) = \frac{1}{K}$). The player *only explores* without using the collected information, and this strategy fails dramatically for any nontrivial problem (*i.e.*, linear regret). Indeed it obtains a linear (mean) regret $R_T = \frac{1}{K}\sum_{k=1}^{K} \Delta_k T$ which gives $R_T \propto T$ for any problem with at least one sub-optimal arm (*i.e.*, all nontrivial problems, ruling out the case where $\mu_1 = \mu_2 = \cdots = \mu_K$).

– The "*Follow-the-Leader*" strategy consists in first playing once each arm, then always playing $A(t) \in \arg\max \widehat{\mu_k}(t)$. The player *only exploits* the collected information, and this strategy can fail dramatically, *i.e.*, obtain linear regret in some problems. Indeed consider $K = 2$ Bernoulli arms of means $\mu_1 = 1/2$ and $\mu_2 = \varepsilon$ where $\varepsilon < 1/2$, then with probability $\varepsilon/2$ the player observes a reward of 0 for arm 1 then 1 for arm 2 on the first rounds, and so she will play arm 2 for the $T-2$ remaining rounds, giving a linear (mean) regret $R_T \geq \frac{\varepsilon}{2}\left(\frac{1}{2} - \varepsilon\right)(T-1)$.

Simple efficient strategies: ε-greedy and Explore-then-Exploit. As illustrated by the two previous examples, an efficient strategy needs to solve the trade-off between exploration and exploitation. The two following solutions both consist in splitting the T time steps into T_0 steps of exploration and $T - T_0$ steps of exploitation.

for $t = 1, 2, \ldots, T$ **do**
  Sample a value uniformly in $[0, 1]$: $U_t \sim \mathcal{U}([0, 1])$
  if $U_t < \varepsilon$ (i.e., *with probability* ε) **then**
    Play uniformly at random $A(t) \sim \mathcal{U}(\{1, \ldots, K\})$ `// Explore`
  else
    Play uniformly among the arms of maximal empirical mean:
    $A(t) \sim \mathcal{U}(\arg\max_{1 \leq k \leq K} \widehat{\mu_k}(t))$ `// or Exploit`
  Observe a reward $r(t)$, and update $X_k(t)$, $N_k(t)$ and $\widehat{\mu_k}(t)$
end

Algorithm 2.1: A simple efficient strategy, the ε-greedy algorithm.

– The ε-greedy strategy (in Algorithm 2.1) consists in alternating exploration and exploitation at a certain ratio [ACBF02]. Fix $0 < \varepsilon < 1$, then at each round, with probability ε the player selects an arm uniformly at random (exploration) and with probability $1 - \varepsilon$ the arm with highest empirical mean is selected (exploitation). On the one hand, if ε is constant, then the (mean) regret still grows linearly, as it is lower bounded by $(\varepsilon \frac{1}{K} \sum_{k=1}^{K} \Delta_k)T$. In average, $T_0 = \varepsilon T$ steps are spent on exploration. On the other hand, if a lower-bound d on the positive gaps is known beforehand, we can consider a sequence $(\varepsilon_t)_{t \in \mathbb{N}^*}$ decreasing with time t, for instance $\varepsilon_t = \varepsilon_0/t$ with $\varepsilon_0 = 6K/d^2$, for a constant $0 < d < \min_{k:\Delta_k > 0} \Delta_k$. Then it was shown in [ACBF02] that the regret of ε-greedy is of the order of $K \ln(T)/d + o(T)$, which leads to an order-optimal regret of $\mathcal{O}(K \ln(T))$, but this is not satisfactory, as $\min_k \Delta_k$ needs to be known in advance, which is usually not the case for real applications. Here again, an average of $T_0 \leq \varepsilon_0 \ln(T)$ steps are spent on exploration.

– The "Explore-then-Exploit" strategy (in Algorithm 2.2), presented for instance in [BCB12], first explores uniformly the K arms for T_0 time steps, then only exploits the arm identified as the best arm after these first T_0 steps (*i.e.*, one of the arms with highest empirical means, after T_0/K samples of each arm). Usually we restrict to T_0 being a multiple of K.

for $t = 1, 2, \dots, T$ **do**
  if $t \leq T_0$ **then**
    Play sequentially $A(t) \in 1 + (t \mod K)$ `// Explore`
  else
    if $t = T_0$ **then**
      Pick one arm $A(T_0) = k$ uniformly among the arms of maximal empirical mean: $A(t) \sim \mathcal{U}(\arg\max_{1 \leq k \leq K} \widehat{\mu_k}(T_0))$ `// then Exploit`
    Play the same arm $A(t) = A(T_0)$
  Observe a reward $r(t)$, and update $X_k(t)$, $N_k(t)$ and $\widehat{\mu_k}(t)$
end

Algorithm 2.2: A simple efficient strategy, the Explore-then-Exploit algorithm.

Here again, if a lower-bound $d > 0$ on the positive gaps is known beforehand, one can find a tuning of T_0 that gives a logarithmic regret, as stated in Theorem 2.10 below. It proves that the "explore-then-exploit" strategy can also obtain an order-optimal regret, $R_T \leq K(4/d^2)(1 + \ln(d^2 T/4)) = \mathcal{O}(K \ln(T))$, if it is tuned with a fixed time T_0 using prior knowledge on the problem (*i.e.*, d) and the horizon T.

Theorem 2.10. *For any instance I with K arms with Bernoulli distributions in $[0, 1]$, of means $\mu_1, \dots, \mu_k$, and any horizon $T > K$, and if $d \leq \Delta = \min_k \Delta_k$ is known, let $T_0 = ((2K)/d^2) \ln(d^2 T/(2K))$. Then the Explore-then-Exploit algorithm with parameter T_0 verifies the following finite-time regret bound*

$$R_T^{\text{Explore-then-Exploit}} \leq \frac{2K}{d^2} \ln\left(\frac{d^2 T}{2K}\right) = \mathcal{O}\left(\frac{K \ln(T)}{\Delta^2}\right). \tag{2.5}$$

Proof. If p denotes the probability that the chosen arm is not optimal, the algorithm suffers from a linear regret for the first T_0 rounds, then with probability p it suffers from a linear regret for the remaining $T - T_0$ rounds, and with probability $1 - p$ it suffers no regret. Thus we have $R_T \leq (\max_{k:\Delta_k > 0} \Delta_k) T_0 + p(T - T_0)$. We then prove that $p \leq 2K \exp(-T_0 d^2/4)$.

We use Hoeffding's inequality from [Hoe63], reminded below in Lemma 2.11. First for the case of two arms: if $\mu_1 = \mu_2 + \Delta$, then $p = \mathbb{P}(\widehat{\mu_1} < \widehat{\mu_2}) \leq \mathbb{P}(\widehat{\mu_1} < \mu_1 - \Delta/2) + \mathbb{P}(\widehat{\mu_2} > \mu_2 + \Delta/2)$, and both terms can be bounded by using Hoeffding's inequality with a (non-random) number of samples $n \leq T_0/K$, to obtain $p \leq 2\exp(-T_0 \Delta^2/(2K))$. Then for $K \geq 2$ arms, a simple union bound on the sub-optimal arms gives $p \leq 2(K-1)\exp(-T_0 d^2/(2K))$, if d is a lower-bound on the positive gaps Δ_k.

So this bound on p gives $R_T \leq KT_0 + 2K\exp(-T_0 d^2/(2K))T$ (as $\max_{k:\Delta_k>0} \Delta_k \leq 1$ and $T - T_0 \leq T$). Optimizing the right hand-side on T_0 gives $T_0 = ((2K)/d^2)\ln(d^2T/(2K))$. □

Lemma 2.11. *Let $Z_1, \dots, Z_n$ be n* i.i.d. *samples from a Bernoulli distribution of parameter $\mu \in [0,1]$ (where n is fixed), of empirical mean $\widehat{Z_n} \doteq \frac{1}{n}\sum_{i=1}^n Z_i$,* Hoeffding's inequality *gives*

$$\begin{cases} \forall x < \mu, & \mathbb{P}(\widehat{Z_n} < x) \leq \exp(-2n(x-\mu)^2), \\ \forall x > \mu, & \mathbb{P}(\widehat{Z_n} > x) \leq \exp(-2n(x-\mu)^2). \end{cases} \tag{2.6}$$

An extension of this strategy is to consider not a fixed time T_0 but a random time τ at which exploration stops. This time τ must be a *stopping time*[3], in the sense that it is a measurable random variable, dependent of the past observations. The strategy is then referred to as "explore-then-commit" (ETC), and the idea is to use a statistical test at every time step t, and stop as soon as enough samples were collected to effectively identify the best arm with a certain confidence level δ. Choosing $\delta \propto 1/T$ and using a lower-bound d on the gaps typically lead to an order-optimal algorithm, as shown in [GKL16].

For both cases, the strategy obtains sub-optimal regret if it is tuned independently of the problem at hand, but can be tuned to be efficient (*i.e.*, with logarithmic regret) if a lower-bound on the gaps Δ_k is known. As such, this weakness makes the presented strategies inapplicable on an unknown problem, and so they are less interesting from a practical point-of-view.

2.4.2 The optimism principle and index policies: UCB_1, kl-UCB etc

A large family of algorithms are index based, as they compute an index $U_k(t)$ on each arm k at time t, and they play the arm that maximizes their index, *i.e.*, $A(t) = \arg\max_k U_k(t)$. If more than one indexes maximize $(U_k(t))_k$, the arm is chosen from the set, usually in a uniformly random manner: $A(t) \sim \mathcal{U}(\arg\max_k U_k(t))$ (using the external randomness, as explained above). The Algorithm 2.3 below details a generic index policy, that includes well known and efficient algorithms such as UCB_1, kl-UCB and many others.

The UCB_1 index policy: using Hoeffding's inequality to build confidence intervals. Let us consider another approach for adaptive exploration, known as "optimism under uncertainty": assume each arm is as good as it can possibly be given the observations so far, and choose the best arm based on these optimistic estimate. This intuition took roots in [LR85], and later lead to the UCB_1 algorithm, analyzed in [ACBF02] for bounded rewards.

[3] See Chapter 3 of [LS19], and we use this notion again in Section 7.5.

for $t = 1, 2, \dots, T$ **do**
  if $t \leq K$ **then**
    Play arm $A(t) = t$;
  else
    For each arm, compute the index $U_k^{\mathcal{A}}(t)$;
    Play arm $A(t)$ uniformly among the arms of maximal index:
    $A(t) \sim \mathcal{U}(\arg\max_{1 \leq k \leq K} U_k^{\mathcal{A}}(t))$;
  Observe a reward $r(t)$ and update $X_k(t)$, $N_k(t)$ and $\widehat{\mu_k}(t)$;
end

Algorithm 2.3: A generic index policy $\mathcal{A}$, using indexes $U_k^{\mathcal{A}}(t)$ (*e.g.*, UCB_1, kl-UCB etc).

For a parameter α, the UCB indexes are computed as follows, as a sum of the *average reward* $\widehat{\mu_k}(t) \doteq \frac{X_k(t)}{N_k(t)}$ and a *confidence radius* $\xi_k(t) \doteq \sqrt{\alpha \frac{\ln(t)}{N_k(t)}}$.

$$U_k^{\mathrm{UCB}_1}(t) = \mathrm{UCB}_k(t) \doteq \underbrace{\frac{X_k(t)}{N_k(t)}}_{\text{Exploitation } \widehat{\mu_k}(t)} + \underbrace{\sqrt{\alpha \frac{\ln(t)}{N_k(t)}}}_{\text{Exploration } \xi_k(t)}. \tag{2.7}$$

This selection rule $A(t) \sim \mathcal{U}(\arg\max_{1 \leq k \leq K} U_k^{\mathcal{A}}(t))$ makes sense for the following reasons: an arm k is chosen at step t because it has a large $\mathrm{UCB}_k(t)$, which can happen for two reasons. i) Because the average reward $\widehat{\mu_k}(t)$ is large, in which case this arm is likely to have a high mean reward μ_k, ii) and/or because the confidence radius $\xi_k(t)$ is large, in which case this arm has not been explored much. Either reason makes this arm worth choosing. One can also observe that $\xi_k(t) \to \infty$ if $t \to \infty$ while $N_k(t) \ll \ln(t)$, which can be used to prove that the UCB_1 algorithm tries all arms at least $\Omega(\ln(T))$ times (in average). Furthermore, these two terms $\widehat{\mu_k}(t)$ and $\xi_k(t)$ in the UCB defined in (2.7) respectively represent *exploitation* and *exploration*, and summing them up is a natural way of dealing with the exploitation/exploration trade-off. The constant parameter α in $\xi_k(t)$ also controls this trade-off, and the theoretical analysis suggests to restrict to $\alpha \geq 1/2$, and to choose $\alpha = 1/2$ for optimal uniform performance (*i.e.*, on all problems, [ACBF02]).

We present the regret bound, which was first stated in [ACBF02], and to explain how Hoeffding's inequality is used we prove it below. Note that for the rest of the manuscript, we use the kl-UCB algorithm (and more subtle concentration inequality) whenever we analyze the regret of a newly introduced algorithm (*i.e.*, in Chapters 6 and 7), but we think the simpler proof of UCB_1 is enlightening for the reader. This has the advantage of being non asymptotic.

Theorem 2.12 (Regret bound for UCB_1). *For any instance I with K arms with bounded distributions in $[0,1]$, of means $\mu_1,\dots,\mu_k$, and any horizon $T > K$, the UCB_1 algorithm with its parameter[4] $\alpha = 2$ verifies the following finite-time regret bound*

$$R_T^{\mathrm{UCB}_1}(I) \leq \left(\sum_{k:\Delta_k>0} \frac{8}{\Delta_k}\right)\ln(T) + \sum_{k:\Delta_k>0}\Delta_k\left(1+\frac{\pi^2}{3}\right). \tag{2.8}$$

Proof. We focus on bounded distributions in $[0,1]$, for which Hoeffding's inequality gives the inequality (2.6), as stated above in Lemma 2.11. Thanks to the regret decomposition from Proposition 2.4, we can focus on bounding $\mathbb{E}[N_k(T)]$ for any sub-optimal arm k.

The first trick consists in writing the following, which is true for any $n \geq 1$:

$$N_k(T) = 1 + \sum_{t=K+1}^{T} \mathbb{1}(A(t)=k) \leq 1 + n + \sum_{t=n}^{T} \mathbb{1}(A(t)=k, N_k(t)\geq n). \tag{2.9}$$

Remember that $\mathrm{UCB}_k(t) = \widehat{\mu_k}(t) + \xi_k(t)$ for any arm k. According to the Algorithm 2.3 (see line 6), a sub-optimal arm k can be chosen only if $\mathrm{UCB}_k(t) \geq \mathrm{UCB}_{k^*}(t)$. Both $\widehat{\mu_k}(t)$ and $\xi_k(t)$ use $n = N_k(t)$ samples of arm k, but as (2.9) above started to isolate $N_k(t)$, we add the freedom of considering different number of samples (using n), so we introduce the notation $\widehat{\mu}_{k,n}(t)$ and $\xi_{k,n}(t)$ where $N_k(t)$ is replaced with n if $n \geq N_k(t)$, *i.e.*, $\widehat{\mu}_{k,n(t)} = \frac{1}{n}\sum_{s=1}^{t-1} r(s)\mathbb{1}(A(s)=k, N_k(s)\leq n)$ and $\xi_{k,n}(t) = \sqrt{2\ln(t)/n}$. Thus, we can continue from (2.9) and write

$$\begin{aligned}
N_k(T) &\leq 1 + n + \sum_{t=n}^{T} \mathbb{1}(A(t)=k, N_k(t)\geq n) \\
&\leq 1 + n + \sum_{t=n}^{T} \mathbb{1}(\widehat{\mu}_{k^*,N_{k^*}(t)}(t) + \xi_{k^*,N_{k^*}(t)}(t) < \widehat{\mu}_{k,N_k(t)}(t) + \xi_{k,N_k(t)}(t), N_k(t)\geq n) \\
&= 1 + n + \sum_{t=n}^{T} \mathbb{1}\left(\min_{0<n_{k^*}\leq t} \widehat{\mu}_{k^*,n_{k^*}}(t) + \xi_{k^*,n_{k^*}}(t) < \max_{n<n_k\leq t} \widehat{\mu}_{k,n_k}(t) + \xi_{k,n_k}(t)\right)
\end{aligned} \tag{2.10}$$

So two union bounds, on n_{k^*} for the $\min$ and on n_k for the $\max$, give two sums

$$N_k(T) \leq 1 + n + \sum_{t=n}^{T}\sum_{n_{k^*}=1}^{t}\sum_{n_k=n}^{t} \mathbb{1}\left(\widehat{\mu}_{k^*,n_{k^*}}(t) + \xi_{k^*,n_{k^*}}(t) < \widehat{\mu}_{k,n_k}(t) + \xi_{k,n_k}(t)\right) \tag{2.11}$$

[4] For simplicity we present the theorem and its proof in the restricted case of $\alpha = 2$. More details on this proof can be found for instance in Section 1.3 of [Sli19], while for instance Chapter 2 of [BCB12] Theorem 2.1) and Chapter 7 of [LS19] (Theorem 7.2) both give more general proofs, in particular for any value of $\alpha \geq \frac{1}{2}$.

Now, at time t, this event $\widehat{\mu}_{k^*,n_{k^*}}(t) + \xi_{k^*,n_{k^*}}(t) < \widehat{\mu}_{k,n_k}(t) + \xi_{k,n_k}(t)$ implies at least one of the following three events:

$$\begin{cases} I_1 &\doteq (\widehat{\mu}_{k^*,n_{k^*}}(t) \leq \mu_{k^*} - \xi_{k^*,n_{k^*}}(t)), \\ I_2 &\doteq (\widehat{\mu}_{k,n_k}(t) \geq \mu_k + \xi_{k,n_k}(t)), \\ I_3 &\doteq (\mu_{k^*} < \mu_k + 2\,\xi_{k,n_k}(t)). \end{cases}$$

- For the first two events I_1 and I_2, we carefully fixed the number of samples so they are no longer random (they are respectively to n_{k^*} and n_k), we can use Hoeffding's inequality to obtain $\mathbb{P}(I_j) \leq 1/t^4$ (for $j = 1, 2$).
- For the last event I_3, observe that $\mu_{k^*} < \mu_k + 2\xi_{k,n_k}(t)$ means $\Delta_k - 2\sqrt{2\ln(t)/n_k} < 0$, where we remind the notation of the gap $\Delta_k \doteq \mu_{k^*} - \mu_k$. Thus if $n_k \geq \left\lceil \frac{8\ln(T)}{\Delta_k^2} \right\rceil \geq \left\lceil \frac{8\ln(t)}{\Delta_k^2} \right\rceil$ (as $T \geq t$), then this inequality actually cannot happen: $\mathbb{P}(\Delta_k - 2\sqrt{2\ln(t)/n_k} < 0) = 0$, so as soon as $n_k \geq \frac{8\ln(T)}{\Delta_k^2}$, $\mathbb{P}(I_3) = 0$.

Taking the expectation of $N_k(T)$ from (2.10), and setting $n = n_T \doteq \lceil \frac{8\ln(T)}{\Delta_k^2} \rceil$ thus gives

$$\begin{aligned} \mathbb{E}[N_k(T)] &\leq 1 + \frac{8\ln(T)}{\Delta_k^2} + \sum_{t=n_T}^{T} \sum_{n_{k^*}=1}^{t} \sum_{n_k=n_T}^{t} \mathbb{P}\left(\widehat{\mu}_{k^*,n_{k^*}}(t) + \xi_{k^*,n_{k^*}}(t) < \widehat{\mu}_{k,n_k}(t) + \xi_{k,n_k}(t)\right) \\ &\leq 1 + \frac{8\ln(T)}{\Delta_k^2} + \sum_{t=n_T}^{T} \sum_{n_{k^*}=1}^{t} \sum_{n_k=n_T}^{t} \big(\underbrace{\mathbb{P}(I_1)}_{\leq 1/t^4} + \underbrace{\mathbb{P}(I_2)}_{\leq 1/t^4} + \underbrace{\mathbb{P}(I_3)}_{=0}\big) \\ &\leq 1 + \frac{8\ln(T)}{\Delta_k^2} + \sum_{t=n_T}^{T} \sum_{n_{k^*}=1}^{t} \sum_{n_k=n_T}^{t} 2\frac{1}{t^4} \end{aligned}$$

We actually have that $\sum_{n_{k^*}=1}^{t} \sum_{n_k=n_T}^{t} 2\frac{1}{t^4} \leq 2 \sum_{n_{k^*}=1}^{t} \frac{1}{t^3} \leq 2\frac{1}{t^2}$, whose sum for $t = 1$ to ∞ is $2\frac{\pi^2}{6}$.

$$\leq \frac{8\ln(T)}{\Delta_k^2} + 1 + 2\sum_{t=1}^{T} \frac{1}{t^2} \leq \frac{8\ln(T)}{\Delta_k^2} + 1 + 2\sum_{t=1}^{\infty} \frac{1}{t^2} \leq \frac{8\ln(T)}{\Delta_k^2} + 1 + \frac{\pi^2}{3}. \tag{2.12}$$

To sum up, we obtain the following finite-time bound on $N_k(T)$ for any sub-optimal arm k

$$\mathbb{E}[N_k(T)] \leq \frac{8\ln(T)}{\Delta_k^2} + \left(1 + \frac{\pi^2}{3}\right).$$

By using the regret decomposition from Proposition 2.4, this gives

$$R_T^{\mathrm{UCB}_1} = \sum_{k:\Delta_k>0} \Delta_k \mathbb{E}[N_k(T)]$$

$$\leq \sum_{k:\Delta_k>0} \frac{8}{\Delta_k}\ln(T) + \sum_{k:\Delta_k>0} \Delta_k \left(1+\frac{\pi^2}{3}\right) = \sum_{k:\Delta_k>0} \frac{8}{\Delta_k}\ln(T) + o(\ln(T))\,.$$

□

We see in this Theorem 2.12 that UCB_1 has the advantage of not relying on any prior knowledge of the problem difficulty, of being anytime and computationally simple, for both memory and time aspects. Moreover, UCB_1 achieves an order-optimal problem-dependent regret upper bound in $\mathcal{O}((\sum_{k:\Delta_k>0}\frac{1}{\Delta_k})\ln(T))$, meaning that it matches the asymptotic regret lower-bound of Lai and Robbins up-to a constant factor [LR85] (see the definition above in page 33). UCB_1 requires a constant storage capacity for each arm (storing $X_k(t)$ and $N_k(t)$ require two integers or a `float` and an integer, *i.e.*, $\mathcal{O}(1)$), giving a storage capacity of $\mathcal{O}(K)$, independently of the horizon T. It also needs to perform some mathematical operations, but a square-root and a logarithm are cheap, thus it costs a $\mathcal{O}(1)$ constant time for each arm and time step, thus a time $\mathcal{O}(KT)$ for the T time steps.

We use UCB_1 as the base building block for other policies in Chapter 5, for these reasons. Moreover, the UCB_1 algorithm has the advantage of being easy to explain and understand, and its decisions can be interpreted clearly: by reading the values of $\widehat{\mu_k}(t)$ and $\mathrm{UCB}_k(t)$, anyone can see why an arm was chosen at anytime. This is why it is used in the proof-of-concept demonstration presented in Section 5.3.

The kl-UCB index policy. The kl-UCB algorithm follows the same spirit as the UCB_1 algorithm presented above, it is an index policy (see Algorithm 2.3), which also builds upper confidence bounds on the unknown mean of each arm. The KL-UCB algorithm was first proposed in [GC11] for one-dimensional exponential families, and then the kl-UCB algorithm was introduced in [CGM+13] for bounded rewards. In all this thesis, we either restrict to exponential families or to bounded rewards in $[0,1]$, for which we use the fact that they are sub-Bernoulli, thus we prefer to only present kl-UCB.

Instead of using a confidence radius $\xi_k(t)$ based on Hoeffding's inequality, the kl-UCB algorithm rather uses Chernoff's concentration inequality for the considered exponential family [C+52, Che81]. We remind that we consider rewards bounded in $[0,1]$. Consider an exploration function $f(t)$, that is typically chosen as $f(t) \doteq \ln(t) + c\ln(\ln(t))$ for the theoretical analyses (with $c \geq 3$), and $f(t) \doteq \ln(t)$ in practice, then the kl-UCB indexes are defined by

$$U_k^{\text{kl-UCB}}(t) \doteq \sup_{q\in[0,1]} \left\{ q : \mathrm{kl}\left(\frac{X_k(t)}{N_k(t)}, q\right) \leq \frac{f(t}{N_k(t)} \right\}. \tag{2.13}$$

For Bernoulli distributions, kl-UCB builds tighter confidence intervals than UCB_1, in the sense that $U_k^{\text{kl-UCB}}(t) < U_k^{\text{UCB}}(t)$ but with the same probability coverage. This is justified by

Pinkser's inequality, which gives $\mathrm{kl}(x, y) \geq 2(x-y)^2$. The KL-UCB and kl-UCB algorithms achieve finite-time regret logarithmic upper-bounds on their regret, and have been proven to be asymptotically optimal, respectively for one-dimensional exponential families and for binary rewards [GC11, CGM+13]. In particular, we highlight that kl-UCB achieves a finite-time regret upper-bound, that matches the asymptotical lower-bound of Lai and Robbins [LR85] for Bernoulli distributed problems, which is our main focus in both Chapters 6 and 7.

A note about the implementation of kl-UCB algorithms. Implementing this kind of policy requires to implement two things. The first one is usually easy: one has to implement $\mathrm{kl}(x, y)$ the Kullback-Leibler divergence of the considered one-dimensional family, for instance kl for Bernoulli distributions has a closed form and is easy to compute. The second one is less obvious: one has to solve the optimization problem in (2.13). Any iterative algorithm for numerical optimization of one-dimensional functions can be used (*e.g.*, see [BV04] for a survey), but as the $\mathrm{kl}(x, \bullet)$ function is usually convex (for any x), two practical and mathematically correct solutions are Newton's method or a bisection search. The search space for q can be restricted to $[X_k(t)/N_k(t), 1]$ instead of $[0, 1]$, and for simplicity and efficiency, in this case a naive bisection search works well. For instance, a precision level of $\varepsilon = 10^{-8}$ is enough for numerical simulations, and typically the bisection search terminates in between 5 to 20 steps.

If we perform numerical simulations with kl-UCB algorithms, we are interested in having efficient implementations, and ideally kl-UCB should not be significantly slower than UCB. The bottleneck of the performance is the computations of the KL functions and the optimization problem, and we note that our library SMPyBandits implements the two parts in both a naive Python implementation (file `kullback.py`) and in a Python module written in a C file[5], in an optimized way (file `kullback_py3.c`). For the supported families of distributions (including Bernoulli, Gaussian, exponential and Poisson), we wrote both a naive Python and an optimized CPython version of their Kullback-Leibler divergence (*i.e.*, $\mathrm{KL}(x, y)$) and a bisection search for the optimization problem for the kl-UCB index (*i.e.*, $\sup_q \mathrm{KL}(x, q) \leq z$).

Variants on UCB_1. Many variants of the UCB_1 algorithms have been studied in the multi-armed bandits literature. For instance, UCB-H replaces the $\ln(t)$ by a $\ln(T)$ (as well as kl-UCB-H), and it actually corresponds to the first algorithm analyzed in [ACBF02]. Using an estimator for the variance of the arms' samples gives UCB-V, which was proven to be efficient against Gaussian distributions with unknown variance. Other variants include UCB^+, $\mathrm{UCB}^\dagger$ from [Lat18], UCBoost, and many more. All these variants are usually comparable to the original UCB_1 algorithm, in terms of time and memory complexity, and they achieve improved regret upper bounds in the same setting or some extensions of the initial setting.

[5] We also wrote an intermediate implementation that uses Cython [BBS+19], to have a file with a syntax closer to Python, while gaining from almost the same performance speed-up as with the optimized C version, see file `kullback_cython.pyx`. These implementations are also published an independent Python package, on `GitHub.com/Naereen/Kullback-Leibler-divergences-and-kl-UCB-indexes` (also on Pypi), as well as a Julia package, on `GitHub.com/Naereen/KullbackLeibler.jl`.

2.4.3 Bayesian policies

Thompson sampling is the oldest known MAB algorithms, dating back from the first paper by Thompson in 1933 [Tho33]. It became popular since its asymptotical and finite-time analyses in [AG12, KKM12]. Thompson sampling uses a Bayesian point of view: instead of building confidence intervals on the means of the arms like UCB_1 does, it starts with a prior $\pi_k(0)$ on the K distributions (*e.g.*, a flat uniform prior), and then after every observation $(k, r(t))$ it updates the posterior distribution of the arm k with a new data $r(t)$, from $\pi_k(t)$ to $\pi_k(t+1)$. Thompson sampling makes its decision at time t by first sampling a random sample $s_k \sim \pi_k(t)$, and then playing according to the "optimism under uncertainty" philosophy if these samples represent the arms (expected) quality, *i.e.*, $A(t) \in \arg\max_k s_k$.

For problems with Bernoulli distributions on the K arms, the best choice of prior is a Beta distribution, that starts as an initially uniform prior (*i.e.*, $\forall k, \pi_k(0) \doteq \mathrm{Beta}(1,1)$), and maintains a distribution $\pi_k(t) \doteq \mathrm{Beta}(X_k(t)+1, N_k(t)-X_k(t)+1)$, as $X_k(t)$ counts the number of successes observed on arm k, and $N_k(t) - X_k(t)$ counts the number of failures. We detail the Thompson sampling algorithm in this case, below in Algorithm 2.4, as it corresponds to the case used in Chapter 5 in Section 5.2.4. In this setting, as well as for one-dimensional exponential families, Thompson sampling was proven to achieve finite-time and asymptotical optimal problem-dependent bounds [KKM12, AG12].

for $t = 1, 2, \dots, T$ **do**
  For each arm, sample $s_k(t) \sim \pi_k(t-1)$ from the posterior of arm k, $\pi_k(t-1) = \mathrm{Beta}(X_k(t-1)+1, N_k(t-1) - X_k(t-1) + 1)$;
  Play arm $A(t)$ uniformly among the arms of maximal random sample: $A(t) \sim \mathcal{U}(\arg\max_{1 \leq k \leq K} U_k(t))$;
  Observe a reward $r(t)$ and update $X_k(t)$ and $N_k(t)$;
end

Algorithm 2.4: Thompson Sampling for Bernoulli rewards, with Beta prior/posteriors.

Bayes-UCB from [KCG12] also uses the Bayesian point of view, updated like for Thompson sampling, but used in a different way. Instead of sampling from the posteriors and playing the arms with maximum sample, Bayes-UCB computes the $(1 - 1/(t(\ln(t))^5)$ quantile of each arm, at time t, and plays the arm with the largest quantile. It was also proven to achieve an asymptotical optimal problem-dependent bound for binary (Bernoulli) bandits [KCG12]. Bayes-UCB is comparable to Thompson sampling in terms of memory complexity, but it can be slower, as computing a quantile is generally more costly than just sampling from a distribution.

We mention a third Bayesian algorithm for curiosity, AdBandits introduced in [TdSCC13], because it has not gained any popularity despite its good empirical performance. AdBandits

follows the same assumptions as Thompson sampling, and for instance for Bernoulli problems it uses a Beta posterior on each arm. It uses a random mixture of two algorithms: with a certain probability it follows Thompson sampling decision rule, otherwise it samples the arm with highest empirical mean (*i.e.*, forced exploitation). It was proposed in the small article [TdSCC13] and illustrated on empirical simulations, but no theoretical analysis was given. We illustrate in Section 3.3 that it can achieve good performance in practice.

Finally, we would like to mention that a recent work [KT19] presented an approach that closes the gap between the two aforementioned point-of-views, frequentist algorithms such as UCB and Bayesian algorithms such as Thompson sampling. The authors of [KT19] showed that their Randomized Confidence Bound (RCB) algorithm can achieve the same regret upper bounds as UCB_1 or Thompson sampling, with uniformly distributed perturbations. Their RCB algorithm ressembles UCB_1, and builds the same confidence interval $[\mathrm{LCB}_k(t), \mathrm{UCB}_k(t)]$ on arm k at time t (the lower confidence bound is $\mathrm{LCB}_k(t) \doteq \widehat{\mu_k}(t) - \xi_k(t)$), but instead of maximizing the UCB, a random sample is simply taken on each interval $s_k \sim \mathcal{U}([\mathrm{LCB}_k(t), \mathrm{UCB}_k(t)])$, and the played arm is the one maximizing this sample, *i.e.*, $A(t) \in \arg\max_k s_k$.

2.4.4 Other policies

We can briefly mention other families of policies.

BESA (Best Empirical Sampled Average) was introduced in [BMM14], in order to fix a simple observation: if arm 1 has 100 samples and arm 2 has 50 samples, it should make more sense to only use 50 samples of arm 1 to compute and compare their empirical means. Based on this idea, the BESA algorithm for $K = 2$ arms is quite simple: at each time step, if arms 1 and 2 have respectively n_1 and n_2 samples, and if $n_1 > n_2$ (for instance), first it sub-samples n_2 observations from n_1, then it computes the mean of these observations, and play the arm maximizing this mean (now that there is the same number of observations for both arms, it makes more sense to compare these quantities). It was analyzed partially, for the two-armed case it was proven to be asymptotically optimal for one-dimensional exponential families, and the authors illustrated that it can be very efficient empirically. However, analyzing it in the generic case was found to be difficult, and it is still an open problem.

Policies for adversarial bandits. Another important family of bandits algorithms are the algorithms proposed for the adversarial setting [ACBFS02]. The first of them is the Exp3 policy, for "*Exp*onential weights for *Exp*loitation and *Exp*loration", which is an example of the well-known *multiplicative weights update algorithm*[6], a family of algorithms developed since the 1950s, and applied to a wide range of different domains. The Exp3 policy maintains weights $w_k(t)$ on the K arms, and at time t it samples an arm from the distribution which is a mixture of

[6] For more details, see this article by J. Kun, `JeremyKun.com/2017/02/27/the-reasonable-effectiveness-of-the-multiplicative-weights-update-algorithm`. The survey [AHK12] gives more details.

$\boldsymbol{w}(t) = [w_1(t), \dots, w_K(t)]$ and the uniform distribution, *i.e.*, $\mathbb{P}(A(t) = k) \doteq (1-\gamma)w_k(t) + \gamma\frac{1}{K}$. The weights are initially uniform, *i.e.*, $w_k(0) = 1/K$, and then at each time after observing a reward $Y_{k,t}$ from arm k, Exp3 updates the weight of the chosen arm multiplicatively, using $w_k(t+1) = w_k(t) \times \exp(\widehat{r_k}(t)/(\gamma N_k(t)))$. The weights are then renormalized, to have a sum $\sum_k w_k(t+1) = 1$. This notation $\widehat{r_k}(t)$ means an unbiased estimator of the reward $r(t) = Y_{k,t}$, that is, $\widehat{r_k}(t) = r(t)/\mathbb{P}(A(t) = k)$. Like for the ε-greedy policy, the parameter γ can be constant, or can be a non-increasing sequence $(\gamma_t)_{t\in\mathbb{N}^*}$. It was proven in [ACBFS02] that Exp3 with constant parameter γ achieves $R_T = \mathcal{O}\left(\sqrt{KT\ln(T)}\right)$ problem-independent regret, while using a decreasing sequence, such as $\gamma_t = \sqrt{\ln(K)/K}\ln(t)/t$ gives an order-optimal problem-independent regret upper-bound of $\mathcal{O}\left(\sqrt{KT}\right)$. A short proof of this results and more details on Exp3 are given in [BCB12]. Many other policies have been proposed for adversarial bandits, like Follow-the-Perturbed-Leader or Follow-the-Regularized-Leader for linear adversarial bandits, and we refer to Parts III and VI of [LS19] for more details.

Hybrid policies. As explained before, in the last few years, the MAB research community has been interested in finding algorithms which achieves both a problem-dependent logarithmic and a minimax upper-bounds. We present here some solutions that are index-based (see Algorithm 2.3). The first example is MOSS from [AB09], or kl-UCB^{++} in [MG17]. If we denote $g(t,T,K) = \ln^+(y(t)(1+\ln^+(y(t))^2))$, and $y(t) = \frac{T}{Kt}$, with $\ln^+(x) = \max(0, \ln(x))$, then they use the following indexes:

$$U_k^{\text{MOSS}}(t) \doteq \frac{X_k(t)}{N_k(t)} + \max\left(0, \sqrt{\frac{\ln\left(\frac{t}{KN_k(t)}\right)}{N_k(t)}}\right).$$

$$U_k^{\text{kl-UCB}^{++}}(t) \doteq \sup_{q\in[0,1]}\left\{q : \text{kl}\left(\frac{X_k(t)}{N_k(t)}, q\right) \leq \frac{g(N_k(t),T,K)}{N_k(t)}\right\}.$$

Both algorithms are index policies, but they are not anytime. For any K, T, and problem instances I in a certain family $\mathcal{I}$ (*e.g.*, with Bernoulli distributions), they satisfy regret bounds like the following, for two constants $c_{\mathcal{A}} \geq 1$ and $c'_{\mathcal{A}} \geq 1$, that depend on the algorithm, and a constant C_I that depend on the problem instance only: $R_T^{\mathcal{A}} \leq \min(c_{\mathcal{A}}\sqrt{KT}, c'_{\mathcal{A}} C_I \ln(T))$.

More recently, the kl-UCB-switch from [GHMS18] is the first algorithm to be proven to obtain simultaneously a distribution-free regret bound of optimal order $\sqrt{KT}$, and a distribution-dependent regret bound of optimal order as well, by matching the $C_I \ln(T)$ asymptotic lower-bound by [LR85]. It is an index policy that uses modified versions of the indexes of kl-UCB$^+$ for arms that are not sampled much (see [Hon19] for more details), and of MOSS$^+$ for the other arms. If the two indexes are defined by $U_k^{\text{MOSS+}}(t) \doteq \frac{X_k(t)}{N_k(t)} + \max(0, \sqrt{\ln\left(\frac{T}{KN_k(t)}\right)/N_k(t)})$ and $U_k^{\text{KL-UCB+}}(t) \doteq \sup_{q\in[0,1]}\left\{q : \text{kl}\left(\frac{X_k(t)}{N_k(t)}, q\right) \leq \ln(\frac{T}{KN_k(t)})/N_k(t)\right\}$,

and if $f(T,K) = \lfloor (T/K)^\gamma \rfloor$ for $\gamma = 1/5$, then kl-UCB-switch uses the index defined as follows:

$$U_k^{\text{kl-UCB-switch}}(t) \doteq \begin{cases} U_k^{\text{KL-UCB+}}(t) & \text{if } N_k(t) \leq f(T,K), \\ U_k^{\text{MOSS+}}(t) & \text{if } N_k(t) > f(T,K). \end{cases}.$$

Finally, it is worth mentioning the Exp3^{++} algorithm, as a recent variant of Exp3 that uses an adaptive tuning of its parameters, proposed by [SL17]. It is anytime, and it was also proven to obtain good "best-of-both-world" performance.

2.4.5 Comparison of the main algorithms on an example Bernoulli problem

We finish this Section 2.4 by illustrating the performance of different algorithms, on the small MAB problem used in the online demonstration shown above (see Figures 2.2 and 2.3). We consider $K = 5$ arms following Bernoulli distributions, of means $\mu_1 = 0.6, \mu_2 = 0.2, \mu_3 = 0.55, \mu_4 = 0.7, \mu_5 = 0.5$ (unknown to the algorithms), and first a horizon $T = 100$ (like in the online demo) then a larger value of $T = 10000$. The best arm is μ_4 and the smallest gap is $\Delta = 0.1$, thus a lower-bound on the gaps is taken as $d = \Delta$.

The different algorithms being compared are the following, in the order they were presented above: first we include the pure-exploration and pure-exploitation algorithms, then the ε-greedy (with $\varepsilon_t = \varepsilon_0/t$ and $\varepsilon_0 = 6K/d^2 = 3000$) and Explore-then-Commit (with $T_0 = K4/d^2 \ln(d^2 T/4) = 2000 \ln(T/400)$) algorithms from Section 2.4.1, which both uses a tuning based on a prior knowledge of Δ (that gives large values of ε_0 and T_0 yielding linear regret for small horizon). We then include efficient algorithms, that do not need prior knowledge of the T (they are anytime) nor Δ (they are robust and efficient on unknown problems): UCB_1 (with $\alpha = 1$), kl-UCB (with Bernoulli $\text{kl} = \text{KL}_{\mathcal{B}}$), and Thompson sampling (with Beta posteriors and flat uniform priors).

We first give in Table 2.1 the cumulated rewards as well as the estimated regrets of the different algorithms, *for one simulation*. First, the rewards are computed as $\frac{1}{N}\sum_{j=1}^{N}\sum_{t=1}^{T} r_{A(t)}^{(j)}(t)$, where $r_k^{(j)}(t)$ means the reward stream of the different runs $j = 1, \dots, N$. Then the estimated regret is *not* computed as $\frac{1}{N}\sum_{j=1}^{N}\sum_{t=1}^{T} r_{k^*}^{(j)}(t) - r_{A(t)}^{(j)}(t)$, as this first formula could give a negative regret and is more noisy, but as $\mu^* T - \frac{1}{N}\sum_{j=1}^{N}\sum_{k=1}^{K} \mu_k N_k^{(j)}(T)$, as this later formula gives a more robust estimator, as noted the proof of Proposition 2.4 (in Page 32 above). It shows that the performance can fluctuate a lot, as on both cases the pure exploitation strategy was very lucky and obtains close-to-optimal performance, even though we proved that it suffers from a linear mean regret.

Then in Table 2.2 we show the *results of the average on* $N = 1000$ *independent runs*. We also include in Figures 2.4, 2.5 below the mean cumulated rewards and mean regrets as functions of the current time step t, for $T = 10000$ (and $N = 1000$). The reward of the best arm is also

Algorithms	Rewards	Regret for $T = 100$	Rewards	Regret for $T = 10000$
Pure exploration	46	20.9	5171	1886.4
Pure exploitation	**65**	**1.15**	**6997**	**0.95**
ε-greedy	50	20.9	6657	382.2
Explore-then-Commit	49	15	5766	1199.8
UCB_1	63	10.3	6920	78.4
kl-UCB	56	12.4	6922	70.2
Thompson sampling	51	12.2	6949	44.2

Table 2.1 – Cumulated rewards and regret, for horizons $T = 100$ and $T = 10000$, *for only one run of the simulation*, for different algorithms.

plotted in Figure 2.4, and it serves as an *upper-bound* to illustrate convergence of the average rewards (*i.e.*, $\frac{1}{t}(r(1) + \cdots + r(t))$), which should converge to μ^* when $t \to \infty$ for efficient algorithms. Conversely, we also add the Lai & Robbins' logarithmic *lower-bound* on regret ($C_I \ln(t)$ from Theorem 2.8) on the regret plots in Figure 2.5. It should not be surprising that the black line of the lower-bound is *above* the values of the regret as the lower-bound is only asymptotic. We can clearly identify the behavior of the different strategies: the three efficient strategies indeed achieve a sub-linear regret (see Figure 2.5b), that looks logarithmic, as supported by the theory, while the naive strategies achieve linear regret. The two simple strategies also achieve sub-linear regret but are less efficient: both ε-greedy and E-t-C starts as pure exploration, respectively until ε_0/t becomes smaller than 1 and until $t > T_0$, then they usually identify correctly the best arm and start to catch up with the best policies.

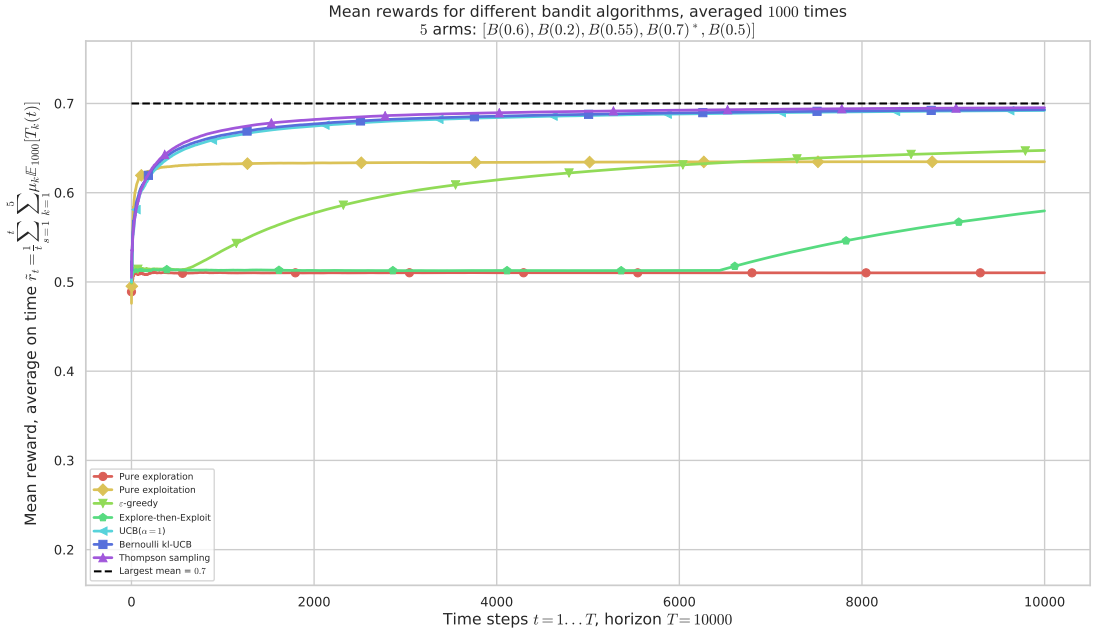

Figure 2.4 – Average of the cumulated rewards, as function of t, for $T = 10000$ and $N = 1000$.

Algorithms	Rewards	Regret for $T = 100$	Rewards	Regret for $T = 10000$
Pure exploration	51	19	5099	1900
Pure exploitation	62	8.3	6349	653
ε-greedy	51	18.7	6460	542
Explore-then-Commit	57	12.9	5795	1207
UCB_1	**60**	**9.8**	6921	79
kl-UCB	61	9.3	6927	72
Thompson sampling	**60**	**9.6**	**6951**	**49**

Table 2.2 – Cumulated rewards and regret, for horizons $T = 100$ and $T = 10000$, *averaged over* $N = 1000$ *independent simulations* $(j = 1, \dots, N)$, for different algorithms.

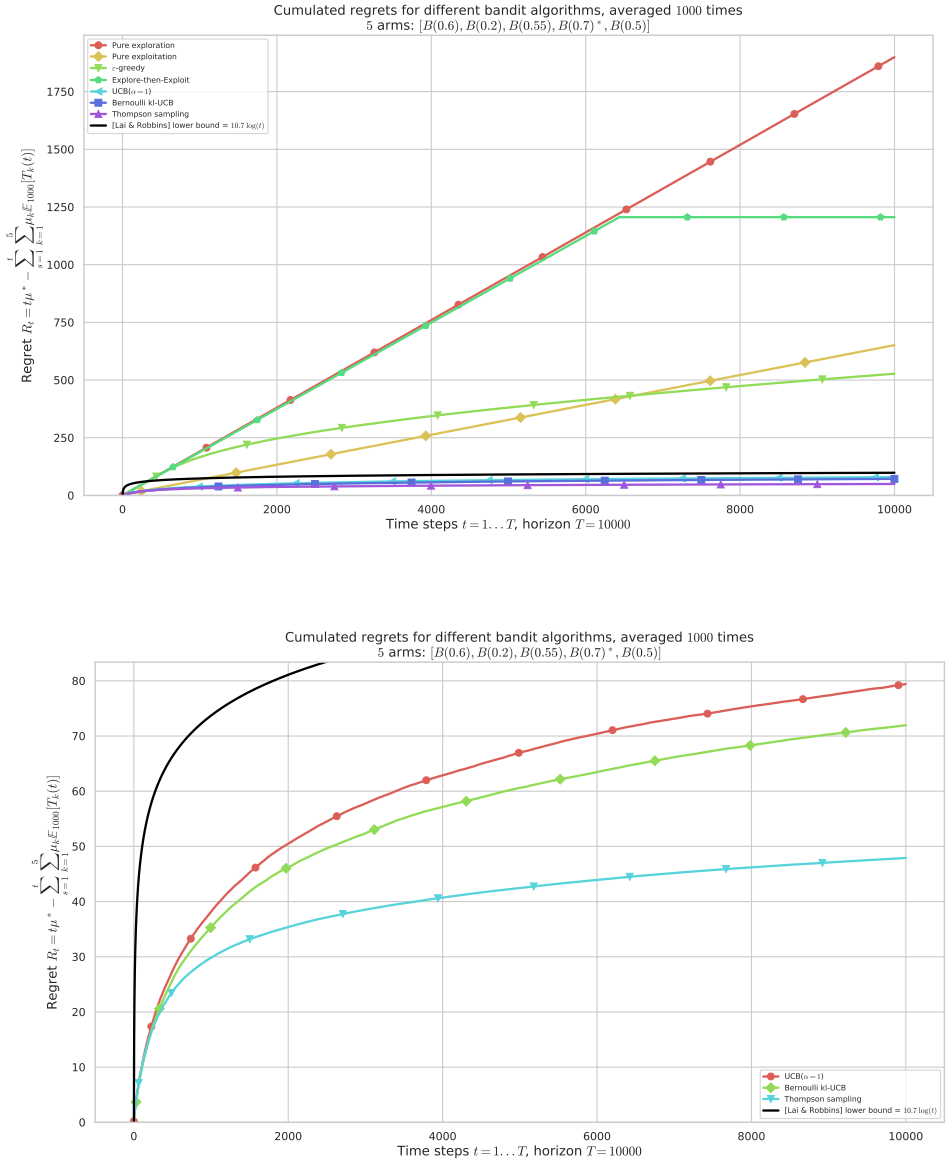

Figure 2.5 – Mean regret R_t as function of t for $T = 10000$ and $N = 1000$. The 3 most efficient algorithms: UCB_1, kl-UCB and Thompson Sampling achieve logarithmic regret.

2.4.6 Summary of this review of MAB algorithms

We gave an overview of the most well known families of MAB algorithms, designed and analyzed for the single-player case of the stationary and stochastic bandit model. Except the naive and simplest strategies given as introductory examples, most of the policies presented above are order-optimal for at least one of the models of binary or bounded rewards, or one-dimensional exponential families, and some of them are known to be asymptotically optimal in different settings. We illustrated the performance of two naive, two simple and three efficient strategies, on the example of Bernoulli-distributed problem used for the online demonstration from Section 2.1. This also serves as a first example of simulation performed with our library SMPyBandits, before its presentation in the next chapter. In the rest of this thesis, we mainly use UCB_1 or Thompson sampling when simplicity and realistic deployment is favored in Chapter 5, and kl-UCB when we focus on mathematical developments in Chapters 6 and 7.

2.5 Conclusion

In this chapter, we presented the multi-armed bandit model, by restricting to a finite number of arms and real-valued rewards. Our main focus is binary or bounded rewards, or one-dimensional exponential families of distributions, and stochastic and stationary problems. By showcasing a small interactive demonstration made available online, we presented the notations used in all this thesis. We then used the Bernoulli-distributed problem underlying this demonstration to present numerical simulations, comparing some algorithms using our Python open-source library SMPyBandits, that is presented in details in the next Chapter 3.

We generalize this MAB model in Chapter 5, by studying decentralized learning of a large set of independent players, all having different random activation times. This extension is significantly harder than the base model presented in this chapter, and it is too complicated to analyze. This model is more generic and realistic, and as such more suitable for applications to Internet of Things (IoT) networks, where arms model orthogonal wireless channels, players model communicating devices (*i.e.*, IoT end-devices) and rewards model successes or failures of a wireless packet sent by a device. We take a more formal approach in the rest of the thesis, first by considering $M \leq K$ devices facing a stationary environment, that is an IoT network of K orthogonal frequency channels, in a decentralized way in Chapter 6, and then by considering a single device facing a non-stationary (piece-wise stationary) problem in Chapter 7. For both directions, we present natural extensions of the base model, and we detail our contributions that obtained state-of-the-art results, for the two problems of stationary multi-players and single-player piece-wise stationary bandits.

Chapter 3

SMPyBandits: an exhaustive Python library to simulate MAB problems

SMPyBandits is a library that has been developed in the Python language since the beginning of this PhD. It is designed to allow easy and fast numerical simulations on single-player and multi-players Multi-Armed Bandits (MAB) algorithms. Its name stands for *S*ingle- and *M*ulti-*P*layer *Bandits* in P*y*thon. To the best of the authors' knowledge, it is the most exhaustive open-source implementation of state-of-the-art algorithms and different kinds of MAB models. This chapter details the organization of the library and what it implements in terms of arm distributions, models, algorithms and visualizations. Then we use it to perform a numerical comparison of the main state-of-the-art single-player bandit algorithms, and a study to compare time and memory costs of some of the most well-known and most widely used MAB algorithms. Note that almost all the numerical simulations used in the rest of the thesis are based on SMPyBandits.

1. Beautiful is better than ugly.
3. Simple is better than complex.
The Zen of Python, by Tim Peters (in PEP20).

Contents

3.1 Introduction

I started the development of the SMPyBandits library in December 2016, and I worked on it actively in 2017 and 2018. It is a Python package, designed to allow easy and fast numerical simulations on single-player and multi-players Multi-Armed Bandits (MAB) algorithms. This library is by far the most exhaustive open-source implementation of state-of-the-art algorithms and different kinds of MAB models, according to the authors' knowledge. It aims at being simple to use and maintain, and has a clean and well documented codebase, and it uses the popular open-source Python language. It allows fast prototyping of simulations, with an easy configuration system and command-line options to customize experiments. Experiment results are saved in an optimized binary format (HDF5) as well as high quality plots of useful visualizations. More than two years of active development have shown how easy it can be to add new algorithms, new arm distributions, and new bandit models (*e.g.*, Markov or non-stationary). It is hosted on GitHub, and uses the state-of-the-art development technologies, by using two online services of continuous integration to run automated tests and to build its online documentation.

SMPyBandits stands for *S*ingle- and *M*ulti-*P*layer *Bandits* in P*y*thon. The library does not aim at being blazing fast or optimized in terms of memory usage, as it comes with a Python implementation [Fou17], and uses only standard open-source Python packages (*i.e.*, no hard to install dependencies). Some critical parts are also available as a `C` Python extension, and the just-in-time Numba compiler [I+17] is used whenever it is possible, so we can note that we optimized the time efficiency of what could be (easily) optimized. However if simulation speed really matters, one should rather refer to less exhaustive but faster implementations, like for example [Lat16a] in `C++` or [Raj17] in Julia. Note that both are not maintained anymore, and contain just a few algorithms for the simple stationary MAB model.

In this Chapter 3, we start by presenting in Section 3.2 the organization of the library. We use the library to compare the most famous and most efficient single-player MAB algorithms in Section 3.3, then we discuss in Section 3.4 about the time and memory costs the same algorithms. The take away messages are two-fold: from a practical point-of-view, it is usually advised to use the simplest algorithm and we advise to use UCB (as we do in the next Chapter 5), and that for theoretical works where optimality of the MAB algorithm is analyzed, we advise to use kl-UCB (as we do in the next Chapters 6 and 7). Finally, in Appendix 3.6 we include some small files showing how to use the library, and we conclude with some details regarding the use of parallel computing to speed-up simulations.

References. The code for SMPyBandits is hosted at `GitHub.com/SMPyBandits/SMPyBandits`, its documentation is at `SMPyBandits.GitHub.io`, and all the library is freely publicly released under the MIT open-source license. This chapter is based on the article [Bes18].

3.2 Presentation of the library

We start by explaining how SMPyBandits simulates MAB problems, by detailing its components: MAB problems (single- or multi-players), and reward distributions. We then detail how it implements MAB algorithms (*e.g.*, UCB), and what kind of information is displayed, saved and plotted after a batch of simulations of bandit problems. The main goal of the library is to be easily able to simulate MAB algorithms (*e.g.*, three algorithms like UCB, kl-UCB and Thompson sampling) on one or more bandit models (single- or multi-players) defined by the number of arms K and their distributions $(\nu_k)_{k\in[K]}$, for some time steps that range from $t = 1$ to the horizon T. After the simulation, the library then displays statistical summary of the (mean) rewards accumulated by each algorithm, as well as regret and other visualizations. The same problem is simulated for N independent repetitions (*e.g.*, $N = 100$) in order to show mean results with low variances.

3.2.1 Single- and multi-players MAB problems

For the classical single-player stochastic MAB model, as defined in Chapter 2, a stochastic MAB problem is defined by $K \geq 2$ distributions $(\nu_k)_{k\in[K]}$ (also called arms), used to generate the *i.i.d.* samples $Y_{k,t} \sim \nu_k, \forall t$. An agent chooses arm $A(t) \in [K]$ at time t and observes the reward $r(t) = Y_{A(t),t}$ without knowing the other (hidden) rewards (in opposition to the full-information setting where $(Y_{1,t}, \dots, Y_{K,t})$ is observed). Her goal is to maximize $\sum_{t=1}^{T} r(t)$, which require to trade-off between exploring the unknown K arms, exploiting the arm which is currently estimated to be the best one.

Simulation loop for single-player MAB. Any simulation library targeting single-player bandit problems must implement at least three components: reward distributions, MAB algorithms, and a simulation loop that essentially looks like this. First, initialize the MAB problem and one or more algorithms, Then, for $t = 1$ to $t = T$ (known beforehand), repeat the following block (for each algorithm). Ask algorithm $\mathcal{A}$ her chosen arm $A(t)$, then sample a (random) reward $r(t)$ (*i.i.d.*) from distribution $\nu_{A(t)}$, and finally feeds the observation $(A(t), r(t))$ to the algorithm. At the end, compute the cumulated reward, the regret, then plot visualizations etc. Note that the second step should be repeated a large number of times (*e.g.*, $N = 100$), in order to study *mean* regret and not only the regret in one single trajectory. If one wants to compare algorithms on a same problem, it is possible to sample all the rewards $(Y_{k,t})_{k\in[K],t\in[T]}$ before-hand, and store them so that for each repetition of the simulation, the randomness from the environment (*i.e.*, the rewards) has the same impact on all the algorithms (with the option `configuration["cache_reward"] = True`).

Simulation loop for multi-players MAB. For Cognitive Radio dealing with OSA problems and other applications, an extension is to consider $M \geq 2$ players, interacting on the same K arms. Whenever two or more players select the same arm at the same time (*e.g.*, for OSA, the same frequency channel), they all suffer from a radio collision. Different collision models have been proposed, and the simplest one consists in giving a 0 reward to each colliding players. Without any centralized supervision or coordination between players, they must learn to access the M best resources (*i.e.*, arms with highest means) without collisions. We refer to Chapter 6 which introduces the multi-players bandit model.

SMPyBandits implements all the collision models found in the literature (in the module `Environment.CollisionModels`), as well as all the algorithms known by the authors (in the module `PoliciesMultiPlayers`). In particular, it includes `rhoRand` from [AMTA11], `MEGA` from [AM15], `MusicalChair` from [RSS16], and our state-of-the-art algorithms `RandTopM` and `MCTopM` from [BK18a], and more recent solutions. For comparison, realistic (*e.g.*, UCB for multiple play) or full-knowledge *centralized* algorithms are also implemented.

Any simulation library targeting multi-players bandit problems must implement at least another component: a simulation loop that essentially looks like this. First, initialize the MAB problem with M players, and one or more cohorts of M players (one player is one algorithm, usually M times the same one), For $t = 1$ to $t = T$ (known beforehand), repeat the following block (for each cohort). Ask each player $\mathcal{A}^j$ her chosen arm $A^j(t)$, then query the collision model to know which player will get a zero reward (for a collision) and which player will get a random reward from the environment. Then, sample (random) feedback $Y_{k,t}$ (*i.i.d.*) from distributions ν_k, and compute the rewards $r^j(t)$ from the random feedback using the collision model. Finally, feed the observation $(A^j(t), Y_{A^j(t),t}, r^j(t))$ to player j, for all the M players, The default collision model is the most widely studied in the literature, where a player encounters a collision (*i.e.*, received a zero reward $r^j(t) = 0$) if she is not the only one to have chosen an arm $k = A^j(t)$, otherwise $r^j(t) = Y_{A^j(t),t}$ if she is the only one playing this arm. At the end, compute the accumulated reward, the regret, then plot visualizations etc.

3.2.2 Reward distributions

We focus on one dimensional distributions (*i.e.*, $r(t) \in \mathbb{R}$), implemented in the `Arms` module. The library supports discrete distributions: *Bernoulli* (`Bernoulli`), *binomial* (`Binomial`), *Poisson* (`Poisson`), and a generic *discrete* distribution (`DiscreteArm`), as well as continuous distributions, which can be truncated to an interval $[a, b]$ or have unbounded support ($\mathbb{R}$): *exponential* (`Exponential`), *gamma* (`Gamma`), *Gaussian* (`Gaussian`) and *uniform* (`Uniform`). The default is to use the same distribution for the K arms, as this is the setting studied in the literature, but it also possible to mix them. For instance the following code in Code 3.1 creates three arms, following Bernoulli distributions, with respective means $0.1, 0.5, 0.9$, and a `MAB`

object which encapsulates the problem. We give another example for *truncated* Gaussian distributions on $[0, 1]$, and a visualization of a histogram of 10000 rewards, below in Figure 3.1.

```python
from SMPyBandits.Arms import *
from SMPyBandits.Environment import MAB

arm1 = Bernoulli(0.1) ; arm2 = Bernoulli(0.5) ; arm3 = Bernoulli(0.9)
bernoulli_problem = MAB([arm1, arm2, arm3])

# but also
means = [0.1, 0.5, 0.9]
bernoulli_problem = MAB({'arm_type': Bernoulli, 'params': means})

gaussian_problem = MAB({'arm_type': Gaussian, 'params': means})
gaussian_problem.plotHistogram()  # display the histogram shown below
```

Code Example 3.1 – Example of Python code to create Bernoulli and Gaussian arms, a MAB problem with $K = 3$ arms, and to plot a histogram of rewards, with SMPyBandits.

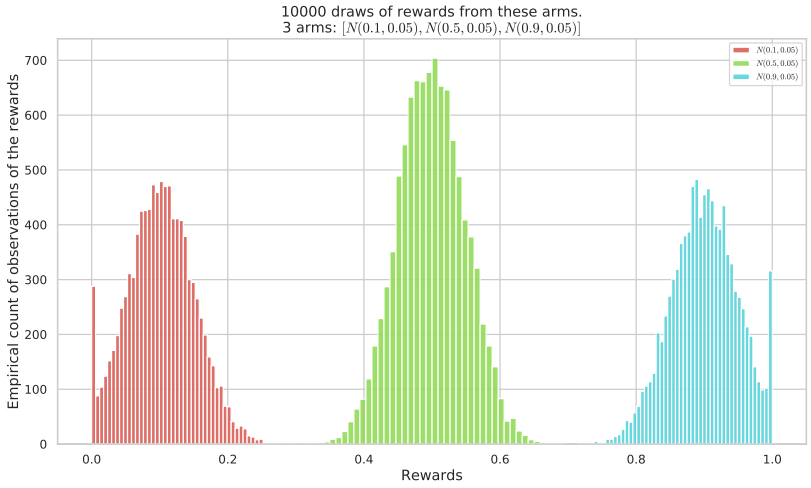

Figure 3.1 – Histogram of 10000 *i.i.d.* rewards obtained from three arms with a Gaussian distribution truncated to $[0, 1]$, of respective means 0.1 (in red), 0.5 (in green) and 0.9 (in blue).

For more details, an interested reader can refer to the following Jupyter notebook [K+16]: SMPyBandits.GitHub.io/notebooks/Easily_creating_MAB_problems.html.

We have not yet added support for higher dimensional distributions of rewards, such as linear bandits, but it would be an interesting extension of SMPyBandits. However, note that our library does support finite-state real-valued Markov MAB models, where arms correspond to Markov chains [Nor98], in the two *rested*/*restless* variants, as introduced by [AVW87b].

3.2.3 Multi-Armed Bandits algorithms

SMPyBandits is a complete open-source implementation of single-player (classical) bandit algorithms, containing over 65 algorithms (in the module `Policies`). It uses a well-designed hierarchical structure and class inheritance scheme (as detailed on the various UML diagrams shown on the `uml_diagrams` folder) to minimize redundancy in the codebase. For instance, most existing algorithms are index policies (see Algorithm 2.3), and new ones are easily written by inheriting from the `IndexPolicy` class (`Policies.IndexPolicy`). For instance the code specific to UCB_1 (with $\alpha = 2$) is as written and fully documented in a file as short as this:

```python
from numpy import sqrt, log          # mathematical functions
from IndexPolicy import IndexPolicy  # base class

class UCB(IndexPolicy):
    """ The UCB policy for bounded bandits.
    Reference: [Lai & Robbins, 1985], [Auer et al. 2020]. """

    def computeIndex(self, arm):
        r""" Compute the current index :math:`U_k(t)`, at time t (:attr:`self.t`)
        and after :math:`N_k(t)` pulls of arm k (``arm``):

        .. math:: U_k(t) = \frac{X_k(t)}{N_k(t)} + \sqrt{\frac{2 \log(t)}{N_k(t)}}.
        """
        if self.pulls[arm] < 1:     # forced exploration in the first steps
            return float('+inf')
        else:                       # or compute UCB index
            estimated_mean = self.rewards[arm] / self.pulls[arm]
            exploration_bias = sqrt((2 * log(self.t)) / self.pulls[arm])
            return estimated_mean + exploration_bias
```

Code Example 3.2 – Code defining the UCB_1 algorithm, as a simple example of an Index Policy.

3.2.4 Summary of the features

With this numerical framework, simulations can run on a single CPU or a multi-core machine using joblib [Var17], and summary plots are automatically saved as high-quality PNG, PDF and EPS, using matplotlib [Hun07] and seaborn [W+17]. Raw data from each simulation is also saved in an HDF5 file, using h5py [C+18], an efficient and compressed binary format, to allow easy post-mortem manipulation of any simulation results. Making new simulations

is very easy, one only needs to write a configuration script (`configuration.py`), without needing a complete knowledge of the internal code architecture.

3.2.5 Documentation of the library

A complete documentation, for each algorithm and the entire codebase, is available online at `SMPyBandits.GitHub.io`. It uses the Sphinx software [B+18], and the content is directly written in the Python files as docstrings (in `"""..."""`, see in the example of Code 3.2 given above), so users have access to the documentation from within their IDE or the Python console. The most interesting component of the library is the many MAB algorithms being implemented: for each of them, the documentation gives a reference to a research paper (*e.g.*, [ACBF02] for `UCB` in Code 3.2), as well as a bird-eye view of its behavior. For most algorithms, especially for index policies, the internal variables of the implementation are carefully linked to the notations of each paper, and formulas explaining the way the algorithm selects its arm are usually given. Whenever it is needed, we also included warnings or information about the empirical performance of the more costly algorithms.

The documentation also contains extensive examples of all intermediate numerical functions, that are also used as tests (using `doctest.testmod` from the standard library). For example, Figure 3.2 below show two screenshots from the documentation. We show the main page, and the list of algorithms in the `Policies` module.

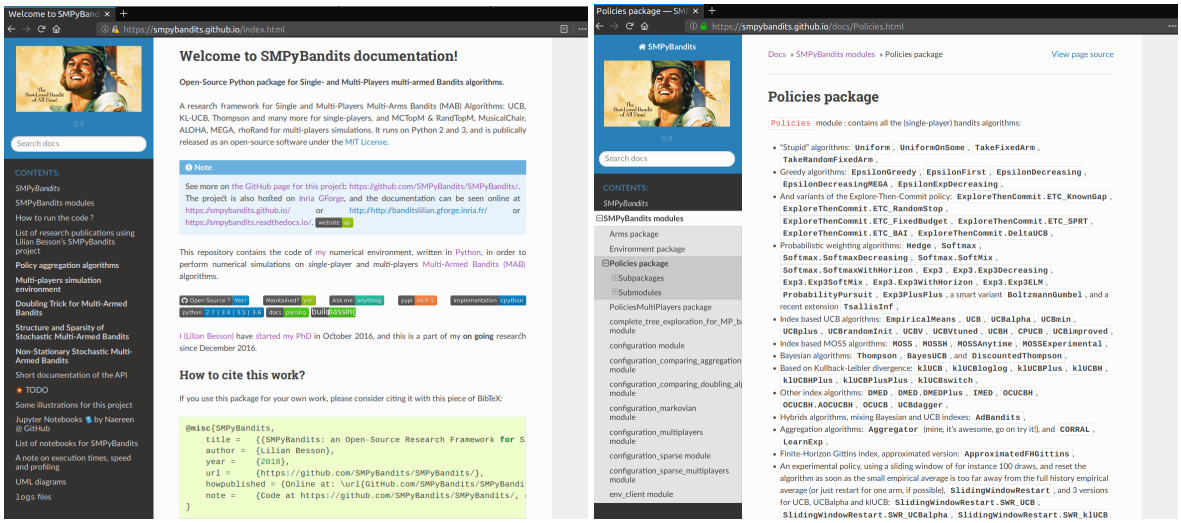

Figure 3.2 – Screenshots from two pages of the documentation: the homepage (`SMPyBandits.GitHub.io`), and a list of all the algorithms in the `Policies` module.

3.2.6 How to run experiments?

We show how to install SMPyBandits, and an example of how to run a simple experiment. See this page `SMPyBandits.GitHub.io/How_to_run_the_code.html` for more details. SMPyBandits is also available on Pypi, see `pypi.org/project/SMPyBandits`, you can install it directly with `sudo pip install SMPyBandits`, or from a `virtualenv` [BP+16]. This bash code shows how to clone the code, and install the requirements for Python 3 (once):

```
# 1. get the code in the folder you want
$ git clone https://GitHub.com/SMPyBandits/SMPyBandits.git
$ cd SMPyBandits.git
# 2. install the requirements
$ pip install -r requirements.txt
```

Code Example 3.3 – Example of Bash code to download and install dependencies of SMPyBandits.

Simulations are easily executed, *e.g.*, Code 3.4 shows how to start $N = 1000$ repetitions of a simple non-Bayesian Bernoulli-distributed problem, for $K = 9$ arms, a horizon of $T = 10000$ and on 4 CPU. It takes about 20 min, on a 4-core 64-bit GNU/Linux laptop. Environment variables (`N=1000` etc) in the command line are not required, but they are convenient.

```
# 3. run a single-player simulation
$ BAYES=False ARM_TYPE=Bernoulli N=1000 T=10000 K=9 N_JOBS=4 \
  MEANS=[0.1,0.2,0.3,0.4,0.5,0.6,0.7,0.8,0.9] \
  python3 main.py configuration.py
```

Code Example 3.4 – Example of Bash code to run a simple experiment with SMPyBandits.

3.2.7 Example of a simulation and illustration

A small script `configuration.py` is used to import the arm classes (`Arms` module), the policy classes (`Policies` module) and define the problems and the experiments. Choosing the algorithms to include is done by changing the `configuration["policies"]` list in the `configuration.py` file. For instance, one can compare the standard anytime kl-UCB algorithm (class `klUCB` in `Policies` module) against the non-anytime variant kl-UCB^{++} algorithm (`klUCBPlusPlus`), and also UCB with $\alpha = 1$ (`UCB`) and Thompson sampling (`Thompson`) with a Beta posterior (`Posterior.Beta`)).

```
configuration["policies"] = [
    { "archtype": klUCB, "params": { "klucb": klucbBern } },
    { "archtype": klUCBPlusPlus, "params": {"horizon": T, "klucb": klucbBern}},
    { "archtype": UCBalpha, "params": { "alpha": 1 } },
    { "archtype": Thompson, "params": { "posterior": Beta } }
]
```

Code Example 3.5 – Example of Python code to configure the list of algorithms tested on a problem.

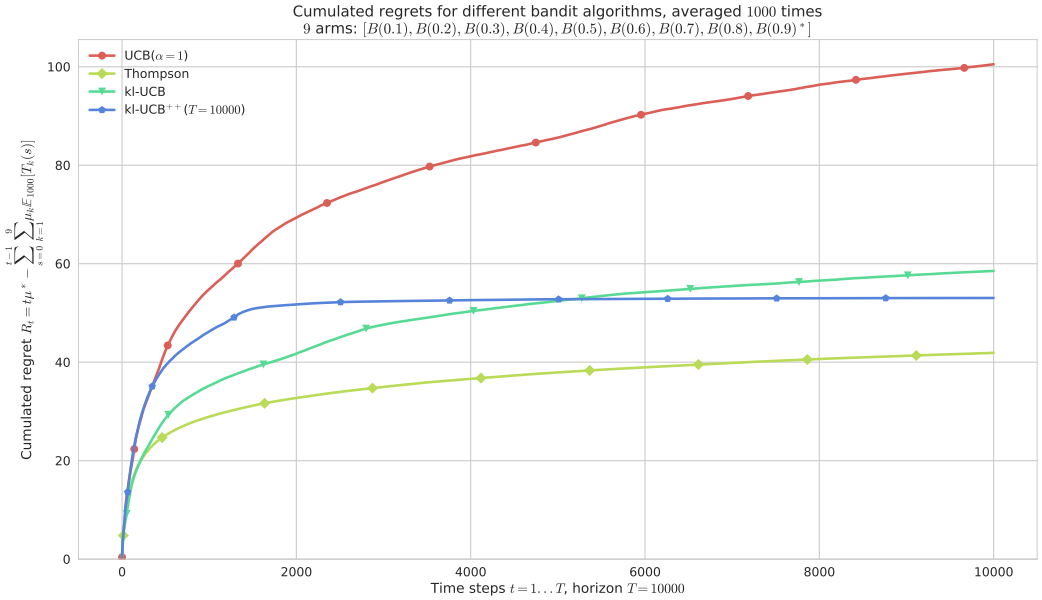

Figure 3.3 – Example of a single-player simulation showing the average regret of four algorithms (UCB, kl-UCB^{++}, kl-UCB and Thompson sampling). They all perform very well: each algorithm is known to be order-optimal (*i.e.*, its regret is proven to match the lower-bound up-to a constant), and each but UCB is known to be asymptotically optimal (*i.e.*, with the constant matching the lower-bound).

Running the simulation as shown above will save figures in a sub-folder, as well as save data (pulls, rewards, regret and other data) in a HDF5 file[1] [C+18]. Figure 3.3 above shows the average regret for these 4 algorithms. The Figure 3.4 below shows the histogram of regret obtained at the end of the experiment (*i.e.*, R_T) for the same example.

3.2.8 Dependencies on other Python libraries

This library is written in Python [Fou17], for versions 2.7+ or 3.4+, using `matplotlib` [Hun07] for 2D plotting, `numpy` [vdWCV11] for data storing, random number generations and opera-

[1] For example, this simulation produced this HDF5 file
GitHub.com/SMPyBandits/SMPyBandits/blob/master/plots/paper/example.hdf5

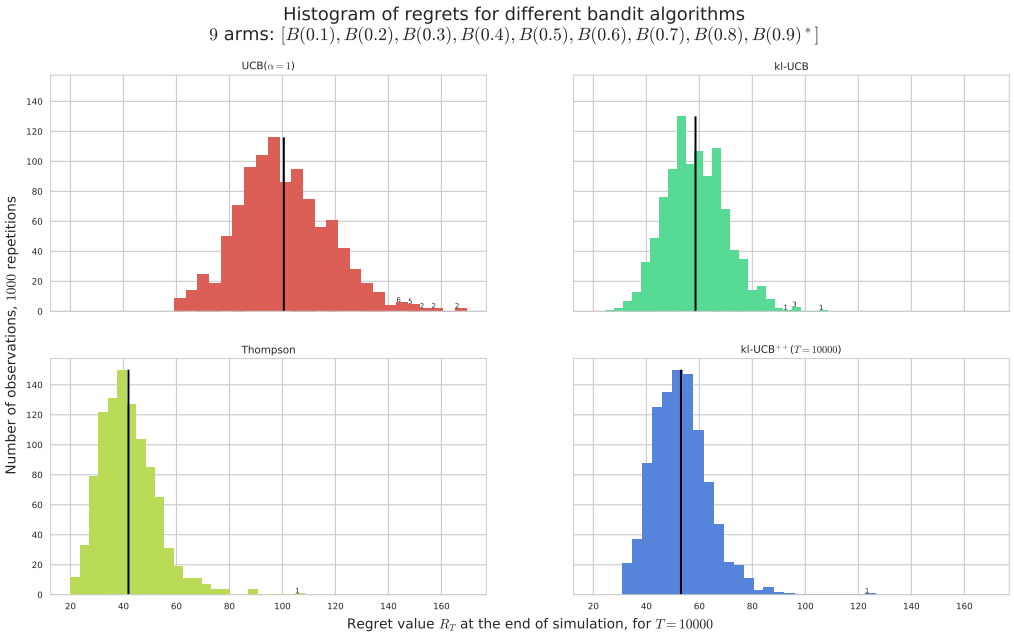

Figure 3.4 – Histogram of regret for the same experiment as of Figure 3.3. For instance, Thomson sampling is very efficient in average (in green), and UCB shows a larger variance (in red).

tions on arrays, `scipy` [JOP+01] for statistical and special functions, and `seaborn` [W+17] for clean plotting and colorblind-aware colormaps.

Optional dependencies include `joblib` [Var17] for parallel simulations, `numba` [I+17] for automatic speed-up on small functions (using a Just-in-Time compiler), `sphinx` [B+18] for generating the documentation, `virtualenv` [BP+16] for launching simulations in isolated environments, and `jupyter` [K+16] used with `ipython` [PG07] to experiment with the code.

All the quoted libraries are free and open-source and can be installed in one command using the `pip` (`pip.PyPa.io`) or `conda` (`conda.anaconda.org`) package manager. When SMPyBandits is installed using `pip install SMPyBandits`, the dependencies are of course automatically installed if not already present.

3.2.9 Continuous integration with Read the Docs and Travis CI

Since 2017 and 2018, SMPyBandits is using two online continuous integration (CI) services, to automatically build and host its documentation, and to automatically test the library on some numerical simulations. These CI services are free for open-source works, and are both triggered whenever a modification of the codebase is sent to the hosting platform GitHub.

Read the Docs. Since 2017, we have been using the free web service provided by Read the Docs (`ReadTheDocs.org`). Read the Docs allows to automatically build the documentation after every commit. This allows to regularly check that the library is well formatted and can be imported correctly, as well as keeping the online documentation up-to-date. Moreover, they offer to host the documentation online, at `SMPyBandits.ReadTheDocs.io`. For more details, see `ReadTheDocs.org/projects/SMPyBandits`. Since its first use, the service did about 180 builds, and about 10% of them were useful to detect newly introduced issues or bugs in the code. The build is configured using the `.readthedocs.yml` file in SMPyBandits main folder, and it builds the documentation in about two minutes. I have also been building the documentation manually on a weekly basis, to also host it on `SMPyBandits.GitHub.io` thanks to GitHub pages. In the last two years, the documentation saw about 20000 unique visits, while the GitHub project have been visited about 4500 unique visits.

Travis CI. Since 2018, we use the free web service provided by Travis CI (`Travis-CI.org`). It allows to automatically run short numerical simulations after every commit, in order to check that each modification on any part of the codebase does not break anything, as well as giving an up-to-date example of log files that shows online the results of different examples of experiments. The tests cover all the main models and almost all the algorithms implemented in SMPyBandits, and it has been proven very useful to quickly find and fix new bugs. For more details, see `Travis-CI.org/SMPyBandits/SMPyBandits`. Since its first use, the service did about 190 builds, and about 30% of them were useful to detect newly introduced issues or bugs in the code. The build is configured using the `.travis.yml` file in SMPyBandits main folder, and it runs numerical experiments with a short horizon (*e.g.*, $T = 100$) and a small number of repetitions (*i.e.*, $N = 4$), but covering all the different models implemented by SMPyBandits (and even including some that are not covered in this chapter, like the Markov model, or the sparse multi-players model). Builds typically run for 15 minutes, and Travis CI have been proven to be very useful in our development process.

3.2.10 List of research works using SMPyBandits

SMPyBandits has been used for the following research articles since 2017, and it is used for the previous and the next chapters of this thesis (except in Chapter 5). We give a link to a page on the documentation, that gives detailed instructions to reproduce the results presented in this research paper, details about the models and the notations, and bibliographic references.

- In [BKM18] and in Chapter 2 above, we used SMPyBandits to illustrate and compare different aggregation algorithms. We designed a variant of the Exp4 algorithm for online aggregation of experts [BCB12], called `Aggregator`. The documentation page is on `SMPyBandits.GitHub.io/Aggregation.html`

- In [BK18a] and in Chapter 6 below, we used SMPyBandits for all the simulations for multi-players bandit algorithms. We designed the two `RandTopM` and `MCTopM` algorithms and proved than they obtain logarithmic regret in the usual setting, and outperform significantly the previous state-of-the-art solutions (*i.e.*, `rhoRand`, `MEGA` and `MusicalChair`). Similarly, see the page `SMPyBandits.GitHub.io/MultiPlayers.html`
- In [BK18b], we used SMPyBandits to illustrate and compare different "doubling trick" schemes. `SMPyBandits.GitHub.io/DoublingTrick.html`
- In [BK19b] and [BK19a], and in Chapter 7 below, we used SMPyBandits for piece-wise stationary MAB models (only for the single-player case). We illustrate and compare different algorithms designed for this family of non-stationary problems. We designed the `GLRklUCB` policy, and implemented most of the state-of-the-art passive or active adaptive policies, both adversarial- or stochastic-based, designed to tackle the piece-wise stationary MAB problems. We also implemented a large benchmark of different piece-wise stationary problems. See `SMPyBandits.GitHub.io/NonStationary.html`

3.3 Experimental comparisons of state-of-the-art algorithms

In this section, we use the SMPyBandits library to compare experimentally various state-of-the-art (single-player) algorithms on some MAB problems. We first detail the list of different algorithms that we compare. We then give the results of the numerical experiments, in terms of mean regret at the end of the experiment of different horizons T. Additional results in terms of real measurements of time and memory are given and discussed in the next Section 3.4.

3.3.1 Experimental setup: algorithms and problems

We consider the 9 following algorithms, and 7 more are described in Appendix 3.6.1. For each of them, we give a bibliographic reference, that corresponds to a recent article studying it and not the first one which introduced it. We give the chosen tuning of its parameters, for parametric algorithms. Algorithms that are "not anytime" use the exact value of the horizon T, and when increasing values of T are studied for the same problem, they use the correct successive values. For reproducibility, we also give in "`typewriter font`" the name of the corresponding class in the `Policies` module in SMPyBandits (*e.g.*, UCB_1 is `Policies.UCBalpha`).

1. ε-greedy [BCB12] (`EpsilonDecreasing`), using $\varepsilon_t = \varepsilon_0/t$, and $\varepsilon_0 = 0.1$ (chosen arbitrarily). It has a very small cost in terms of time and memory, but it usually achieves linear regret in practice, despite of the theoretical regret bound.

2. Explore-then-Commit (`ETC_KnownGap`), that knows the horizon, and a lower-bound on the gap between arms (chosen arbitrarily as $\delta = 0.01$, valid for all problems). Similarly to ε-greedy, it has a very small footprint in terms of time and memory, but most of the times it only obtains large (linear) regret.

3. Exp3^{++} from [SL17] (`Exp3PlusPlus`), using $\alpha = 3$ and $\beta = 256$ as advised.

4. UCB_1 from [ACBF02] (`UCBalpha`), shown in Algorithm 2.3 above, using $\alpha = 1$. It achieves order-optimal problem-dependent bounds with a $\mathcal{O}(K \ln(T)/\Delta^2)$ regret.

5. kl-UCB from [CGM+13] (`klUCB`), also shown in Algorithm 2.3 above, using the Bernoulli KL divergence and the corresponding kl-UCB indexes (coded as `kullback.klucbBern`). It is computationally more costly that UCB, even if empirically we found that even in the worst cases kl-UCB is no more than one order of magnitude slower than UCB.

6. Thompson sampling from [KKM12] (`Thompson`), using a Beta prior and posterior, initially uniform (*i.e.*, $\pi_k(0) = \mathrm{Beta}(1, 1)$). It is efficient in terms of storage, and even if K random samples must be sampled from the arms posteriors at each time step t, Thompson sampling is not much slower than UCB, if the random number generator used for the simulations is efficient (it is the case for SMPyBandits, as we use `numpy.random` module which relies on highly optimized C or Cython code).

7. Bayes-UCB from [KCG12] (`BayesUCB`), using a Beta prior and posterior, initially uniform, *i.e.*, $\pi_k(0) = \mathrm{Beta}(1, 1)$. It is comparable to Thompson sampling in terms of memory complexity, but slower as computing a quantile is more costly than sampling from a distribution. But in particular for Bernoulli distributed arms and for Beta posteriors and priors, Bayes-UCB is only about twice as slow as Thompson sampling.

8. AdBandits from [TdSCC13] (`AdBandits`), using $\alpha = 1$. In practice, it is usually (slightly) more efficient than both Thompson sampling and Bayes-UCB in terms of regret, it is comparable in terms of computation times, but costs more memory.

9. BESA (Best Empirical Sampled Average) from [BMM14], which is implemented with a binary tournament, written in a naive but efficient way (*i.e.*, not using recursive functions, by using the `BESA` class with the `"non_recursive"=True` option). But the extension to $K > 2$ arms is still costly in terms of both time and memory, as illustrated below, and blows-up exponentially when K increases.

We focus on the most well known algorithms, discussed in Section 2.4, and two others that are efficient but less known (AdBandits and BESA). To highlight that SMPyBandits implements many other MAB algorithms proposed in recent works, we detail in Appendix 3.6.1 7 other algorithms. They are more recent (*e.g.*, 3 from 2018 and 2 from 2019) and are usually more complex, or based on a different point-of-view. The numerical results presented below include

these extra algorithms, to justify empirically that despite their respective qualities, and despite being very efficient, it is reasonable to focus on UCB and kl-UCB in the rest of this thesis, as they stay comparable with or more efficient than other recent algorithms, but are simpler to implement (*e.g.*, when comparing UCB to `ApproximatedFHGittins` or MOSS-Anytime) to manipulate theoretically (*e.g.*, when comparing kl-UCB to BESA, PHE or RCB).

Randomly sampled problems. For brevity, we prefer to focus on a single kind of distributions (Bernoulli), but similar results were observed for other distributions, in particular for (possibly truncated) Gaussian distributions.

For a fixed number of arms $K \geq 2$, instead of simulating a large number of times the same problem, we generate a new random problem for each independent run. We consider a randomly generated vector of means, each being sampled uniformly at random in $[0, 1]$, with a minimum gap of $\Delta^{\min}$, as well as minimum and maximum values of $\mu_{\min}$ and $\mu_{\max}$, that is denoted by $\boldsymbol{\mu} \sim \mathcal{E}(\Delta^{\min}, \mu_{\min}, \mu_{\max})$. This space $\mathcal{E}_{\Delta^{\min}}$ is defined as $\{\boldsymbol{\mu} \in [\mu_{\min}, \mu_{\max}]^K : \min_{k \neq k'} |\mu_k - \mu_{k'}| \geq \Delta^{\min}\}$. We use $\mu_{\min} = \Delta^{\min}$ and $\mu_{\max} = 1 - \Delta^{\min}$, and the value used for $\Delta^{\min}$ is 0.1 for $K \leq 3$ (for "easy" problems), and $\frac{1}{3K}$ for $K \geq 5$ (for "harder" problems).

Other parameters of the experiments. On the one hand, we fix $K = 8$ and we consider increasing values for the horizon, from $T = 1000$ to $T = 50000$. On the other hand, we fix $T = 5000$ and we consider as well an increasing number of arms, from $K = 2$ to $K = 32$. For all experiments, we run $N = 1000$ independent simulations. We show in Code 3.6 in the Appendix below more details about how to run these experiments.

3.3.2 Experiments results

We give in Figures 3.5 and 3.6 below the results of the experiments.

Summary of the experiments. We are able to check empirically that the regret of all the efficient algorithm indeed scales as predicted by the theory, that is linearly in the number of arms, and logarithmically in the horizon, *i.e.*, $R_T = \mathcal{O}(K \ln T)$. The main take-away message is the following: in all the rest of this thesis, we focus on two algorithms depending if simplicity or efficiency is favored:

- UCB is used in the more applied Chapter 5, when simplicity is favored,
- kl-UCB is used, in the two more theoretical Chapters 6 and 7, when we analyze mathematically the performance of an algorithm that is running on top of a classical stationary MAB policy, like our two contributions, MCTopM and GLR.

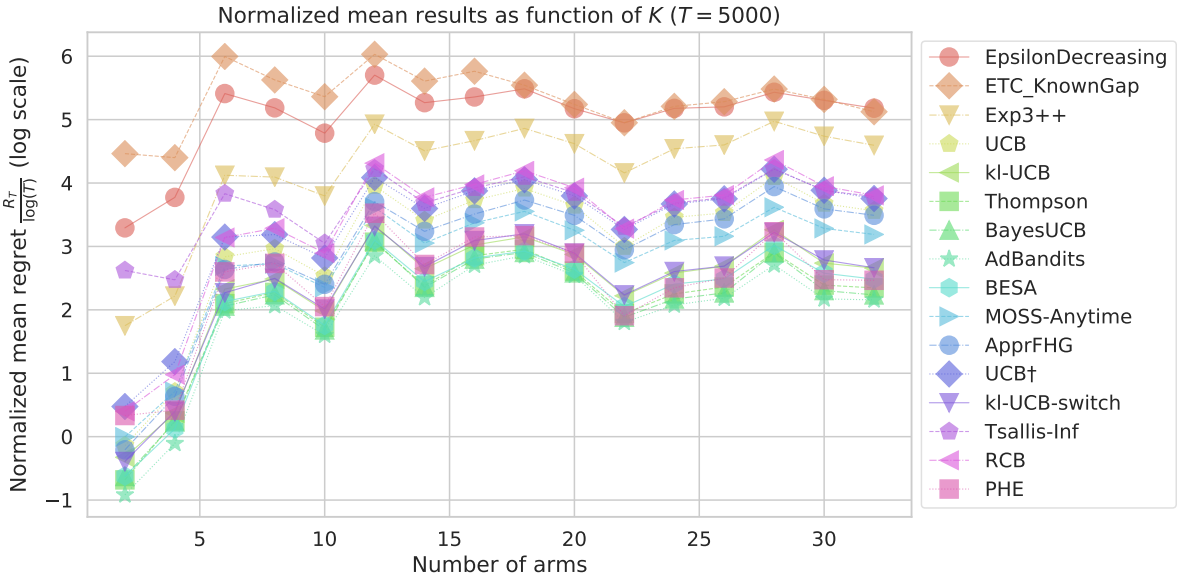

Figure 3.5 – Regret vs different values of K ($R_T / \ln(T)$), for $T = 5000$ and for 16 algorithms. The y-axis is in log-scale. All algorithms appear to have a regret slowly growing with respect to K, as predicted by the regret bounds which are linear with respect to the number of arms. Bayesian algorithms appear to be the most efficient, and kl-UCB as well as UCB are also seen to be efficient. Both the ε-greedy and Explore-then-Commit algorithms performed poorly, actually they achieve linear regret.

3.4 Comparing real measurements of time and memory costs

In this section, we report additional experiment results from the simulations described in the previous Section 3.3. Instead of studying on the efficiency of the algorithms (*i.e.*, their regret), we report results of real measurements in terms of computational time as well as memory storage. While the results reported in the previous section should not depend on the implementation of the different algorithms, the results in this section concern real measurements of both time and memory consumptions of the simulation software used for these simulations. Hence, the reported results highly depend on many factors, including how the code is written, and where and when it is run. We take precautions to ensure the fairness of the comparison between the different algorithms, as detailed in Appendix 3.6.2.

3.4.1 Computational time

In Figure 3.7, we can see that Bayesian algorithms appear to be the most efficient (*i.e.*, in the bottom left corner), and kl-UCB is very close to their best empirical performances. UCB, algorithms that were proven to perform similarly to UCB (*i.e.*, PHE and RCB), and other index policies inspired by UCB (ApprFHG, UCB†) enjoy very similar performances: a larger regret than Bayesian algorithms and kl-UCB, but a shorter running time. This observation highlights

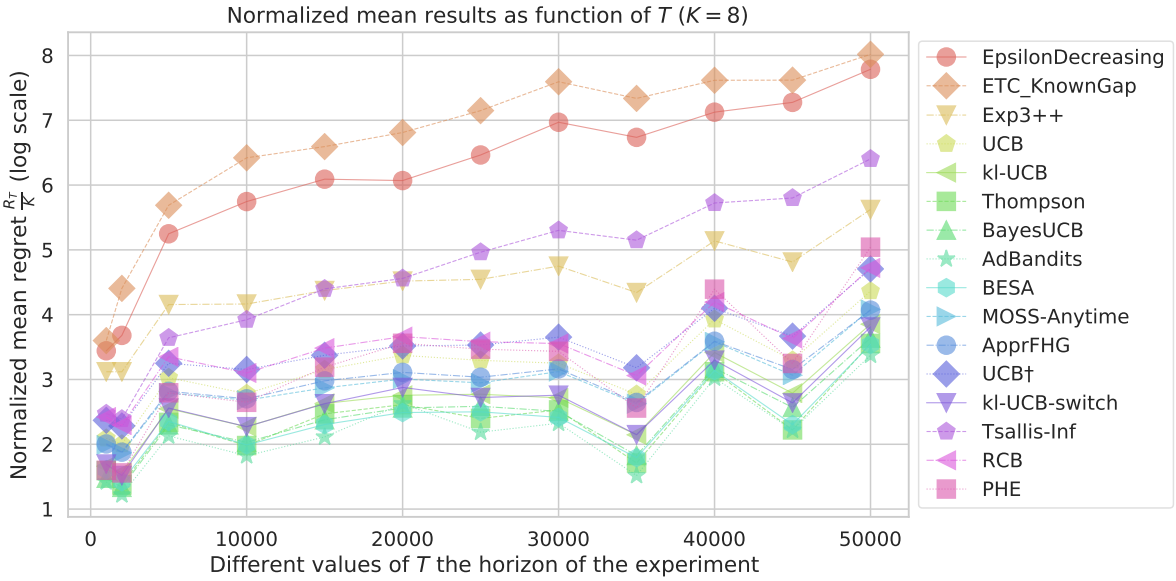

Figure 3.6 – Regret vs different values of T (R_T/K), for $K = 32$ and for 16 algorithms. All efficient algorithms appear to have a logarithmic regret with respect to the horizon, as predicted. The respective ranking of all the algorithms also appears to remain preserved for different values of T, which is also backed-up by theoretical results: if two algorithms $\mathcal{A}$ and $\mathcal{A}'$ has a regret close to their regret bounds, of the form $R_T \leq \mathcal{O}(K \ln(T))$, and the bound for $\mathcal{A}$ use a smaller constant than the bound for $\mathcal{A}'$, $\mathcal{A}$ should obtain a smaller regret than $\mathcal{A}'$ no matter the horizon. Bayesian algorithms appear to be the most efficient, and kl-UCB as well as UCB are also shown to be efficient. Finally, we also observe once more that both ε-greedy and Explore-then-Commit performed poorly, achieving linear regret.

an interesting trade-off between having a small regret, and being fast and computationally efficient. We also observe that BESA has a low regret but is much slower than all the other algorithms, because its complexity is exponentially growing wrt K the number of arms.

Moreover, in the two Figures 3.8 and 3.9, we are able to check empirically that the computational time of all the efficient algorithm indeed scales as predicted by the theory, that is linearly in the number of arms in the horizon, *i.e.*, $\mathcal{T}_T = \mathcal{O}(KT)$.

3.4.2 Memory cost

Like for the computational cost discussed above, in Figure 3.10, we can see that Bayesian algorithms like Thompson sampling again appear to be the most efficient (*i.e.*, in the bottom left corner), and kl-UCB is close to their best empirical performances. UCB and other index policies inspired by UCB (ApprFHG, UCB†) enjoy very similar performances: a larger regret than Bayesian algorithms and kl-UCB, but a similar memory cost. This time, there is no clear trade-off between optimality in terms of regret and memory cost, and based on simply this Figure 3.10, one could advise to use Thompson sampling rather than kl-UCB.

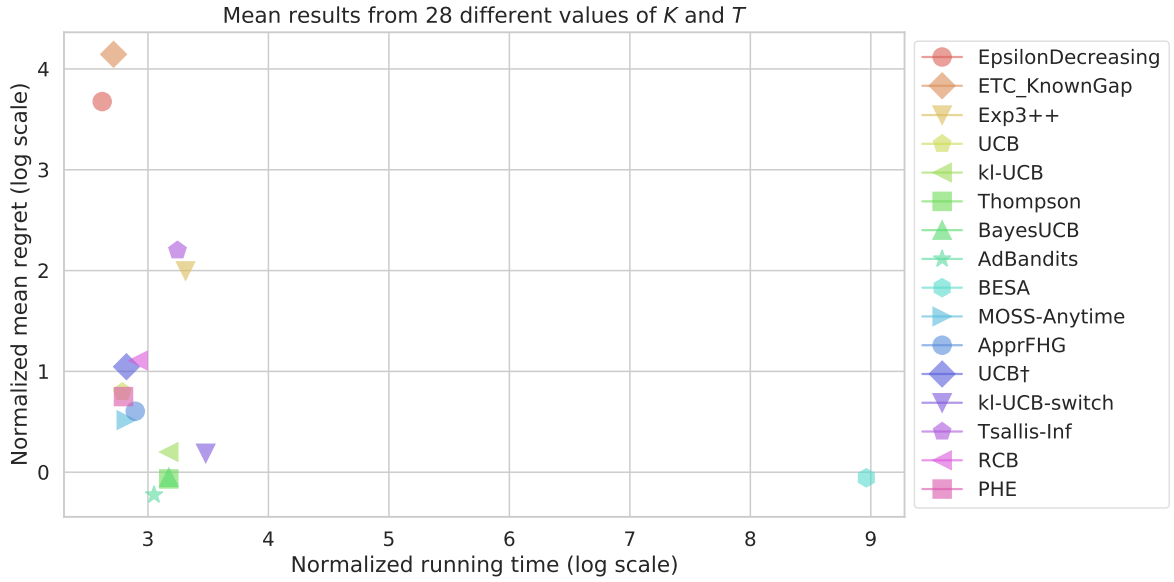

Figure 3.7 – Normalized mean regret vs normalized running time (in micro-seconds), aggregating the results from different values of K and T, for 16 algorithms. Both the x-axis and y-axis are in log-scale. UCB and kl-UCB are among the best algorithms, while AdBandits, Thompson sampling and Bayes-UCB slightly outperform them in terms of regret, and have similar running times.

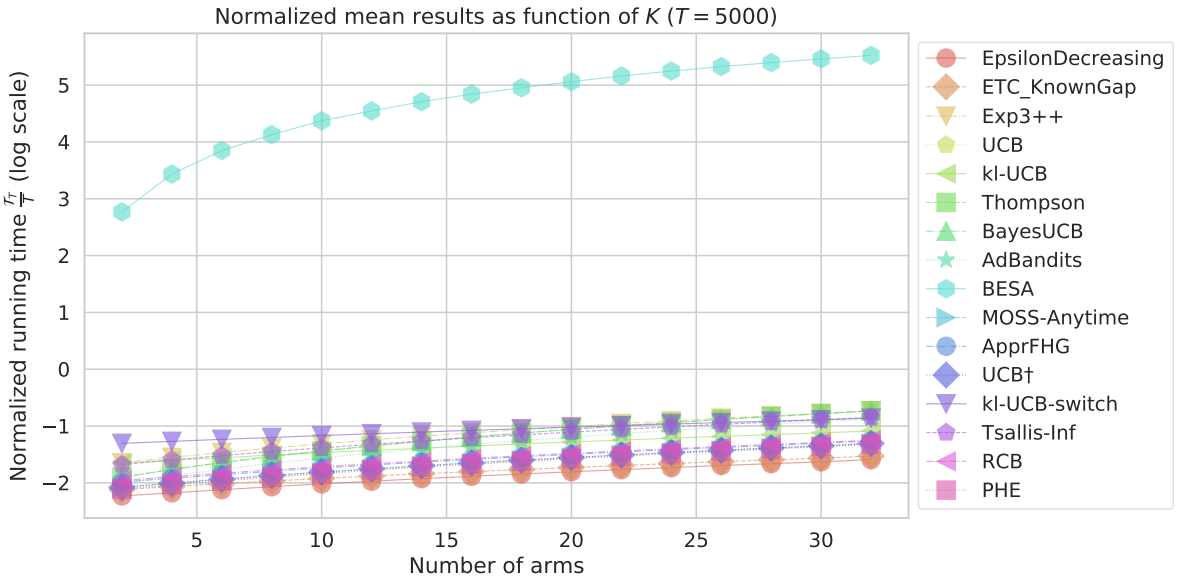

Figure 3.8 – Normalized running time vs different values of K ($\mathcal{T}_T/T$), for $T = 5000$ and for 16 algorithms. y-axis is in log-scale. All algorithms except BESA has a linear normalized running time, meaning that for K arms they use a computation time proportional to K, as predicted: $\mathcal{T}_T = \mathcal{O}(KT)$.

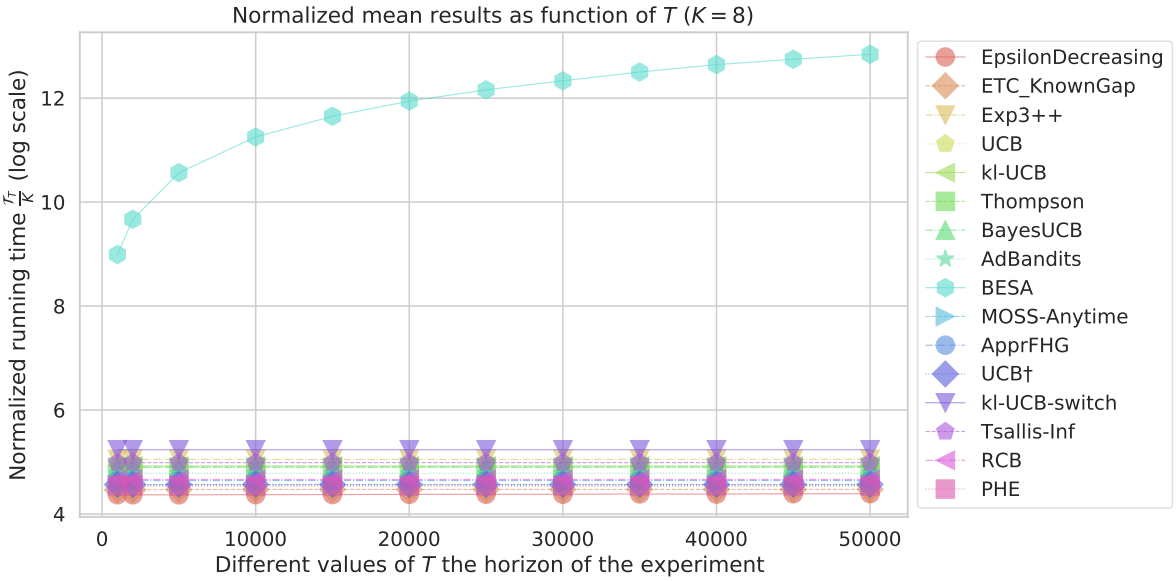

Figure 3.9 – Normalized running time vs different values of T ($\mathcal{T}_T/T$), for $K = 32$ and for 16 algorithms. y-axis is in log-scale. All algorithms except BESA has a constant normalized running time, meaning that for T rounds they use a computation time proportional to T, as predicted: $\mathcal{T}_T = \mathcal{O}(KT)$.

Moreover, in the two Figures 3.11 and 3.12, we are able to check empirically that the memory cost of all the efficient algorithm indeed scales as predicted by the theory, that is linearly in the number of arms but independently of the horizon, *i.e.*, $\mathcal{M}_T = \mathcal{O}(K)$.

Conclusion. The simplest (but most efficient) algorithms have a time complexity at each time step $t \in [T]$ bounded by $\mathcal{O}(K)$, independently of t, and thus have a total time complexity bounded by $\mathcal{T}_T = \mathcal{O}(KT)$, as well as a memory cost proportional to the number of arms but independent of the horizons, *i.e.*, bounded by $\mathcal{M}_T = \mathcal{O}(K)$.

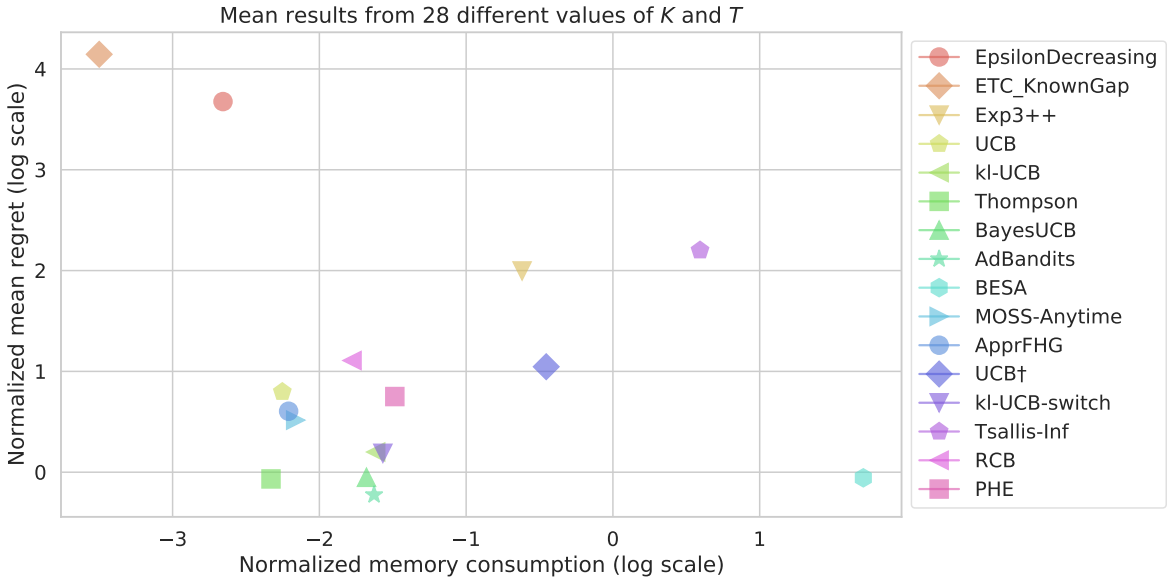

Figure 3.10 – Normalized mean regret vs normalized memory costs (in bytes), aggregating the results from different values of K and T, for 16 algorithms. Both the x-axis and y-axis are in log-scale. Thompson sampling appears as the best algorithm in this visualization, while UCB has the advantage of being memory efficient, and kl-UCB obtains similar performances.

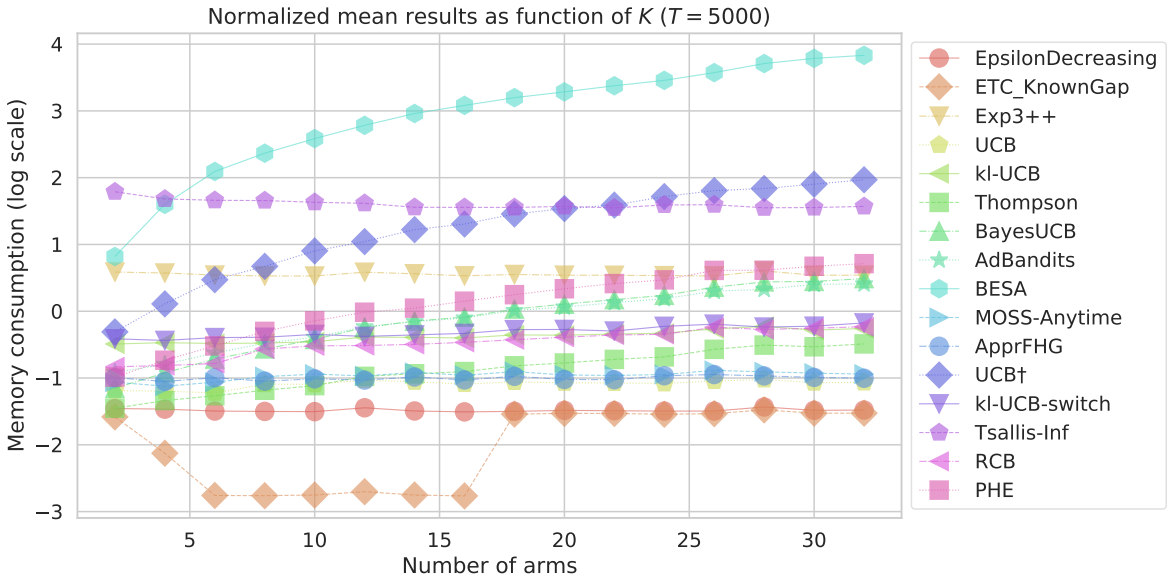

Figure 3.11 – Normalized memory cost vs different values of K ($\mathcal{M}_T/K$), for $T = 5000$ and for 16 algorithms. y-axis is in log-scale. All algorithms (except BESA) has an almost constant memory cost, meaning that for K arms they use a storage proportional to K, as predicted: $\mathcal{M}_T = \mathcal{O}(K)$.

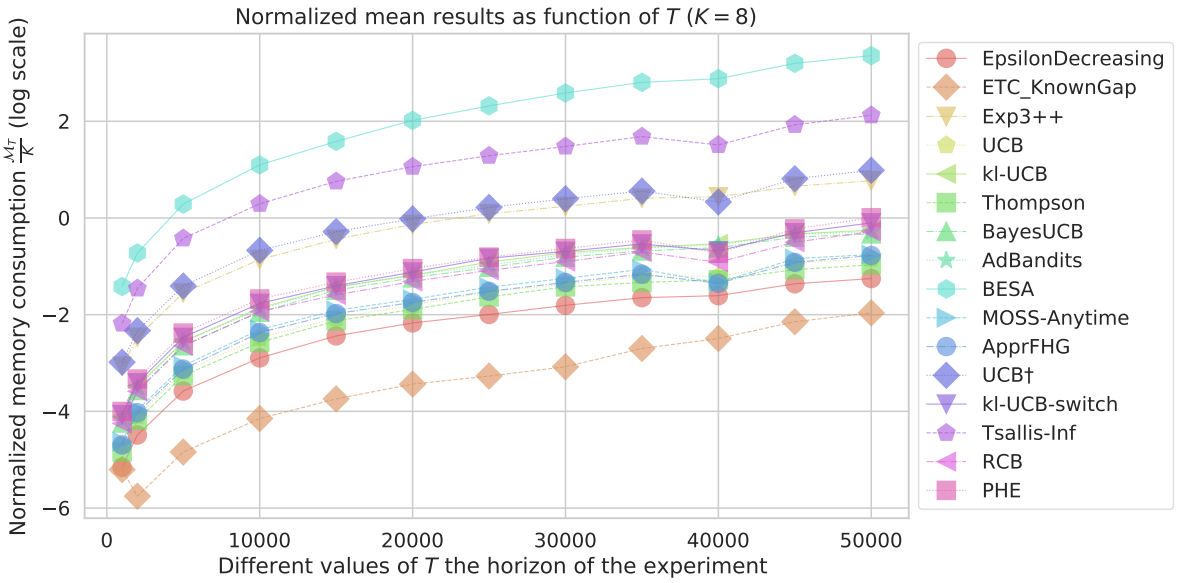

Figure 3.12 – Normalized memory cost vs different values of T ($\mathcal{M}_T/K$), for $K = 32$ and for 16 algorithms. y-axis is in log-scale. All algorithms have a growing normalized memory cost, meaning that for T rounds they use a computation time almost independent of T, as predicted: $\mathcal{M}_T = \mathcal{O}(K)$.

We also shown a trade-off between optimality in terms of regret, and efficiency in terms of time complexity or memory cost. Our position regarding this trade-off is motivated by Occam's razor principle. On the one hand, if the algorithm should be implemented on a cognitive radio device that has limited hardware capacity (for instance), one can reasonably aim at the simplest yet order-optimal algorithms, and we advise to use UCB and algorithms running on top of this simple index policy, as we do in Chapter 5. On the other hand, if one is more interested in the mathematical developments and wants to prove the tightest possible regret upper bounds, aiming at more efficient but more complex algorithms is interesting, and we chose the kl-UCB algorithm as the base bandit policy for our works in Chapters 6 and 7.

3.5 Conclusion

We chose to present here the Python library SMPyBandits in this chapter, rather than in the Appendix, because all the numerical experiments on single-player multi-armed bandits in Chapter 4, and on more sophisticated models in the last two Chapters 6 and 7 are built on SMPyBandits. We detailed the three following main points of our library:

- (i) The purpose of SMPyBandits is to easily implement numerical simulations of stochastic or piece-wise stochastic problems of single- or multi-players multi-armed bandits. SMPyBandits is distributed on GitHub and Pypi freely, under an open-source license, and it is extensively documented (at `SMPyBandits.GitHub.io`). Our library allows any researcher to easily run numerical simulations of different kinds of multi-armed bandit problems, requiring only a small knowledge of Python thanks to its documentation, its well-designed API, and many examples of simulation scripts and configuration files included.

- (ii) We detailed how SMPyBandits is implementing arms, problems, algorithms, and use these components to implement a simulation loop, with various visualizations being performed after the simulation. As far as now, SMPyBandits is restricted to the finite-arm case, but it supports a wide range of arms distributions. Different kinds of models are implemented, from stationary single-player to piece-wise stationary multi-players with different collision models. One of the main qualities of the library is that it is quite exhaustive, as all the main families of algorithms covering these different models have been implemented, even very recent algorithms from the literature, as we followed the active research from December 2016 to June 2019. More than 65 algorithms or variants of algorithms are implemented for the single-player case, 5 for the experts aggregation problem, about 15 for the multi-players case, and about 20 for the piece-wise stationary problem. All the codebase is fully documented, and the library is using continuous integration to run automated tests on the code after every modification. When comparing algorithms on a problem, the main performance measure is the regret, but the library

also computes, stores and visualizes other measures, such as best-arm selection rate, mean cumulated reward, as well as real time or memory costs.

(iii) Finally, we presented how to use SMPyBandits, if one wants to run some pre-designed simulations or design new simulations. Running a simulation is very easy, and different examples showed that the main parameters such as the time horizon T or the number of repetitions can be configured directly from the command line when running the Python script, or by modifying the code. Designing a new simulation requires to have a basic knowledge of Python, but not to dive into the implementation of the library.

We want to conclude by highlighting that a significant amount of time during my PhD was devoted to the development of SMPyBandits, and as such the library, its documentation and this chapter are considered an important contribution of this thesis. Our library is used for the numerical simulations in the rest of this document, except Chapter 5. We also used it in other publications not included in this thesis, like our work on doubling tricks [BK18b].

Perspectives

An interesting task that I would have liked to complete is to interface the library with a web-based interactive demonstration, in order to allow anyone to launch simulations without any knowledge of programming. It is already possible to reproduce some of the experiments presented in this thesis, by following the instructions given in the documentation (see Section 3.2.10), by using the Jupyter notebooks [K+16] made available[2].

Finally, the most exciting thing that could happen to our SMPyBandits library would be to see it gaining popularity! Its documentation has seen already about 25000 visits, the project on GitHub had 130 stars in November 2019, and based on the features requested and the emails received about it, we counted between ten to twenty researchers in other labs who use or used SMPyBandits. While this is a good start, we believe that the library is mature and interesting enough to hope to see it being used by more people. We have submitted a summary paper presenting SMPyBandits [Bes18] to the MLOSS track of the Journal of Machine Learning Research (JMLR), and we hope that it will be accepted, as it would give more visibility to this work. As a personal note, I would like to continue working on SMPyBandits, and implement the most interesting requested features, as well as maintain it, and possibly continue to add recent algorithms by following actively the research in this community. I would also love to be able to teach an under-graduate course on reinforcement learning and bandits in the future, and to use my library as a support to illustrate a course and its practical sessions.

[2] These notebooks are hosted on both the GitHub repository of SMPyBandits and on my website on `perso.crans.org/besson/PhD/notebooks/`. They can be used locally if you install the library, but can also be used on cloud platforms, like Binder `mybinder.org/v2/gh/SMPyBandits/SMPyBandits/master` or Google Colab `colab.research.google.com/github/SMPyBandits/SMPyBandits/tree/master/notebooks/`

3.6 Appendix

We give in this appendix more details regarding the numerical experiments presented in Section 3.3 and 3.4 above, for the other algorithms used in our benchmark, and details on the methodology used to measure the time and memory.

3.6.1 Additional details about numerical experiments in Section 3.3

This Appendix section starts by describing 7 more algorithms that are also compared with the 9 presented above in Section 3.3.

10. MOSS-Anytime from [DP16], using $\alpha = 1$ (`MOSSAnytime`), is an anytime variant of MOSS [BS12], using an adaptive tuning of its parameter. It obtains good "best of both world" performances, meaning that it achieves $\mathcal{O}(K \ln(T)/\Delta^2)$ regret for problem-dependent bounds, and $\mathcal{O}(\sqrt{KT})$ for problem-independent bounds. Empirically, it performs usually similarly to UCB, and is slightly more costly in terms of both time and memory.

11. Approximated Finite-Horizon Gittins from [Lat16b] (`ApproximatedFHGittins`), using $\alpha = 1$, mimics the UCB algorithm but uses a more complicated function to compute the upper confidence bounds. It achieves order-optimal problem-dependent bounds with a $\mathcal{O}(K \ln(T)/\Delta^2)$ regret. Empirically, it performs usually similarly to UCB and MOSS-Anytime, and is slightly more costly in terms of both time and memory.

12. UCB† from the same author [Lat18] (`UCBdagger`), using $\alpha = 1$, mimics the UCB algorithm but uses a much more complicated function to compute the upper confidence bounds, and uses more storage. It also achieves order-optimal problem-dependent bounds with a $\mathcal{O}(K \ln(T)/\Delta^2)$ regret. Empirically, it performs usually similarly to UCB and MOSS-Anytime, and is slightly more costly in computation time, but it is much more costly in terms of memory.

13. Anytime variant of kl-UCB-switch from [GHMS18] (`klUCBswitchAnytime`), is a very recent variant of KL-UCB [CGM+13]. It mimics the KL-UCB algorithm but uses a much more complicated function to compute the upper confidence bounds, and uses more storage. It is anytime, and was proven to obtain good "best of both world" performances, meaning that it achieves an asymptotically optimal $\mathcal{O}(\ln(T))$ regret for problem-dependent bounds, and $\mathcal{O}(\sqrt{KT})$ for problem-independent bounds. Empirically, it usually outperforms (slightly) kl-UCB in terms of regret, and costs about the same memory, but it is slower.

14. Tsallis-Inf from [ZS19] (`TsallisInf`), using $\alpha = 1/2$ (it seems to be the most efficient of the algorithms described in the article). It is based on the online mirror descent

algorithm with a Tsallis entropy regularizer, and it is anytime. It was also proven to obtain good "best of both world" performances. Empirically, we were unable to find any problem where it performs as well as UCB (or any other efficient algorithm), and we are confident that our implementation is correct[3]. TSALLIS-INF is also slower than UCB (about as slow as kl-UCB-switch), and costs an-order-of-magnitude more memory.

15. RCB (Randomized Confidence Bound) from [KT19] (`RCB`), using $\alpha = 1$ and perturbations uniformly sampled in $[0, 1]$. We prefer to use the simplest of the algorithms described in the article. It was analyzed and found to be order-optimal for problem-dependent bounds, and empirically we found that it is usually performs slightly worse than UCB, in terms of regret, time and memory. It is included because it remains comparably efficient with the other state-of-the-art algorithms, and because the key message from [KT19] is very interesting: "the optimism embedded in UCB can be replaced by simple randomization".

16. PHE (Perturbed-History Exploration) from [KSGB19] (`PHE`), using a perturbation scale of 0.5 as advised. The algorithm adds $\mathcal{O}(t)$ *i.i.d.* pseudo-rewards to its history in round t, and then pulls the arm with the highest estimated value in its perturbed history. It was also analyzed and found to be comparable with UCB. Like RCB, PHE was found to be empirically slightly worse than other state-of-the-art algorithms. Interestingly, its time and memory consumption stay constant with respect to the step number t and the horizon T, because generating and summing t pseudo-rewards from a Bernoulli distribution can actually be done in $\mathcal{O}(1)$ time and space, by using efficient sampling methods for sampling from a Binomial distribution.

How to run such experiments. We give below in Code 3.6 a Bash command to run the experiments presented in Sections 3.3 and 3.6.1 above. It uses `for` loops and environment variables from Bash, and not Python, mainly for concision, but we could also have done the same by writing a Python script that calls the `main.py` script for these values of T and K.

3.6.2 Methodology details for measurements of time and memory

The results reported in Section 3.4 highly depend on many factors, including how the code is written, and where and when it is run. We detail both below:

Quality and optimization of the code: The same level of optimization is used in all the codebase of SMPyBandits, and most of the time, the code is pure and naive Python and was not

[3] Despite a serious amount of time spent on this implementation, maybe it has some bug which explains the poor empirical performance obtained by TSALLIS-INF in our simulations. Exploring in more details this kind of algorithms is very interesting, as algorithms based on online mirror descent make a rich connection between multi-armed bandit and online convex optimization [H+16], and a short-term future work in SMPyBandits will be to explore different values of α for Tsallis entropy regularization, or other families of regularization.

```
$ for T in $(seq 5000 5000 50000); do \
    DEBUG=False NOPLOTS=False SAVEALL=True N_JOBS=-1 N=1000 BAYES=True \
    T=$T   K=8  python3 main.py configuration.py \
    && cp logs/main_py3_log.txt logs/main_py3_log__N1000_BAYES_T{T}_K8.txt \
  done
$ for K in $(seq 2 2 32); do \
    DEBUG=False NOPLOTS=False SAVEALL=True N_JOBS=-1 N=1000 BAYES=True \
    T=5000 K=$K python3 main.py configuration.py \
    && cp logs/main_py3_log.txt logs/main_py3_log__N1000_BAYES_T5000_K{K}.txt \
  done
```

Code Example 3.6 – Bash code to run the large-scale experiments presented in Sections 3.3 and 3.6.1, for $K = 8$ and $T \in \{5000, \dots, 50000\}$ and $T = 5000$ and $K \in \{2, \dots, 32\}$.

optimized. Mathematical functions (*e.g.*, $\sqrt{\bullet}, \ln$) and random numbers used are using `numpy` and `numpy.random` modules [vdWCV11], which are based on C and Cython code [BBS+19] and can be considered highly efficient. Computations of Kullback-Leibler and indexes for kl-UCB algorithms are based on a compiled CPython extension written in C [Fou17] and can also be considered highly efficient. As we can safely affirm that the code of the different algorithms has the same level of optimization, the comparison is fair, and we do not favor any algorithm in their implementation in SMPyBandits.

About the experimental environment: the exact measurements used for the figures displayed below highly depend on the machine used for the simulation, the version of the language and its libraries (see above in Section 3.2.8 for details about SMPyBandits), as well as the number of CPU cores being used (here, we used 12 cores in a 12-core desktop) etc. As long as the different algorithms and simulations are performed on the same environment, the comparison we make from them are fair and do make sense.

About the measurement protocol. To be precise, we used the two following approaches to measure the real time and memory costs of the different algorithms.

For time, we used the `time.time()` function from Python's standard library, that gives the current time in micro-seconds. In the `Evaluator` object of SMPyBandits, before launching the "for" loop on $t \in [T]$ for one algorithm, the system time is stored, and when the loop is finished, the time used for this loop is the current system time minus the starting time. This measurement gets averaged on the $N = 100$ (independent) repetitions, and consistently measure the time efficiency of the algorithms.

For memory, we use two different approaches whether the code runs on a UNIX or a Windows system. On UNIX, the `resource` module allows to measure the memory of the current process, and by counting the difference in memory used by the `Evaluator` object

before and after the "for" loop, we can track the memory used by the algorithm to store all its interior variables.

In both cases, the "for" loop takes some time and stores many variables, but the only difference in terms of both time or memory between two algorithms is explained by the difference in the implementation of the algorithms.

Comparing measurements. But what is important in these simulation results is not the exact values, but rather to compare the costs of the different algorithms, and thus only the relative difference in terms of time and memory costs are important. Relative difference for costs do not depend much on the code and the machine used for the simulation. The computation time is *normalized*, that is it is divided by the horizon, to count the (average) time used by an algorithm at time t from $t = 1$ to $t = T$, while the memory cost is *not normalized*. Thus, we can check that efficient algorithms have a running time independent on the horizon T, instead of just observing a linear dependency, and we can check that efficient algorithms have a memory cost independent on the horizon. All the considered algorithms in this Chapter are efficient in this aspect, but in Chapter 7 we study algorithms that essentially have to store, and run computations, on an increasing number of observations (*e.g.*, CUSUM-UCB), so their computation cost at time t increases (linearly) with t, and thus they are more costly. We can also check that efficient algorithms have a running time and a memory cost linear in the number of arms K, while more complex algorithms like BESA suffer from an exponential blow-up of their complexity when K increases.

Normalizing data. The two figures below regret normalized data, in the following way. For each algorithm, we ran simulations to obtain its (empirical) regret, computation time and space requirement, for different problems with different values of K and T. Simply considering the average of such measurements makes no sense, as for instance two values of the regret for $T = 1000$ or $T = 50000$ do not have the same order of magnitude. We know that efficient algorithms are expected to follow these patterns:

- The final regret R_T should scale as $\mathcal{O}(K \ln(T))$,
- The total computation time $\mathcal{T}_T$ should scale as $\mathcal{O}(KT)$ (*i.e.*, a computation time of $\mathcal{O}(K)$ for each time step t),
- The total memory cost $\mathcal{M}_T$ should scale as $\mathcal{O}(K)$, independent of the horizon.

Thus, on the one hand, when we show aggregated results from all the different values of K and T, we normalized the data by dividing the regrets by $K \ln(T)$, the times by KT and the memory by K. On the other hand, when we plot a quantity (R_T, $\mathcal{T}_T$, $\mathcal{M}_T$) as a function of T (resp. of K) we only normalize by K (resp. by T).

Chapter 4

Expert aggregation for online MAB algorithms selection

The review of MAB algorithms given in the previous Chapter 2 showed that there is a large collection of different algorithms designed for different kinds of bandit problems. In this chapter, we discuss the question of online algorithm selection. We tackle the question of how to select a particular bandit algorithm when a practitioner is facing a particular (unknown) bandit problem. Instead of always choosing a fixed algorithm, or running costly benchmarks before real-world deployment of the chosen algorithm, another solution could be to select a few candidate algorithms, where at least one is expected to be very efficient for the given problem, and use online algorithm selection to automatically and dynamically decide the best candidate. We propose an extension of the Exp4 algorithm for this problem, that we called Aggregator, and illustrate its performance on some bandit problems.

– Y'a toujours au moins deux solutions à un problème.
Élias de Kelliwic'h, interprété par Bruno Fontaine,
Kaamelott, Livre III, Épisode 67 "La Potion de Fécondité II".

Contents

4.1 Different approaches on algorithm selection

For any real-world applications of MAB algorithms, several solutions have been explored based on various models, and for any model, typically there are many algorithms available, as we have seen above. We gave in Section 2.4 an overview of the main families of algorithms designed to tackle stochastic MAB problems, and we mainly focused on the UCB_1, kl-UCB and Thompson sampling algorithms. But a rich research literature has produced many different algorithms tackling the MAB problem, as suggested for instance by the length of the reference book [LS19]. Thus, when a practitioner is facing a problem where MAB algorithms could be used, it is not an easy task to decide which algorithm to implement. It is hard to predict which solution could be the best for real-world conditions at every instant, and even by assuming a stationary environment, when one is facing a certain problem but has limited information about it, it is hard to know beforehand which algorithm can be the best solution.

In this chapter, we first present two naive approaches for selecting an algorithm when facing a new problem, and then we detail the online approach that uses a "leader" MAB algorithm running on top of a pool of "followers" algorithms, and we present our contribution that is a new "leader" algorithm based on $\mathrm{Exp4}$.

Publication. This chapter is based on our article [BKM18].

Outline. This chapter is organized as follows. First, we give more motivations in the rest of this section, then we explain how to combine such stationary MAB algorithms and aggregate them. We present the proposed algorithm, called $\mathrm{Aggregator}$, in Section 4.2, Finally, we present numerical experiments in Section 4.3, on Bernoulli and non-Bernoulli MAB problems, comparing the regret of several algorithms against different aggregation algorithms. Theoretical guarantees are shortly discussed in Section 4.4.

4.1.1 Motivation for online algorithm selection

Many different learning algorithms have been proposed by the machine learning community, and most of them depend on several parameters, for instance α for UCB_1, the prior for Thompson sampling or Bayes-UCB, the kl function for kl-UCB etc. Every time a new MAB algorithm $\mathcal{A}$ is introduced, it is compared and benchmarked on some bandit instances, parameterized by $\boldsymbol{\mu} = (\mu_1, \dots, \mu_K)$, usually by focusing on its expected regret $R_T^{\mathcal{A}}$. For a known and specific instance, simulations help to select the best algorithm in a pool of algorithms, but when one wants to tackle an *unknown* real-world problem, one expects to be efficient against *any* problem, of any size and complexity in a certain family: ideally one would like to use an algorithm that can be applied identically against any problem of such family.

Naive approaches. On the one hand, a practitioner can decide to pick one algorithm, maybe because it seems efficient on other problems, or maybe because it is simple enough to be used in its application. It might be unrealistic to implement complicated algorithms on limited hardware such as embedded chips in a very low-cost IoT end-device, and for instance a practitioner could choose to only consider the UCB_1 algorithm (or other low-cost algorithms). On the other hand, if prior knowledge on the application at hand is available, one could implement some benchmarks, and compare a set of algorithms on different problems. If a leader appears clearly, it is then possible to choose it for the application.

Illustrative example. For instance, if you know that the considered problem can either have K arms with very close means, or one optimal arm far away from the other, two versions of UCB_1 will perform quite differently in the two problems: using a large α, *i.e.*, favoring exploration, will give low regret in the first case and high regret in the second case, while using a low α, *i.e.*, favoring exploitation, will obtain opposite performances. A first approach can be to use an intermediate value, as $\alpha = 1/2$ suggested by theory, but another approach could be to consider an aggregated vote of different versions of UCB_1, each running with a different value of α (*e.g.*, in a logarithmic grid), and let a "leader" learning algorithm decide which value of α is the best *for the problem at hand*.

4.1.2 Online algorithm selection with expert aggregation

The online approach is interesting in the case where the computation power or memory storage of the application is not a limitation factor, but where one cannot run benchmarks before deploying the application. We consider a fixed set of algorithms, and we use another learning algorithm on top of this set, to learn *on the fly* which one should be trusted more, and eventually, used on its own.

The aggregation approach is especially interesting if we know that the problem the application will face is one of a few known kinds of problems. In such cases, if there are N different sorts of problems, and if the practitioner has prior knowledge on it, she can use the naive approach by selecting algorithm $\mathcal{A}_i$ which should perform well on problem i, for $i \in [N]$. Then she can use the aggregation of $\mathcal{A}_1, \dots, \mathcal{A}_N$ when facing an unknown problem. To the best of the authors' knowledge, aggregation algorithms, such as $\mathrm{Exp4}$ which dates back from 2002 [ACBF02], have actually never been used in practice for stochastic MAB problems. For instance, if we look at the applications of MAB for Opportunistic Spectrum Access, like it was proposed in [JEMP09, JEMP10, JMP12], online selection of MAB algorithms was never discussed, and usually the considered algorithm is simply UCB_1, with no discussion regarding this choice.

4.1.3 Aggregating bandit algorithms

We assume to have $N \geq 2$ MAB algorithms, $\mathcal{A}_1, \dots, \mathcal{A}_N$, and let $\mathcal{A}_{\text{aggr}}$ be an aggregation algorithm, which runs the N algorithms in parallel (with the same slotted time), and use them to choose its arms based on a voting from their N decisions. $\mathcal{A}_{\text{aggr}}$ depends on a pool of algorithms and a set of parameters. We would like that $\mathcal{A}_{\text{aggr}}$ performs almost as well as the best of the $\mathcal{A}_a$, with a good choice of its parameters, independently of the MAB problem. Ideally $\mathcal{A}_{\text{aggr}}$ should perform similarly to the best of the $\mathcal{A}_a$. To simplify the presentation, we restrict in Algorithm 4.1 to bandit algorithms that give deterministic recommendations: one arm is chosen with probability 1 and the others with probability 0. However, both Exp4 and Aggregator can be adapted to aggregate randomized bandit algorithms, *i.e.*, algorithms that output a probability distribution $q(t) = (q_k(t))_{k\in[K]}$ over the K arms at each time step, and draw the next selected arm according to this distribution. For instance, Thompson sampling uses its posterior distribution, or UCB can use a distribution with a mass of $1/n$ on the $n \geq 1$ arms of maximal index, and a mass of 0 on the other arms.

The aggregation algorithm maintains a probability distribution π^t on the N algorithms $\mathcal{A}_a$, starting from a uniform distribution. The probability of trusting the decision made by algorithm $\mathcal{A}_a$ at time t is thus π^t_a. $\mathcal{A}_{\text{aggr}}$ then simply performs a weighted vote on its algorithms: it first decides whom to trust by sampling $a \in [N]$ from π^t, then follows $\mathcal{A}_a$'s decision: $a \sim \pi^t, A_{\text{aggr}}(t) = A(t) = A_a(t)$. We prove below that it is equivalent to first let all the algorithms decide their arm, *i.e.*, $A_a(t)$, and then to compute $\forall k \in [K], p^t_k \doteq \sum_{a=1}^N \pi^t_a \times \mathbb{1}(\{A_a(t) = k\})$, the weighted probability that one of the N aggregated algorithms chose arm k, and finally to sample $A(t) \sim \pi^t$.

Proposition 4.1. *The two following sampling schemes for the aggregated algorithm* $\mathcal{A}_{\text{aggr}}[\mathcal{A}_1, \dots, \mathcal{A}_N]$ *are equivalent,* i.e., *they give the same distribution on the action chosen by* $\mathcal{A}_{\text{aggr}}$*,* $A_{\text{aggr}}(t) = A(t)$*.*

1. *Sample* $a(t) \sim \pi^t$ *first, then trusts* $\mathcal{A}_{a(t)}$*'s decision:* $A_{\text{aggr}}(t) = A(t) = A_{a(t)}(t)$*,*
2. *Let* $A_a(t)$ *be the arm chosen by algorithm* $\mathcal{A}_a$ *(sampled from* q^t_a*), for each* $a \in [N]$*, and compute* $\forall k \in [K], p^t_k \doteq \sum_{a=1}^N \pi^t_a \times \mathbb{1}(A_a(t) = k)$*. Then, play* $A_{\text{aggr}}(t) = A(t) \sim p^t$*.*

Proof. For any fixed time step $t \in [T]$, we denote respectively $P(t)$ and $P'(t)$ the distribution of action of the aggregated algorithm $\mathcal{A}_{\text{aggr}}$ at time t, respectively under the first and second sampling scheme. Let $q^t_a \in \Delta_K$ be the distribution of the chosen action by algorithm $\mathcal{A}_a$ (for $a \in [N]$), that depends on the past observations (as well as some external randomness, see Section 2.1). The first sampling scheme gives $P_k(t) = \mathbb{P}(A_{\text{aggr}}(t) = k) = \mathbb{P}(\cup_{a=1}^N A_{\text{aggr}}(t) = A_a(t) = k, a(t) = a) = \sum_{a=1}^N \mathbb{P}(A_a(t) = k)\mathbb{P}(a(t) = a) = \sum_{a=1}^N q_{a,k}(t)\pi^t_a$,

by independence of $a(t) \sim \pi^t$ and $A_i(t) \sim q_i(t)$ (for all i). The second sampling scheme gives $P'_k(t) = \mathbb{P}(A_{\text{aggr}}(t) = k) = \mathbb{E}[p^t_k]$ by definition, and $\mathbb{E}[p^t_k] = \sum_{a=1}^N \pi^t_a \mathbb{E}[\mathbb{1}(A_a(t) = k)] = \sum_{a=1}^N \pi^t_a \mathbb{P}(A_a(t) = k) = \sum_{a=1}^N q_{a,k}(t)\pi^t_a$. Thus we showed that $P_k(t) = P'_k(t)$, so the two sampling schemes are equivalent, as claimed. □

The main questions are then to know what observations (*i.e.*, arms and rewards) should be given as feedback to which algorithms, and how to update the trusts at each step, and our proposal Aggregator differs from Exp4 on these very two points. The considered aggregation algorithms are special cases of the well-known *multiplicative weights update algorithm*.

4.2 The Aggregator algorithm

The Aggregator algorithm is detailed in Algorithm 4.1. At every time step, after having observed a reward $r(t) = Y_{A(t),t}$ for its chosen action $A(t)$, the algorithm updates the trust probabilities from π^t to π^{t+1} by a multiplicative exponential factor (using the learning rate and the *unbiased* reward). Only the algorithms $\mathcal{A}_a$ who advised the last decision get their trust updated, in order to trust more the "reliable" algorithms.

Unbiased estimate of the rewards. The reward estimate is unbiased in the following sense. If one had access to the samples $Y_{k,t}$ for all arms k, the reward incurred by algorithm a at time t would be $r^a(t) = Y_{A_a(t),t}$. But we are not in the full information setting (see [CBL06]), but in the bandit setting, so only one of the samples $Y_{k,t}$ can be observed, $r(t) = Y_{A(t),t}$. This quantity can only be observed for those algorithms a for which $A^t_a = A(t)$. However, by dividing by the probability of observing this recommendation, one obtains an unbiased estimate of $r^a(t)$. More precisely, if we define the estimate by

$$\widehat{r^a}(t) \doteq \frac{Y_{A_a(t),t}}{p^t_{A_a(t)}} \mathbb{1}(A_a(t) = A(t)), \tag{4.1}$$

then it satisfies $\mathbb{E}_{O_t}[\widehat{r^a}(t)|O_t] = Y_{A_a(t),t}$, for all a, where the expectation is taken conditionally to the history of observations up to round t, O_t. Observe that $\widehat{r^a}(t) = 0$ for all algorithms a such that $A_a(t) \neq A(t)$.

An important feature of Aggregator is the feedback provided to each underlying bandit algorithm, upon the observation of arm $A(t)$. Rather than updating only the trusted algorithms (that is the algorithms which would have drawn arm $A(t)$) with the observed reward $r(t)$, we found that updating each algorithm with the (original) reward observed for arm $A(t)$ improves the performance drastically. As expected, the more feedback they get, the faster the underlying algorithms learn, and the better the aggregation algorithm is. This intuition is backed up by theory explained in [MM11].

Input: N bandit algorithms, $\mathcal{A}_1, \dots, \mathcal{A}_N$, with $N \geq 2$
Input: A sequence of learning rates, $(\eta_t)_{t\geq 1}$, *e.g.*, $\eta_t = \ln(N)/(tK)$
Data: Initial uniform distribution, $\pi^0 = \mathcal{U}([N])$
Result: $\mathcal{A}_{\text{aggr}} = \text{Aggregator}[\mathcal{A}_1, \dots, \mathcal{A}_N]$
for $t = 1, \dots, T$ **do** `// At every time step`
  for $a = 1, \dots, N$ **do** `// Can be parallel`
    $\mathcal{A}_a$ updates its internal state (e.g., UCB indexes);
    It chooses $A_a(t) \in [K]$;
  end
  Let $p_k^t \doteq \sum_{a=1}^{N} \pi_a^t \times \mathbb{1}(A_a(t) = k),\ \forall k \in [K]$;
  Then $\mathcal{A}_{\text{aggr}}$ chooses arm $A(t) \sim p^t$;
  Give *original* reward $(A(t), r(t))$ to *each* $\mathcal{A}_a$ (maybe *not* on its chosen arm);
  Compute an *unbiased* estimate of the reward, $\widehat{r}(t) = r(t)/p^t_{A(t)}$;
  for $a = 1, \dots, N$ **do**
    if $\mathcal{A}_a$ *was trusted*, i.e., $A_a(t) = A(t)$ **then**
      $\pi_a^{t+1} = \exp(\eta_t \widehat{r}(t)) \times \pi_a^t$; `// Trusted more`
    else
      $\pi_a^{t+1} = \pi_a^t$; `// Do not update the trust now`
    end
  Renormalize the new weights π^{t+1}: $\pi^{t+1} \doteq \pi^{t+1} / \sum_{a=1}^{N} \pi_a^{t+1}$.
end

Algorithm 4.1: The Aggregator algorithm, aggregating N MAB algorithms $\mathcal{A}_1, \dots, \mathcal{A}_N$.

Regarding the update of π^t, one can note that the trust probabilities are not all updated before the normalization step, and an alternative would be to increase π_a if $A_a(t) = A(t)$ and to *decrease it otherwise*. It would not be so different, as there is a final renormalization step, and empirically this variation has little or no impact on the performance of Aggregator.

Comparison with Exp4**.** The Exp4 algorithm dates from [ACBFS02], and for instance it is also well explained in Section 4.2 of [BCB12]. It is similar to Aggregator, presented in Algorithm 4.1, but differs in the two following points. The first difference is that $a \sim \pi^t$ is sampled first and the arm chosen by $\mathcal{A}_a$ is trusted, whereas Aggregator needs to listen to the N decisions to perform the updates on π^t. Then, Exp4 gives back an observation (*i.e.*, a pair arm, reward) only to the last trusted algorithm whereas Aggregator gives it to all algorithms. The second difference is that after having computed the reward estimate $\widehat{r^a}(t)$, Exp4 updates the estimated cumulative reward for each algorithm, $\widetilde{R}_a(t) = \sum_{s=1}^{t} \widehat{r^a}(t) \times \mathbb{1}(A_a^s = A_{\text{aggr}}^s)$. Instead of updating π^t multiplicatively as we do for our proposal, Exp4 recomputes it, proportionally to $\exp(\eta_t \widetilde{R}_a(t))$. Note that there is no difference for the case of constant learning rates, and it does not differ much for decreasing learning rates as well.

We also note that Exp4 uses *losses* instead of rewards, with $\ell(t) = 1 - r(t)$, but this is only a change of vocabulary. A learner can equivalently play to maximize its cumulated rewards or to minimize its cumulated losses. Most works on using expert advice and game theory usually prefer to think about losses, as for instance the book [CBL06].

How to choose η_t. The sequence of non-negative learning rates $(\eta_t)_{t\geq 1}$ used by Exp4 can be arbitrary. It can be constant but should be non-increasing [BCB12, Theorem 4.2]. If the horizon T is known (and fixed), they advise to use $\eta_t \doteq \eta = 2\ln(N)/(TK)$. However, for real-world communication problems, it can be considered unrealistic to assume a fixed and known time horizon. For more discussion on this hypothesis, we refer to Section 1 of our article [BK18b]. Thus we prefer an alternative horizon-free choice of learning rates, $\eta_t \doteq \ln(N)/(tK)$ suggested by [BCB12]. It is non-increasing, and it is obtained by minimizing the upper-bound on the regret derived in [BCB12, pp48]. We compared both approaches empirically, and the second one usually performs better. We also stick to this sequence $(\eta_t)_{t\geq 1}$ of decreasing learning rates for Aggregator.

4.3 Experiments on simulated MAB problems

We focus on *i.i.d.* MAB problems, with $K = 9$ arms. Similar behaviors are observed for other values, *e.g.*, trying up-to $K = 100$ gave the same results. For Bernoulli problem, the first one uses $\boldsymbol{\mu} = [0.1, \dots, 0.9]$, and is considered as a "simple" problem. The second one is divided in three groups: 2 very bad arms ($\mu = 0.01, 0.02$), 5 average arms ($\mu = 0.3$ to 0.6) and 3 very good arms ($\mu = 0.78, 0.8, 0.82$), and it is considered as a "harder" problem. The horizon is set to $T = 20000$ (but its value is unknown to all algorithms), and simulations are repeated 1000 times, to estimate the expected regret. This empirical estimation of the expected regret R_T is plotted below, as a function of T, comparing some algorithms $\mathcal{A}_1, \dots, \mathcal{A}_N$ (for $N = 6$), and their aggregation with Aggregator (displayed in orange bold), using the parameter-free learning rate sequence, $\eta_t \doteq \ln(N)/(tK)$.

Lower-bound. The Lai & Robbins' logarithmic lower-bound [LR85] is also plotted. It corresponds to the second case in Theorem 2.7. It is crucial to note that the lower-bound is only asymptotic, and as such one should not be surprised to see regret curves smaller than the lower-bound (*e.g.*, for the easier Bernoulli problem in Figure 4.1)

Comparing the algorithms against the same realizations. Note that for each of the $N = 1000$ simulations, we choose to generate all the rewards beforehand, *i.e.*, one full matrix $(Y_{k,t})_{k\in[K],t\in[T]}$, for each of the N repetitions, in order to compare the algorithms on the same realizations of the MAB problem. Similar plots and similar results are obtained if this choice

is not made, but it makes more sense to compare them against the same randomization. Note that this choice is the default in SMPyBandits, but the other possibility is implemented as well, by changing `cache_rewards` to `true` or `false` in the `configuration` dictionary. We refer to the online documentation for explanations on all these details.

We compare the Aggregator algorithm, as well as other aggregation algorithms, Exp4 from [BCB12], CORRAL from [ALNS17] and LearnExp from [AHK17], all with their default parameters. The aggregated algorithms consist in: a naive uniform exploration (to have at least one algorithm with bad performances, *i.e.*, linear regret, that is *not* included in the plots to reduce clutter), UCB with $\alpha = 1/2$, three kl-UCB algorithms (resp. with Bernoulli, Gaussian and exponential kl functions), and Bayes-UCB and Thompson sampling with uniform prior.

Figures 4.1 and 4.4 are in semilog-y scale, this helps to see that the best algorithms can be an *order of magnitude* more efficient than the worst, and the Aggregator performs similarly to the best ones, when the other aggregation algorithms are usually amongst the worst. Figure 4.5 is in semilog-x scale to show that the regret of efficient algorithms are indeed logarithmic.

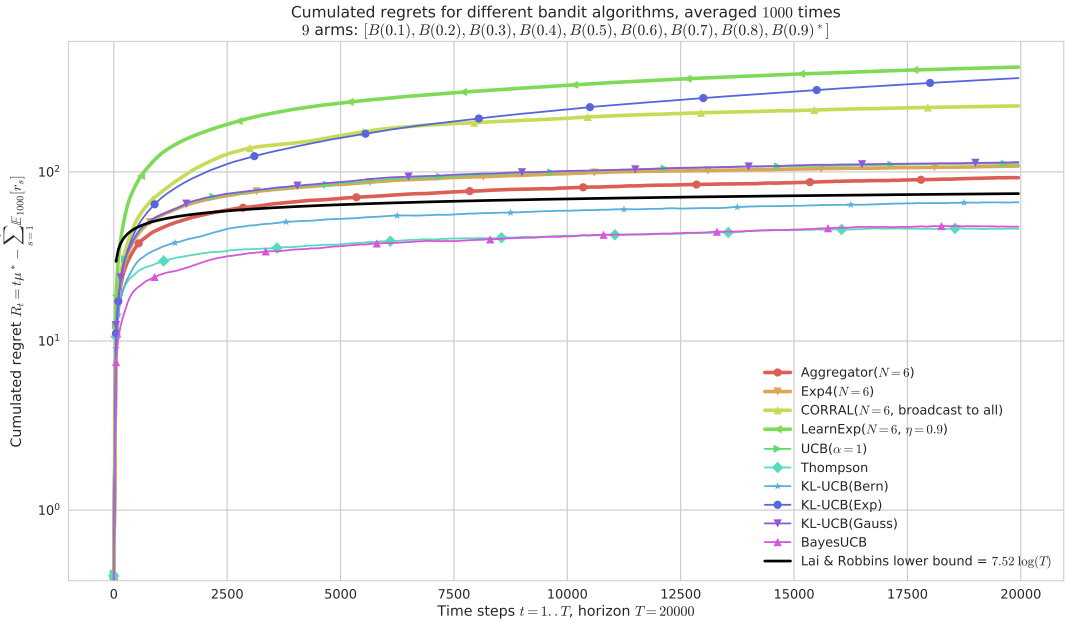

Figure 4.1 – On a "simple" Bernoulli problem (semilog-y scale). Aggregator is in **bold red**.

For Bernoulli problems (Figures 4.1 and 4.2), UCB with $\alpha = 1/2$, Thompson sampling, Bayes-UCB and kl-UCB$^+$ (with the binary kl function) all perform similarly, and Aggregator is found to be as efficient as all of them. For Gaussian and exponential arms, rewards are truncated into $[0, 1]$, and the variance of Gaussian distributions is fixed to $\sigma^2 = 0.05$ for all arms, and can be known to the algorithms (the kl function is adapted to this one-dimensional exponential family). Figure 4.3 uses only Gaussian arms, with a large gap between their

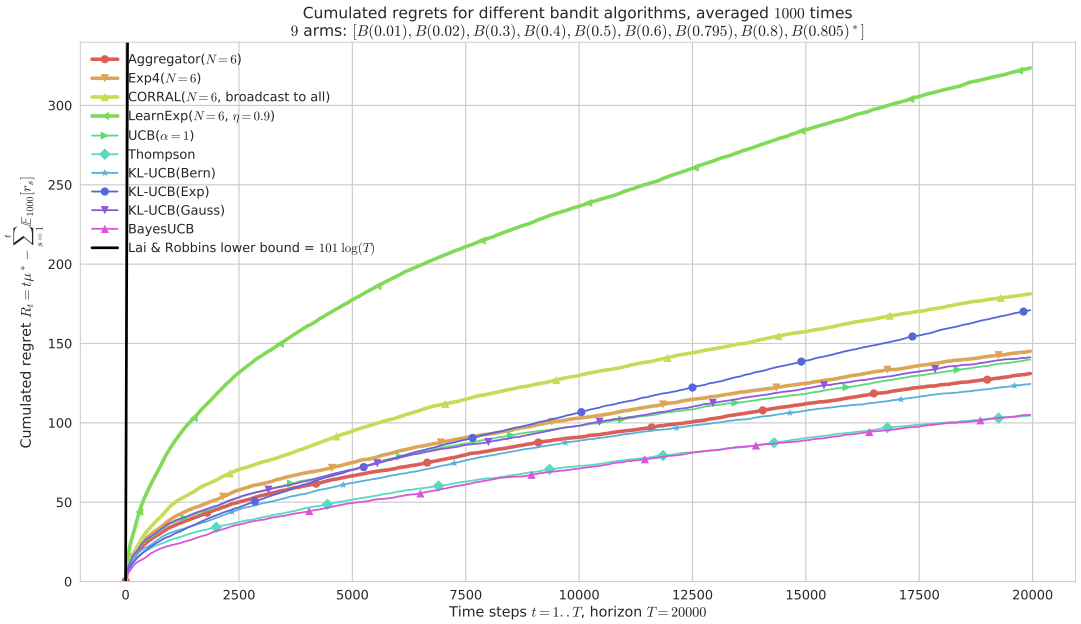

Figure 4.2 – On a "harder" Bernoulli problem, they all have similar performances, except LearnExp, and our proposal Aggregator outperforms its competitors.

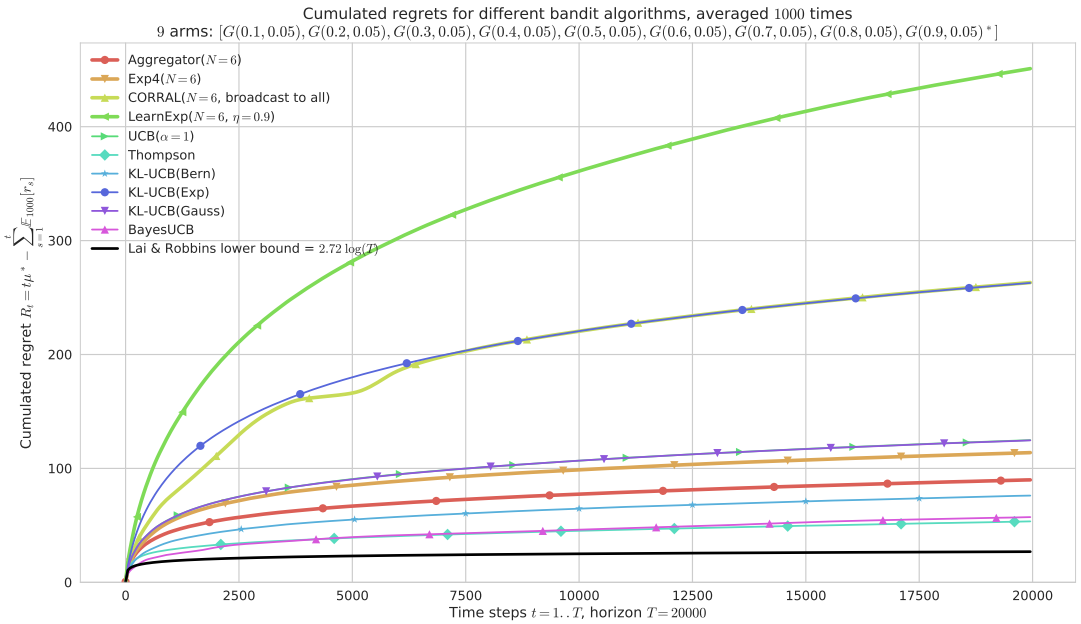

Figure 4.3 – On an "easy" Gaussian problem, only Aggregator shows reasonable performances, thanks to Bayes-UCB and Thompson sampling.

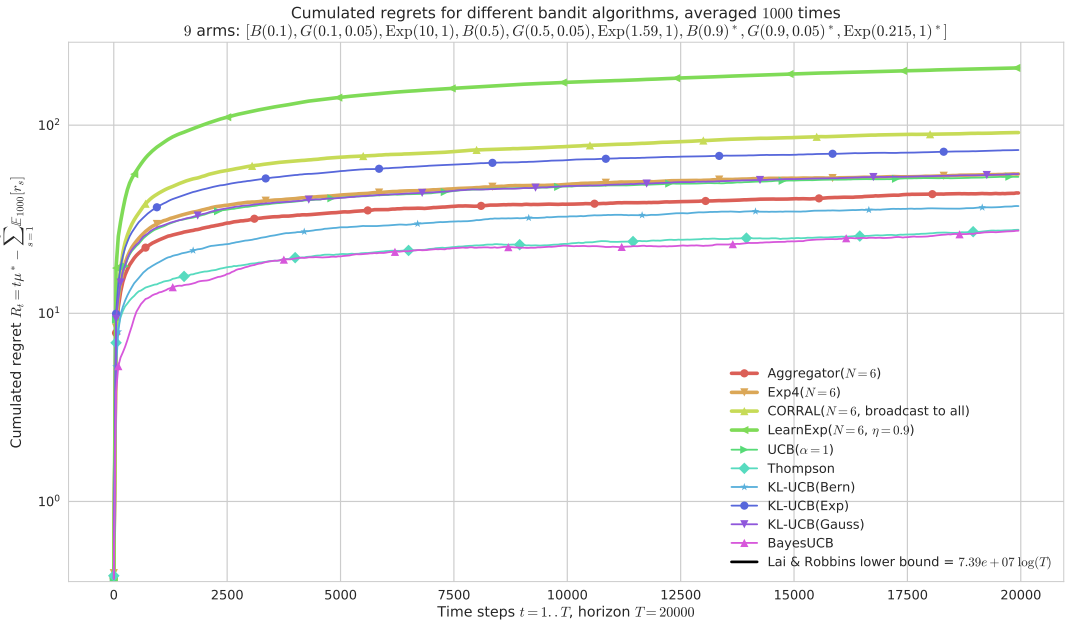

Figure 4.4 – On a harder problem, mixing Bernoulli, Gaussian, Exponential arms, with 3 arms of each type with the *same mean*.

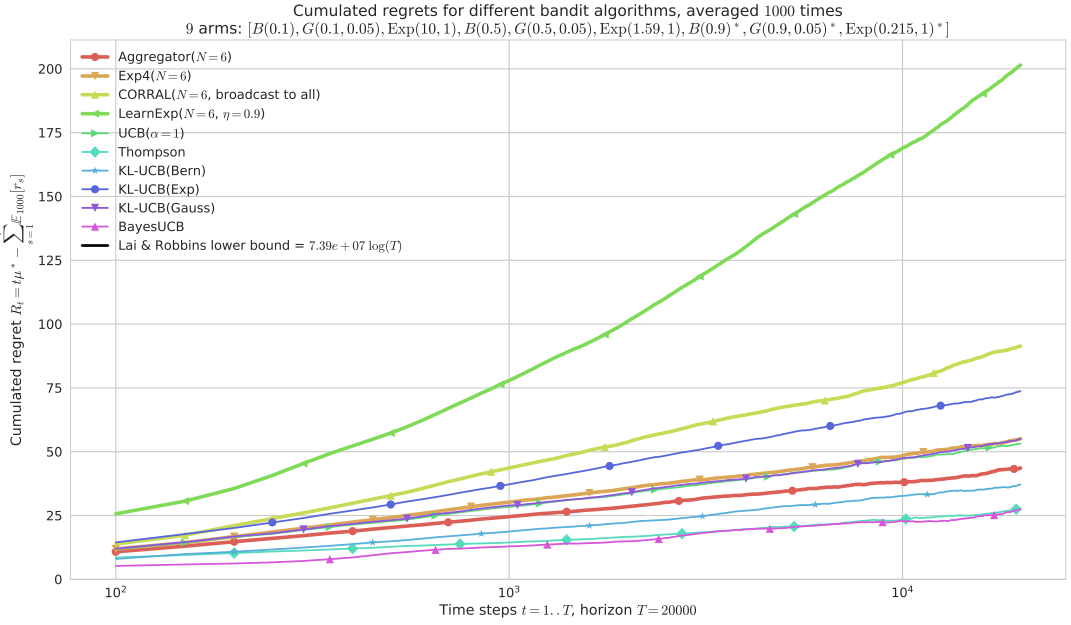

Figure 4.5 – The semilog-x scale clearly shows the logarithmic growth of the regret for the best algorithms and our proposal Aggregator, even in a hard "mixed" problem (*cf.* Figure 4.4).

means and a relatively small variance, giving an "easy" problem. And Figure 4.4 shows a considerably harder "mixed" problem, when the distributions are no longer in the same one-dimensional exponential family and so the Lai & Robbins' lower-bound no longer holds.

For each of the 4 problems considered, the Aggregator algorithm is the best of all the aggregation algorithms, and its regret is close to the best of the aggregated algorithms. Especially in difficult problems with mixed distributions, Aggregator showed to be more efficient that Exp4 and orders of magnitude better than the other reference aggregation algorithms LearnExp and CORRAL (see Figures 4.4 and 4.5).

Reproducibility. The experiments in this section are based on our library SMPyBandits, and the page `SMPyBandits.GitHub.io/Aggregation.html` gives instructions to reproduce them.

4.4 Conclusion – Towards theoretical guarantees

The Aggregator does not have satisfying theoretical guarantees in terms of regret R_T, unlike many bandit algorithms. Another notion, the *adversarial regret*, denoted by $\overline{R_T}$, measures the difference in terms of rewards, between the aggregation algorithm $\mathcal{A}_{\text{aggr}}$ and the best aggregated algorithm $\mathcal{A}_a$. This is in contrast with the (classical) regret, which measure the difference with the best fixed-arm strategy (Definition 2.3). Thus, even if the aggregated algorithms have logarithmic (classical) regret, having an adversarial regret scaling as $\sqrt{T}$ does not permit to obtain a logarithmic (classical) regret for the aggregation algorithm. Under some additional hypotheses, [BCB12, Theorem 4.2] proves that Exp4 has a bounded adversarial regret, $\overline{R_T} \leq 2\sqrt{TN\ln(K)}$, with the good choice of the learning rate sequence $(\eta_t)_{t\geq 1}$.

The proposed algorithm follows quite closely the architecture of Exp4, and a similar bound for Aggregator is expected to hold. This would be a first theoretical guarantee, but not satisfactory as we saw above that simple algorithms (like UCB) have regrets scaling as $\ln(T)$ [ACBF02, BCB12], not $\sqrt{T}$. Regret bounds in several different settings are proven for the CORRAL algorithm [ALNS17], but no logarithmic upper-bound can be obtained from their technique, even in the simplest setting of stochastic bandits. However, Aggregator seems to have a (finite-horizon) logarithmic regret in all the experiments we performed, for both Bernoulli and non-Bernoulli problems (*e.g.*, Gaussian, exponential and Poisson distributions).

Part II

Multi-Armed Bandit Models for Internet of Things Networks

Chapter 5

Improving Spectrum Usage of IoT Networks with Selfish MAB Learning

After detailing in Part I the MAB model, we now come back to our main question of interest. In this chapter, we focus on wireless networks following the hypotheses common to present and future Internet of Things (IoT) networks exposed in Chapter 1. Our goal is to show that the IoT devices can automatically learn to increase their battery life and their successful transmission rates, without changing anything on the IoT standard side. We propose two models of IoT networks, composed of many independent IoT end-devices, that can use low-cost Reinforcement Learning (RL) algorithms in order to learn how to improve their spectrum access. Decentralized RL for IoT lets the devices use acknowledgements sent back by their Base Station as a reward, instead of sensing feedback like for OSA. We consider many independent "dynamic" devices, each communicating with a small probability at every instant. Simulations show that dynamic devices can greatly improve their spectrum efficiency, by using MAB algorithms like UCB. We also developed a proof-of-concept using USRP platforms, for a real-world validation of this approach. In a second step, we consider a second model where a dynamic device has to (try to) retransmit a message, in case of a failed first transmission, up-to a fixed number of retransmissions. We compare heuristics based on UCB, and simulations confirm that the non-naive heuristics also significantly improve the network efficiency.

Contents

5.1 Introduction and motivations for MAB learning for IoT Networks

After the first chapters that presented the model of MAB, we go back to the initial problems studied in this thesis, and thus we focus on Internet of Things (IoT) networks. As explained in the introduction in Chapter 1, unlicensed bands are more and more used and considered for mobile and LAN (Local Area Network) and for Internet of Things communication standards. This heavy use of unlicensed bands, in particular with the expected exponential growth of the number of IoT devices, will cause performance drop, due to radio collisions that could even compromise IoT promises.

Efficient Medium Access Control (MAC) policies allow devices to avoid interfering traffic and can significantly reduce the spectrum contention problem in unlicensed bands. As end-devices battery life is a key constraint of IoT networks, and as IoT networks are decentralized, because the devices initiate transmissions, this leads to IoT protocols using as low signaling overhead as possible and simple ALOHA-based mechanisms. In this chapter, we analyze the performance of Multi-Armed Bandits (MAB) algorithms, that could be used in combination with a time-frequency slotted ALOHA-based protocol. We highlight that even without changing anything on the level of IoT standards, our proposal is just an add-on capability that can be used on a unit-per-unit basis. We consider the UCB[ACBF02], and the Thompson-Sampling (TS) algorithms [Tho33, AG12, KKM12], for the first model. For the demonstration as well as for the second model, without loss of generality, we preferred to focus on heuristics based on the simplest algorithm (*i.e.*, UCB), to give a clear presentation of the different ideas explored to solve the problem of learning in order to retransmit efficiently.

We present in Section 5.2 how the MAB algorithms can be used in a unlicensed but frequency- and time-slotted IoT network. Several devices are using bandit algorithms, and the assumptions made by the stochastic bandit algorithms are not satisfied: as several agents learn simultaneously and their activation processes are random, their behavior is not stationary. As far as we know, we provide the first practical study to confirm robustness of the use of stochastic bandit algorithms for decision making in IoT networks with a large number of intelligent devices in the network, which makes the environment "strongly not stationary". This specific context makes it very hard to give mathematical proofs of convergence and of efficiency of bandit algorithms (that is why we relax the hypothesis and only consider up-to $M \leq K$ players in Chapter 6). We then validate the model with a hardware implementation on real radio signals, detailed in Section 5.3. We conclude this chapter by presenting in Section 5.4 an extension of this model to take into account another aspect of the ALOHA protocol, that is the possibility for dynamic devices to retransmit their packets if the *Ack* was not received.

Publications. This chapter is mainly based on our articles [BBM+17, BBM18, BBM19, BBMVM19, MB19, MBDT19].

5.2 Selfish learning for many dynamic devices with low activation probabilities in an IoT network

As explained before in Chapter 1, the future IoT networks will require to support more and more communicating devices. In this section, we show that intelligent devices in unlicensed bands can use MAB learning algorithms to improve spectral resource exploitation. We evaluate the performance of two classical MAB learning algorithms, UCB and Thomson Sampling, to handle the decentralized decision-making of Spectrum Access, applied to IoT networks. We mean by *decentralized* that learning is performed on the device side, and is spread on the totality of the devices in a network. We also evaluate the learning performance when the number of intelligent end-devices grows.

The aim of this section is to assess the potential gain of learning algorithms in IoT scenarios, even when the number of intelligent devices in the network increases, and the network usage is more and more fluctuating. To do that, we suppose an IoT network made of two types of devices: *static devices* that use only one channel (fixed in time), and *dynamic devices* that can choose the channel for each of their transmissions. Static devices form an interfering traffic, which could be generated by devices using other standards as well. Note that instead of assuming that each static device uses a fixed channel, we could also assume a looser hypothesis: if each static device uses a fixed sub-set of the K channels, and a purely uniform random access in its set of considered channels, then *in average* the observed occupancy of the K channels can be modeled as if it were occupied by (more) static devices using only one channel. So this first hypothesis is actually not constraining. We first evaluate the probability of collision if the dynamic devices randomly select their channels (that is, a naive approach), and if a centralized controller would optimally distribute all of them in the channels at the beginning of the scenario. This second approach is ideal, but not realistic for the most common situation of decentralized co-located IoT networks, and it is just used here as a reference. Then, these three reference scenarios allow to evaluate the performance of bandit algorithms, such as UCB and TS, in a decentralized network, in terms of successful communications rate, as it reflects the network efficiency. We show that these algorithms have near-optimal performance, even when the proportion of end-devices increases and the interfering traffic from other devices becomes less and less stochastic, more and more fluctuating and unpredictable.

5.2.1 System model and notations

We present our system model, which consists of one gateway and many IoT devices, using a frequency- and time- slotted protocol.

One gateway and many devices. We consider the system model presented in Figure 5.1, where a set of devices all sends up-link packets to a (unique) network gateway. Messages

can be sent in a fixed number $K \geq 2$ of wireless channels, that are assumed to be orthogonal, that is, a message in channel k will not cause collision to a message in another channel $j \neq k$. The communication between IoT devices and this gateway is done through a simple pure acknowledged ALOHA-based protocol where devices transmit up-link packets of fixed duration whenever they want. We mean here by ALOHA-based that *devices do not use sensing*, and *we do not consider retransmissions of packets* (we relax this hypothesis in Section 5.4).

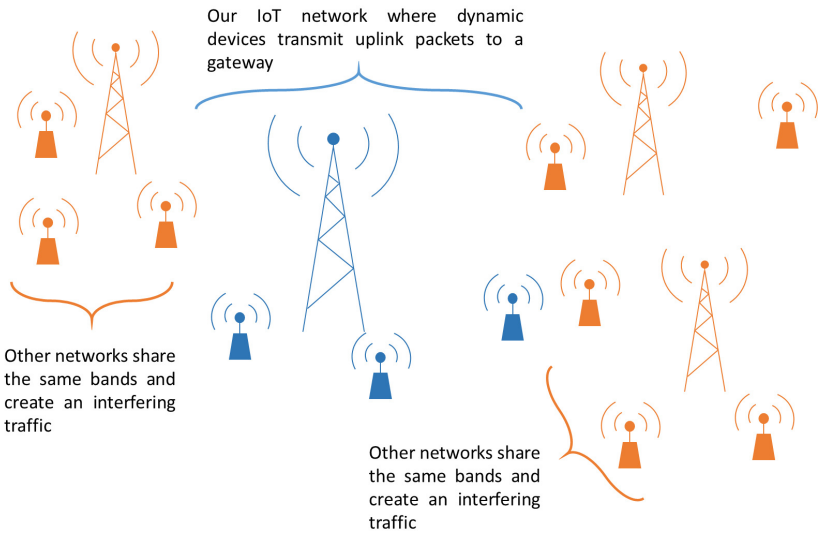

Figure 5.1 – In our system model, some dynamic devices (in the IoT network in blue) transmit packets to a gateway and suffer from the interference generated by neighboring networks (in orange left/right).

The devices can transmit their packets in one of the K channels. In the case where the gateway –of the corresponding IoT network– receives an up-link message in one channel, it transmits an acknowledgement to the end-device in the same channel, after a fixed delay. This is realistic in IoT networks such as networks based on LoRaWAN. In a more general setting, if there were more than one gateway in the same IoT network being considered, the network would reply to the device by letting only one gateway sends back an acknowledgement. The natural choice is for the network to send this acknowledgement by the gateway which received the up-link message. For simplicity but without loss of generality, we consider a network with only one gateway, but still it is important to observe the distinction between the gateway, which is simply a RF node, and the IoT network in charge of receiving, handling, and replying to the incoming up-link messages from the IoT devices being paired in the network.

These communications operate in unlicensed ISM bands and, consequently, they can suffer from interference generated by uncoordinated co-localized and/or neighboring networks (two are shown in orange in Figure 5.1, in left or right). This interfering traffic is uncontrolled, and is most likely unevenly distributed over the K different channels, as each IoT protocol or IoT network can choose to use a different subset of channels. In order to simulate networks designed for the IoT, we consider a protocol **with no sensing** and no repetition of up-link

messages. The gateway is in charge of sending back an acknowledgement, after some fixed-time delay, to any device paired with this gateway in this network (*i.e.*, in blue in Figure 5.1) which succeeded in sending an up-link packet. By considering a small number of orthogonal wireless channels, and a unique PHY layer configuration (*i.e.*, modulation, waveform, etc), and in case of a non-uniform traffic in the different channels, the device can improve their usage of the network if they are able to *learn* on the fly the best channels to use, that is, the most vacant one. Indeed, in this model, the *quality* of the channels (*i.e.*, the resources) are identified by their vacancy, or one minus their occupancy rates.

We note that MAB learning has also started to be applied to also optimize the PHY layer parameters, see for instance [KAF+18] which followed our article [BBM+17], but in this thesis we chose to restrict to the spectrum access problem and thus we only consider MAB models where the arms correspond to orthogonal frequency bands.

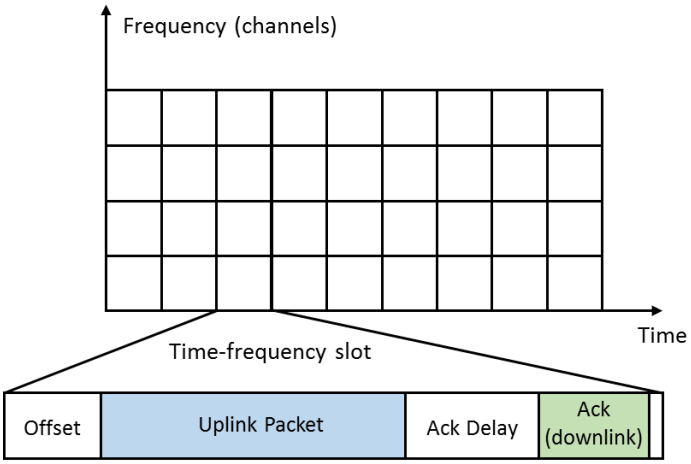

Figure 5.2 – The considered time-frequency ALOHA-based communication protocol [Abr70, Rob75]. Each frame is composed by a fixed duration up-link slot in which the end-devices transmit their (up-link) packets. If a packet is well received, the gateway replies by transmitting an *Ack*, after the ack delay.

Slotted protocol. For simplicity, and as in all this thesis, we only consider a discrete protocol (*i.e.*, slotted). As illustrated in Figure 5.2, we suppose a slotted protocol, in both time and frequency. All devices share a synchronized time, and know in advance K, the finite number of available RF channels. In each time slot, the devices try to send packets to the unique gateway, which listens continuously to all channels, following an ALOHA-based communication protocol [Abr70, Rob75], with no sensing. Each time slot is divided in two parts: first for up-link communications in which data packets are sent by end-devices to the gateway. In one channel, if only one packet is sent in this part of the slot, the gateway can decode it and sends an acknowledgement to the device in the second part (on the same channel). If two or more devices send an up-link packet in the same slot, the up-link packets collide, and the

acknowledgement (*Ack*) is not transmitted. In this case, we say that there is a *collision* in this time slot. In other words, if the gateway cannot successfully decode the incoming (up-link) messages because they were corrupted by collisions, it does not send any *Ack* back. This way, no collision can occur on the down-link messages, easing the analysis of collisions.

Static vs dynamic devices. We make the following assumptions on the network. We assume that there are two types of end-devices in the network:

- *Static* end-devices are identical, and each of them uses only *one* channel to communicate with the gateway, with no loss of generality. Their choice is assumed to be fixed in time (*i.e.*, stationary). The traffic generated by these devices is considered as an interfering traffic for other devices.
- *Dynamic* (or *smart*) end-devices can use all the available channels, by quickly changing their communication channel at any time slot, following a Machine Learning policy. For that end, they use their history of successes or failures of their past communication they experienced in each channel, to learn about channel availability. We also assume that the dynamic end-devices can run simple embedded decision making algorithms, and have limited but reasonable computing as well as storage capacities. Note that of course we assume a limited storage capacity, so no device stores the full history of communications successes and failures, but they only store average rates (which can be stored using two integers for each of the K channels). Our goal is to propose a learning algorithm than can be implemented by each dynamic device, in a decentralized and independent manner, in order to improve their successful communications rate automatically.

We further assume that there are $K \geq 2$ channels, $D \geq 0$ dynamic end-devices, and $S \geq 0$ static devices with $0 \leq S_k \leq S$ static devices in channel $k \in [K]$ (so $S = \sum_{k=1}^{K} S_k$).

Random emission patterns. We suppose that all devices follow the same emission pattern, being fixed in time, and we choose to model it as a simple Bernoulli process: all devices have the same probability to send a packet in any (discrete) temporal slot, and we denote $p \in (0, 1)$ this probability. The parameter p essentially controls the frequency of communication for each device, once the time scale is fixed, and $1/p$ is proportional to the *duty cycle*. For instance, for IoT devices sending messages with a duration of 1 second and possibly at every second, then on a daily basis we have $p = 1/(12 \times 60 \times 60) \simeq 1.5 \times 10^{-5}$. In the experiments below, p is about 10^{-3}, because in a crowded network p should be smaller than $K/(S + D)$ for all devices to communicate successfully (in average).

Some assumptions on the network occupation. We focus on *dense networks*, in which the number of devices $S + D$ is very large compared to K (for instance, about 1000 to 100000, while K is about 4 to 256). As this problem is only interesting if devices are able to communicate reasonably efficiently with the gateway, we assume that devices only communicate occasionally,

i.e., with a low *duty cycle*, as it is always considered for IoT. Note that even unlicensed bands have such limitations, as for instance this is a strict requirement for any device using the 868 MHz ISM band in Europe (and its regulation also enforces a maximum transmission power, but we do not consider power transmission in this work). We prefer this choice rather than non-crowded networks, *i.e.*, where $S + D \leq K$, as the former makes more sense for realistic IoT networks.

On the opposite, imagine if there were only $K = 4$ channels being occupied by $D+S = 100$ devices, each communicating with a high rate of $p = 1/10$, with a non-zero occupancy in each channel (*i.e.*, $\forall k, S_k > 0$). Then, almost all time slots will lead to collisions in all channels, for a uniformly random access scheme, and thus the network efficiency (*i.e.*, successful communications rate) will be so close to zero that using learning algorithms cannot improve much. Such scenario is not our target of interest, and thus we prefer to only consider feasible scenarios where p is smaller than $K/(S + D)$, in order to *have an average of active devices not larger*[1] *than the number of channels*.

Link with the MAB model. All devices follow a Bernoulli emission process. Consider the network from the point of view of one dynamic device: every time a dynamic device has to communicate with the gateway, it has to choose one channel (at each transmission $t \geq 1, t \in \mathbb{N}$), denoted as $A(t) = k \in [K]$. Then, the dynamic device waits in this channel $A(t)$ for an acknowledgement sent by the gateway, during a certain period (*e.g.*, 5 seconds for the example considered above). Before sending another message (*i.e.*, at time $t + 1$), the dynamic device knows if it received or not this *Ack* message. For this reason, selecting channel (or arm) k at time t yields a (random) feedback, called a (binary) *reward*, $r(t) \doteq Y_{k,t} \in \{0, 1\}$, being 0 if no *Ack* was received before the next message, or 1 if *Ack* was successfully received. The goal of the dynamic device is to minimize its packet loss ratio, or equivalently, to maximize its number of successful transmissions, or its cumulative reward, $\sum_{t=1}^{T} r(t)$, which is the usual objective in MAB problems (see Section 2.1).

This problem is a special case of the stochastic MAB with Bernoulli distributions. Contrarily to many previous works done in the CR field and for Opportunistic Spectrum Access [JEMP10, JMP12], the reward $r(t)$ does *not* come from a sensing phase before sending the t-th message, as it would do for any "listen-before-talk" model. In our model, rewards rather come from receiving or not an acknowledgement from the gateway, between the t-th and $t+1$-th messages. A reward of one indicates that the acknowledgement was received on time, and a reward of zero indicates the opposite.

The problem parameters are $S_1, \ldots, S_K$ which represent the (stationary) occupancy of the channels by the static devices, and they are unknown to each dynamic device, so to maximize their cumulated rewards, they must learn the distributions of the channels, in order to be able to progressively improve their respective successful communications rate. The goal is

[1] In Chapter 6 we simply consider the case of $p = 1$ and $M = D \leq K$ dynamic devices, referred to as *players*.

thus to propose a simple sequential algorithm to be applied identically and independently by each dynamic device, in a fully distributed setting (each device runs its own algorithm, from its observations), in order to minimize collisions and maximize the fraction of successful transmissions of all the dynamic devices. This requires to tackle the so-called *exploration-exploitation dilemma*: a device has to try all channels a sufficient number of times to get a robust estimate of their qualities, while not selecting the worst channels too many times. Before presenting the MAB algorithms used in the experiments, we present some simple baseline (reference) policies.

5.2.2 Three reference policies

We present three different policies that can be used to assess the efficiency of the learning algorithms presented later on. The first one is naive but can be used in practice, while the two others are very efficient but require full knowledge on the system (*i.e.*, an oracle) and are thus unpractical. They are however useful for our numerical simulations, and are used as references, to show that our MAB-based approaches quickly learn to perform almost optimally. Their short names are used in the legend on Figures 5.3, 5.5), and are given in "quotes" in the corresponding paragraphs.

1st - Naive policy: Random Channel Selection ("Random")

We derive here the probability of having a successful transmission, for a dynamic device, in the case where all the dynamic devices make a purely random channel selection (*i.e.*, uniform on $i \in [K]$). This reflects a naive policy that could be implemented by all the dynamic devices, and it provides a reference scenario to compare against. Note that even nowadays this is still the solution implemented for real IoT devices deployed in new LoRaWAN networks.

In this case, for one dynamic device, a successful transmission happens if it is the only device to choose channel k, at that time slot. the S_k static devices in each channel k are assumed to be independent, and static and dynamic devices are assumed to *not* transmit at each time t with a fixed probability $1-p$, so probability of successful transmission is computed as follows.

$$\mathbb{P}(\text{success}|\text{sent}) = \sum_{k=1}^{K} \underbrace{\mathbb{P}(\text{success}|\text{sent in channel } k)}_{\text{No one else sent in channel } k} \underbrace{\mathbb{P}(\text{sent in channel } k)}_{=1/K, \text{ by uniform choice}} \tag{5.1}$$

All dynamic devices follow the same policy in this case, so the probability of transmitting at that time in channel k for any dynamic device is p/K, and there are $D-1$ other dynamic devices. As they are independent, the probability that no other dynamic device sent in k is $q = \mathbb{P}(\bigcap_{j=1}^{D-1} \text{device } j \text{ did not send in } k) = \prod_{j=1}^{D-1} \mathbb{P}(\text{device } j \text{ did not send in } k)$. And $\mathbb{P}(\text{device } j \text{ sent in } k) = p \times 1/K$, by uniform choice on channels and the Bernoulli emission

hypothesis. So $q = \prod_{j=1}^{D-1}(1-p/K) = (1-p/K)^{D-1}$. Thus we can conclude,

$$\begin{aligned}\mathbb{P}(\text{success}|\text{sent}) &= \sum_{k=1}^{K} \underbrace{(1-p/K)^{D-1}}_{\text{No other dynamic device}} \times \underbrace{(1-p)^{S_k}}_{\text{No static device}} \times \frac{1}{K} \\ &= \frac{1}{K}\left(1-\frac{p}{K}\right)^{D-1} \sum_{k=1}^{K}(1-p)^{S_k}. \end{aligned} \tag{5.2}$$

This probability (5.2) is constant wrt time, and easy to compute numerically. Comparing the successful transmission rate of any policy against this naive policy is important, as any efficient learning algorithm should outperform it, maybe after a long enough initial learning period.

2nd - (Unachievable) Optimal oracle policy ("Optimal")

We investigate here the optimal policy that can be achieved if the dynamic devices have a perfect knowledge of the distribution of static devices $(S_k)_k$, and a fully centralized decision making[2] is possible. We want to find the stationary distribution of devices into channels that maximizes the probability of having a successful transmission.

If the oracle chooses a fixed configuration of dynamic devices, it means that for each dynamic device the oracle affects it to a unique channel for all time steps. Then there is a number D_k of devices affected to channel k being fixed in time (*i.e.*, stationary), and thus this probability is computed as before:

$$\begin{aligned}\mathbb{P}(\text{success}|\text{sent}) &= \sum_{k=1}^{K} \mathbb{P}(\text{success}|\text{sent in channel } k)\ \mathbb{P}(\text{sent in channel } k) \\ &= \sum_{k=1}^{K} \underbrace{(1-p)^{D_k-1}}_{D_k-1 \text{ others}} \times \underbrace{(1-p)^{S_k}}_{\text{No static device}} \times \underbrace{D_k/D}_{\text{Sent in channel } k}. \end{aligned} \tag{5.3}$$

Consequently, an optimal allocation vector $(D_1, \ldots, D_K) \in \mathbb{R}^K$ is a solution of the following real-valued constraint optimization problem:

$$\arg\max_{D_1,\ldots,D_K} \sum_{k=1}^{K} D_k(1-p)^{S_k+D_k-1}, \tag{5.4a}$$

$$\text{such that} \sum_{k=1}^{K} D_k = D, \tag{5.4b}$$

$$D_k \geq 0 \qquad \forall k \in [K]. \tag{5.4c}$$

[2] This optimal policy needs an *oracle* seeing the entire system, and affecting all the dynamic devices, once and for all, for a fixed stationary scenario, in order to avoid any signaling overhead. This is not possible in IoT contexts as several completely independent networks may operate in a single place.

Proposition 5.1. *The* Lagrange multipliers *method* [BV04] *can be used to solve the constraint real-valued maximization problem introduced in equation* (5.4)*. It gives a closed form expression for the* (*unique*) *optimal solution* $D_k^*(\lambda)$*, depending on the system parameters, and the unknown Lagrange multiplier* $\lambda \in \mathbb{R}$*.*

$$D_k^*(\lambda) = \left(\frac{1}{\ln(1-p)} \left[\mathcal{W}\left(\frac{\lambda \mathrm{e}}{(1-p)^{S_k - 1}} \right) - 1 \right] \right)^+ . \tag{5.5}$$

Proof.

- In a realistic scenario, we can assume that $D_k \leq \frac{-2}{\ln(1-p)} \approx \frac{2}{p}, \quad \forall k \in [K]$. For such values for D_k, the objective function $f : (D_1, \ldots, D_K) \mapsto \sum_{k=1}^K D_k (1-p)^{S_k + D_k - 1}$ is concave as the sum of concave functions[3].
- The Lagrange multipliers method can be applied to the optimization problem (5.4a), with a concave objective function f, linear equality constraints (5.4b) and linear inequality constraints (5.4c). The strong duality condition is satisfied in this case [BV04], so finding the saddle points will be enough to find the maximizers.

More details are given in Section 5.6.1 in the Appendix of this Chapter. □

Where in the equation (5.5), $(a)^+ \doteq \max(a, 0)$, and $\mathcal{W}$ denotes the $\mathcal{W}$-Lambert function which is the reciprocal bijection of $x \mapsto xe^x$ on $\mathbb{R}^+ = [0, +\infty)$ (which can be computed numerically in an efficient manner, [CGH+96]). Moreover, condition (5.4b) implies that the Lagrange multiplier λ is the solution of the constraint $\sum_{k=1}^K D_k^*(\lambda) = D$. This single constraint can be solved numerically, with simple one-dimensional root finding algorithms.

Note that solving the optimization problem provides the optimal *real values* $(D_k^*)_k$, which have to be rounded to find the optimal *integer* number of devices for channel k. Any rounding choice will give about the same distribution, up-to a difference of only one device by channel, and so we chose to round from below for the first channels: $\widehat{D_k} = \lfloor D_k^* \rfloor$ for $1 \leq k < K$, and $\widehat{D_K} = D - \sum_{k=1}^{K-1} \widehat{D_k}$.

3rd - A greedy approach of the oracle strategy ("Good sub-optimal")

We propose a *sequential* approximation of the optimal policy: the third solution is a sub-optimal naive policy, simple to set up, but also unpractical as it also needs an oracle. End-devices are iteratively inserted in the channels with the lowest load (*i.e.*, the index k minimizing $S_k + D_k(\tau)$ at global time step τ). Once the number of devices in each channel is computed, the probability of sending successfully a message is also given by equation (5.3). This is the

[3] It is worth noting that f is neither concave nor quasi-concave on $[0, \infty)^K$ [Lue68, Yaa77].

policy that would be used by dynamic devices if they were inserted one after the other, and if they had a perfect knowledge of the channel loads.

5.2.3 Sequential policies based on bandit algorithms

While the stochastic MAB model has been used to describe some aspects of Cognitive Radio systems, it is in principle not suitable for our IoT model, due to the non-stationarity of the channels occupancy, caused partly by the learning policy used by dynamic devices, but mainly by their random activation processes. In our model, every dynamic device implements its own learning algorithm, *independently*. For one device, the time t refers to the number of times it accessed the network (following its Bernoulli transmission process, *i.e.*, its duty cycle), *not* the total number of time slots from the beginning, as rewards are only obtained after a transmission, and IoT devices only transmit sporadically, due to low transmission duty cycles.

Using a bandit algorithm for IoT devices. The IoT application is challenging in that there are *multiple* players (the dynamic devices) interacting with the *same* arms (the channels), without any centralized communication (they do not even know the total number of dynamic devices). We propose algorithms in which each dynamic device ignores all the other one and implements a learning algorithm to play a bandit game. In each time slot, if it has to communicate (which happens with probability p), then it chooses a channel and it receives a reward 1 if the transmission is successful, 0 otherwise. Each device aims at maximizing the sum of the rewards collected during its communication instants, which shall indeed maximize the fraction of successful transmissions. Besides the modified time scale (rewards are no longer collected at every time step), this looks like a usual bandit problem. However, it cannot be modeled as a stochastic MAB, as the rewards are (unfortunately) *not i.i.d.*: they not only depend on the (stationary, *i.i.d.*) behavior of the static devices, but also on the behavior of other dynamic devices, that is not stationary (because of learning and random activation of each device). Despite this, we show in the next subsection that running a stochastic bandit algorithm for each device based on its own rewards is surprisingly successful.

Considered algorithms. The two algorithms we consider are UCB ("UCB" in the figures) and Thompson sampling (TS) ("Thompson-sampling"), and they are presented in Section 2.4. The UCB algorithm uses $\alpha = 1/2$ in our experiments. The TS algorithm is known to be empirically efficient, and for these reasons it has been used successfully in various applications, including problems from Cognitive Radio [TCLM16, MTC+16], and also in previous work on decentralized IoT-like networks [DMP16].

***Adversarial* bandit algorithms?** Instead of using MAB algorithms assuming a stochastic hypothesis on the system, we could try to use MAB algorithms designed to tackle a more general problem, that makes no hypothesis on the interfering traffic. The *adversarial MAB* algorithms is a broader family, of which a well-known and efficient example is the $\mathrm{Exp3}$ algorithm [ACBF02, BCB12]. Empirically, the $\mathrm{Exp3}$ algorithm turned out to perform significantly worse than both UCB and TS in the same experiments, therefore we did not report results here.

5.2.4 Numerical results

We suppose a network with $S + D = 2000$ end-devices, and one IoT gateway. Each device sends packets following a Bernoulli process, of probability $p = 10^{-3}$ (*e.g.*, this is realistic: one packet sent about every 20 minutes, for time slots of $1\mathrm{s}$). The RF band is divided in $K = 10$ channels. Each static device only uses one channel, and their uneven distribution in the 10 channels is chosen as $(S_1, \cdots, S_K) = S \times (0.3,\ 0.2,\ 0.1,\ 0.1,\ 0.05,\ 0.05,\ 0.02,\ 0.08,\ 0.01,\ 0.09)$, to keep the same proportions when S decreases. The dynamic devices have access to all the channels, and use learning algorithms. We simulate the network during 10^6 discrete time slots, during which each device transmits on average 1000 packets (*i.e.*, the learning time is about 1000 steps, for each algorithm). We tried similar experiments with other values for K and this distribution vector, and results were similar for non-homogeneous repartitions.

Clearly, the problem is less interesting for a homogeneous distribution, as all channels are equivalent for dynamic devices, and so even with D small in comparison to S, the system behaves like in Figure 5.3d, where the performance of the five approaches are very close.

First results. Figure 5.3 presents the successful transmission rate as a function of time. The two MAB algorithms, UCB and Thompson Sampling (TS), are compared against the naive random policy (which is outperformed easily by the MAB algorithms), and the two (optimal and greedy) oracle policies (which outperform slightly the MAB algorithms). The results are displayed when 10%, 30%, 50% and 100% of the traffic is generated by dynamic devices.

We can see in Figure 5.3 that the TS algorithm (in red $+$) outperforms the UCB algorithm (in blue $*$), when the number of end-devices is below 50%. When the number of end-devices is higher, both algorithms have almost the same performance, and perform well after a small number of transmissions (*i.e.*, they show quick convergence). Moreover, we can see in Figures 5.3a, 5.3b, and 5.3c that both have better success rate than the random policy and the probability of successful transmission is between the optimal oracle and sub-optimal oracle policies. For instance, for 10% of dynamic devices, after about 1000 transmissions, using UCB over the naive uniform policy improved the successful transmission rate from 83% to 88%, and using Thompson Sampling improved it to 89%. Increasing the number of end-devices decreases the gap between the optimal and random policies: as expected intuitively, the more

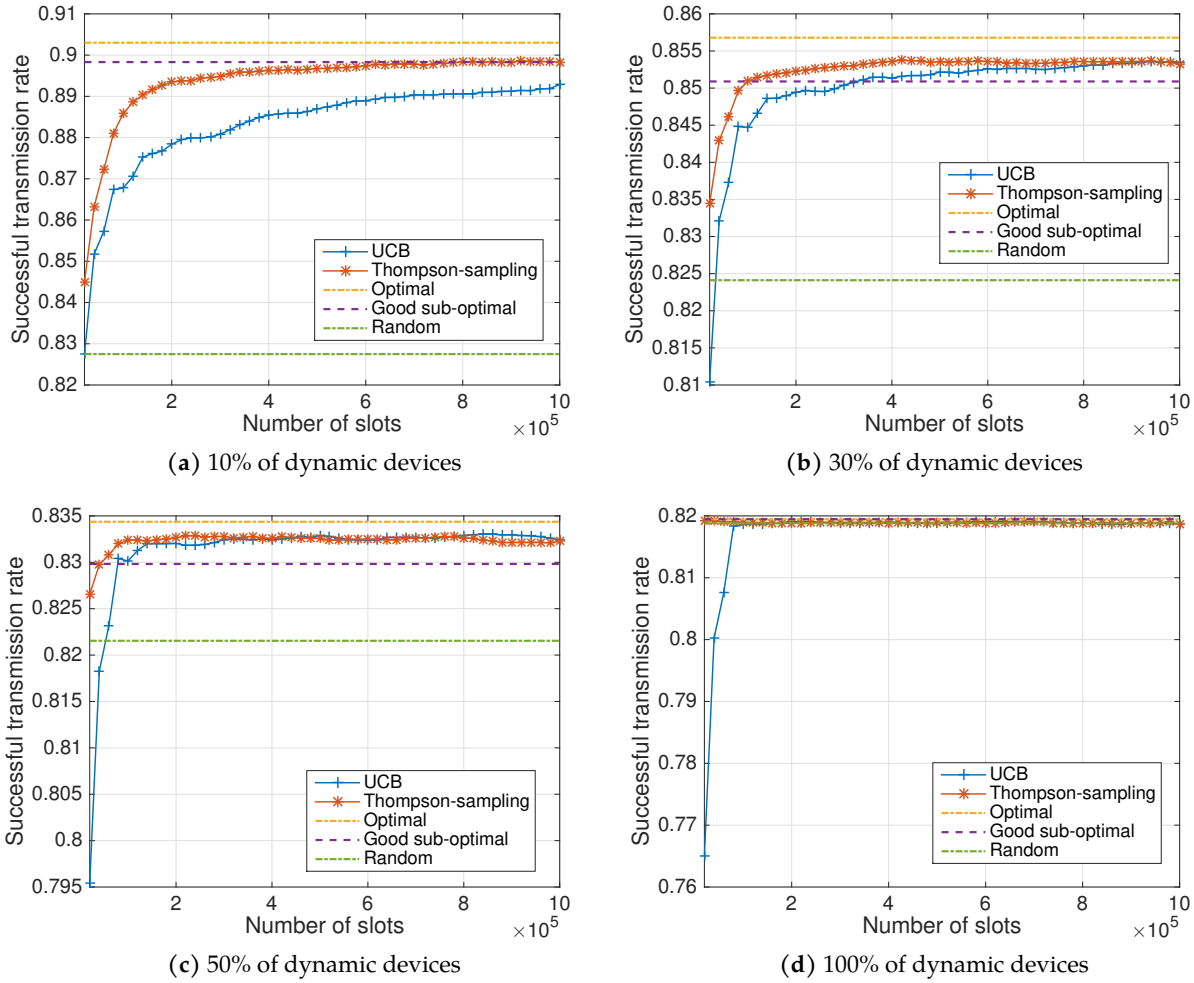

(**a**) 10% of dynamic devices

(**b**) 30% of dynamic devices

(**c**) 50% of dynamic devices

(**d**) 100% of dynamic devices

Figure 5.3 – Performance of two MAB algorithms, UCB in blue and Thompson Sampling in red, compared to extreme reference policies without learning or oracle knowledge, when the proportion of dynamic end-devices in the network increases, from 10% to 100%.

dynamic devices, the less useful are learning algorithms, and basically for networks with only dynamic devices, the random policy is as efficient as the optimal one, as seen in Figures 5.3d and on the right end side of Figure 5.4.

Successful transmission rate as a function of the number of dynamic devices. To better assess the evolution of the optimal policy compared to the random one, we have displayed on Figure 5.4 the evolution of the gain, in terms of successful transmission rate, provided by the optimal oracle and the two learning policies, after 10^6 time slots, *i.e.*, about 1000 transmissions for each IoT device. We can see that when the proportion of end-devices is low (*e.g.*, 1% of devices are dynamic), the optimal policy provides an improvement of 16% compared to random channel selection. The TS algorithm always provides near-optimal performance, but

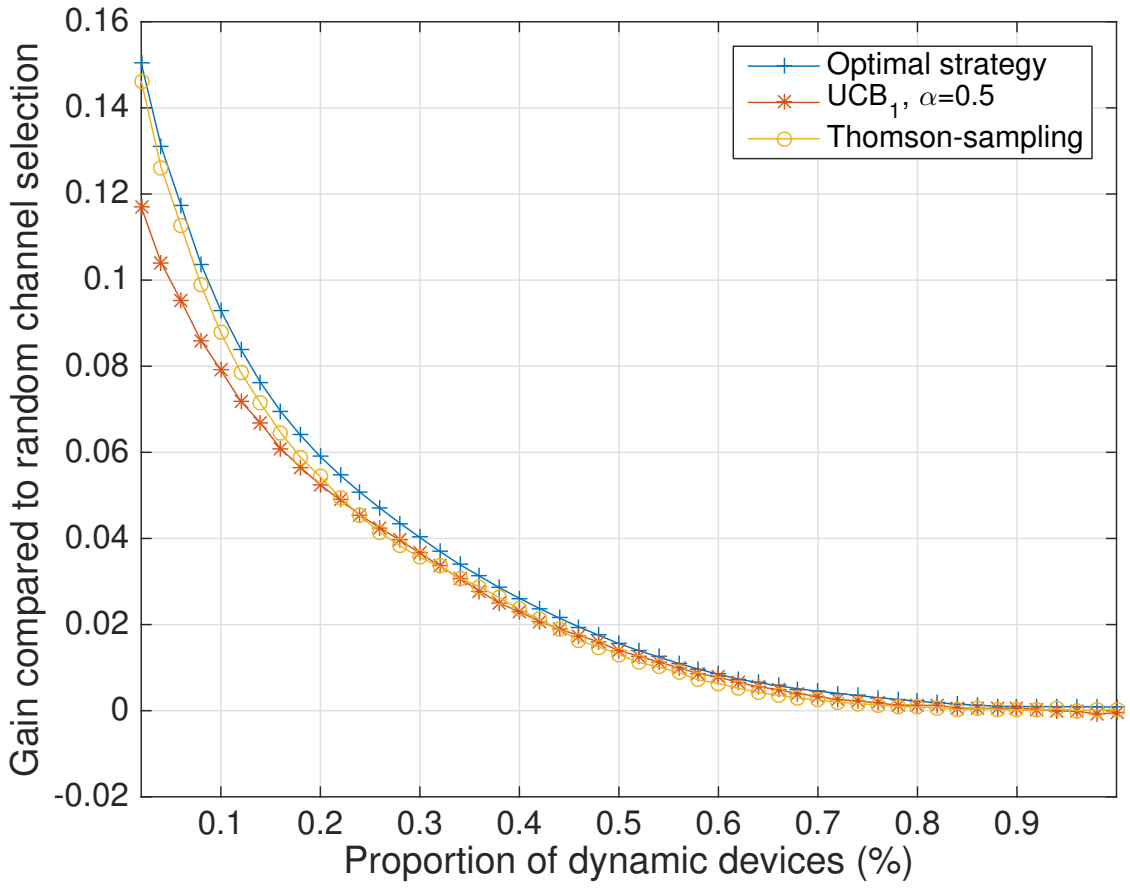

Figure 5.4 – Learning with UCB and Thomson Sampling, with many dynamic devices. The learning gain, for each device, decreases with the proportion of dynamic devices in the network. Note that the values (16% etc) depend on the distribution of static devices into the K channels (*i.e.*, $S_1, \dots, S_K$) but the general profile of this plot does *not* depend much on these parameters.

the UCB algorithm has a slower rate of convergence and performs consequently worse after 1000 transmissions, for instance it only provides a gain of 12% for the same proportion of dynamic devices (1%), for the considered values of $S_1, \dots, S_K$.

Figure 5.4 also shows that learning keeps near-optimal performance even when the proportion of devices becomes large. Note that when this proportion increases, the assumptions of a stochastic MAB model are clearly violated, and there is no mathematical justification for the efficiency of TS and UCB algorithms. Hence, it is surprising to have near optimal performance with stochastic MAB algorithms applied to partly or fully dynamic scenarios.

A safety check. We include another simulation in Figure 5.5, with a uniform distribution of static devices (*i.e.*, $\forall k, S_k = S/K$), to check that learning approach (here, only UCB) also gives interesting gain of performance, and achieve a close-to optimal successful transmission rate.

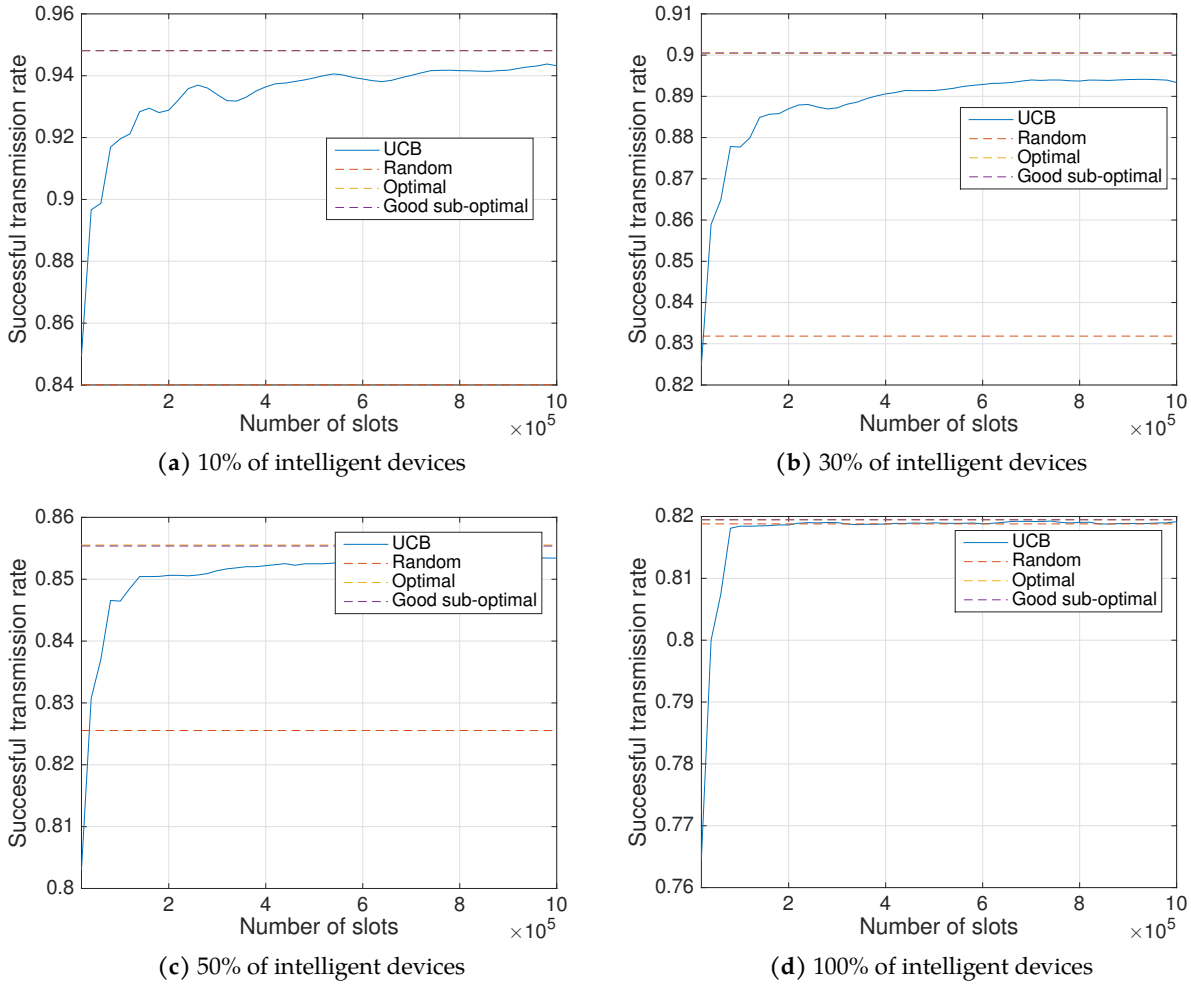

(**a**) 10% of intelligent devices

(**b**) 30% of intelligent devices

(**c**) 50% of intelligent devices

(**d**) 100% of intelligent devices

Figure 5.5 – Performance of the UCB bandit algorithm for the special case of uniform distribution of the static devices, when the proportion of intelligent devices in the network increases, from 10% to 100%.

Except for the limit case of 100% of dynamic devices, which corresponds to Figures 5.3d and 5.5d, where the uniform access performs as well as the optimal oracle solution, the MAB-based approach almost instantly outperforms the baseline.

Reproducibility. The simulation code used for the experiments in Section 5.2.4 is for MATLAB or GNU Octave, and it was written in collaboration with Rémi Bonnefoi, in May 2017. Instructions to reproduce our experiments are given, and the code is open-sourced under the MIT License, at `Bitbucket.org/scee_ietr/rl_slotted_iot_networks`.

5.3 Proof-of-concept of our model for real-world validation

In this section, we present a demonstration showcased at the International Conference on Telecommunication (ICT) in June 2018 [BBM18, BBM19], implementing a proof-of-concept (PoC) of the model introduced in Section 5.2. As far as we know, this is the first demonstration of running learning algorithms on the end-device side for Internet of Things networks, in real radio conditions, as highlighted it in our paper [MB19].

This PoC implements an IoT network the following way: one base station, one or several intelligent (*i.e.*, learning) devices, embedding the proposed solution, and a traffic generator that emulates radio interference from many other devices. Intelligent devices communicate with the base station with a wireless ALOHA-based protocol with acknowledgements, which does not require any specific overhead for the learning. Similarly to the previous section, network access is modelled as a discrete sequential decision making problem, and using the framework and algorithms from MAB learning, we show that intelligent devices can improve their access rate to the network, by using low complexity and decentralized algorithms, such as UCB and Thompson Sampling. This solution could be added in a straightforward and costless manner in most IoT networks, such as LoRaWAN networks, just by adding this feature at the higher level of the MAC layer, in all or only some of the devices, without any modification on the network side, and no signalling overhead for the devices.

Related works. This work is new for the IoT context, but previous works have similarly implemented proof-of-concepts to show that Reinforcement Learning (RL) algorithms can be used within real-world wireless communications. Starting from 2010, the works of W. Jouini and C. Moy [JEMP09, JEMP10, JMP12] were among the first ones to propose to use RL for Cognitive Radio, especially MAB and the UCB algorithm, and proof-of-concepts were developed with C. Robert from 2013 [RMZ14, Moy14]. Between 2015 and 2017, C. Moy, N. Modi and S. Darak (of our team SCEE) continued to work on this direction [DNMP16, DMP16, DMNM16, KDY+16]. Since 2017, S. Darak and his team at IIIT Delhi (India) have been quite active in the research on CR using MAB, and some of their recent works are illustrated with real-world demo using USRP and the MATLAB/Simulink system [KYDH18, SKHD18, JKYD18].

5.3.1 Context of this demonstration

We describe the way we implemented a demo where we evaluate MAB algorithms, used in combination with a pure ALOHA-based protocol, such as the ones employed in LPWAN. This demonstration is the first implementation which aims at assessing the potential gain of MAB learning algorithms in IoT scenarios. We use a test-bed designed in 2017 by the SCEE team at the Rennes campus of CentraleSupélec [Bod17, Appendix 3], containing different USRP

boards [Ett], controlled by a single laptop running the GNU Radio software [GNUb], and where the intelligence of each device corresponds to a learning algorithm, implemented as a GNU Radio block [GNUa] and written in Python or C++.

In our demo, we consider a simple wireless network, that reproduces the model of Section 5.2, consisting of one base station (*i.e.*, radio access point), and a certain interfering background traffic, assumed to be stationary (*i.i.d.*), which is generated by end-devices communicating in other networks. Some dynamic intelligent devices (end-user or autonomous devices) try to communicate with the base station, with a low-overhead protocol. This communication can be done in different channels which are also shared by devices using other networks. Once the base station receives a packet transmitted by a dynamic device in one channel (*i.e.*, if no collision occurred), it transmits back to it an acknowledgement in the same channel, after a fixed-time delay, as it is done in the LoRaWAN standard. This *Ack* allows the device to learn about the channel quality (*i.e.*, mean availability) and thus, to use learning algorithms for the purpose of best channel selection.

We can generate scenarios with different parameters (number of channels, interfering traffic load on each channel, etc) in order to evaluate the performance of learning in various settings. Moreover, we compare the performance of learning strategies with that of the random uniform access to channels, which is the current state-of-the-art of commercial LPWAN solutions [RKS17]. This allows to check that in case of uniform traffic, when there is nothing to learn, the intelligent devices at least do not reduce their successful communications rate in comparison to the naive devices. This also shows that in case of non-uniform stationary traffic, MAB learning algorithms indeed help to increase the global efficiency of the network by improving the success rate of the intelligent devices. The benefits are twice and of primary importance for IoT networks: the proposed approach can mitigate RF collisions, and enhance intelligent device battery lifetime if they do retransmissions.

5.3.2 Physical model and user interface of our GNU Radio implementation

In this section, we present the implementation of MAB algorithms in the model of IoT networks presented in Section 5.2.1. We first describe the simplified physical layer of this demo, then we present our GNU Radio implementation.

Physical layer and protocol. We implement a simple PHY/MAC layers solution, in order to demonstrate the possibility of improvement of the performance of IoT communications in unlicensed bands. We could have used any physical layer and any ALOHA-based protocol. We choose to implement our own physical layer and protocol, for both clarity and conciseness, and because developing a complete IoT network protocol stack is no more my research work and would have fall outside of the scope of this thesis.

Regarding the physical layer, we consider a QPSK constellation (*Quadrature Phase-Shift Keying*, *e.g.*, see references in [Bod17]). Moreover, we use simplified packets composed of two parts. The first part is the *preamble* which is used for the purpose of synchronization (phase correction). Then, we have the *index* of the user, which is a sequence of QPSK symbols. For example, this index can be a simple QPSK symbol ($\pm 1 \pm 1j$), or a sequence of QPSK symols if the PoC has to consider more users. With ℓ QPSK symbols, we can indeed fit at most $4^\ell/2 = 2^{2\ell-1}$ devices, and not 4^ℓ due to the use of a conjugate index to send back acknowledgements from the base station. Once the base station receives an up-link packet, it detects this index and transmits an acknowledgement which has the same frame structure, but where the index is the conjugate of the index of the up-link packet ($z \mapsto \overline{z}$, *e.g.*, $1 + j \mapsto 1 - j$). Thanks to this index, we can have several devices communicating with the same base station. In turn, the end-device that receives the acknowledgement demodulates it, and checks if the index is the conjugate of its own index. In this case, the *Ack* was sent for him, and it knows that its packet has been received and decoded correctly by the base station.

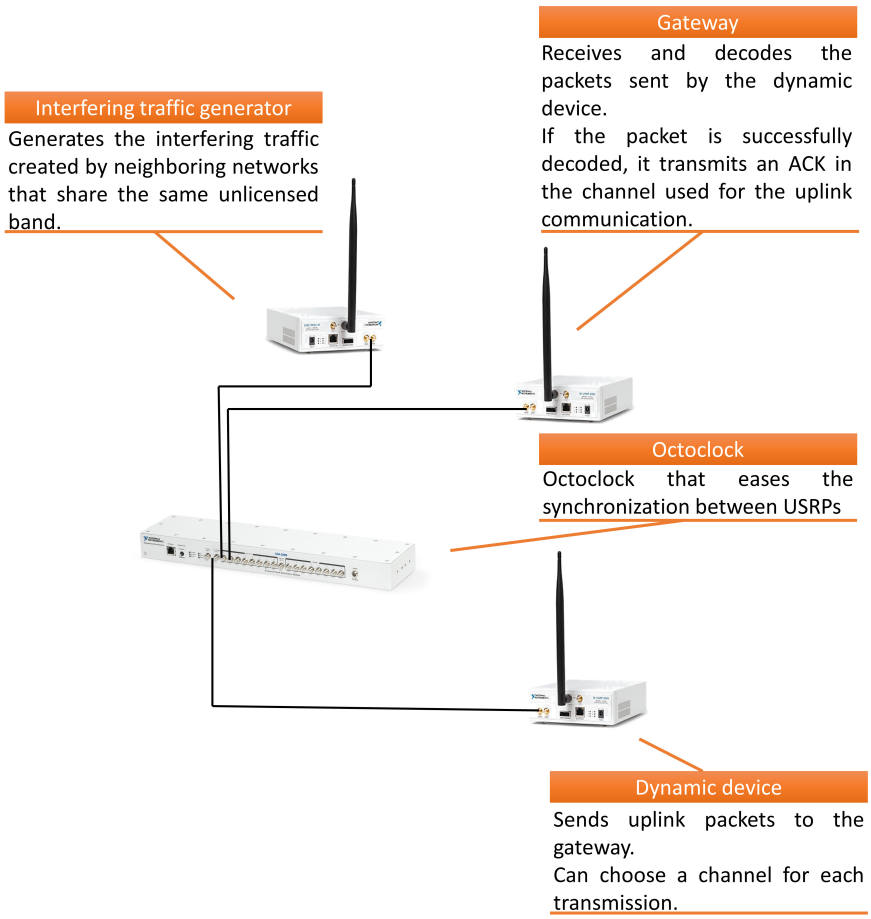

Figure 5.6 – Schematic of our implementation that presents the role of each USRP platform.

Figure 5.7 – Two pictures showing the SCEE test-bed [Bod17, Appendix 3], taken in 2018.

Equipment. We use USRP N210 boards [Ett], from Ettus Research (National Instrument), with version 4 of their FPGA system and version 5.1 of the RBX system. As illustrated in Figure 5.6, the implementation is composed of at least 3 USRP: the base station, a traffic generator which emulates the interfering traffic (made by surrounding static devices), and at least one dynamic device. Each dynamic device has its own USRP and its own learning algorithm.

The boards have their own power supply, and are all connected to a local Ethernet switch, itself connected to a single laptop, running GNU/Linux and Ubuntu. The pictures in Figure 5.7 show the test-bed used for these experiments. To ease the synchronization in both time and frequency between the boards representing the dynamic devices and the base station, we use an Octoclock [Oct], also a product of Ettus Research, and coaxial cables connecting every platform to the Octoclock for time (PPS) and frequency synchronization, but this is not mandatory.

Details about our implementation. We used the GNU Radio Companion software (GRC, version 3.7 in 2017), and a laptop runs a GRC design to configure and control each USRP platform. As such, one laptop can run in parallel the control program of any number of boards[4]. The GNU Radio software provides the framework and tools to build and run software radio or just general signal-processing applications. GNU Radio applications are flow-graphs: a series of signal processing blocks connected together to describe a data flow. For maximum efficiency, we wrote all of our blocks in `C++`. These flow-graphs can be written in either `C++` or the Python programming language. The GNU Radio infrastructure is written entirely in `C++`, and many of the user tools are written in Python. GNU Radio Companion is a graphical user interface (UI) used to develop GNU Radio applications: GRC is effectively a Python code-generation tool. When a flow-graph is compiled in GRC, a Python code is produced, which can be executed to connect to the USRP, create the desired GUI windows and widgets, and create and connect the blocks in the flow-graph.

Illustrations of the flow-graph for the three components of the presented demonstration are included in Appendix 5.6.2, in Figures 5.15, 5.16 and 5.17.

User Interface. We have designed a user interface in order to visualize the results obtained with the experimental demonstration. This user interface is shown in Figure 5.8. We can see that it is made of three parts, one for each USRP, as highlighted in circled red numbers.

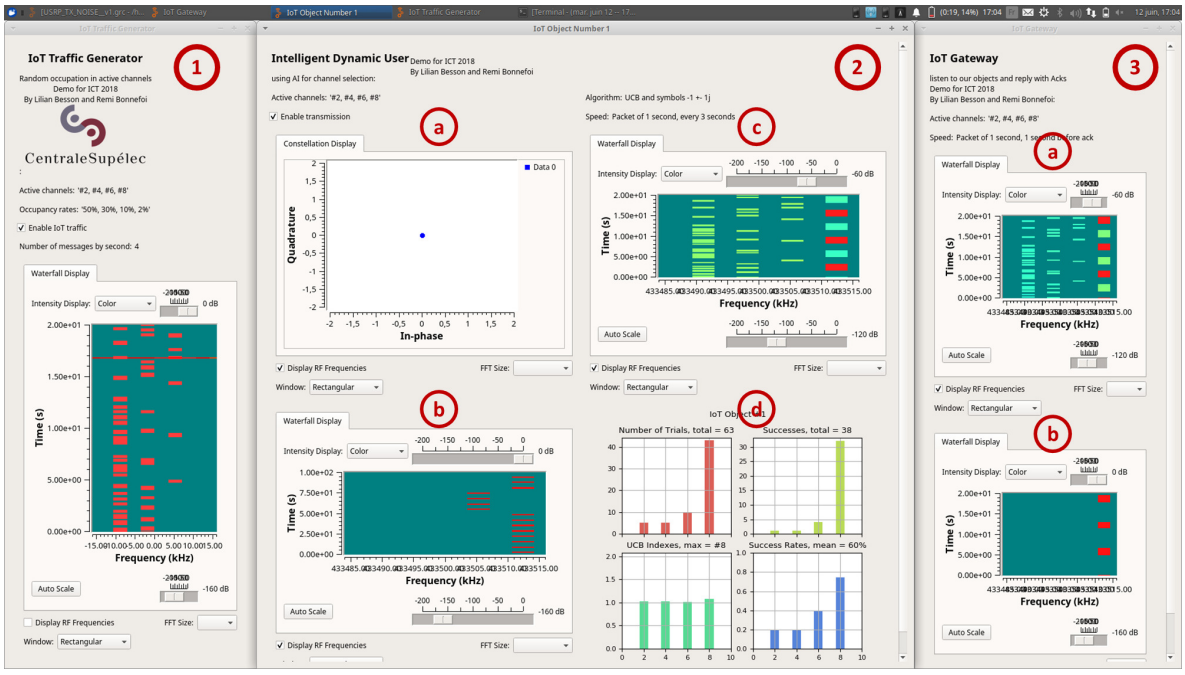

Figure 5.8 – User interface of our demonstration.

[4] Even if in practice, maximum efficiency is kept as long as there is not more than one GRC design by CPU core.

1. The first part is the interface of the IoT traffic generator, where we see the traffic generated by this USRP, presented in a waterfall view in the time vs frequency domain. Messages of the random traffic, generated by surrounding static devices, are shorter in time by purpose (they could be coming from other IoT standard), in order to distinguish them from an intelligent device traffic on the "waterfall" visualizations of the traffic.

2. The second part is the interface of the intelligent device which is made of four parts. At the top left, we observe the constellation of the transmitted packet (a). At the bottom left, we have a time/frequency view of the lasts packets transmitted by the device (b). We can see, in this view that the device transmitted its last 9 packets in channels $\#3$ and $\#4$. Then, at the top right of this interface (c), we can see the traffic observed by this device, where we have the interfering traffic (green), the up-link packets transmitted by this device (red) and the acknowledgements sent by the base station (blue). Colors in the "waterfall" represent the RF power level received at the device antenna. Hot colors are for closer elements, as for instance the device Tx antenna (reception) is close to the device Rx antenna (transmission), and consequently for the device waterfall these signals are colored in red (see graph (c) in part 2). Finally, at the bottom right (d), we have four histograms showing the performance indicators of the chosen MAB algorithm (number of transmissions, number of successful transmissions, UCB indexes and success rates, in each channel).

3. The last part is the interface of the base station, where we can see the traffic observed by the base station (a) and the channels in which the last acknowledgements have been sent (b). The observed traffic is coherent with (c) of part 2, as the elements are very close the one from the others on the test-bed. Colors may change, as they depend on the exact distance between the different transmitters and receivers. See more details in [MB19].

5.3.3 Experimental results

We compare in this PoC the two algorithms described in Section 2.4 (UCB and Thompson sampling) against a uniform access algorithm, that uniformly selects its channel at random. Note that we could run more algorithms, but with no real added-valued in terms of validation of the proposed learning-based approach, which is our goal. For one dynamic device, three algorithms are compared by their mean successful communications rates, on a horizon of $T = 2000$ communication slots, and were using three algorithms: uniform random access (in cyan), Thompson Sampling ("TS", in green) and UCB (in red).

In Figure 5.9 below, we show the results averaged on 10 repetitions using the same conditions. Each experiment has been done on a duration of about half a day, due to the IoT sporadic transmission mode that we want to respect (like in the model of Section 5.2). However, we make devices generate one message every 5 seconds, in order to artificially speed up the

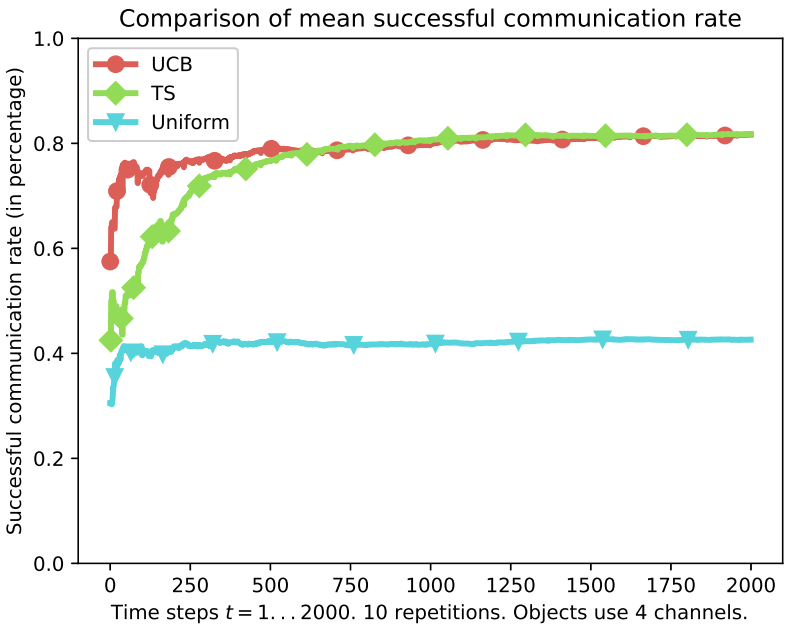

Figure 5.9 – Less than 400 communication slots (*i.e.*, less than 100 trials in each channel) are sufficient for the two learning devices (UCB and Thompson Sampling) to reach a successful communications rate close to 80%, which is **twice as much** as the non-learning (uniform) device, which stays around 40% of success. Similar gains of performance were obtained in other scenarios.

process and with no loss of generality (as we are using real hardware). Learning can be useful only when there is a large enough difference between "good" and "bad" channels, Each device was learning to access 4 different non-overlapping channels, that we chose to have occupancy rates of $(\mu_k)_k = [15\%, 10\%, 2\%, 1\%]$. Note that a maximum occupancy rate of 15% could seem not so high, but indeed it is, because for a pure ALOHA access mode, a naive dynamic device only obtains about 40% success rate, under such occupancy of the channels (see the "uniform" plot in Figure 5.9). The occupancy rate of a channel, which denotes the mean occupancy, is implemented using the traffic generator, to emulate the presence of S_i static devices with emission probability p (that is, $\mu_i = S_i \times p$ here).

When facing the same stationary background traffic, we see that the learning devices are both quickly more efficient than the naive uniform device. We obtain an improvement in terms of successful communications rate from 40% to about 60% in only 100 communications (about 16 min), and up-to 80% in only 400 communications. In stationary environments, both the TS and UCB algorithms are efficient and converge quickly, resulting in a strong decrease in collisions and failed communication slots. UCB is faster to learn but eventually TS gives a (slightly) better average performance.

Similar results are obtained for overlapping channels, when dynamic devices are learning in the presence of multiple devices, all using the same learning algorithm. However, our

experimental test-bed cannot run hundreds of intelligent devices. Empirical results confirm the simulations presented in Section 5.2 (see Figure 5.4). Such results are very encouraging, and illustrate well the various strong possibilities of MAB learning applied to IoT networks.

Availability of data and materials. The source code of our demonstration is fully available online, open-sourced under GPLv3 license, at `bitbucket.org/scee_ietr/malin-multi-arm-bandit-learning-for-iot-networks-with-grc/`. It contains both the GNU Radio Companion flowcharts and blocks, with ready-to-use `Makefiles` to easily compile, install and launch the demonstration. The demonstration only requires a laptop and open-source free softwares, as the laptop should run a GNU/Linux distribution (like Ubuntu or Debian), in addition to USRP platforms from Ettus Research.

Video. As depicted in Figure 5.10 below, we realized a 6-minute **video** to sum-up our demonstration and advertise our work online, and it is available on the YouTube hosting platform, at `youtu.be/HospLNQhcMk`. The video shows examples of 3 dynamic devices learning simultaneously, confirming the results of Figure 5.9 for overlapping channels. It also shows the connections between the USRP boards, the Octoclock, the master laptop etc, completing the presentation of the SCEE test-bed already shown in Figure 5.7.

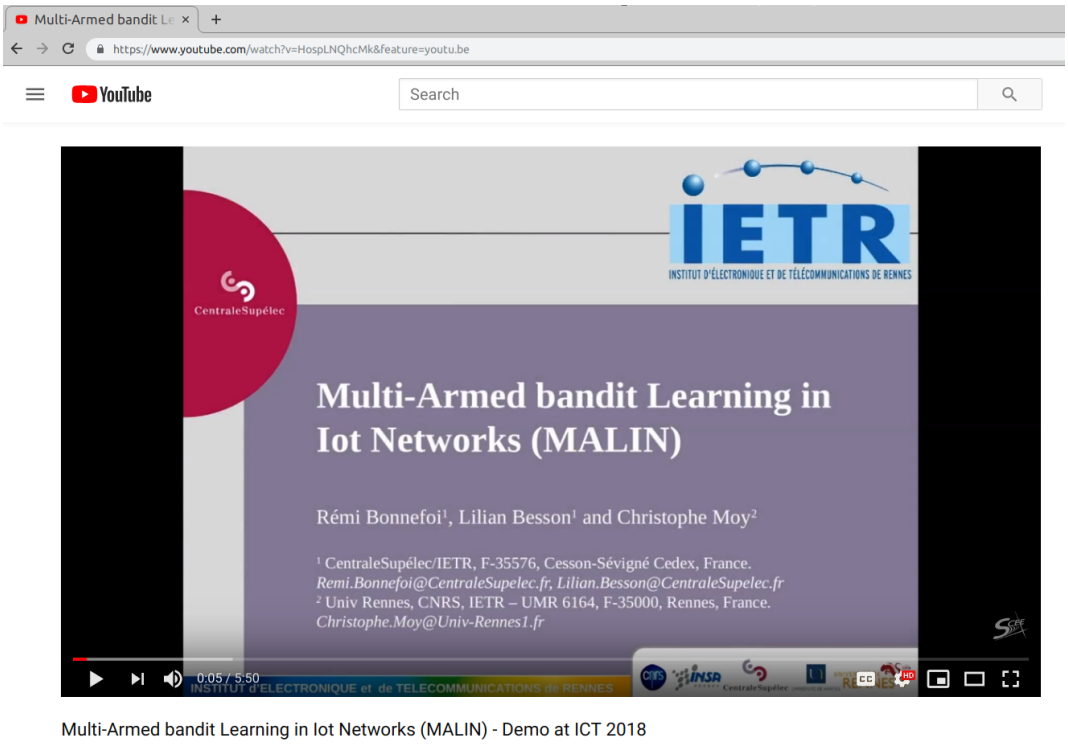

Figure 5.10 – Screenshot of the **video** of our demonstration, `youtu.be/HospLNQhcMk`.

5.4 Extending the model to account for retransmissions

We presented in Section 5.2 low-cost algorithms following well-known approaches, such as Upper-Confidence Bound (UCB), and we have reported encouraging results. When considering the application of MAB algorithms for slotted wireless protocols in a decentralized manner, other recent directions of research include theoretical analysis, like what we present in the next Chapter 6, or realistic empirical PoC like in [RMZ14, DMNM16, DNMP16, KDY+17] or the previous Section 5.3, and finally applications to multi-hoping networks [MTC+16, TCLM16] or other kinds of networks [AC18, WCN+19, WBMB+19]. None of the mentioned works discuss the impact of retransmissions on the performance of MAB learning algorithms.

In this section, we extend the previous model to take into account the possibility for retransmissions of a message after a collision. This is of major importance as most protocols for real-world IoT networks can use retransmissions, it is for instance the case of the LoRaWAN standard [RKS17]. As before, we propose and evaluate different learning strategies based on MAB algorithms. However, the price to be paid is a shorter battery lifetime for IoT devices. So this approach would be used only for devices with strong delivery constraints (*e.g.*, for healthcare applications), or that can refuel their energy over time (*e.g.*, for robotic applications).

We want to assess the performance of MAB algorithms for channel selection in LPWA networks operating in unlicensed bands, while taking into account the impact of retransmissions on the network performance. For this reason, several decision making strategies are applied after a first retransmission (*i.e.*, when a collision occurs). The proposed approach employs contextual information provided by the number of retransmissions, and is again implemented independently by each device, so that no coordination among them is needed. Moreover, our UCB-based heuristics again show low complexity, which make them suitable for being embedded in LPWA devices, like in the previous sections.

The contributions of this section can be thus summarized as follows. Firstly, we provide a close form approximation of the radio collision probability after a first retransmission. By doing this, we highlight the need to develop a learning approach for channel selection upon collision. Secondly, different heuristics are proposed to cope with retransmissions. Lastly, we conduct simulations in order to compare the performance of the proposed heuristics with a naive uniform random approach, and a UCB strategy (*i.e.*, without any learning for the retransmissions, that is, the same channel is used for retransmission).

5.4.1 Presentation of the model with retransmissions

LPWA network. Like in the previous sections of this chapter, we consider an LPWA network [RKS17], composed of a gateway and a large number of end-devices that regularly send short data packets, where K channels ($K > 1$) are available for the transmission of their packets.

We assume that this network is constituted by two types of devices: On the one hand, we have *static* devices that operate in one channel[5] in order to communicate with the gateway. On the other hand, there are IoT devices, that possess the additional advantage of being able to select any of the K available channels to perform their transmissions.

Like in the previous model presented in Section 5.2, regardless the type of devices, each of them follows a slotted ALOHA protocol [Rob75], and has a probability $p > 0$ to transmit a packet in a time slot. We make the hypothesis that the transmission is successful if the channel is available, otherwise it fails upon radio collision. The novelty compared to the previous model is that in case of RF (up-link or down-link) collision that prevents the devices from receiving the *Ack* from the gateway, these devices will attempt to retransmit their packet up-to $\mathrm{MaxBackOff}$ times[6], with $\mathrm{MaxBackOff} \in \mathbb{N}^*$. It is important to note that, every retransmission is carried out after a random back-off time, uniformly distributed in $\{0, \ldots, m-1\}$, where $m \in \mathbb{N}^*$ is the length of the back-off interval (note the difference between m and $\mathrm{MaxBackOff}$).

Model of IoT devices. The aforementioned contention process can be described by a Markov chain model [Nor98] similar to the one presented in [YFE12], as it is depicted in Figure 5.11. When a device has a packet to transmit, it goes from an idle state to a transmission state, while considering retransmissions due to different collision probabilities, $p_c, p_{c1}, \ldots, p_{c\mathrm{MaxBackOff}-2}$, at each $\mathrm{MaxBackOff}$ back-off stage. At each time slot, a transition from an idle state to a transmission state (denoted as `Trans.`) occurs if a packet transmission is required, while waiting states (denoted as `Wait`), correspond to a m back-off interval.

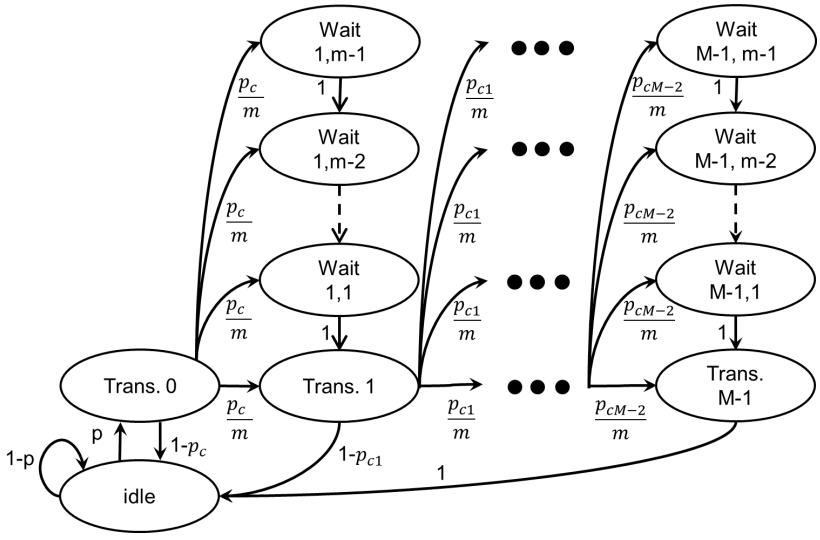

Figure 5.11 – The Markov model of the behavior of all devices paired to the considered IoT network using the ALOHA protocol. *Note*: $\mathrm{MaxBackOff}$ is written M, to have smaller and simpler labels.

[5] Note that, for unlicensed bands, this definition also encompasses any device following a different standard or trying to establish communication with gateways of other networks.

[6] We denote it $\mathrm{MaxBackOff}$ instead of M like we did in our paper [BBMVM19], as M is used in next Chapter 6.

A device aims to select a channel with the highest probability of successful transmissions, for which it uses a reinforcement learning approach, again formulated as a MAB problem. Contrarily to what may appear at first sight, *the goal is not to minimize the number of retransmissions*, but to maximize the probability of successful transmission, considering both the first transmission of a message and the retransmissions of the same message. Indeed, the objective of each device is to *maximize its battery life by minimizing its* ***total*** *number of transmissions*. We address the problem of channel selection taking into account the described Markov model for the retransmissions of end-devices. It motivates this section for which we consider the number of retransmissions, carried out by each device.

5.4.2 Motivations for the proposed approach

We consider IoT devices with a constraint on their QoS, imposing the successful delivery of their messages. When such an IoT device experiments a collision, it goes in a back-off state to retransmit the same packet on the same or another channel. If all devices remain in the same channel for retransmissions, it is a well-known result that it could result in a sequence of successive collisions with the same packets' devices that previously collided. Thus, it seems interesting to consider in the decision making policy the possibility for a device to retransmit in a different channel. One of our motivations to develop new MAB algorithms for the considered problem is this option of using a different communication channel between the first transmission and the next retransmissions.

By considering this possibility, the device will have to learn more, thus, we expect the learning time to be longer, but it could be possible that the final performance gain increases too, in terms of network performance. We present in Section 5.4.5 an analysis to check this performance gain, for various heuristics based on the UCB algorithm. Here after, we start by presenting a mathematical derivation that backups this idea. To do so, we study the collision probabilities considering the Markov process depicted in Figure 5.11, and foresee the impact of using bandit strategies, as well as setting guidelines for the design of heuristic approaches.

Probability of collision at a second transmission slot. It is well known [Abr70, Rob75] that having a collision during an access time can be overcome by a retransmission procedure (this can take several retransmission attempts). Our goal here is to obtain a mathematical approximation of the collision probability at the second transmission slot p_{c1}, as a function of the first collision probability p_c. We make two approximations $\mathcal{H}_1$ and $\mathcal{H}_2$ defined as (they are hypotheses on which the rest of this section is built),

- $\mathcal{H}_1$: The probability p_{c1}, is composed by the sum of two probabilities: i) the probability of colliding consecutively twice, *i.e.*, the devices that collide at a given time slot and collide again when retransmitting their packets, and ii) the probability of collision among

devices that did not collide in the same previous collision. Moreover, we suppose that the number of devices involved in a collision is small in comparison to the total number of devices. This is very realistic as a very small proportion of devices transmit at the same period, due to their low duty cycle.

- $\mathcal{H}_2$: The total number of back-off stages at time t is constant, and it is assumed to be large enough to consider that no device will ever be in the last failure state (this case is the one on the right side in Figure 5.11), after $\mathrm{MaxBackOff}$ successive failed retransmissions (otherwise, its battery life can be threatened if it does not have re-fueling capabilities).

Considering one device and one channel, we denote x_t^i the probability that it is transmitting a packet for the $(i+1)$-th time in a given time slot t (with $i \in \{0, \ldots, \mathrm{MaxBackOff} - 1\}$), and we denote $x_t = \sum_{i=0}^{\mathrm{MaxBackOff}-1} x_t^i$ the probability that it transmits a packet (*i.e.*, just the sum on i of x_t^i). We consider $N > 0$ active devices following the same policy.

We assume to be in the steady state [Nor98], in the Markov chain model depicted in Figure 5.11, and thus the probabilities no longer depend on the slot number t (*i.e.*, $\forall t, x_t = x$). Therefore, the probability that this device has a collision at the first transmission is p_c, and has the following expression

$$p_c = 1 - (1-x)^{N-1} \iff x = 1 - (1-p_c)^{\frac{1}{N-1}}. \tag{5.6}$$

Moreover, from (5.6) we define the probability $p_{cp}(n)$ that involves the collision of n packets sent by each IoT device (for any $1 \leq n \leq N-1$), during the first transmission slot, and is defined by $p_{cp}(n) = \binom{N-1}{n} x^n (1-x)^{N-1-n}$. As explained above, if an IoT device experiences a collision at the first transmission, it proceeds for the retransmission of its packet after a random back-off interval. We denote p_{ca} the probability to have a collision with a packet involved in the previous collision. Under the $\mathcal{H}_1$ assumption, the number of packets involved in the same previous collision remains very small in comparison to the total number of devices that may transmit during this time. In other words, this collision probability does not depend on previous retransmissions and is equal to p_c. So, the probability that the same device's packet experiences again a collision at the second time slot is

$$p_{c1} = p_{ca} + (1 - p_{ca})\, p_c. \tag{5.7}$$

If the device has a collision at the first attempt, we consider $p_{bp}(n)$ the probability that it has a collision with *exactly* n packets (for any $1 \leq n \leq N-1$), and that *at least one* of the n devices involved in this first collision chooses the same back-off interval,

$$p_{bp}(n) = \binom{N-1}{n} x^n (1-x)^{N-1-n} \left[1 - \left(1 - \frac{1}{m}\right)^n\right]. \tag{5.8}$$

Besides, p_{ca} is the conditional probability of collision with a packet sent by a device involved in the previous collision given that the packet experienced collision at its first transmission. Hence, under hypothesis $\mathcal{H}_2$, we can use Bayes theorem and the law of total probability to relate p_{ca} with $p_{bp}(n)$, and the different probabilities that a device experienced a collision during the first slot and has the same back-off interval for its retransmission is, $p_{ca} = \frac{1}{p_c}\sum_{n=1}^{N-1} p_{bp}(n)$. Therefore, the expression of p_{ca} is

$$\begin{aligned}&\frac{1}{p_c}\sum_{n=1}^{N-1}\binom{N-1}{n}x^n\,(1-x)^{N-1-n}\left[1-\left(1-\frac{1}{m}\right)^n\right]\\&=1-\frac{1}{p_c}\sum_{n=1}^{N-1}\binom{N-1}{n}x^n\,(1-x)^{N-1-n}\left(1-\frac{1}{m}\right)^n.\end{aligned}\tag{5.9}$$

Once again under $\mathcal{H}_1$, assuming that the number of devices involved in the first collision is small compared to $N-1$, the first $N_0 \ll N-1$ terms of the sum in (5.9) are predominant. We derive $p_{ca} \simeq 1 - \frac{1}{p_c}\sum_{n=1}^{N_0}\binom{N-1}{n}x^n\,(1-x)^{N-1-n}\left(1-\frac{1}{m}\right)^n$. Moreover, for these terms, n is small compared to $N-1$, and so $N-1-n$ can be approximated to $N-1$. Thus it gives,

$$p_{ca} \simeq 1 - \frac{(1-x)^{N-1}}{p_c}\sum_{n=1}^{N_0}\binom{N-1}{n}x^n\left(1-\frac{1}{m}\right)^n.\tag{5.10}$$

Assuming $\mathcal{H}_1$ amounts to consider that $x \ll 1$. As a consequence, the sum in equation (5.10) can be supplemented by negligible terms,

$$p_{ca} \simeq 1 - \frac{(1-x)^{N-1}}{p_c}\sum_{n=1}^{N-1}\binom{N-1}{n}x^n\left(1-\frac{1}{m}\right)^n.\tag{5.11}$$

The binomial theorem expands the sum in (5.11), so we can rewrite the expression of p_{ca}

$$p_{ca} \simeq 1 - \left(\frac{1}{p_c}-1\right)\left[1+\left(1-(1-p_c)^{\frac{1}{N-1}}\right)\left(1-\frac{1}{m}\right)\right]^{N-1}.\tag{5.12}$$

Finally, our approximation of p_{c1} can be obtained by inserting (5.12) in (5.7).

$$\begin{aligned}p_{c1} &= p_{ca} + (1-p_{ca})\,p_c = (1-p_c)p_{ca} + p_c\\&\simeq (1-p_c)\,(1-\left(\frac{1}{p_c}-1\right)\left[1+\left(1-(1-p_c)^{\frac{1}{N-1}}\right)\left(1-\frac{1}{m}\right)\right]^{N-1} + p_c.\end{aligned}\tag{5.13}$$

Behavior analysis of p_c and p_{c1} In order to assess the proposed approximation, we suppose a unique channel where all the devices follow the same contention Markov process. We simulate an ALOHA protocol with a maximum number of retransmissions $\mathrm{MaxBackOff} = 10$, a maximum back-off interval $m = 10$, and a transmission probability $p = 10^{-3}$. In Figure 5.12,

we show the collision probabilities for different number of devices N (from $N = 50$ to $N = 400$), for both p_c and p_{c1}. We can verify that the obtained approximation is very precise for lower values $p_{c1} \leq 30\%$ (*i.e.*, red and orange curves are quite close). Moreover, a significant gap between p_{c1} and p_c, of up-to 10%, can be observed, which suggests us to resort to MAB algorithms for the channel selection for both the first transmission and next retransmissions.

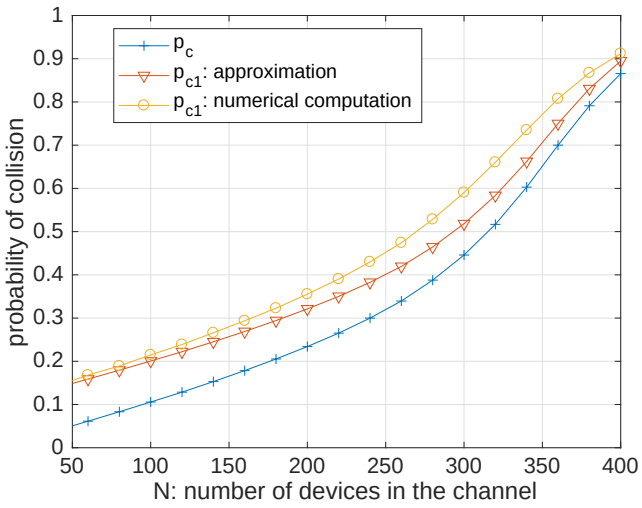

Figure 5.12 – Our approximation (in red) of p_{c1} (in orange), probability of collision at the second transmission, is more precise for smaller N. We also include p_c (in blue).

Learning is useful for non-congested networks. It is worth highlighting that, if we write (5.7) as $p_{c1} = p_c + p_{ca}\,(1 - p_c)$, then it is obvious that p_{c1} is always larger than p_c (as $p_{ca}\,(1 - p_c) > 0$). But for large values of p_c, $p_{ca}\,(1 - p_c) \simeq 0$ so the gap gets small, and for small values of p_c the gap is significant. Moreover, we can verify (*e.g.*, numerically or by differentiating) that the gap decreases when p_c increases (for fixed N and m). This backups mathematically the observation we made from Figure 5.12: the smaller the p_c, the larger is the gap between p_c and p_{c1}. We interpret this fact in two different situations:

- On the one hand, in a congested network, when devices suffer from a large probability of collision on their first transmission (*i.e.*, p_c is not so small), then $p_{c1} \simeq p_c$ and so devices cannot really hope to reduce their collision probabilities even if the use a different channel for retransmission.

- On the other hand, if p_c is small enough, *i.e.*, in a network not yet too congested, then the derivation above shows that $p_{c1} > p_c$, meaning that the possible gain of retransmitting in a different channel that the one used for the first transmission can be large, in terms of collision probability (*e.g.*, up-to 10% in this experimental setting). In other words, when learning can be useful (small p_c), learning to retransmit in a different channel can have a large impact on the global collision rate, thus justifying our approach.

5.4.3 The first heuristic: UCB unaware of retransmissions

This first heuristic we propose is unaware of retransmission: the same channel is used for retransmissions. The UCB algorithm is implemented independently by each device, we denote it "first-stage" UCB, and we present it in Algorithm 5.1. It is the same algorithm as the Algorithm 2.3 in Section 2.4.2 (using the same UCB indexes as we defined them in equation (2.7)), but we write it again to make clear the difference with first transmission and retransmission of messages. Note that a device using this first approach is only able to select a channel for the first transmission (using UCB, line 3-5), and then it uses the same channel for all the corresponding retransmissions of a packet (if retransmissions happen, line 7-8).

1 **for** $t = 1, \dots, T$ **do**
2 **if** *First packet transmission* **then**
3 Compute $\forall k, U_k(t) = \widehat{\mu_k}(t) + \sqrt{\alpha \ln(t)/N_k(t)}$;
4 Transmit in channel $A(t) \sim \mathcal{U}(\arg\max_k U_k(t))$;
5 Reward $r(t) = 1$, if *Ack* is received, else 0;
6 **else** `// Retransmit in same channel`
7 j $\leftarrow$ last channel selected by first-stage UCB;
8 Transmit in channel $A(t) = j$;
9 **end**

Algorithm 5.1: First-stage UCB and retransmission in same channel ("Only UCB").

More formally, for one device, let $N_k(t)$ be the number of times the channel k (for $k \in [K]$) was selected up-to time $t-1$, for $t \geq 1$ for any $t \in \mathbb{N}$, $N_k(t) = \sum_{\tau=1}^{t-1} \mathbb{1}(A(\tau) = k)$. The empirical mean estimator $\widehat{\mu_k}(t)$ of channel k is defined as $\widehat{\mu_k}(t) = \frac{1}{N_k(t)} \sum_{\tau=1}^{t-1} r(\tau) \mathbb{1}(A(\tau) = k)$, where $r(t) = Y_{k,t}$ is the reward obtained after transmission in channel k at time t. The upper confidence bound in each channel k is defined as $U_k(t) = \widehat{\mu_k}(t) + \sqrt{\alpha \ln(t)/N_k(t)}$. Finally, the transmission channel at time step t is $A(t) \sim \mathcal{U}(\arg\max_k U_k(t))$.

Small warning about notations: local (device) time vs global (gateway) time. In the algorithms presented in this chapter, the time step t does not refer to the *global* time step (as seen from the gateway), but rather the current number of up-link transmissions (or retransmissions) that was carried out by the device. Each device wakes up whenever it has to send some data, following its own emission process (we restrict to a Bernoulli process of small probability, *e.g.*, $p = 10^{-3}$), and whenever it wakes up, it sends its packet, and will send again for at most MaxBackOff times (*e.g.*, MaxBackOff $= 10$) until it receives an *Ack*. In other words, the time steps t in the following algorithms denote the number of up-link packets sent by the device, and these up-link transmissions or retransmissions can happen at different (global or real-world) times. The local index t is independent on

the global time (*i.e.*, the time of the gateway), and IoT device does not need to care about this difference. From the device point-of-view, the learning occurs at successive times (whenever the device wakes up), regardless of the global time.

5.4.4 Heuristics to (try to) learn how to retransmit efficiently

A device that implements the UCB algorithm is led to focus its transmissions and retransmissions in the channel which is currently identified as the best. As explained above in Section 5.4.2, focusing in one channel could increase the collision probability in retransmissions. We describe here the proposed heuristics for the channel selection in a retransmission. It is carried out taking into account that a device can incorporate a different channel selection strategy while being in a back-off state. Hence, a natural question is to evaluate whether using this additional contextual information can improve the performance of a learning policy.

For that end, all of our heuristics comprise two stages: the first stage is a UCB algorithm employed for the first attempt to transmit, and the second stage is another algorithm used for channel selections for the next retransmissions. We present below four heuristics for this second stage. Their short names (with their colors) are used in the legend on Figures 5.13, 5.14), and are given in "quotes" in the corresponding paragraphs.

Uniform random retransmission "(Random"). In this first proposal, the device uses a random channel selection, following a uniform distribution (on $[K]$). It is described below in Algorithm 5.2. More precisely, the first-stage UCB use rewards built from the acknowledgments that the device received or not for its first-stage transmission, but do not use any feedback about any of the retransmissions of any message.

```
for t = 1, ..., T do
    if First packet transmission then
        Use first-stage UCB as in Algorithm 5.1;
    else                                          // Random retransmission
        Transmit in channel A(t) ~ U(1, ..., K);
end
```

Algorithm 5.2: Heuristic: uniform random retransmission "(Random").

UCB **for retransmission ("UCB").** Instead of applying a random channel selection for retransmission, another heuristic is to use a second UCB algorithm in the second stage. In other words, we expect that this algorithm is able to learn the best channel to retransmit a

packet. It is described in Algorithm 5.3, and it is still a practical approach, since the storage requirements and time complexity remains linear w.r.t. the number of channels K (*i.e.*, $\mathcal{O}(K)$). Note that, we use the subscript $(^r)$ to denote the variables $\widehat{\mu}^r(t)$, $B_k^r(t)$ and $U_k^r(t)$, related to the UCB algorithm employed for the retransmission.

for $t = 1, \dots, T$ **do**
  if *First packet transmission* **then**
    Use first-stage UCB as in Algorithm 5.1;
  else `// Packet retransmission with the other` UCB^r
    Compute $\forall k, U_k^r(t) = \widehat{\mu_k}^r(t) + \sqrt{\alpha \ln(t)/N_k^r(t)}$;
    Transmit in channel $C^r(t) \sim \mathcal{U}(\arg\max_k U_k^r(t))$;
    Reward $r^r(t) = 1$, if *Ack* is received, else 0;
end

Algorithm 5.3: Heuristic: UCB for retransmission ("UCB").

K different UCBs for retransmission ("K UCB") Another heuristic is to not use the same algorithm no matter where the collision occurred, but to use K different second-stage UCB algorithms. It means that after a failed first transmission in channel j, the device relies on the j-th algorithm to decide its retransmission. The corresponding algorithm is depicted in Algorithm 5.4. Each of these algorithms are denoted using the subscript $(^j)$, for $j \in [K]$.

for $t = 1, \dots, T$ **do** `// At every time step`
  if *First packet transmission* **then**
    Use first-stage UCB as in Algorithm 5.1;
  else `// Packet retransmission with one of the` K UCB^j
    j $\leftarrow$ last channel selected by first-stage UCB;
    Compute $\forall k, U_k^j(t) = \widehat{\mu_k}^j(t) + \sqrt{\alpha \ln(t)/N_k^j(t)}$;
    Transmit in channel $A^j(t) \sim \mathcal{U}(\arg\max_k U_k^j(t))$;
    Reward $r^j_{A^j(t)}(t) = 1$ if *Ack* is received, else 0;
end

Algorithm 5.4: Heuristic: K different UCBs for retransmission ("K UCB").

Although, this approach increases the complexity and storage requirements (now, of order $\mathcal{O}(K^2)$). For the LPWA networks of interest, such as LoRaWAN, the cost of its implementation is still affordable, since a small number of channels is used. For instance, for $K = 4$ channels, the memory to store $K + 1 = 5$ algorithms is of the order of the requirements to store one.

Note that for other networks this heuristic could not be practical. The storage requirements and time complexity is now quadratic in K, and as such we no longer consider this heuristic to be a practical proposal in some LPWA networks, as for instance Sigfox networks consist in a large number of very narrow-band channels (*e.g.*, $K = 128$). But for LoRaWAN networks with $K = 4$, storing $K + 1 = 5$ algorithms does not cost much more than storing 2.

Delayed UCB for retransmission ("Delayed UCB"). This last heuristic is a composite of the random retransmission (Algorithm 5.2) and the UCB retransmission (Algorithm 5.3) approaches. Instead of starting the second stage UCB directly from the first retransmission, we introduce a fixed delay $\Delta \in \mathbb{N}$, $\Delta \geq 1$, and start to rely on the second stage UCB after Δ transmissions. The selection for the first steps is handled with the random retransmission.

The idea behind this delay is to allow the first stage UCB to start learning the best channel, before starting the second stage UCB (see details in Algorithm 5.5). The number of transmissions to wait before applying the second algorithm is denoted by Δ, it has to be fixed before-hand[7]. Note that, we use the subscript $(^d)$ to denote the variables related to the delayed second-stage UCB algorithm.

for $t = 1, \dots, T$ **do** `// At every time step`
  if *First packet transmission* **then**
    Use first-stage UCB as in Algorithm 5.1;
  else if $t \leq \Delta$ **then** `// Random retransmission`
    Transmit randomly in a channel $A(t) \sim \mathcal{U}(1, \dots, K)$.
  else `// Packet retransmission with delayed UCB`^{d}
    Compute $\forall k, U_k^d(t) = \widehat{\mu_k}^d(t) + \sqrt{\alpha \ln(t)/N_k^d(t)}$;
    Transmit in channel $A^d(t) \sim \mathcal{U}(\arg\max_k U_k^d(t))$;
    Reward $r^d_{A^d(t)}(t) = 1$ if *Ack* is received, else 0;
end

Algorithm 5.5: Heuristic: delayed UCB for retransmission ("Delayed UCB").

Other ideas that we did not explore. Instead of considering a first-stage UCB followed by a random channel retransmission, we could have considered a random first-stage channel retransmission followed by a second-stage UCB. This was not considered in our study [BBMVM19], and we preferred to not add it to the experiments presented below, for three reasons: to avoid clutter in the plots, to win some time as these experiments had to run for

[7] Choosing the value of Δ could be done by extensive benchmarks but such approach goes against the reinforcement learning idea: a heuristic should work against any problem, without the need to simulate the problem before-hand to find a good value of some internal parameter. As such, we only consider a delay of $\Delta = 100$ in our experiments, and we did not try to optimize it.

quite a long time, but mainly because the first-stage channel selection is most important one as we illustrate by the large difference in terms of performance between the uniform channel selection and the "Only UCB" heuristic, below in Figures 5.13 and 5.14.

Using another bandit policy? We could have chosen any bandit algorithm for the "first stage" component used in this Section, and for simplicity and clarity we focused on a simple but efficient one (UCB). We believe that the same empirical results, but more importantly, the same conclusions, could be given if we used Bayes-UCB or other bandit algorithm for the base building block in the different heuristics proposed in this section. Our goal here was not to optimize on the bandit policy (as we presented in Section 3.3 some numerical simulations doing precisely this), but rather to compare the different heuristics, for a fixed bandit policy (for which we preferred to use UCB for simplicity).

5.4.5 Numerical results

We simulate our network considering N devices following the contention Markov process described in Section 5.4.1, and a LoRaWAN standard with $K = 4$ channels, as in Section 5.2. Each device is set to transmit with a fixed probability $p = 10^{-3}$, *i.e.*, a packet about every 20 minutes for time slots of 1 s. For the evaluation of the proposed heuristics, a total number of $T = 20 \times 10^4$ time slots is considered, and the results are averaged over 1000 independent random simulations.

In a first scenario, we consider a total number of $N = 1000$ IoT devices, with a non-uniform distribution of static devices given by $10\%, 30\%, 30\%, 30\%$ for the four channels. In other words, the channels are occupied[8] respectively 10%, 30%, 30%, and 30% of time, and the contention Markov process considered is given by $\mathrm{MaxBackOff} = 5$, and $m = 5$. In Figure 5.13, we show the successful transmission rate versus the number of slots, for all the proposed heuristics.

A first result is that all the heuristics clearly outperform the non-learning approach that simply uses random channel selection for both transmissions and retransmissions (*i.e.*, the "no UCB" curve in black), which is (still) the current state-of-the-art in IoT networks. The improvement of the heuristics over the non-learning approach is clear, and for every heuristic that uses a kind of learning mechanism it can be observed that the successful transmission rate increases rapidly (or equivalently the PLR decreases). Moreover, all of these approaches show a fast convergence making them suitable for the targeted application. It is also worth mentioning that the employment of the same UCB algorithm for retransmissions, denoted

[8] Note that we consider higher occupancy rates that the ones considered previously in Section 5.3, because the goal of this experimental section is to evaluate our approach that uses learning to optimize the way each device retransmits its packets. We need to have a large enough probability p_c of retransmission if we want to see a difference between the different learning heuristics, which is why we consider a network more densely occupied than the one considered in Section 5.3.

here as "Only UCB", achieves a better performance, while a "Random" retransmission features a slight degradation. This result can be explained as follows: the loss of performance related to the separation of information for several algorithms is greater than the gain obtained by considering the first transmissions and retransmissions separately.

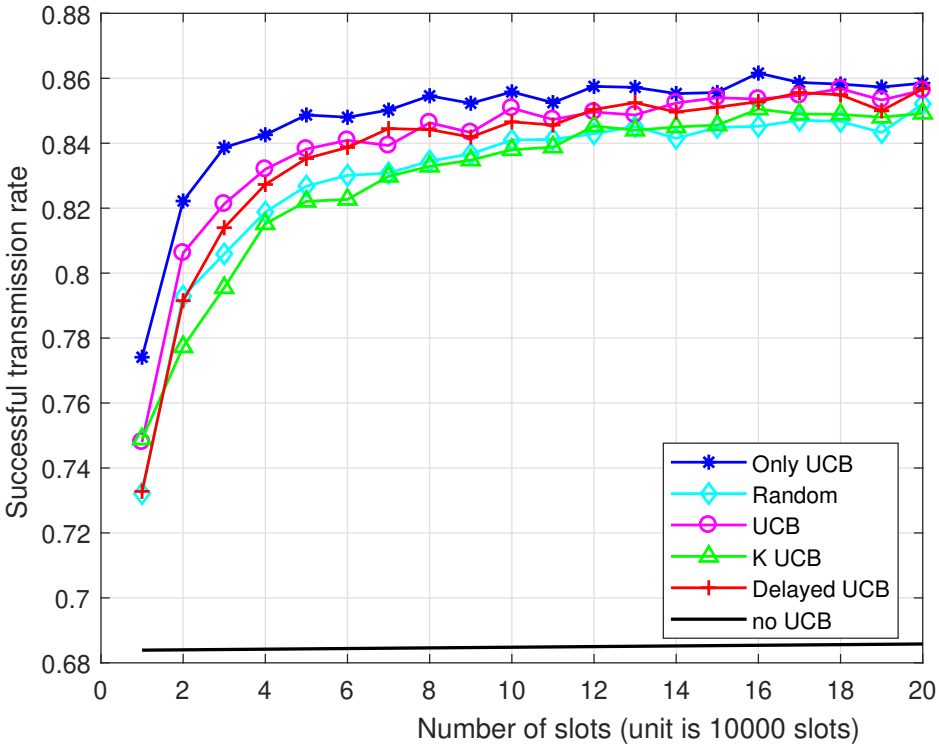

Figure 5.13 – Comparison between the exposed heuristics for the retransmission:" Only UCB", "Random", "UCB", "K UCB", and "Delayed UCB". The usage of the same learning policy for transmissions and retransmission is named "Only UCB", whereas the usage of a random channel selection, for both transmission and retransmission, is labeled as "no UCB". First scenario: learning helps but learning to retransmit smartly is not needed, as we observe that the random retransmission heuristic achieves similar performance than the others. We considered $N = 1000$ static IoT devices, that occupy the 4 channels in a static way leading to mean occupancy rates of $10\%, 30\%, 30\%, 30\%$.

We also consider in these experiments the case of an ALOHA protocol using $\mathrm{MaxBackOff} = 5$, and $m = 10$, a statistic distribution of the devices about $40\%, 30\%, 20\%, 10\%$ for the four channels, and $N = 2000$ IoT devices. The corresponding results are depicted in Figure 5.14. In this case the successful transmission rate is degraded compared with achieved results in Figure 5.13. We can explain this by the fact that we are considering in this network an increased number of devices, which increases the collision probability. It is important to highlight, that the "Random" retransmission heuristic shows a poor performance in comparison to the other heuristics, and it can be attributed to the fact that the number of retransmission is increased, and consequently a learning approach is able to take advantage of it. Furthermore, the "UCB",

"K UCB" and "Delayed UCB" heuristics behave similarly to "Only UCB", after a similar convergence time.

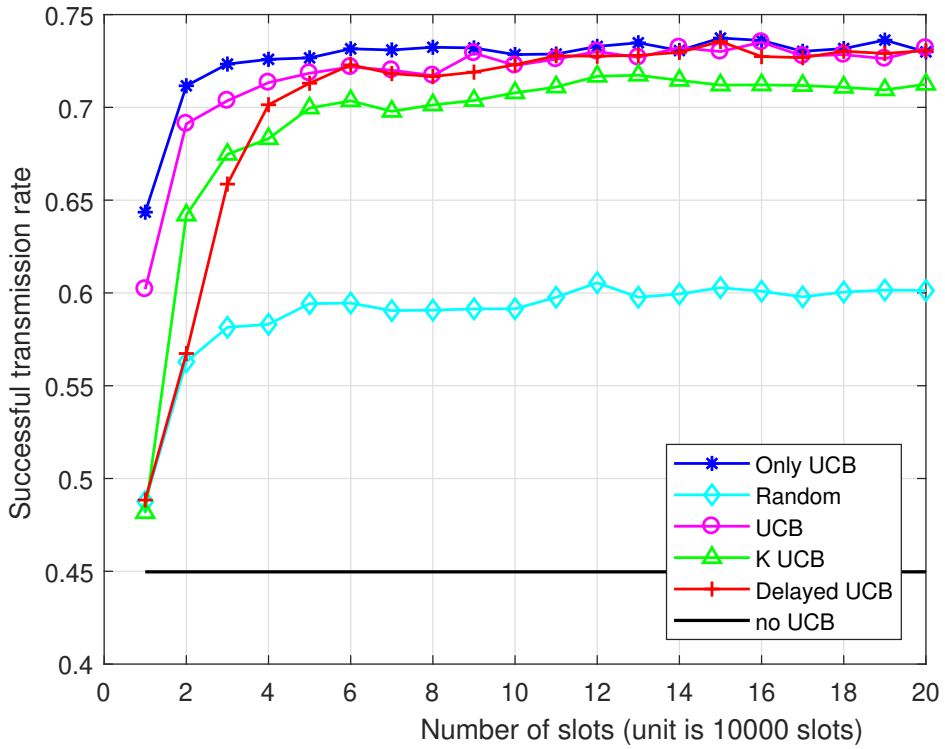

Figure 5.14 – Second scenario: learning helps a lot (a gain of 30% in terms of collision probability), and learning to retransmit smartly is needed. We observe that the random retransmission achieves poor performance compared to the others. We considered $N = 2000$ static IoT devices, that occupy the 4 channels in a static way leading to mean occupancy rates of $10\%, 30\%, 30\%, 30\%$.

The conclusions we can draw from these results are twofold. Firstly, MAB learning algorithms are very useful to reduce the collision rate in LPWA networks, a gain of up-to 30% of successful transmission rate is observed after convergence. Secondly, using learning mechanisms for retransmissions can be a simple yet efficient and interesting way to reduce collisions in IoT networks, even in networks with massive deployments of IoT as this can be checked in Figure 5.14, where the random retransmission heuristic is greatly outperformed by the any of the UCB-based approaches, that use learning for channel selection during the retransmission procedure. With 10% to 30% occupancy rates the considered example of IoT network can indeed be considered as an IoT network with a massive deployment of devices.

Reproducibility. The source code (MATLAB or Octave) used for the simulations and the figures of this section is open-sourced under the MIT License. It was written in collaboration with Rémi Bonnefoi and Julio César Mango-Vasquez, in the summer 2018, and is published at `Bitbucket.org/scee_ietr/ucb_smart_retrans`.

5.5 Conclusion – Towards theoretical guarantees

We focused in this chapter on models of IoT networks, and we proposed to use classical stationary multi-armed bandit learning algorithms implemented in a selfish and decentralized manner by each of the dynamic devices in the IoT network. We presented two models of wireless IoT networks, without relying on the feedback provided by spectrum sensing, and inspired by the ALOHA protocol. We proposed two versions, with or without retransmissions of up-link packages in case of collisions. We conclude that this learning-based approach is efficient, as it allows the IoT devices to automatically and independently increase their successful transmission rates.

It is also quite surprising that stochastic MAB algorithms can be of any use in such non-stationary applications. Unfortunately, it turned out to be of extreme difficulty to analyze analytically the considered model with thousands of independent devices, all communicating and learning in their own (random) time scales. That is why we focus on two different simplifications of this model in the next chapters, for which we are able to provide a rigorous theoretical analysis.

Multi-Players MAB. On the one hand, we are actually able to analyze a simpler model, if we assume to have at most $M \leq K$ devices with a transmission probability of $p = 1$. Instead of the experiment-driven direction pursued in this chapter, another possibility is to consider a *multi-players MAB* model to describe our problem. The main difference between the two models is the fact that in Chapter 5, $M \gg K$ devices transmit their messages at every time step, by following a random activation process (with a fixed transmission probability $p < 1$). If static and dynamic devices that have to transmit at a fixed time are denoted *active devices*, then their random activation patter makes the number of active devices an (unpredictable) random variable. Analyzing multi-players MAB models under this hypothesis is much harder, and is left as a future work. We study the case of $M \leq K$ devices learning independently to play a K-armed bandit in the next Chapter 6.

Non-stationary MAB. On the other hand, while it is hard to analyze the models of this chapter because of the unpredictable behaviors of the IoT devices' activation patterns and the evolving number of active devices, we are also able to analyze a simpler model, if we focus on a single player accessing a network which is assumed to be *piece-wise stationary*, that are bandit problems which are stationary on "long enough" intervals, of unknown locations and lengths. We then study this second direction in Chapter 7.

5.6 Appendix

5.6.1 Proof of Proposition 5.1

We include here the missing details of the proof of Proposition 5.1. First, we need to justify that the objective function is quasi-convex, in each of its coordinates. Then, we develop the computation of $D_i^*(\lambda)$, as a closed form expression of the system parameters (K, p), the distribution of static devices $(S_1, \dots, S_K)$ and the Lagrange multiplier λ.

Quasi-convexity.

- For $0 < \gamma < 1$, the function $g(x) \doteq x\gamma^x$ is quasi-convex on $[0, \infty)$, *i.e.*, $g(\eta x + (1-\eta)y) \leq \max(g(x), g(y))$ for any $x, y \in [0, \infty)$ and $\eta \in [0, 1]$ (definition from [Lue68]). Indeed, $g(\eta x + (1-\eta)y) = \eta\left[x(\gamma^x)^\eta\right]\gamma^{((1-\eta)y)} + (1-\eta)\left[y(\gamma^y)^{1-\eta}\right]\gamma^{\eta x}$, and $\gamma^{((1-\eta)y)} \leq 1$ and $\gamma^{\eta x} \leq 1$. But also $(\gamma^x)^\eta \leq \gamma^x$ as $\eta \leq 1$, and the same holds for $(\gamma^y)^{1-\eta} \leq \gamma^y$. So $g(\eta x + (1-\eta)y) \leq \eta(x\gamma^x) + (1-\eta)(y\gamma^y)$ which is a convex combination of $x\gamma^x$ and $y\gamma^y$, so smaller than the larger of the two values, and so $g(\eta x + (1-\eta)y) \leq \max(x\gamma^x, y\gamma^y)$.
- The function $f(D_1, \dots, D_K) \doteq \sum_{i=1}^{K} D_i(1-p)^{S_i+D_i-1}$ is quasi-convex in each of its coordinates, on $[0, \infty)^K$, as a sum of component-wise quasi-convex functions (with $\gamma = (1-p) \in (0, 1)$, thanks to the first point). □

Derivation of the Lagrange multiplier solution. Let us now prove the expression for D_i^* given above in (5.5).

- If $\boldsymbol{D} \doteq (D_1, \dots, D_K)$, the Lagrangian is denoted $\mathcal{L}(\boldsymbol{D}, \lambda) \doteq f(\boldsymbol{D}) + \lambda(D - \sum_{i=1}^{K} D_i)$, and its derivative w.r.t. D_i is $\frac{\partial}{\partial D_i}\mathcal{L}(\boldsymbol{D}, \lambda) = (1-p)^{S_i+D_i-1} + \ln(1-p)D_i(1-p)^{S_i+D_i-1} - \lambda$.
- So the gradient is zero $\frac{\partial}{\partial D_i}\mathcal{L}(\boldsymbol{D}, \lambda)|_{D_i=D_i^*} = 0$ iff D_i^* satisfies $(1-p)^{D_i^*}(1+\ln(1-p)D_i^*) = \lambda/(1-p)^{S_i-1}$. Let $x = \ln(1-p)D_i^*$ this is equivalent to $\mathrm{e}^x(1+x) = \lambda/(1-p)^{S_i-1}$ and with $y = 1 + x$, we get $\mathrm{e}^y y = \lambda\mathrm{e}/(1-p)^{S_i-1}$.
- By using the $\mathcal{W}$-Lambert function $\mathcal{W}$ [CGH+96], reciprocal of $y \mapsto \mathrm{e}^y y$, we get $x = y - 1 = \mathcal{W}(\lambda\mathrm{e}/(1-p)^{S_i-1}) - 1$. So the gradient of the Lagrangian is zero iff $D_i^* = \max(0, x/\ln(1-p)) = \left[\frac{1}{\ln(1-p)}\mathcal{W}(\lambda\mathrm{e}/(1-p)^{S_i-1}) - 1\right]^+$, because D_i^* has to be non-negative. This gives the i-th coordinate of the unique saddle point of $f(\boldsymbol{D})$, and so the unique solution to the maximization problem (5.4a), thanks to [Lue68, Theorem 1]. □

5.6.2 Illustration of the GNU Radio Companion Flowcharts

For the curious reader, we wanted to include here an illustration and a description of the three components of the demonstration we presented above in Section 5.3.

The code corresponding to the following components is written in `C++` and `Python` for the hand-written blocks, and using the GUI of the GNU Radio Companion software. The flow-graphs are saved as XML files, and the complete code of our proof-of-concept is fully available online, open-sourced under GPLv3 license, at `bitbucket.org/scee_ietr/malin-multi-arm-bandit-learning-for-iot-networks-with-grc/`.

Random traffic generator

Figure 5.15 shows the **random traffic generator** flow-graph. `Generator` is the only hand-written block, which is configured with a list of active channels, a list of occupancy rate, and constants about the PHY layer (preamble length and data length). It uses one USRP equipped with one antenna, as it only emits data (by using the "UHD: USRP" block in"Sink" mode).

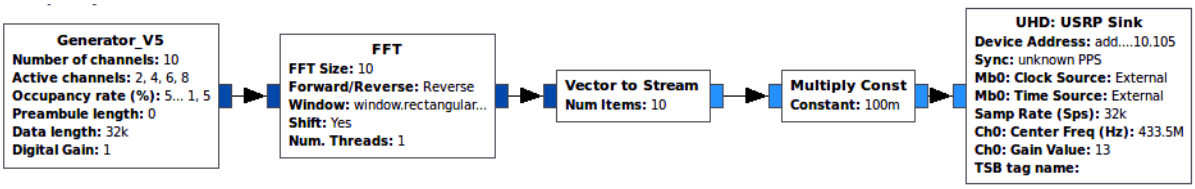

Figure 5.15 – The **random traffic generator** flow-graph.

IoT base station

The **IoT base station** is presented in Figure 5.16 below. We wrote the following blocks:

- 1) the `Demodulator` block, which is configured with a list of detection threshold (on the received power),
- 2) the `Check_ack` block, which is configured with a maximum block error and an accepted error rates (to decide when a message is close enough to an acknowledgement),
- and finally 3) the `send_ack` block, which is configured with the list of active channels, and knowledge about the PHY layer (delay before sending the Ack and its length).

All blocks need to know the constants about the PHY layer (preamble length and data length). The base station uses one USRP board equipped with two antennas, to emit and receive data (by using "Sink" and "Source" modes).

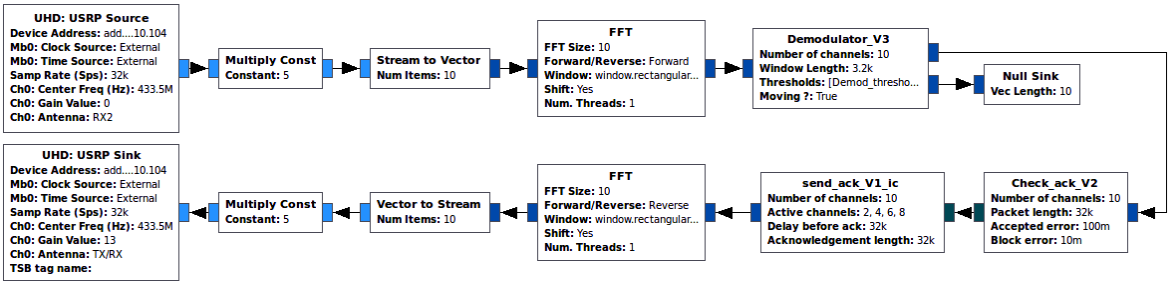

Figure 5.16 – The **IoT base station** flow-graph.

IoT dynamic device

Figure 5.17 below shows the **IoT dynamic device** flow-graph. The hand-written blocks are

- 1) the `Renormalized_ack` block, which is configured with the list of active channels and extra knowledge about the PHY layer (preamble length, message length, and a threshold to tune detection of the incoming Ack),
- 2) the `Demodulator` and 3) the `Check_ack` blocks, both shared with the IoT gateway,
- and finally 4) the `generator_SU` block, which embeds the UCB or Thompson Sampling algorithm, and which is configured with the list of active channels.

Most blocks need to know constants about the PHY layer (preamble length and data length). Any of the IoT dynamic devices also uses one USRP board equipped with two antennas, to emit and receive data ("Sink" and "Source" modes).

We note the difference between the base station and the end-devices. The base station uses its Rx antenna to scan the entire range of the K channels, at all time steps ; while dynamic devices use their Rx antennas only to listen for the acknowledgement sent by the base station if it received and decoded its up-link packet. After each transmission, the dynamic device listens to one channel during a certain time interval, in the channel used for up-link transmission.

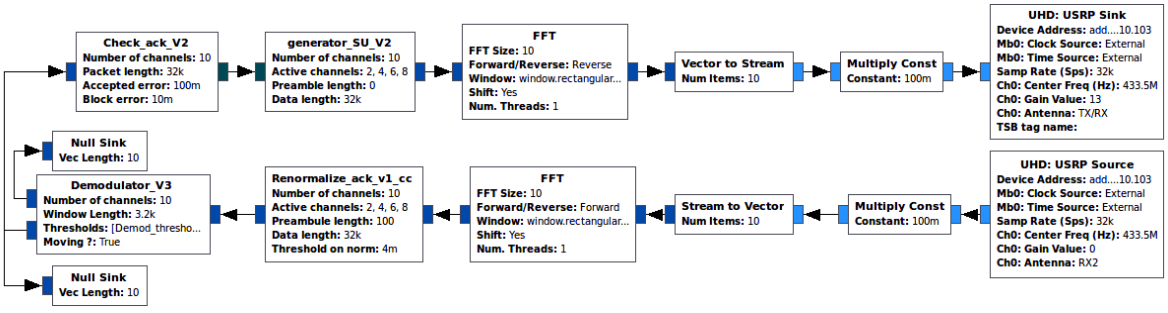

Figure 5.17 – The **IoT dynamic device** flow-graph.

Chapter 6

Multi-Players Multi-Armed Bandits

In this chapter, we are interested in a more formal approach to the decentralized learning problem presented of many end-devices accessing the same IoT wireless network than in the previous Chapter 5. We restrict to the easiest case of at most $M \leq K$ devices using a network with K orthogonal frequency channels. Each device has data to transmit at every instant, that is we restrict to the case of an activation probability of $p = 1$, under the hypothesis of random activation patterns of Chapter 5. We discuss three feedback levels that give variants of the multi-players MAB model previously studied in the literature, and we define the centralized regret as a measure of performance of multi-player bandits algorithms. Using a decomposition of the centralized system regret, we start by explaining the intuition about the expected behavior of any efficient decentralized algorithm, and then we propose $\mathrm{RandTopM}$ and MCTopM, two new orthogonalization schemes. Combining them with the $\mathrm{kl\text{-}UCB}$ index policy gives efficient algorithms, that achieve state-of-the-art performance in terms of their regret, which is also backed up by numerical simulations. We conclude by reviewing different extensions of the multi-players models.

Contents

6.1 Motivations for multi-players MAB models

As we saw in Chapters 1 and 5, a crucial step for the development of Cognitive Radio is to insert *multiple* smart devices (at least $M \geq 2$), in the *same* environment, or background traffic. In this Chapter 6, we are interested in a more formal approach to the decentralized learning problem presented in the previous Chapter 5. Such networks can be modelled using a decentralized multi-players multi-armed bandit problem, where arms are channels and players are dynamic IoT devices. The decentralized hypothesis means that the central base station (or gateway) does not given any direct order to the devices, they are all in charge of deciding the channel they each want to use at each time step. Moreover, the devices are independent and do not directly communicate with each other either. We show that dynamic end-devices are able to use limited feedback sent by the gateway to learn to find orthogonal affectations of the group of end-devices to the best radio channels, automatically and without explicit communication with each other. In other words, the end-devices are able to learn to cooperate efficiently, in a completely decentralized and autonomous manner.

We consider M identical dynamic IoT devices, communicating with a unique gateway, in K orthogonal channels and in an acknowledgment-based wireless protocol slotted in time. A perfect time and frequency synchronization is assumed, and some *i.i.d.* background traffic is assumed to be non-uniformly distributed in the K channels. As before, if two or more devices decide to use the same channel at the same time, a *collision* arises and none of sent up-link packet can be received by the gateway. Unfortunately, it is very hard to formally analyze the IoT network models we presented in Chapter 5, mainly because of the random activation process of all the dynamic (*i.e.*, learning) devices. Even if there are many identical bandit algorithms learning independently and in a decentralized way, the difficulty mainly comes from the fact that all of them are only communicating at some (random) time steps, and at each time step the number of communicating devices is random and unpredictable.

Mainly for these two reasons, for this Chapter 6 we prefer to only consider at most $M \leq K$ devices, communicating at each time step. Note that in the model of Chapter 5, this hypothesis $M \leq K$ corresponds to choosing a probability of activation of $p = 1$, as we assumed that (in average) no more than K devices should be active at the same step. We start by reviewing previous works on multi-players MAB models, which all considered the easier case of *sensing feedback*. But in the model studied in this chapter, each device also uses a Multi-Armed Bandit algorithm, to maximize its number of successful communications, by using the received acknowledgement *Ack* as a (random) binary reward after each up-link message (*i.e.*, at each time step). With the presence of a central controller that can assign the devices to different channels, this amounts to choosing at each time step *several* arms of a MAB in order to maximize the global rewards, and can thus be viewed as an application of the multiple-play bandit, introduced by [AVW87a] and recently studied by [KHN15]. They essentially proved that

existing algorithms can be easily extended to the multiple-play case, with provable guarantees on their regret. Due to the communication cost implied by a central controller, a more relevant model is the *decentralized multi-players* multi-armed bandit model, introduced by [LZ10] and further studied shortly after in [AMT10, AMTA11], in which players select arms individually and collisions may occur, that yield a loss of reward. Further algorithms were proposed in similar models by [TL12] and [KNJ12] (under the assumption that each arm is a Markov chain), and by [AM15, AM16] and [RSS16] for *i.i.d.* arms. In the point of view of the wireless protocol, each time frame is separated as before in a *sensing* phase (during which the device senses for the background traffic), an *up-link* phase (during which the device sends a packet to the gateway if it sensed the chosen channel to be free), and a *down-link* phase (during which it waits for an *Ack* from the gateway). In this first model, the binary reward is 1 only if the channel was sensed to be free of background traffic **and** if *Ack* was received, and the device has access to both information. We present two algorithms, $\mathrm{RandTopM}$ and MCTopM, based on the combination of an efficient MAB index policy (we chose $\mathrm{kl\text{-}UCB}$) and a smart orthogonalization procedure, based on a random hoping procedure called Musical Chair. Like in previous works, we consider the centralized system regret (multi-players regret), or simply referred to as regret. We start by showing an improved asymptotical regret lower-bound for any algorithm of a certain class. We then analyze the MCTopM algorithm and we show that its regret upper-bound is logarithmic, improving over the previous state-of-the-art. We also present extensive numerical simulations that show that our proposal outperforms all previous solutions and is much more efficient in this easier model of sensing feedback with a fixed and known number of players M accessing $K \geq M$ channels.

The goal for every player is to select most of the time one of the M best arms, without colliding too often with other players. A first difficulty relies in the well-known trade-off between *exploration* and *exploitation*: players need to explore all the arms to estimate their means, while trying to focus on the best arms to gain as many rewards as possible. The decentralized setting considers wireless protocol with no direct or explicit exchange of information between players, and assumes that the players only know K and M. To avoid collisions, players should furthermore find orthogonal configurations, *i.e.*, the M players use the M best arms without any collision, without explicitly communicating[1] with each other. Hence, in that case the trade-off is to be found between exploration, exploitation *and* low collisions.

All these above-mentioned works are motivated by the OSA problem, in which it is assumed that *sensing* occurs, that is, each smart device observes the availability of a channel (*i.e.*, a reward from the arm) *before* trying to transmit and possibly experiment a collision with other smart devices. However some real radio networks do not use sensing at all, *e.g.*,

[1] One must now be careful about this aspect when stating that "no explicit communications are allowed between players" in the model, as [BP18] proved that even in the no sensing case, the "communication trick" can be used to exchange information between players, by generating collisions at some pre-agreed times. We discuss this work more in details at the end of this chapter, in Section 6.7.3.

emerging standards currently or recently developed for *Internet of Things* (IoT) networks, such as LoRaWAN. Thus, to take into account these new applications, algorithms with additional constraints on the available feedback have to be proposed, within the multiple-player MAB model. Especially, the typical approach that combines a (single-player) bandit algorithm based on the sensing information –to learn the quality of the channels while targeting the best ones– with a low-complexity decentralized collision avoidance protocol, is no longer possible. Our article [BK18a] was the first to study this other model of multi-players bandits for the "no sensing" case, for which we only proposed a heuristic, the naive Selfish strategy as it was already used in Chapter 5. Even if empirical simulations showed that Selfish-kl-UCB performs very well, it is a mistake to only consider mean regret, as we found on numerical simulations as well as formal derivation on a simple example of $K = M = 2$ that the Selfish heuristic can have a linear regret with a low probability (and so asymptotically it has linear expected regret and fails to solve "no sensing" multi-players MAB problems). We do not propose any other efficient algorithm, but our work presented in April 2018 has strongly inspired two articles published shortly after [LM18, BP18]. They confirmed our findings that Selfish can have a linear regret, and they both proposed new algorithms. We include some numerical simulations to compare some of them, and we present in details the current state-of-the-art of research on multi-players MAB models without sensing.

Outline. The rest of this chapter is organized as follows. We first introduce the multi-players bandit model with three feedback levels in Section 6.2. We define the regret, and then present a useful decomposition in Section 6.3. The Selfish, RandTopM and MCTopM algorithms are introduced in Section 6.4, for which we present a theoretical analysis in Section 6.5. We report the results of an experimental study in Section 6.6. Finally, we present in Section 6.7 a review of the recent literature which studies variants of the model presented in this Chapter. For some extensions, we discuss how to adapt our proposals and illustrate the empirical performances of such modification of MCTopM-kl-UCB, leaving theoretical analyses as future works.

Publication. This chapter is mainly based on our article [BK18a].

6.2 Three feedback levels for the multi-players bandit model

Similarly to what is presented in Chapter 2, we consider a K-armed Bernoulli bandit model, of horizon $T \geq 2$, in which arm k is a Bernoulli distribution with mean $\mu_k \in [0, 1]$. We denote $(Y_{k,t})_{t\in[T]}$ the *i.i.d.* (binary) *reward stream* for arm k, that satisfies $\mathbb{P}(Y_{k,t} = 1) = \mu_k$ and that is independent from the other rewards streams.

Generalization to other distributions. However we mention that our lower bound and all our algorithms (and their analysis) could be extended to one-dimensional exponential

families (just like for the kl-UCB algorithm of [CGM+13]). For simplicity, we focus on the Bernoulli case, that is also the most relevant for Cognitive Radio problems, by considering channels' availabilities as a source of binary rewards.

In the multi-players MAB setting, there are $M \in [K]$ players (or agents), that have to make decisions at some pre-specified time instants. At time step $t \in \mathbb{N}, t \geq 1$, player j selects an arm $A^j(t)$, independently from the other players' selections.

Definition 6.1. *A* collision *occurs at time t if at least two players choose the same arm. We introduce the two events, for $j \in [M]$ and $k \in [K]$,*

$$C^j(t) \doteq \{\exists j' \neq j : A^{j'}(t) = A^j(t)\} \quad \text{and} \quad C_k(t) \doteq \left\{\#\{j : A^j(t) = k\} > 1\right\}, \tag{6.1}$$

that respectively indicate that a collision occurs at time t for player j ($C^j(t)$, j in superscript), and that a collision occurs at time t on arm k ($C_k(t)$, k in subscript).

Each player j then receives (and observes) the *binary rewards* $r^j(t) \in \{0, 1\}$,

$$r^j(t) \doteq Y_{A^j(t),t} \, \mathbb{1}(\overline{C^j(t)}). \tag{6.2}$$

In other words, she receives the reward of the selected arm if she is the only one to select this arm, and a reward zero otherwise. This provides another reason to focus on the Bernoulli model. It is the hardest model, in the sense that receiving a reward zero is *not enough* to detect collisions. For other models, the data streams $(Y_{k,s})_s$ are usually continuously distributed, with no probability mass at the value of zero (*e.g.*, Gaussian). Hence receiving $r^j(t) = 0$ directly gives $\mathbb{1}(C^j(t)) = 1$. Note that other models for rewards loss have also been proposed in the literature, for instance the reward could be randomly allocated to one of the players selecting it. To stay consistent with the model presented in the previous Chapter 5, and for simplicity, we preferred to focus on full reward occlusion in this chapter.

A multi-players MAB strategy is formally defined as a tuple $\mathcal{A} = (\mathcal{A}_1, \ldots, \mathcal{A}_M)$ of arm selection strategies for of each of the M players, and the goal is to propose a strategy that maximizes the total reward of the system, under some constraints. First, each player j should adopt a *sequential* strategy $\mathcal{A}_j$, that decides which arm to select at time t based on *previous observations*. Previous observations for player j at time t always include the previously chosen arms $A^j(s)$ and received rewards $r^j(s)$ for $s < t$, but may also include the *sensing information* $Y_{A^j(t),t}$ or the *collision information* $C^j(t)$. More precisely, depending on the application, one may consider the following three observation models, (I), (II) and (III).

If the arms have continuous distributions (or are such that $\mathbb{P}(Y_{k,s} = 0) = 0$), the *sensing information* $Y_{A^j(t),t}$ and *collision information* $C^j(t)$ can always be extracted from the reward

information. But for Bernoulli distributions, one may consider the following three observation models, that are not equivalent:

(I) **Simultaneous sensing and collision**: player j observes $Y_{A^j(t),t}$ *and* $C^j(t)$. We note that this first model was never previously studied, but we do not focus on it because of its unrealistic aspect, and its simplicity (it is easier than the following model, for which we obtain good theoretical results).

(II) **Sensing, then collision**: player j observes $Y_{A^j(t),t}$, *then* observes the reward, and thus also $C^j(t)$ only if $Y_{A^j(t),t} = 1$. This common setup, studied for example by [AMTA11, RSS16], is relevant to model the OSA problem: the device first checks for the presence of primary users in the chosen channel, if this channel is free ($Y_{A^j(t),t} = 1$), the transmission is successful ($r^j(t) = 1$) if no collision occurs with other smart devices ($\overline{C^j(t)}$).

(III) **No sensing**: player j only observes the reward $r^j(t)$. For IoT networks, this reward can be interpreted as an acknowledgement from a Base Station, received when a communication was successful. A lack of acknowledgment may be due to a collision with a device from the background traffic ($Y_{A^j(t),t} = 0$), or to a collision with one of the other players ($C^j(t)$). However, the sensing and collision information is censored. Recently, our work presented in Chapter 5 [BBM+17] presented the first (bandit-based) algorithmic solutions under this (harder) feedback model, in a slightly different setup, more suited to large scale IoT applications. As explained above, this third model was found to be too general to analyze mathematically, and we did not present theoretical results of convergence of the algorithms considered in Chapter 5.

Under each of these three models, we define $\mathcal{F}_t^j$ to be the filtration generated by the observations gathered by player j up to time t (which contains different information under models (I), (II) and (III)). While a *centralized* algorithm may select the vector of actions for all players $(A^1(t), \dots, A^M(t))$ based on all the observations from $\bigcup_j \mathcal{F}_{t-1}^j$, under a *decentralized* algorithm the arm selected at time t by player j only depends on the past observation of this player. More formally, $A^j(t)$ is assumed to be $\mathcal{F}_{t-1}^j$-measurable.

Definition 6.2. *We denote by μ_1^* the best mean, μ_2^* the second best etc, and by M-*best *the (non-sorted) set of the indices of the M arms with largest mean* (best arms)*: if $\mu_1^* = \mu_{k_1}, \dots, \mu_M^* = \mu_{k_M}$ then M-best $= \{k_1, \dots, k_M\}$. Similarly, M-*worst *denotes the set of indices of the $K - M$ arms with smallest means* (worst arms)*, $[K] \setminus M$-best.*

Note that they are both uniquely defined whenever $\mu_M^* > \mu_{M+1}^*$.

Following a natural approach in the bandit literature, like in Section 2.3, we evaluate the performance of a multi-players strategy using the *expected regret* (later simply referred to as

regret), that measures the performance gap with respect to the best possible strategy. The regret of the strategy $\mathcal{A}$ at horizon T is the difference between the cumulated reward of an oracle strategy, assigning in this case the M players to M-best, and its cumulated reward:

Definition 6.3. *The excepted centralized multi-players regret is defined by*

$$R_T^{\mathcal{A}}(\boldsymbol{\mu}, M) \doteq \left(\sum_{k=1}^{M} \mu_k^*\right) T - \mathbb{E}_{\mu}\left[\sum_{t=1}^{T}\sum_{j=1}^{M} r^j(t)\right]. \tag{6.3}$$

With this definition, maximizing the expected sum of global reward of the system is indeed equivalent to minimizing the regret, and we investigate the best possible *regret rate* of a decentralized multi-players algorithm in the next section.

6.3 Decomposing the multi-player regret to get an intuition for the design of efficient decentralized algorithms

In this section, we provide a useful decomposition of the regret (Lemma 6.5) that permits to establish a new problem-dependent lower bound on the regret (Theorem 6.8), and also provides key insights on the derivation of regret upper bounds (Lemma 6.9).

Warning. The regret lower bound that we gave in [BK18a] is not applicable to any algorithm, as it was discovered by E. Boursier and V. Perchet. As they explain in Section 2.4 in [BP18], the proof we gave in the Appendix of our paper [BK18a] was wrong in just one step. The results stated in this section are now correct, thanks to the modifications that we added here, that is, to consider this information term $\mathcal{I}_{\boldsymbol{\mu},\boldsymbol{\lambda}}(\mathcal{A}_j, T)$. The cost for this modification is to restrict the lower-bound to a smaller class of algorithms, which *should* contain RhoRand, RandTopM and MCTopM, but not the two algorithms proposed SIC-MMAB from [BP18] and Multiplayer Explore-then-Commit (M-ETC) from [KM19]. Proving that the proposed algorithms are in this class is left as an open question.

6.3.1 A useful regret decomposition

We introduce additional notations in the following definition.

Definition 6.4. *Let* $N_k^j(T) \doteq \sum_{t=1}^T \mathbb{1}(A^j(t) = k)$, *and denote* $N_k(T) \doteq \sum_{j=1}^M N_k^j(T)$ *the* number of selections *of arm* $k \in [K]$ *by any player* $j \in [M]$, *up to time* T.

Let $\mathcal{C}_k(T)$ *be the* number of colliding players *on arm* $k \in [K]$ *up to horizon* T:

$$\mathcal{C}_k(T) \doteq \sum_{t=1}^T \sum_{j=1}^M \mathbb{1}(C^j(t))\mathbb{1}(A^j(t) = k). \tag{6.4}$$

Note that when n *players choose arm* k *at time* t, *this counts as* n *collisions, not just one. So* $\mathcal{C}_k(T)$ *counts the total* number of colliding players *rather than the number of collision events. Hence there is small abuse of notation when calling it a number of collisions.*

We now provide a regret decomposition for any bandit instances with a strict gap between the M best arms and the other arms (*i.e.*, $\mu_M^* > \mu_{M+1}^*$).

Lemma 6.5. *For any bandit instance* $\boldsymbol{\mu} \in \mathcal{P}_M \doteq \left\{\boldsymbol{\mu} \in [0,1]^K : \mu_M^* > \mu_{M+1}^*\right\}$, *it holds that*

$$R_T^{\mathcal{A}}(\boldsymbol{\mu}, M) = \underbrace{\sum_{k \in M\text{-worst}} (\mu_M^* - \mu_k)\mathbb{E}_\mu[N_k(T)]}_{\text{(a)}} \tag{6.5}$$
$$+ \underbrace{\sum_{k \in M\text{-best}} (\mu_k - \mu_M^*)(T - \mathbb{E}_\mu[N_k(T)])}_{\text{(b)}} + \underbrace{\sum_{k=1}^K \mu_k \mathbb{E}_\mu[\mathcal{C}_k(T)]}_{\text{(c)}}.$$

In this decomposition, term (a) counts the lost rewards due to sub-optimal arms *selections* ($k \in M$-worst), *term (b) counts the number of times the* best arms *were* not *selected* ($k \in M$-best), *and term (c) counts the weighted number of collisions, on* all arms.

Proof. Using the definition of regret $R_T^{\mathcal{A}}(\boldsymbol{\mu}, M)$ from (6.3), denoted here R_T, and this collision indicator $\eta^j(t) \doteq \mathbb{1}(\overline{C^j(t)})$,

$$R_T = \left(\sum_{k=1}^M \mu_k^*\right) T - \mathbb{E}_\mu\left[\sum_{t=1}^T \sum_{j=1}^M Y_{A^j(t),t}\eta^j(t)\right] = \left(\sum_{k=1}^M \mu_k^*\right) T - \mathbb{E}_\mu\left[\sum_{t=1}^T \sum_{j=1}^M \mu_{A^j(t)}\eta^j(t)\right]$$

The last equality comes from the linearity of expectations, and the fact that $\mathbb{E}_\mu[Y_{k,t}] = \mu_k$ (for all t, from the *i.i.d.* hypothesis), and the independence with $A^j(t)$, $\eta^j(t)$ and $Y_{k,t}$ (observed *after* playing $A^j(t)$). So $\mathbb{E}_\mu[Y_{A^j(t),t}\eta^j(t)] = \sum_k \mathbb{E}_\mu[\mu_k \mathbb{1}(A^j(t), t)\eta^j(t)] = \mathbb{E}_\mu[\mu_{A^j(t)}\eta^j(t)]$. And so

$$R_T = \mathbb{E}_\mu\left[\sum_{t=1}^T \sum_{j \in M\text{-best}} \mu_j - \sum_{t=1}^T \sum_{j=1}^M \mu_{A^j(t)}\eta^j(t)\right]$$

$$= \left(\frac{1}{M} \sum_{j \in M\text{-best}} \mu_j \right) - \sum_{k=1}^{K} \sum_{j=1}^{M} \mu_k \mathbb{E}_\mu \left[N_k^j(T) \right] + \sum_{k=1}^{K} \mu_k \mathbb{E}_\mu \left[\mathcal{C}_k(T) \right].$$

For the first term, we have $TM = \sum_{k=1}^{K} \sum_{j=1}^{M} \mathbb{E}_\mu \left[N_k^j(T) \right]$, and if we denote $\overline{\mu}^* \doteq \frac{1}{M} \sum_{j \in M\text{-best}} \mu_j$ the average mean of the M-best arms, then,

$$= \sum_{k=1}^{K} \sum_{j=1}^{M} (\overline{\mu}^* - \mu_k) \mathbb{E}_\mu \left[N_k^j(T) \right] + \sum_{k=1}^{K} \mu_k \mathbb{E}_\mu \left[\mathcal{C}_k(T) \right].$$

If $\overline{\Delta_k} \doteq \overline{\mu}^* - \mu_k$ is the gap between the mean of the arm k and the M-best average mean, and if M^* denotes the index of the worst of the M-best arms (*i.e.*, $M^* = \arg\min_{k \in M\text{-best}}(\mu_k)$), we can split $[K]$ into three disjoint sets $M\text{-best} \cup M\text{-worst} = (M\text{-best} \setminus \{M^*\}) \cup \{M^*\} \cup M\text{-worst}$

$$= \sum_{k \in M\text{-best} \setminus \{M\}} \overline{\Delta_k} \mathbb{E}_\mu \left[N_k(T) \right] + \overline{\Delta_{M^*}} \mathbb{E}_\mu \left[N_{M^*}(T) \right]$$
$$+ \sum_{k \in M\text{-worst}} \overline{\Delta_k} \mathbb{E}_\mu \left[N_k(T) \right] + \sum_{k=1}^{K} \mu_k \mathbb{E}_\mu \left[\mathcal{C}_k(T) \right].$$

But for $k = M^*$, $N_{M^*}(T) = TM^* - \sum_{k \in M\text{-best} \setminus \{M\}} \mathbb{E}_\mu \left[N_k(T) \right] - \sum_{k \in M\text{-worst}} \mathbb{E}_\mu \left[N_k(T) \right]$, so by recombining the terms, we obtain,

$$= \sum_{k \in M\text{-best} \setminus \{M\}} (\overline{\Delta_k} - \overline{\Delta_{M^*}}) \mathbb{E}_\mu \left[N_k(T) \right] + \overline{\Delta_{M^*}} TM^*$$
$$+ \sum_{k \in M\text{-worst}} (\overline{\Delta_k} - \overline{\Delta_{M^*}}) \mathbb{E}_\mu \left[N_k(T) \right] + \sum_{k=1}^{K} \mu_k \mathbb{E}_\mu \left[\mathcal{C}_k(T) \right].$$

The term $\overline{\Delta_k} - \overline{\Delta_{M^*}}$ simplifies to $\mu_{M^*} - \mu_k$, and so $\overline{\Delta_{M^*}} = \frac{1}{M} \sum_{k=1}^{M} \mu_k - \mu_{M^*}$ by definition of $\overline{\mu}^*$. And for $k = M^*$, $\mu_{M^*} - \mu_k = 0$, so the first sum can be written for $k = 1, \dots, M$ only, soIt

$$R_T = \sum_{k \in M\text{-best}} (\mu_{M^*} - \mu_k) \mathbb{E}_\mu \left[N_k(T) \right] + \sum_{k \in M\text{-best}} (\mu_k - \mu_{M^*}) T$$
$$+ \sum_{k \in M\text{-worst}} (\mu_{M^*} - \mu_k) \mathbb{E}_\mu \left[N_k(T) \right] + \sum_{k=1}^{K} \mu_k \mathbb{E}_\mu \left[\mathcal{C}_k(T) \right]$$

And so we obtain the decomposition with three terms (a), (b) and (c).

$$R_T = \sum_{k \in M\text{-best}} (\mu_k - \mu_{M^*}) \left(T - \mathbb{E}_\mu \left[N_k(T) \right] \right)$$
$$+ \sum_{k \in M\text{-worst}} (\mu_{M^*} - \mu_k) \mathbb{E}_\mu \left[N_k(T) \right] + \sum_{k=1}^{K} \mu_k \mathbb{E}_\mu \left[\mathcal{C}_k(T) \right].$$

Which is exactly the decomposition we wanted to prove. □

The regret decomposition in Lemma 6.5 is valid for both centralized and decentralized algorithms. For centralized algorithms, due to the absence of collisions, (c) is obviously zero, and (b) is non-negative, as $N_k(T) \leq T$. For decentralized algorithms, (c) may be significantly large, and term (b) may be negative, as many collisions on arm k may lead to $N_k(T) > T$ (which is counter intuitive with such notations). However, a careful manipulation of this decomposition shows that the regret is always lower bounded by term (a). Figure 6 in Appendix F of [BK18a] illustrates two cases of $M < K$ and $M = K$, and the different impact of the three terms (a), (b) and (c) on the regret.

Lemma 6.6. *For any strategy $\mathcal{A}$ and $\boldsymbol{\mu} \in \mathcal{P}_M$, the regret is lower-bounded by (a):*

$$R_T^{\mathcal{A}}(\boldsymbol{\mu}, M) \geq \sum_{k \in M\text{-worst}} (\mu_M^* - \mu_k) \mathbb{E}_\mu[N_k(T)].$$

Proof. Note that term (c) is clearly lower bounded by 0 but it is not obvious for (b) as there is no reason for $N_k(T)$ to be upper bounded by T (it counts the selections of arm k by *all* the players, and for instance if player 1 is fixed on arm 1 and player 2 plays it at least once, then $N_1(T) \geq T + 1$). Let $N_k^!(T) \doteq \sum_{t=1}^T \mathbb{1}(\exists! j, A^j(t) = k)$, where the notation $\exists!$ stands for "there exists a unique". Then $N_k(T) = \sum_{t=1}^T \sum_{j=1}^M \mathbb{1}(A^j(t) = k)$ can be decomposed as

$$N_k(T) = \sum_{t=1}^T \mathbb{1}(\exists! j, A^j(t) = k) + \sum_{t=1}^T \sum_{j=1}^M c_{k,t} \mathbb{1}(A^j(t) = k) = N_k^!(T) + C_k(T).$$

We focus on the two terms (b) + (c) from the decomposition of $R_T^{\mathcal{A}}(\boldsymbol{\mu}, M)$ from Lemma 6.5,

$$\begin{aligned}
(b) + (c) &= \sum_{k \in M\text{-best}} (\mu_k - \mu_M^*)(T - \mathbb{E}_\mu[N_k^!(T)]) + \sum_{k \in M\text{-best}} \mu_M^* \mathbb{E}_\mu[C_k(T)] \\
&\quad + \sum_{k=1}^M \mu_k \mathbb{E}_\mu[C_k(T)] - \sum_{k \in M\text{-best}} \mu_k \mathbb{E}_\mu[C_k(T)] \\
&= \sum_{k \in M\text{-best}} (\mu_k - \mu_M^*)(T - \mathbb{E}_\mu[N_k^!(T)]) + \sum_{k \in M\text{-best}} \mu_M^* \mathbb{E}_\mu[C_k(T)] + \sum_{k \in M\text{-worst}} \mu_k \mathbb{E}_\mu[C_k(T)] \\
&= \sum_{k \in M\text{-best}} (\mu_k - \mu_M^*)(T - \mathbb{E}_\mu[N_k^!(T)]) + \sum_{k=1}^M \min(\mu_M^*, \mu_k) \mathbb{E}_\mu[C_k(T)].
\end{aligned}$$

And now both terms are non-negative, as $N_k^!(T) \leq T$, $\min(\mu_M^*, \mu_k) \geq 0$, and $C_k(T) \geq 0$, so (b) + (c) ≥ 0 which proves that $R_T^{\mathcal{A}}(\boldsymbol{\mu}, M) = (a) + (b) + (c) \geq (a)$, as wanted. □

6.3.2 An improved asymptotic lower bound on the regret

Similarly to what we present above in Section 2.3, we use the Kullback-Leibler divergence kl to express this lower bound. We first introduce the assumption under which we derive a regret lower bound, that generalizes the assumption of uniform efficiency given in Definition 2.6, a classical assumption made by [LR85] in single-player bandit models.

Definition 6.7. *An algorithm $\mathcal{A}$ is* **strongly uniformly efficient** *if for all $\boldsymbol{\mu} \in \mathcal{P}_M$,*

$$\forall a \in (0,1), R_T^{\mathcal{A}}(\boldsymbol{\mu}, M) \underset{T\to+\infty}{=} o(T^\alpha), \tag{6.6}$$

$$\text{and } \forall a \in (0,1), \forall j \in [M], k \in M\text{-best}, \quad \frac{T}{M} - \mathbb{E}_\mu[N_k^j(T)] \underset{T\to+\infty}{=} o(T^\alpha). \tag{6.7}$$

Having a small regret on every problem instance (*i.e.*, being uniformly efficient) is a natural assumption, that rules out policies tuned to perform well only on specific instances (*e.g.*, fixed-armed policies). From this assumption $R_T^{\mathcal{A}}(\boldsymbol{\mu}, M) = o(T^\alpha)$ and the decomposition of Lemma 6.5 one can see[2] that for every $k \in M\text{-best}$, $T - \mathbb{E}_\mu[N_k(T)] = o(T^\alpha)$, and so

$$\sum_{j=1}^{M} \left(\frac{T}{M} - \mathbb{E}_\mu[N_k^j(T)] \right) = o(T^\alpha). \tag{6.8}$$

The additional assumption in (6.7) further implies some notion of *fairness*, as it suggests that each of the M players spends on average the same amount of time on each of the M best arms. Note that this assumption is satisfied by any strategy that is invariant under every permutation of the players, *i.e.*, for which the distribution of the observations under $\mathcal{A}_\sigma = (\mathcal{A}_{\sigma(1)}, \dots, \mathcal{A}_{\sigma(M)})$ is independent from the choice of permutation $\sigma \in \Sigma_M$ of the set $\{1, \dots, M\}$. In that case, it holds that $\mathbb{E}_\mu[N_k^j(T)] = \mathbb{E}_\mu[N_k^{j'}(T)]$ for every arm k and $(j, j') \in [M]$, hence (6.7) and (6.8) are equivalent, and strong uniform efficiency is equivalent to standard uniform efficiency. Note that the algorithms studied in Section 6.4 are permutation invariant, and MCTopM-kl-UCB is thus an example of strongly uniformly efficient algorithm, as we prove in Section 6.5 that its regret is logarithmic on every instance $\mu \in \mathcal{P}_M$.

About fairness. In the proofs of the regret bounds for RhoRand in [AMTA11], the authors briefly mention that their policy is invariant under permutation and that this yields a certain fairness guarantee, but without formalizing it more. The notion of fairness defined above can be interpreted as a "cooperative fairness", opposed to the notion of "arm fairness" that has been studied in a few papers on single-player stochastic MAB. For instance, [PGNN19] requires that

[2] With some arguments used in the proof of Lemma 6.6 to circumvent the fact that (b) may be negative.

each arm must be sampled at least a given fraction of bandit game, *i.e.*, $\forall k, \mathbb{E}[N_k(T)] \geq r_k T$, where the constraint vector $[r_1, \dots, r_K] \in [0,1]^K$ is known by the algorithm.

Collision information. The following notations and the hypothesis on the collision information term (6.9) comes from Appendix E of [KM19]. Similarly to what we did in Section 2.1, consider the observations O_t^j that player j gathered after t rounds of its algorithm $\mathcal{A}_j$ for a fixed player $j \in [M]$, defined as $O_t^j \doteq \left(U^j(1), Y_{A^j(1),1}, C^j(1), \dots, U^j(t), Y_{A^j(t),t}, C^j(t)\right)$, where $U^j(t)$ denotes some external source of randomness useful to select $A^j(t+1)$. For instance, an algorithm based on ranks and UCB indexes, like RhoRand, when two arms have the same maximum index the decision is an $\arg\max$, and ties are usually broken by a uniform random selection among the arms with maximum index.

Fix a problem $\boldsymbol{\mu}$, then introduce an alternative model parameterized by $\boldsymbol{\lambda}$, with a small difference between $\boldsymbol{\mu}$. Fix a sub-optimal arm k and $\varepsilon > 0$, and $\lambda_k = \mu_M^* + \varepsilon$ and $\lambda_\ell = \mu_\ell$ for any $\ell \neq k$. We denote $\mathbb{P}_{\boldsymbol{\mu}}^{O_t^j}$ the distribution of the vector O_t^j under the model $\boldsymbol{\mu}$ when using algorithm $\mathcal{A}_j$. Then we introduce the *collision information term* as:

$$\mathcal{I}_{\boldsymbol{\mu},\boldsymbol{\lambda}}(\mathcal{A}_j, T) \doteq \sum_{t=1}^{T} \mathrm{KL}(\mathbb{P}_{\boldsymbol{\mu}}^{C_t|O_{t-1}^j}, \mathbb{P}_{\boldsymbol{\lambda}}^{C_t|O_{t-1}^j}). \tag{6.9}$$

For a *decentralized strategy* $\mathcal{A}$ that has access to the sensing information (*i.e.*, ruling out model (III)), and satisfies $\mathcal{I}_{\boldsymbol{\mu},\boldsymbol{\lambda}}(\mathcal{A}_j, T) = o(\ln(T))$, we now state a problem-dependent asymptotic lower bound on the number of sub-optimal arms selections. The additional hypothesis on $\mathcal{I}_{\boldsymbol{\mu},\boldsymbol{\lambda}}(\mathcal{A}, T)$ essentially says that "the collisions do not bring too much information on the arm means". The theorem stated below is proven in the Appendix of [BK18a], and it also yields an asymptotic logarithmic lower bound on the regret.

Theorem 6.8. *Under observation models (I) and (II), consider a strongly uniformly efficient* decentralized *policy $\mathcal{A} = (\mathcal{A}_1, \dots, \mathcal{A}_M)$ and a problem $\boldsymbol{\mu} \in \mathcal{P}_M$. Furthermore, if $\mathcal{A}_j$ satisfies $\mathcal{I}_{\boldsymbol{\mu},\boldsymbol{\lambda}}(\mathcal{A}_j, T) = o(\ln(T))$, then*

$$\forall j \in [M],\ \forall k \in M\text{-worst},\quad \liminf_{T\to\infty} \frac{\mathbb{E}_\mu[N_k^j(T)]}{\ln(T)} \geq \frac{1}{\mathrm{kl}(\mu_k, \mu_M^*)}. \tag{6.10}$$

And so if $\mathcal{A}_1, \dots, \mathcal{A}_M$ all satisfy this hypothesis, from Lemma 6.6, it follows that

$$\liminf_{T\to+\infty} \frac{R_T^{\mathcal{A}}(\boldsymbol{\mu}, M)}{\ln(T)} \geq M \times \left(\sum_{k \in M\text{-worst}} \frac{(\mu_M^* - \mu_k)}{\mathrm{kl}(\mu_k, \mu_M^*)} \right). \tag{6.11}$$

Observe that the regret lower bound (6.11) is tighter than the state-of-the-art lower bound in this setup, given by [LZ10], that states that

$$\liminf_{T\to+\infty} \frac{R_T^{\mathcal{A}}(\boldsymbol{\mu}, M)}{\ln(T)} \geq \sum_{k\in M\text{-worst}} \left(\sum_{j=1}^{M} \frac{(\mu_M^* - \mu_k)}{\mathrm{kl}(\mu_k, \mu_j^*)} \right), \tag{6.12}$$

as for every $k \in M$-worst and $j \in [M]$, $\mathrm{kl}(\mu_k, \mu_j^*) \geq \mathrm{kl}(\mu_k, \mu_M^*)$. It is worth mentioning that [LZ10] considered the more general assumption for $\mathcal{A}$ that there exists some numbers (a_k^j) such that $a_k^j T - \mathbb{E}_\mu[N_k^j(T)] = o(T^\alpha)$ whereas in Definition 6.7 we make the choice $a_k^j = 1/M$. Our result could be extended to this case, but we chose to keep the notation simple and focus on *fair allocation* of the optimal arms between players. We also highlight that the proof of the bound of [LZ10] contained the same mistake as our proof in [BK18a], but by using the same hypothesis and modification in the proof, it is applicable to the same class of algorithms as our Theorem 6.8 (*i.e.*, algorithms $\mathcal{A}$ such that $\mathcal{I}_{\boldsymbol{\mu},\lambda}(\mathcal{A}_j, T) = o(\ln(T))$).

Price of decentralized learning. Interestingly, our lower bound is exactly a multiplicative constant factor M away from the lower bound given by [AVW87a] for centralized algorithms (which is clearly a simpler setting). This intuitively suggests the number of players M as the (multiplicative) *"price of decentralized learning"*. However, to establish this regret bound, we lower bounded the number of collisions by zero, which may be too optimistic. Indeed, for an algorithm to attain the lower bound (6.11), the number of selections of each sub-optimal arm should match the lower bound (6.10) *and* term (b) and term (c) in the regret decomposition of Lemma 6.5 should be negligible compared to $\ln(T)$.

To the best of the authors' knowledge, no algorithm has been shown to experience only $o(\ln(T))$ collisions in expectation so far, for every $M \in \{2, \dots, K\}$ and $\boldsymbol{\mu} \in \mathcal{P}_M$. The best candidate would be the Sic-MMAB algorithm [BP18], whose number of collisions is proven to be $\mathcal{O}((\ln(T))^2) = o(\ln(T))$ in high probability (Lemma 8), but not $o(\ln(T))$ in expectation. Since our article [BK18a], we kept as a future work the question of finding a lower bound on the minimal number of collisions experienced by any strongly uniformly efficient decentralized algorithm. Such result would thus be a nice complement to our Theorem 6.8.

6.3.3 Towards regret upper bounds

A natural approach to obtain an upper bound on the regret of an algorithm is to upper bound separately each of the three terms defined in Lemma 6.5. The following result shows that term (b) can be related to the number of sub-optimal selections and the number of collisions that occurs on the M best arms.

Lemma 6.9. *The term (b) in Lemma 6.5 is upper bounded as*

$$(b) \leq (\mu_1^* - \mu_M^*)\Big(\sum_{k \in M\text{-worst}} \mathbb{E}_\mu[N_k(T)] + \sum_{k \in M\text{-best}} \mathbb{E}_\mu[C_k(T)] \Big). \tag{6.13}$$

Proof. Recall that we want to upper bound $(b) \doteq \sum_{k \in M\text{-best}} (\mu_k - \mu_{M*}) \left(T - \mathbb{E}_\mu[N_k(T)]\right)$. First, we observe that, for all $k \in M$-best, $T - \mathbb{E}_\mu[N_k(T)] \leq T - \mathbb{E}_\mu\left[\sum_{t=1}^T \mathbb{1}(\exists j : A^j(t) = k)\right] = \mathbb{E}_\mu\left[\sum_{t=1}^T \mathbb{1}(\forall j, A_j(t) \neq k)\right] = \mathbb{E}_\mu\left[\sum_{t=1}^T \mathbb{1}(k \notin \widehat{S}_t)\right]$, where we denote by $\widehat{S}_t = \{A^j(t), j \in [M]\}$ the set of selected arms at time t (with no repetition). With this notation one can write

$$\begin{aligned}(b) &\leq (\mu_1 - \mu_{M^*}) \sum_{k \in M\text{-best}} \left(T - \mathbb{E}_\mu[N_k(T)]\right) \leq (\mu_1 - \mu_{M^*}) \mathbb{E}_\mu \left[\sum_{k \in M\text{-best}} \sum_{t=1}^T \mathbb{1}(k \notin \widehat{S}_t) \right] \\ &= (\mu_1 - \mu_{M^*}) \mathbb{E}_\mu \left[\sum_{t=1}^T \sum_{k \in M\text{-best}} \mathbb{1}(k \notin \widehat{S}_t) \right].\end{aligned}$$

The quantity $\sum_{k \in M\text{-best}} \mathbb{1}(k \notin \widehat{S}_t)$ counts the number of optimal arms that have not been selected at time t. For each mis-selection of an optimal arm, there either exists a sub-optimal arm that has been selected, or an arm in M-best on which a collision occurs. Hence

$$\sum_{k \in M\text{-best}} \mathbb{1}(k \notin \widehat{S}_t) = \sum_{k \in M\text{-best}} \mathbb{1}(C_k(t)) + \sum_{k \in M\text{-worst}} \mathbb{1}(\exists j : A^j(t) = k),$$

which yields

$$\mathbb{E}_\mu \left[\sum_{t=1}^T \sum_{k \in M\text{-best}} \mathbb{1}(k \notin \widehat{S}_t) \right] \leq \sum_{k \in M\text{-best}} \mathbb{E}_\mu\left[\mathcal{C}_k(T)\right] + \sum_{k \in M\text{-worst}} \mathbb{E}_\mu\left[N_k(T)\right]$$

and Lemma 6.9 follows. □

This result can also be used to recover Proposition 1 from [AMTA11], giving an upper bound on the regret that only depends on the *expected number of sub-optimal selections*, $\mathbb{E}_\mu[N_k(T)]$ for $k \in M$-worst, and the *expected number of colliding players on the optimal arms*, $\mathbb{E}_\mu[\mathcal{C}_k(T)]$ for $k \in M$-best. Note that, in term (c) the number of colliding players on the sub-optimal arm k may be upper bounded as $\mathbb{E}_\mu[\mathcal{C}_k(T)] \leq M\mathbb{E}_\mu[N_k(T)]$.

In the next section, we present an algorithm that has a logarithmic regret, by controlling its sub-optimal selections, while ensuring that the number of sub-optimal selections is matching the lower bound of Theorem 6.8.

6.4 New algorithms for multi-players bandits

Regardless of whether sensing is or not possible, we start by presenting formally in Section 6.4.1 the Selfish heuristic, as it was used by all the IoT devices in the first model presented in Chapter 5. It does not use an orthogonalization strategy as the collisions are directly accounted for in the UCB-like indices that are used by each device to select its channel (*i.e.*, by each player to select its arm, in the bandit vocabulary). Selfish can also be used under observation model (III) –*without sensing*, and without the knowledge of M. It was conjectured in [BK18a] that Selfish can suffer linear regret, and later confirmed in [LM18, BP18]. When sensing is possible, that is under observation models (I) and (II), most existing strategies build on a *single-player bandit algorithm* (usually an *index policy*) that relies on the sensing information, together with an *orthogonalization strategy* to deal with collisions. Following this approach, we introduce two new algorithms, RandTopM and MCTopM, in Section 6.4.2.

> **Remark.** We want to strengthen the fact that in all the proposed algorithms, the players do *not* know their numbers $j \in [M]$, and they do not need to know it to achieve low regret. This would be an unrealistic hypothesis, as explained in Section 6.7.1 below.

6.4.1 The Selfish heuristic, with or without "sensing"

Under observation model (III) no sensing information is available and the previous algorithms cannot be used, as the sum of sensing information $S_k^j(t)$ and thus the empirical mean $\widehat{\mu}_k^j(t)$ cannot be computed, hence neither the indices $U_k^j(t)$. However, one can still define a notion of *empirical reward* received from arm k by player j, by introducing

$$\widetilde{S_k}^j(t) \doteq \sum_{t=1}^{T} r^j(t) \mathbb{1}(A^j(t) = k) \quad \text{and letting} \quad \widetilde{\mu_k}^j(t) \doteq \widetilde{S_k}^j(t) \,/\, N_k^j(t). \tag{6.14}$$

Note that $\widetilde{\mu_k}^j(t)$ is no longer meant to be an unbiased estimate of μ_k as it also takes into account the collision information, that is present in the reward. Based on this empirical reward, one can similarly defined modified indices as (where $f(t) = \mathcal{O}(\ln(t))$ is an exploration function)

$$\widetilde{U_k}^j(t) \doteq \begin{cases} \widetilde{\mu_k}^j(t) + \sqrt{f(t)/(2N_k^j(t))} & \text{for UCB,} \\ \sup\left\{ q \in [0,1] : N_k^j(t) \times \mathrm{kl}(\widetilde{\mu_k}^j(t), q) \leq f(t) \right\} & \text{for kl-UCB.} \end{cases} \tag{6.15}$$

Given any of these two index policies (UCB or kl-UCB), the Selfish algorithm is then playing like a single-player index policy (see Algorithm 2.3) $A^j(t) \in \mathcal{U}(\arg\max_{k\in[K]} \widetilde{U_k}^j(t-1))$. The name "selfish" comes from the fact that each player is targeting, in a "selfish" way, the

arm that has the highest index, instead of accepting to target only one of the M best. The reason that this may work precisely comes from the fact that $\widetilde{U_k}^j(t)$ is no longer an upper-confidence on μ_k, but some hybrid index that simultaneously increases when a transmission occurs and decreases when a collision occurs. This behavior is easier to be understood for the case of Selfish-UCB in which, letting $N_k^{j,C}(t) = \sum_{s=1}^t \mathbb{1}(C^j(t))$ be the number of collisions on arm k, one can show that the hybrid Selfish index induces a penalty proportional to the fraction of collision on this arm and the quality of the arm itself:

$$\widetilde{U_k}^j(t) = U_k^j(t) - \underbrace{\left(\frac{N_k^{j,C}(t)}{N_k^j(t)}\right)}_{\text{fraction of collisions}} \underbrace{\left(\frac{1}{N_k^{j,C}(t)} \sum_{t=1}^{T} Y_{A^j(t),t} \mathbb{1}(C^j(t)) \mathbb{1}(A^j(t) = k)\right)}_{\text{estimate of } \mu_k}. \tag{6.16}$$

From a bandit perspective, it looks like each player is using a stochastic bandit algorithm (UCB or kl-UCB) when interacting with K arms that give a feedback (the reward, and not the sensing information) that is far from being *i.i.d.* from some distribution, due to the collisions. As such, the algorithm does not appear to be well justified, and one may rather want to use adversarial bandit algorithms like Exp3 [ACBFS02], that do not require a stochastic (*i.i.d.*) assumption on arms. However, we found out empirically that Selfish is doing surprisingly well when using UCB-like indexes, greatly outperforming Selfish based on Exp3, like what we found in Chapter 5 in harder settings.

We illustrate in Section 6.5.3 that Selfish does have a (very) small probability to fail (badly), for some problem with small K, which precludes the possibility of a logarithmic regret for any problem. In most cases, it empirically performs similarly to all the algorithms described before, and usually outperforms RhoRand, even if it neither exploits the sensing information, nor the knowledge of the number of players M. Practitioners may still be interested by the algorithm, especially for Cognitive Radio applications in which sensing is hard or cannot be considered. In fact, we used the Selfish heuristic in Chapter 5, in the different models, using UCB or Thompson sampling as the underlying policy. Thus we propose next our main contribution, the MCTopM algorithm, proved to be asymptotically optimal for the identification of sub-optimal arms (when using kl-UCB), attaining order-optimal logarithmic regret, and outperforming all the other algorithms for the "sensing case".

6.4.2 Two new strategies based on indices and orthogonalization

The approaches we now describe for multi-players bandits can be used in combination with any index policy (see Algorithm 2.3), but we restrict our presentation to UCB algorithms, for which strong theoretical guarantees can be obtained. In particular, we focus on two types of indices: UCB_1 [ACBF02] and kl-UCB [CGM+13]. For player $j \in [M]$ denote $S_k^j(t) \doteq \sum_{s=1}^t Y_{k,s} \mathbb{1}(A^j(t) = k)$ the current sum of rewards obtained for arm k, then $\widehat{\mu}_k^j(t) \doteq S_k^j(t)/N_k^j(t)$

(if $N_k^j(t) \neq 0$) is the empirical mean of arm k, and thus one can define the index

$$U_k^j(t) \doteq \begin{cases} \widehat{\mu}_k^j(t) + \sqrt{f(t)/(2N_k^j(t))} & \text{for UCB,} \\ \sup\left\{q \in [0,1] : N_k^j(t) \times \mathrm{kl}(\widehat{\mu}_k^j(t), q) \leq f(t)\right\} & \text{for kl-UCB,} \end{cases} \tag{6.17}$$

where $f(t)$ is some *exploration function*, usually taken to be $\ln(t)$ in practice, and slightly larger in theory (*e.g.*, $f(t) = \ln(t) + 3\ln(\ln(t))$), which ensures that $\mathbb{P}(U_k^j(t) \geq \mu_k) \gtrsim 1 - 1/t$ (see [CGM+13]). A classical (single-player) UCB algorithm aims at the arm with the largest index, as presented above in Section 2.4.2. However, if each of the M players selects the arm with the largest UCB, all the players will end up colliding most of the time on the best arm. To circumvent this problem, several coordination mechanisms have emerged, that rely on *ordering* the indices and targeting *one of* the M-best indices.

Two ideas for orthogonalization. On the one hand, the TDFS algorithm [LZ10] relies on the player agreeing in advance on the time steps at which they will target each of the M best indices. Even though some alternative without pre-agreement are proposed, they are quite complicated and we prefer to focus on other approaches. On the other hand, the RhoRand algorithm [AMTA11] relies on randomly selected *ranks*. More formally, letting $\pi(k, \mathbf{U})$ be the index of the k-th largest entry in a vector $\mathbf{U}$, in RhoRand each player maintains at time t an internal rank $R^j(t) \in [M]$ and selects at time t, $A^j(t) \doteq \pi\left(R^j(t), [U_\ell^j(t)]_{\ell \in [K]}\right)$. If a collision occurs, a new rank is drawn uniformly at random, $R^j(t+1) \sim \mathcal{U}([M])$.

Our two proposals. We now propose two alternatives to this strategy, that do not rely on ranks and rather randomly fix themselves on one *arm* in $\widehat{M^j}(t)$, that is defined as the set of arms that have the M largest indices (at the current time t and for player j),

$$\widehat{M^j}(t) \doteq \left\{\pi\left(k, \{U_\ell^j(t)\}_{\ell \in [K]}\right), k = 1, \dots, M\right\}. \tag{6.18}$$

The RandTopM **algorithm.** We precisely state the first proposal below in Algorithm 6.1. RandTopM is essentially a refinement over RhoRand, to not use the indirection of ranks, and a simpler version of MCTopM. The difference with MCTopM is that the latter introduces a concept of a "Chair", by considering a binary "being fixed" state $s^j(t)$, as presented in Algorithm 6.2 below. In RandTopM, player j is always considered "not fixed", and a *collision always forces a uniform sampling of the next arm* from $\widehat{M^j}(t)$.

The MCTopM **algorithm.** The second proposal MCTopM is stated below as Algorithm 6.2, it is a slightly more complex extension of the RandTopM algorithm. From there on, we focus on MCTopM as it is easier to analyze and performs better. Both algorithms ensure that

Let $A^j(0) \sim \mathcal{U}([K])$ and $C^j(0) = \text{False}$
for $t = 1, \dots, T$ **do**
  if $A^j(t-1) \notin \widehat{M^j}(t)$ **then**
    if $C^j(t-1)$ **then** // collision at previous step
      $A^j(t) \sim \mathcal{U}\left(\widehat{M^j}(t)\right)$ // randomly switch
    else // randomly switch on an arm that had smaller UCB
      $A^j(t) \sim \mathcal{U}\left(\widehat{M^j}(t) \cap \left\{k : U_k^j(t-1) \leq U^j_{A^j(t)}(t-1)\right\}\right)$
  else
    $A^j(t) = A^j(t-1)$ // stays on the same arm
  Play arm $A^j(t)$, get new observations (sensing and collision),
  Compute the indices $U_k^j(t+1)$ and set $\widehat{M^j}(t+1)$ for next step.
end

Algorithm 6.1: The RandTopM decentralized learning policy (for an index policy U^j).

player j always selects at time $t+1$ an arm from $\widehat{M^j}(t)$. When a collision occurs for a player implementing the RandTopM algorithm, that player randomly switches arm within $\widehat{M^j}$, while MCTopM uses a more sophisticated mechanism, that is reminiscent of "Musical Chair" (MC) and inspired by the work of [RSS16]: players tend to fix themselves on arms ("chairs") and ignore future collision when this happens.

Let $A^j(0) \sim \mathcal{U}([K])$ and $C^j(0) = \text{False}$ and $s^j(1) = \text{False}$
for $t = 1, \dots, T$ **do**
  if $A^j(t-1) \notin \widehat{M^j}(t)$ **then** // transition (3) or (5)
    $A^j(t) \sim \mathcal{U}\left(\widehat{M^j}(t) \cap \left\{k : U_k^j(t-1) \leq U^j_{A^j(t)}(t-1)\right\}\right)$ // not empty
    $s^j(t) = \text{False}$ // aim at an arm with a smaller UCB at $t-1$
  else if $C^j(t-1)$ and $\overline{s^j(t-1)}$ **then** // collision and not fixed
    $A^j(t) \sim \mathcal{U}\left(\widehat{M^j}(t)\right)$ // transition (2)
    $s^j(t) = \text{False}$
  else // transition (1) or (4)
    $A^j(t) = A^j(t-1)$ // stay on the previous arm
    $s^j(t) = \text{True}$ // become or stay fixed on a "chair"
  Play arm $A^j(t)$, get new observations (sensing and collision),
  Compute the indices $U_k^j(t+1)$ and set $\widehat{M^j}(t+1)$ for next step.
end

Algorithm 6.2: The MCTopM decentralized learning policy (for an index policy U^j).

More precisely, under MCTopM, if player j did not encounter a collision when using arm k at time t, then she marks her current arm as a "chair" ($s^j(t) = \text{True}$), and will keep using it even

if collisions happen in the future (lines 9-11). As soon as this "chair" k is no longer in $\widehat{M_j}(t)$, a new arm is sampled uniformly from a subset of $\widehat{M^j}(t)$, defined with the previous indices $U^j(t)$ (lines 3-5). The subset enforces a certain inequality on indices, $U^j_{k'}(t-1) \leq U^j_k(t-1)$ and $U^j_{k'}(t) \geq U^j_k(t)$, when switching from $k = A^j(t-1)$ to $k' = A^j(t)$. This helps to control the number of such changes of arm, as shown in Lemma 6.13. The considered subset is never empty as it contains at least the arm replacing the $k \in \widehat{M^j}(t-1)$ in $\widehat{M^j}(t)$. Collisions are dealt with only for non-fixed players j, and when the previous arm is still in $\widehat{M^j}(t)$. In this case, a new arm is sampled uniformly from $\widehat{M^j}(t)$ (lines 6-8). This stationary aspect helps to minimize the number of collisions, as well as the number of switches of arm. The five different transitions (1), (2), (3), (4), (5) refer to the notations used in the analysis of MCTopM (in the next section), and they are illustrated in Figure 6.1 below.

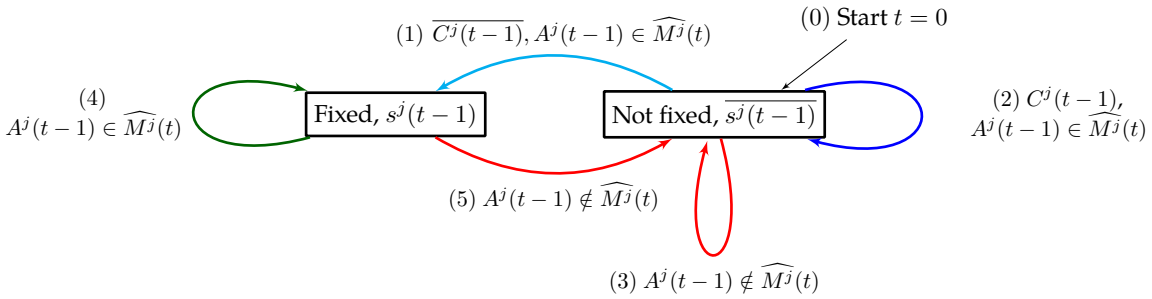

Figure 6.1 – Player j using MCTopM, represented as "state machine" with 5 transitions. Taking one of the five transitions means playing one round of the Algorithm 6.2, to decide $A^j(t)$ using information of previous steps.

6.5 Finite-time upper-bound on the regret of MCTopM

We now focus on obtaining positive results for the algorithms we proposed in Section 6.4 above. Section 6.5.1 gives an asymptotically optimal analysis of the expected number of sub-optimal draws for our two proposals RandTopM and MCTopM as well as for RhoRand, when they are combined with kl-UCB indices, and then we restrict to the most efficient algorithm MCTopM, by proving in Section 6.5.2 that it achieves a logarithmic number of collisions and regret. Finally, Section 6.5.3 shortly discusses a negative result regarding Selfish.

6.5.1 Common analysis for RandTopM- and MCTopM

Lemma 6.10 gives a finite-time upper bound on the expected number of draws of a sub-optimal arm k for any player j, that holds for both RandTopM-kl-UCB and MCTopM-kl-UCB. Our improved analysis also applies to RhoRand. Explicit expressions for C_μ, D_μ can be found in the proof given below.

Lemma 6.10. *For any $\boldsymbol{\mu} \in \mathcal{P}_M$, let player $j \in [M]$ use the* RandTopM-, MCTopM- *or* RhoRand-kl-UCB *decentralized policy with exploration function $f(t) \doteq \ln(t) + 3\ln(\ln(t))$. Then for any sub-optimal arm $k \in M$-worst there exists problem-dependent constants $C_{\boldsymbol{\mu}}, D_{\boldsymbol{\mu}} > 0$ such that*

$$\mathbb{E}_{\mu}[N_k^j(T)] \leq \frac{\ln(T)}{\mathrm{kl}(\mu_k, \mu_M^*)} + \underbrace{C_{\boldsymbol{\mu}}\sqrt{\ln(T)} + D_{\boldsymbol{\mu}}\ln(\ln(T)) + 3M + 1}_{=o(\ln(T))}. \tag{6.19}$$

It is important to notice that the leading constant in front of $\ln(T)$ is the same as in the constant featured in Equation (6.10) of Theorem 6.8. This result proves that the lower bound on sub-optimal selections is asymptotically matched for the three considered algorithms. This is a strong improvement in comparison to the previous state-of-the-art results [LZ10, AMTA11].

Proof. Fix $k \in M$-worst and a player $j \in [M]$. The key observation is that for MCTopM, RandTopM as well as the RhoRand algorithm, it holds that

$$\Big(A^j(t) = k\Big) = \Big(A^j(t) = k, \exists m \in M\text{-best} : U_m^j(t) < U_k^j(t)\Big). \tag{6.20}$$

For each algorithm, the arm selected at time t always belongs to the set $\widehat{M^j}(t)$ of arms with M largest indices. Selecting the sub-optimal arm k at time t implies that $k \in \widehat{M^j}(t)$, and that one of the arms in M-best must be excluded from $\widehat{M^j}(t)$, because there are M arms in both M-best and $\widehat{M^j}(t)$. In particular, arm k must have a larger index than this particular arm m.

Thanks to (6.20) and if $\mathbb{P}_{\boldsymbol{\mu}}$ denote here the probability under model $\boldsymbol{\mu}$, it is easy to decompose the number of selections of arm k by user j up to round T as

$$\begin{aligned}\mathbb{E}_{\mu}[N_k^j(T)] &= \mathbb{E}_{\mu}\left[\sum_{t=1}^{T} \mathbb{1}\left(A^j(t) = k\right)\right] = \sum_{t=1}^{T} \mathbb{P}_{\boldsymbol{\mu}}\left(A^j(t) = k\right). \\ &= \sum_{t=1}^{T} \mathbb{P}_{\boldsymbol{\mu}}\left(A^j(t) = k, \ \exists m \in [M] : \ U_{m^*}^j(t) < U_k^j(t)\right).\end{aligned}$$

Considering the relative position of the upper-confidence bound $U_{m^*}^j(t)$ and the corresponding mean $\mu_m^* = \mu_{m^*}$, one can write the decomposition

$$\begin{aligned}\mathbb{E}_{\mu}[N_k^j(T)] \leq &\sum_{t=1}^{T} \mathbb{P}_{\boldsymbol{\mu}}\left(\exists m_1 \in [M] : \ U_{m_1^*}(t) < \mu_m^*\right) + \\ &\sum_{t=1}^{T} \mathbb{P}_{\boldsymbol{\mu}}\left(A^j(t) = k, \ \exists m_2 \in [M] : \ U_{m_2^*}(t) \leq U_k(t), \forall m_3 \in [M] : \ U_{m_3{}^*}(t) \geq \mu_{m_3}^*\right)\end{aligned}$$

$$\mathbb{E}_\mu[N_k^j(T)] \leq \sum_{m_1=1}^{M}\sum_{t=1}^{T}\mathbb{P}_{\boldsymbol{\mu}}\left(U_{m_1^*}(t) < \mu^*_{m_1}\right) + \sum_{t=1}^{T}\mathbb{P}_{\boldsymbol{\mu}}\left(A^j(t)=k,\ \ \exists m_2\in[M]:\ \mu^*_{m_2}\leq U_k(t)\right)$$
$$\leq \sum_{m_1=1}^{M}\sum_{t=1}^{T}\mathbb{P}_{\boldsymbol{\mu}}\left(U_{m_1^*}(t) < \mu^*_{m_1}\right) + \sum_{t=1}^{T}\mathbb{P}_{\boldsymbol{\mu}}\left(A^j(t)=k,\ \mu_{M^*}\leq U_k(t)\right) \tag{6.21}$$

where the last inequality (for the first term) comes from the fact that μ_{M^*} is the smallest of the μ_{m^*} for $m \in [M]$.

Now each of the two terms in the right hand side of (6.21) can directly be upper bounded using tools developed by [CGM+13] for the analysis of kl-UCB. The leftmost term in (6.21) can be controlled using Lemma 6.11 below that relies on a self-normalized deviation inequality, whose proof exactly follows from the proof of Fact 1 in Appendix A of [CGM+13].

Lemma 6.11. *For any arm k, if $U_k^j(t)$ is the* kl-UCB *index with exploration function $f(t) = \ln(t) + 3\ln(\ln(t))$, then $\sum_{t=1}^{T}\mathbb{P}_{\boldsymbol{\mu}}\left(U_k^j(t) < \mu_k\right) \leq 3 + 4\mathrm{e}\ln(\ln(T))$.*

The rightmost term in (6.21) can be controlled using Lemma 6.12, that is a direct consequence of the proof of Fact 2 in Appendix A of [CGM+13]. Denote $\mathrm{kl}'(x,y)$ the derivative of the function $x \mapsto \mathrm{kl}(x,y)$ (for any fixed $y \neq 0, 1$).

Lemma 6.12. *For any arms k and k' such that $\mu_{k'} > \mu_k$, if $U_k^j(t)$ is the kl-UCB index with exploration function $f(t)$,*

$$\sum_{t=1}^{T}\mathbb{P}_{\boldsymbol{\mu}}\left(A^j(t)=k, \mu_{k'}\leq U_k^j(t)\right) \leq \frac{f(T)}{\mathrm{kl}(\mu_k,\mu_{k'})} + \sqrt{2\pi}\sqrt{\frac{\mathrm{kl}'(\mu_k,\mu_{k'})^2}{\mathrm{kl}(\mu_k,\mu_{k'})^3}}\sqrt{f(T)}$$
$$+ 2\left(\frac{\mathrm{kl}'(\mu_k,\mu_{k'})}{\mathrm{kl}(\mu_k,\mu_{k'})}\right)^2 + 1. \tag{6.22}$$

Putting things together, one obtains the non-asymptotic upper bound

$$\mathbb{E}_\mu\left[N_k^j(T)\right] \leq \frac{\ln(T)+3\ln(\ln(T))}{\mathrm{kl}(\mu_k,\mu_{M^*})} + \sqrt{2\pi}\sqrt{\frac{\mathrm{kl}'(\mu_k,\mu_{M^*})^2}{\mathrm{kl}(\mu_k,\mu_{M*})^3}}\sqrt{\ln(T)+3\ln(\ln(T))}$$
$$+ 2\left(\frac{\mathrm{kl}'(\mu_k,\mu_{M^*})}{\mathrm{kl}(\mu_k,\mu_{M^*})}\right)^2 + 4M\mathrm{e}\ln(\ln(T)) + 3M + 1, \tag{6.23}$$

which yields Lemma 6.10, with explicit constants $C_{\boldsymbol{\mu}}$ and $D_{\boldsymbol{\mu}}$. □

As announced, Lemma 6.13 controls the number of switches of arm that are due to the current arm leaving $\widehat{M^j}(t)$, for both RandTopM and MCTopM. It essentially proves that lines 3-5 in Algorithm 6.2 (when a new arm is sampled from the non-empty subset of $\widehat{M^j}(t)$) happen a logarithmic number of times. The proof of this result is given below.

Lemma 6.13. *For any $\boldsymbol{\mu} \in \mathcal{P}_M$, any player $j \in [M]$ using* RandTopM- *or* MCTopM-kl-UCB, *and any arm k, it holds that*

$$\sum_{t=1}^{T} \mathbb{P}\left(A^j(t) = k, k \notin \widehat{M^j}(t)\right) = \left(\sum_{k', \mu_{k'} < \mu_k} \frac{1}{\mathrm{kl}(\mu_k, \mu_{k'})}\right) \ln(T) \left(\sum_{k', \mu_{k'} > \mu_k} \frac{1}{\mathrm{kl}(\mu_{k'}, \mu_k)}\right) \ln(T) + o(\ln(T)). \tag{6.24}$$

Proof. We analyze the case when the current arm leaves the set $\widehat{M^j}$ (Line 4):

$$\begin{aligned}
&\sum_{t=1}^{T} \mathbb{P}\left(A^j(t) = k, k \notin \hat{M}^j(t)\right) \\
&\leq \sum_{t=1}^{T} \mathbb{P}\left(A^j(t) = k, k \notin \hat{M}^j(t), A^j(t+1) \in \widehat{M^j}(t) \cap \{k' : U^j_{k'}(t-1) \leq U^j_k(t-1)\}\right) \\
&\leq \sum_{t=1}^{T} \sum_{k' \neq k} \mathbb{P}\left(A^j(t) = k, A^j(t+1) = k', U^j_{k'}(t) \geq U^j_k(t), U^j_{k'}(t-1) \leq U^j_k(t-1)\right) \\
&= \sum_{k' \neq k} \underbrace{\sum_{t=1}^{T} \mathbb{P}\left(A^j(t) = k, A^j(t+1) = k', U^j_{k'}(t) \geq U^j_k(t), U^j_{k'}(t-1) \leq U^j_k(t-1)\right)}_{\doteq N_{k'}}
\end{aligned}$$

Now, to control $N_{k'}$, we distinguish two cases. If $\mu_k < \mu_{k'}$, one can write

$$N_{k'} \leq \sum_{t=1}^{T} \mathbb{P}\left(U^j_{k'}(t) \leq \mu_{k'}\right) + \sum_{t=1}^{T} \mathbb{P}\left(A^j(t) = k, U^j_k(t-1) \geq \mu_{k'}\right)$$

The first sum is $o(\ln(T))$ by Lemma 6.11. To control the second sum, we apply the same trick that led to the proof of Lemma 6.12 in [CGM+13]. Letting $\mathrm{kl}^+(x, y) \doteq \mathrm{kl}(x, y)\mathbb{1}(x \geq y)$, and $\widehat{\mu}^j_{k,s}$ be the empirical mean of the s first observations from arm k by player j, one has

$$\sum_{t=1}^{T} \mathbb{P}\left(A^j(t) = k, U^j_k(t-1) \geq \mu_{k'}\right)$$

$$= \mathbb{E}\left[\sum_{t=1}^{T}\sum_{s=1}^{t-1} \mathbb{1}\Big(A^j(t)=k, N_k^j(t-1)=s\Big)\mathbb{1}\Big(s\times \mathrm{kl}^+\left(\widehat{\mu}_{k,s}^j, \mu_k\right) \leq f(t)\Big)\right]$$

$$\leq \mathbb{E}\left[\sum_{s=1}^{T} \mathbb{1}\Big(s\times \mathrm{kl}^+\left(\widehat{\mu}_{k,s}^j, \mu_k\right) \leq f(T)\Big) \sum_{t=s-1}^{T} \mathbb{1}\Big(A^j(t)=k, N_k^j(t-1)=s\Big)\right]$$
$$\leq \sum_{s=1}^{T} \mathbb{P}\left(s\times \mathrm{kl}^+\left(\widehat{\mu}_{k,s}^j, \mu_k\right) \leq f(T)\right), \tag{6.25}$$

where the last inequality uses that for all s,

$$\sum_{t=s-1}^{T} \mathbb{1}\Big(A^j(t)=k, N_k^j(t-1)=s\Big) = \sum_{t=s-1}^{T} \mathbb{1}\Big(A^j(t)=k, N_k^j(t)=s+1\Big) \leq 1.$$

From (6.25), the same upper bound as that of Lemma 6.12 can be obtained using the tools from [CGM+13], which proves that for $T\to\infty$,

$$N_{k'} = \frac{\ln(T)}{\mathrm{kl}(\mu_k, \mu_{k'})} + o(\ln(T)).$$

If $\mu_k > \mu_{k'}$, we rather use that $N_{k'} \leq \sum_{t=1}^{T} \mathbb{P}\left(U_k^j(t) \leq \mu_k\right) + \sum_{t=1}^{T} \mathbb{P}\left(A^j(t+1)=k', U_{k'}^j(t) \geq \mu_k\right)$, and similarly Lemma 6.11 and a slight variant of Lemma 6.12 to deal with the modified time indices yields $N_{k'} = \frac{\ln(T)}{\mathrm{kl}(\mu_{k'}, \mu_k)} + o(\ln(T))$. Summing over k' yields the result. □

6.5.2 Regret analysis of MCTopM with kl-UCB indexes

For MCTopM, we are furthermore able to obtain a logarithmic regret upper bound, by proposing an original approach to control the number of collisions under this algorithm. First, we can bound the number of collisions by the number of collisions for players not yet "fixed on their arms" ($\overline{s^j(t)}$), that we can then bound by the number of changes of arms.

Lemma 6.14. *For any $\boldsymbol{\mu} \in \mathcal{P}_M$, if all players use the* MCTopM-kl-UCB *decentralized policy, and $M \leq K$, then the total average number of collisions (on all arms) is upper-bounded by*

$$\mathbb{E}_\mu\left[\sum_{k=1}^{K} \mathcal{C}_k(T)\right] \leq M^2(2M+1)\left(\sum_{\substack{a,b=1,\dots,K\\ \mu_a<\mu_b}} \frac{1}{\mathrm{kl}(\mu_a,\mu_b)}\right)\ln(T) + o(\ln T). \tag{6.26}$$

Note that this bound is in $\mathcal{O}(M^3)$, which significantly improves over the $\mathcal{O}\Big(M\binom{2M-1}{M}\Big)$ bound, proven by [AMTA11] for RhoRand. The obtained bound is worse than the $\mathcal{O}(M^2)$ proven by [RSS16] for Musical Chair. However, unlike Musical Chair, our algorithm does not need any prior knowledge on the problem complexity, at it is indeed not very satisfying from an applicative point of view to require a prior knowledge of $\mu^*_M - \mu^*_{M+1}$.

Proof. A key feature of both the RandTopM and MCTopM algorithms is Lemma 6.13, that states that the probability of switching from some arm because this arm leaves $\widehat{M^j}(t)$ is small.

Figure 6.1 presented above provides a schematic representation of the execution of the MCTopM algorithm, that has to be exploited in order to properly control the number of collisions. The sketch of the proof is the following: by focusing only on collisions in the "not fixed" state, bounding the number of transitions (2) and (3) is enough. Then, we show that both the number of transitions (3) and (5) are small: as a consequence of Lemma 6.13, the average number of these transitions is $\mathcal{O}(\ln T)$. Finally, we use that the length of a sequence of consecutive transitions (2) is also small (on average smaller than M), and except for possibly the first one, starting a new sequence implies a previous transition (3) or (5) to arrive in the state "not fixed". This gives a logarithmic number of transitions (2) and (3), and so gives $\mathbb{E}_\mu[\sum_k \mathcal{C}_k(T)] = \mathcal{O}(\ln T)$, with explicit constants depending on $\boldsymbol{\mu}$ and M.

As in Algorithm 6.2, $s^j(t-1)$ is the event that player j decided to fix herself on an arm at the end of round $t-1$. Thus $s^j(0)$ is false, and $s^j(t)$ is defined inductively from $s^j(t-1)$ as

$$s^j(t) = \Big(s^j(t-1) \cup \Big(\overline{s^j(t-1)} \cap \overline{C^j(t-1)}\Big)\Big) \cap \Big(A^j(t) \in \widehat{M^j}(t-1)\Big). \tag{6.27}$$

For the sake of clarity, we now explain Figure 6.1 in words. At step t, if player j is not fixed ($\overline{s^j(t-1)}$), she can have three behaviors when executing MCTopM. She keeps the same arm and goes to the other state $s^j(t)$ with transition (1), or she stays in state $\overline{s^j(t)}$ in two cases. Either she sampled $A^j(t)$ uniformly from $\widehat{M^j}(t) \cap \{m : U^j_m(t-1) \leq U^j_k(t-1)\}$ with transition (3), in case of collision and if $A^j(t-1) \in \widehat{M^j}(t)$, or she sampled $A^j(t)$ uniformly from $\widehat{M^j}(t)$ with transition (2), if $A^j(t-1) \notin \widehat{M^j}(t)$. In particular, note that (3) is executed and not (2) if $\overline{C^j(t-1)}$. Transition (3) is a uniform sampling from $\widehat{M^j}(t)$ (the "Musical Chair" step).

For player j and round t, we now introduce a few events that are useful in the proof. First, for every $x = 1, 2, 3, 4, 5$, we denote $I^j_x(t)$ the event that a transition of type (x) occurs for player j after the first t observations (*i.e.*, in round t, to decide $A^j(t)$). Formally they are defined by

$$\begin{aligned}
I^j_1(t) &\doteq \Big(\overline{s^j(t-1)}, \overline{C_j(t-1)}, A^j(t-1) \in \widehat{M^j}(t)\Big), \\
I^j_2(t) &\doteq \Big(\overline{s^j(t-1)}, C_j(t-1), A^j(t-1) \in \widehat{M^j}(t)\Big), \quad \text{and} \quad I_3(t) \doteq \Big(\overline{s^j(t-1)}, A^j(t-1) \notin \widehat{M^j}(t)\Big), \\
I_3(t) &\doteq \Big(s^j(t-1), A^j(t-1) \in \widehat{M^j}(t)\Big), \quad \text{and} \quad I_5(t) \doteq \Big(s^j(t-1), A^j(t-1) \notin \widehat{M^j}(t)\Big).
\end{aligned}$$

Then, we introduce $\widetilde{C^j}(t)$ as the event that a collision occurs for player j at round t if she is not yet fixed on her arm, that is $\widetilde{C^j}(t) \doteq \left(C^j(t), \overline{s^j(t)}\right)$.

A key observation is that $C^j(t)$ implies $\bigcup_{j'=1}^{M} \widetilde{C^{j'}}(t)$, as a collision necessarily involves at least one player $j' \in [K]$ not yet fixed on her arm ($\overline{s^{j'(t-1)}}$). Otherwise, if they are all fixed, *i.e.*, for all j', $s^{j'}(t-1)$, then by definition of $s^j(t-1)$, none of the player changed their arm from $t-1$ to t, and none experienced any collision at time $t-1$ so by induction there is no collision at time t. Thus, $\sum_{j=1}^{M} \mathbb{P}(C^j(t))$ can be upper bounded by $M \sum_{j=1}^{M} \mathbb{P}(\widetilde{C^j}(t))$ (union bound), and it follows that if $\mathcal{C}(T) \doteq \sum_{k=1}^{K} \mathcal{C}_k(T)$ then

$$\mathbb{E}_\mu[\mathcal{C}(T)] \leq M \sum_{j=1}^{M} \sum_{t=1}^{T} \mathbb{P}(\widetilde{C^j}(t)).$$

We can further observe that $\widetilde{C^j}(t)$ implies a transition (2) or (3), as a transition (1) cannot happen in case of collision. Thus another union bound gives

$$\sum_{t=1}^{T} \mathbb{P}(\widetilde{C^j}(t)) \leq \sum_{t=1}^{T} \mathbb{P}(I_2^j(t)) + \sum_{t=1}^{T} \mathbb{P}(I_3^j(t)). \tag{6.28}$$

In the rest of the proof we focus on bounding the number of transitions (2) and (3).

Let $N_x^j(T)$ be the random variable denoting the number of transitions of type (x). Neglecting the event $\overline{s^j(t-1)}$ for $x = 3$ and $s^j(t)$ for $x = 5$, one has

$$\mathbb{E}_\mu[N_x^j(t)] = \sum_{t=1}^{T} \mathbb{P}(I_x^j(t)) \leq \sum_{t=1}^{T} \mathbb{P}\left(A^j(t-1) \notin \widehat{M^j}(t)\right) \leq \sum_{t=1}^{T} \sum_{k=1}^{K} \mathbb{P}\left(A^j(t-1) = k, k \notin \widehat{M^j}(t)\right), \tag{6.29}$$

which is $\mathcal{O}(\ln T)$ (with known constants) by Lemma 6.13. In particular, this controls the second term in the right hand side of (6.28).

To control the first term $\sum_{t=1}^{T} \mathbb{P}(I_2^j(t))$ we introduce three sequences of random variables, the starting times $(\theta_i)_{i\geq 1}$ and the ending times $(\tau_i)_{i\geq 1}$ (possibly larger than T), of sequences during which $I_2(s)$ is true for all $s \in [\theta_i, \ldots, \tau_i - 1]$, but not before and not after, that is $\forall i \in \{1, \ldots, n(T)\}, \overline{I_2^j(\theta_i - 1)} \cap \bigcap_{t=\theta_i}^{\tau_i - 1} I_2^j(t) \cap \overline{I_2^j(\tau_i)}$ with $n(T)$ the number of such sequences, *i.e.*, $n(T) \doteq \inf\{i \geq 1 : \min(\theta_i, \tau_i) \geq T\}$ (or 0 if θ_1 does not exist). If $\theta_i = 1$, the first sequence does not have term $\overline{I_2^j(\theta_i - 1)}$.

Now we can decompose the sum on $t = 1, \ldots, T$ with the use of consecutive sequences,

$$\mathbb{E}_\mu[N_2^j(t)] = \mathbb{E}_\mu\left[\sum_{t=1}^{T} \mathbb{1}\left(I_2^j(t)\right)\right] = \mathbb{E}_\mu\left[\sum_{i=1}^{n(T)} \left(\sum_{t=\theta_i}^{\tau_i - 1} 1 + \sum_{t=\tau_i}^{\theta_{i+1}-1} 0\right)\right] = \mathbb{E}_\mu\left[\sum_{i=1}^{n(T)} (\tau_i - \theta_i)\right].$$

Both $n(T)$ and $\tau_i - \theta_i \geq 0$ have finite averages for any i (as $\tau_i - \theta_i \leq T$), and $n(T)$ is a *stopping time* with respect to the past events (that is, $\mathcal{F}_T^j$), thus we can use Wald's Lemma [Wal45], to obtain a decomposition with two terms (α) and (β), $\mathbb{E}_\mu[N_2^j(t)] \leq \mathbb{E}_\mu[n(T)] \times \max_{i \geq 1} \mathbb{E}_\mu[\tau_i - \theta_i]$.

(α) To control $\mathbb{E}_\mu[n(T)]$, we can observe that the number of sequences $n(T)$ is smaller than 1 plus the number of times when *a sequence begins* (1 plus because maybe the game starts in a sequence). And beginning a sequence at time θ_i implies $\overline{I_2^j(\theta_i - 1)} \cap I_2^j(\theta_i)$, which implies a transition of type (3) or (5) at time $\theta_i - 1$, as player j is in state "not fixed" at time θ_i (transitions (1) and (4) are impossible). As stated above, $\mathbb{E}_\mu[N_x^j(T)] = \mathcal{O}(\ln T)$ for both $x = 3$ and $x = 5$, and so $\mathbb{E}_\mu[n(T)] = \mathcal{O}(\ln T)$ also.

(β) To control $\mathbb{E}_\mu[\tau_i - \theta_i]$, a simple argument can be used. The union of events $\bigcup_{t=\theta_i}^{\tau_i - 1} I_2^j(t)$ implies $C^j(t)$ for $\tau_i - \theta_i$ consecutive times. The very structure of RandTopM gives that in this sequence of transitions (2), the successive collisions (*i.e.*, $C^j(t-1) \cap C^j(t)$) implies that each new arm $A^j(t)$ for $t \in \{\theta_i, \tau_i - 1\}$ is selected uniformly from $\widehat{M^j}(t)$, a set of size M with at least one available arm. Indeed, as there is $M - 1$ other players, at time t *at least* one arm in $\widehat{M^j}(t)$ is not selected by any player $k' \neq k$, and so player j has *at least* a probability $1/M$ to select a free arm, which implies $\overline{C^j(t)}$, and so implies the end of the sequence. In other words, the average length of sequences of transitions (2), $\mathbb{E}_\mu[\tau_i - \theta_i]$, is bounded by the expected number of failed trial of a repeated Bernoulli experiment, with probability of success larger than $1/M$ (by the uniform choice of $A^j(t)$ in a set of size M with at least one available arm). We recognize the mean of a geometric random variable, of parameter $\lambda \geq 1/M$, and so $\mathbb{E}_\mu[\tau_i - \theta_i] = \frac{1}{\lambda} \leq \frac{1}{1/M} = M$.

This finishes the proof as $\mathbb{E}_\mu[N_2^j(T)] = \sum_{t=1}^T \mathbb{P}(I_2^j(t)) = \mathcal{O}(\ln T)$ and so $\sum_{t=1}^T \mathbb{P}(\widetilde{C^j}(t) \cap (A^j(t) = k)) = \mathcal{O}(\ln T)$ and finally $\mathbb{E}_\mu[\mathcal{C}(T)] = \sum_{k=1}^K \mathbb{E}_\mu[\mathcal{C}^k(T)] = \mathcal{O}(\ln T)$ also.

We can be more precise about the constants, by using the previous arguments successively.

$$
\begin{aligned}
\mathbb{E}_\mu[\mathcal{C}(T)] &\leq M \sum_{j=1}^M \left(\sum_{t=1}^T \mathbb{P}(I_2^j(t)) + \sum_{t=1}^T \mathbb{P}(I_3^j(t)) \right) = M \left(\sum_{j=1}^M \mathbb{E}_\mu[N_2^j(T)] + \mathbb{E}_\mu[N_3^j(T)] \right) \\
&\leq M^2 \left(\mathbb{E}_\mu[n(T)] \mathbb{E}_\mu[\theta_i - \tau_i] \right) + M^2 \mathbb{E}_\mu[N_3^1(T)] \\
&\leq M^2 (1 + \mathbb{E}_\mu[N_3^1(T)] + \mathbb{E}_\mu[N_5^1(T)]) M + M^2 \mathbb{E}_\mu[N_3^1(T)] \\
&\leq 2M^3 \mathbb{E}_\mu[N_3^1(T)] + o(\ln T) + M^2 \sum_{\substack{a,b=1,\dots,K \\ \mu_a < \mu_b}} \frac{\ln(T)}{\mathrm{kl}(\mu_a, \mu_b)} + o(\ln T) \\
&\leq \left(2M^3 + M^2 \right) \sum_{\substack{a,b=1,\dots,K \\ \mu_a < \mu_b}} \frac{\ln(T)}{\mathrm{kl}(\mu_a, \mu_b)} + o(\ln T) \,.
\end{aligned}
$$

Thus we prove the desired inequality, with explicit constants depending only on $\boldsymbol{\mu}$ and M.

$$\sum_{k=1}^{K} \mathbb{E}_{\mu}[\mathcal{C}^k(T)] = \mathbb{E}_{\mu}[\mathcal{C}(T)] \leq M^2 (2M+1) \sum_{\substack{a,b=1,\dots,K \\ \mu_a<\mu_b}} \frac{\ln(T)}{\mathrm{kl}(\mu_a,\mu_b)} + o(\ln T) \,. \tag{6.30}$$

□

Logarithmic switching cost for MCTopM**.** While Lemma 6.14 bounds the number of collisions, another consequence of our proof is that we have also bounded the (expected) number of *switches of arms*, $\mathrm{SC}^{\mathcal{A}}(T) = \sum_{t=1}^{T-1} \mathbb{P}(A^j(t+1) \neq A^j(t))$. We controlled the total number of transitions (2), (3) and (5) (see Figure 6.1), which are the only transitions when a player can change its arm. Thus, the total number of arm switches is also logarithmic, if the M players use MCTopM-kl-UCB. This additional guarantee was never clearly stated for previous works, like RhoRand. Even though minimizing the number of arms switching was not a goal, this guarantee is appealing, in particular for Cognitive Radio applications, where switching arms means re-configuring a radio hardware, an operation that costs energy. An algorithm guaranteeing a small number of switches is thus interesting, and for instance [DMNM16] studied the empirical impact of the number of hardware reconfigurations on the battery life of a dynamic end-devices. This work highlighted a trade-off between minimizing regret and minimizing the number of switches of arms. On a more experimental note, it was shown in [DMNM16] that the previous state-of-the-art policy for multi-players bandits, RhoRand, could be tuned to run in batches, in order to reduce by a certain multiplicative factor its switching cost while multiplying its regret by the same factor. While such ideas can interest a practitioner, they does not change the asymptotic behavior of $\mathrm{SC}^{\mathcal{A}_1,\dots,\mathcal{A}_M}(T)$, which is $\Theta(\ln(T))$ for any efficient policy. We also note that introducing explicit *switching costs* in the regret, like it was done in previous works like [TRY17] for single-player bandits, could also be fruitful.

Logarithmic Regret for MCTopM**.** Now that the sub-optimal arms selections and the collisions are both proven to be at most logarithmic in Lemmas 6.10 and 6.14 above, it follows from our regret decomposition (Lemma 6.5) together with Lemma 6.9 that the regret of MCTopM-kl-UCB is logarithmic. More precisely, we obtain a finite-time problem-depend upper bound on the regret of this algorithm.

Theorem 6.15. *If all M players use* MCTopM-kl-UCB*, and $M \leq K$, then for any problem $\boldsymbol{\mu} \in \mathcal{P}_M$, there exists a problem dependent constant $G_{M,\boldsymbol{\mu}}$, such that the regret satisfies:*

$$R_T^{\mathcal{A}}(\boldsymbol{\mu}, M) \leq G_{M,\boldsymbol{\mu}} \ln(T) + o(\ln T) \,. \tag{6.31}$$

Moreover, the dependency of the constant regarding the number of players is $G_{M,\boldsymbol{\mu}} = \mathcal{O}(M^3)$.

Strong uniform efficiency. As soon as $R_T = \mathcal{O}(\ln(T))$ for all problems, MCTopM is clearly proven to be uniformly efficient, as $\ln(T)$ is $o(T^\alpha)$ for any $\alpha \in (0, 1)$. And as justified after Definition 6.7 (page 145), uniform efficiency and invariance under permutations of the users implies strong uniform efficiency, and so MCTopM satisfies Definition 6.7.

6.5.3 Discussion on Selfish

The analysis of the Selfish algorithm is harder, but we obtained some understanding of the behavior of this algorithm, that seems to be doing surprisingly well in many contexts, as in our experiments with $K = 9$ arms and in extensive experiments not reported in this section. However, a disappointing result is that we found simple problems, usually with small number of arms, for which the algorithm may fail. For example with $M = 2$ or $M = 3$ players competing for $K = 3$ arms, with means $\boldsymbol{\mu} = [0.1, 0.5, 0.9]$, the histograms in Figure 6.2 suggest that with a small probability, the regret R_T of Selfish-kl-UCB can be very large.

In the Appendix E of our article [BK18a], we explained when such situations may happen, and we included a conjectured (constant, but small) lower bound on the probability that Selfish experience collision almost at every round. This result would then prevent Selfish from having a logarithmic regret. However, it is to be noted that the lower bound of Theorem 6.8 does not apply to the censored observation model (III) under which Selfish operates. The SIC-MMAB algorithm proposed in [BP18] answers the question we left open last year in [BK18a], of whether logarithmic regret is at all possible for the "no sensing" case (model (III)). They confirmed that Selfish-UCB can indeed suffer linear regret, and proposed an algorithm based on a "communication trick" to achieve logarithmic regret for this harder model (III).

6.6 Experimental results for multi-player bandits with sensing

In all the numerical simulations, we focus on the model with sensing, *i.e.*, model (I) or (II). We illustrate here the empirical performances of the algorithms presented in Section 6.4, used in combination with the UCB or kl-UCB indices. The analysis given in Section 6.5 was focusing on kl-UCB, because it is well known that it is more efficient both in practice and in theory. To illustrate this, we first show below the result of some experiments comparing different algorithms that use either the UCB or the kl-UCB indexes. Our proposed algorithms, MCTopM, RandTopM and Selfish are bench-marked against the state-of-the-art RhoRand algorithm.

We also include a (unrealistic) centralized multiple-play kl-UCB algorithm, as defined by [AVW87a], essentially to check that the *"price of decentralized learning"* is not too large. Centralized multiple-play index policies are very similar to single-player index policies (see Algorithm 2.3), they work by computing an index $U'_k(t)$ for each arm $k \in [K]$, and then sort

the arm by decreasing index, and affect the M players to the M arms with highest index. They are based on a central supervision, as a single algorithm is in charge of deciding the arms used by the M players, and as such they are both unrealistic to set-up in practice, and falling outside of our focus that is on decentralized algorithms.

First experiment: UCB vs kl-UCB. The first experiment is considering $K = 9$ arms, with means $\boldsymbol{\mu} = [0.1, 0.2, \dots, 0.9]$, and $M = 3$ then 6 then 9 players. Note that here and as in all this section we consider different algorithms that know the number of players M (see Section 6.7.1 below for a discussion on the case when M could be unknown). Performance is measured with the *expected* regret up to horizon $T = 10000$, estimated based on 1000 repetitions on the same bandit instance.

Algorithm	**Index policy**	$M = 3$ players	$M = 6$	$M = 9$
Centralized multiple-play	UCB	321 ± 30	233 ± 25	0
	kl-UCB	94 ± 17	68 ± 18	0
Selfish	UCB	1263 ± 157	3694 ± 387	12420 ± 404
	kl-UCB	243 ± 31	743 ± 113	3005 ± 492
RhoRand	UCB	1455 ± 208	4775 ± 463	11794 ± 1083
	kl-UCB	394 ± 96	2385 ± 412	7057 ± 1053
RandTopM	UCB	1020 ± 92	2899 ± 418	470 ± 346
	kl-UCB	258 ± 43	902 ± 234	551 ± 520
MCTopM	UCB	980 ± 76	1466 ± 132	43 ± 13
	kl-UCB	$\mathbf{248 \pm 40}$	$\mathbf{410 \pm 54}$	$\mathbf{42 \pm 10}$

Table 6.1 – Regret for all orthogonalization policies and different numbers of players. Using kl-UCB is much more efficient than using UCB, for multi-players bandit (here in a simple problem with $K = 9$ arms).

We report in Table 6.1 above the results in terms of mean regret, plus or minus one standard deviation. The conclusions are three fold: first we observe for any of the compared algorithms, using kl-UCB is always (much) better than using UCB. Second, we observe that our proposal MCTopM is outperforming the state-of-the-art RhoRand policy, and performs closely to the centralized (unrealistic) approach. Third we observe in the last column, when $M = K = 9$, that MCTopM is achieving constant regret, as we proved that the regret upper-bound of Theorem 6.15 is indeed $\mathcal{O}(1)$ if there is no arms in M-worst, and it shows that the orthogonalization scheme proposed for MCTopM is very efficient, especially in comparison to previous state-of-the-art approaches using ranks. Additional experiments and illustrations are given below. We illustrate below the (empirical mean) regret R_t as a function of time and not only results in terms of empirical mean regret R_T at the end of the bandit game.

The purpose of this work is not to optimize on the index policy, but rather propose new ways of using indices in a decentralized setting, and as we observed in Table 6.1 that using kl-UCB rather than UCB indices always yield better practical performance, from now on we only report results for kl-UCB.

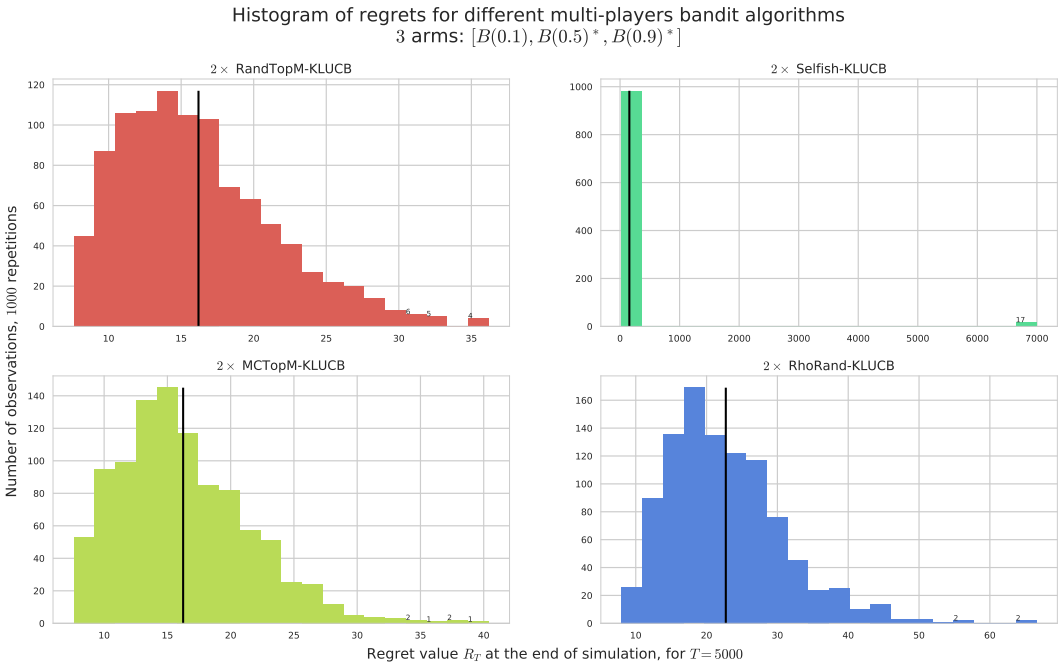

Figure 6.2 – Regret for $M = 2$ players, $K = 3$ arms, horizon $T = 5000$, 1000 repetitions and $\boldsymbol{\mu} = [0.1, 0.5, 0.9]$. Axis x is for regret (different scale for each part), and the green curve for Selfish shows a small probability of having a linear regret (17 cases of $R_T \geq T$, out of 1000). The regret for the three other algorithms is very small for this problem, always smaller than 100 here.

Other experiments. We now present more results for two bandit instances. The first instance is a small problem with $K = 3$ arms and means $\boldsymbol{\mu} = [0.1, 0.5, 0.9]$, for the case of $M = 2$ players. It is used to illustrate that in some unlucky runs, Selfish can suffer a linear regret, as illustrated in Figure 6.2. The second instance considers $K = 9$ arms with means $\boldsymbol{\mu} = [0.1, 0.2, \dots, 0.9]$, three cases are presented: $M = 6$ in Figure 6.3, and for the two limit cases $M = 2$ and $M = 9 = K$ in Figure 6.4. We also include histograms showing the *distribution* of the final regret R_T, as this allows to check if the regret is indeed small for *each* run of the simulation. We also include the *asymptotic* lower bound from Theorem 6.8 on regret plots.

We also compared our algorithms to with MEGA [AM15] and Musical Chair [RSS16], in the presence of sensing, *i.e.*, observation model (II), for which they were developed. Yet these two algorithms were found to both be very hard to use efficiently in practice, and we show in Figure 6.5 that they perform poorly in comparison to RhoRand, RandTopM and MCTopM. MEGA needs a careful tuning of *five* parameters (c, d, p_0, α and β) to attain reasonable performances. No good guideline for tuning them is provided and using *cross validation*, as suggested by [AM15], can be considered out of the scope of *online* sequential learning. Musical Chair consists of a random exploration phase of length T_0 after which the players quickly converge to orthogonal strategies targeting the M best arms. With probability at least $1 - \delta$, its regret is proven to be "constant" (of order $\ln(1/\delta)$). The theoretical minimal value

for T_0 depends on δ, on the horizon T and on a lower bound ε on the gap $\Delta = \mu^*_M - \mu^*_{M+1}$, and the practical tuning is hard too.

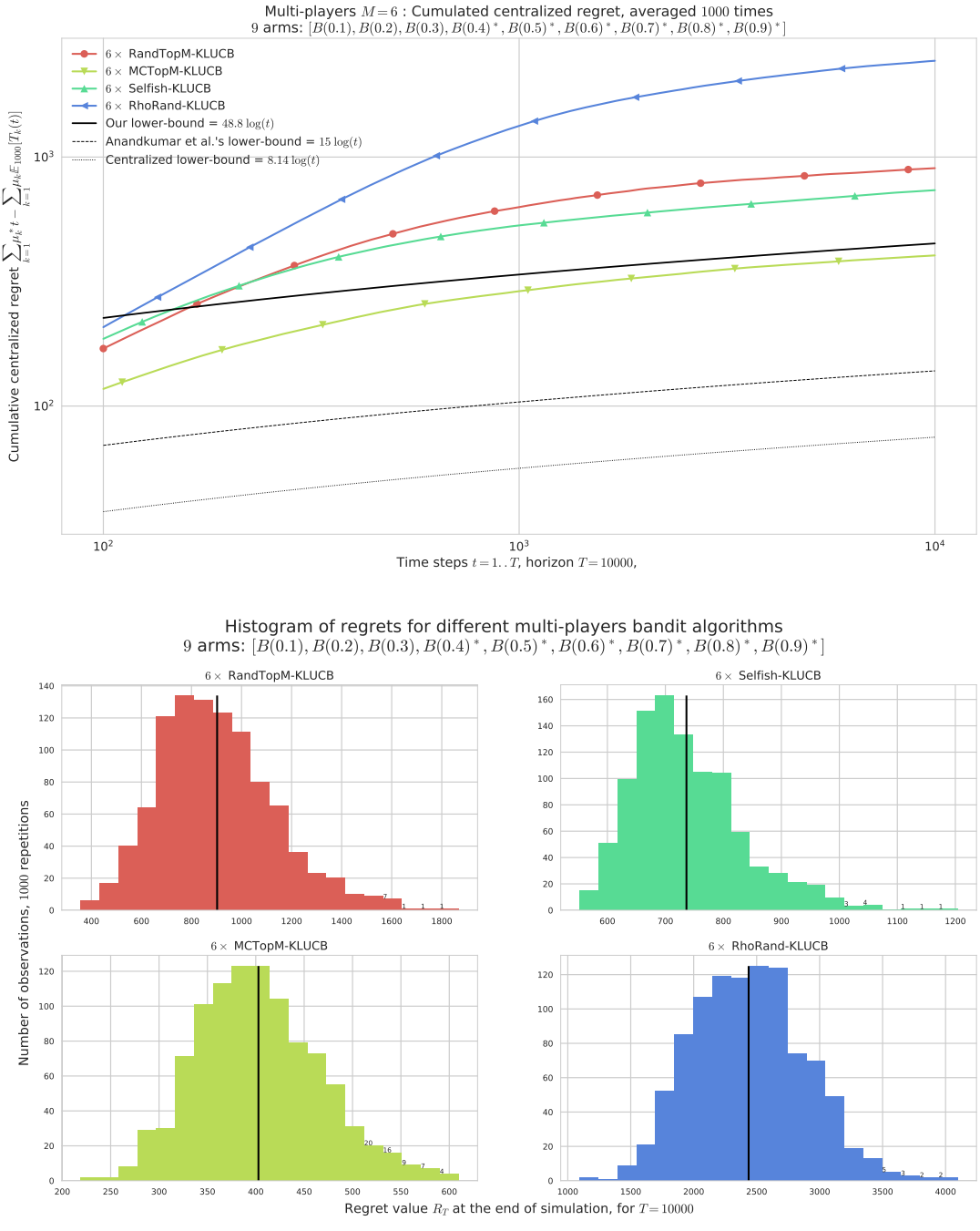

Figure 6.3 – Regret (in log-log scale), for $M = 6$ players for $K = 9$ arms, horizon $T = 5000$, for 1000 repetitions on problem $\boldsymbol{\mu} = [0.1, \dots, 0.9]$. RandTopM (in light green) outperforms Selfish (in green), both clearly outperform RhoRand. The regret of MCTopM is logarithmic, empirically with the same slope as the lower bound. The x axis on the regret histograms have different scale for each algorithm.

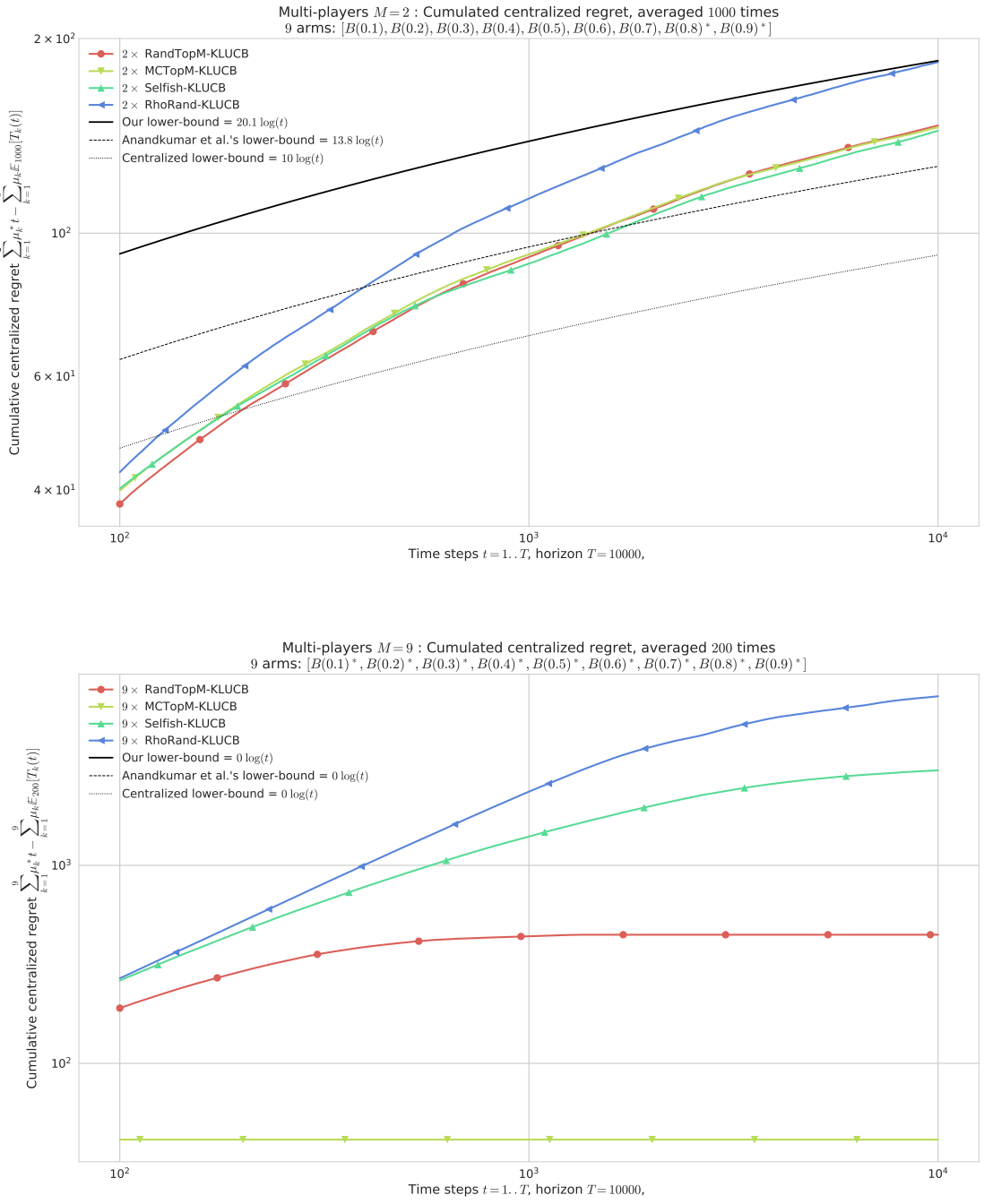

Figure 6.4 – Regret (in log-log scale), for $M = 2$ and 9 players for $K = 9$ arms, horizon $T = 5000$, for problem $\boldsymbol{\mu} = [0.1, \dots, 0.9]]$ for problem $\boldsymbol{\mu} = [0.1, \dots, 0.9]$. In different settings, RandTopM (in light green) and Selfish (in green) can outperform each other, and always outperform RhoRand. MCTopM is always among the best algorithms, and for M not too small, its regret seems logarithmic with a constant matching the lower bound.

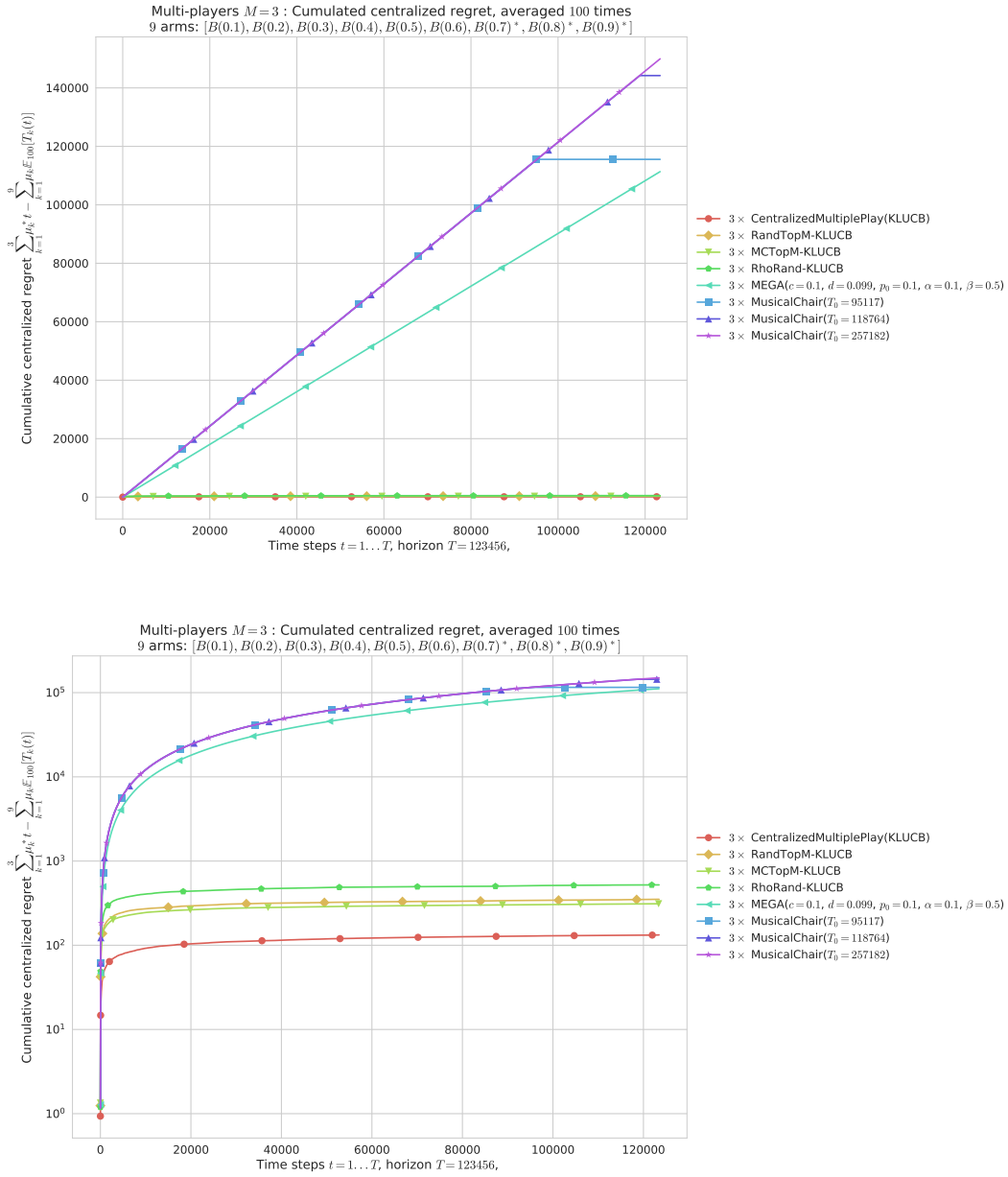

Figure 6.5 – Regret for $M = 3$ players for $K = 9$ arms, horizon $T = 123456$, for 100 repetitions on problem $\mu = [0.1, \dots, 0.9]$. With a perfect knowledge on the horizon and the gap ($\Delta = 0.1$ here) and by using the parameters suggested from their respective articles, MEGA and Musical Chair perform badly, even in this simple setting. The first two Musical Chair instances use the optimal T_0 value from [RSS16], with ε taken slightly smaller than the gap Δ ($\varepsilon = 0.99\Delta$), and respectively with $\delta = 0.5$ and $\delta = 0.1$, for which the regret can be bounded with probability 0.5 and 0.9 respectively. The third instance uses the optimal T_0 corresponding to $\delta = 1/T$, that is guaranteed to have an expected regret of order $\ln(T)$. The log-y scale is used to easily differentiate between the different algorithms, and highlight that our proposal (in light green ∇) outperform both MEGA and Musical Chair by three orders of magnitudes!

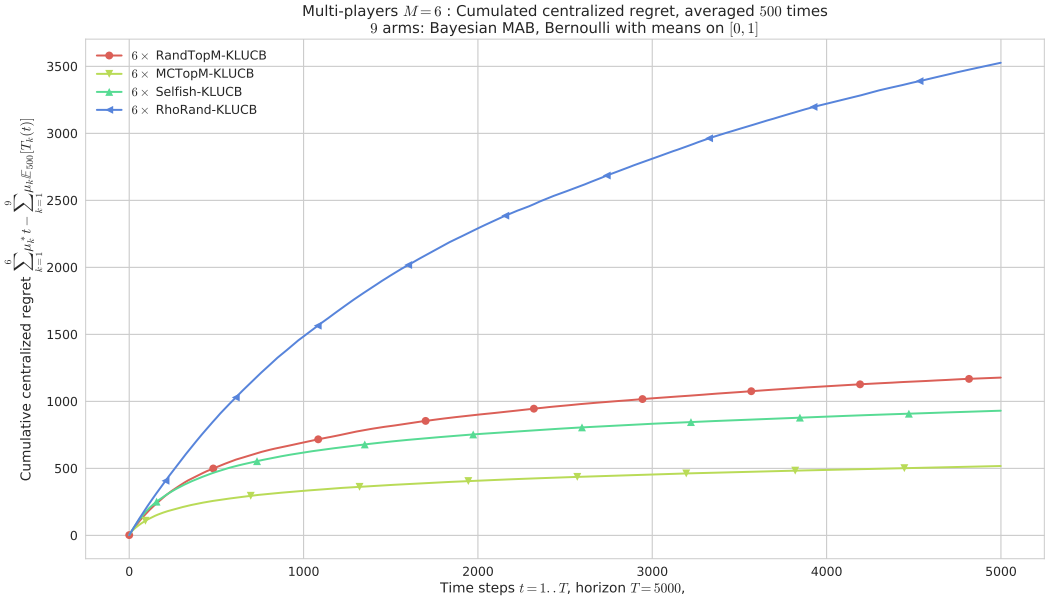

Figure 6.6 – Regret for $M = 6$ players, $K = 9$ arms, horizon $T = 5000$, against 500 problems $\boldsymbol{\mu}$ uniformly sampled in $[0,1]^K$. RhoRand (top blue) is outperformed by the other algorithms (and the gain increases with M). MCTopM (bottom green) outperforms all the other algorithms in most cases.

Uniformly sampled problems. Experiments with a different problem for each repetition, that is uniformly sampled $\boldsymbol{\mu} \sim \mathcal{U}([0,1]^K)$, are also considered, in Figure 6.6 and 6.7. This helps to check that no matter the *complexity* of the considered problem (one measure of complexity being the constant in our lower bound), MCTopM performs similarly or better than all the other algorithms, and Selfish outperforms RhoRand in most cases. Figure 6.6 is a good example of outstanding performances of MCTopM and Selfish in comparison to RhoRand. Empirically, our proposals were found to always outperform RhoRand, and except for Selfish that can fail badly on problems with small K, we verified that MCTopM outperforms the state-of-the-art algorithms in many different problems, and is more and more efficient as M and K grows.

Note that more numerical experiments were conducted for the article [BK18a], and in particular the last pages of the paper show more figures, in other settings.

Reproducibility. The experiments in this chapter use our library SMPyBandits, and the page `SMPyBandits.GitHub.io/MultiPlayers.html` gives instructions to reproduce them.

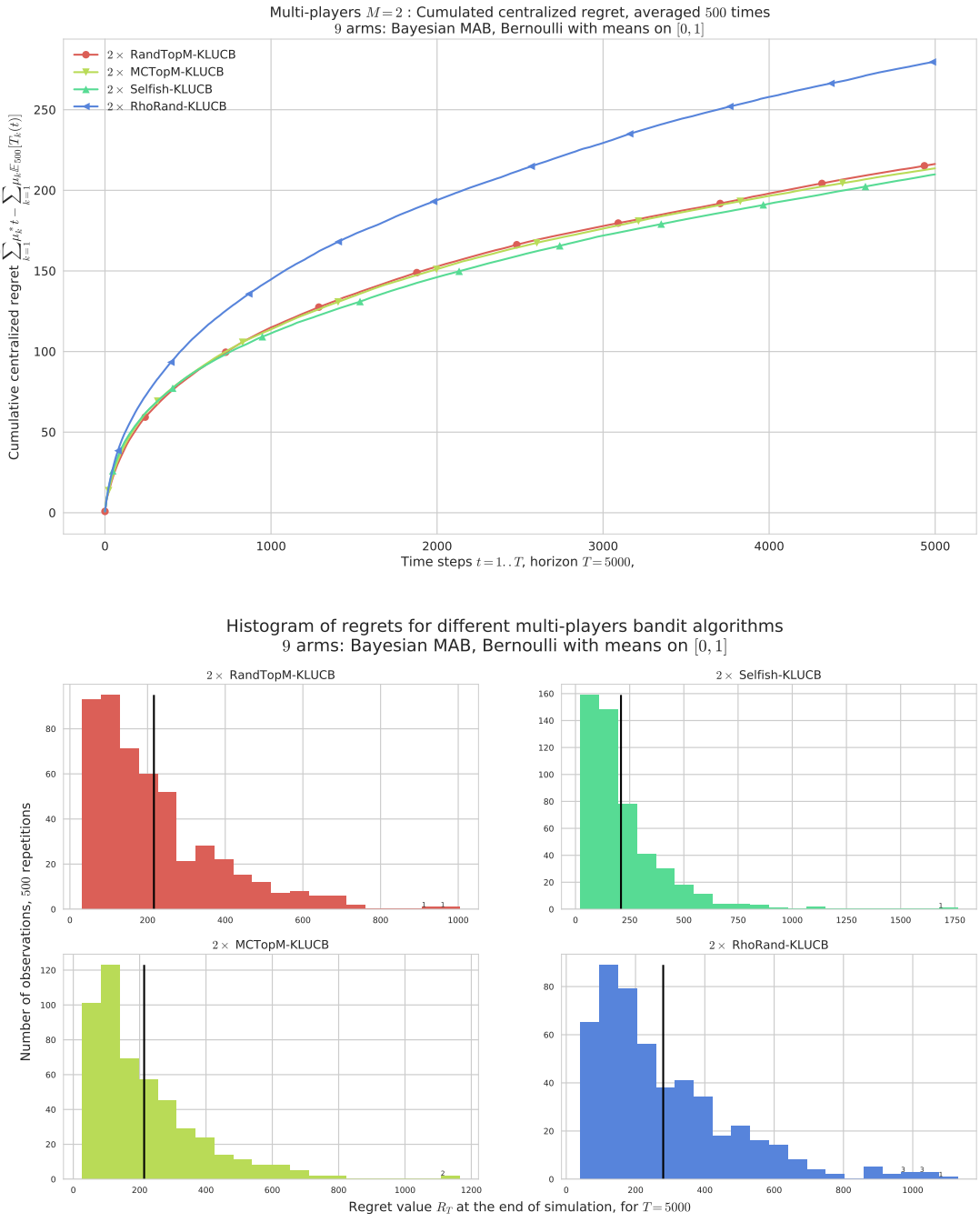

Figure 6.7 – Regret for $M = 2$ players, $K = 9$ arms, horizon $T = 5000$, against 500 problems $\boldsymbol{\mu}$ uniformly sampled in $[0,1]^K$. RhoRand (top blue) is outperformed by the other algorithms (and the gain increases when M increases), which all perform similarly in such configurations. Note that the (small) tail of the histograms come from complicated problems $\boldsymbol{\mu}$ and not failure cases.

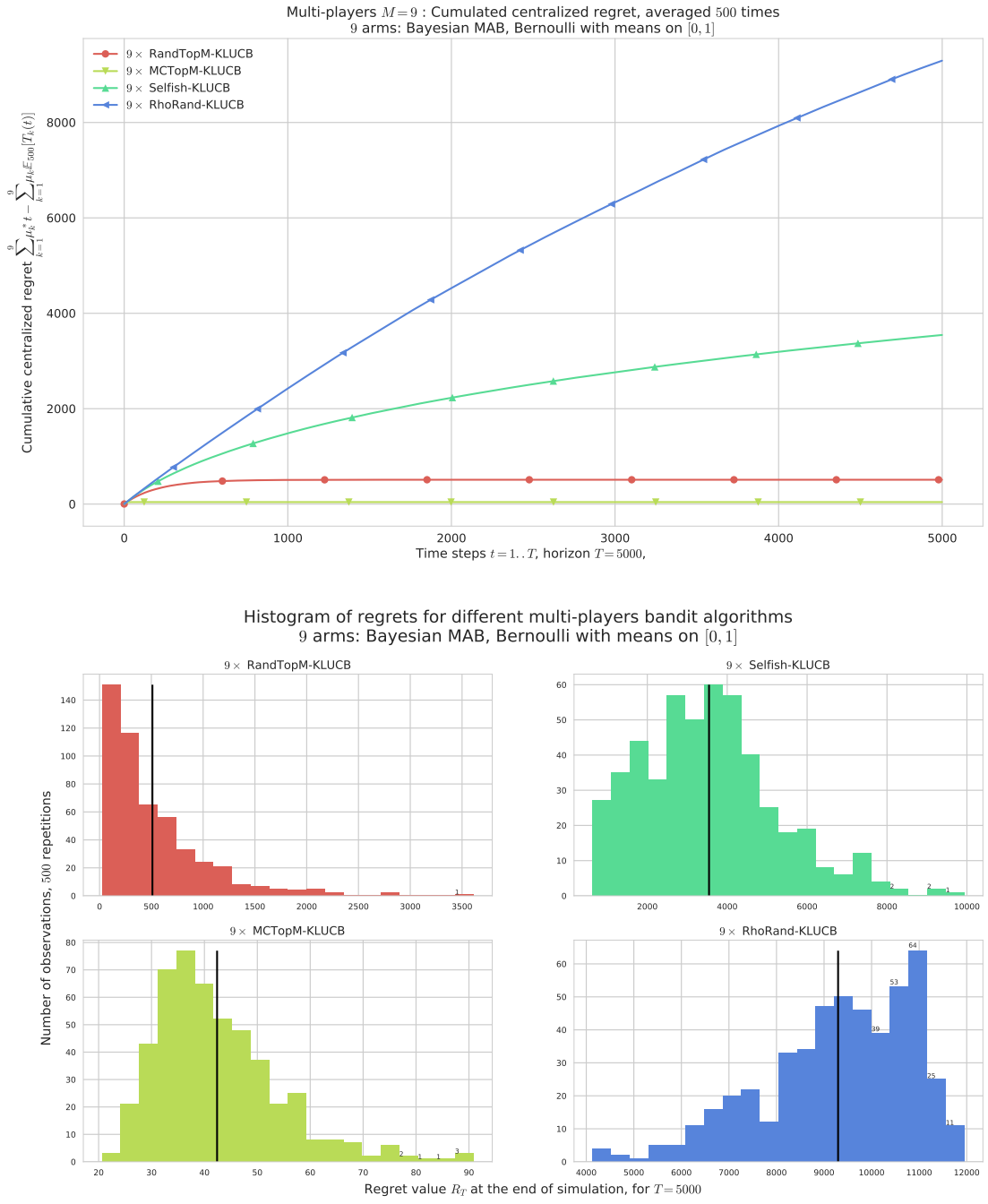

Figure 6.8 – Regret for $M = K = 9$, horizon $T = 5000$, against 500 problems $\boldsymbol{\mu}$ uniformly sampled in $[0,1]^K$. This extreme case $M = K$ shows the drastic difference of behavior between RandTopM (red) and MCTopM (light green), with constant regret, and RhoRand (blue) and Selfish (green), with large regret.

6.7 Literature review of extensions of the multi-player MAB model

Before concluding this chapter, we review many extensions to the three models presented above in Section 6.2 that were introduced in recent literature. We wanted to highlight that the community has been quite active on research on multi-players bandits in the last 10 years, but especially active since last spring 2018. For instance, our article [BK18a] was the first to propose the "no sensing" case, and it was studied by (at least) two independent group of researchers since its publication in April 2018 [BP18, LM18]. Another example is the model with different arm means among players, who was initially studied in [AMT10, KNJ12] and then more recently in [BL18, KM19].

Many extensions of the simpler model of multi-players bandits have been considered. The number of players M can be fixed but initially unknown to the players, the sensing information can be absent (like the model (III) presented above), there could be communications between players (happening at each time step or only occasionally), or M could evolve over time to model the possibility of arrivals or departures of players (*i.e.*, connection's and disconnections of devices in a wireless networks). Also inspired by real-world wireless networks, the arm means may vary among players, for instance to model players located at different distance of the gateway, and we can also consider networks with some "jammers" whose purpose is not to communicate to the gateway in a collaborative way, like the M devices, but to interfere with the communications of the M devices.

Finally, we can also be interested by models where M stays fixed, but the environment evolves, for instance with abrupt changes in the means of arms. This last model makes a good connection between this chapter and the next one, and an exciting future work is to further study this model in order to tackle this kind of problems by merging our contributions for stationary multi-players bandits and for non-stationary single-player bandits.

6.7.1 Unknown (fixed) number of players

In the model we presented above, we assumed the number of players M to be fixed in time during the learning process. Without removing this hypothesis (we study this case below in Section 6.7.2), it is interesting to remark that we made no hypothesis on whether the players can know this value M or not. Our proposals, $\mathrm{RandTopM}$ and MCTopM, both assume to know M beforehand, like it was done for their main inspiration, $\mathrm{RhoRand}$.

Performance of our proposals for a wrong value of M. We can start by asking whether the most efficient algorithm, MCTopM-kl-UCB, is still efficient if it uses a value M' different from the real number of players M. Even though we did not include numerical simulations for this case in Section 6.6 above, we did some tests, which confirmed two disappointing

results that were also proven analytically. First, the three algorithms ($\mathrm{RhoRand}$, $\mathrm{RandTopM}$ and MCTopM) give linear regret if they are using a value M' strictly smaller than M (and if $\mu^*_{M-1} > \mu^*_M$), as players will converge to play about $T - \mathcal{O}(\ln(T))$ times the $M-1$ best arms, leading to at least one collision most of the time, and thus a linear regret. Second, if the M players falsely use a value $M' > M$, then there is also a certain (fixed) probability to achieve a linear regret. Indeed, imagine one player ($M = 1$) running MCTopM with the false knowledge of $M' = 2$, and if it learned to accurately identify the set of the 2 best arms, then the MCTopM orthogonalization scheme can make it play the worst of the two arms, and as $M = 1$ this player will never encounter any collision, thus playing this sub-optimal arm for about $T - \mathcal{O}(\ln(T))$ times, also leading to linear regret.

Interpretation of the hypothesis of knowing M for real-world networks. One could criticize our approach if we study a wireless networks with no central coordination from the gateway, in particular where the devices cannot be assigned to a channel or be assigned a unique ID by the gateway when they first log in the network. Then in such networks, if one wants to apply an algorithm like $\mathrm{MCTopM\text{-}kl\text{-}UCB}$, the M devices need to know their number M, and have to receive it from the gateway, as it is the only part of this example of network which known M. It seems unrealistic to ask the gateway to send the fixed value M to each device, and not a unique ID to each device, for instance $\mathrm{id}^j \in [K]$.

If the M players each have a unique ID, then a simple explore-then-commit algorithm (see Section 2.4.1), running on top of a round-Robin phase can achieve order-optimal regret. If the players know the time horizon T, then they can fix a confidence level δ. For the first T_0 time steps, the M players will use a simple round-Robin game, using their (unique) ID to stay orthogonal: player j starts at arm j, then $j+1$, then cycle in $[K]$. They encounter no collision in these time steps, and then user j targets the j-th best arm among the set of M-best arm. If T_0 is large enough, all players have built the same estimate of the ranking of the arms (and not only correctly identified the set of M-best arms), with high probability (at least δ), and thus they will also encounter no collision and no regret from after time T_0. The mean regret of such approach is easily bounded by $R_T \leq MT_0 + (1-\delta)(T - T_0)$, so by using $\delta = 1 - 1/T$, $R_T = \mathcal{O}(T_0)$. By calibrating T_0 based on δ (which needs prior knowledge of T, see the proof we gave in Section 9) and the minimal gap Δ between $M\text{-best}$ and $M\text{-worst}$, one can show, using similar arguments as used by [RSS16] for the Musical Chair policy, that with large probability a constant regret is obtained. A logarithmic regret can be obtained from the same bound, proving the order-optimist of this simple approach, if we assume that user j knows it is user number j. Without giving more details, we let the interested refer to what is explained for the algorithms presented in [DH18, JKYD18, KDH+19]. These works assume a prior knowledge of Δ, or other measures of the difficulty of the problem, and as such we do not find them comparable with the approach chosen here.

Two ideas to estimate M. Some works studied the same model as model (II) "with sensing", under the hypothesis that players do not know in the value of M. As illustrated above, if we consider algorithms building on the same ideas as RhoRand or MCTopM, it seems mandatory to first build an estimate of the value of M then run the initial algorithm that assumed a perfect knowledge of M. Two possible directions exist to estimate M on the fly.

The first idea comes from [AMTA11], and the intuition behind it is quite simple, even if the mathematical derivations are not. All players will build an estimate $\widehat{M}^j(t)$ of the number of players, that start by $\widehat{M}^j(0) = 1$. As soon as one collision is observed, a player knows that $M \geq 2$, so $\widehat{M}^j(t+1) = 2$. Then, based on probabilistic computations on the expected number of collisions if there were m players, all following the same strategy (*e.g.*, RhoRand in the case of), and because the formula is simple to compute for different m, the authors proposed a statistical test of the hypothesis $M \leq \widehat{M}^j(t)$ against $M > \widehat{M}^j(t)$ which is expressed as a simple comparison of the current number of collisions (since last update of $\widehat{M}^j(t)$) against a threshold. If a player observed "too many" collisions (that are unlikely to be caused by only $\widehat{M}^j(t) - 1$ other players), then she increases her current estimate $\widehat{M}^j(t+1) = \widehat{M}^j(t) + 1$.

The second idea comes from [RSS16], and suppose to know beforehand both the horizon T and a certain measure of the difficulty of the problem (*i.e.*, a lower bound on the minimal gap between two means). If all the M players start to play for a long enough time T_0 uniformly at random among all the K arms, then the (expected) number of collisions observed $\mathbb{E}[\mathcal{C}^j_{T_0}]$ by any player j is a (relatively simple) function of M. By knowing K and T_0 and if all players use the same mechanism, then they can invert the formula to obtain the most likely estimate of M which explained the observations of $\mathcal{C}^j_{T_0}$ collisions. This second approach works empirically very fine, but it requires a fine tuning of the stopping time T_0. J. Rosenski and O. Shamir and L. Szlak study the performance of their algorithm with high-probability bounds [RSS16], and the tuning of T_0 they propose depends on prior knowledge on the problem. For this reason, we are not fond of this approach, as this hypothesis is quite unrealistic if one wants to apply this kind of algorithms for real-world wireless networks. We note that all the following works assume some sort of prior knowledge on the difficulty of the problem: [KDY+17, KYDH18, SKHD18, JKYD18, DH18, KDH+19, TPHD19].

Extension of our proposals to learn the value of M. Similarly to what was proposed for the RhoEst algorithm in [AMTA11], we could have worked on proposing and analyzing an extension of our proposals that could efficiently learn the value of M the number of players. We implemented this RhoEst policy in our library SMPyBandits [Bes19], as well as this mechanism for RandTopM and MCTopM. Building from the theoretical analysis given for RhoEst in [AMTA11], and the analysis of MCTopM-kl-UCB, we believe it is possible to show that the aforementioned extension also achieves sub-linear regret without requiring players to know M in the beginning of the bandit game. More precisely, we believe that

MCTopM-kl-UCB can still give order-optimal logarithmic regret if M players use it, and this extension of Theorem 6.15 is not included due to space constraints. Writing its proof and performing more simulations are left as possible future work.

Simulations. We consider a bandit problem with $K = 9$ arms, of means $0.1, \dots, 0.9$, and three different cases of $M = 3, 6, 9$ players, for 100 independent repetitions and a horizon of $T = 10000$. As before, we include the centralized multiple-play kl-UCB as an unachievably efficient baseline, the Selfish-kl-UCB algorithm as a heuristic which does not require to know M. Then we compare the RhoRand, RandTopM and MCTopM algorithms, using kl-UCB, which know M beforehand, with their extensions implementing the same algorithm as RhoEst, to estimate M on the fly.

Algorithms	**Hyp. on M**	$M = 3$ players	$M = 6$ players	$M = 9$ players
Centralized multiple-play	Known M	$\mathbf{92 \pm 20}$	$\mathbf{70 \pm 16}$	$\mathbf{0}$
Selfish	Don't need M	250 ± 34	735 ± 85	3010 ± 472
RhoRand	Known M	417 ± 103	2481 ± 449	6639 ± 1035
	Estimate M	1422 ± 1051	9030 ± 1922	7264 ± 1009
RandTopM	Known M	268 ± 45	941 ± 217	437 ± 367
	Estimate M	688 ± 614	4256 ± 2701	1155 ± 544
MCTopM	Known M	244 ± 39	401 ± 55	44 ± 13
	Estimate M	563 ± 546	1560 ± 1293	618 ± 29

Table 6.2 – Mean regret $\pm$ 1 std-dev, for different algorithms on the same problem with $M = 3, 6, 9$, comparing algorithms which knows M against algorithms which estimate M on the fly. All use kl-UCB.

One can observe in Table 6.2 the empirical performances of different algorithms in an example problem, in each case of low, medium and maximum number of players ($M = 3, 6, 9$ for $K = 9$ arms). The three algorithms RhoRand, RandTopM and MCTopM all suffer from similar increase on their regret when they have to estimate M on the fly (written "Estimate M" in red, in Table 6.2). Our proposals are still much more efficient than RhoRand when using the procedure to estimate M described from [AMTA11]. For the two non-extreme cases ($M = 3, 6$), the performance drop when having to estimate M is quite large, and consistent on the different algorithms.
The extreme case of $M = K$ players is of highest interest, as MCTopM achieves a very small regret (proven to be $\mathcal{O}(1)$ as it is just the expected time of the orthogonalization process), while the same algorithm with unknown M suffers from a much larger regret. In this extreme case, RhoRand and its extension both perform very closely, as expected, and much worse than MCTopM. Additional simulations, for increasing time horizons T, confirmed the expected order-optimal regret of this extension of MCTopM-kl-UCB.

6.7.2 Arrival and departures of players: the "dynamic setting"

As reminded above, the model assumes that the number of players M remains fixed during all the bandit game. However, in real-world wireless networks, when players model communicating devices connected to a single gateway, devices can arrive or leave the network at any time. The existing previous work on multi-players bandit models are all motivated by possible applications to wireless networks, but most of them assume M to be fixed. The first work studying the relaxation of this hypothesis is [RSS16], where this case is called the "dynamic setting". If the arrival or departures of players is not random, but determined in advance while still being unknown to any player, the natural notion of regret is the following, where the expectation $\mathbb{E}[\bullet]$ is capturing the randomness in the sensing information, as well as in the players' decisions (*i.e.*, collisions):

$$R_T^{\mathrm{dyn}} \doteq \sum_{t=1}^{T} \sum_{k=1}^{M(t)} \mu_k^* - \mathbb{E}\left[\sum_{t=1}^{T} \sum_{j=1}^{M(t)} r^j(t)\right]. \tag{6.32}$$

In [RSS16], the authors explain that if the model allows arrival or departures of players at *any time step*, then the game is much harder, and sub-linear regret is most likely un-achievable, if we consider the natural extension of the definition of regret as in the model presented in Section 6.2 above. But this negative results depends on how arrival of players are modeled: if an arriving player has no prior memory of the previous observations, *i.e.*, if it model a new device, then if there is no restriction on the number or frequency of arrival or departures, we can most likely prove that sub-linear regret is not achievable in general. A simple but extreme example shows that regret has to be linear for any bandit strategy (in the observation model with sensing). Consider $K = 2$ Bernoulli-distributed arms of means $\mu_1 = \mu_2 = 1/2$, and one player is always active and play any bandit strategy (*e.g.*, $\mathrm{MCTopM\text{-}kl\text{-}UCB}$). Every time step, another player is either arriving, without any knowledge of the problem (*e.g.*, it is a fresh and new IoT device). Then no matter the strategy of these new players, even if they all play $\mathrm{MCTopM\text{-}kl\text{-}UCB}$ for instance, if they play a uniformly efficient strategy there is a non-zero probability that player 1 suffers from a collision at each time step, thus resulting in linear centralized system regret.

The authors of [RSS16] also assume that the players all know a lower-bound L on the length of all the intervals during which arrival or departures of players are allowed. A naive idea, if L is large enough, is simply to restart the underlying algorithm every L time steps, in order to directly benefit from the theoretical guarantees of the "static setting" (where M stays constant). Unfortunately this idea yields a large regret if the length of "static" intervals L is too small. Applied to the $\mathrm{Musical\,Chair}$ algorithm, the authors in [RSS16] call this basic extension Dynamic $\mathrm{Musical\,Chair}$Under the simple hypothesis that the overall number of players entering and leaving the game is sub-linear in T (*i.e.*, a $o(T)$), they analyze the regret

of Dynamic Musical Chair and prove it is also sub-linear (see Theorem 2 in Section 3.4). Under the same hypothesis, and if the lower-bound L is known before-hand and is large enough, then we could also apply the same idea as from [RSS16] to our approach. We believe that we could easily prove a sub-linear regret bound, if all players run MCTopM-kl-UCB, and if currently active players restart their memory of the past observations every L time steps. As the regret guarantee is stronger (*i.e.*, smaller regret upper-bound) for MCTopM than Musical Chair, we also believe that in this "slowly varying" dynamic setting, applying the idea of Dynamic Musical Chair from [RSS16] to MCTopM would also give a small regret upper-bound.

After being introduced in [RSS16], some more recent works studied the case of arrival or departures of players, usually referred to as "dynamic setting" or "dynamic case". For instance, [BP18] studies in Section 4 the first algorithm proposed for the dynamic case under the no-sensing model. They study the same notion of regret as the one proposed in [RSS16] and given above in (6.32), see Equation (10) in Section 4.2.1. With the assumption of a non-decreasing number of players, *i.e.*, if only arrivals of players are considered, they prove a regret upper-bound of the Dyn-MMAB algorithm in Theorem 3 . If all arriving players are using their Dyn-MMAB algorithm, the "dynamic" regret is bounded by $\mathcal{O}(M^2 K \ln(T)/\mu^*_M)$, if $M = M(T)$ is the total number of players involved in the problem.

6.7.3 Without sensing information

We presented in Section 6.2 the model (III), without sensing information. Players can only observe $Y_{k,t}$, the product of the *i.i.d.* random sensing information from arm k and of the no-collision indicator. This model seems harder than the model with sensing information, and even though the proposal Selfish works fine in simulations (in terms of average regret), we proved that it can yield linear regret. In our paper [BK18a] as well as in the previous sections, it was left as a future work to know if an algorithm can achieve sub-linear regret in this harder model without sensing information.

Inspired by the publication of our article [BK18a], E. Boursier and V. Perchet studied this question in the following summer 2018 [BP18]. Their main contribution is an answer to the aforementioned open problem, as they showed that the model without sensing information is essentially not harder than the model with sensing information. Similarly, G. Lugosi and A. Mehrabian studied the same problem [LM18]. In both works, the authors detail algorithms that give a logarithmic system regret, if $M \leq K$ players all independently implement the proposed solution.

The "communication trick". The recent work [BP18] proposed an idea they called the "communication trick". It essentially allow any player to send one bit to all the others, at some pre-agreed time steps, with no modification on the model. Thanks to this "communication

trick", recent research efforts have been more focus on studying the basic model –without explicit communications between players–, while proposing algorithms that can rely on some communication between players. This trick essentially use the fact that the players share a synchronized time, thus they can use a collision as a way to directly exchange one bit of information between two players. Such process is slow and not efficient, as all but two players must do nothing when player i is sending a bit to player j, but it does build a communication protocol in the model without explicit communication between players. We note that this "communication trick" is used for instance in [KM19], and we let the interested reader refer to these two recent works [BP18, KM19].

Estimating collisions through uniform exploration. [LM18] gives a first algorithm with expected regret of $\mathcal{O}(MK\ln(T)/\Delta^2)$, if $\Delta = \mu^*_M - \mu^*_{M+1} \neq 0$, achieving a better dependency regarding M when compared to our result (our bound is $\mathcal{O}(M^3)$) but at the cost of (much) larger constants hidden in the $\mathcal{O}$ notation, and a non-fully explicit algorithms which usually obtain bad (or worse) empirical performance. Then they study an interesting extension that works also if $\Delta = 0$ or if Δ is so close than the bound in $1/\Delta^2$ becomes useless for "small horizons". This behavior is well known for classical bandits, where bounds of the form $\ln(T)/\Delta^2$ become worse than a linear regret T if Δ is very small (*i.e.*, $\Delta \ll \sqrt{\ln(T)/T}$). For this extension, their proposed algorithm is proven to achieve $\mathcal{O}\Big(K^2M(\ln(T))^2/\mu + KM\min(\sqrt{T\ln(T)}, \ln(T)/\Delta')\Big)$ regret, if μ is a lower-bound on μ^*_M and $\Delta' = \max(\Delta, \min\{|\mu^*_M - \mu^*_i| : \mu^*_M > \mu^*_i\})$ (that both have to be known beforehand by the algorithm). The proposed algorithms in [LM18] are all based on the Musical Chair algorithm from [RSS16], and the curious reader should read for instance their Algorithm 2 (page 15) for more details.

The results presented in [LM18] are based on some hypotheses, for instance the tuning they propose for the length g of the uniform exploration phase in the beginning of their "Musical Chair"-like algorithm is based on a prior knowledge of the horizon T. In Section 4 they explain how to relax the assumptions of their results. For the same example, the "doubling trick" technique can be used to obtain a regret upper bound for an algorithm unaware of the value of T, within a constant multiplicative factor of the upper bound given for the algorithm aware of T (Section 4.1). Because the regret bound is of the form $\mathcal{O}\Big(\sqrt{T}\ln(T)\Big)$, a simple "doubling trick" of increasing horizons of lengths $T_i = 2^i$ works well, as proposed in [CBL06] and as studied in depth in our article [BK18b]. They also study in Section 4.3 an extension of the model for the case with more players than arms, but we do not give more details on this aspect. Their definition of a centralized regret for this case is an interesting and natural generalization of the definition, and they also proposed an algorithm achieving $\mathcal{O}(MK\ln(T)\exp(4M/K)/\Delta^2)$ regret in this case. Finally, they also proposed in Section 4.4 an extension of their algorithm to estimate the number of players M, which is analyzed as for the Musical Chair algorithm in [RSS16], and also achieve logarithmic regret. Note that it is significantly harder to estimate M without collision information, and Algorithm 3 in page 24 is quite complex. We did not

implement it, and it would be interesting to run some numerical simulations in order to validate it empirically.

About Selfish-UCB **inefficiency.** It is also proven in Appendix A of [BP18] that Selfish-UCB has a linear regret, in the theoretical case, with a very neat argument from number theory (using Lindemann-Weierstrass theorem). As we conjectured, there is a gap between the theoretical result and its practical consequence, as the Theorem 4 they gave is only valid for real-valued number, and not for hardware-represented floating point number. Their proof is supporting what we illustrated in Figure 4 in [BK18a]. Their argument is essentially to prove that for Selfish-powered players using the simple UCB-indexes, with a probability p at time t (both independent from T), two players might have the same number of pulls and the same observed rewards for each arm. In that case, the two players would pull the same arms and thus collide for a long time, until they reach a "tie breaking point" where they could choose different arms thanks to a random tie breaking rule (*e.g.*, if two values of their UCB indexes are the same, the $\arg\max$ is a uniform random choice among the two arms). They prove that it is unlikely to encounter any of these "tie breaking points", in theory if the UCB indexes are real-valued number (that can be rational or irrational).

Additional numerical simulations. To illustrate the difficulty of the "no sensing" case, we illustrate here the performances of different algorithms designed specifically for this setting. As above, we consider a bandit problem with $K = 9$ arms, of means $0.1, \dots, 0.9$, and three different cases of $M = 3, 6, 9$ players, for $N = 100$ independent repetitions, and horizon $T = 10000$. We include the Selfish-kl-UCB algorithm as a heuristic, as well as the Improved Musical Chair algorithm from [LM18] and Sic-MMAB from [BP18]. It is also interesting to add the centralized multiple-play kl-UCB is included as an unrealistic efficient baseline, as it does not use the sensing information but only the joint information (the reward) $r^j(t)$, because it directly affects the player in an orthogonal configuration and thus never encounters any collision (thus $r^j(t) = Y_{t,A^j(t)}$ for each j, t). For the two other algorithms, we use the advised tuning of their parameters: for Sic-MMAB, we used $T_0 = \lceil K \ln(T) \rceil$, for Improved-MC, we used $c = 1$ which gives $g = 235$, whereas in the paper the authors use $c = 128$ for their analysis. We found empirically no difference when using different values of the constant c or g, and unfortunately the regret of Improved-MC was always found to be linear[3].

We give in Table 6.3 the mean regret obtained for these different algorithms, and we observe a drastic difference between the unrealistic centralized algorithm, which achieves a very small regret, the heuristic Selfish-kl-UCB which achieve small mean regret (but is small to fail in theory and in some instances), and the two other algorithms. We were unable

[3] For instance Improved-MC obtained a mean regret 12150 for $T = 10000$, for $M = 3, K = 9$, but seeing one value for one horizon does not mean anything, and we also experimented with larger values of T and found a similar linear behavior.

to find any bug in our implementation of Improved Musical Chair from [LM18] and all the different tuning of c (or g) explored gave the same disappointing result (*i.e.*, linear regret). The Sic-MMAB algorithm performs better than the Selfish heuristic for the extreme case of $M = K$, but its large regret in this case shows that the orthogonalization protocol developed by [BP18] is not fast to converge (for illustration, for the same problem for $M = K = 9$ for the "sensing" case, MCTopM-kl-UCB achieves a mean regret of about 40, two orders of magnitude smaller!). Further empirical evaluation would be needed to fully understand the situation, and a first future work would be to either fix our implementation of the algorithm proposed by [LM18] or propose an efficient modification, and illustrate in some problems that it can indeed achieve sub-linear regret (maybe it does but only for large horizons, even if we did try larger values of T like up-to $T = 200000$).

Algorithms \ Number of players	$M = 3$	$M = 6$	$M = 9$
Centralized Multiple play kl-UCB	$\mathbf{91 \pm 21}$	$\mathbf{70 \pm 16}$	$\mathbf{0 \pm 0}$
Selfish-kl-UCB	249 ± 35	728 ± 94	2953 ± 501
Sic-MMAB	1705 ± 340	3915 ± 300	1713 ± 52
Improved Musical Chair	12149 ± 60	22341 ± 77	27462 ± 85

Table 6.3 – Comparison of the mean regret $\pm$ 1 std-dev, for different algorithms, on the same problem with $M = 3, 6, 9$ players, for the "no sensing" case. More work is needed on our implementation on Improved Musical Chair. The results on Sic-MMAB confirm the numerical experiments of [BP18].

6.7.4 With direct communication or coordination between players

In the models of IoT networks considered in this thesis, we assume that *the different IoT devices cannot communicate with each other*, and can only communicate with their gateway. This hypothesis is realistic, mostly for energy consumption and spectrum efficiency reasons. Of course, we can relax it, and in practice in some families of wireless networks, communication between devices are possible. Note that this extension is *not* considering a graph of distributed agents all playing cooperatively to solve a unique bandit game, like it is studied in the "*graph bandit*" problem [Val16]. We are interested here by an extension of the model where players can send some bits to one or all the other players, at some or every time steps.

Clearly, the problem is easier by allowing communication, and it is quite immediate to see that the communication capacity between players must be limited otherwise the problem is already known and solved. Indeed, imagine that at each time step t, all the M players could share an unbounded number of bits with the other players, at no cost (even if this hypothesis is clearly unrealistic for wireless networks). Then they can share all their observations, and they can all run the same multiple-plays MAB algorithm [AVW87a], like for instance the extension of Thompson sampling for multiple-plays studied in [KHN15], or extensions of KL-UCB from [LKC17]. In this setting, a logarithmic regret is easily obtained, and the regret

upper-bound of the two aforementioned algorithms asymptotically achieve the lower-bound from [AVW87a].

A more interesting extension is thus to limit the communication between players, either to a small number of bits or just one bit, at every or only some time steps. We identified that the state-of-the-art on this direction of research consists in the two very recent works [TZZ19] and [WHCW19]. Distributed pure exploration is studied in [TZZ19], where the proposed new lower bounds for the regret of any algorithm for the distributed best arm identification problem, under the fixed time or fixed confidence settings. The also propose effective algorithms that asymptotically match their lower-bounds (up-to logarithmic factors, in some cases). The second work studies distributed learning for (not necessarily stochastic) multi-armed bandits as well as linear bandits [TZZ19]. For a distributed K-armed bandit with M agents, they developed two protocols achieving near-optimal regret $\mathcal{O}(\sqrt{MKT\ln(T)})$, and requiring little communication cost, one is independent of the time horizon T and use $\mathcal{O}(M\ln(T))$ communications, and the other is independent of the number of arms K and use $\mathcal{O}(MK\ln(M))$ communications. Their model and algorithms fit in the distributed, decentralized framework we advertise in all this thesis, and this last work is very interesting.

Additionally, after the recent work [BP18] introduced the "communication trick", some recent research efforts have been more focus on studying the basic model –without explicit communications between players–, while proposing algorithms that can rely on some communication between players. This "communication trick" is used for instance in [KM19]. Due to space constraint, we let the interested reader refer to these last two works [BP18, KM19] as they are both solid, and well explained.

Another line of research is to consider models that are closer to realistic wireless communication networks, as it is done in [AM16, AM18]. Explaining in details their model and proposed solutions is out of the scope of this thesis, but we sum-up the contributions of the latest [AM18]. They address several aspects of the challenge of communication networks shared by many users simultaneously: learning unknown stochastic network characteristics, sharing resources with other users while keeping coordination overhead to a minimum. The solution they proposed combines Multi-Armed Bandit learning with a lightweight signalling-based coordination scheme, and ensures convergence to a stable allocation of resources. Their work considers single-user level algorithms for two scenarios: an unknown fixed number of users, and a dynamic number of users, both for different arms means for each user. Analytic performance guarantees, proving convergence to stable marriage configurations, are presented for both setups. Similarly to our work, the algorithms are based on a system-wide perspective, rather than focusing on single user welfare.

6.7.5 With different arm utilities among players

In the multi-players model presented in this chapter, we assume that the arm distributions are the same for all the players. For cognitive radio applications, where arms model channels and players are radio devices, it can be unrealistic to consider that two players, maybe located at different distances from the gateway or equipped with different hardwares, encounter the same mean quality when accessing the same channel. Motivated by this weakness, some researchers studied an interesting extension of the model of interest, considering multi-players MAB models with different arms distributions among players. Starting in 2012 by [KNJ12] where arms are Markov chain, this model was studied more actively recently, in two articles published in 2018 [DH18, BL18] and two more in 2019 [KM19, TPHD19].

In such models, instead of considering K arms characterized by a vector of distributions, $(\nu_k)_{1\leq k\leq K}$, if there is M players we consider a *matrix of distributions*, $(\nu_k^j)_{1\leq k\leq K, 1\leq j\leq M}$. Two users j and j' can experience different utilities for the same arm k, *i.e.*, $\nu_k^j \neq \nu_k^{j'}$. The goal stays the same, each player wants to maximize its cumulated reward, with or without explicit communications between players, with or without sensing information, but always without central supervision. Like before, maximizing the rewards of each player simultaneously is maybe not possible. As soon as the matrix is not invariant under permutation of the users, the problem nature changes fundamentally: instead of finding an optimal orthogonal assignment of the M players to the M-best arms, the goal of the system is now to reach an equilibrium position, also referred to as a stable marriage. Assignment are also called matching, and total (mean) reward of an assignment is its utility. Such equilibrium position means that the utility obtained by the M player cannot be increased by swapping two users. Indeed imagine just $M = 3$ players and $K = 3$ arms, and Bernoulli distributions of means $[0.1, 0.5, 0.5]$, $[0.1, 0.5, 0.5]$ and $[0.9, 0.5, 0.1]$ for player 1, 2 and 3. Then two optimal affectations of players to arms are $[3, 2, 1]$ or $[2, 3, 1]$, both giving the same utility of 1.9.

In this extension, performance is still evaluated by a system regret, now defined as the difference between the sum of the cumulated rewards by the M players, and the utility of any matching. The question is to know if it is possible to obtain a logarithmic –or even sub-linear– regret in this problem is more difficult that for the model presented in Section 6.2. This question was first answered in [BL18], and proposed an algorithm based on alternating three phases, and increasing their lengths after the end of each epoch (2^p for the p-th epoch). First, players explore in order to estimate the expectations of the arm rewards ; then players use their "Game of Thrones" dynamics (GoT, inspired by Musical Chair [RSS16]) and play the optimal solution most of the time ; finally players play the action they played most of the time in the recent GoT phases. They proved that their GoT algorithm achieves a regret of $\mathcal{O}((\ln(T))^{2+\kappa})$, for any positive constant κ, as small as possible, if κ is known by the algorithm.

Until the very recent work of [KM19], it was unknown if a logarithmic regret was possible. They proposed an algorithm that is based on two phases: first, players will learn M and learn orthogonal ranks, using the "communication trick" of [BP18], and then one player is elected as a leader and the others are followers. This second step, after initialization, is also using epoch of increasing lengths 2^p. Until the optimal solution, each epoch is alternating three phases. Followers start by a Round-Robin uniform exploration with no collision, then they use the "communication trick" to communicate their samples to the leader, and finally they start an exploitation phase until the end of the game if the leader player tells them so. The leader can thus collect enough samples from all arms and all players, and is able to solve iteratively the stable marriage problem, and sends back the successive estimate of the solution to the players. In the easiest case when their is a unique optimal matching, their algorithm Multiplayer Explore-Then-Commit (M-ETC) is the first one to achieve logarithmic regret, in the form of $R_T = \mathcal{O}\left(MK\ln(KT) + KM^3\ln(MKT)/\Delta + KM^2(\ln(M\ln(KT)/\Delta))^2\right)$, if Δ is defined as the gap between the utility of the best matching and the utility of that of the matching with second best utility. In the generic case, their algorithm M-ETC with Elimination achieves a regret of $\mathcal{O}((\ln(T))^{1+\kappa})$ for any positive constant κ.

Finally, we note that previous works all focused on the "sensing" case, but most likely sub-linear regret can be achieve by decentralized algorithms that leverage the same techniques as introduced by [BP18, LM18] for the "no sensing case". We conclude by noting that this model was recently studied by two very recent other works, [DH18, TPHD19], who obtained results comparable to the results from the two works presented above. They both also study the case of dynamic settings, with arrival or departures of players, as presented in Section 6.7.2. Both articles [DH18, TPHD19] use the terminology of ad-hoc networks, and they compare empirically their proposal with some previous works, while [KM19] do not include numerical simulations, and while [BL18] illustrate the performance of their GoT algorithm on a simple example, they do not compare with other algorithms. It would be interesting to compare empirically all the different approaches. Another interesting directions are to study the possible extension of this model with different arm utilities by players to the non-stationary case, or real-world validation of such decentralized algorithms in real IoT networks.

6.7.6 Modeling more closely a real wireless network

We simply quote here three recent articles which proposed a similar approach of using decentralized reinforcement learning algorithms on the device-side on wireless networks, but proposed models closer to the reality of wireless networks. The first work is [NC17], which proposes to use a decentralized learning based on deep learning, in the "no sensing" case, but in a model where the users have to learn not only the channels to use for their up-link messages (only from the feedback through the acknowledgements, like in Section 5.2), but where they have to learn the whole "spectrum access actions". The work of [AM18] is

discussed above for the case with communicating players, and their model is very interesting from the point-of-view of real-world wireless communication protocols.

Finally, the very recent work of [ZBLN19] is the first one to present experiments of reinforcement learning done on simulated LTE and 5G channels. The mathematics behind their model are actually quite close to the model, but they explain it in terms of OFDMA and Quality-of-Service (QoS). Their algorithm is essentially based on a pre-agreement of the M players, that will deterministically run an alternation of exploration phase, auction phase and exploitation phase, of (exponentially) increasing durations. By diving into the details of the modulation and giving explicitly the form of the up-link messages sent by the devices, the authors are able to set-up two different up-link packets, to efficiently perform the auction phase (see Figure 2). They prove a regret upper-bound of the order $R_T = \mathcal{O}(\ln(T))$, with no special care regarding the constants, but we can also note that their algorithm require a prior knowledge of $\Delta_{\min}$ a problem-dependent constant (Theorem 3).

6.7.7 Can MAB learning also be used to learn the rank for RhoRand ?

Similarly to the proof-of-concept of applying MAB learning in an IoT network that we presented in Section 5.3, in [DNMP16, DMP16], the authors study the same model and focused on the RhoRand policy, for the OSA case. It was the state-of-the-art back in 2016, and the authors combine it with UCB or kl-UCB, as well as an extension using Bayes-UCB from [KCG12]. Their idea is to use the same skeleton as RhoRand, that is to assign a *rank* to each player, and make players change their rank after any collision. But instead of selecting a new rank uniformly at random among $[M]$, they proposed to use a "second-stage" learning policy, based on Bayes-UCB, to (try to) learn the best rank while still exploring each rank from time to time. This is a very natural idea: use a bandit algorithm to balance the exploration/exploitation aspect of rank selection, instead of a random hoping. This algorithm is named RhoLearn, and it is implemented in SMPyBandits, where it can use Bayes-UCB, or any of the 65 or more bandit algorithms available in the library. Even if no theoretical guarantee backs up this idea of second-stage learning with Bayes-UCB, empirical simulations found that it can be efficient. We illustrate this in Table 6.4 below, where we consider the same problem as described above in Section 6.7.3 (Table 6.3). We include different RhoLearn algorithms, that uses kl-UCB, Bayes-UCB or Exp3 for the second-stage learning, and we include both the centralized multiple-play version of kl-UCB and MCTopM-kl-UCB for comparison.

6.7.8 With malicious jammers

In all this chapter and the previous research literature, another common hypothesis is that all the M players are pursuing the same goal, and are all behaving nicely by following the same algorithm. Distributed algorithms proposed in the literature aim to maximize the

Algorithm \ Number of players	$M = 3$	$M = 6$	$M = 9$
Centralized multiple-play kl-UCB	$\mathbf{92 \pm 20}$	$\mathbf{70 \pm 16}$	$\mathbf{0}$
RhoRand-kl-UCB	417 ± 103	2481 ± 449	6639 ± 1035
RhoLearn-kl-UCB + kl-UCB	546 ± 190	1172 ± 295	1416 ± 347
RhoLearn-kl-UCB + Bayes-UCB	561 ± 219	1204 ± 394	1363 ± 331
RhoLearn-kl-UCB + Exp3	529 ± 175	1659 ± 331	5134 ± 976
MCTopM-kl-UCB	244 ± 39	401 ± 55	44 ± 13

Table 6.4 – Comparing RhoRand and RhoLearn on a simple MP-MAB problem with $K = 9$ arms.

network throughput by ensuring orthogonal channel allocation for the SU. However, these algorithms work under the assumption that all the SU faithfully follow the algorithms which may not always hold due to the decentralized nature of the network. In the paper [SKHD18], the authors study for the first time distributed algorithms that are robust against malicious behavior, also called *jamming attack*. They consider both the cases of *jammers* launching coordinated and uncoordinated attacks, and consider a set of J jammers. In the coordinated attack, the jammers select non-overlapping channels to attack in each time slot and can significantly increase the number of collisions for SU. They setup the problem in each scenario as a multi-players bandit and develop algorithm, and their analysis shows that when the SU faithfully implement proposed algorithms, the regret is constant with high probability. They validate their claims through extensive synthetic experiments and also through a realistic USRP. Their synthetic experiments consider different cases, for different values of K the number of channels, M the number of players and J the number of jammers.

6.7.9 Towards non-stationary multi-players MAB models

Since the beginning of this thesis, all the studied bandit problems were stationary: the rewards coming from choosing arm k are *i.i.d.* and follow the same distribution ν_k. The next Chapter 7 is focused on the piece-wise stationary bandit model, a relaxation of this hypothesis.

When we were working on multi-players bandits, in Autumn 2017 and 2018 [BK18a], we left the study of the piece-wise stationary case as a future work, and shortly after we were excited to see that three independent works tackling this question were published, in December 2018 [WS18a] and in February 2019 [ALK19, BV19]. Without diving too much into the details, we review here these three works. Without a more serious analysis, we conjecture that it should not be difficult to merge the regret lower-bound for stationary *multi-players* MAB (Theorem 6.8) and the lower-bound for *piece-wise stationary* single-player MAB from [GM11]. We conjecture that any reasonable decentralized bandit algorithm must suffer a regret at least $\Omega(M\sqrt{K\Upsilon_T T})$ for $M \leq K$ players, K arms, and Υ_T stationary intervals.

Extending the single-player case. On the one hand, piece-wise stationary multi-players MAB can be tackled by extending algorithms developed for the single-player case. In [WS18a], the authors study exactly the same multi-players bandit model as our model, and they propose two distributed algorithms that can efficiently be used by $M \leq K$ players to achieve sub-linear regret for piece-wise stationary problems, essentially by considering it as a harder case of a stationary problem.

The proposed the RR-SW-UCB# algorithm, which combines their SW-UCB# algorithm, previously proposed in [WS18b], and a Round-Robin hoping, under the assumption that each user $j \in [M]$ knows its ID j (we criticize this unrealistic assumption in Section 6.7.1 above). The SW-UCB# algorithm is discussed more in details in the literature review of Chapter 7 below. If Υ_T is bounded by $\Upsilon_T = \mathcal{O}(T^\gamma)$, for a known γ but an unknown Υ_T, they prove for instance in Theorem 2 [WS18a] that the expected cumulative regret of their RR-SW-UCB# algorithm is bounded by $R_T = \mathcal{O}\left(T^{\frac{1+\gamma}{2}} \ln(T)\right)$ (what we call the centralized system regret). This bound is of the same order as the bound obtained by the same authors for the SW-UCB# algorithm in [WS18b] for the single-player case. If $\Upsilon_T = \mathcal{O}(T^\gamma)$, this bound is comparable to the results obtained for most of the research literature on piece-wise stationary bandits (earlier works like D-UCB in [GM11] have the $\ln(T)$ outside the square root, while more recent works all improved this aspect and have the $\ln(T)$ in the square root, like for instance our algorithm GLR-klUCB in [BK19b] and presented in Chapter 7). Even if their analysis is not explicit regarding the constant, in the case where $\Upsilon_T = \mathcal{O}(T^\gamma)$ for a known γ, their regret upper-bound actually matches the conjectured lower-bound, up to a logarithmic factor $\ln(T)$.

And finally, even though numerical simulations in their papers [WS18b, WS18a] are interesting and confirm the regret upper-bounds, they do not compare with any other algorithm, and thus a future work can be to study this direction in more details. Sadly, a major drawback of their work is that assume that player $j \in [M]$ knows its index j, and as we explained above this small hypothesis is actually quite strong, as it allows players to be already orthogonal, and it reduces greatly the difficulty of the decentralized bandit problem.

In the adversarial setting. On the other hand, another possibility is to extend ideas developed for the adversarial setting. In [ALK19], the authors essentially consider the piece-wise stationary as an easier case of an adversarial problem. The recent work [BV19] also proposes a decentralized algorithm that can achieve sub-linear regret ($\mathcal{O}(T^{3/4})$) under an adversarial multi-players bandit model.

In [ALK19], the authors build on the Musical Chair algorithm from [RSS16], to let the M players converge to a ranking in an efficient and decentralized way (cf. Algorithm 1), and they apparently discovered the "communication trick" independently from [BP18] to use (virtual) communications between players to set up a "coordinator" player and $M-1$ "followers" (running respectively their Algorithms 2 and 3). Their key algorithmic technique

is to imitate the idealized case where there is full communication between the players. Then, to address the no-communication constraint, we enforce the players to keep the same decisions (arms) within long periods of time (blocks). This gives them the chance to coordinate between themselves via a simple protocol that uses collisions as a primitive, yet effective manner of communication.

Their proposal is using the Exp3 algorithm from [ACBFS02] on a combinatorial problem: they consider "meta" arms that are affectations of the M players to M distinct arms among the K arms. As soon as the "coordinator" can effectively use one algorithm to decide the arms played by all the M players, they show that the regret will grow as $R_T = \mathcal{O}\Big(M^{4/3}K^{2/3}(\ln(K))^{1/3}T^{2/3}\Big)$ as shown in Theorem 4.1 (they used K for M the number of players, and N for K the number of arms). This bound is much worse than the one obtained for the first article [WS18a], but is more general, and it is much worse than the bound of $\mathcal{O}\Big(\sqrt{KT\ln(K)}\Big)$ obtained for Exp3 for the single-player adversarial setting in [ACBFS02]. Note that this bound in $T^{2/3}$ is of the same order as the one given in [AM15], for the MEGA algorithm. However, we note that the dependency in M is surprisingly better for their result than for the regret upper-bound for MCTopM-kl-UCB (which scales in M^3 in Theorem 6.15).

Moreover, at first sight, this idea of "meta" arms implies an exponential blowup in terms of computational and storage cost, as there is $\binom{M}{K}$ such "meta arms", but the authors provide in Section 4.1 and Lemma 4.1 [ALK19] an interesting discussion regarding the time efficiency of their proposed algorithm, and they show it can stay polynomial in M and K by leveraging techniques from the Determinental Point Processes (DPP, see [GBV18] and references therein for a good introduction). In this second work also, we can note the poor experimental section, as the proposed algorithm is only compared against the Musical Chair algorithm, in "easy" problems (small number of break-points Υ_T). Despite being more complicated than other approaches, their algorithm "`C & P`" should not be too hard to implement by ourselves, and studying its empirical performance is an interesting future work.

6.8 Conclusion

To sum up, we presented in this chapter three variants of Multi-Players Multi-Armed Bandits, with different levels of feedback being available to the decentralized players, under which we proposed efficient algorithms. The two easiest models are the ones with sensing information (*i.e.*, for OSA), for which our theoretical contribution improves both the state-of-the-art upper and lower bounds on the regret. In the absence of sensing, we also provide some motivation for the practical use of the interesting Selfish heuristic, a simple index policy based on hybrid indices that are directly taking into account the collision information, like in Chapter 5.

We also reviewed various variants of this model and we discussed the related literature, which has proven to be very active in the last two years. For some models, we explained why our approach does not work efficiently without modifications, but we detailed and illustrated how to adapt MCTopM to other settings. For example, it assumes to know the number of players M before-hand, but we illustrated that a previously introduced technique to estimate M on the run can also be applied to our proposal and give satisfactory empirical performances. Further works would be required to adapt the theoretical analysis to these various extensions, such as the "dynamic" case which allows arrivals or departures of devices, and which is especially interesting for Cognitive Radio applications.

– Victoriae mundis et mundis lacrima.
Bon, ça ne veut absolument rien dire, mais je trouve que c'est assez dans le ton.
Le Roi Loth, interprété par François Rollin,
Kaamelott, Livre IV, "Le désordre et la nuit".

– C'est pas moi qu'explique mal, c'est les autres qui sont cons !
Perceval, interprété par Franck Pitiot,
Kaamelott, Livre IV, "Perceval Fait Raitournelle".

Chapter 7

Piece-Wise Stationary Bandits

In this last chapter, we are also interested in a more formal approach to the decentralized learning problem presented in Chapter 5. Instead of keeping the stationary hypothesis but considering $2 \leq M \leq K$ devices accessing a wireless networks with K orthogonal frequency channels, as we did in Chapter 6, we are now interested in another direction of formal analysis of the intractable models of IoT networks of Chapter 5. We study a generalization of the single-player stationary bandit model, to account for possible non-stationarity of the rewards. We review existing works on piece-wise stationary MAB models, then we study the Generalized Likelihood Ratio Test (GLRT) for bounded or sub-Bernoulli distributions. We are able to prove finite-time guarantees for our test, on its *false alarm probability* and *detection delay*, and can be combined with an efficient bandit policy (kl-UCB), to propose an efficient algorithm for piece-wise stationary problems, GLR-klUCB. We analyze its regret, and show that it achieves state-of-the-art finite-time regret bounds. Finally, we showcase numerical experiments on which our approach outperform other state-of-the-art solutions.

Contents

7.1 Motivations for non stationary MAB models

As highlighted in Chapters 1 and 5 for cognitive radio applications, as well as other applications such as recommender systems, the assumption that the arms distribution *do not change over time* may be a big limitation. Indeed, in cognitive radio or IoT networks, new devices can enter or leave the network, which impacts the availability of the radio channel they use to communicate, making it non stationary. And for instance in online recommendation, the popularity of items is also subject to trends. Hence, there has been some interest on how to take those *non-stationary* aspects into account within a multi-armed bandit model.

A first possibility to cope with non-stationary is to model the decision making problem as an *adversarial bandit problem* [ACBFS02]. Under this model, rewards are completely arbitrary and are not assumed to follow any probability distribution. For adversarial environments, the pseudo-regret, which compares the accumulated reward of a given strategy with that of the best fixed-arm policy, is often studied. The pseudo regret of the Exp3 algorithm has been shown to be $\mathcal{O}(\sqrt{KT})$, which matches the lower bound given by [ACBFS02]. However, this model is a bit too general for the considered applications, where reward distributions do not necessarily vary at every round. For these reasons, an intermediate model, called the *piece-wise stationary MAB*, has been introduced in Section 8 of the seminal paper [ACBFS02]. They propose a simple extension of the Exp3 policy, referred to as Exp3.S, that uses exponential weights like Exp3 tweaked with an adaptive forced exploration probability to passively adapt to changes. It was shown that Exp3.S attains a regret of $\mathcal{O}(\sqrt{KTS\ln(KT)})$, when comparing with an arbitrary sequence of comparators that does not switch for more than $S-1$ times. Running their algorithm over the non-stationary problem, and picking their comparators sequence as the best arm in each stationary interval, one can already get $\sqrt{\Upsilon_T T\ln(T)}$ regret, and the only prior knowledge needed to run the Exp3.S algorithm is T and Υ_T. Moreover, Exp3.S is efficient in terms of both storage and computation time, and is simple to implement.

It could seem that the problem is considered as solved by the Exp3.S algorithm, but it was actively studied since the seminal paper [ACBFS02]. Two main reasons explain the dynamic research on this problem: first, it is well known that despite their qualities, exponential-weights algorithms like Exp3 can usually be greatly outperformed by UCB-based algorithms, for stochastic problems, and so it is expected that Exp3.S can be outperformed by other algorithms, thus any practical application might benefit from algorithms that are more efficient than Exp3.S. The second reason is that passively adaptive algorithms function as black-box models: they do not try to detect changes and do not explain why they changed from one arm to another. A lot of the recent research has been focused on actively adaptive algorithms, precisely because they allow to interpret their decisions, by detecting changes on arms with statistical tests. The piece-wise stationary MAB model has then been studied by [KS06] and [YM09]. This model is sometimes referred to as the abruptly changing [WS18b], or switching

environments [MS13]. In this model, described in full details in Section 7.2, the (random) reward of arm k at round t has some mean $\mu_k(t)$, that is constant on intervals between two *break-points*, and the regret is measured with respect to the *current* best arm $k_t^* \doteq \arg\max_i \mu_k(t)$.

Outline. We introduce the model in Section 7.2, and we review related works in Section 7.3. In Section 7.4, we study the Generalized Likelihood Ratio test for sub-Bernoulli distributions (B-GLRT) as a change-point Detector (CPD) algorithm. We introduce the two variants of GLR-klUCB algorithm in Section 7.5, where we also present upper bounds on their regret. The unified regret analysis is given in Section 7.6, we prove one result in Section 7.7. We discuss numerical experiments in Section 7.8, with more details in the Appendix 7.10.

Publications. This chapter is based on our articles [BK19b, BK19a].

7.2 The piece-wise stationary bandit model

A *piece-wise stationary bandit model* generalizes the model of Chapter 2. It is characterized by a set of K arms, and a horizon T. A (random) stream of rewards $(Y_{k,t})_{t\in[T]}$ is associated to each arm $k \in [K]$. We assume that the rewards are bounded, and without loss of generality we assume that $Y_{k,t} \in [0,1]$. We denote by $\mu_k(t) \doteq \mathbb{E}[Y_{k,t}]$ the mean reward of arm k at round t. At each round t, a decision maker has to select an arm $A(t) \in [K]$, based on her past observations, and receives the corresponding reward $r(t) \doteq Y_{A(t),t}$. At time t, we denote by k_t^* an optimal arm, *i.e.*, an arm with maximal expected reward $\mu_{k_t^*}(t) \doteq \max_k \mu_k(t)$ (possibly not unique).

A policy $\mathcal{A}$ chooses the next arm to play based on the sequence of past plays and obtained rewards. Like for stationary problems (see Definition 2.3 in Chapter 2), the performance of $\mathcal{A}$ is measured by its (piece-wise stationary) *regret*, the difference between the expected reward obtained by an oracle policy playing an optimal arm k_t^* at time t (that can change at each round), and that of the policy $\mathcal{A}$. We use the same notation as the regret for stationary problem without ambiguity, as in this chapter we only consider the following definition,

$$R_T^{\mathcal{A}} \doteq \mathbb{E}\left[\sum_{t=1}^{T} \left(\mu_{k_t^*}(t) - \mu_{A(t)}(t)\right)\right]. \tag{7.1}$$

In the piece-wise *i.i.d.* model, we furthermore assume that a relatively small *number of break-points* Υ_T (wrt the horizon T, *i.e.*, $\Upsilon_T = o(T)$), which is defined by

$$\Upsilon_T \doteq \sum_{t=1}^{T-1} \mathbb{1}\left(\exists k \in [K] : \mu_k(t) \neq \mu_k(t+1)\right). \tag{7.2}$$

If we denote $\tau^{(0)} \doteq 0$, we define the i-th break-point by $\tau^{(i)} \doteq \inf\{t > \tau^{(i-1)} : \exists k : \mu_k(t) \neq \mu_k(t+1)\}$ for $i \in [\Upsilon_T]$. Hence for $t \in [\tau^{(i)} + 1, \tau^{(i+1)}]$, that is on any stationary segments, the rewards $(Y_{k,t})$ associated to each arm k are *i.i.d.* (hence the name *piece-wise stationary*).

Note than when a break-point occurs, we do not assume that all the arms means change, but that *there exists* an arm whose mean has changed. Depending on the application, many scenarios can be meaningful: changes can occur on all arms simultaneously (due to some exogenous event), or only one or a few arms change at each break-point. For instance, for a cognitive radio application in a IoT-like network, we can imagine that all the devices of one company (or network provider) use a fixed (or a subset of) channel(s), and on a particular day in a city, if the company deploys a lot of new devices, then one (or some) channel(s) see their mean occupancy rates abruptly change.

We define NC_k the *number of change-points* on arm k by $\mathrm{NC}_k \doteq \sum_{t=1}^{T-1} \mathbb{1}\left(\mu_k(t) \neq \mu_k(t+1)\right)$, which is clearly bounded by $\mathrm{NC}_k \leq \Upsilon_T$, but there can be an arbitrary difference between these two quantities for some arms. If $C_T \doteq \sum_{k=1}^{K} \mathrm{NC}_k$ is the total number of change-points on the arms, we have $C_T \in \{\Upsilon_T, \Upsilon_T + 1, \ldots, K\Upsilon_T\}$. We illustrate the two extreme cases in problems 1 and 2 presented in Figures 7.1 and 7.2 below.

An interesting interpolation. The piece-wise stationary bandit model can be viewed as an interpolation between stationary and adversarial models, as the stationary model corresponds to $\Upsilon_T = 0$ (*i.e.*, one stationary segment), while some adversarial models can be considered as a special (worst) case, with $\Upsilon_T = T - 1$ (when considering an adaptive or an oblivious adversary). However, typical analyzes of algorithms designed for the piece-wise stationary model assume a small number of changes, typically $\Upsilon_T = o(\sqrt{T})$. Note that the adversarial model of [ACBFS02] is quite powerful, and the authors presented in Section 8 of their paper the Exp3.S algorithm for the piece-wise stationary problem, as explained in Section 7.1 above.

Two examples of problems. To illustrate the model, we give here two examples of piece-wise stationary problems used for the numerical experiments presented in Section 7.8.

Problem 1. We consider $K = 3$ arms changing $\Upsilon_T = 4$ times until $T = 5000$. The arm means $(\mu_k(t))_{k\in[K],t\in[T]}$ are shown in Figure 7.1 below. Note that changes happen on only one arm (*i.e.*, $C_T = \Upsilon_T = 4$), and the optimal arm changes once at $\tau_2^{(1)} = 2000$.

Problem 2. This problem is close to Problem 1, with a minimum optimality gap of 0.1 (at any time, the smallest difference between two means is at least 0.1), and illustrated in Figure 7.2. However, all arms change at every break-point (*i.e.*, $C_T = K\Upsilon_T = 12$), with identical gaps of 0.1 for arms 0 and 1, and of 0.2 for arm 2 (between two break-points, the mean change of $+0.1$ for arm 0 and -0.1 for arm 1 and -0.2 for arm 2). The first optimal

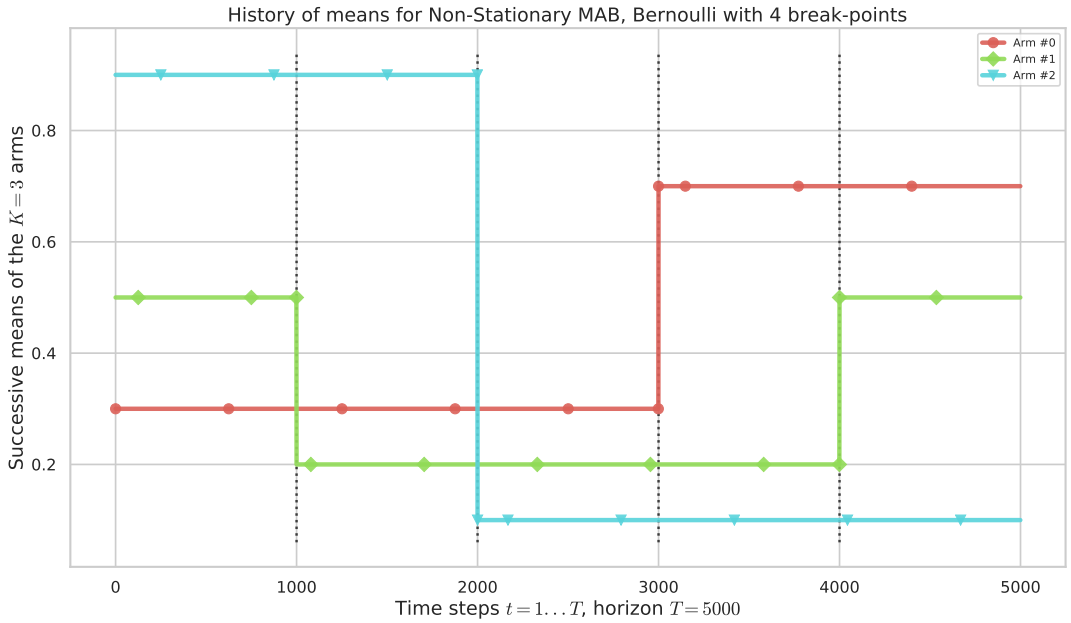

Figure 7.1 – Problem 1: $K = 3$ arms with $T = 5000$, and $\Upsilon = 4$ changes occur on only one arm at a time (*i.e.*, $C = 4$). The means are in $[0, 1]$, and there are $C + 1 = 5$ stationary intervals of equal lengths. Some changes do not modify the optimal arm (*e.g.*, at $T = 1000$ and $T = 4000$) and others do.

arm decreases at every change (2 with ∇ markers), and one arm stays the worst (1 with $\diamond$ markers).

7.3 Review of related works

We review previous works that studied the piece-wise stationary bandit model, or variants of this model. To the best of the authors' knowledge, all the previous works are based on the idea of combining a classical bandit policy, such as Thompson sampling, UCB or Exp3, with a strategy to account for changes in arms' distributions. Following the vocabulary used in previous works, we make the distinction between *passively* and *actively* adaptive strategies. On the one hand, actively adaptive strategies monitor the arms' rewards, by using change detection algorithms [BN93], and reset the history of pulls and rewards of one or all the arms as soon as a change is detected. On the other hand, passively adaptive strategies use a (fixed) discount factor or a limited memory size, while most active strategies use a growing memory.

Passively adaptive algorithms. Their common idea is to adapt a classical policy into forgetting old rewards. If the forgetting behavior is done efficiently, then the policy can efficiently focus mostly on the most recent rewards, and passively adapt to changes whenever they

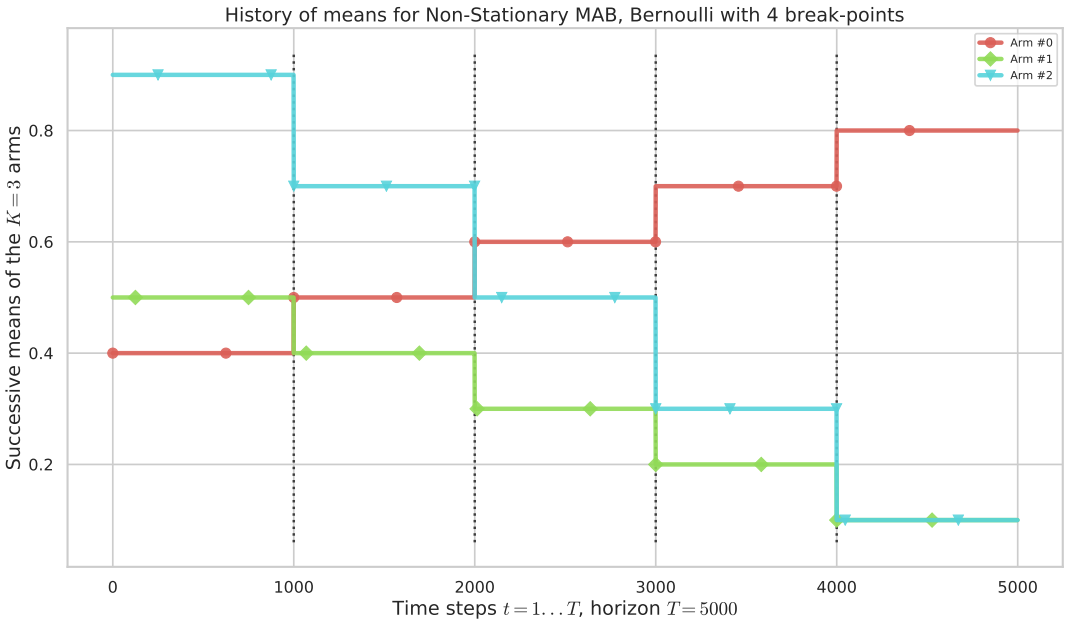

Figure 7.2 – Problem 2: $K = 3$ arms with $T = 5000$, and $\Upsilon = 4$ changes occur on all arms (*i.e.*, $C = 12$). The means are again in $[0, 1]$, and there are also $C + 1 = 5$ stationary intervals of equal lengths.

happen. The Discounted UCB (D-UCB) algorithm is an adaptation of the UCB algorithm, first introduced in [KS06]. It works by decreasing all the past rewards by a discount factor $\gamma \in (0, 1)$, when receiving a new reward from an arm, so that the recent rewards weight more in the (discounted) empirical means, that are used for the computation of its UCB indexes. The regret of D-UCB was proven to be upper-bounded by $\mathcal{O}(\sqrt{\Upsilon_T T \ln(T)})$ in [GM11], with a tuning $\gamma = 1 - \sqrt{\Upsilon_T / T}/4$, dependent on Υ_T. The Sliding-Window UCB (SW-UCB), proposed by [GM11], uses a sliding window of a fixed size τ, to store only the most τ recent rewards for each arm. They prove that tuning its window-size to $\tau = 2\sqrt{T \ln(T)/\Upsilon_T}$, gives a bound on the regret of SW-UCB of the form $\mathcal{O}(\sqrt{\Upsilon_T T \ln(T)})$.

Both D-UCB and SW-UCB build on a stationary policy, but for example Exp3.S from [ACBFS02] builds on the Exp3 policy, which is designed for the adversarial case. Exp3.S actually achieves a good regret upper-bound, of the form $\mathcal{O}(\sqrt{K \Upsilon_T T})$, with no additional prior knowledge except that of T and Υ_T. It constitutes a good baseline for the numerical experiments in Section 7.8, even if we did find that Exp3.S performs worse that the most of the other approaches based on extending stationary bandit algorithms (*e.g.*, SW-UCB). Similarly, previous works showed that older algorithms have no or weaker regret guarantees, and have been proven to be less efficient empirically, or are designed for more specific settings.

The idea of using a simple discount factor, as for D-UCB, was recently adapted to a Bayesian policy, with the Discounted Thompson sampling (DTS) algorithm presented by [RK17]. Even

if no theoretical guarantee was given, it can be empirically very efficient, but we found that DTS is not robust on the choice of if its discount factor $\gamma \in (0,1)$, contrarily to what was highlighted in the paper. The DTS algorithm can perform well in practice, for instance with $\gamma = 0.75$ on Problems 1 and 2 (see Section 7.8). In general, we found that passively adaptive approaches can be efficient when their parameters are well tuned, but our experiments show that actively adaptive algorithms perform significantly better.

Actively adaptive algorithms. A first line of research uses frequentist change-point detectors [BN93], combined with stationary policies, usually index policies like UCB. When using an efficient change-point Detector (CD) algorithm with an efficient index policy, these approaches usually perform more efficiently than the passively algorithms. The Adapt-EVE algorithm from [HGB+06] used a Page-Hikley (PH) Test and the UCB policy, but no theoretical guarantee was given. The Windowed-Mean Shift algorithm from [YM09] is more generic and combines any efficient bandit policy with a CD test based on a sliding window, but their approach is not applicable to the bandit setting of interest in this chapter, as they consider side observations. The Exp3.R algorithm from [AF15, AFM17] combines a CD algorithm with Exp3, and the history of all arms are reset as soon as a sub-optimal arm is detecting to become optimal. A regret bound of $\mathcal{O}(\Upsilon_T \sqrt{T \ln(T)})$ was proven, even when Υ_T is known.

Two recent and related works use the two-sided CUSUM CD algorithm for CUSUM-UCB in [LLS18] and a specific and simpler CD algorithm for the Monitored UCB (M-UCB) algorithm introduced in [CZKX19]. The CUSUM test is rather complicated and it is parametric: it uses the first M samples (for a fixed $M \in \mathbb{N}^*$) from one arm to compute an average $\widehat{u_0}$, and then builds two random walks, using the remaining observations for this arm. A change is detected when one of the random walks crosses a threshold h. It requires the tuning of three parameters, M and h as well as a drift correction parameter $\varepsilon \in (0,1)$. The PH test, also studied in [LLS18], is similarly complex, and we found in numerical experiments that PHT-UCB performs very similarly to CUSUM-UCB. Even if it has the advantage of not requiring a parameter M, it has no theoretical guarantee, so we do not include PHT-UCB in the experiments presented below. In comparison, M-UCB uses a much simpler test, based on the w most recent observations on one arm (for a fixed and even number $w \in 2\mathbb{N}^*$), and compares with a fixed threshold h the difference of the sum of rewards for the first half and the second half. It is numerically much simpler, and has the advantage of using only a bounded memory (of order $\mathcal{O}(Kw)$ for K arms). Both approaches also introduced a mechanism to force a uniform exploration of each arm, parameterized by $\omega \in (0,1)$ (note that it is called α in both papers, but we rename it ω in this chapter to avoid clutter with α of UCB_1 in (2.7)).

When all their parameters are tuned correctly, both approaches are proven to achieve good regret upper-bounds, of order $\mathcal{O}(K\sqrt{\Upsilon_T T \ln(KT)})$. As both results are valid under (slightly) different assumptions, we consider the two results to be the current state-of-the-art.

As for previous works, tuning their parameters requires to know both the horizon T and the number of break-points Υ_T. But most importantly it requires a prior knowledge of the problem difficulty, by assuming to know a lower bound on both the length of stationary segments (*e.g.*, L for M-UCB) or on the changes on the means of arms (*e.g.*, ε for CUSUM). CUSUM-UCB achieves a better regret upper bound, of the order of $\mathcal{O}(\sqrt{\Upsilon_T T \ln(T/\Upsilon_T)})$, but *only* for Bernoulli distributions, and when its 4 parameters $(\omega, \varepsilon, M, h)$ are tuned based on problem-dependent knowledge. M-UCB achieves a regret bounded by $\mathcal{O}(\sqrt{\Upsilon_T T \ln(T)})$, for bounded distributions, and when its 4 parameters (ω, b, w, γ) are also tuned based on a problem-dependent knowledge of $\tilde{\delta}$ and L (see Assumption 1 and Remark 1 in [CZKX19]).

On the one hand, CUSUM-UCB performs *local restarts* using this test, to reset the history of *one arm* for which the test detects a change. On the other hand, M-UCB performs *global restarts* using this test, to reset the history of *all arms* whenever the test detects a change *on one* of the arms. Compared to CUSUM-UCB, note that M-UCB is numerically much simpler as it only uses a sub-linear memory (wrt T), of order $\mathcal{O}(Kw)$ for K arms (as w grows with T).

Another interesting recent work is [AGO18], where the authors propose an efficient algorithm, AdSwitch, for the two-armed case ($K = 2$). It proceeds in episodes, starting a new episode whenever the algorithm detects a change in one of the arms. Each episode consists of three phases, estimation, exploitation then exploration. First, an estimation phase where both arms are played alternatingly until their means can be distinguished. Then follows an exploitation phase, and finally with some low probability, an exploration phase is started that checks whether a change has occurred. Similarly to what previous approaches did (*e.g.*, CUSUM uses a threshold ε), this phase checks for changes of a certain minimum magnitude, but the innovation in this work is that this algorithm does not need any prior knowledge of the minimum magnitude. Instead, it uses geometrically decreasing magnitudes $d_k = 2^{-i}$, meaning that even difficult changes should be detected, possibly in a later episode, as each episode only considers a few different values of d_k. They prove that their algorithm achieves a regret bound of $\mathcal{O}(\ln(T)\sqrt{\Upsilon_T T})$, without a prior knowledge of Υ_T. However, this work as two drawbacks: first, the algorithm currently only applies to two arms, and the generalization does not seem straightforward. Then, the theoretical result is valid for "sufficiently large constants C_1 and C_2", with a large constant C hiding in the $\mathcal{O}(\bullet)$ notation. We did some experiments with AdSwitch, even if it is not included in the benchmark presented below in Section 7.8. It uses two parameters C_1, C_2 that are set at large values for the theoretical analysis, and while we explored numerically different choices, it seemed that setting $C_1 = C_2 = 1$ gave the best performance (which is outside of the comfort zone of the theoretical analysis). Even for this tuning, and for problems with just $K = 2$ arms, empirically this policy is performing poorly in comparison to other policies based on active CD detection and kl-UCB indexes.

Expert aggregation. Another line of research on actively adaptive algorithms uses a Bayesian point of view. A Bayesian CD algorithm is combined with Thompson Sampling in [MS13], and more recently [AMF17] introduced the Memory Bandit algorithm. It is presented as efficient empirically, but no theoretical guarantee are given for these two works, and due to its complexity, we do not include it in our experiments. The idea behind Memory Bandit is to use an expert aggregation algorithm, like Exp4 from [ACBF02] or our Aggregator algorithm from Chapter 4 [BKM18], modified to efficiently aggregate a growing number of experts, using techniques presented in [MM17]. A new expert is introduced at each time step, and experts correspond to different Thompson sampling algorithms, each using a different history of pulls and rewards. Intuitively, after a change-point the newest experts will soon become the most efficient, as they are learning by using rewards drawn from the new distribution(s). Note that obtaining regret bounds for these methods is still an open-problem, and as they are computationally more costly, we chose to not include them in our experiments.

Slowly-varying model. A different setting where the quantity of interest is not Υ_T but the total variational budget V_T, was introduced by [BGZ14], for which they proposed the REXP3 algorithm. The total variation budget V_T is defined as $\sum_{t=1}^{T-1}\sum_{k=1}^{K} D(\nu_k(t), \nu_k(t+1))$, for a certain measure of difference D, which measures how much the two distributions of any arm k have changed from time t to time $t+1$. Two examples can be the total variation distance $\|\cdot\|_{TV}$ or the Kullback-Leibler divergence. The REXP3 algorithm can also be qualified as passively adaptive: it is based on (non-adaptive) restarts of the EXP3 algorithm. As the total variational budget satisfies $\Delta^{\text{change}}\Upsilon_T \leq V_T \leq \Upsilon_T$, with Δ^{change} the minimum magnitude of a change-point, their regret bound of order of $\mathcal{O}(V_T^{1/3}T^{2/3})$ is actually weaker than existing results in our setting.

The slowly-varying model is quite different from the setting we are considering in this chapter, and even if the most recent works on this model are very interesting [WS18b], we preferred to focus on the piece-wise stationary (also called abruptly changing) model, hence we do no include any of these algorithms in the experiments presented in Section 7.8.

Another point-of-view on prior knowledge of Υ_T. In this chapter, like in our two main inspirational works [CZKX19, LLS18], we assume that the algorithm knows in advance the number of break-points Υ_T. Another interesting point-of-view is the one presented by [WS18b, WS18a], where the authors assume that there exists a number $\nu \in (0,1)$ for which $\Upsilon_T = o(T^\nu)$, and they also assume that any algorithm tackling such problems can know in advance the value of ν (or an upper-bound on ν), in order to tweak its parameters from this value ν, but cannot know the exact value of Υ_T. This interpretation is interesting too, but empirically we found that the SW-UCB# algorithm proposed in [WS18b] performs comparably to SW-UCB, and thus we did not include it in the experiments presented below in Section 7.8.

Adversarial or non-stationary contextual bandits. For contextual bandits, two very recent works are [LWAL18] and [CLLW19]. While both works target a more general setting, their algorithms are also applicable to non-contextual bandits, *i.e.*, classical bandits like the model studied in this chapter. From Table 1 in [LWAL18], one can see that their two algorithms Exp4.S and Ada-ILTCB recover the same regret guarantees as we do, in the non-contextual case: that is, a $\mathcal{O}(\Upsilon_T\sqrt{T})$ regret without knowing the number of changes and $\mathcal{O}(\sqrt{\Upsilon_T T})$ with this knowledge. We discuss both these algorithms: first, in the non-contextual case, Exp4.S actually reduces to Exp3.S, which we discussed above. Then, the Ada-ILTCB algorithm is however a less appealing candidate for the setting of this chapter, for the following reason. This algorithm requires as input a parameter L which needs to be an upper bound on the largest stationary sequence in the problem, in order for its regret to scale as $\Upsilon_T\sqrt{L}$ (neglecting K and $\ln$ factors). It is claimed that the tuning $L = T/\Upsilon_T$ yields the optimal bound $\sqrt{\Upsilon_T T}$. However, this tuning is only possible in a "balanced" instance without stationary sequence longer than T/Υ_T. In a piece-wise stationary instance with a stationary sequence of length $T/2$, one cannot get better than $\mathcal{O}(\Upsilon_T\sqrt{T})$ regret, by setting $L = T/2$ (see for instance the problem 4 in our benchmark below in Section 7.8), and as such the regret bound of Ada-ILTCB appears much worse than the announced $\mathcal{O}(\sqrt{\Upsilon_T T})$ bound. Besides, no experiments are reported by [LWAL18], and the Ada-ILTCB algorithm seems much more complicated to implement than other alternatives, so we prefer to not include it in the experiments presented later.

Positioning of our results. The two algorithms CUSUM-UCB and M-UCB are both analyzed under some reasonable assumptions on the problem parameters –the means $(\mu_k(t))$– mostly saying that the break-points are sufficiently far away from each other. However, the proposed guarantees only hold for parameters *tuned using some prior knowledge of the means*. Indeed, while in both cases the threshold h can be set as a function of the horizon T and the number of break-points Υ_T (also needed by previous approaches to obtain the best possible bounds), the parameter ε for CUSUM and w for M-UCB require the knowledge of Δ^{change} the smallest magnitude of a change-point. In this chapter, we propose *the first algorithm that does not require this knowledge*, and still attains a $\mathcal{O}(\sqrt{\Upsilon_T T \ln(T)})$ regret. Moreover we propose the first comparison of the use of local and global restarts within an adaptive algorithm, by studying two variants of the proposed algorithm. In others words, if we want to apply our proposal to piece-wise stationary problems such as problem 1 or 2 presented above (see Figures 7.1, 7.2), it only needs to know beforehand that $T = 5000$ and $\Upsilon_T = 4$ for these examples, but it does not need to know the amplitude of changes $\Delta^{\text{change}} = \max_{k,t} |\mu_k(t) - \mu_k(t+1)|$ nor the optimality gap or a bound on the optimality gap at any time step $\Delta^{\text{opt}} = \max_{k,k'} |\mu_k(t) - \mu_{k'}(t)|$.

Moreover, we can use the two problems 1 and 2 to illustrate the expected empirical behavior of GLR-klUCB. Problem 1 has only *local changes*, meaning that at any change-point, only one arm sees its distribution change, while problem 2 has only *global changes*, meaning that all

arms see their distribution change at each change-point. They illustrate the two extreme cases of having $C_T = \Upsilon_T$ (for problem 1) and $C_T = K\Upsilon_T$ (for problem 2).

- On the one hand, we expect the *local restart* variant of GLR-klUCB to outperform the *global restart* variant for problem 1, as the intuition suggests that it is sub-optimal to reinitialize the memory of the observations of the $K - 1$ arms whose distributions did not change after a change-point is detected (as the *global restart* variant does).
- On the other hand, we expect the *global restart* variant to outperform the *local restart* variant for problem 2, as detecting a change on any arm is enough to know that all arms changed and to reinitialize the memory of all arms, and thus the intuition suggests that it is sub-optimal to reinitialize only the memory of the observation of the arm on which the change-point was detected (as the *local restart* variant does).

Of course, in a given environment, without additional prior knowledge on the difficulty of the problem at hand, the algorithm cannot know which situation is more likely to happen, between having only local changes ($C_T = \Upsilon_T$) or only global changes ($C_T = K\Upsilon_T$), or any intermediate setting between the two extreme cases. Thus we do not believe to be able to design a policy that could be uniformly better than the two variants of GLR-klUCB. Surprisingly, numerical experiments show that the *local* variant of GLR-klUCB actually outperforms the *global* variant for both problem 1 and 2, as shown below in Table 7.2, and in other problems as shown in Table 7.3. Understanding this difference in terms of numerical performance of the two variants is left as future work. Finally, on the practical side, we can note that while the proposed B-GLRT test is more complex to implement than the test used by M-UCB, we propose two heuristics to speed it up while not losing much in terms of regret, in Appendix 7.10.3.

About kl-UCB. Our proposal GLR-klUCB is inspired by both the M-UCB and CUSUM-UCB algorithms [LLS18, CZKX19]. Previous works focused on using UCB, but we propose to use kl-UCB instead, as it is known to be more efficient for Bernoulli rewards as well as for a more generic case of bounded or one-dimensional exponential families [CGM+13]. Theoretical results for [LLS18] and [CZKX19] were only given for UCB, but they suggested that extending the results to kl-UCB (or other efficient stationary policies) should not be difficult. For a fair comparison, we therefore chose to compare the different change-point detector algorithms combined with kl-UCB. We also include in Table 7.1 a comparison of the performance of different algorithms when using UCB or kl-UCB indexes, in order to illustrate that using a more efficient index policy always improves performance, as predicted.

7.4 The Bernoulli GLRT change-point Detector

Sequential change-point detection has been extensively studied in the statistical community, from the 1930s with pioneer works like [Wil38] and later on with seminal works like [Bar59, SV95]. We refer to the book [BN93] for a survey. In this section, we are interested in detecting changes on the mean of a probability distribution with bounded support.

Assume that we collect independent samples $X_1, X_2, \dots$ all from some distributions supported in $[0, 1]$. We want to discriminate between two possible scenarios: all the samples come from distributions that have a common mean μ_0, or there exists a *change-point* $\tau > 1$ such that $X_1, \dots, X_\tau$ have some mean μ_0 and $X_{\tau+1}, X_{\tau+2}, \dots$ have a different mean $\mu_1 \neq \mu_0$. A sequential change-point detector is a *stopping time*[1] $\hat{\tau}$ with respect to the filtration $\mathcal{F}_t \doteq \sigma(X_1, \dots, X_t)$ such that $(\hat{\tau} < \infty)$ means that we reject the hypothesis $\mathcal{H}_0 : (\exists \mu_0 \in [0, 1] : \forall t \in \mathbb{N}^*, \mathbb{E}[X_t] = \mu_0)$.

Generalized Likelihood Ratio tests date back to the seminal work of [Wil38], and were for instance studied for change-point detection by [Bar59, SV95]. Exploiting the fact that bounded distribution are $(1/4)$-sub Gaussian (*i.e.*, their moment generating function is dominated by that of a Gaussian distribution with the same mean and a variance $1/4$), the (Gaussian) GLRT, recently studied in depth by [Mai19], and can be used for this problem. We propose instead to exploit the fact that bounded distributions are also dominated by Bernoulli distributions.

Definition 7.1 (Sub-Bernoulli distributions)**.** *We call a* sub-Bernoulli distribution *any distribution ν that satisfies $\ln \mathbb{E}_{X\sim\nu}\left[e^{\lambda X}\right] \leq \phi_\mu(\lambda)$ with $\mu \doteq \mathbb{E}_{X\sim\nu}[X]$ and $\phi_\mu(\lambda) \doteq \ln(1 - \mu + \mu e^{\lambda})$ is the log moment generating function of a Bernoulli distribution with mean μ, for any $\mu \in [0, 1]$.*

Lemma 1 of [CGM+13] establishes that any bounded distribution supported in $[0, 1]$ is a sub-Bernoulli distribution. As explained in Section 2.1.2, this work can be applied to any bounded distribution without loss of generality, as a reward in $r \in [a, b]$ can clearly be mapped to $[0, 1]$ simply by using $r' = (r - a)/(b - a)$. We assume that both the decision maker and the algorithm know beforehand the values of a and b.

7.4.1 Presentation of the test

If the samples (X_t) were all drawn from a Bernoulli distribution, this change-point detection problem would reduce to a simple parametric sequential test of $\mathcal{H}_0 : (\exists \mu_0 : \forall t \in \mathbb{N}^*, X_t \overset{\text{i.i.d.}}{\sim} \mathcal{B}(\mu_0))$, against the alternative $\mathcal{H}_1 : (\exists \mu_0 \neq \mu_1, \tau \in \mathbb{N}^* : X_1, \dots, X_\tau \overset{\text{i.i.d.}}{\sim} \mathcal{B}(\mu_0)$ and $X_{\tau+1}, X_{\tau+2}, \dots \overset{\text{i.i.d.}}{\sim} \mathcal{B}(\mu_1))$.

[1] Stopping times are for instance presented formally in Chapter 3 of [LS19].

The Generalized Likelihood Ratio statistic for this test is defined by

$$\mathrm{GLR}(n) \doteq \frac{\sup\limits_{\mu_0,\mu_1,\tau<n} \ell(X_1,\dots,X_n;\mu_0,\mu_1,\tau)}{\sup\limits_{\mu_0} \ell(X_1,\dots,X_n;\mu_0)}, \tag{7.3}$$

where $\ell(X_1,\dots,X_n;\mu_0)$ and $\ell(X_1,\dots,X_n;\mu_0,\mu_1,\tau)$ respectively denote the *likelihoods* of the first n observations under a model in $\mathcal{H}_0$ and $\mathcal{H}_1$. High values of this statistic tend to indicate rejection of $\mathcal{H}_0$. By using the form of the likelihood for Bernoulli distributions, this statistic can be written with the binary relative entropy kl, defined by $\mathrm{kl}(x,y) \doteq x\ln\left(\frac{x}{y}\right) + (1-x)\ln\left(\frac{1-x}{1-y}\right)$ for $x,y\in[0,1]$ (with the usual convention that $t\ln(t)\doteq 0$ if $t=0$). Indeed, we show below in Appendix 7.10.2 that for Bernoulli distributions, we have

$$\ln \mathrm{GLR}(n) = \sup_{s\in[n-1]} \left[s\times \mathrm{kl}\left(\widehat{\mu}_{1:s},\widehat{\mu}_{1:n}\right) + (n-s)\times \mathrm{kl}\left(\widehat{\mu}_{s+1:n},\widehat{\mu}_{1:n}\right)\right]. \tag{7.4}$$

where for $s\leq s'$, $\widehat{\mu}_{s:s'} \doteq \frac{1}{s-s'+1}\sum_{t=s}^{s'} X_t$ denotes the average of the observations $X_s,\dots,X_{s'}$. This motivates the following definition of the Bernoulli GLRT change-point detector.

Definition 7.2. *The Bernoulli GLRT (B-GLRT) change-point detector with threshold function $\beta(n,\delta)$ is the stopping time $\widehat{\tau}_\delta$ defined by*

$$\widehat{\tau}_\delta \doteq \inf\left\{ n\in\mathbb{N}^* : \sup_{s\in[n-1]} \left[s\times \mathrm{kl}\left(\widehat{\mu}_{1:s},\widehat{\mu}_{1:n}\right) + (n-s)\times \mathrm{kl}\left(\widehat{\mu}_{s+1:n},\widehat{\mu}_{1:n}\right)\right] \geq \beta(n,\delta)\right\}. \tag{7.5}$$

with the convention that we enforce $\left[s\times \mathrm{kl}\left(\widehat{\mu}_{1:s},\widehat{\mu}_{1:n}\right) + (n-s)\times \mathrm{kl}\left(\widehat{\mu}_{s+1:n},\widehat{\mu}_{1:n}\right)\right] = 0$ *whenever we have $\widehat{\mu}_{1:s}=\widehat{\mu}_{s+1:n}$, in particular if $\widehat{\mu}_{1:n}\in\{0,1\}$, then $\widehat{\mu}_{1:s}=\widehat{\mu}_{s+1:n}=\widehat{\mu}_{1:n}\in\{0,1\}$.*

Asymptotic properties of the GLRT for change-point detection have been studied by [LX10] for Bernoulli distributions and more generally for any one-parameter exponential family $\mathcal{E}$, for which the GLR test is defined as in (7.5), but with $\mathrm{kl}(x,y)$ replaced by the Kullback-Leibler divergence $\mathrm{kl}_{\mathcal{E}}(x,y)$ between two elements in that exponential family that have mean x and y (see Definition 2.1). For example, the Gaussian GLR studied by [Mai19] corresponds to the stopping time (7.5) with the quadratic divergence $d(x,y)=2(x-y)^2$, when the variance is set to $\sigma^2=1/4$, and non-asymptotic properties of this test are given for any $(1/4)$-subGaussian samples. Note that Pinsker's inequality gives that $\mathrm{kl}(x,y)\geq 2(x-y)^2$, hence the B-GLRT may stop earlier that the Gaussian GLR. In the next section, we provide new non-asymptotic results about the B-GLRT under the assumption that the samples (X_t) come from a sub-Bernoulli distribution, which in particular holds for any distribution supported in $[0,1]$.

7.4.2 Non-asymptotic properties of the B-GLRT

When used for a bandit problem, the two main properties of a sequential change-point detection test are its *false alarm probability* and its *detection delay*. A small false alarm probability ensures that no detection occurs before it should (*i.e.*, no useless detection occur on stationary segments), and a small detection delay ensures that, if the stationary segments are long enough, then every change-points on every arm will be detected after a short enough amount of samples from that arm. We give below two lemmas: Lemma 7.3 bounds the false alarm probability for a certain choice of threshold function, and Lemma 7.5 bounds the detection delay if there are enough samples before the change-point.

False alarm probability. In Lemma 7.3 below, we propose a choice of the threshold function $\beta(n, \delta)$ under which the probability that there exists a *false alarm* under *i.i.d.* data is as small as we want. To define β, we first introduce the function $\mathcal{T}$, defined for $x > 0$ by

$$\mathcal{T}(x) \doteq 2\widetilde{h}\left(\frac{h^{-1}(1+x) + \ln(2\zeta(2))}{2}\right), \tag{7.6}$$

where for $u \geq 1$ we define $h(u) \doteq u - \ln(u)$ and its inverse $h^{-1}(u)$, we define $\widetilde{h}(x) \doteq \mathrm{e}^{1/h^{-1}(x)} h^{-1}(x)$ if $x \geq h^{-1}(1/\ln(3/2))$ and $\widetilde{h}(x) \doteq (3/2)(x - \ln(\ln(3/2)))$ otherwise, for any $x \geq 0$, and with the value $\zeta(2) = \pi^2/6$. Even if it does not have a closed form expression, the function $\mathcal{T}$ is easy to compute numerically. The inverse h^{-1} can be computed using $\mathcal{W}$, the Lambert $\mathcal{W}$ function [CGH+96], which is the inverse of $x \mapsto x\mathrm{e}^x$, as $h^{-1}(x) = -\mathcal{W}(-\mathrm{e}^{-x})$.

The use of $\mathcal{T}$ for the construction of concentration inequalities that are uniform in time is detailed in [KK18], where tight upper bound on this function $\mathcal{T}$ are also given: $\mathcal{T}(x) \simeq x + 4\ln\left(1 + x + \sqrt{2x}\right)$ for $x \geq 5$ and $\mathcal{T}(x) \sim x$ when x is large.

Lemma 7.3. *For a probabilistic model $P = \mathbb{P}_{\mu_0}$ under which $X_t \in [0, 1]$, and $\forall t, \mathbb{E}_P[X_t] = \mu_0$, the B-GLRT test $\widehat{\tau}_\delta$ (from Definition 7.2) satisfies $\mathbb{P}_{\mu_0}(\widehat{\tau}_\delta < \infty) \leq \delta$, with the threshold*

$$\beta(n, \delta) \doteq 2\mathcal{T}\left(\frac{\ln(3n\sqrt{n}/\delta)}{2}\right) + 6\ln(1 + \ln(n)). \tag{7.7}$$

Proof. Lemma 7.3 is presented for bounded distributions and is actually valid for any sub-Bernoulli distribution. It could also be presented for more general distributions satisfying

$$\mathbb{E}[\mathrm{e}^{\lambda X}] \leq \mathrm{e}^{\phi_\mu(\lambda)} \quad \text{with} \quad \mu = \mathbb{E}[X], \tag{7.8}$$

where $\phi_\mu(\lambda)$ is the log moment generating of some one-dimensional exponential family $\mathcal{E}$. The Bernoulli divergence $\mathrm{kl}(x,y)$ would be replaced by the corresponding divergence $\mathrm{kl}_{\mathcal{E}}$ in that exponential family. Let us go back to the Bernoulli case with divergence $\mathrm{kl}(x,y)$. We first have

$$s \times \mathrm{kl}\left(\widehat{\mu}_{1:s}, \widehat{\mu}_{1:n}\right) + (n-s) \times \mathrm{kl}\left(\widehat{\mu}_{s+1:n}, \widehat{\mu}_{1:n}\right) = \inf_{\lambda \in [0,1]} \left[s \times \mathrm{kl}\left(\widehat{\mu}_{1:s}, \lambda\right) + (n-s) \times \mathrm{kl}\left(\widehat{\mu}_{s+1:n}, \lambda\right)\right].$$

Hence the probability of a false alarm occurring is upper bounded as

$$\begin{aligned}
\mathbb{P}_{\mu_0}\left(T_\delta < \infty\right) &\leq \mathbb{P}_{\mu_0}\left(\exists s \in \mathbb{N}^*, n \in \mathbb{N}^*, s < n : s\,\mathrm{kl}\left(\widehat{\mu}_{1:s}, \widehat{\mu}_{1:n}\right) + (n-s)\,\mathrm{kl}\left(\widehat{\mu}_{s+1:n}, \widehat{\mu}_{1:n}\right) > \beta(n,\delta)\right) \\
&\leq \mathbb{P}_{\mu_0}\left(\exists s \in \mathbb{N}^*, n \in \mathbb{N}^*, s < n : s\,\mathrm{kl}\left(\widehat{\mu}_{1:s}, \mu_0\right) + (n-s)\,\mathrm{kl}\left(\widehat{\mu}_{s+1:n}, \mu_0\right) > \beta(n,\delta)\right) \\
&\leq \sum_{s=1}^{\infty} \mathbb{P}_{\mu_0}\left(\exists n > s : s\,\mathrm{kl}\left(\widehat{\mu}_{1:s}, \mu_0\right) + (n-s)\,\mathrm{kl}\left(\widehat{\mu}_{s+1:n}, \mu_0\right) > \beta(n,\delta)\right) \\
&= \sum_{s=1}^{\infty} \mathbb{P}_{\mu_0}\left(\exists r \in \mathbb{N}^* : s\,\mathrm{kl}\left(\widehat{\mu}_{s}, \mu_0\right) + r\,\mathrm{kl}\left(\widehat{\mu}'_{r}, \mu_0\right) > \beta(s+r,\delta)\right),
\end{aligned}$$

where $\widehat{\mu}_s$ and $\widehat{\mu}'_r$ are the empirical means of respectively s and r *i.i.d.* observations with mean μ_0 and distribution ν, that are independent from the previous ones. As ν is sub-Bernoulli, the conclusion follows from Lemma 7.4 below and from the definition of $\beta(n,\delta)$, if we denote $F(x) \doteq \ln(1+\ln(x))$,

$$\begin{aligned}
&\mathbb{P}_{\mu_0}\left(T_\delta < \infty\right) \\
&\leq \sum_{s=1}^{\infty} \mathbb{P}_{\mu_0}\left(\exists r \in \mathbb{N}^* : s\,\mathrm{kl}\left(\widehat{\mu}_{s}, \mu_0\right) + r\,\mathrm{kl}\left(\widehat{\mu}'_{r}, \mu_0\right) > 6F(s+r) + 2\mathcal{T}\left(\frac{\ln(3(s+r)^{3/2}/\delta)}{2}\right)\right) \\
&\leq \sum_{s=1}^{\infty} \mathbb{P}_{\mu_0}\left(\exists r \in \mathbb{N}^* : s\,\mathrm{kl}\left(\widehat{\mu}_{s}, \mu_0\right) + r\,\mathrm{kl}\left(\widehat{\mu}'_{r}, \mu_0\right) > 3F(s) + 3F(r) + 2\mathcal{T}\left(\frac{\ln(3s^{3/2}/\delta)}{2}\right)\right)
\end{aligned}$$

And so we have $\mathbb{P}_{\mu_0}\left(T_\delta < \infty\right) \leq \sum_{s=1}^{\infty} \exp(-\frac{\ln(3s^{3/2}/\delta)}{2}) = \sum_{s=1}^{\infty} \frac{\delta}{3s^{3/2}} \leq \delta$. □

Lemma 7.4. *Consider a one-dimensional exponential family $\mathcal{E}$, and let ν_μ be the unique distribution in this family that has mean μ, with moment generating function $\phi_\mu(\lambda) = \mathbb{E}_{X\sim\nu_\mu}[e^{\lambda X}]$. Let $\mathrm{kl}_{\mathcal{E}}(\mu,\mu') \doteq \mathrm{KL}(\nu_\mu, \nu_{\mu'})$ be the KL divergence associated to $\mathcal{E}$. Let $(X_i)_{i\in\mathbb{N}^*}$ and $(Y_k)_{i\in\mathbb{N}^*}$ be two independent* i.i.d. *processes, with respective means μ and μ', such that $\mathbb{E}[e^{\lambda X_1}] \leq \mathrm{e}^{\phi_\mu(\lambda)}$ and $\mathbb{E}[e^{\lambda Y_1}] \leq \mathrm{e}^{\phi_{\mu'}(\lambda)}$. Denote $\widehat{\mu}_s \doteq \frac{1}{s}\sum_{i=1}^{s} X_i$ and $\widehat{\mu}'_r \doteq \frac{1}{r}\sum_{i=1}^{r} Y_k$. Then for every $s, r \in \mathbb{N}^*$ we have,*

$$\mathbb{P}\left(\exists r \in \mathbb{N}^* : s\,\mathrm{kl}_{\mathcal{E}}\left(\widehat{\mu}_s, \mu\right) + r\,\mathrm{kl}_{\mathcal{E}}\left(\widehat{\mu}'_r, \mu'\right) > 3\ln(1+\ln(s)) + 3\ln(1+\ln(r)) + 2\mathcal{T}\left(\frac{x}{2}\right)\right) \leq \mathrm{e}^{-x}, \tag{7.9}$$

where $\mathcal{T}$ is the function defined in (7.6).

Proof. This Lemma 7.4 is proven in Appendix 7.10.2. □

Detection delay. Another key feature of a change-point detector is its *detection delay* under a model in which a change from mean μ_0 to mean μ_1 occurs at time τ. We already observed that from Pinsker's inequality, the B-GLRT stops earlier than a Gaussian GLR. Hence, we can leverage some techniques from [Mai19] to upper bound the detection delay of the B-GLRT. Letting $\Delta = |\mu_0 - \mu_1|$, one can essentially establish that for τ larger than $(1/\Delta^2)\ln(1/\delta)$ (*i.e.*, enough samples before the change), the delay can be of the same magnitude (*i.e.*, enough samples after the change). In the bandit analysis in Section 7.6, the detection delay will be crucially used to control the probability of the good event (in Lemma 7.13 and the corresponding Lemma not included here, but given in Appendix of [BK19b]).

Lemma 7.5. *For a probabilistic model $P' = \mathbb{P}_{\mu_0,\mu_1,\tau}$ under which $X_t \in [0,1]$, and $\forall t \leq \tau, \mathbb{E}_{P'}[X_t] = \mu_0$, $\forall t > \tau, \mathbb{E}_{P'}[X_t] = \mu_1$, the B-GLRT test satisfies*

$$\mathbb{P}_{\mu_0,\mu_1,\tau}(\widehat{\tau}_\delta \geq \tau + u) \leq \exp\left(-\frac{2\tau u}{\tau+u}\left(\max\left[0, \Delta - \sqrt{\frac{\tau+u}{2\tau u}\beta(\tau+u,\delta)}\right]\right)^2\right). \quad (7.10)$$

where $\Delta = |\mu_0 - \mu_1|$ denotes the gap of the change-point.

Proof. It is actually not used as such in the proofs of the regret upper bounds given below, because a similar but more specific result is used and proven in the proofs. For instance, see below in Section 7.7.2 (more specifically, in page 218). □

For a threshold β chosen as in the Lemma 7.3, a consequence of the Lemma 7.5 is that if the break-point τ happens after about $\mathcal{O}(\Delta^{-2}\ln(1/\delta))$ samples, the detection time will be of the same magnitude (with high probability). In other words, if the B-GLRT test gathers enough samples before a change-point, its delay $\widehat{\tau}_\delta$ is of order $\mathcal{O}(\Delta^{-2}\ln(1/\delta))$, with high probability.

7.4.3 Practical considerations

Lemma 7.3 provides the first non-asymptotic control of false alarm for the B-GLRT employed for bounded data. However, the threshold (7.7) is not fully explicit as the function $\mathcal{T}(x)$ can only be computed numerically. Note that for sub-Gaussian distributions, results from [Mai19] show that the smaller and more explicit threshold $\beta(n,\delta) = \left(1+\frac{1}{n}\right)\ln\left(\frac{3n\sqrt{n}}{\delta}\right)$, can be used to prove an upper bound of δ for the false alarm probability of the GLR, with quadratic divergence $d(x,y) = 2(x-y)^2$. For the B-GLRT, numerical simulations suggest that the threshold (7.7) is a bit conservative (see Appendix 7.10.4), and in practice we recommend to keep only the leading term and use $\beta(n,\delta) = \ln(3n^{3/2}/\delta) = \ln(3) + 3/2\ln(n) - \ln(\delta)$.

Also note that, as any test based on scan-statistics, the B-GLRT can be costly to implement as at every time step t, it considers all previous time steps as a possible position for a change-point

(*i.e.*, $s \in [n-1]$ if there are n samples). Thus, it can be interesting in practice to down-sample the possible values of both n and s, that is to use a large stopping time, defined by

$$\widetilde{\tau}_\delta = \inf\left\{ n \in \mathcal{N} : \sup_{s \in \mathcal{S}_n} \left[s \times \mathrm{kl}\left(\widehat{\mu}_{1:s}, \widehat{\mu}_{1:n}\right) + (n-s) \times \mathrm{kl}\left(\widehat{\mu}_{s+1:n}, \widehat{\mu}_{1:n}\right) \right] \geq \beta(n,\delta) \right\}, \quad (7.11)$$

for subsets $\mathcal{N}$ and $\mathcal{S}_n$. Following the proof of Lemma 7.3, we can easily see that this variant obtains the same false-alarm control. However, the detection delay may be slightly increased. In Appendix 7.10.3 we show that using these practical tweaks has little impact on the regret of the bandit strategy introduced below, while speeding up its computation time.

7.5 A new algorithm for piece-wise stationary bandits

We start by giving the pseudo-code of our algorithm, and by explaining every part, then we give its finite-time regret upper bounds, for the two variants of using local or global restarts. The analysis in both cases is using a unified proof technique, that we present before giving more details about the proof of half of the results (the other proof can be found in [BK19b]).

We now present the GLR-klUCB algorithm, which combines a bandit algorithm with a change-point detector running on each arm. It also needs a third ingredient, some forced exploration parameterized by $\omega \in (0,1)$ to ensure that each arm is sampled enough and in order to also be able to detect changes on arms currently under-sampled by the bandit algorithm. GLR-klUCB combines the kl-UCB algorithm, as it is given and analyzed by [CGM+13], with the B-GLRT change-point detector introduced in Section 7.4. This algorithm, formally stated as Algorithm 7.1, can be used in any bandit model with bounded rewards, and we expect it to be very efficient at least for Bernoulli distributions, which are the most relevant for our applications of interest (see Chapter 1 and 5).

When does GLR-klUCB restart? The GLR-klUCB algorithm can be viewed as a kl-UCB algorithm allowing for some *restarts* on the different arms. A restart happens when the B-GLRT change-point detector detects a change on the arm k that has been played (line 9). To be fully specific, $\mathrm{GLR}_\delta(Z_1, \dots, Z_n) = \mathrm{True}$ if and only if

$$\sup_{s \in [n-1]} \left[s \times \mathrm{kl}\left(\frac{1}{s}\sum_{i=1}^{s} Z_k, \frac{1}{n}\sum_{i=1}^{n} Z_k \right) + (n-s) \times \mathrm{kl}\left(\frac{1}{n-s}\sum_{i=s+1}^{n} Z_k, \frac{1}{n}\sum_{i=1}^{n} Z_k \right) \right] \geq \beta(n,\delta), \quad (7.12)$$

with $\beta(n,\delta)$ defined in (7.7), or $\beta(n,\delta) = \ln(3n^{3/2}/\delta)$, as we recommend in practice (see Section 7.4.3). We remind that in this notation, if $\widehat{Z}_{1:s} = \widehat{Z}_{s+1:n}$ (*i.e.*, if all observations $Z_1, \dots, Z_n$ are equal), then we set the left-hand side of (7.12) to 0, and the B-GLRT cannot detect a change-point. We define the (kl-UCB like) index used by our algorithm, by denoting $\tau_k(t)$ the last restart that happened for arm k before time t, $n_k(t) \doteq \sum_{s=\tau_k(t)+1}^{t} \mathbb{1}(A(s) = k)$ the

1 **Input:** *Parameters*: exploration rate $\omega \in (0,1)$, confidence level $\delta > 0$
2 **Input:** *Option*: **Local** or **Global** restart
3 **initialization:** $\forall k \in [K]$, $\tau_k = 0$ and $n_k = 0$;
4 **for** $t = 1, 2, \ldots, T$ **do**
5 | **if** $t \mod \left\lfloor \frac{K}{\omega} \right\rfloor \in [K]$ **then** `// forced exploration`
6 | | $A(t) = t \mod \left\lfloor \frac{K}{\omega} \right\rfloor$;
7 | **else**
8 | | $A(t) \in \mathcal{U}\left(\arg\max_{k \in [K]} \mathrm{UCB}_k(t)\right)$, with $\mathrm{UCB}_k(t)$ defined in (7.13);
9 | Play arm $A(t)$: $n_{A(t)} = n_{A(t)} + 1$;
10 | Observe the reward $Y_{A(t),t}$: $Z_{A(t),n_{A(t)}} = Y_{A(t),t}$;
11 | **if** $\mathrm{GLR}_\delta(Z_{A(t),1}, \ldots, Z_{A(t),n_{A(t)}}) = \mathit{True}$ **then** `// change-point is detected`
12 | | **if** ***Global*** *restart* **then**
13 | | | $\forall k \in [K], \tau_k = t$ and $n_k = 0$; `// restart all arms`
14 | | **else**
15 | | | $\tau_{A(t)} = t$ and $n_{A(t)} = 0$; `// restart only this arm`
16 **end**

Algorithm 7.1: The GLR-klUCB algorithm, with **Local** or **Global** restarts.

number of selections of arm k, and $\widehat{\mu}_k(t) \doteq \frac{1}{n_k(t)} \sum_{s=\tau_k(t)+1}^{t} Y_{k,s} \mathbb{1}(A(s) = k)$ their empirical mean (if $n_k(t) \neq 0$). With the exploration function $f(t) \doteq \ln(t) + 3\ln(\ln(t))$ if $t > 1$ and $f(t) = 0$ otherwise, the index is defined using the binary relative entropy kl as

$$\mathrm{UCB}_k(t) \doteq \max\left\{q \in [0,1] : n_k(t) \times \mathrm{kl}\left(\widehat{\mu}_k(t), q\right) \leq f(t - \tau_k(t))\right\}. \tag{7.13}$$

Two options for restarts. For this algorithm, we simultaneously investigate two possible behaviors: *global restart* (reset the history of all arms once a change was detected on one of them, line 11), and *local restart* (reset only the history of the arm on which a change was detected, line 13), which are the two different options in Algorithm 7.1. Under local restart, in the general case the times $\tau_k(t)$ are not equal for all arms, hence the index policy associated to (7.13) is *not* a standard UCB algorithm, as each index uses a *different exploration rate* $f(t - \tau_k(t))$. It is important to highlight that in the CUSUM-UCB algorithm, which is the only existing algorithm based on local restart, the UCB indexes are defined differently[2]: $f(t - \tau_k(t))$ is replaced by $f(n_t)$ with $n_t \doteq \sum_{k=1}^{K} n_k(t)$.

Threshold function β. We present in Appendix 7.10.4 numerical simulations that compare different choices of threshold functions β. We compare the non-explicit function used in

[2] This alternative is currently not correctly supported by theory, as we found mistakes in the analysis of CUSUM-UCB: the main problem resides in the use of Hoeffding's inequality with a *random* number of observations and a *random* threshold to obtain Eq. (31)-(32) in the paper [LLS18].

Lemma 7.3 (that makes use of a numerical approximation of the function $\mathcal{T}$), with the simpler value $\beta(n,\delta) = \ln(3n\sqrt{n}/\delta)$, as well as two other choices. To sum-up these simulations, they validate the use of a simpler and more explicit threshold, thus we recommend in practice to use $\beta_1(n,\delta) = \ln(3n\sqrt{n}/\delta)$.

Forced exploration. GLR-klUCB (lines 3-5) generalizes the deterministic exploration proposed for M-UCB by [CZKX19], whereas CUSUM-UCB performs a uniform random exploration. Both approaches are parameterized by $\omega \in (0,1)$. More precisely, CUSUM-UCB samples arm k with probability ω/K at each time step, and M-UCB uses a deterministic scheme, to force exploring the K arms: when the time since the last restart, $t-\tau$, is found to be in $[K]$ modulo $\lceil 1/\omega \rceil$. Both solutions ensure that all arms are sampled enough on each stationary sequence, so that the CD algorithm has enough *i.i.d.* samples to detect changes. A consequence of this forced exploration is given in Proposition 7.6 below.

Proposition 7.6. *For every pair of instants $s \leq t \in \mathbb{N}^*$ between two restarts on arm k,* i.e., *for a $i \in [NC_k]$, one has $\tau_k^{(i)} = \tau_k(t) < s \leq t < \tau_k^{(i+1)}$, it holds that $n_k(t) - n_k(s) \geq \lfloor \frac{\omega}{K}(t-s) \rfloor$.*

Proof. We consider one arm $k \in [K]$, and when the GLR-klUCB algorithm is running, we consider two time steps $s \leq t \in \mathbb{N}^*$, chosen between two restart times for that arm k. Lines 3-4 state that $A(u) = u \mod \lceil \frac{K}{\omega} \rceil$ if $u \mod \lceil \frac{K}{\omega} \rceil \in [K]$, thus we directly find

$$\begin{aligned}
n_k(t) - n_k(s) &= \sum_{u=s+1}^{t} \mathbb{1}(A(u) = k) \\
&\geq \sum_{u=s+1}^{t} \mathbb{1}\left(A(u) = k, A(u) = u \mod \left\lceil \frac{K}{\omega} \right\rceil\right) \\
&\geq \sum_{u=s+1}^{t} \mathbb{1}\left(k = u \mod \left\lceil \frac{K}{\omega} \right\rceil\right) \\
&= (t - (s+1) + 1) / \left\lceil \frac{K}{\omega} \right\rceil \geq \left\lfloor \frac{\omega}{K}(t-s) \right\rfloor.
\end{aligned}$$

□

Other forced exploration schemes? We present in Appendix 7.10.5 numerical simulations that compare three different options of forced exploration schemes. We compare the uniformly random exploration used by CUSUM-UCB, against the deterministic scheme used in Algorithm 7.1, and against a more complicated scheme based on *tracking* and inspired by [GK16]. To sum-up these simulations, the deterministic scheme gives an efficient change-point detection algorithm, and an efficient GLR-klUCB policy. As it is the simplest one to handle in our proofs, this is the one we chose for Algorithm 7.1.

7.6 Finite-time upper-bounds on the regret of GLR-klUCB

This section gives the finite-time regret bounds for the two variants, and interpretations of both results. We include only one proof, as the other is given in [BK19b].

7.6.1 Results for GLR-klUCB using *global restarts*

Recall that $\tau^{(i)}$ denotes the position of the i-th break-point and let $\mu_k^{(i)}$ be the mean of arm k on the segment between the i- and $(i+1)$-th break-point: $\forall t \in \{\tau^{(i-1)}+1, \dots, \tau^{(i)}\}, \mu_k(t) = \mu_k^{(i)}$. Let $i^* = \arg\max_k \mu_k^{(i)}$ and the largest gap at break-point i as $\Delta^{(i)} \doteq \max_{k\in[K]} |\mu_k^{(i)} - \mu_k^{(i-1)}| > 0$.

Assumption 7.7. *Define* $d^{(i)} \doteq d^{(i)}(\omega, \delta) \doteq \left\lceil \frac{4K}{\omega\left(\Delta^{(i)}\right)^2}\beta(T,\delta) + \frac{K}{\omega} \right\rceil$. *Then* we assume that there are enough samples between two global change-points. *In other words, we assume for all change* $i \in [\Upsilon_T]$, $\tau^{(i)} - \tau^{(i-1)} \geq 2\max(d^{(i)}, d^{(i-1)})$.

Assumption 7.7 is easy to interpret, and it is actually a standard assumption in non-stationary bandits. It requires that the distance between two consecutive break-points is large enough: how large depends on the magnitude of the largest change that happen at those two break-points. Under this assumption, we provide in Theorem 7.8 a finite time problem-dependent regret upper bound. It features the algorithm's parameters ω and δ, the KL-divergence terms $\mathrm{kl}(\mu_k^{(i)}, \mu_{k^*}^{(i)})$ expressing the hardness of the (stationary) MAB problem between two break-points, and the $\Delta^{(i)}$ terms expressing the hardness of the change-point detection problem in the i-th segment.

Theorem 7.8. *For* ω *and* δ *for which Assumption 7.7 is satisfied, the regret of* GLR-klUCB *with parameters* ω *and* δ *based on* ***Global*** *Restart satisfies the following* finite-time *regret bound*

$$R_T \leq 2\sum_{i=1}^{\Upsilon_T} \frac{4K}{\omega\left(\Delta^{(i)}\right)^2}\beta(T,\delta) + \omega T + \delta(K+1)\Upsilon_T + \sum_{k=1}^{K} \sum_{\substack{i=1,\dots,\Upsilon_T \\ \mu_k^{(i)} \neq \mu_{k^*}^{(i)}}} \frac{\left(\mu_{k^*}^{(i)} - \mu_k^{(i)}\right)}{\mathrm{kl}\left(\mu_k^{(i)}, \mu_{k^*}^{(i)}\right)} \ln(T) + \underline{\mathcal{O}}\left(\sqrt{\ln(T)}\right). \tag{7.14}$$

Warning: We highlight that *this result is finite-time* and not asymptotic, but if it uses the notation $\underline{\mathcal{O}}\left(\sqrt{\ln(T)}\right)$ for simplicity. This last term $\underline{\mathcal{O}}(\dots)$ does not mean the whole inequality is only valid for $T \to \infty$, but it rather means that at finite time, the inequality is valid with

the last term being a function $g(T)$, which is upper-bounded by a certain $c_0 \times \sqrt{\ln(T)}$, from a certain time T_0 (*i.e.*, $\forall T \geq T_0$). It is also the case of the next Theorem 7.11.

Corollary 7.9. *For "easy" problems satisfying the corresponding Assumption 7.7, let Δ^{opt} denote the smallest value of a sub-optimality gap on one of the stationary segments, and Δ^{change} be the smallest magnitude of any change-point on any arm, then the regret of* GLR-klUCB *with parameters ω and δ based Global Restarts satisfies*

1. *Choosing $\omega = \sqrt{\ln(T)/T}$, $\delta = 1/\sqrt{T}$ (with no prior knowledge of Υ_T) gives*

$$R_T = \mathcal{O}\left(\frac{K}{\left(\Delta^{change}\right)^2} \Upsilon_T \sqrt{T \ln(T)} + \frac{(K-1)}{\Delta^{opt}} \Upsilon_T \ln(T) \right), \tag{7.15}$$

2. *Choosing $\omega = \sqrt{\Upsilon_T \ln(T)/T}$, $\delta = 1/\sqrt{\Upsilon_T T}$ (with prior knowledge of Υ_T) gives*

$$R_T = \mathcal{O}\left(\frac{K}{\left(\Delta^{change}\right)^2} \sqrt{\Upsilon_T T \ln(T)} + \frac{(K-1)}{\Delta^{opt}} \Upsilon_T \ln(T) \right). \tag{7.16}$$

7.6.2 Results for GLR-klUCB using Local Restarts

Some new notations are needed to state a regret bound for GLR-klUCB using *local restarts*, and to distinguish notations between the results for the two variants (local and global restarts), we denote ℓ instead of i for the indexes of change-points. We let $\tau_k^{(\ell)}$ denote the position of the ℓ-th change-point *for arm k*: $\tau_k^{(\ell)} = \inf\{t > \tau_k^{(\ell-1)} : \mu_k(t) \neq \mu_k(t+1)\}$, with the convention $\tau_k^{(0)} = 0$, and let $\overline{\mu}_k^{(\ell)}$ be the ℓ-th value for the mean of arm k, such that $\forall t \in [\tau_k^{(\ell-1)}+1, \tau_k^{(\ell)}],\ \mu_k(t) = \overline{\mu}_k^{(\ell)}$. We also introduce the gap $\Delta_k^{(\ell)} = \overline{\mu}_k^{(\ell)} - \overline{\mu}_k^{(\ell-1)} > 0$.

Assumption 7.10. *Define $d_k^{(\ell)} \doteq d_k^{(\ell)}(\omega, \delta) \doteq \left\lceil \frac{4K}{\omega \left(\Delta_k^{(\ell)}\right)^2} \beta(T, \delta) + \frac{K}{\omega} \right\rceil$. Then* we assume that there are enough samples between two local change-points. *In other words, we assume that for all arm k and all change-point of that arm $\ell \in [N C_k]$, $\tau_k^{(\ell)} - \tau_k^{(\ell-1)} \geq 2\max(d_k^{(\ell)}, d_k^{(\ell-1)})$.*

Assumption 7.10 is easy to interpret, as Assumption 7.7, but it is non standard the literature, and to the best of the authors' knowledge, this analysis is the first one to consider such assumption on the problem difficulty. It requires that any two consecutive change-points *on a given arm* are sufficiently spaced (relatively to the magnitude of those two change-points). Under that assumption, Theorem 7.11 provides a regret upper bound that scales with similar quantities as that of Theorem 7.8, except that the number of break-points Υ_T is replaced with the *total* number of change-points $\mathrm{C}_T \doteq \sum_{k=1}^{K} N C_k$, which verifies $\Upsilon_T \leq \mathrm{C}_T \leq K \Upsilon_T$.

Theorem 7.11. *For ω and δ for which Assumption 7.10 is satisfied, the regret of* GLR-klUCB *with parameters ω and δ based on Local Restart satisfies the following* finite-time *regret bound*

$$R_T \leq 2\sum_{k=1}^{K}\sum_{\ell=1}^{NC_k}\frac{4K}{\omega\left(\Delta_k^{(\ell)}\right)^2}\beta(T,\delta)+\omega T+2\delta \mathrm{C}_T+\sum_{k=1}^{K}\sum_{\ell=1}^{NC_k}\frac{\ln(T)}{\mathrm{kl}(\overline{\mu}_k^{(\ell)},\mu_{i,\ell}^*)}+\underline{\mathcal{O}}\left(\sqrt{\ln(T)}\right), \quad (7.17)$$

where $\mu_{i,\ell}^* \doteq \inf\left\{\mu_{k_t^*}(t) : \mu_{k_t^*}(t) \neq \overline{\mu}_k^{(\ell)}, t \in [\tau_k^{(\ell)}+1, \tau_k^{(\ell+1)}]\right\}$.

Like for the first Theorem 7.8, we highlight that *this result is finite-time*. The proof of GLR-klUCB with *local restarts* is not included, but it can be found in the Appendix of [BK19b], as it is quite similar to the proof for *global restarts* given above. The main difficulty relies in defining the "good event" $\mathcal{E}_T$, and proving that it happens with high probability (by showing that the complementary event $\mathcal{E}_T^c$ is highly unlikely). We can directly obtain different regret upper-bounds for different choices of the two parameters ω and δ. We prefer to state the four cases, as this highlights the modularity of our analysis given by Theorem 7.11.

Corollary 7.12. *For "easy" problems satisfying the corresponding Assumption 7.10, with Δ^{opt} and Δ^{change} defined as in Corollary 7.9, then the regret of* GLR-klUCB *with parameters ω and δ based Local Restarts satisfies*

1. *Choosing $\omega = \sqrt{\ln(T)/T}$, $\delta = 1/\sqrt{T}$ (with no prior knowledge of Υ_T or C_T) gives*

$$R_T = \mathcal{O}\left(\frac{K}{\left(\Delta^{change}\right)^2}\mathrm{C}_T\sqrt{T\ln(T)}+\frac{\mathrm{C}_T}{\left(\Delta^{opt}\right)^2}\ln(T)\right), \quad (7.18)$$

2. *Choosing $\omega = \sqrt{\Upsilon_T\ln(T)/T}$, $\delta = 1/\sqrt{\Upsilon_T T}$ (with prior knowledge of Υ_T and "optimist" guess $\Upsilon_T \simeq \mathrm{C}_T \ll K\Upsilon_T$) gives*

$$R_T = \mathcal{O}\left(\frac{K^2}{\left(\Delta^{change}\right)^2}\sqrt{\Upsilon_T T\ln(T)}+\frac{K\Upsilon_T}{\left(\Delta^{opt}\right)^2}\ln(T)\right), \quad (7.19)$$

3. *Choosing $\omega = \sqrt{\mathrm{C}_T\ln(T)/T}$, $\delta = 1/\sqrt{\mathrm{C}_T T}$ (with prior knowledge of C_T) gives*

$$R_T = \mathcal{O}\left(\frac{K}{\left(\Delta^{change}\right)^2}\sqrt{\mathrm{C}_T T\ln(T)}+\frac{\mathrm{C}_T}{\left(\Delta^{opt}\right)^2}\ln(T)\right), \quad (7.20)$$

4. *Choosing $\omega = \sqrt{K\Upsilon_T\ln(T)/T}$, $\delta = 1/\sqrt{K\Upsilon_T T}$ (with prior knowledge of Υ_T and "pessimist" guess $\mathrm{C}_T \simeq K\Upsilon_T$) gives*

$$R_T = \mathcal{O}\left(\frac{K}{\left(\Delta^{change}\right)^2}\sqrt{\mathrm{C}_T T\ln(T)}+\frac{\mathrm{C}_T}{\left(\Delta^{opt}\right)^2}\ln(T)\right). \quad (7.21)$$

7.6.3 Interpretation and comparison of the results

The regret bounds we obtain for the two variants of GLR-klUCB, in Theorems 7.8 and 7.11 respectively, both show that there exists a tuning of ω and δ as a function and T *and the number of changes* such that the regret is of order $\mathcal{O}_h(K\sqrt{\Upsilon_T T\ln(T)})$ and $\mathcal{O}_h(K\sqrt{\mathrm{C}_T T\ln(T)})$ respectively, where the $\mathcal{O}_h$ notations ignore the gap terms. For very particular instances such that $\Upsilon_T = \mathrm{C}_T$, *i.e.*, at each break-point only one arm changes (*e.g.*, problem 1 from Figure 7.1), the theory advocates the use of local restarts. Indeed, while the regret guarantees obtained are similar, those obtained for local restarts hold for a wider variety of problems as Assumption 7.10 is less stringent than Assumption 7.7. Besides those specific instances, our results are essentially worse for *local* than for *global restarts*. However, we only obtain regret upper bounds – thus providing a theoretical safety net for both variants of our algorithm, and the practical story is different, as discussed in Section 7.8. Indeed, we find that GLR-klUCB performs better with local restarts, uniformly on all problems.

One can note that with the tuning of ω and δ prescribed by Corollaries 7.9 and 7.12, the regret bounds of GLR-klUCB hold for problem instances for which two consecutive break-points (or change-points on an arm) are separated by more than (about) $\sqrt{T\ln(T)}/(\Delta^{\text{change}})^2$ rounds. Hence those guarantees are valid on "easy" problems only, with "few" changes of "large" magnitudes, in particular they do not hold for the harder problems 3 or 5 presented in Section 7.8. However, this does not prevent our algorithms from performing well on more realistic instances, as shown by the numerical experiments, for instance with problem 3 presented in the next Section 7.8. And M-UCB [CZKX19] is also analyzed for the same type of unrealistic assumptions, while its practical performance is illustrated beyond those.

7.7 Proof of the regret upper-bounds

This section starts by giving a unified analysis of regret of the two variants of GLR-klUCB, then we give the proof of the finite-time regret bound for the variant using *global restarts*. The proof of the other variant using *local restarts* follows the skeleton of the unified analysis, and it can be found in Appendix E of [BK19b].

7.7.1 Sketch of the unified regret analysis

We emphasize that our approach is significantly different from those proposed by [CZKX19] for M-UCB and by [LLS18] for CUSUM-UCB. Recall that in this Chapter, the regret is defined as $R_T \doteq \mathbb{E}\left[\sum_{t=1}^{T}(\mu_{k_t^*}(t) - \mu_{A(t)}(t))\right]$. First, we introduce $\mathcal{D}(T,\omega)$ the (deterministic) set of time steps at which the forced exploration is performed before time T (see lines 3-4 in Algorithm 7.1), and as we observe that $\mu_{k_t^*} - \mu_{A(t)} \leq 1$ because rewards are assumed to be bounded in $[0,1]$, we can write a first decomposition of the regret, first without the expectation defining the

mean regret:

$$\begin{aligned}
&\sum_{t=1}^{T}(\mu_{k_t^*}(t) - \mu_{A(t)}(t)) \\
&\qquad \leq \sum_{t=1}^{T} \mathbb{1}(t \in \mathcal{D}(T,\omega)) + \sum_{t=1}^{T}(\mu_{k_t^*}(t) - \mu_{A(t)}(t))\mathbb{1}\left(t \notin \mathcal{D}(T,\omega), \mathrm{UCB}_{A(t)}(t) \geq \mathrm{UCB}_{k_t^*}(t)\right) \\
&\qquad \leq \omega T + \sum_{t=1}^{T} \mathbb{1}\left(\mathrm{UCB}_{k_t^*}(t) \leq \mu_{k_t^*}(t)\right) + \sum_{k=1}^{K}\sum_{t=1}^{T}(\mu_{k_t^*}(t) - \mu_k(t))\mathbb{1}\left(A(t)=k, \mathrm{UCB}_k(t) \geq \mu_{k_t^*}(t)\right).
\end{aligned}$$

Introducing some *good event* $\mathcal{E}_T$, to be specified in each case, and its complementary $\mathcal{E}_T^c$, one can write the following decomposition, that highlights two important terms (A) and (B)

$$\begin{aligned}
R_T \leq T\mathbb{P}\left(\mathcal{E}_T^c\right) + \omega T + \underbrace{\mathbb{E}\left[\mathbb{1}(\mathcal{E}_T)\sum_{t=1}^{T}\mathbb{1}\left(\mathrm{UCB}_{k_t^*}(t) \leq \mu_{k_t^*}(t)\right)\right]}_{(A)} \\
+ \underbrace{\mathbb{E}\left[\mathbb{1}(\mathcal{E}_T)\sum_{t=1}^{T}(\mu_{k_t^*}(t) - \mu_{A(t)}(t))\mathbb{1}\left(\mathrm{UCB}_{A(t)}(t) \geq \mu_{k_t^*}(t)\right)\right]}_{(B)}.
\end{aligned} \tag{7.22}$$

Each analysis requires to define an *appropriate good event*, stating that *some* change-points are detected within a reasonable delay. Each regret bound then follows from upper bounds on term (A), term (B), and on the failure probability $\mathbb{P}(\mathcal{E}_T^c)$. To control (A) and (B), we split the sum over consecutive segments, $[\tau^{(i)}+1, \tau^{(i+1)}]$ for *global restarts* and $[\tau_k^{(i)}+1, \tau_k^{(i+1)}]$ for each arm k for *local restarts*, and use elements from the analysis of kl-UCB from [CGM+13].

The tricky part of both proofs, which crucially exploits Assumption 7.7 or 7.10, is actually to obtain an upper bound on $\mathbb{P}(\mathcal{E}_T^c)$. For example for *local restarts* (Theorem 7.11), the good event is defined as $\mathcal{E}_T(\omega,\delta) \doteq \left(\forall k \in [K], \forall \ell \in [\mathrm{NC}_k], \widehat{\tau}_k^{(\ell)} \in \left[\tau_k^{(\ell)}+1, \tau_k^{(\ell)} + d_k^{(\ell)}\right]\right)$, where $\widehat{\tau}_k^{(\ell)}$ is defined as the ℓ-th change detected by the algorithm on arm k, and $d_k^{(\ell)} = d_k^{(\ell)}(\omega,\delta)$ is defined in Assumption 7.10. Introducing the event $\mathcal{C}_k^{(\ell)} \doteq \left\{\forall j \leq \ell, \widehat{\tau}_k^{(\ell)} \in \left[\tau_k^{(j)}+1, \tau_k^{(j)} + d_k^{(j)}\right]\right\}$, that all the changes up to the ℓ-th have been detected, a union bound yields this decomposition

$$\mathbb{P}(\mathcal{E}_T(\omega,\delta)^c) \leq \sum_{k=1}^{K}\sum_{\ell=1}^{\mathrm{NC}_k} \underbrace{\mathbb{P}\left(\widehat{\tau}_k^{(\ell)} \leq \tau_k^{(\ell)} \mid \mathcal{C}_k^{(\ell-1)}\right)}_{(a)} + \sum_{k=1}^{K}\sum_{\ell=1}^{\mathrm{NC}_k} \underbrace{\mathbb{P}\left(\widehat{\tau}_k^{(\ell)} \geq \tau_k^{(\ell)} + d_k^{(\ell)} \mid \mathcal{C}_k^{(\ell-1)}\right)}_{(b)}. \tag{7.23}$$

- Term (a) is related to the control of probability of false alarm, which is given by Lemma 7.3 for a change-point detector running in isolation. Observe that under the bandit algorithm, the change-point detector associated to arm k is based on (possibly much) less than $t - \tau_k(t)$ samples from arm k, which makes false alarm even less likely to occur. Hence, it is easy to show that $(a) \leq \delta$.

- Term (b) is related to the control of the detection delay, which is more tricky to obtain under the GLR-klUCB adaptive sampling scheme, when compared to a result like Lemma 7.5, or Theorem 6 in [Mai19] for the change-point detector running in isolation. More precisely, we need to leverage the forced exploration to be sure we have enough samples for detection, thanks to Proposition 7.6. This explains why delays defined in Assumption 7.10 are scaled by $1/\omega$. Using some elementary calculus and a concentration inequality given in Lemma 7.14, we can finally also prove that $(b) \leq \delta$.

Finally by controlling terms (a) and (b), the "bad event" is unlikely: $\mathbb{P}(\mathcal{E}_T^c) \leq 2\mathrm{C}_T\delta$. By putting together the three pieces, that are a bound on (A), (B) and $\mathbb{P}(\mathcal{E}_T^c)$, we obtain the desired finite-time upper-bound on the regret of GLR-klUCB.

7.7.2 Proof for GLR-klUCB with *global restarts*

The proof uses these notations: let $\widehat{\tau}^{(i)}$ be the i-th change detected by the algorithm, leading to the i-th (full) restart and let $\widehat{\tau}(t)$ be the last time before t that the algorithm restarted. We denote $n_k(t) \doteq \sum_{s=\tau(t)+1}^{t} \mathbb{1}(A(s) = k)$ the number of selections of arm k since the last (global) restart, and $\widehat{\mu}_k(t) \doteq \frac{1}{n_k(t)} \sum_{s=\tau(t)+1}^{t} Y_{k,s}\mathbb{1}(A(s) = k)$ their empirical average (if $n_k(t) \neq 0$).

As explained before, our analysis relies on the general regret decomposition (7.22), with the following appropriate good event. Let $d^(i)$ be defined as in Assumption 7.7, we define

$$\mathcal{E}_T(\delta) \doteq \left(\forall i \in [\Upsilon_T], \widehat{\tau}^{(i)} \in \left[\tau^{(i)} + 1, \tau^{(i)} + d^{(i)}\right]\right). \tag{7.24}$$

Under the good event, all the change-points are detected within a delay at most $d^{(i)}$. From Assumption 7.7, as the period between two changes are long enough, if $\mathcal{E}_T(\delta)$ holds, then for all change k, we have $\tau^{(i)} \leq \widehat{\tau}^{(i)} \leq \tau^{(i+1)}$. So we can prove the following.

Lemma 7.13. *The "bad event" $\mathcal{E}_T(\delta)$ defined in (7.24) is unlikely: $\mathbb{P}(\mathcal{E}_T^c(\delta)) \leq \delta(K+1)\Upsilon_T$.*

We now turn our attention to upper bounding the two terms (A) and (B) in (7.22).

Upper bound on term (A).

$$\begin{aligned}
(A) &\leq \mathbb{E}\left[\mathbb{1}(\mathcal{E}_T)\sum_{t=1}^{T}\mathbb{1}\left(n_{k_t^*}(t)\,\mathrm{kl}\left(\widehat{\mu}_{k_t^*}(t), \mu_{k_t^*}(t)\right) \geq f(t-\tau(t))\right)\right] \\
&\leq \sum_{i=1}^{\Upsilon_T}\mathbb{E}\left[\mathbb{1}(\mathcal{E}_T)\sum_{t=\tau^{(i)}+1}^{\tau^{(i+1)}}\mathbb{1}\left(n_{k^*}(t)\,\mathrm{kl}\left(\widehat{\mu}_{k^*}(t), \mu_{k^*}^{(i)}\right) \geq f(t-\widehat{\tau}(t))\right)\right] \\
&\leq \sum_{i=1}^{\Upsilon_T}\mathbb{E}\left[d^{(i)} + \mathbb{1}(\mathcal{E}_T)\sum_{t=\widehat{\tau}^{(i)}+1}^{\tau^{(i+1)}}\mathbb{1}\left(n_{k^*}(t)\,\mathrm{kl}\left(\widehat{\mu}_{k^*}(t), \mu_{k^*}^{(i)}\right) \geq f(t-\widehat{\tau}^{(i)})\right)\right]
\end{aligned}$$

$$\leq \sum_{i=1}^{\Upsilon_T} d^{(i)} + \sum_{i=1}^{\Upsilon_T} \mathbb{E}\left[\mathbb{1}(\mathcal{C}^{(i)}) \sum_{t=\widehat{\tau}^{(i)}}^{\tau^{(i+1)}} \mathbb{1}\left(n_{k^*}(t)\,\mathrm{kl}\left(\widehat{\mu}_{k^*}(t), \mu_{k^*}\right) \geq f(t-\widehat{\tau}^{(i)})\right)\right],$$

where we introduce the event $\mathcal{C}^{(i)}$ that all the changes up to the i-th have been detected:

$$\mathcal{C}^{(i)} = \left\{\forall j \leq k, \widehat{\tau}^{(j)} \in \{\tau^{(j)}+1, \ldots, \tau^{(j)}+d^{(j)}\}\right\}. \tag{7.25}$$

Clearly, $\mathcal{E}_T \subseteq \mathcal{C}^{(i)}$ and $\mathcal{C}^{(i)}$ is $\mathcal{F}_{\widehat{\tau}^{(i)}}$-measurable. Observe that conditionally to $\mathcal{F}_{\widehat{\tau}^{(i)}}$, when $\mathcal{C}^{(i)}$ holds, $\widehat{\mu}_{k^*}(t)$ is the average of samples that have all mean $\mu_{k^*}^{(i)}$. Thus, introducing $\widehat{\mu}_s$ as a sequence of *i.i.d.* random variables with mean $\mu_{k^*}^{(i)}$, one can write

$$\begin{aligned}
&\mathbb{E}\left[\mathbb{1}(\mathcal{C}^{(i)}) \sum_{t=\widehat{\tau}^{(i)}}^{\tau^{(i+1)}} \mathbb{1}\left(n_{k^*}(t)\,\mathrm{kl}\left(\widehat{\mu}_{k^*}(t), \mu_{k^*}^{(i)}\right) \geq f(t-\widehat{\tau}^{(i)})\right) \middle| \mathcal{F}_{\widehat{\tau}^{(i)}}\right] \\
&= \mathbb{1}(\mathcal{C}^{(i)}) \sum_{t=\widehat{\tau}^{(i)}}^{\tau^{(i+1)}} \mathbb{E}\left[\mathbb{1}\left(n_{k^*}(t)\,\mathrm{kl}\left(\widehat{\mu}_{k^*}(t), \mu_{k^*}^{(i)}\right) \geq f(t-\widehat{\tau}^{(i)})\right) \mid \mathcal{F}_{\widehat{\tau}^{(i)}}\right] \\
&\leq \mathbb{1}(\mathcal{C}^{(i)}) \sum_{t'=1}^{\tau^{(i+1)}-\widehat{\tau}^{(i)}} \mathbb{P}\left(\exists s \leq t' : s\,\mathrm{kl}(\widehat{\mu}_s, \mu_{k^*}^{(i)}) \geq f(t')\right) \\
&\leq \sum_{2=1}^{T} \frac{1}{t\ln(t)} \leq \ln(\ln(T)),
\end{aligned}$$

where the last but one inequality relies on the concentration inequality given in Lemma 2 of [CGM+13], for the choice $f(t) = \ln(t) + 3\ln(\ln(t))$. The last inequality comes from a sum-integral comparison, as $\int_1^T \frac{1}{t\ln(t)}\mathrm{d}t = \ln(\ln(T))$. Finally, the law of total expectation gives

$$(A) \leq \sum_{i=1}^{\Upsilon_T} \left[d^{(i)} + \ln(\ln(T))\right]. \tag{7.26}$$

Upper bound on term (B)**.** We let $\widetilde{\mu}_{k,s}^{(i)}$ denote the empirical mean of the first s observations of arm k made after time $t = \widehat{\tau}^{(i)}+1$. Rewriting the sum in t as the sum of consecutive intervals $[\tau^{(i)}+1, \tau^{(i+1)}]$, we obtain

$$\begin{aligned}
(B) &\leq \mathbb{E}\Big[\mathbb{1}(\mathcal{E}_T) \sum_{i=1}^{\Upsilon_T} \sum_{t=\tau^{(i)}}^{\tau^{(i+1)}} \left(\mu_{k^*}^{(i)} - \mu_{A(t)}^{(i)}\right) \mathbb{1}\left(\mathrm{UCB}_{A(t)}(t) \geq \mu_{k^*}^{(i)}\right)\Big] \\
&\leq \sum_{i=1}^{\Upsilon_T} \mathbb{E}\Big[\mathbb{1}(\mathcal{E}_T)\widehat{\tau}^{(i)} + \mathbb{1}(\mathcal{E}_T) \sum_{t=\widehat{\tau}^{(i)}+1}^{\tau^{(i+1)}} \left(\mu_{k^*}^{(i)} - \mu_{A(t)}^{(i)}\right) \mathbb{1}\left(\mathrm{UCB}_{A(t)}(t) \geq \mu_{k^*}^{(i)}\right)\Big] \\
&\leq \sum_{i=1}^{\Upsilon_T} d_k^{(i)} + \sum_{k=1}^{K} \mathbb{E}\Big[\mathbb{1}(\mathcal{E}_T) \sum_{t=\widehat{\tau}^{(i)}+1}^{\tau^{(i+1)}} \left(\mu_{k^*}^{(i)} - \mu_k^{(i)}\right) \mathbb{1}\left(A(t)=k, \mathrm{UCB}_k(t) \geq \mu_{k^*}^{(i)}\right)\Big]
\end{aligned}$$

$$
\begin{aligned}
&\leq \sum_{i=1}^{\Upsilon_T} d_k^{(i)} + \sum_{k=1}^{K}\sum_{i=1}^{\Upsilon_T}\left(\mu_{k^*}^{(i)} - \mu_k^{(i)}\right) \times \\
&\qquad \mathbb{E}\Big[\mathbb{1}(\mathcal{E}_T) \sum_{t=\widehat{\tau}^{(i)}+1}^{\tau^{(i+1)}} \sum_{s=1}^{t-\widehat{\tau}^{(i)}} \mathbb{1}\left(A(t)=k, n_k(t)=s\right) \mathbb{1}\left(s\,\mathrm{kl}(\widetilde{\mu}_{k,s}^{(i)}, \mu_{k^*}^{(i)}) \leq f(\tau^{(i+1)} - \widehat{\tau}^{(i)})\right)\Big] \\
&\leq \sum_{i=1}^{\Upsilon_T} d_k^{(i)} + \sum_{k=1}^{K}\sum_{i=1}^{\Upsilon_T}\left(\mu_{k^*}^{(i)} - \mu_k^{(i)}\right) \mathbb{E}\Big[\mathbb{1}(\mathcal{E}_T) \sum_{s=1}^{n_k(\tau^{(i+1)})} \mathbb{1}\left(s\,\mathrm{kl}(\widetilde{\mu}_{k,s}^{(i)}, \mu_{k^*}^{(i)}) \leq f(\tau^{(i+1)} - \tau^{(i)})\right)\Big] \\
&\leq \sum_{i=1}^{\Upsilon_T} d_k^{(i)} + \sum_{k=1}^{K}\sum_{i=1}^{\Upsilon_T}\left(\mu_{k^*}^{(i)} - \mu_k^{(i)}\right) \mathbb{E}\Big[\mathbb{1}(\mathcal{C}^{(i)}) \sum_{s=1}^{n_k(\tau^{(i+1)})} \mathbb{1}\left(s\,\mathrm{kl}(\widetilde{\mu}_{k,s}^{(i)}, \mu_{k^*}^{(i)}) \leq f(\tau^{(i+1)} - \tau^{(i)})\right)\Big].
\end{aligned}
$$

Conditionally to $\mathcal{F}_{\widehat{\tau}^{(i)}}$, when $\mathcal{C}^{(i)}$ holds, for $s \in [n_k(\tau^{(i+1)})]$, $\widetilde{\mu}_{k,s}^{(i)}$ is the empirical mean from *i.i.d.* observations of mean $\mu_k^{(i)}$. Therefore, introducing $\widehat{\mu}_s$ as a sequence of *i.i.d.* random variables with mean $\mu_k^{(i)}$, it follows from the law of total expectation that

$$
(B) \leq \sum_{i=1}^{\Upsilon_T} d^{(i)} + \sum_{k=1}^{K}\sum_{i=1}^{\Upsilon_T}\left(\mu_{k^*}^{(i)} - \mu_k^{(i)}\right) \sum_{s=1}^{\tau^{(i+1)}-\tau^{(i)}} \mathbb{P}\left(s \times \mathrm{kl}(\widehat{\mu}_s, \mu_{k^*}^{(i)}) \leq f(\tau^{(i+1)} - \tau^{(i)})\right).
$$

If $\mu_{k^*}^{(i)} > \mu_k^{(i)}$ by definition, we can use the analysis of kl-UCB from [CGM+13] to further upper bound the right-most part, and we obtain

$$
(B) \leq \sum_{i=1}^{\Upsilon_T} d^{(i)} + \sum_{k=1}^{K}\sum_{i=1}^{\Upsilon_T} \mathbb{1}\left(\mu_k^{(i)} \neq \mu_{k^*}^{(i)}\right) \left[\frac{\left(\mu_{k^*}^{(i)} - \mu_k^{(i)}\right)}{\mathrm{kl}(\mu_k^{(i)}, \mu_{k^*}^{(i)})} \ln(T) + \mathcal{O}\left(\sqrt{\ln(T)}\right)\right]. \tag{7.27}
$$

Combining the regret decomposition (7.22) with Lemma 7.13 and the two upper bounds of (A) in (7.26) and of (B) in (7.27),

$$
R_T \leq 2\sum_{i=1}^{\Upsilon_T} \frac{4K}{\omega\left(\Delta^{(i)}\right)^2}\beta(T,\delta) + \omega T + \delta(K+1)\Upsilon_T + \sum_{k=1}^{K} \sum_{i:\mu_k^{(i)} \neq \mu_{k^*}^{(i)}} \frac{\left(\mu_{k^*}^{(i)} - \mu_k^{(i)}\right)}{\mathrm{kl}\left(\mu_k^{(i)}, \mu_{k^*}^{(i)}\right)} \ln(T) + \mathcal{O}\left(\sqrt{\ln(T)}\right),
$$

which concludes the proof. □

Controlling the probability of the good event: proof of Lemma 7.13

Recall that $\mathcal{C}^{(i)}$ defined in (7.25) is the event that all the break-points up to the k-th have been correctly detected. Using a union bound, one can write

$$
\mathbb{P}(\mathcal{E}_T^c) \leq \sum_{i=1}^{\Upsilon_T} \mathbb{P}\left(\widehat{\tau}^{(i)} \notin \{\tau^{(i)}+1, \ldots, \tau^{(i)} + d^{(i)}\} \,\middle|\, \mathcal{C}^{(i-1)}\right)
$$

And thus we can split between a term corresponding to a false alarm and a term corresponding to a bounded detection delay,

$$\mathbb{P}(\mathcal{E}_T^c) \leq \sum_{i=1}^{\Upsilon_T} \underbrace{\mathbb{P}\left(\widehat{\tau}^{(i)} \leq \tau^{(i)} \mid \mathcal{C}^{(i-1)}\right)}_{(a)} + \sum_{i=1}^{\Upsilon_T} \underbrace{\mathbb{P}\left(\widehat{\tau}^{(i)} \geq \tau^{(i)} + d^{(i)} \mid \mathcal{C}^{(i-1)}\right)}_{(b)}.$$

The final result follows by proving that $(a) \leq K\delta$ and $(b) \leq \delta$, as detailed below.

Upper bound on (a): controlling the false alarm. We have $\widehat{\tau}^{(i)} \leq \tau^{(i)}$, which implies that there exists an arm whose associated change-point detector has experienced a false-alarm, *i.e.*,

$$\begin{aligned}(a) &\leq \mathbb{P}(\exists k \in [K], \exists s < t \leq n_k(\tau_k^{(i)}) : s\,\mathrm{kl}\left(\widehat{\mu}_{k,1:s}^{(i-1)}, \widehat{\mu}_{k,1:t}^{(i-1)}\right) \\ &\qquad + (t-s)\,\mathrm{kl}\left(\widehat{\mu}_{k,s+1:t}^{(i-1)}, \widehat{\mu}_{k,1:t}^{(i-1)}\right) > \beta(t,\delta) \mid \mathcal{C}^{(i-1)}) \\ &\leq \sum_{k=1}^{K} \mathbb{P}\left(\exists s < t : s\,\mathrm{kl}(\widehat{\mu}_{1:s}, \mu_k^{(i-1)}) + (t-s)\,\mathrm{kl}(\widehat{\mu}_{s+1:t}, \mu_k^{(i-1)}) > \beta(t,\delta)\right),\end{aligned}$$

where the last inequality simply comes from a union bound on $k \in [K]$, and with $\widehat{\mu}_{s:s'} \doteq \sum_{r=s}^{s'} Z_{i,r}$ where $Z_{i,r}$ is an *i.i.d.* sequence with mean $\mu_k^{(i-1)}$. Indeed, conditionally to $\mathcal{C}^{(i-1)}$, the $n_k(\tau^{(i)})$ successive observations of arm k arm starting from $\widehat{\tau}^{(i)}$ are *i.i.d.* with mean $\mu_k^{(i-1)}$. Using Lemma 7.4, term (a) is upper bounded by $K\delta$. □

Upper bound on term (b): controlling the delay. From the definition of $\Delta^{(i)}$, there exists an arm k such that $\Delta^{(i)} \doteq |\mu_k^{(i)} - \mu_k^{(i-1)}|$. We shall prove that it is unlikely that the change-point detector associated to this arm k does not trigger within the delay $d^{(i)}$.

First, it follows from Proposition 7.6 that there exists $\bar{t} \in \{\tau^{(i)}, \dots, \tau^{(i)} + d^{(i)}\}$ such that $n_k(\bar{t}) - n_k(\tau^{(i)}) = \overline{r}$, where $\overline{r} \doteq \lfloor \frac{\omega}{K} d^{(i)} \rfloor$ (as the mapping $t \mapsto n_k(t) - n_k(\tau^{(i)})$ is non-decreasing, is 0 at $t = \tau^{(i)}$ and its value at $\tau^{(i)} + d^{(i)}$ is larger than $\overline{r}$). Using the inclusion $\left(\widehat{\tau}^{(i)} \geq \tau^{(i)} + d^{(i)}\right) \subseteq \left(\widehat{\tau}^{(i)} \geq \bar{t}\right)$, the event $\left(\widehat{\tau}^{(i)} \geq \tau^{(i)} + d^{(i)}\right)$ further implies that

$$n_k(\tau^{(i)})\,\mathrm{kl}\left(\widetilde{\mu}_{i,n_k(\tau^{(i)})}^{(i-1)}, \widetilde{\mu}_{i,n_k(\bar{t})}^{(i-1)}\right) + \overline{r}\,\mathrm{kl}\left(\widetilde{\mu}_{i,n_k(\tau^{(i)}):n_k(\bar{t})}^{(i-1)}, \widetilde{\mu}_{i,n_k(\bar{t})}^{(i-1)}\right) \leq \beta(n_k(\tau^{(i)}) + \overline{r}, \delta),$$

where $\widetilde{\mu}_{k,s}^{(i-1)}$ denotes the empirical mean of the s first observation of arm k since the $(i-1)$-th restart $\widehat{\tau}^{(i-1)}$ and $\widetilde{\mu}_{i,s:s'}^{(i-1)}$ the empirical mean that includes observation number s to number s'. Conditionally to $\mathcal{C}^{(i-1)}$, $\widetilde{\mu}_{i,n_k(\tau^{(i)})}^{(i-1)}$ is the empirical mean of $n_k(\tau^{(i)})$ *i.i.d.* replications of mean $\mu^{(i-1)}$, whereas $\widetilde{\mu}_{i,n_k(\tau^{(i)}):n_k(\bar{t})}^{(i-1)}$ is the empirical mean of $\overline{r}$ *i.i.d.* replications of mean $\mu_k^{(i)}$.

Moreover, Proposition 7.6 shows that $n_k(\tau^{(i)})$ is bounded in a certain interval, $n_k(\tau^{(i)}) \in \left[\left\lfloor \frac{\omega}{K}\left(\tau^{(i)} - \widehat{\tau}^{(i-1)}\right)\right\rfloor, \left(\tau^{(i)} - \widehat{\tau}^{(i-1)}\right)\right]$. Conditionally to $\mathcal{C}^{(i-1)}$, by using Assumption 7.7, we

can prove that $d^{(i-1)} \leq (\tau^{(i)} - \tau^{(i-1)})/2$, and thus we obtain furthermore that

$$n_k(\tau^{(i)}) \in \left\{ \left\lfloor \frac{\omega}{2K}(\tau^{(i)} - \tau^{(i-1)}) \right\rfloor, \dots, \tau^{(i)} - \tau^{(i-1)} \right\} \doteq \mathcal{I}_i.$$

Introducing $\widehat{\mu}_{a,s}$ (resp. $\widehat{\mu}_{b,s}$) the empirical mean of s *i.i.d.* observations with mean $\widehat{\mu}_k^{(i-1)}$ (resp. $\widehat{\mu}_k^{(i)}$), such that $\widehat{\mu}_{a,s}$ and $\widehat{\mu}_{b,r}$ are independent, it follows that

$$(b) \leq \mathbb{P}\left(\exists s \in \mathcal{I}_i : s \,\mathrm{kl}\left(\widehat{\mu}_{a,s}, \frac{s\widehat{\mu}_{a,s} + \overline{r}\widehat{\mu}_{b,\overline{r}}}{s+\overline{r}} \right) + \overline{r}\,\mathrm{kl}\left(\widehat{\mu}_{b,\overline{r}}, \frac{s\widehat{\mu}_{a,s} + \overline{r}\widehat{\mu}_{b,\overline{r}}}{s+\overline{r}} \right) \leq \beta(s+\overline{r},\delta) \right),$$

where we used the following property on means of $x = y + z$ observations Z_i: $\widetilde{\mu}_{1:x} = \widetilde{\mu}_{1:y+z} = \frac{1}{y+z}\sum_{i=1}^{y+z} Z_i = \frac{1}{y+z}\left(y\widetilde{\mu}_{1:y} + z\widetilde{\mu}_{y+1:z}\right)$, with $x = n_k(\bar{t}) = y + z = n_k(\tau^{(i)}) + \overline{r}$, in order to compute $\widetilde{\mu}^{(i-1)}_{i,n_k(\bar{t})} = \left(n_k(\tau^{(i)})\widetilde{\mu}^{(i-1)}_{i,n_k(\tau^{(i)})} + \overline{r}\widetilde{\mu}^{(i-1)}_{i,n_k(\tau^{(i)}):n_k(\bar{t})} \right) / (n_k(\tau^{(i)}) + \overline{r})$.

Using Pinsker's inequality, and introducing the gap $\Delta_k^{(i)} \doteq \mu_k^{(i-1)} - \mu_k^{(i)}$ (which is such that $\Delta^{(i)} = |\Delta_k^{(i)}|$), one can write

$$\begin{aligned}
(b) &\leq \mathbb{P}\left(\exists s \in \mathcal{I}_i : \frac{2s\overline{r}}{s+\overline{r}} \left(\widehat{\mu}_{a,s} - \widehat{\mu}_{b,\overline{r}}\right)^2 \leq \beta(s+\overline{r},\delta) \right) \\
&\leq \mathbb{P}\left(\exists s \in \mathbb{N} : \frac{2sr}{s+r} \left(\widehat{\mu}_{a,s} - \widehat{\mu}_{b,s} - \Delta_k^{(i)}\right)^2 \geq \beta(s+r,\delta) \right) \\
&+ \mathbb{P}\left(\exists s \in \mathcal{I}_i : \frac{2s\overline{r}}{s+\overline{r}} \left(\widehat{\mu}_{a,s} - \widehat{\mu}_{b,\overline{r}} - \Delta_k^{(i)}\right)^2 \leq \beta(s+\overline{r},\delta), \frac{2s\overline{r}}{s+\overline{r}} \left(\widehat{\mu}_{a,s} - \widehat{\mu}_{b,\overline{r}}\right)^2 \leq \beta(s+\overline{r},\delta) \right)
\end{aligned}$$

Using Lemma 7.14 stated in Appendix 7.10.2, and a union bound, the first term in the right hand side is upper bounded by δ (as $\beta(r+s,\delta) \geq \beta(r,\delta) \geq \ln(3s\sqrt{s}/\delta)$). For the second term, we use the observation

$$\frac{2s\overline{r}}{s+\overline{r}} \left(\widehat{\mu}_{a,s} - \widehat{\mu}_{b,\overline{r}} - \Delta_k^{(i)}\right)^2 \leq \beta(s+\overline{r},\delta) \quad \Rightarrow \quad |\widehat{\mu}_{a,s} - \widehat{\mu}_{b,\overline{r}}| \geq |\Delta_k^{(i)}| - \sqrt{\frac{s+\overline{r}}{2\overline{r}s}\beta(s+\overline{r},\delta)}$$

and, using that $\Delta^{(i)} = |\Delta_k^k|$, one obtains

$$(b) \leq \delta + \mathbb{P}\left(\exists s \in \mathcal{I}_i : \Delta^{(i)} \leq 2\sqrt{\frac{s+\overline{r}}{2s\overline{r}}\beta(s+\overline{r},\delta)} \right). \tag{7.28}$$

Define $s_{\min} \doteq \left\lfloor \frac{\omega}{K}(\tau^{(i)} - \tau^{(i-1)})/2 \right\rfloor$. Using the fact that the two mappings $s \mapsto (s+\overline{r})/s\overline{r}$ and $s \mapsto \beta(s+\overline{r},\delta)$ are respectively decreasing and increasing in s, one has, for all $s \in \mathcal{I}_i$,

$$2\frac{s+\overline{r}}{s\overline{r}}\beta\left(s+\overline{r},\delta\right) \quad \leq \quad 2\frac{s_{\min}+\overline{r}}{s_{\min}\overline{r}}\beta\left(T,\delta\right) \leq \frac{4\beta(T,\delta)}{\left\lfloor \frac{\omega}{K}d^{(i)} \right\rfloor},$$

where the last inequality follows from the fact that $\overline{r} \leq s_{\min}$ as $d^{(i)} \leq (\tau^{(i)} - \tau^{(i-1)})/2$ by Assumption 7.7. Now the definition of $d^{(i)}$ readily implies that $\left\lfloor \frac{\omega}{K} d^{(i)} \right\rfloor > \frac{4\beta(T,\delta)}{(\Delta^{(i)})^2}$, which yields

$$\forall s \in \mathcal{I}_i, \ \ 2\frac{s+\overline{r}}{s\overline{r}}\beta(s+\overline{r},\delta) \leq \left(\Delta^{(i)}\right)^2.$$

Hence, the probability in the right-hand side of (7.28) is zero, which yields $(b) \leq \delta$. □

7.8 Experimental results for piece-wise stationary bandits

In this section we report results of numerical simulations performed on synthetic data, in order to compare the performance of GLR-klUCB against other state-of-the-art approaches, on some piece-wise stationary bandit problems. For simplicity, we restrict to rewards generated from Bernoulli distributions, even if GLR-klUCB can be applied to any bounded distributions.

We report results obtained on five different piece-wise stationary bandit problems, illustrated in Figures 7.1 and 7.2 above, and Figures 7.5, 7.6 and 7.7 below. We present regret tables and regret plots, for which the mean regret was estimated using 1000 independent runs.

Algorithms and parameters tuning. We include in this study two algorithms designed for the classical stationary MAB, kl-UCB [GC11], and Thompson sampling [AG12, KKM12], and an "oracle" version of kl-UCB, that we call Oracle-Restart. This algorithm knows the exact locations of the break-points, and restarts kl-UCB at those locations (without any delay).

Then, we compare our algorithms to several competitors designed for a piece-wise stationary model. For a fair comparison, all algorithms that use UCB as a sub-routine were adapted to use kl-UCB instead, which yields better performance[3]. Moreover, all the algorithms are tuned as described in the corresponding paper, using in particular the knowledge of the number of break-points Υ_T and the horizon T. We first include three *passively adaptive algorithms*: Discounted kl-UCB (D-kl-UCB, [KS06]), with discount factor $\gamma = 1 - \sqrt{\Upsilon_T/T}/4$, Sliding-Window kl-UCB (SW-kl-UCB, [GM11]) using window-size $\tau = 2\sqrt{T\ln(T)/\Upsilon_T}$ and Discounted Thompson sampling (DTS, [RK17]) with discount factor $\gamma = 0.95$. For this last algorithm, the discount factor $\gamma = 0.75$ suggested by the authors was performing significantly worse on the problem instances we tried. More precisely, we found that $\gamma \leq 0.95$ gives better performances for short-term problems (problems $1, 2, 4$) and $\gamma \geq 0.95$ is better suited for long experiments (problems $3, 5$). Additionally, we include the Exp3.S algorithm from [ACBFS02], setting its parameters as in the Corollary 8.3 of the paper: $\omega = 1/T$ and $\gamma = \min(1, \sqrt{K(\Upsilon_T \ln(KT) + \mathrm{e})/((\mathrm{e}-1)T)})$, based on a prior knowledge of T and Υ_T.

[3] [LLS18, CZKX19] both mention that extending their analysis to the use of kl-UCB should not be too difficult.

The main goal here is to compare against *actively adaptive algorithms*. We include CUSUM-klUCB, tuned with $M = 150$ and $\varepsilon = 0.1$ for easy problems $(1, 2, 4)$ and $\varepsilon = 0.001$ for hard problems $(3, 5)$, and with $h = \ln(T/\Upsilon_T)$, $\omega = \sqrt{\Upsilon_T \ln(T/\Upsilon_T)/T}$, as suggested in the paper [LLS18]. Finally, we include M-klUCB, tuned with $w = 150$, based on a prior knowledge of the problems as the formula using $\delta_{\min}$ given in [CZKX19] is too large for small horizons (on all the problem instances), a threshold $b = \sqrt{w \ln(2KT)}$ and $\gamma = \sqrt{\Upsilon_T K(2b + 3\sqrt{w})/(2T)}$ as suggested by Remark 4 in the paper [CZKX19].

For GLR-klUCB, we explore the two different options with **Local** and **Global** restarts, using respectively $\delta = 1/\sqrt{\Upsilon T}, \omega = \omega_0\sqrt{\Upsilon_T \ln(T)/T}$ and $\delta = 1/\sqrt{K\Upsilon_T T}, \omega = \omega_0\sqrt{K\Upsilon_T \ln(T)/T}$ from Corollaries 7.9 and 7.12. Both choices of ω appear to be too large empirically, as they come from minimizing the regret upper-bound rather than the regret itself, thus the constant is set to $\omega_0 = 0.05$. We show in Appendix G of [BK19b] a sensitivity analysis on ω, which concludes to a robustness regarding this parameter, with similar regret as soon as $\omega \leq 0.1$. We do not use a constant δ_0 to change the confidence level to $\delta = \delta_0\delta_T$, as we verified empirically that $\delta_0 = 1$ is uniformly better for different problems. To speed up the simulations, two optimizations are used, with $\Delta n = \Delta s = 10$, and CUSUM also uses the first trick with $\Delta n = 10$ (see Appendix 7.10.3 for more details).

Time and memory costs of GLR-klUCB. Finally, we mention that we discuss in details in Appendix F of [BK19b] about the time and memory complexities of GLR-klUCB, and the other algorithms considered for the numerical experiments. To sum up, at every time step the CPD algorithm needs a time $\mathcal{O}(n_i) = \mathcal{O}(d_{\max})$, and at the end, the time complexity of CUSUM-klUCB as well as GLR-klUCB is $\mathcal{O}(KTd_{\max})$, which can be up-to $\mathcal{O}(KT^2)$, much more costly than $\mathcal{O}(KT)$ for kl-UCB for instance. Our proposal GLR-klUCB requires a storage of the order of $\mathcal{O}(Kd_{\max})$ and a running time of the order of $\mathcal{O}(KTd_{\max})$. We validated the two bounds experimentally, with results presented in Tables 2 and 3 in [BK19b].

Examples of detection delays *on one run* for two simple problems. Before giving larger results that compare our approach against other algorithms, we consider the two problems 1 and 2 presented above in Figures 7.1 and 7.2 (for $T = 5000$). *For one (random) simulation*, we give below examples of the efficiency of the change-point detection algorithm used by GLR-klUCB as well as CUSUM-klUCB and M-klUCB, by showing the times at which they detect a change and reinitialize their memory of observations of one or all the arms. As shown below, in the experiments summary, the three algorithms based on change-point detection obtain sub-linear regret, but they have different behaviors. The test in M-UCB usually detects less changes, while the test in CUSUM-UCB usually detects more changes and even unnecessary changes. On the examples presented below as well as large scale examples,

all the tests appear to have no (or a small number of) false alarm, and always a small detection delay for changes that are "easy enough" to be efficiently detected.

Problem 1 has only local changes, and important changes, that denote here changes on the current optimal arm, happen only at $t = 2000$ when arm 2 becomes sub-optimal (μ_2 goes from 0.9 to 0.1) and arm 0 becomes optimal, and at $t = 3000$ when arm 0 stays optimal but sees its mean change from 0.3 to 0.7. Other changes concern arm 1 at $t = 1000$ and $t = 4000$.

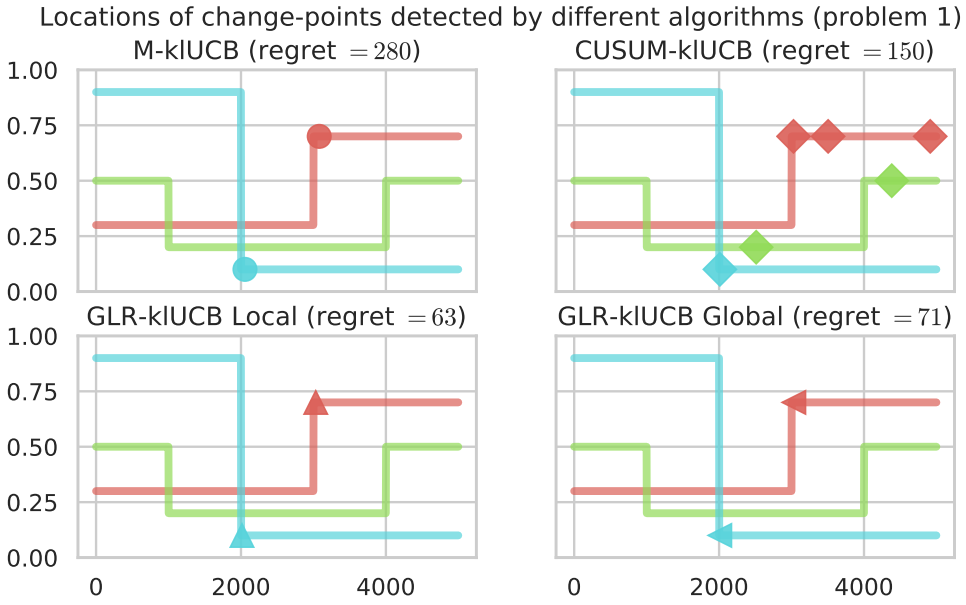

Figure 7.3 – Locations of the detected change-points for four algorithms on Problem 1.

Figure 7.3 displays the locations of the successively detected change-points by four algorithms, 1) M-klUCB, 2) CUSUM-klUCB, 3) GLR-klUCB with *local restart*, 4) GLR-klUCB with *global restart*. In this "easy" problem, all algorithms correctly detect the important changes, except CUSUM which detected a change on arm 1 (in red) twice after the change-point located at $t = 3000$. The three other algorithms have a very small delay, for instance only 9 samples from arm 0 (in blue) after its change at time $t = 2000$ are enough for the GLR test to detect a change. Very small delays are possible only after having collected a lot of samples of the arm which changed, and for instance the same algorithm obtains a delay of 32 samples from arm 1 for the next change at $t = 3000$, because this arm was sampled less. On this problem, while M-klUCB detects the same changes as GLR-klUCB, with larger but comparable delays, it is seen to obtain a larger regret than the two GLR variants, simply because the tuning of its forced exploration probability (*i.e.*, ω) makes it explore sub-optimal arms more often.

Problem 2 has only global changes, and important changes happen only at $t = 1000$ when arm 2 sees its mean change from 0.9 to 0.7, then at $t = 2000$ when it becomes sub-optimal (μ_2

goes from 0.7 to 0.5) and arm 0 becomes optimal, and at $t = 3000$ and $t = 4000$ when arm 0 stays optimal but sees its mean change from 0.6 to 0.7 and then from 0.7 to 0.8.

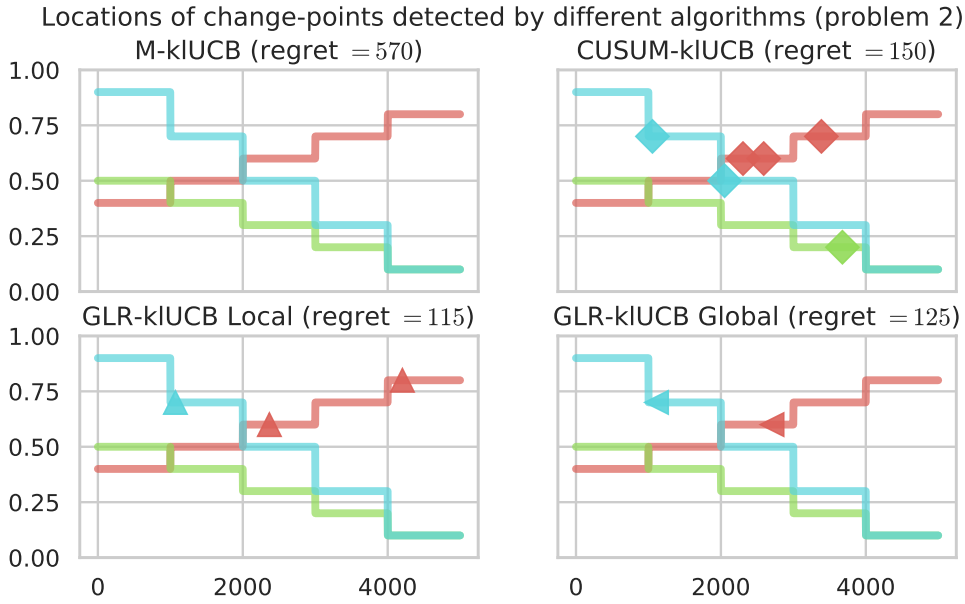

Figure 7.4 – Locations of the detected change-points for four algorithms on Problem 2.

Like for the first problem, we illustrate the behavior of the same four algorithms in Figure 7.4. In this other problem, the difference between M-klUCB and CUSUM-klUCB is clear: the first algorithm fails to detect any change, leading to a large regret, while the second one detects the changes that happen on the currently optimal arm and some other changes. Drawing conclusions on their behavior from a single simulation is meaningless, as this example of behavior is counter intuitive: On the one hand, CUSUM uses local restarts, and it should be less efficient than global restarts for this problem, as changes are all global. On the other hand, M-klUCB uses global restarts, but here it fails to detect any change. The two GLR-klUCB variants correctly detect the important changes, and we observe that their delays to detect a change can vary, mainly due to the randomness (we remind that we illustrate only one repetition of the simulation here). For instance, after the change on arm 1 (in red), the *local restart* detects it at time $t = 2376$ and the *global restart* detects it at time $t = 2701$.

In these two examples, we compare the two variants of GLR-klUCB, with the two state-of-the-art policies CUSUM-klUCB and M-klUCB, that are all based on combining kl-UCB with a change-point detection algorithm. The results given above should be taken carefully, they only have the purpose of being an illustration of the possible behaviors of these algorithms, as they are the results of *only one* (*random*) *simulation*! But it is still interesting to compare the final regret in one run, as given above, with the mean regret for 1000 independent runs, as given below in Table 7.2. The values change, but the ranking stays the same: GLR-klUCB

outperforms both CUSUM-klUCB and M-klUCB, and the test based on CUSUM seems more efficient than the test based of M-klUCB in the problems at hand.

Illustrations of the rest of the benchmark. We continue here the presentation of the other problems of our benchmark, after Figures 7.1 and 7.2 above for the two problems 1 and 2.

Problem 3. (see Figure 7.5) This problem is harder, with $K = 6$, $\Upsilon_T = 8$ and $T = 20000$. At every break-point, almost all arms change, and means are bounded in $[0.01, 0.07]$. The gaps Δ are much smaller than for the first problems, with amplitudes ranging from 0.02 to 0.001. Note that the assumptions of the regret upper bounds for GLR-klUCB are violated, as well as the assumptions for the analysis of M-UCB and CUSUM-UCB. It is interesting to say that this problem is inspired from Figure 3 of [CZKX19], where the synthetic data was obtained from manipulations on a real-world database of clicks from *Yahoo!*. The details fall outside of the scope of this section, and are well explained in the paper [CZKX19].

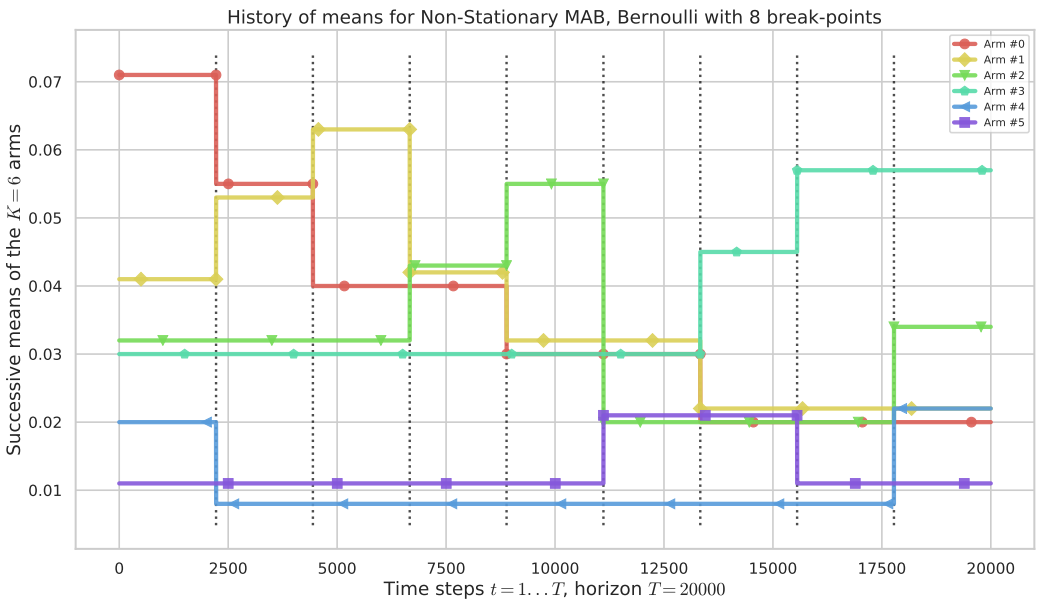

Figure 7.5 – Problem 3: $K = 6$, $T = 20000$, $C = 19$ changes occur on most arms at $\Upsilon = 8$ break-points.

Problem 4. Like problem 1, it uses $K = 3$ arms, $\Upsilon = 4$ change-points and $T = 5000$, but the stationary sequences between successive change-points no longer have the same length, as illustrated in Figure 7.6. Classical (stationary) algorithms such as kl-UCB can be "tricked" by large enough stationary sequences, as they start by learning with a large confidence the optimal arm, and then fail to adapt to a new optimal arm after a change-point. We observe below in Table 7.3 that they can suffer higher regret when the change-points are more spaced out, like for instance for this problem starting with a longer stationary sequence of length $T/2$.

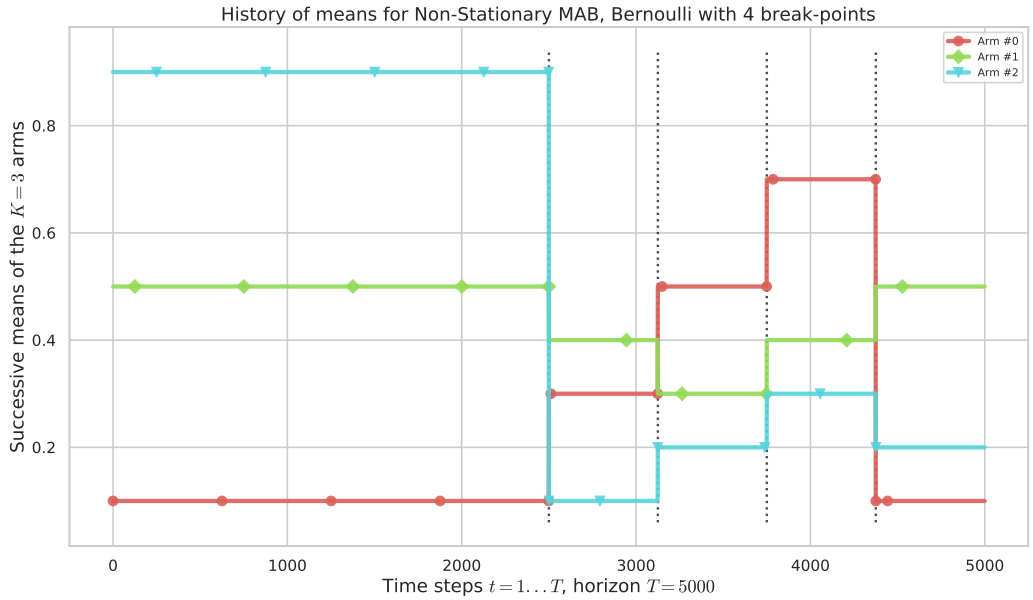

Figure 7.6 – Problem 4: $K = 3$, $T = 5000$, $C = 12$ changes occur on all arms at $\Upsilon = 4$ break-points.

Problem 5. Like problem 3, this harder problem is inspired from synthetic data obtained from a real-world database of clicks from *Yahoo!*, but from another competitor paper, see Figure 3 from [LLS18]. It is a much harder piece-wise stationary problem, with $\Upsilon = 81$ change-points on $K = 5$ arms for a longer horizon of $T = 100000$. Some arms change at almost every time steps, for a total number of break-points $C = 179$, but the optimal arm is almost always the same one (arm 0, with •). It is a good benchmark to see if the actively adaptive policies do not detect *too many changes*, as the Oracle-Restart policy suffers higher regret in comparison to kl-UCB. Means are also bounded in $[0.01, 0.07]$, with small gaps of amplitude in $[0.001, 0.02]$, as shown in Figure 7.7.

First experiment: UCB vs kl-UCB. Similarly to what is presented in Chapter 6 in Table 6.1, we start by some experiments that justify the focus on the kl-UCB index policy. Indeed, the purpose of this work is not to optimize on the index policy, but rather propose new ways of using indices for piece-wise stationary problems. We run two experiments on **problems 1** and **2**, with a horizon of $T = 20000$ and 1000 independent repetitions, for which we compare UCB against kl-UCB, for CUSUM-, M-, GLR and the oracle policy. We report in Table 7.1 below the results (in terms of mean regret), and we observe that using kl-UCB rather than UCB indices always yields better practical performance.

Thus it is fair to compare our proposal against the modified versions of the two algorithms CUSUM- and M- that use the kl-UCB index policy instead of UCB, as they perform uniformly

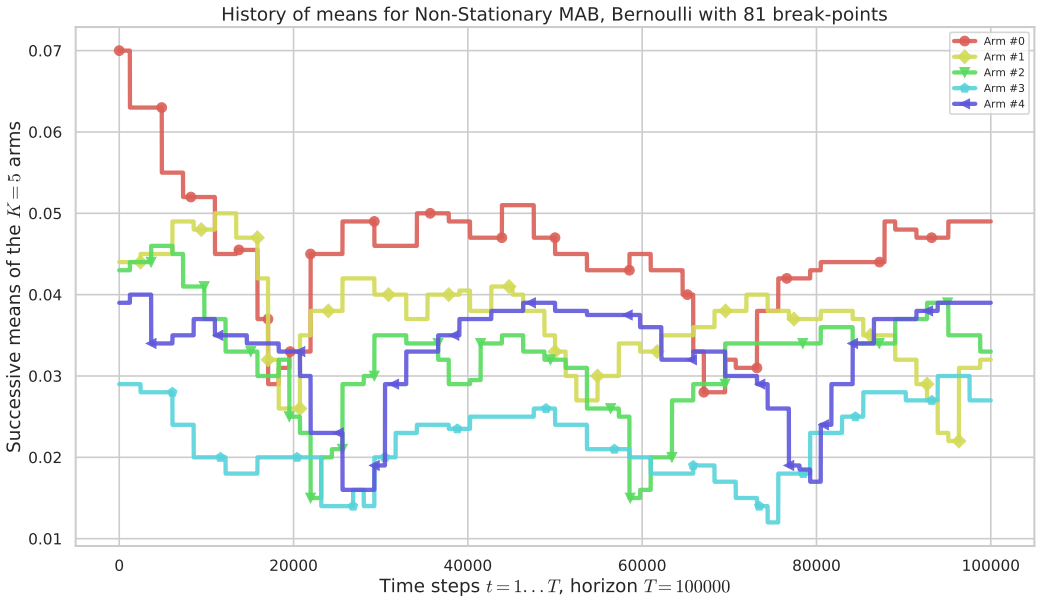

Figure 7.7 – Pb 5: $K = 5$, $T = 100000$, $C = 179$ changes occur on some arms at $\Upsilon = 81$ break-points.

better with kl-UCB than with UCB (the same tendency was observed on all other problems). We also note that, without surprise, the oracle policy also performs (much) better with kl-UCB than with UCB. Consequently, from now on we only report results for kl-UCB.

Algorithm	Index policy	Problem 1	Problem 2
Oracle-Restart	UCB	216	219
	kl-UCB	**54**	**67**
M-	UCB	878	2040
	kl-UCB	817	1485
CUSUM	UCB	439	381
	kl-UCB	304	316
GLR (Local)	UCB	191	232
	kl-UCB	**132**	**186**

Table 7.1 – Mean regret $\pm$ 1 std-dev, on problems 1 and 2 with $T = 5000$. We conclude that using kl-UCB is much more efficient than using UCB, for non-stationary bandit.

Results on the entire benchmark. The two Tables 7.2 and 7.3 show the final regret R_T obtained for each algorithm. Results highlighted in **bold** show the best non-oracle algorithm for each experiment, with GLR-klUCB being the best non-oracle strategy for problems 1 and 2. Thompson sampling and kl-UCB are efficient, and better than Discounted-kl-UCB which is inefficient. DTS and SW-kl-UCB can sometimes be more efficient than their stationary counterparts, but perform worse than the Oracle and most actively adaptive algorithms. For

kl-UCB indexes, M- and CUSUM- outperform the previous algorithms, but GLR- is often better. On these problems, GLR-klUCB with **Local** restarts is always more efficient than with **Global** restarts. Note that on problem 2, all means change at every break-point, hence one could expect the Global variant to be more efficient, yet the experiments show the superiority of Location variant on every instance. The Exp3.S algorithm was found to outperform other algorithms based on Exp3, including recent variants like Exp3^{++} [SL17] or Exp3.R from [AFM17]. Exp3.S usually performs similarly to M-klUCB, but it is greatly outperformed by the oracle algorithm, by GLR-klUCB and by CUSUM-klUCB.

Algorithms \ Problems	Pb 1	Pb 2 ($T = 5000$)	Pb 3 ($T = 20000$)
Oracle-Restart kl-UCB	$\mathbf{37 \pm 37}$	$\mathbf{45 \pm 34}$	$\mathbf{257 \pm 86}$
Exp3.S	352 ± 51	310 ± 62	665 ± 93
kl-UCB	270 ± 76	162 ± 59	529 ± 148
Discounted-kl-UCB	1456 ± 214	1442 ± 440	1376 ± 37
SW-kl-UCB	177 ± 34	182 ± 34	1794 ± 71
Thompson sampling	493 ± 175	388 ± 147	1019 ± 245
DTS	209 ± 38	249 ± 39	2492 ± 52
M-klUCB	290 ± 29	534 ± 93	645 ± 141
CUSUM-klUCB	148 ± 32	152 ± 42	$\mathbf{490 \pm 133}$
GLR-klUCB(Local)	$\mathbf{74 \pm 31}$	$\mathbf{113 \pm 34}$	513 ± 97
GLR-klUCB(Global)	97 ± 32	134 ± 33	621 ± 103

Table 7.2 – Mean regret $\pm$ 1 std-dev, on problems 1, 2 (with $T = 5000$) and 3 ($T = 20000$).

Algorithms \ Problems	Pb 4 ($T = 5000$)	Pb 4 ($T = 10000$)	Pb 5
Oracle-Restart kl-UCB	$\mathbf{68 \pm 40}$	$\mathbf{86 \pm 50}$	126 ± 54
Exp3.S	551 ± 63	860 ± 109	723 ± 121
kl-UCB	615 ± 74	1218 ± 123	106 ± 36
SW-kl-UCB	202 ± 33	322 ± 47	228 ± 27
Discounted-kl-UCB	911 ± 210	1741 ± 200	2085 ± 910
Thompson sampling	756 ± 65	1476 ± 137	$\mathbf{88 \pm 39}$
DTS	250 ± 39	481 ± 58	238 ± 24
M-klUCB	337 ± 46	544 ± 47	116 ± 36
CUSUM-klUCB	267 ± 69	343 ± 94	117 ± 34
GLR-klUCB(Local)	$\mathbf{99 \pm 32}$	$\mathbf{128 \pm 42}$	149 ± 34
GLR-klUCB(Global)	128 ± 32	185 ± 47	152 ± 32

Table 7.3 – Mean regret $\pm$ 1 std-dev. Problem 4 use $K = 3$ arms, and a first long stationary sequence. Problem 5 use $K = 5$, $T = 100000$ and is much harder with $\Upsilon = 82$ break-points and $C = 179$ changes.

We highlight that the best non-oracle strategies are actively adaptive, thus the experiments confirm that an efficient bandit algorithm (*e.g.*, kl-UCB) combined with an efficient change-point detector (*e.g.*, GLR) provides efficient strategies for the piece-wise stationary model.

Regret plots. We show below on Figure 7.8 and additional in Appendix 7.10.1 the simulation results for the five problems. The results of Tables 7.2 and 7.3 focus on the value of R_T at the end of each bandit game, but it is also interesting to observe two plots for each experiment. First, we show the mean regret as a function of time (*i.e.*, R_t for $t \in [T]$), for 9 of the considered algorithms (as they are outperformed by the others, Exp3.S and Discounted-kl-UCB are not included in order to avoid clutter). Efficient stationary algorithms, like TS and kl-UCB, typically suffer a linear regret after a change on the optimal arm, if they had "too" many samples before the change-points (*e.g.*, on Figure 7.8 and even more on Figures 7.11 and 7.13). This illustrates the conjecture that classical algorithms can suffer linear regret even on simple piece-wise stationary problems.

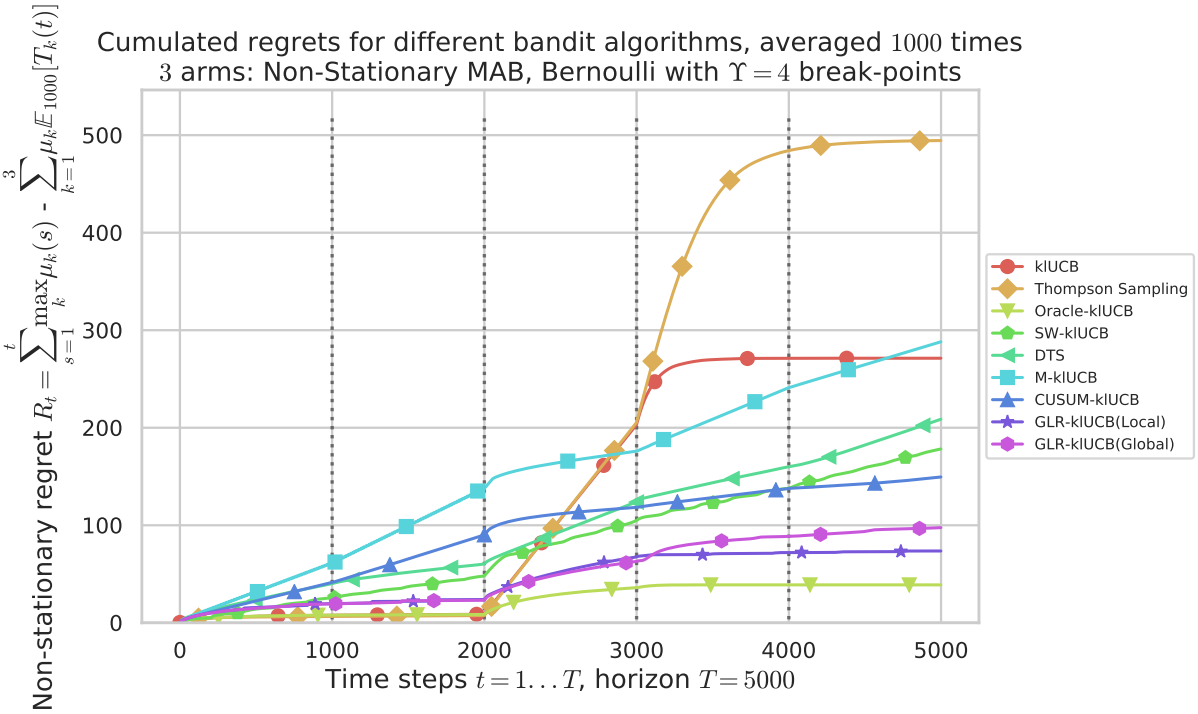

Figure 7.8 – Mean regret as a function of time, R_t for horizon $T = 5000$, for problem 1.

On simple problems, like problem 1, all the algorithms being designed for piece-wise stationary environments perform similarly, but as soon as the gaps are smaller or there are more changes, we observe that GLR-klUCB can outperform the two other actively adaptive algorithms CUSUM-klUCB and M-klUCB (*e.g.*, on Figure 7.9), and performs much better than passively adaptive algorithms DTS and SW-kl-UCB (*e.g.*, on Figure 7.12). Our approach is the algorithm which performs the closer to the oracle for problem 4.

Finally, in the case of hard problems, like problems 3 and 5, that have a lot of changes but where the optimal arm barely changes, we verify in Figure 7.13 that kl-UCB and TS can outperform the oracle policy. Indeed the oracle policy is sub-optimal as it restarts as soon

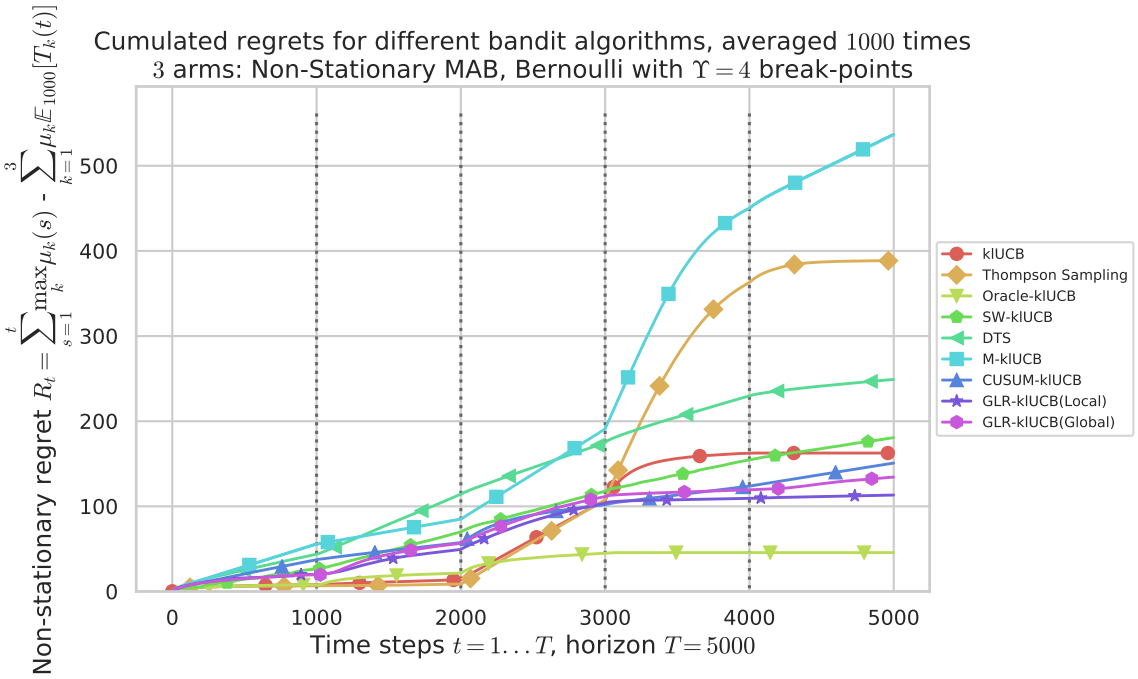

Figure 7.9 – Mean regret as a function of time, R_t for horizon $T = 5000$, for problem 2.

as one arm change but is unaware of the meaningful changes, and stationary policies which quickly identify the best arm will play it most of the times, achieving a smaller regret. We note that, sadly, all actively adaptive policies fail to outperform stationary policies on such hard problems, because they do not observe enough rewards from each arm between two restarts (*i.e.*, the Assumptions 7.7 and 7.10 for the two Theorems 7.8 and 7.11 are not satisfied). We can also verify that the two options, **Local** and **Global** restart, for GLR-klUCB, give close results, and that the **Local** option is always better.

We also show the empirical distribution of the regret R_T, on Figure 7.10 below. It shows that algorithms efficient in terms of regret also have a small variance on their regret.

Reproducibility. The experiments in this chapter use SMPyBandits, and the instructions to reproduce them are given on `SMPyBandits.GitHub.io/NonStationaryBandits.html`.

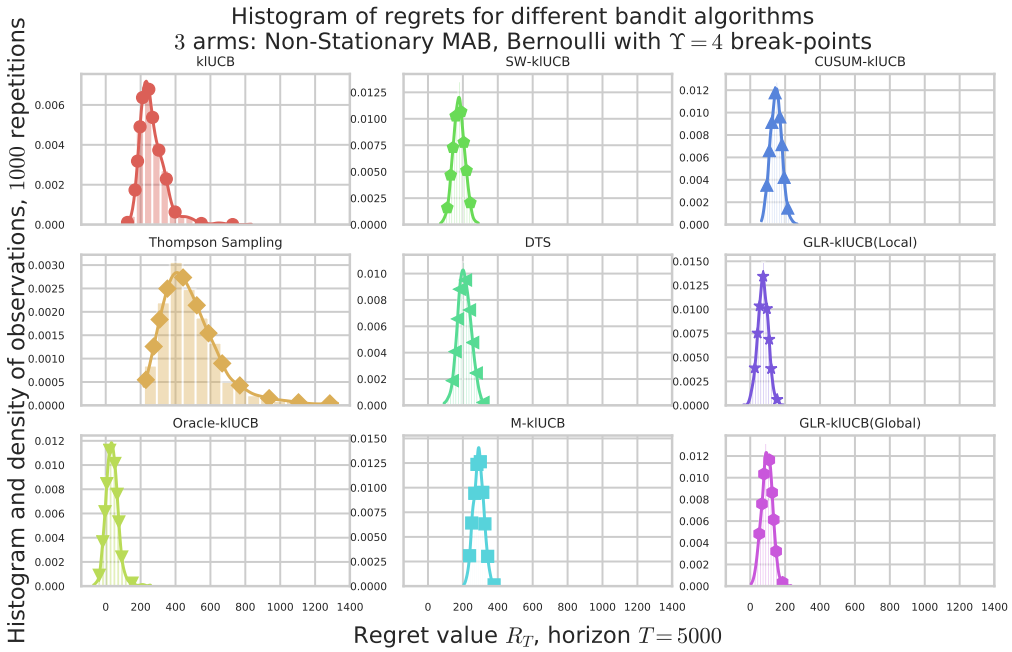

Figure 7.10 – Histograms of the distributions of regret R_T ($T = 5000$) for problem 1.

7.9 Conclusion

In this chapter, we studied and presented the piece-wise stationary bandit model, starting by reviewing existing works. We proposed a new algorithm for this problem, GLR-klUCB, which combines the kl-UCB algorithm with the Bernoulli GLR change-point detector. This actively adaptive method attains state-of-the-art regret upper-bounds when tuned with a prior knowledge of the number of changes Υ_T, but *without any other prior knowledge on the problem*, unlike its best two competitors, CUSUM-UCB and M-UCB, that require to know a lower bound on the smallest magnitude of a change. We also gave numerical evidence of the efficiency of our proposal.

This chapter was an interesting direction of analysis of the intractable model from Chapter 5, of independent end-devices running embedded MAB learning algorithms to improve their spectrum access in an IoT network. Instead of dealing with the multi-players aspect, as we did in the previous Chapter 6, we dealt in Chapter 7 about the non-stationary aspect. Different kinds of non-stationary bandit models have been considered in the literature, including adversarial, slowly-varying or abruptly-changing bandits, and as found the later to be the most appropriate to model non-stationarity of cognitive radio networks, we focus on abruptly-changing or piece-wise stationary bandit problems. Our proposed algorithm achieves state-of-the-art results for this model, by requiring a weaker prior knowledge on the problem difficulty when compared with its best competitors. An important future work is to investigate whether actively adaptive approaches can attain an order-optimal $\mathcal{O}(\sqrt{\Upsilon_T T})$ regret upper-

bound without the knowledge of Υ_T the number of break-point. Another possible future work is to propose an algorithm that could blindly adapt to both the slowly-varying and the abruptly-changing models, as well as being efficient against stationary models.

As suggested by the "dynamic case" of multi-players bandits presented in Chapter 6, another promising direction of future work is to study non-stationary distributed multi-players bandits. A natural extension of the model presented in this chapter is to consider non-communicating players cooperating in a decentralized way to play the same bandit game, as it was proposed recently in [WS18a]. The authors build on their recent work [WS18b] and show that a regret bounded by $\mathcal{O}(\sqrt{T^{\frac{1+\nu}{2}}\ln(T)})$ can still be achieved by M players, in the number of breaking points is $\Upsilon_T = \mathcal{O}(T^{\nu})$. Their algorithm assume that player j knows its ID $j \in [M]$ as well as ν, and removing these hypotheses is an interesting direction of future work. Furthermore, a promising direction is to directly try to join our contributions from Chapters 6 and 7, and propose an efficient algorithm using three parts: $\mathrm{kl\text{-}UCB}$ indexes for arm selection, MCTopM for orthogonalization (*i.e.*, dealing with collisions), and $\mathrm{GLR\text{-}klUCB}$ for non-stationarity (*i.e.*, dealing with abrupt changes).

7.10 Appendix

We start by including figures as complementary illustrations to the numerical results presented in Section 7.8 above. We then give some additional useful results, along with their proofs, and then we give complementary numerical experiments to justify some choices made in the presentation of our proposal GLR-klUCB.

7.10.1 Additional figures

We give here plots showing the mean regret R_t as a function of time, and histograms of the distributions of the final regret R_T, for the different problems of our benchmark. Figures 7.8 and 7.10 above show that our two proposals are efficient against problem 1, and Figure 7.9 concerns problem 2. Then we show similar results for problem 4 in Figure 7.11.

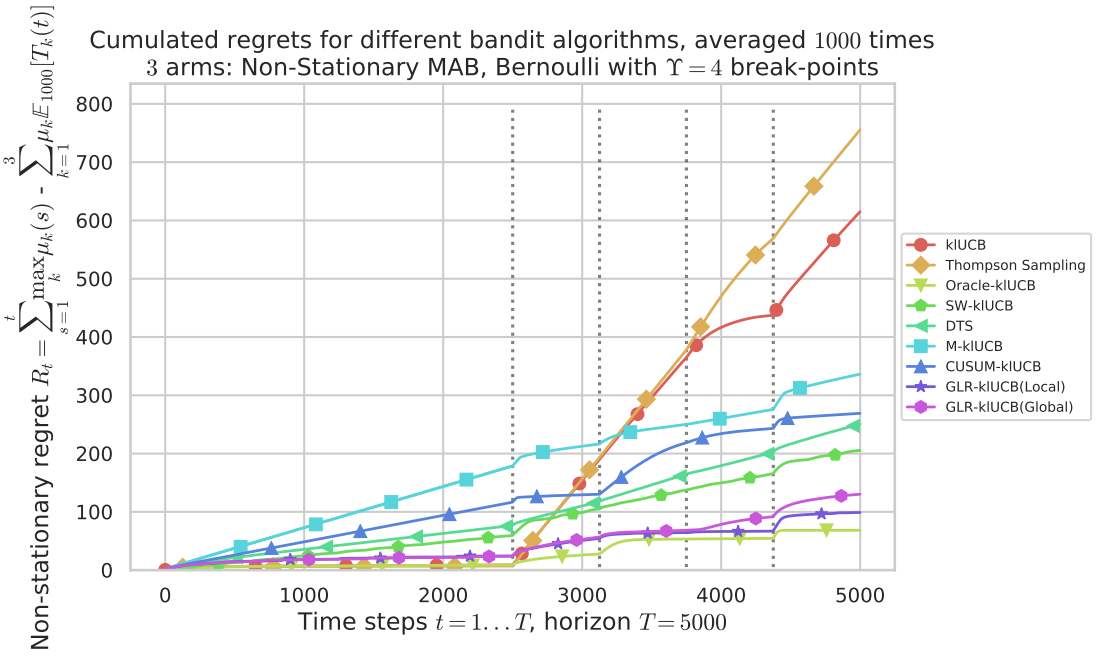

Figure 7.11 – Mean regret as a function of time, R_t for horizon $T = 5000$, for problem 4. We see that after a "long enough" stationary interval, the algorithms designed for stationary problems lose track of the best arm, and suffer from linear regret for a long period (*e.g.*, Thompson sampling in yellow ⋄).

For harder problems, like problems 3 and 5, the stationary policy kl-UCB can outperform actively adaptive strategies, if the stationary intervals are too short or if the gap between arms are too small. In other words, we illustrate in Figures 7.12 and 7.13 that while the actively adaptive strategies can be very efficient when applied to problems that are not too difficult to track, they can become sub-optimal for difficult problems.

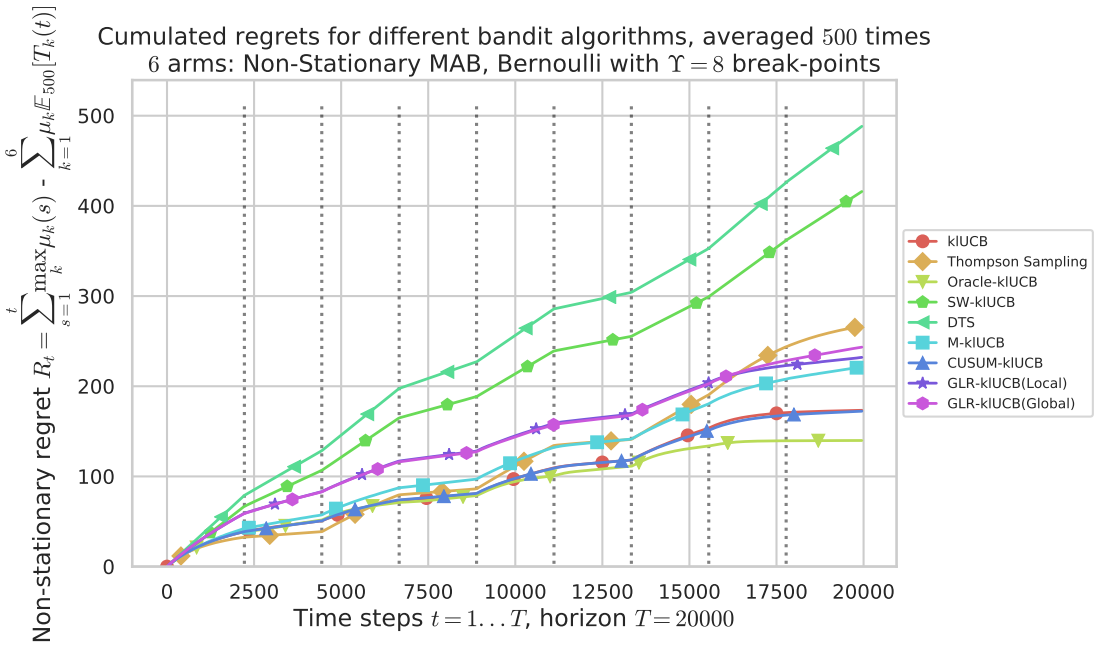

Figure 7.12 – Mean regret as a function of time, R_t for horizon $T = 20000$, for problem 3.

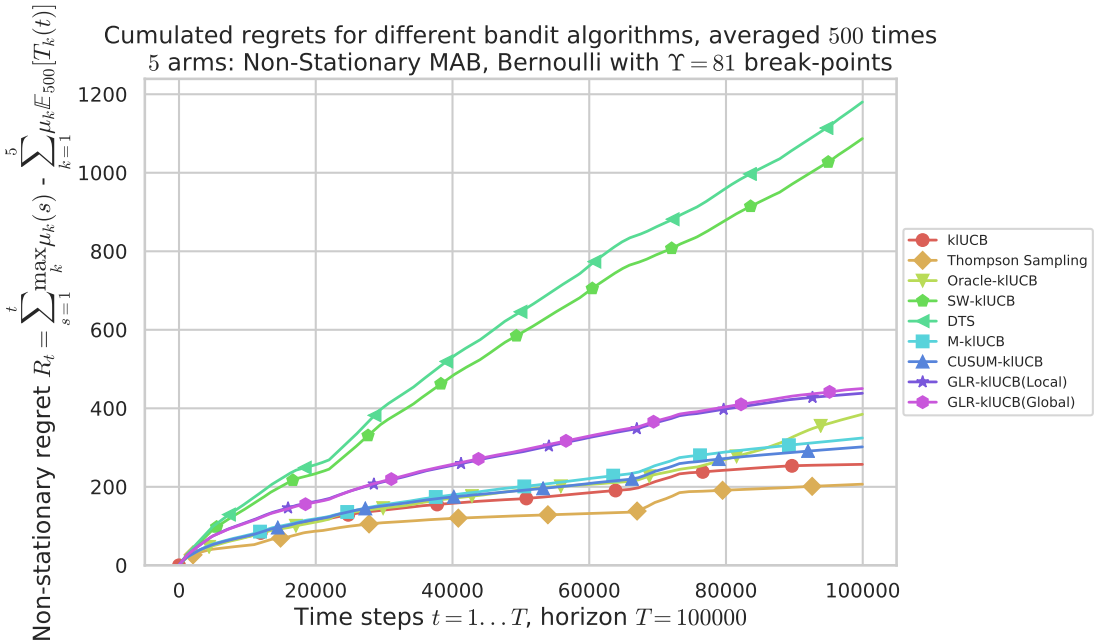

Figure 7.13 – Mean regret as a function of time, R_t for horizon $T = 100000$, for problem 5.

7.10.2 Omitted proofs

This Appendix gives some proofs omitted in the main text of this chapter. The remaining missing proofs can be found in the article [BK19b].

Simplified expression for the GLR statistic

First, we consider the denominator in the expression of $\mathrm{GLR}(n)$ (7.3), that is the $\sup$ on μ_0. We have $\ell(X_1,\dots,X_n;\mu_0) = \prod_{i=1}^{n} \ell(X_i;\mu_0)$ by independence of the observations X_i, and $\ell(X_i;\mu_0) = \mu_0^{X_i}(1-\mu_0)^{1-X_i}$ for Bernoulli distributions. Therefore, taking the logarithm gives

$$\begin{aligned}
\ln\left[\ell(X_1,\dots,X_n;\mu_0)\right] &= \sum_{i=1}^{n} \ln\left[\ell(X_i;\mu_0)\right] = \sum_{i=1}^{n} X_i \ln(\mu_0) + (1-X_i)\ln(1-\mu_0) \\
&= \ln(\mu_0) \times \left(\sum_{i=1}^{n} X_i\right) + \ln(1-\mu_0) \times \left(n - \sum_{i=1}^{n} X_i\right) \\
&= n\left(\widehat{\mu}_{1:n}\ln(\mu_0) + (1-\widehat{\mu}_{1:n})\ln(1-\mu_0)\right).
\end{aligned}$$

For a constant $a \in [0,1]$, let $h(x) \doteq a\ln(x) + (1-a)\ln(1-x)$ on $(0,1)$, and we are trying to solve $\sup_{x\in[0,1]} h(x)$. If $a = 0$ or $a = 1$, h is maximum at $x = a$. Now if $a \neq 0$, As h is of concave and of class $\mathcal{C}^1$, we can just differentiate and find the root of its derivative, $h'(x) = a/x - (1-a)/(1-x)$, so $h'(x) = 0$ if and only if $x = a$. Thus in all cases, $\sup_{x\in[0,1]} h(x) = h(a)$. Here, we have $a = \widehat{\mu}_{1:n}$, and thus we solved the $\sup_{\mu_0}$ optimization problem found in the denominator of the $\mathrm{GLR}(n)$ expression. By replacing $\mu_0 = \widehat{\mu}_{1:n}$, we obtained the following (unique) solution,

$$\sup_{\mu_0} \ln\left[\ell(X_1,\dots,X_n;\mu_0)\right] = n\left(\widehat{\mu}_{1:n}\ln(\widehat{\mu}_{1:n}) + (1-\widehat{\mu}_{1:n})\ln(1-\widehat{\mu}_{1:n})\right). \tag{7.29}$$

Now let us consider the nominator of the $\mathrm{GLR}(n)$ expression, that is the $\sup$ on μ_0, μ_1, τ. We can again work with log-likelihoods, and so we have

$$\begin{aligned}
&\ln\left[\ell(X_1,\dots,X_n;\mu_0,\mu_1,\tau)\right] \\
&= \sum_{i=1}^{\tau} X_i\ln(\mu_0) + (1-X_i)\ln(1-\mu_0) + \sum_{i=\tau+1}^{n} X_i\ln(\mu_1) + (1-X_i)\ln(1-\mu_1) \\
&= s\big(\widehat{\mu}_{1:s}\ln(\mu_0) + (1-\widehat{\mu}_{1:s})\ln(1-\mu_0)\big) \\
&\quad + (n-s)\big(\widehat{\mu}_{s+1:n}\ln(\mu_1) + (1-\widehat{\mu}_{s+1:n})\ln(1-\mu_1)\big).
\end{aligned}$$

Because we solved in (7.29) the $\sup$ for the denominator, we have

$$\mathrm{GLR}(n) = \frac{\sup\limits_{\mu_0,\mu_1,\tau<n} \ell(X_1,\dots,X_n;\mu_0,\mu_1,\tau)}{\exp\left[n\left(\widehat{\mu}_{1:n}\ln(\mu_0) + (1-\widehat{\mu}_{1:n})\ln(1-\mu_0)\right)\right]},$$

$$= \sup_{\mu_0,\mu_1,\tau<n} \frac{\ell(X_1,\dots,X_n;\mu_0,\mu_1,\tau)}{\exp\left[n\left(\widehat{\mu}_{1:n}\ln(\widehat{\mu}_{1:n}) + (1-\widehat{\mu}_{1:n})\ln(1-\widehat{\mu}_{1:n})\right)\right]},$$
$$= \exp\Big[\sup_{\mu_0,\mu_1,\tau<n}\Big[\ln\Big[\frac{\ell(X_1,\dots,X_n;\mu_0,\mu_1,\tau)}{\exp\left[n\left(\widehat{\mu}_{1:n}\ln(\widehat{\mu}_{1:n}) + (1-\widehat{\mu}_{1:n})\ln(1-\widehat{\mu}_{1:n})\right)\right]}\Big]\Big]\Big],$$

When the last equation comes from the fact that $\exp$ is increasing. Thus by taking the logarithm of both sides, we obtain

$$\begin{aligned}\ln \mathrm{GLR}(n) &= \sup_{\mu_0,\mu_1,\tau<n}\Big[\ln\Big[\frac{\ell(X_1,\dots,X_n;\mu_0,\mu_1,\tau)}{\exp\left[n\left(\widehat{\mu}_{1:n}\ln(\widehat{\mu}_{1:n}) + (1-\widehat{\mu}_{1:n})\ln(1-\widehat{\mu}_{1:n})\right)\right]}\Big]\Big],\\ &= \sup_{\mu_0,\mu_1,s\in[n-1]}\Big[s\big(\widehat{\mu}_{1:s}\ln(\mu_0) + (1-\widehat{\mu}_{1:s})\ln(1-\mu_0)\big)\\ &\qquad + (n-s)\big(\widehat{\mu}_{s+1:n}\ln(\mu_1) + (1-\widehat{\mu}_{s+1:n})\ln(1-\mu_1)\big)\\ &\qquad - n\big(\widehat{\mu}_{1:n}\ln(\widehat{\mu}_{1:n}) + (1-\widehat{\mu}_{1:n})\ln(1-\widehat{\mu}_{1:n})\big)\Big].\end{aligned}$$

By linearity and independence, we can separate the joint optimization problem on μ_0, μ_1, s in two optimizations problems for μ_0, s and μ_1, s, that can first be solved explicitly for μ_0 (resp. μ_1) and then left to be solved for s. By definition, $n\,\widehat{\mu}_{1:n} = \sum_{i=1}^{n} X_i = s\,\widehat{\mu}_{1:s} + (n-s)\,\widehat{\mu}_{s+1:n}$, so the right hand side (negative) part involving $\widehat{\mu}_{1:n}$ can be distributed in the two left hand side (positive) terms, which are both handled similarly. For instance for μ_0, we use the same computation as above with the function h to find the optimum: $\widehat{\mu}_{1:s}\ln(\mu_0) + (1-\widehat{\mu}_{1:s})\ln(1-\mu_0)$ is optimum for $\mu_0 = \widehat{\mu}_{1:s}$. Similarly, the term for μ_1 gives that $\sup_{\mu_1} \widehat{\mu}_{s+1:n}\ln(\mu_1) + (1-\widehat{\mu}_{s+1:n})\ln(1-\mu_1)$ is attained for $\mu_1 = \widehat{\mu}_{s+1:n}$. Finally, by replacing the two expressions of the solutions for μ_0 and μ_1, we obtain

$$\begin{aligned}\ln \mathrm{GLR}(n) = \sup_{s\in[n-1]}\Big[&s \times \Big(\widehat{\mu}_{1:s}\ln(\widehat{\mu}_{1:s}) + (1-\widehat{\mu}_{1:s})\ln(1-\widehat{\mu}_{1:s})\\ &\qquad - \widehat{\mu}_{1:s}\ln(\widehat{\mu}_{1:n}) + (1-\widehat{\mu}_{1:s})\ln(1-\widehat{\mu}_{1:n})\Big)\\ +(n-s) &\times \Big(\widehat{\mu}_{s+1:n}\ln(\widehat{\mu}_{s+1:n}) + (1-\widehat{\mu}_{s+1:n})\ln(1-\widehat{\mu}_{s+1:n})\\ &\qquad - \widehat{\mu}_{s+1:n}\ln(\widehat{\mu}_{1:n}) + (1-\widehat{\mu}_{s+1:n})\ln(1-\widehat{\mu}_{1:n})\Big)\Big].\end{aligned}$$

We conclude by recognizing the expressions of $s \times \mathrm{kl}(\widehat{\mu}_{1:s}, \widehat{\mu}_{1:n})$ and $(n-s) \times \mathrm{kl}(\widehat{\mu}_{s+1:n}, \widehat{\mu}_{1:n})$.

Proof of Lemma 7.4.

Using the same construction as in the proof of Theorem 14 in [KK18], one can prove that for every $\lambda \in I$ (for an interval I), there exists a non-negative super-martingale $M^{\lambda}(s)$ with respect to the filtration $\mathcal{F}_t \doteq \sigma(X_1,\dots,X_t)$ that satisfies $\mathbb{E}[M^{\lambda}(s)] \leq 1$ and

$$\forall s \in \mathbb{N}^*,\ \ M^{\lambda}(s) \geq \mathrm{e}^{\lambda[s\,\mathrm{kl}(\widehat{\mu}_s,\mu) - 3\ln(1+\ln(s))] - g(\lambda)}$$

for some function $g : I \to \mathbb{R}$. This super-martingale is of the form $M^\lambda(s) \doteq \int \mathrm{e}^{\eta \sum_{i=1}^{s} X_i - \phi_\mu(\lambda) s} d\pi(\eta)$, for a well-chosen probability distribution π, and the function g can be chosen to be any

$$\begin{array}{rcl} g_\xi : [0; 1/(1+\xi)] & \longrightarrow & \mathbb{R} \\ \lambda & \mapsto & \lambda(1+\xi)\ln\left(\dfrac{\pi^2}{3(\ln(1+\xi))^2}\right) - \ln(1-\lambda(1+\xi)) \end{array}$$

for a parameter $\xi \in [0, 1/2]$.

Similarly, if we denote $\mathcal{F}'_r$ the filtration $\sigma(Y_1, \dots, Y_r)$, there exists an independent super-martingale $W^\lambda(r)$ w.r.t. the filtration $\mathcal{F}'_r$, such that

$$\forall r \in \mathbb{N}^*, \;\; W^\lambda(r) \geq \mathrm{e}^{\lambda[r\,\mathrm{kl}(\widehat{\mu}'_r, \mu) - 3\ln(1+\ln(r))] - g(\lambda)},$$

for the same function $g(\lambda)$. In the terminology of [KK18], the two following processes are g-DCC (for Doob-Cramér-Chernoff), $\boldsymbol{X}(s) \doteq s\,\mathrm{kl}(\widehat{\mu}_s, \mu) - 3\ln(1+\ln(s))$ and $\boldsymbol{Y}(s) \doteq r\,\mathrm{kl}(\widehat{\mu}_r, \mu) - 3\ln(1+\ln(r))$, as for both processes Doob's inequality can be applied in combination with the Cramér-Chernoff method to obtain deviation inequalities that are uniform in time.

Here we have to modify the technique used in the Lemma 4 of [KK18] in order to take into account the two stochastic processes, and the presence of super-martingales instead of martingales (for which Doob inequality still works). One can write

$$\begin{aligned} &\mathbb{P}(\exists r \in \mathbb{N}^* : s\,\mathrm{kl}\left(\widehat{\mu}_s, \mu\right) + r\,\mathrm{kl}\left(\widehat{\mu}'_r, \mu'\right) > 3\ln(1+\ln(s)) + 3\ln(1+\ln(r)) + u) \\ &\leq \mathbb{P}\left(\exists r \in \mathbb{N}^* : M^\lambda(s) W^\lambda(r) > \mathrm{e}^{\lambda u - 2g(\lambda)}\right) \\ &= \lim_{n\to\infty} \mathbb{P}\left(\exists r \in [n] : M^\lambda(s) W^\lambda(r) > \mathrm{e}^{\lambda u - 2g(\lambda)}\right) \\ &= \lim_{n\to\infty} \mathbb{P}\left(\sup_{r\in[n]} M^\lambda(s) W^\lambda(r) > \mathrm{e}^{\lambda u - 2g(\lambda)}\right). \end{aligned}$$

Using that $\widetilde{M}(r) \doteq M^\lambda(s) W^\lambda(r)$ is a super-martingale with respect to the filtration $\widetilde{\mathcal{F}}_r \doteq \sigma(X_1, \dots, X_s, Y_1, \dots, Y_r)$, one can apply Doob's maximal inequality to obtain

$$\begin{aligned} \mathbb{P}\left(\sup_{r\in[n]} M^\lambda(s) W^\lambda(r) > \mathrm{e}^{\lambda u - 2g(\lambda)}\right) &\leq \mathrm{e}^{-(\lambda u - 2g(\lambda))} \mathbb{E}[\widetilde{M}(1))] \\ &= \mathrm{e}^{-(\lambda u - 2g(\lambda))} \mathbb{E}[M^\lambda(s) W^\lambda(1)] \\ &\leq \mathrm{e}^{-(\lambda u - 2g(\lambda))}, \end{aligned}$$

using that $M^\lambda(s)$ and $W^\lambda(1)$ are independent and have an expectation smaller than 1.

Putting things together yields

$$\mathbb{P}\left(\exists r \in \mathbb{N}^* : s\,\mathrm{kl}\left(\widehat{\mu}_s, \mu\right) + r\,\mathrm{kl}\left(\widehat{\mu}'_r, \mu'\right) > 3\ln(1+\ln(s)) + 3\ln(1+\ln(r)) + u\right) \leq \mathrm{e}^{-\left(\lambda u - 2g_\xi(\lambda)\right)},$$

for any function g_ξ defined above. The conclusion follows by optimizing for both λ and ξ, using Lemma 18 in [KK18].

A concentration result involving two arms

The following result is useful to control the probability of the good event in our two regret analyzes. Its proof follows from a straightforward application of the Cramér-Chernoff method [BLM13], and is given below.

Lemma 7.14. *Let $\widehat{\mu}_{i,s}$ be the empirical mean of $s \in \mathbb{N}^*$ i.i.d. observations with mean μ_i, for $i \in \{a, b\}$, that are σ^2-sub-Gaussian. Define $\Delta \doteq \mu_a - \mu_b$. Then for any $s, r > 0$, we have*

$$\mathbb{P}\left(\frac{s\,r}{s+r}\left(\widehat{\mu}_{a,s} - \widehat{\mu}_{b,r} - \Delta\right)^2 \geq u\right) \leq 2\exp\left(-\frac{u}{2\sigma^2}\right). \tag{7.30}$$

Proof of Lemma 7.14. We first note that

$$\begin{aligned}
&\mathbb{P}\left(\frac{s\,r}{s+r}\left(\widehat{\mu}_{a,s} - \widehat{\mu}_{b,r} - \Delta\right)^2 \geq u\right) \\
&\leq \mathbb{P}\left(\widehat{\mu}_{a,s} - \widehat{\mu}_{b,r} \geq \Delta + \sqrt{\frac{s+r}{sr}u}\right) + \mathbb{P}\left(\widehat{\mu}_{b,r} - \widehat{\mu}_{a,s} \geq -\Delta + \sqrt{\frac{s+r}{sr}u}\right),
\end{aligned} \tag{7.31}$$

and those two quantities can be upper-bounded similarly using the Cramér-Chernoff method.

Let (X_i) and (Y_i) be two *i.i.d.* sequences that are σ^2-sub-Gaussian with mean μ_1 and μ_2 respectively. Let n_1 and n_2 be two integers and $\widehat{\mu}_{1,n_1}$ and $\widehat{\mu}_{2,n_2}$ denote the two empirical means based on n_1 observations from X_i, and n_2 observations from Y_i respectively. Then for every $\lambda > 0$, as $x \mapsto \exp(\lambda x)$ is increasing, if $p \doteq \mathbb{P}\left(\widehat{\mu}_{1,n_1} - \widehat{\mu}_{2,n_2} \geq \mu_1 - \mu_2 + x\right)$, we have

$$\begin{aligned}
p &\leq \mathbb{P}\left(\frac{1}{n_1}\sum_{i=1}^{n_1}(X_i - \mu_1) - \frac{1}{n_2}\sum_{i=1}^{n_2}(Y_i - \mu_2) \geq x\right) \\
&= \mathbb{P}\left(\exp\left(\lambda\left(\frac{1}{n_1}\sum_{i=1}^{n_1}(X_i - \mu_1) - \frac{1}{n_2}\sum_{i=1}^{n_2}(Y_i - \mu_2)\right)\right) \geq \exp(\lambda x)\right).
\end{aligned}$$

And so thanks to Markov's inequality, we obtain

$$\begin{aligned} p &\leq \exp(-\lambda x)\mathbb{E}\left[\exp\left(\lambda\frac{1}{n_1}\sum_{i=1}^{n_1}(X_i-\mu_1)\right)\right]\mathbb{E}\left[\exp\left(-\lambda\frac{1}{n_2}\sum_{i=1}^{n_2}(Y_i-\mu_2)\right)\right] \\ &= \exp\left(-\lambda x + n_1\phi_{X_1-\mu_1}\left(\frac{\lambda}{n_1}\right) + n_2\phi_{Y_1-\mu_2}\left(-\frac{\lambda}{n_2}\right)\right) \\ &\leq \exp\left(-\lambda x + \frac{\lambda^2\sigma^2}{2n_2} + \frac{\lambda^2\sigma^2}{2n_1}\right), \end{aligned}$$

where the last inequality uses the sub-Gaussian property, on the two centered variables $X_1-\mu_1$ and $Y_1-\mu_2$. In order to obtain the tightest bound on the left-hand side probability, we can look for the value of λ that minimizes the right-hand side of the inequality yields. By differentiating and by convexity, we find the value

$$\lambda \doteq \frac{1}{2}\frac{x}{\sigma^2/(2n_1)+\sigma^2/(2n_2)}$$

which yields the tighter inequality on this probability,

$$p = \mathbb{P}\left(\widehat{\mu}_{1,n_1} - \widehat{\mu}_{2,n_2} \geq \mu_1 - \mu_2 + x\right) \leq \exp\left(-\frac{n_1 n_2}{n_1+n_2}\frac{x^2}{2\sigma^2}\right).$$

Using this inequality twice in the right hand side of (7.31) concludes the proof. □

7.10.3 Two numerical optimization tricks for GLR-klUCB

As the main weakness of GLR-klUCB is its numerical efficiency, we suggest here two simple ideas to drastically speed-up its computation time.

1. The *first optimization*, parameterized by a constant $\Delta n \in \mathbb{N}^*$, is the following idea. We can test for statistical changes not at all time steps $t \in [T]$ but only every Δn time steps (*i.e.*, for t satisfying $t \mod \Delta n = 0$). In practice, instead of sub-sampling for the *time* t, we propose to sub-sample for the number of samples of arm i before calling GLR to check for a change on arm i, that is, $n_i(t)$ in Algorithm 7.1. Note that the first heuristic using Δn can be applied to M-UCB as well as CUSUM-UCB and PHT-UCB, with similar speed-up and typically leading to similar consequences on the algorithm performance.

2. The *second optimization* is in the same spirit, and uses a parameter $\Delta s \in \mathbb{N}^*$. When running the GLR test with data $Z_1, \ldots, Z_t$, instead of considering every splitting time steps $s \in [t]$, in the same spirit, we can skip some and test not at all time steps s but only every Δs time steps.

The new GLR test is using the stopping time $\widetilde{T_\delta}$ defined in (7.11), with $\mathcal{T} = \{t \in [T], t \mod \Delta n = 0\}$ and $\mathcal{S}_t = \{s \in [t], s \mod \Delta s = 0\}$. The goal is to speed up the computation time of every call to the GLR test (*e.g.*, choosing $\Delta s = 10$, every call should be about 10 times faster), and to speed up the overhead cost of running the tests on top of the index policy (kl-UCB), by testing for changes *less* often (*e.g.*, choosing $\Delta n = 10$ should speed up the all computation by a factor 10).

Empirical validation of these optimization tricks. We consider the problem 1 presented above (Figure 7.1), with $T = 5000$ and 100 repetitions, and we give the means ($\pm$ 1 standard-deviation) of both regret and computation time of GLR-klUCB with **Local** restarts, for different parameters Δn and Δs, in Table 7.4 below. The other parameters of GLR-klUCB are chosen as $\delta = 1/\sqrt{K \Upsilon_T T}$ and $\omega = 0.1\sqrt{K \ln(T)/T}$ (from Corollary 7.12). The algorithm analyzed in Section 7.6 corresponds to $\Delta n = \Delta s = 1$.

Δn \ Δs	1	5	10	20
1	44 ± 29	44 ± 28	50 ± 31	53 ± 28
5	48 ± 29	41 ± 30	44 ± 28	47 ± 31
10	51 ± 32	43 ± 26	47 ± 28	46 ± 29
20	46 ± 31	46 ± 34	46 ± 31	49 ± 31

Δn \ Δs	1	5	10	20
1	**50 s $\pm$ 4.5 s**	11.1 s $\pm$ 1.2 s	5.8 s $\pm$ 0.5 s	3.3 s $\pm$ 0.3 s
5	17.9 s $\pm$ 1.6 s	5.08 s $\pm$ 3.3 s	2.5 s $\pm$ 0.3 s	1.7 s $\pm$ 0.2 s
10	14.9 s $\pm$ 1.9 s	3.47 s $\pm$ 0.4 s	2.1 s $\pm$ 0.2 s	1.4 s $\pm$ 0.2 s
20	12.1 s $\pm$ 1.1 s	3.02 s $\pm$ 0.3 s	1.9 s $\pm$ 0.2 s	**0.2 s $\pm$ 0.1 s**

Table 7.4 – Effects of the two optimizations parameters Δn and Δs, on the mean regret R_T (top) and mean computation time (bottom) for GLR-klUCB on a simple problem. Using the optimizations with $\Delta n = \Delta s = 20$ does not reduce the regret much but speeds up the computations by about a **factor 50**.

On the same problem, the Oracle-Restart kl-UCB obtained a mean regret of 37 for a running time of 711 ms, while kl-UCB obtained a regret of 270 for a time of 587 ms. In comparison with the two other efficient approaches, M-kl-UCB obtained a regret of 290 for a time of 943 ms, and CUSUM-klUCB obtained a regret of 148 for a time of 46 s. This shows that our proposal is very efficient compared to stationary algorithms, and comparable to the state-of-the-art actively adaptive algorithm. Moreover, this shows that two heuristics efficiently speed-up the computation times of GLR-klUCB. Choosing small values, like $\Delta n = 20, \Delta s = 20$, can speed-up GLR-klUCB, making it fast enough to be comparable to recent efficient approaches like M-UCB and even comparable to the oracle policy. It is very satisfying to see that these optimizations do not reduce much the regret of GLR-klUCB, as it still outperforms most state-of-the-art algorithms, and significantly reduces the computation time as wanted. With such numerical optimization, GLR-klUCB is not significantly slower than kl-UCB while being much more efficient for piece-wise stationary problems.

7.10.4 Comparison of different threshold functions β

We compare different threshold functions, $\beta_i(n, \delta)$ for $i \in \{1, 2, 3, 4\}$, that can be used in the B-GLRT test used for the GLR-klUCB algorithm (see the details in equation (7.12) and in Algorithm 7.1). In the B-GLRT test, there is a sup optimization problem on $s \in [n-1]$, and this sup is compared with the threshold $\beta(n, \delta)$. The threshold function given in (7.7) was chosen to obtain Lemma 7.3, that is a false alarm probability bounded by δ. We note that we also considered the possibility of using a threshold that could be a function of both n the sample size as well as $s \in [n-1]$ the "splitting index" between means $\widehat{\mu}_{1:s}$ and $\widehat{\mu}_{s+1:n}$. We did some preliminary experiments to explore this direction and did not find a significant difference, in terms of numerical efficient of the resulting GLR-klUCB algorithm, and mathematically the analysis presented in Section 7.4.2 is simpler to follow if the threshold are uniform on s.

- β_1 The first variant is the one we advised to use in practice for GLR-klUCB, it is very simple to compute numerically: $\beta_1(n, \delta) \doteq \ln\left(\frac{3n^{3/2}}{\delta}\right) = -\ln(\delta) + \ln(3) + 3/2\ln(n)$.
- β_2 The second variant is smaller without this power $3/2$: $\beta_2(n, \delta) \doteq \ln\left(\frac{1}{\delta}\right) + \ln(1 + \ln(n))$.
- β_3 The third variant is using the function $\mathcal{T}$, as introduced by (7.6). The function $\mathcal{T}$ is computed with a numerical approximation[4] of the Lambert function $\mathcal{W}$, as explained in Section 7.4.2, $\beta_3(n, \delta) \doteq 2\mathcal{T}\left(\frac{\ln(2n^{3/2})/\delta}{2}\right) + 6\ln(1 + \ln(n))$.
- β_4 The forth variant is using the function $\widetilde{\mathcal{T}}(x) = x + 4\ln(1 + x + \sqrt{2x})$, as a simple approximation of $\mathcal{T}(x)$, which is valid and quite accurate as soon as $x \geq 5$, $\beta_4(n, \delta) \doteq 2\widetilde{\mathcal{T}}\left(\frac{\ln(2n^{3/2})/\delta}{2}\right) + 6\ln(1 + \ln(n))$.

As before, we consider the three problems 1, 2 and 4, with time horizon $T = 5000$, and we present in Table 7.5 the mean results of 100 independent runs. We only consider the variant of GLR-klUCB based on **Local restarts**, and we used the parameters ω_T, δ_T as given by the Corollary 7.12, and with the deterministic exploration scheme.

Threshold function	Problem 1	Problem 2	Problem 4
$\beta_1(n, \delta)$	$\mathbf{70 \pm 30}$	109 ± 32	99 ± 29
$\beta_2(n, \delta)$	73 ± 28	99 ± 32	$\mathbf{88 \pm 32}$
$\beta_3(n, \delta)$	77 ± 27	$\mathbf{89 \pm 32}$	134 ± 35
$\beta_4(n, \delta)$	77 ± 30	101 ± 30	135 ± 30

Table 7.5 – Mean regret $\pm$ 1 standard-deviation, for different choices of threshold function $\beta(n, \delta)$, on three problems of horizon $T = 5000$, for GLR-klUCB.

As we could expect, the four choices give comparable results, as well as β_3 and β_4. The first two choices give better performance in most cases, and they are computationally less costly. We note that the threshold β_1 is closer mathematically to the threshold β_3, that was

[4] The Lambert $\mathcal{W}$ function is available in Python as `scipy.special.lambertw` from `scipy` [JOP+01].

used in the analysis, and thus it is the one we advise to use in practice. The sum-up of these experiments is that a practitioner should use the simplest and most explicit threshold β_1, instead of the more complicated one that was used for the analysis. Therefore, the choice of threshold function $\beta_1(n, \delta) \doteq \ln\left(3n^{3/2}/\delta\right)$ for GLR-klUCB presented in Algorithm 7.1 is validated by these experiments.

7.10.5 Comparison of mechanisms used to enforce uniform exploration

We compare different exploration mechanisms that can be used to enforce a sufficient exploration of all arms in the GLR-klUCB algorithm. All options are parameterized by a constant $\omega \in (0, 1)$, which essentially represents the fraction of time steps spent in the forced exploration, either in average or in total.

1. The **deterministic exploration** corresponds to the one described in Algorithm 7.1. At time t, if $t \mod \left\lfloor \frac{K}{\omega} \right\rfloor \in [K]$, then the arm $A_t = t \mod \left\lfloor \frac{K}{\omega} \right\rfloor$ is played. It is the simplest, both to compute numerically and to handle mathematically, as the proof of Proposition 7.6 is short and simple. Its deterministic nature makes it the easiest choice for the proof skeleton given in Section 7.7.1, as the set $\mathcal{D}(T, \omega)$ used in the decomposition (7.22) of the regret is deterministic, and thus it greatly simplifies the manipulation of expectations and random events. Note that this mechanism is also the one used by M-UCB [CZKX19].

2. The **uniform random exploration** is the one proposed for CUSUM-UCB [LLS18]. At time t, a random arm is played with probability ω/K. That is, first we sample a boolean variable from a Bernoulli law of mean ω, so that 1 indicates a random play (with proba. ω), and 0 indicates a play using the UCB indexes (with proba. $1 - \omega$). Then if it is a random play, arm $i \in [K]$ is selected uniformly at random (with probability $1/K$), and arm $A_t = i$ is played. Proving a result like Proposition 7.6 is not much harder for this second mechanism, but the difficulty lies in extending the proof skeleton we give in Section 7.7.1 to have a random set $\mathcal{D}(T, \omega)$.

3. The **tracking-based exploration** mechanism is inspired by the tracking trick used in [GK16], and it is actually quite intuitive. At any time t, instead of having a uniform probability of forcing an exploration of every arm, it can make sense to force exploring arms that are currently not explored enough. This way, we actively enforce that each arm have enough samples. At time t, the goal is for any arm i to have been sampled more than $\omega \times (t - \tau_i)$ time, if $t - \tau_i$ represents the number of time steps since the last restart on this arm i. So the tracking-based exploration samples an arm i uniformly at random among the set of arms i such that $n_i(t) < \omega(t - \tau_i)$, if it is not empty, otherwise it plays according to the UCB indexes. Numerically, it is not much more complicated than the two previous solutions. It was the first direction we pursued for our analysis, but

we dropped it since mathematically, it was harder to prove a result like Proposition 7.6, and it was also harder to incorporate the randomness of this exploration scheme in the regret decomposition (7.22).

Note that the analysis we gave in Section 7.6 is based on the deterministic exploration, but with a careful handling of random events and if we prove a result similar to Proposition 7.6, we believe our analysis could also be extended to another exploration mechanism.

As before, we consider the three problems 1, 2 and 4, with time horizon $T = 5000$, and we present in Table 7.6 the mean results of 100 independent runs. We include the two variants of GLR-klUCB, based on **Local restarts** or **Global restarts**, for which we used the parameters ω_T, δ_T as given by the two Corollaries 7.9 and 7.12.

Exploration mechanism	Variant	Problem 1	Problem 2	Problem 4
Deterministic exploration	Local	$\mathbf{68 \pm 33}$	116 ± 36	99 ± 33
	Global	97 ± 28	134 ± 36	131 ± 32
Uniform random exploration	Local	74 ± 30	$\mathbf{108 \pm 33}$	106 ± 31
	Global	91 ± 30	134 ± 33	129 ± 33
Tracking-based exploration	Local	73 ± 32	104 ± 33	$\mathbf{89 \pm 29}$
	Global	96 ± 26	133 ± 32	120 ± 30

Table 7.6 – Mean regret $\pm$ 1 standard-deviation, for different choices of exploration mechanisms, on three problems of horizon $T = 5000$, for GLR-klUCB, with local or global restarts.

As expected, all options give similar results, and each of the three options was found to outperform the two others in one of the three problems considered for these experiments (problems 1, 2 and 4). The result highlighted in **bold** in Table 7.6 shows the best algorithm in each problem. We note that in terms of its average regret on the different problems, the tracking-based exploration is the best choice. The sum-up of these experiments is that it is sufficient to use the simplest exploration scheme based on a deterministic exploration, rather than a more complicated exploration scheme based on tracking. Therefore, our choice of the deterministic exploration scheme for GLR-klUCB presented in Algorithm 7.1 is validated by these experiments.

– Par exemple, vous prenez aujourd'hui. Vous comptez sept jours. Ça vous emmène dans une semaine. Et bien on sera exactement le même jour qu'aujourd'hui… À une vache près, hein… C'est pas une science exacte.
Karadoc, interprété par Jean-Christophe Hembert,
Kaamelott, Livre II, "Sept cent quarante-quatre".

Chapter 8

General Conclusion and Perspectives

Conclusion on our contributions

We started this manuscript by detailing the historical, scientific and technical contexts of our research during this PhD. We explained the problems that motivate and justify our works. The main question we studied was *"Can we adapt the decision making tools, already successfully applied to Cognitive Radio for Opportunistic Spectrum Access, to the specific needs of CR for the (future) Internet of Things networks?"* We first gave a strong theoretical background on the reinforcement learning model considered in this thesis, that is the multi-armed bandit model. We then focused on our problems of solving the spectrum scarcity issue in unlicensed bands, in the context of the future Internet of Things networks. We worked on extending to the specificities of such IoT networks the ideas underlying the previously studied applications of machine learning to solve the spectrum scarcity issue in licensed networks.

Our main contribution to answer our problematic is a model of Internet of Things networks, based on an ALOHA-like protocol slotted in time and frequency, and that considers one IoT base station serving a large number of devices following the IoT constraints (low-cost, low duty cycle, long range etc). In such a IoT network, we focused on many dynamically reconfigurable IoT end-devices, that are able to run low-cost and low-complexity decision making algorithms, embedded on each device using their limited computational and storage capacities. We proposed two models, whether the considered IoT standard enforces the devices to try to retransmit a few times their up-link packet in case of a failed transmission (*i.e.*, a collision with other devices), or to drop their packet after a failed transmission (*i.e.*, with or without retransmission). Both models are realistic, and for both cases we proposed to use multi-armed bandit (MAB) algorithms, such as UCB or Thompson sampling, in order that the numerous IoT devices improve their spectrum access scheme, on their own, by learning which of the K frequency channels are the less occupied ones by the environmental traffic (in average).

The approach we thus advocate is to use low-complexity MAB algorithms such as kl-UCB or Thompson sampling, or variants tuned to be robust in slowly-evolving non-stationary scenario (*e.g.*, Sliding-Window UCB, Discounted-Thompson, or actively adaptive algorithm such as the one of Chapter 7, GLR-kl-UCB). For a company that manufactures IoT end-devices, it is very simple and cheap in terms of both hardware and software costs to implement such MAB algorithms on the low-cost embedded processors, and equip all the produced IoT devices with this capacity of using online machine-learning for their spectrum access. The embedded decision-making algorithm automatically improves the channel selection of each device, in a fully decentralized way. It also increases the total number of successful up-link transmissions, and thus this increases the Quality of Service of the considered IoT application. Finally, such algorithm also allows more devices to be served by the same IoT gateway. Another consequence is a reduced energy consumption and an increased battery life for the IoT end-devices.

The advocated approach also has the advantage of not requiring to change anything on the IoT standard, as the only modification happens on the device side, by letting it actively decide the channels it uses for up-link transmissions, instead of relying on a naive uniform channel access. We also note that this approach can easily be used to allow the IoT devices to optimize by themselves other parameters of their wireless communications on the fly, as the multi-armed bandit framework is not restricted to be applied to the selection of frequency channel but can be applied to any exploration-exploitation problem with a finite set of possible options. The solution we propose can thus be easily extended to also select dynamically other parameters such as the coding rate or spreading factor of a LoRa network (*e.g.*, [KAF+18]), the emission power in a NOMA standard, or any other discrete-valued parameters that have an impact on the successful transmissions rates and can be optimized on the device's side by using reinforcement learning.

Moreover, from a theoretical point-of-view, even though it was found hard to propose a rigorous analysis of our model of IoT networks, because of the large number of devices having different random and unpredictable activation patterns, our contributions also include an analysis of two restricted models. On the one hand, we considered a model where the devices have data to transmit at each time step, relaxing the hypothesis of a random activation process (with a small probability, as IoT devices have low duty cycles), and thus by restricting to the case of at most $M \leq K$ devices using a wireless standard with K orthogonal frequency channels. This first model is similar to the multi-player bandit model studied in the last 10 years, and for stationary and stochastic environments we were able to propose an efficient algorithm, MCTopM. Our proposed algorithm performs very well in practice and we obtained interesting guarantees on its regret, as well as on the number of radio collisions and on radio reconfigurations that the devices will suffer if they all implement our solution. On the other hand, we studied a model that focuses on only one device but relaxes the hypothesis of stationarity on the surrounding radio traffic, and considers that is can be stationary in consecutive intervals of time, of unknown durations. This second model is similar to the piece-

wise stationary (or abruptly-changing) bandit model studied since the 2000s, and we solved it by proposing a new actively adaptive bandit policy, for which we obtained state-of-the-art results, in terms of its regret and its false alarm probability and delay of detection.

Finally, from an application point-of-view, we also presented a realistic implementation of a proof-of-concept of our first model of IoT network, that was used to validate empirically the proposed approach. We showed that the IoT devices can effectively use a multi-armed bandit algorithm to automatically learn to favor certain frequency channels over others, and finally to optimize their spectrum access, to reduce their number of failed transmissions. Our proposed approach is to use decentralized reinforcement learning algorithms, directly embedded on the IoT end-devices, in order to improve their spectrum access and channel selection schemes. We confirmed from both numerical simulations and a validation on real radio traffic and real hardware that our proposal is an excellent candidate to start to solve the spectrum scarcity issue for unlicensed bands, that is cheap and easy to deploy.

Perspectives

The works presented in each chapter suggest possible directions of future studies.

For our models of IoT networks. The first model presented in Section 5.2 could easily be generalized with two probabilities p_S and p_D, if the S static and D dynamic devices have different transmission patterns, and less easily with a different probability per device. Also, other emission patterns could be considered, instead of a Bernoulli process for each user. In this entire Chapter 5, we prefer to consider that all the devices have the same activation probability, to keep the notations and the model as simple as possible. Moreover, for the sake of simplicity we supposed that all devices use the same standard. Future works could consider more realistic interference scenarios and IoT networks, with non-slotted time, more than one base station etc. Another extension could be to consider not a Bernoulli activation process (or any random process), but a fixed rate of transmission, *e.g.*, one transmission a day. In this case, additionally to deciding the channel for communication (*i.e.*, *where* to communicate), each device could thus also have to decide *when* to communicate. However, this clearly leads to a much larger action space, as there are many time slots in one day (for example), and thus we believe that as soon as the action space becomes too large in this extension, the simple MAB-based learning approach could be no longer appropriate. It is well-known in the MAB literature that the larger the action space, the slower is the convergence speed of any stationary MAB algorithms. Thus, it could be exciting to study the possible application of *contextual* MAB [LCLS10, LWAL18] or structured MAB [CMP17] models and algorithms for this extension.

For multi-player bandits. The study on multi-players bandits in Chapter 6 suggests several further research directions. First, one could investigate the notion of *optimal algorithms* in the decentralized multi-players model with sensing information. So far we provided the first matching upper and lower bound on the expected number of sub-optimal arms selections, which suggests some form of (asymptotic) optimality. However, sub-optimal draws turn out to not be the dominant terms in the regret, both in our upper bounds and in practice. Thus a promising future work is to identify some notion of *minimal number of collisions*. This could be similar to what a recent work [WHCW19] studied for the minimal amount of communication needed to achieve logarithmic regret, in a similar model that authorizes direct communications between players.

We also presented many extensions of the multi-players bandit model in Section 6.7, and even if some have already been implemented, an important future work is to implement the most interesting ones in SMPyBandits (see tickets 120, 124, 185). From the point-of-view of the theoretical analysis, we are especially interested by first extending our proposed algorithm MCTopM to the case of an unknown number of players. Then we could also address the most interesting extension for the application to wireless networks, *i.e.*, the "dynamic case" which allows for arrivals and departures of players in the multi-player bandit game.

Regarding non-stationary bandits. We believe that the new proof technique of Chapter 7 could be used to analyze GLR-klUCB under less stringent assumptions than the one made in this chapter (and in previous works), that would require only a few "meaningful" changes to be detected. This promising research direction is left for future work, but the hope is that the regret would be expressed in terms of the number of such meaningful changes, instead of the number of break-points Υ_T. We shall moreover investigate whether actively adaptive approaches can attain a $\mathcal{O}(\sqrt{\Upsilon_T T})$ regret upper-bound without the knowledge of Υ_T. We also believe that combining change-point *localization* with an efficient change-point detection algorithm, such as GLR-klUCB, could lead to an interesting class of more efficient algorithms. Another very interesting future work is to study possible extensions of our approach, especially to the slowly-varying model, as studied in [BGZ14, LRC+16, WS18b], or to other models such as the rotting bandit model [SLC+19], which is interesting for many applications even if it does not seem directly usable for the cognitive radio setting.

For our library SMPyBandits. A few tasks are left on SMPyBandits, a first one could be to implement new variants of the single-player stochastic models, as well as variants for the multi-players or the non-stationary cases. For more details, see the issue tickets at `GitHub.com/SMPyBandits/SMPyBandits/issues/`. A second interesting task could be to add support for the "dynamic case" of multi-players bandits to allow arrivals or departures of players (ticket 124).

Unifying multi-player and non-stationary bandits. A natural next step after this thesis is to study non-stationary distributed multi-players bandits, to unify the models from Chapter 6 and 7. A natural extension of the non-stationary model is to consider non-communicating players cooperating in a decentralized way to play the same bandit game, as it was proposed recently in [WS18a]. We could also build on the proof technique used in this paper, even if we are interested in removing the hypothesis that player j knows its ID $j \in [M]$ before starting to play. A promising direction is to directly try to join our contributions from Chapter 6 and 7, and propose an efficient algorithm using three parts: kl-UCB indexes for arm selection, MCTopM for orthogonalization (*i.e.*, dealing with collisions), and the Bernoulli GLR break-point detector for non-stationarity (*i.e.*, dealing with abrupt changes). The three parts should be inter-connected, the same way we built MCTopM-kl-UCB and GLR-klUCB, by connecting two of the three components together. We propose a simple idea to incorporate the detected change-points by B-GLR test in the orthogonalization procedure MCTopM: whenever a change-point is detected, the player is no longer "fixed" on its chosen arm. Even if we already obtained promising results on preliminary numerical simulations, analyzing such a strategy that combines MCTopM, GLR and kl-UCB is left as a challenging future work.

Finally, I would be very interested in looking at a unique "unified" algorithm that can be used in all the different settings studied in this thesis, and maybe others, and automatically adapt to the setting at hand. For instance, even if GLR-klUCB is very efficient for piece-wise stationary problems, its forced exploration makes it sub-optimal for stationary problems. Another example is for multi-players bandits, where MCTopM-kl-UCB performs sub-optimally on piece-wise stationary problems. One approach to obtain a unified "master" algorithm could be to use expert aggregation on the different state-of-the-art algorithms presented in this thesis, and as each one was proven to be efficient in one setting, the resulting aggregated algorithm would also be efficient in each of the different settings. As this approach does not seem theoretically promising, as illustrated in Section 4.4, a preferred approach could be to design a "unified" algorithm which adapts automatically to the kind of problem it is facing.

Je vous remercie d'avoir lu cette thèse. Merci de me signaler toute erreur par courriel ou sur GitHub :
Thanks for reading this document. Please notify me about any mistake by e-mail or on GitHub:
↪ GitHub.com/Naereen/phd-thesis/issues/new
↪ Lilian.Besson@{Crans.org, Inria.fr, live.fr}

– Les rêves, ça se compare pas…
Le Roi Arthur, interprété par Alexandre Astier,
Kaamelott, Livre VI, Épisode 9, "Dies Irae".

Appendix A

About Doubling Tricks for Multi-Armed Bandits

This appendix quickly presents the contributions of another publication that was not presented in the main text of this thesis. We studied doubling tricks and their possible uses for multi-armed bandits, between fall 2017 and spring 2018, and we wrote an article [BK18b] which was rejected at the COLT 2018 conference, and unfortunately we lacked the time to improve it and resubmit it to another conference.

Motivations for anytime algorithms. As introduced in Chapter 2, an online reinforcement learning algorithm is *anytime* if it does not need to know in advance the horizon T of the experiment. Depending on the context of the practical application of interest, it might be unrealistic to assume to know in advance T. We give two examples to illustrate where this prior knowledge can be realistic or not. On the one hand, consider clinical trials: it is likely that the number of patients is known before starting the trial, and for this model we refer to all the research that studies the setting of fixed-time best-arm identification [ABM10, GK16]. On the second hand, consider cognitive radio and decentralized MAB learning implemented on IoT devices (like we present it in Chapter 5): usually a learning step corresponds to an up-link and then down-link message sent and received by the IoT device, and so the time horizon T denotes the total number of such messages. While it can be assumed that the device will run for instance for 10 years (as it is advertised by some companies [CVZZ16]), many kinds of application such as medical sensors or connected fields cannot predict the number of total communications before setting up the device.

For this later range of applications, it is of highest interest to be able to use low-cost MAB algorithms that do not rely on prior knowledge of the problem for which they will be applied, and especially do not need to know the horizon T. In this thesis, while we proposed in Chapter 6 any-time algorithms solving the presented problem of stationary multi-players

bandit, our solution for the problem of non-stationary MAB problem studied in Chapter 7 does rely on a prior knowledge of the horizon T. It is an interesting direction of research to know what is the best approach to fix this weakness: work more and design algorithms that are inherently any-time, or use a generic technique to avoid depending on a prior knowledge of T, and automatically transform our non-anytime approach to make it anytime.

Solution to "patch" a non-anytime algorithm. A well-known technique to obtain an anytime algorithm from any non-anytime algorithm is the "Doubling Trick", as first introduced in [CBL06] and used for instance in [AO10, AGO18]. In the context of adversarial or stochastic multi-armed bandits, the performance of an algorithm is measured by its regret, and we study two families of sequences of growing horizons (geometric and exponential) to generalize previously known results that certain doubling tricks can be used to conserve certain regret bounds. In a broad setting, we prove that a geometric doubling trick can be used to conserve (minimax) bounds in $R_T = \mathcal{O}(\sqrt{T})$ but *cannot* conserve (distribution-dependent) bounds in $R_T = \mathcal{O}(\ln(T))$. We give insights as to why exponential doubling tricks may be better, as they conserve bounds in $R_T = \mathcal{O}(\ln(T))$, and are close to conserving bounds in $R_T = \mathcal{O}(\sqrt{T})$. Interestingly, we prove that they conserve bounds of the mixed form $R_T = \mathcal{O}(T^\gamma (\ln(T))^\delta)$, for $0 < \gamma < 1$ and $\delta > 0$, and so an exponential doubling trick could be used to obtain an anytime version of the algorithm we propose for non-stationary bandits, GLR-klUCB in Chapter 7. However, our study was only focusing on stationary bandit, and it is left as a future work to explore the harder case of piece-wise stationary problems.

In our article [BK18b], we also present numerical experiments in the case of stationary MAB problems, to compare the performance of efficient anytime algorithms, like kl-UCB, against efficient non-anytime algorithms, like kl-UCB^{++} from [MG17], made anytime with different choices of doubling-trick. We conclude that for such problems, if T is not known before, it is always more efficient to use policies that were designed to be anytime that to use a doubling trick. For example, an applicative paper written in 2018, [LLL19], only tested the use of an exponential doubling trick combined with kl-UCB^{++}, but most surely the kl-UCB algorithm would have given better empirical performance as well as more robust results...

To conclude this work, we would need to complete the study of the doubling tricks, and instead of focusing on two families (geometric and exponential), we need to completely characterize the doubling tricks that allow to preserve certain regret bounds. Such doubling is given either by the function mapping the current time t to the current estimate of the horizon $T(t)$, or the sequence $(T_i)_{i \in \mathbb{N}^*}$ of successive estimates of the horizons. We are interested in pursuing this work, in the hope of finding an intermediate sequence, growing faster than a geometric but slower than an exponential doubling sequence, that can preserve both worlds, problem-dependent bounds in $\mathcal{O}(\ln(T))$ and problem-independent bounds in $\mathcal{O}(\sqrt{T})$.

Abbreviations and Notations

Acronyms and Abbreviations

Ack	*Acknowledgement*
ALOHA	*ALOHA* (not an acronym)
BTS	*Base Tranceiver Station* (or *gateway*)
CPU	*Central Processing Unit*
CR	*Cognitive Radio*
DSA	*Dynamic Spectrum Access*
GLR, GLRT	*Generalized Likelihood Ratio*, *Generalized Likelihood Ratio Test*
i.i.d.	*identically and independently distributed* (variables, observations or samples)
IoT	*Internet of Things*
ISM	*Industrial, Scientific and Medical* (bands)
KL	*Kullback-Leibler* (divergence)
klUCB	*Kullback-Leibler Upper Confidence Bound* (algorithm)
LAN	*Local Area Network*
LPWAN	*Low-Power Wide-Area Network*
MAB	*Multi-Armed Bandit*
MAC	*Medium Access Control* (layer)
MCTopM	*Musical-Chair on Top-M* (algorithm)
ML	*Machine Learning*
NB-IoT	*Narrow-Band Internet of Things*
NOMA	*Non-Orthogonal Multiple Access*
OSA	*Opportunistic Spectrum Access*
PHY	*PHYsical* (layer)
PLR	*Packet Loss Ratio*
PU	*Primary User*
QPSK	*Quadrature Phase-Shift Keying*
RAM	*Random Access Memory*

RandTopM	*Random Hoping on Top-M* (algorithm)
RF	*Radio Frequency*
RL	*Reinforcement Learning*
SCEE	*Signal, Communication et Électronique Embarquée* (research team in CentraleSupélec, campus of Rennes)
SNR	*Signal to Noise Ratio*
SU	*Secondary User*
TS	*Thompson Sampling* (algorithm)
UCB	*Upper Confidence Bound* (object or algorithm)
USRP	*Universal Software Radio Peripheral*
WLAN	*Wireless Local Area Network*
wlog	*with loss of generality*
wrt	*with respect to*

Exponents

y^j	Usually denotes a variable depending on a player in Chapter 6 (for $j \in [M]$), or to distinguish between different independent runs in numerical simulations in Chapter 2 (for $j \in [N]$)
$y^{(i)}$, $y^{(\ell)}$	Usually the superscript index (i) or (ℓ) denotes a variable in the i-th stationary interval, under the point-of-views of *global* or *local* changes, in Chapter 7

Greek symbols

α	Denotes the parameter of a UCB algorithm in Chapters 2 and 5
α_0, δ_0	Usually denotes a constant scaling of a parameter of an algorithm, for instance $\varepsilon_t = \varepsilon_0/t$ is used in Chapter 2, or $\alpha = \alpha_0 \alpha_T$ is used in Chapter 7
$\beta(n, \delta)$	Usually denotes a threshold for the statistical (GLR) tests in Chapter 7
$\boldsymbol{\mu}, \boldsymbol{\nu}, \boldsymbol{\lambda}$	Vector of means $(\mu_k) = \mu_1, \ldots, \mu_K$, or vector of distributions $(\nu_k)_k$ or $(\lambda_k)_k$ (characterizing a problem)
Δn, Δs	Parameters of numerical optimization tricks in Chapter 7
Δ	Usually denotes the gap in terms of means of arms, usually between the best and second best arms, in Chapters 2, 6. In Chapter 5 in Algorithm 5.5 it denotes a delay. In Chapter 7, it can denote different gaps (Δ^{opt} and Δ^{change})
δ	Usually denotes a lower-bound on the gap Δ, known beforehandby an algorithm, in Chapters 6, 7. Also denote a confidence level of an algorithm in Section 7.4
γ	Usually denotes a discount factor, *e.g.*, in D-UCB or D-TS in Chapter 7
μ^*, μ_k^*	Mean of the optimal arm (*i.e.*, $\mu^* = \max_k \mu_k$), and mean of the k-th best arm
μ_k, $\mu_k(t)$, μ_k^j, $\mu_k^{(i)}$	Mean of arm k, arm k at time t (in Chapter 7), arm k for user j (in Chapter 6), arm k in the i-th stationary interval (in Chapter 7)
ν_k, $\nu_k(t)$, ν_k^j	Distribution of arm k, arm k at time t, arm k for user j
ω	Denotes a parameter controlling the forced exploration mechanism in Chapter 7

π	It usually denotes the number $\pi \simeq 3.14\ldots$, but it also denotes a probability distribution in Chapter 4 or a permutation in Section 6.4.2
τ	Length of a sliding-window, *e.g.*, in SW-UCB in Chapter 7
τ_k^j, $\tau_k^{(i)}$	Location of a change-point, *e.g.*, the j-th change-point on arm k, in Chapter 7
Υ_T	Number of break-points in a piece-wise stationary MAB problem in Chapter 7. NC_i denotes the number of change-points on arm i, and $C_T = \sum_{i=1}^{K} \mathrm{NC}_i$ the number of change-points on the arms
ε	Usually denotes a small positive real value, *e.g.*, the parameter for the ε-greedy algorithm, or the drift correction parameter for CUSUM in Chapter 7

Indices

x_k	Usually denotes a variable depending on an arm, for $k \in [K]$
$Y_{k,t}$	Usually denotes a variable depending on an arm $k \in [K]$ and on time $t \in [T]$

Roman symbols

$\mathcal{A}$	An algorithm, also referred to as a policy or a strategy. $\mathcal{A}_1, \ldots, \mathcal{A}_N$ denote the N aggregated algorithms in Chapter 4 and $\mathcal{A}_1, \ldots, \mathcal{A}_M$ denotes the algorithms of the M players in Chapter 6
$\mathcal{H}_0$, $\mathcal{H}_1$, $\mathcal{H}_2$	Hypothesis, in Chapters 5 and 7
$\mathcal{T}$	In Chapter 7, denote a function in (7.6) and a set of time steps in Section 7.10.3
$\mathrm{MaxBackOff}$	Maximum number of retransmission of a packet in the ALOHA protocol in Chapter 5
$\mathrm{UCB}_k(t)$	Upper-Confidence Bound (UCB) of arm k at time t for an index policy
$\widehat{\mu}_k(t)$	Empirical mean of rewards obtained for arm k at time t
$A(t)$, $A^j(t)$	Decision of algorithm $\mathcal{A}$ at time $t \in [T]$, $A(t) \in [K]$ (from algorithm $\mathcal{A}$), decision for user $j \in [M]$ in Chapter 6 (from algorithm $\mathcal{A}^j$)
$C_k(t)$, $C^j(t)$	In Chapter 6, collision indicator on arm $k \in [K]$ or for user $j \in [M]$, at time t
$C_{\boldsymbol{\mu}}$, $D_{\boldsymbol{\mu}}$, $G_{M,\boldsymbol{\mu}}$	In Chapter 6, constants depending on the problem parameters only and on M
D, D_k	In Chapter 5, total number of *dynamic* devices in the network or in channel k
$d^{(i)}$, $d^{(\ell)}$	Lower-bound on number of samples for accurate detection of change-points in Chapter 7
i, j	Usually denotes the i-th or j-th player, $i, j \in [M]$ in Chapter 6
K	Number of arms for multi-armed bandit games
k	Usually denotes the k-th arm, $k \in [K]$, mainly used in subscripts
M	Number of player for multi-players bandit games in Chapter 6
m	Maximum length of the back-off interval after a collision, in Chapter 5
N	Usually denotes the number of independent repetitions of the same numerical experiments (*e.g.*, $N = 1000$). In Chapter 5, N denotes the number of IoT (dynamic) devices in the studied network
$N_k(t)$	Number of samples obtained for arm k at time t
O_t, O_t^j	Vector of observations until time t in Chapters 2 and 6 (for player j)

p	In Chapter 5, probability of transmission for the devices following a Bernoulli random emission pattern (*e.g.*, $p = 10^{-5}$)
$r(t)$, $r^j(t)$	Reward obtained at time t, for user j at time t
R_T, $R_T^{\mathcal{A}}$, $R_T^{\mathcal{A}}(I)$	Regret of an algorithm $\mathcal{A}$ for horizon T (on instance I)
S, S_k	In Chapter 5, total number of *static* devices in the network or in channel k
T	Time horizon, the duration of the bandit game (always $T \geq 1$)
t, s, n, r	Time step, $t \in [T]$. Chapter 7 also uses s, n and r, *e.g.*, in the $\sup$ of the stopping times or some technical lemmas
T_0, T_1	Fixed durations of some algorithms based on different phases, *e.g.*, for Explore-then-Exploit or Musical Chair from [RSS16]
$U_k(t)$	Index of arm k at time t for an index policy
$U_k^j(t)$, $U^j(t)$	Index of (arm k) at time t of user j for an index policy in Chapter 6
$Y_{k,t}$	Random sample from the arm k at time t

Mathematical notations

$[K]$, T, $[N]$ etc	For an integer $N \in \mathbb{N}$, $N \geq 0$, $[N]$ denotes the set $\{1, \dots, N\} = \{n \in \mathbb{N} : 1 \leq n \leq N\}$. If the order is important, it is ordered from 1 to N.
$\mathcal{E}$, $\mathcal{E}_T$	Used in Chapter 7 to denote "good events" that happen most of the time
$\mathcal{F}$, $\mathcal{F}_t$	Filtration in a probabilistic model, after $t-1$ prior observations
$\mathcal{W}$	Lambert $\mathcal{W}$ function, the first branch of the inverse of $x \mapsto x\exp(x)$, cf. [CGH+96]
$\mathbb{E}$	Expectation under a probabilistic model
kl	Binary relative entropy, KullBack-Leibler divergence between two Bernoulli distribution: $\mathrm{kl}(x,y) = x\ln(x/y) + (1-x)\ln((1-x)/(1-y))$
$\lfloor\bullet\rfloor$, $\lceil\bullet\rceil$	Floor $\lfloor x\rfloor = \sup\{n \in \mathbb{Z}, n \leq x\}$ and ceil $\lceil x\rceil = \inf\{n \in \mathbb{Z}, x < n\}$ functions
$\mathbb{1}(E)$	Indicator function of an event E ($= 1$ if and only if the event E is true)
$\mathbb{P}$	Probability measure under a probabilistic model
$\widehat{X}$	Usually denotes an "empirical value", a mean or an estimate of a quantity X that depends on time, *e.g.*, $\widehat{\mu_k}$ the empirical mean of arm k
$\widetilde{X}$	Usually denotes another "empirical value" or an estimate of a quantity X that depends on time, *e.g.*, $\widetilde{S}_t$ the set of selected arms in Section 6.4.1. Also denotes a surrogate for a function without a closed form, *e.g.*, $\widetilde{T}$ in Section 7.10.4
$d(x,y)$	Divergence function between two distributions of parameters x and y, in a one-dimensional exponential family, in Chapter 7
E^c	Complement of an event E
f, g, h	Real-valued functions, *e.g.*, the exploration function used for kl-UCB indexes, $f(t) = \ln(t) + 3\ln(\ln(t))$
$o(\bullet)$, $\mathcal{O}(\bullet)$, $\Omega(\bullet)$	Landau notations for positive functions: $f(x) = o(g(x))$ means that $g(x) \neq 0$ and $f(x)/g(x) \to 0$ for $x \to \infty$, $f(x) = \mathcal{O}(g(x))$ means that there exists $x_0, K > 0$ such that $f(x) \leq Kg(x)$ from $x \geq x_0$, and $f(x) = \Omega(g(x))$ means $g(x) = \mathcal{O}(f(x))$
X'	Usually denotes a "wrong value" of a variable X, for instance M' denotes in Section 6.7.1. Also denotes the derivative of a function, *e.g.*, f'

List of Figures

List of Algorithms

List of Code Examples

List of Tables

List of References

[AB09] J-Y. Audibert and S. Bubeck. Minimax Policies for Adversarial and Stochastic Bandits. In *Conference on Learning Theory*, pages 217–226. PMLR, 2009.

[AB10] J.-Y. Audibert and S. Bubeck. Regret Bounds And Minimax Policies Under Partial Monitoring. *Journal of Machine Learning Research*, 11:2785–2836, 2010.

[ABM10] J-Y. Audibert, S. Bubeck, and R. Munos. Best Arm Identification in Multi-Armed Bandits. In *Conference on Learning Theory*, page 13. PMLR, 2010.

[Abr70] N. Abramson. The ALOHA System: Another Alternative for Computer Communications. In *Proceedings of the November 17-19, 1970, Fall Joint Computer Conference*, AFIPS '70 (Fall), pages 281–285, New York, NY, USA, 1970. ACM.

[AC18] A. Azari and C. Cavdar. Self-organized Low-power IoT Networks: A Distributed Learning Approach. In *Global Communications Conference*, Abu Dhabi, UAE, December 2018. IEEE.

[ACBF02] P. Auer, N. Cesa-Bianchi, and P. Fischer. Finite-time Analysis of the Multi-armed Bandit Problem. *Machine Learning*, 47(2):235–256, 2002.

[ACBFS95] P. Auer, N. Cesa-Bianchi, Y. Freund, and R. Schapire. Gambling in a Rigged Casino: The Adversarial Multi-Armed Bandit Problem. In *Annual Symposium on Foundations of Computer Science*, pages 322–331. IEEE, 1995.

[ACBFS02] P. Auer, N. Cesa-Bianchi, Y. Freund, and R. Schapire. The Non-Stochastic Multi-Armed Bandit Problem. *SIAM journal on computing*, 32(1):48–77, 2002.

[AF15] R. Allesiardo and R. Féraud. Exp3 with Drift Detection for the Switching Bandit Problem. In *International Conference on Data Science and Advanced Analytics*, pages 1–7. IEEE, 2015.

[AFM17] R. Allesiardo, R. Féraud, and O.-A. Maillard. The Non-Stationary Stochastic Multi-Armed Bandit Problem. *International Journal of Data Science and Analytics*, 3(4):267–283, 2017.

[AG12] S. Agrawal and N. Goyal. Analysis of Thompson sampling for the Multi-Armed Bandit problem. In *Conference On Learning Theory*, pages 36–65. PMLR, 2012.

[AGO18] P. Auer, P. Gajane, and R. Ortner. Adaptively Tracking the Best Arm with an Unknown Number of Distribution Changes. *European Workshop on Reinforcement Learning*, 2018.

[Agr95] R. Agrawal. Sample mean based index policies by $\mathcal{O}(\ln n)$ regret for the Multi-Armed Bandit problem. *Advances in Applied Probability*, 27(4):1054–1078, 1995.

[AHK12] S. Arora, E. Hazan, and S. Kale. The multiplicative weights update method: a meta-algorithm and applications. *Theory of Computing*, 8(1):121–164, 2012.

[AHK17] S. Adish, H. Hassani, and A. Krause. Learning to Use Learners' Advice. *arXiv preprint arXiv:1702.04825*, 2017.

[ALK19] P. Alatur, K. Y. Levy, and A. Krause. Multi-Player Bandits: The Adversarial Case. *arXiv preprint arXiv:1902.08036*, 2019.

[ALNS17] A. Agarwal, H. Luo, B. Neyshabur, and R. E. Schapire. Corralling a Band of Bandit Algorithms. In *Conference on Learning Theory*, pages 12–38. PMLR, 2017.

[ALVM06] I. F. Akyildiz, W.-Y. Lee, M. C. Vuran, and S. Mohanty. NeXt Generation, Dynamic Spectrum Access, Cognitive Radio Wireless Networks: A Survey. *Computer Networks*, 50(13):2127–2159, 2006.

[AM15] O. Avner and S. Mannor. Learning to Coordinate Without Communication in Multi-User Multi-Armed Bandit Problems. *arXiv preprint arXiv:1504.08167*, 2015.

[AM16] O. Avner and S. Mannor. Multi-User Lax Communications: a Multi-Armed Bandit Approach. In *International Conference on Computer Communications*. IEEE, 2016.

[AM18] O. Avner and S. Mannor. Multi-User Communication Networks: A Coordinated Multi-Armed Bandit Approach. *arXiv preprint arXiv:1808.04875*, 2018.

[AMF17] R. Alami, O.-A. Maillard, and R. Féraud. Memory Bandits: Towards the Switching Bandit Problem Best Resolution. In *Conference on Neural Information Processing Systems*, 2017.

[AMT10] A. Anandkumar, N. Michael, and A. K. Tang. Opportunistic Spectrum Access with multiple users: Learning under competition. In *International Conference on Computer Communications*. IEEE, 2010.

[AMTA11] A. Anandkumar, N. Michael, A. K. Tang, and S. Agrawal. Distributed Algorithms for Learning and Cognitive Medium Access with Logarithmic Regret. *Journal on Selected Areas in Communications*, 29(4):731–745, 2011.

[AO10] P. Auer and R. Ortner. UCB Revisited: Improved Regret Bounds For The Stochastic Multi-Armed Bandit Problem. *Periodica Mathematica Hungarica*, 61(1-2):55–65, 2010.

[AVW87a] V. Anantharam, P. Varaiya, and J. Walrand. Asymptotically efficient allocation rules for the Multi-Armed Bandit problem with multiple plays - Part I: IID rewards. *Transactions on Automatic Control*, 32(11):968–976, 1987.

[AVW87b] V. Anantharam, P. Varaiya, and J. Walrand. Asymptotically efficient allocation rules for the Multi-Armed Bandit problem with multiple plays - Part II: Markovian rewards. *Transactions on Automatic Control*, 32(11):977–982, 1987.

[B+18] G. Brandl et al. Sphinx: Python documentation generator. Online at: `https://sphinx-doc.org`, 2018.

[Bar59] G.A. Barnard. Control charts and stochastic processes. *Journal of the Royal Statistical Society. Series B (Methodological)*, pages 239–271, 1959.

[BBM+17] R. Bonnefoi, L. Besson, C. Moy, E. Kaufmann, and J. Palicot. Multi-Armed Bandit Learning in IoT Networks: Learning Helps Even in Non-Stationary Settings. In *12th EAI Conference on Cognitive Radio Oriented Wireless Network and Communication*, Lisboa, Portugal, 2017.

[BBM18] L. Besson, R. Bonnefoi, and C. Moy. Multi-Arm Bandit Algorithms for Internet of Things Networks: A TestBed Implementation and Demonstration that Learning Helps. Demonstration presented at International Conference on Telecommunications, June 2018.

[BBM19] L. Besson, R. Bonnefoi, and C. Moy. GNU Radio Implementation of MALIN: "Multi-Armed bandits Learning for Internet-of-things Networks". In *Wireless Communications and Networking Conference*, Marrakech, Morocco, April 2019. IEEE. Following a Demonstration presented at International Conference on Telecommunications (ICT) 2018.

[BBMVM19] R. Bonnefoi, L. Besson, J. C. Manco-Vasquez, and C. Moy. Upper-Confidence Bound for Channel Selection in LPWA Networks with Retransmissions. In *MOTIoN Workshop*, Marrakech, Morocco, April 2019. IEEE.

[BBS+19] S. Behnel, R. Bradshaw, Dag S. Seljebotn, G. Ewing, W. Stein, G. Gellner, et al. Cython: C-extensions for python. Online at: https://cython.org, 2019.

[BCB12] S. Bubeck and N. Cesa-Bianchi. Regret Analysis of Stochastic and Non-Stochastic Multi-Armed Bandit Problems. *Foundations and Trends® in Machine Learning*, 5(1):1–122, 2012.

[Bes18] L. Besson. SMPyBandits: an Experimental Framework for Single and Multi-Players Multi-Arms Bandits Algorithms in Python. Preprint, submitted to JMLR MLOSS, https://hal.archives-ouvertes.fr/hal-01840022, 2018.

[Bes19] L. Besson. SMPyBandits: an Open-Source Research Framework for Single and Multi-Players Multi-Arms Bandits (MAB) Algorithms in Python, 2016–2019. Code at https://GitHub.com/SMPyBandits/SMPyBandits/, documentation at https://SMPyBandits.GitHub.io/.

[BGZ14] O. Besbes, Y. Gur, and A. Zeevi. Stochastic Multi-Armed Bandit Problem with Non-Stationary Rewards. In *Advances in Neural Information Processing Systems*, pages 199–207, 2014.

[BK18a] L. Besson and E. Kaufmann. Multi-Player Bandits Revisited. In M. Mohri and K. Sridharan, editor, *Algorithmic Learning Theory*, Lanzarote, Spain, 2018.

[BK18b] L. Besson and E. Kaufmann. What Doubling Trick Can and Can't Do for Multi-Armed Bandits. Preprint, https://hal.archives-ouvertes.fr/hal-01736357, February 2018.

[BK19a] L. Besson and E. Kaufmann. Analyse non asymptotique d'un test séquentiel de détection de ruptures et application aux bandits non stationnaires. *GRETSI*, August 2019. https://hal.archives-ouvertes.fr/hal-02152243.

[BK19b] L. Besson and E. Kaufmann. Combining the Generalized Likelihood Ratio Test and kl-UCB for Non-Stationary Bandits. Preprint, https://hal.archives-ouvertes.fr/hal-02006471, arXiv preprint arXiv:1902.01575, February 2019.

[BKM18] L. Besson, E. Kaufmann, and C. Moy. Aggregation of Multi-Armed Bandits Learning Algorithms for Opportunistic Spectrum Access. In *Wireless Communications and Networking Conference*, Barcelona, Spain, 2018. IEEE.

[BL18] I. Bistritz and A. Leshem. Distributed Multi-Player Bandits: a Game Of Thrones Approach. In *Advances in Neural Information Processing Systems*, pages 7222–7232, 2018.

[BLM13] S. Boucheron, G. Lugosi, and P. Massart. *Concentration Inequalities: A Nonasymptotic Theory of Independence*. Oxford university press, 2013.

[BMM14] A. Baransi, O.-A. Maillard, and S. Mannor. Sub-sampling for Multi-armed Bandits. *Proceedings of the European Conference on Machine Learning*, 2014.

[BN93] M. Basseville and I. Nikiforov. *Detection of Abrupt Changes: Theory And Application*, volume 104. Prentice Hall Englewood Cliffs, 1993.

[Bod17] Q. Bodinier. *Coexistence of Communication Systems Based on Enhanced Multi-Carrier Waveforms with Legacy OFDM Networks*. PhD thesis, CentraleSupélec, 2017.

[BP+16] I. Bicking, PyPA, et al. Virtualenv: a tool to create isolated Python environments. Online at: https://virtualenv.pypa.io, November 2016.

[BP18] E. Boursier and V. Perchet. SIC-MMAB: Synchronisation Involves Communication in Multiplayer Multi-Armed Bandits. *arXiv preprint arXiv:1809.08151*, 2018.

[BR19] D. Bouneffouf and I. Rish. A Survey on Practical Applications of Multi-Armed and Contextual Bandits. *arXiv preprint arXiv:1904.10040, under review by IJCAI 2019 Survey*, 2019.

[BS12] S. Bubeck and A. Slivkins. The Best Of Both Worlds Stochastic And Adversarial Bandits. In *Conference on Learning Theory*, pages 42–1. PMLR, 2012.

[BV04] S. Boyd and L. Vandenberghe. *Convex Optimization*. Cambridge Univ. Press, 2004.

[BV19] M. Bande and V. V. Veeravalli. Adversarial Multi-User Bandits for Uncoordinated Spectrum Access. In *IEEE International Conference on Acoustics, Speech and Signal Processing (ICASSP)*, pages 4514–4518. IEEE, 2019.

[C+52] H. Chernoff et al. A measure of asymptotic efficiency for tests of a hypothesis based on the sum of observations. *The Annals of Mathematical Statistics*, 23(4):493–507, 1952.

[C+18] A. Collette et al. h5py: HDF5 for Python. Online at: `https://www.h5py.org`, 2018.

[CBL06] N. Cesa-Bianchi and G. Lugosi. *Prediction, Learning, and Games*. Cambridge University Press, 2006.

[CGH+96] R. Corless, G. Gonnet, D. Hare, D. Jeffrey, and D. Knuth. On the Lambert W Function. In *Advances in Computational Mathematics*, pages 329–359, 1996.

[CGM+13] O. Cappé, A. Garivier, O.-A. Maillard, R. Munos, and G. Stoltz. Kullback-Leibler Upper Confidence Bounds For Optimal Sequential Allocation. *Annals of Statistics*, 41(3):1516–1541, 2013.

[Che81] H. Chernoff. A note on an inequality involving the normal distribution. *The Annals of Probability*, pages 533–535, 1981.

[CLLW19] Y. Chen, C. Lee, H. Luo, and C. Wei. A New Algorithm for Non-stationary Contextual Bandits: Efficient, Optimal, and Parameter-free. In A. Beygelzimer and D. Hsu, editor, *Conference on Learning Theory*, volume 99, pages 1–30. PMLR, 2019.

[CMP17] R. Combes, S. Magureanu, and A. Proutiere. Minimal Exploration in Structured Stochastic Bandits. In *Advances in Neural Information Processing Systems*, pages 1761–1769, 2017.

[CVZZ16] M. Centenaro, L. Vangelista, A. Zanella, and M. Zorzi. Long-range communications in unlicensed bands: the rising stars in the IoT and smart city scenarios. *Wireless Communications*, 23(5):60–67, 2016.

[CZKX19] Y. Cao, W. Zheng, B. Kveton, and Y. Xie. Nearly Optimal Adaptive Procedure for Piecewise-Stationary Bandit: a Change-Point Detection Approach. In *International Conference on Artificial Intelligence and Statistics*, Okinawa, Japan, 2019.

[DH18] S. J. Darak and M. K. Hanawal. Distributed Learning and Stable Orthogonalization in Ad-Hoc Networks with Heterogeneous Channels. *arXiv preprint arXiv:1812.11651*, 2018.

[DMNM16] S. J. Darak, N. Modi, A. Nafkha, and C. Moy. Spectrum Utilization and Reconfiguration Cost Comparison of Various Decision Making Policies for Opportunistic Spectrum Access Using Real Radio Signals. In *11th EAI Conference on Cognitive Radio Oriented Wireless Network and Communication*, Grenoble, France, 2016.

[DMP16] S. J. Darak, C. Moy, and J. Palicot. Proof-of-Concept System for Opportunistic Spectrum Access in Multi-user Decentralized Networks. *EAI Endorsed Transactions on Cognitive Communications*, 2:1–10, 2016.

[DNMP16] S. J. Darak, A. Nafkha, C. Moy, and J. Palicot. Is Bayesian Multi Armed Bandit Algorithm Superior? Proof of Concept for Opportunistic Spectrum Access in Decentralized Networks. In *11th EAI Conference on Cognitive Radio Oriented Wireless Network and Communication*, Grenoble, France, 2016.

[DP16] R. Degenne and V. Perchet. Anytime Optimal Algorithms In Stochastic Multi Armed Bandits. In *International Conference on Machine Learning*, pages 1587–1595, 2016.

[Ett] Ettus. USRP Hardware Driver and USRP Manual. Online at https://files.ettus.com/manual/page_usrp2.html. Accessed: 2018-09-25.

[Fou17] Python Software Foundation. Python language reference, version 3.6. Online at: https://www.python.org, October 2017.

[GB12] A. Garhwal and P. P. Bhattacharya. A Survey on Dynamic Spectrum Access Techniques for Cognitive Radio. *International Journal of Next-Generation Networks (IJNGN)*, 3(4), 2012.

[GBV18] G. Gautier, R. Bardenet, and M. Valko. DPPy: Sampling Determinantal Point Processes with Python. *arXiv preprint arXiv:1809.07258*, 2018. Code at https://github.com/guilgautier/DPPy. Documentation at https://dppy.readthedocs.io.

[GC11] A. Garivier and O. Cappé. The KL-UCB Algorithm for Bounded Stochastic Bandits and Beyond. In *Conference on Learning Theory*, pages 359–376. PMLR, 2011.

[GGCA11] N. Gupta, O. Granmo-Christoffer, and A. Agrawala. Thompson Sampling for Dynamic Multi Armed Bandits. In *International Conference on Machine Learning and Applications Workshops*, pages 484–489. IEEE, 2011.

[GHMS18] A. Garivier, H. Hadiji, P. Menard, and G. Stoltz. KL-UCB-switch: optimal regret bounds for stochastic bandits from both a distribution-dependent and a distribution-free viewpoints. *arXiv preprint arXiv:1805.05071*, 2018.

[GK16] A. Garivier and E. Kaufmann. Optimal Best Arm Identification with Fixed Confidence. In *PMLR*, volume 49 of *Conference on Learning Theory*, 2016.

[GKL16] A. Garivier, E. Kaufmann, and T. Lattimore. On Explore-Then-Commit Strategies. In *PMLR*, volume 29 of *Advances in Neural Information Processing Systems*, 2016.

[GM11] A. Garivier and E. Moulines. On Upper-Confidence Bound Policies For Switching Bandit Problems. In *Algorithmic Learning Theory*, pages 174–188. PMLR, 2011.

[GNUa] GNU Radio Companion Documentation and Website. Online at https://wiki.gnuradio.org/index.php/GNURadioCompanion. Accessed: 2018-09-25.

[GNUb] GNU Radio Documentation and Website. Online at https://www.gnuradio.org/about/. Accessed: 2018-09-25.

[H+16] E. Hazan et al. Introduction to online convex optimization. *Foundations and Trends® in Optimization*, 2(3-4):157–325, 2016.

[Hay05] S. Haykin. Cognitive Radio: Brain-Empowered Wireless Communications. *Journal on Selected Areas in Communications*, 23(2):201–220, 2005.

[HGB+06] C. Hartland, S. Gelly, N. Baskiotis, O. Teytaud, and M. Sebag. Multi-Armed Bandit, Dynamic Environments and Meta-Bandits. In *NeurIPS 2006 Workshop, Online Trading Between Exploration And Exploitation*, 2006.

[Hoe63] W. Hoeffding. Probability inequalities for sums of bounded random variables. *Journal of the American statistical association*, 58(301):13–30, 1963.

[Hon19] J. Honda. A Note on KL-UCB+ Policy for the Stochastic Bandit. *arXiv preprint arXiv:1903.07839*, 2019.

[Hun07] J. D. Hunter. Matplotlib: a 2D Graphics Environment. *Computing In Science & Engineering*, 9(3):90–95, 2007.

[I+17] Anaconda Inc. et al. Numba, NumPy aware dynamic Python compiler using LLVM. Online at: `https://numba.pydata.org`, 2017.

[JEMP09] W. Jouini, D. Ernst, C. Moy, and J. Palicot. Multi-Armed Bandit Based Policies for Cognitive Radio's Decision Making Issues. In *International Conference Signals, Circuits and Systems*. IEEE, 2009.

[JEMP10] W. Jouini, D. Ernst, C. Moy, and J. Palicot. Upper Confidence Bound Based Decision Making Strategies and Dynamic Spectrum Access. In *International Conference on Communications*, pages 1–5. IEEE, 2010.

[JKYD18] H. Joshi, R. Kumar, A. Yadav, and S. J. Darak. Distributed Algorithm for Dynamic Spectrum Access in Infrastructure-Less Cognitive Radio Network. In *2018 IEEE Wireless Communications and Networking Conference (WCNC)*, pages 1–6, 2018.

[JMP12] W. Jouini, C. Moy, and J. Palicot. Decision Making for Cognitive Radio Equipment: Analysis of the First 10 Years of Exploration. *EURASIP Journal on Wireless Communications and Networking*, 2012(1), 2012.

[JOP+01] E. Jones, T. E. Oliphant, P. Peterson, et al. SciPy: Open source scientific tools for Python. Online at: `https://www.scipy.org`, 2001.

[Jor10] M. Jordan. Stat 260/CS 294. Online at `https://people.eecs.berkeley.edu/~jordan/courses/260-spring10/`, 2010. Chapter 8 covers the exponential family.

[Jou17] W. Jouini. *Contribution to Learning and Decision Making under Uncertainty for Cognitive Radio*. PhD thesis, CentraleSupélec, IETR, Rennes, 2017.

[K+16] T. Kluyver et al. Jupyter Notebooks – a publishing format for reproducible computational workflows. In F. Loizides and B. Schmidt, editors, *Positioning and Power in Academic Publishing: Players, Agents and Agendas*, pages 87–90. IOS Press, 2016.

[KAF+18] R. Kerkouche, R. Alami, R. Féraud, N. Varsier, and P. Maillé. Node-based optimization of LoRa transmissions with Multi-Armed Bandit algorithms. In *International Conference on Telecommunications*, Saint-Malo, France, 2018. J. Palicot and R. Pyndiah.

[KCG12] E. Kaufmann, O. Cappé, and A. Garivier. On Bayesian Upper Confidence Bounds for Bandit Problems. In *International Conference on Artificial Intelligence and Statistics*, pages 592–600, 2012.

[KDH+19] R. Kumar, S. J. Darak, M. K. Hanawal, A. K. Sharma, and R. K. Tripathi. Distributed Algorithm for Learning to Coordinate in Infrastructure-Less Network. *IEEE Communications Letters*, 23(2):362–365, 2019.

[KDY+16] R. Kumar, S. J. Darak, A. Yadav, A. K. Sharma, and R. K. Tripathi. Two-stage Decision Making Policy for Opportunistic Spectrum Access and Validation on USRP Testbed. *Wireless Networks*, pages 1–15, 2016.

[KDY+17] R. Kumar, S. J. Darak, A. Yadav, A. K. Sharma, and R. K. Tripathi. Channel Selection for Secondary Users in Decentralized Network of Unknown Size. *Communications Letters*, 21(10):2186–2189, 2017.

[KHN15] J. Komiyama, J. Honda, and H. Nakagawa. Optimal Regret Analysis of Thompson Sampling in Stochastic Multi-Armed Bandit Problem with Multiple Plays. In *International Conference on Machine Learning*, volume 37, pages 1152–1161. PMLR, 2015.

[KK18] E. Kaufmann and W. M. Koolen. Mixture Martingales Revisited with Applications to Sequential Tests and Confidence Intervals. *arXiv preprint arXiv:1811.11419*, 2018.

[KKM12] E. Kaufmann, N. Korda, and R. Munos. Thompson Sampling: an Asymptotically Optimal Finite-Time Analysis. In *Algorithmic Learning Theory*, pages 199–213. PMLR, 2012.

[KL51] S. Kullback and R.A. Leibler. On Information and Sufficiency. *The Annals of Mathematical Statistics*, 22(1):79–86, 1951.

[KM19] E. Kaufmann and A. Mehrabian. New Algorithms for Multiplayer Bandits when Arm Means Vary Among Players. *arXiv preprint arXiv:1902.01239*, 2019.

[KNJ12] D. Kalathil, N. Nayyar, and R. Jain. Decentralized Learning for Multi-Player Multi-Armed Bandits. In *Conference on Decision and Control*. IEEE, 2012.

[KS06] L. Kocsis and C. Szepesvári. Discounted UCB. In *2nd PASCAL Challenges Workshop*, 2006.

[KSGB19] B. Kveton, C. Szepesvari, M. Ghavamzadeh, and C. Boutilier. Perturbed-History Exploration in Stochastic Multi-Armed Bandits. In *28th International Joint Conference on Artificial Intelligence (IJCAI 2019)*, 2019.

[KT19] B. Kim and A. Tewari. On the Optimality of Perturbations in Stochastic and Adversarial Multi-Armed Bandit Problems. *arXiv preprint arXiv:1902.00610*, 2019.

[KYDH18] R. Kumar, A. Yadav, S. J. Darak, and M. K. Hanawal. Trekking Based Distributed Algorithm for Opportunistic Spectrum Access in Infrastructure-Less Network. In *2018 16th International Symposium on Modeling and Optimization in Mobile, Ad-Hoc, and Wireless Networks (WiOpt)*, pages 1–8, 2018.

[Lat16a] T. Lattimore. Library for Multi-Armed Bandit Algorithms. Online at: `https://github.com/tor/libbandit`, 2016.

[Lat16b] T. Lattimore. Regret Analysis Of The Finite Horizon Gittins Index Strategy For Multi Armed Bandits. In *Conference on Learning Theory*, pages 1214–1245. PMLR, 2016.

[Lat18] T. Lattimore. Refining the confidence level for optimistic bandit strategies. *The Journal of Machine Learning Research*, 19(1):765–796, 2018.

[LBCU+09] M. López-Benítez, F. Casadevall, A. Umbert, J. Pérez-Romero, R. Hachemani, J. Palicot, and C. Moy. Spectral Occupation Measurements and Blind Standard Recognition Sensor for Cognitive Radio Networks. In *2009 4th International Conference on Cognitive Radio Oriented Wireless Networks and Communications*, pages 1–9. IEEE, 2009.

[LCLS10] L. Li, W. Chu, J. Langford, and R. E. Schapire. A Contextual-Bandit Approach to Personalized News Article Recommendation. In *International Conference on World Wide Web*, pages 661–670. ACM, 2010.

[LKC17] A. Luedtke, E. Kaufmann, and A. Chambaz. Asymptotically Optimal Algorithms for Budgeted Multiple Play Bandits. *Machine Learning*, pages 1–31, 2017.

[LLL19] H. Li, J. Luo, and C. Liu. Selfish Bandit based Cognitive Anti-jamming Strategy for Aeronautic Swarm Network in Presence of Multiple Jammert. *IEEE Access*, 2019.

[LLS18] F. Liu, J. Lee, and N. Shroff. A Change-Detection based Framework for Piecewise-stationary Multi-Armed Bandit Problem. In *The Thirty-Second AAAI Conference on Artificial Intelligence (AAAI 2018)*, 2018.

[LM18] G. Lugosi and A. Mehrabian. Multiplayer bandits without observing collision information. *arXiv preprint arXiv:1808.08416*, 2018.

[LR85] T. L. Lai and H. Robbins. Asymptotically Efficient Adaptive Allocation Rules. *Advances in Applied Mathematics*, 6(1):4–22, 1985.

[LRC+16] J. Louëdec, L. Rossi, M. Chevalier, A. Garivier, and J. Mothe. Algorithme de bandit et obsolescence : un modèle pour la recommandation. In *18ème Conférence francophone sur l'Apprentissage Automatique, 2016 (Marseille, France)*, 2016.

[LS19] T. Lattimore and C. Szepesvári. *Bandit Algorithms*. Cambridge University Press, 2019. Draft of Wednesday 1st of May, 2019, https://tor-lattimore.com/downloads/book/book.pdf.

[Lue68] D. G. Luenberger. Quasi-Convex Programming. *SIAM Journal on Applied Mathematics*, 16(5):1090–1095, 1968.

[LWAL18] H. Luo, C. Wei, A. Agarwal, and J. Langford. Efficient Contextual Bandits in Non-stationary Worlds. In S. Bubeck, V. Perchet, and P. Rigollet, editors, *Proceedings of the 31st Conference On Learning Theory*, volume 75 of *Proceedings of Machine Learning Research*, pages 1739–1776. PMLR, 2018.

[LX10] T. L. Lai and H. Xing. Sequential change-point detection when the pre-and post-change parameters are unknown. *Sequential Analysis*, 29(2):162–175, 2010.

[LZ08] K. Liu and Q. Zhao. A Restless Bandit Formulation of Opportunistic Access: Indexablity and Index Policy. In *Annual Communications Society Conference on Sensor, Mesh and Ad-Hoc Communications and Networks Workshops*. IEEE, 2008.

[LZ10] K. Liu and Q. Zhao. Distributed Learning in Multi-Armed Bandit with Multiple Players. *Transaction on Signal Processing*, 58(11):5667–5681, 2010.

[Mai19] O.-A. Maillard. Sequential change-point detection: Laplace concentration of scan statistics and non-asymptotic delay bounds. In *Algorithmic Learning Theory*, 2019.

[MB19] C. Moy and L. Besson. Decentralized Spectrum Learning for IoT Wireless Networks Collision Mitigation. In *ISIoT workshop*, Santorin, Greece, May 2019.

[MBDT19] C. Moy, L. Besson, G. Delbarre, and L. Toutain. Decentralized Spectrum Learning for Radio Collision Mitigation in Ultra-Dense IoT Networks: LoRaWAN Case Study and Measurements. Submitted for a special volume on Machine Learning for Intelligent Wireless Communications and Networking, Annals of Telecommunications, July 2019.

[MG17] P. Ménard and A. Garivier. A Minimax and Asymptotically Optimal Algorithm for Stochastic Bandits. In *Algorithmic Learning Theory*, volume 76, pages 223–237. PMLR, 2017.

[MGMM+15] L. Melián-Gutiérrez, N. Modi, C. Moy, F. Bader, I. Pérez-Álvarez, and S. Zazo. Hybrid UCB-HMM: A Machine Learning Strategy for Cognitive Radio in HF Band. *IEEE Transactions on Cognitive Communications and Networking*, 1(3):347–358, 2015.

[MM99] J. Mitola and G. Q. Maguire. Cognitive Radio: making software radios more personal. *Personal Communications*, 6(4):13–18, 1999.

[MM11] O.-A. Maillard and R. Munos. Adaptive Bandits: Towards the best history-dependent strategy. In *International Conference on Artificial Intelligence and Statistics*, pages 570–578, 2011.

[MM12] J. Marinho and E. Monteiro. Cognitive Radio: Survey on Communication Protocols Spectrum Decision Issues and Future Research Directions. *Wireless Networks*, 18(2):147–164, 2012.

[MM17] J. Mourtada and O.-A. Maillard. Efficient Tracking of a Growing Number of Experts. In *Algorithmic Learning Theory*, volume 76 of *Proceedings of Algorithmic Learning Theory*, pages 1–23, Tokyo, Japan, 2017.

[Mod17] N. Modi. *Machine Learning and Statistical Decision Making for Green Radio*. PhD thesis, CentraleSupélec, IETR, Rennes, 2017.

[Moy14] C. Moy. Reinforcement Learning Real Experiments for Opportunistic Spectrum Access. In *WSR'14*, page 10, Karlsruhe, Germany, 2014.

[MS13] J. Mellor and J. Shapiro. Thompson Sampling in Switching Environments with Bayesian Online Change Detection. In *Artificial Intelligence and Statistics*, pages 442–450, 2013.

[MTC+16] A. Maskooki, V. Toldov, L. Clavier, V. Loscrí, and N. Mitton. Competition: Channel Exploration/Exploitation Based on a Thompson Sampling Approach in a Radio Cognitive Environment. In *International Conference on Embedded Wireless Systems and Networks* (*dependability competition*), Graz, Austria, February 2016.

[NC17] O. Naparstek and K. Cohen. Deep Multi-User Reinforcement Learning for Dynamic Spectrum Access in Multichannel Wireless Networks. In *GLOBECOM 2017 - 2017 IEEE Global Communications Conference*, pages 1–7, 2017.

[Nor98] J. R. Norris. *Markov Chains*, volume 2 of *Cambridge Series in Statistical and Probabilistic Mathematics*. Cambridge University Press, Cambridge, 1998.

[Oct] OctoClock Clock Distribution Module with GPSDO - Ettus Research. Online at https://www.ettus.com/product/details/OctoClock-G. Accessed: 2018-09-25.

[PG07] F. Pérez and B. E. Granger. IPython: a System for Interactive Scientific Computing. *Computing in Science and Engineering*, 9(3):21–29, May 2007.

[PGNN19] V. Patil, G. Ghalme, V. Nair, and Y. Narahari. Stochastic Multi-Armed Bandits with Arm-specific Fairness Guarantees. *arXiv preprint arXiv:1905.11260*, 2019.

[PPS11] K. Patil, R. Prasad, and K. Skouby. A Survey of Worldwide Spectrum Occupancy Measurement Campaigns for Cognitive Radio. In *2011 International Conference on Devices and Communications* (*ICDeCom*), pages 1–5. IEEE, 2011.

[Raj17] V. Raj. A Julia Package for providing Multi Armed Bandit Experiments. Online at: https://github.com/v-i-s-h/MAB.jl, 2017.

[RK17] V. Raj and S. Kalyani. Taming Non-Stationary Bandits: a Bayesian Approach. 2017.

[RKS17] U. Raza, P. Kulkarni, and M. Sooriyabandara. Low Power Wide Area Networks (LPWAN): An Overview. *Communications Surveys Tutorials*, 19(2):855–873, 2017.

[RMZ14] C. Robert, C. Moy, and H. Zhang. Opportunistic Spectrum Access Learning Proof of Concept. In *SDR-WinnComm'14*, page 8, Schaumburg, United States, 2014.

[Rob52] H. Robbins. Some Aspects of the Sequential Design of Experiments. *Bulletin of the American Mathematical Society*, 58(5):527–535, 1952.

[Rob75] L. G. Roberts. ALOHA Packet System With and Without Slots and Capture. *SIGCOMM Computer Communication Review*, 5(2):28–42, 1975.

[RSS16] J. Rosenski, O. Shamir, and L. Szlak. Multi-Player Bandits – A Musical Chairs Approach. In *International Conference on Machine Learning*, pages 155–163. PMLR, 2016.

[SB11] M. Subhedar and G. Birajdar. Spectrum Sensing Techniques in Cognitive Radio Networks: a Survey. *International Journal of Next-Generation Networks*, 3(2):37–51, 2011.

[SB18] R. S. Sutton and A. G. Barto. *Reinforcement Learning: An introduction*. MIT press, 2018.

[SKHD18] S. Sawant, R. Kumar, M. K. Hanawal, and S. J. Darak. Learning to Coordinate in a Decentralized Cognitive Radio Network in Presence of Jammers. In *16th International Symposium on Modeling and Optimization in Mobile, Ad Hoc, and Wireless Networks* (*WiOpt*), Shanghai, China, 2018. IEEE.

[SL17] Y. Seldin and G. Lugosi. An Improved Parametrization and Analysis of the EXP3++ Algorithm for Stochastic and Adversarial Bandits. In *Conference on Learning Theory*, volume 65, pages 1–17. PMLR, 2017.

[SLC+19] J. Seznec, A. Locatelli, A. Carpentier, A. Lazaric, and M. Valko. Rotting Bandits Are No Harder Than Stochastic Ones. *International Conference on Artificial Intelligence and Statistics*, 2019.

[Sli19] A. Slivkins. Introduction to Multi-Armed Bandits. *arXiv preprint arXiv:1904.07272v3*, June 2019.

[SV95] D. Siegmund and E.S. Venkatraman. Using the Generalized Likelihood Ratio Statistic for Sequential Detection of a Change Point. *The Annals of Statistics*, pages 255–271, 1995.

[TCLM16] V. Toldov, L. Clavier, V. Loscrí, and N. Mitton. A Thompson Sampling Approach to Channel Exploration Exploitation Problem in Multihop Cognitive Radio Networks. In *PIMRC*, pages 1–6, Valencia, Spain, September 2016.

[TdSCC13] F. S. Truzzi, V. F. da Silva, A. H. Reali Costa, and F. Gagliardi Cozman. AdBandit: a New Algorithm for Multi-Armed Bandits. *ENIAC*, 2013(1), 2013.

[Tho33] W. R. Thompson. On the Likelihood that One Unknown Probability Exceeds Another in View of the Evidence of Two Samples. *Biometrika*, 25, 1933.

[TL12] C. Tekin and M. Liu. Online Learning in Decentralized Multi-User Spectrum Access with Synchronized Explorations. In *Military Communications Conference*. IEEE, 2012.

[TPHD19] H. Tibrewal, S. Patchala, M. K. Hanawal, and S. J. Darak. Distributed Learning and Optimal Assignment in Multiplayer Heterogeneous Networks. In *IEEE Conference on Computer Communications* (*INFOCOM 2019*), pages 1693–1701. IEEE, 2019.

[TRY17] K. Tomer, L. Roi, and M. Yishay. Bandits with Movement Costs and Adaptive Pricing. In *Conference on Learning Theory*, volume 65, pages 1242–1268. PMLR, 2017.

[TZZ19] C. Tao, Q. Zhang, and Y. Zhou. Collaborative Learning with Limited Interaction: Tight Bounds for Distributed Exploration in Multi-Armed Bandits. *arXiv preprint arXiv:1904.03293*, 2019.

[Val16] M. Valko. *Bandits on Graphs and Structures*. Habilitation thesis to supervise research, École normale supérieure de Cachan, 2016.

[Var17] G. Varoquaux. Joblib: running Python functions as pipeline jobs. Online at: `https://joblib.readthedocs.io`, March 2017.

[vdWCV11] S. van der Walt, C. S. Colbert, and G. Varoquaux. The NumPy Array: A Structure for Efficient Numerical Computation. *Computing in Science & Engineering*, 13(2):22–30, March 2011.

[VMB+10] V. Valenta, R. Maršálek, G. Baudoin, M. Villegas, M. Suarez, and F. Robert. Survey on spectrum utilization in Europe: Measurements, analyses and observations. In *5th EAI Conference on Cognitive Radio Oriented Wireless Network and Communication*, pages 1–5. IEEE, 2010.

[W+17] M. Waskom et al. Seaborn: statistical data visualization. Online at: `https://seaborn.pydata.org`, September 2017.

[Wal45] A. Wald. Some Generalizations of the Theory of Cumulative Sums of Random Variables. *The Annals of Mathematical Statistics*, 16(3):287–293, 1945.

[WBMB+19] F. Wilhelmi, S. Barrachina-Muñoz, B. Bellalta, C. Cano, A. Jonsson, and G. Neu. Potential and pitfalls of multi-armed bandits for decentralized spatial reuse in wlans. *Journal of Network and Computer Applications*, 127:26–42, 2019.

[WCN+19] F. Wilhelmi, C. Cano, G. Neu, B. Bellalta, A. Jonsson, and S. Barrachina-Muñoz. Collaborative spatial reuse in wireless networks via selfish multi-armed bandits. *Ad Hoc Networks*, 2019.

[WHCW19] Y. Wang, J. Hu, X. Chen, and L. Wang. Distributed Bandit Learning: How Much Communication is Needed to Achieve (Near) Optimal Regret. *arXiv preprint arXiv:1904.06309*, 2019.

[Whi88] P. Whittle. Restless bandits: Activity allocation in a changing world. *Journal of Applied Probability*, 25(A):287–298, 1988.

[Wil38] S. S. Wilks. The large-sample distribution of the likelihood ratio for testing composite hypotheses. *The Annals of Mathematical Statistics*, 9(1):60–62, 1938.

[WS18a] L. Wei and V. Srivastava. On Distributed Multi-player Multi-Armed Bandit Problems in Abruptly-Changing Environment. In *Conference on Decision and Control*, pages 5783–5788. IEEE, 2018.

[WS18b] L. Wei and V. Srivatsva. On Abruptly-Changing And Slowly-Varying Multi-Armed Bandit Problems. In *American Control Conference*, pages 6291–6296. IEEE, 2018.

[YA09] T. Yucek and H. Arslan. A Survey of Spectrum Sensing Algorithms for Cognitive Radio Applications. *IEEE Communications Surveys & Tutorials*, 11(1):116–130, 2009.

[Yaa77] M. E. Yaari. A Note on Separability and Quasiconcavity. *Econometrica*, 45(5):1183–1186, 1977.

[YFE12] X. Yang, A. Fapojuwo, and E. Egbogah. Performance Analysis and Parameter Optimization of Random Access Backoff Algorithm in LTE. In *Vehicular Technology Conference*, pages 1–5. IEEE, September 2012.

[YM09] J. Y. Yu and S. Mannor. Piecewise-Stationary Bandit Problems with Side Observations. In *International Conference on Machine Learning*, pages 1177–1184. ACM, 2009.

[Z. 19] Z. Tian and J. Wang and J. Wang and J. Song. Distributed NOMA-Based Multi-Armed Bandit Approach for Channel Access in Cognitive Radio Networks. *IEEE Wireless Communications Letters*, pages 1–4, 2019.

[ZBLN19] S. M. Zafaruddin, I. Bistritz, A. Leshem, and D. Niyato. Distributed Learning for Channel Allocation Over a Shared Spectrum. In *20th IEEE International Workshop on SignalProcessing Advances in Wireless Communications (SPAWC)*, Cannes, France, 2019.

[ZS07] Q. Zhao and B. M. Sadler. A Survey of Dynamic Spectrum Access. *Signal Processing magazine*, 24(3):79–89, 2007.

[ZS19] J. Zimmert and Y. Seldin. An Optimal Algorithm for Stochastic and Adversarial Bandits. In K. Chaudhuri and M. Sugiyama, editors, *Proceedings of Machine Learning Research*, volume 89 of *Proceedings of Machine Learning Research*, pages 467–475. PMLR, 2019.

– Well, my brother has his sword, and I have my mind. A mind needs books *like a sword needs a whetstone, if it is to keep its edge. That is why I read so much, Jon Snow.*
George R. R. Martin, *A Game of Thrones*.

UNIVERSITE BRETAGNE LOIRE / MATHSTIC

CentraleSupélec

Titre : Algorithmes de Bandits Multi-Joueurs pour les Réseaux de l'Internet des Objets

Mots clés : Internet des Objets (IdO), Radio Intelligente, Théorie de l'apprentissage, Apprentissage séquentiel, Apprentissage par renforcement, Bandits multi-bras (BMB), Apprentissage décentralisé, Bandits multi-bras multi-joueurs, Détection des points de changement, Bandits multi-bras non stationnaires

Résumé : Dans cette thèse de doctorat, nous étudions les réseaux sans fil et les appareils reconfigurables qui peuvent accéder à des réseaux de radio intelligente, dans des bandes non licenciées et sans supervision centrale. Nous considérons des réseaux actuels ou futurs de l'Internet des Objets (IdO), avec l'objectif d'augmenter la durée de vie de la batterie des appareils, en les équipant d'algorithmes d'apprentissage machine peu coûteux mais efficaces, qui leur permettent d'améliorer automatiquement l'efficacité de leurs communications sans fil. Nous proposons différents modèles de réseaux de l'IdO, et nous montrons empiriquement, par des simulations numériques et une validation expérimentale réaliste, le gain que peuvent apporter nos méthodes, qui se reposent sur l'apprentissage par renforcement.

Les différents problèmes d'accès au réseau sont modélisés avec des Bandits Multi-Bras (BMB), mais l'analyse de la convergence d'un grand nombre d'appareils jouant à un jeu collaboratif sans communication ni aucune coordination reste délicate, lorsque les appareils suivent tous un modèle d'activation aléatoire. Le reste de ce manuscrit étudie donc deux modèles restreints, d'abord des bandits multi-joueurs dans des problèmes stationnaires, puis des bandits mono-joueur non stationnaires. Nous détaillons également une autre contribution, la bibliothèque Python open-source SMPyBandits pour des simulations numériques de problèmes MAB, qui couvre les modèles étudiés et d'autres.

Title : Multi-Players Bandit Algorithms for Internet of Things Networks

Keywords: Internet of Things (IoT), Cognitive Radio, Learning Theory, Sequential Learning, Reinforcement Learning, Multi-Armed Bandits (MAB), Decentralized Learning, Multi-Player Multi-Armed Bandits, Change Point Detection, Non-Stationary Multi-Armed Bandits

Abstract: In this PhD thesis, we study wireless networks and reconfigurable end-devices that can access Cognitive Radio networks, in unlicensed bands and without central control. We focus on Internet of Things networks (IoT), with the objective of extending the devices' battery life, by equipping them with low-cost but efficient machine learning algorithms, in order to let them automatically improve the efficiency of their wireless communications. We propose different models of IoT networks, and we show empirically on both numerical simulations and real-world validation the possible gain of our methods, that use Reinforcement Learning.

The different network access problems are modeled as Multi-Armed Bandits (MAB), but we found that analyzing the realistic models was intractable, because proving the convergence of many end-devices playing a collaborative game without communication nor coordination is hard, when end-devices all follow random activation patterns. The rest of this manuscript thus studies two restricted models, first multi-players bandits in stationary problems, then non-stationary single-player bandits. We also detail another contribution, SMPyBandits, an open-source Python library for numerical MAB simulations, covering all the studied models and more.